Digitized by the Internet Archive
in 2023 with funding from
Kahle/Austin Foundation

https://archive.org/details/contributionsfro0015unse

Carnegie Institution of Washington

UNIVERSITY OF ARIZONA
STEWARD
OBSERVATORY
TUCSON, ARIZONA

CONTRIBUTIONS

FROM THE

MOUNT WILSON OBSERVATORY

VOLUME XV

NOS. 327–345

WITH FIVE PLATES

DECEMBER, 1926—MAY, 1927

UNIVERSITY OF ARIZONA
LIBRARY

C28
v.15

CONTENTS

NO. PAGE

327. THE ABSOLUTE MAGNITUDES OF GIANT M STARS. *Gustaf Strömberg* 1

328. A STUDY OF THE INFRA-RED SOLAR SPECTRUM WITH THE INTERFEROMETER. *Harold D. Babcock* 11

329. MEASUREMENT OF THE VELOCITY OF LIGHT BETWEEN MOUNT WILSON AND MOUNT SAN ANTONIO. *A. A. Michelson, Assisted by F. Pearson. With an Appendix,* MEASUREMENT OF LENGTH OF LINE USED IN DETERMINATION OF VELOCITY OF LIGHT, by *William Bowie* 35

330. THE SHORT-PERIOD VARIABLE STAR RV CANUM VENATICORUM. *J. Schilt* 57

331. INTERSTELLAR CALCIUM. *Otto Struve* 63

332. THE MOTIONS OF GIANT M STARS. *Gustaf Strömberg* 101

333. SPECTROGRAPHIC ORBITS OF THE TWO COMPONENTS OF BOSS 5683. *Roscoe F. Sanford* 129

334. STARS WHOSE SPECTRA HAVE BRIGHT IRON LINES. *Paul W. Merrill* 135

335. THE NEBULOUS ENVELOPE AROUND NOVA AQUILAE NO. 3. *Edwin Hubble* and *John Charles Duncan* 145

336. TRANSMISSION PROPERTIES OF SOME FILTERS. *Edison Pettit* . . 151

337. ON THE SPECTRA OF DOUBLY AND TREBLY IONIZED TITANIUM (*Ti* III and *Ti* IV). *Henry Norris Russell* and *R. J. Lang* . . . 167

338. INVESTIGATIONS ON PROPER MOTION. TWELFTH PAPER: THE PROPER MOTIONS AND INTERNAL MOTIONS OF MESSIER 2, 13, AND 56. *Adriaan van Maanen* 197

339. ON THE RELATIONS BETWEEN PERIOD, LUMINOSITY, AND SPECTRUM AMONG CEPHEIDS. *Henry Norris Russell* 221

340. ON THE RADIAL VELOCITY AND SPECTRUM OF THE CEPHEID VARIABLE T MONOCEROTIS. *Roscoe F. Sanford* 235

341. RELATED LINES IN THE SPECTRA OF THE ELEMENTS OF THE IRON GROUP. *Henry Norris Russell* 249

342. SERIES AND IONIZATION POTENTIALS OF THE ELEMENTS OF THE IRON GROUP. *Henry Norris Russell* 283

175530

NO. PAGE

343. SECONDARY STANDARDS OF WAVE-LENGTH; INTERFEROMETER MEASUREMENTS OF IRON AND NEON LINES. *Harold D. Babcock* 307

344. THE ARC AND SPARK SPECTRA OF TITANIUM. PART I: THE SPARK SPECTRUM, *Ti* II. *Henry Norris Russell* 335

345. THE ARC AND SPARK SPECTRA OF TITANIUM. PART II: THE ARC SPECTRUM, *Ti* I. *Henry Norris Russell* 381

LIST OF PLATES

NO. FACING PAGE

I. Spectrum of Integrated Sunlight . 33

II. Nova Aquilae No. 3 (1918) 146

III. Arc, Spark, and Vacuum-Spark Spectra of Titanium . 168

IV. Vacuum-Spark Spectrum of Titanium . . . 169

V. Arc and Furnace Spectrum of *Ti* λ4347 to λ4251 . 432

Contributions from the Mount Wilson Observatory, No. 327
Reprinted from the *Astrophysical Journal*, Vol. LXV, pp. 108–116, 1927
Printed in the U.S.A.

THE ABSOLUTE MAGNITUDES OF GIANT M STARS

By GUSTAF STRÖMBERG

ABSTRACT

Derivation of absolute magnitudes from spectroscopic criteria.—The article gives the method and the formulae used in deriving the reduction curves which are the basis of the absolute magnitudes of *giant M stars* published by Adams, Joy, and Humason in *Mt. Wilson Contr.*, No. 319. Provisional curves for each spectral subdivision were formed for each line listed in *Contr.* No. 319 and adjusted to give an accordant system of magnitudes M_1. Systematic corrections, S, to this provisional system then gave the adopted system M_1+S. The absolute magnitudes were derived entirely from the *peculiar motions;* parallactic motions have not been used because of the large dispersion in velocity. Results from trigonometric parallaxes are also given, but the parallaxes are very small and not numerous enough to give the same accuracy that can be obtained from the peculiar motions.

Probable errors and residual systematic corrections.—Figure 1 shows the relation between the computed absolute magnitudes and the provisional magnitudes. The deviations from the line represent the *residual systematic corrections,* S' (Table I), to the adopted magnitudes. In general these are below 0.1 mag. S'_1 and S'_2 are similar corrections for use in deriving mean parallaxes and mean tangential motions. The *probable errors* of individual determinations of an absolute magnitude for the supergiants and the ordinary giants are ± 0.63 and ± 0.45 mag., respectively. These were derived from the dispersion in M, which was obtained from a simple formula, equation (10), which is not influenced by the systematic corrections. This formula is also applicable in cases where no spectroscopic absolute magnitudes are available, in which case τ' is a reduced τ-component.

In *Mount Wilson Contribution*, No. 319,[1] Adams, Joy, and Humason have published the absolute magnitudes, as determined from spectroscopic criteria, of practically all the M stars brighter than apparent magnitude 6.0 and north of declination $-30°$. All of these stars, at least as far as the spectroscopic criteria indicate, are giants. The reduction curves used for the different spectral lines were derived by the writer. The following account gives data regarding the systematic and accidental errors affecting the results.

The general method used by Adams was to select lines which apparently varied with absolute magnitude. As an indication of the general order of absolute magnitude, the reduced proper motion $H=m+5 \log \mu$ was used. The existence of a correlation between line-intensity and H was accepted as an indication that a line could be used for determining the absolute magnitude. The lines finally used are given in the paper cited.

---

[1] *Astrophysical Journal*, 64, 225, 1926.

For each line groups of stars were formed having a small range in line-intensity and spectral subdivision. An approximate mean absolute magnitude was then computed from the peculiar motions by methods explained later on. The resulting reduction curves for the different lines were slightly adjusted with the aid of the correlation data for individual lines, so that all the lines would give, as nearly as possible, the same absolute magnitude. The absolute magnitudes derived from the adjusted curves are denoted by M_1. Corrections to this system were then computed with the aid of additional data which had been obtained in the meantime. The results of this last computation are given below, together with the derivation of the formulae for computing the mean absolute magnitudes and their dispersion.

The following notation is used:

M = the true absolute magnitude of a star; M_1 = the provisional absolute magnitude derived from spectroscopic criteria; S = the systematic correction to a mean M_1 to reduce it to a mean M; Δ = the difference between M and M_1+S for an individual star; m = the apparent visual magnitude from the *Henry Draper Catalogue;* π = the true parallax; π_1 = the spectroscopic parallax derived from the difference M_1-m; τ = a peculiar angular cross-motion, either perpendicular to the great circle toward the assumed solar apex (τ-component), or a proper-motion component along any axis after the parallactic motion projected on this axis, calculated with π_1 as an approximate value of the parallax, has been subtracted; τ' = an angular peculiar motion divided by the parallax π_1 for the same star; τ_m and τ'_m = the average values of τ and τ' taken without regard to sign; θ = average peculiar radial velocity in km/sec., without regard to sign; ϵ = the peculiar linear cross-motion projected on the same axis as τ; k = 4.738 km×year/sec., numerically equal to the mean distance of earth to sun in kilometers divided by the number of seconds in a year.

We have then

$$M=M_1+S+\Delta\ , \tag{1}$$

$$\pi=0.1\times 10^{0.2(M-m)}=\pi_1\sigma\delta\ , \tag{2}$$

where

$$\left.\begin{array}{l}\pi_1=0.1\times 10^{0.2(M_1-m)}\\ \sigma=10^{0.2S}\ ;\qquad \delta=10^{0.2\Delta}\end{array}\right\} \tag{3}$$

$$k\tau=\pi\epsilon=\pi_1\sigma\delta\epsilon\ . \tag{4}$$

The errors Δ are supposed to be distributed according to a normal error function around a zero value, and the dispersion is defined by the equation

$$q^2=\overline{\Delta^2}\ .$$

We have

$$\overline{M}=\overline{M}_1+S\ ,$$

where a bar above a symbol denotes an algebraic mean.

Further,

$$\bar{\delta}=\overline{10^{\ 0.2\Delta}}=\frac{1}{\sqrt{2\pi}\ q}\int_{-\infty}^{+\infty}10^{0.2\Delta}\,e^{-\frac{\Delta^2}{2q^2}}\,d\Delta=A\ . \tag{5}$$

The following relation between A and q is then found:

$$q^2=50\ \text{Mod}\ \log A=21.71\ \log A\ . \tag{6}$$

The approximate formula

$$A=1+\frac{0.02q^2}{\text{Mod}^2}$$

was given in *Contribution* No. 199, page 6,[1] and can be used for q less than about ± 1.0, but the general formula (6) is equally simple.

Before forming means of the equations (4), we must consider the correlations between δ and the other quantities present. The errors Δ arise from several causes. First, there are errors in the measurements of the line intensities; further, the true line intensity may vary, the true absolute magnitude remaining constant; and, finally, the true absolute magnitude may vary while the spectral criteria used remain unaffected. We may thus expect correlations between Δ and M_1 and between Δ and M, the former being particularly marked if the true absolute magnitude varies less than that spectroscopically determined, and the latter, if the reverse is the case. In equation (4) we may thus expect a correlation between δ and π_1, and also between δ and π, and, consequently, between δ and τ. The correlation between absolute magnitude and velocity would produce a correlation between δ and ϵ, but, since the change in mean peculiar radial velocity for the different groups is in this case practically zero, we need not consider the last correlation.

---

[1] *Astrophysical Journal*, **53**, 18, 1921.

Forming the mean for equations (4), disregarding their signs, we find

$$k\tau_m = \bar{\pi}\theta = \overline{\pi_1\delta}\,\sigma\theta\ .$$

We thus obtain

$$\bar{\pi} = \frac{k\tau_m}{\theta} = \overline{\pi_1\delta}\,\sigma = \sigma_1\bar{\pi}_1\ . \tag{7}$$

We cannot here separate $\overline{\pi_1}$ from $\bar{\delta}$.

Dividing equation (4) by π_1 and forming similar means, we find

$$\sigma\bar{\delta}\theta = k\tau'_m\ .$$

Since, by (5), $\bar{\delta}$ is denoted by A, we may write

$$\sigma A = \frac{k\tau'_m}{\theta} = \sigma_2\ . \tag{8}$$

To determine σ and A separately, we must have recourse to moments of second order. First, we derive from a relation analogous to (5),

$$\overline{\delta^2} = \overline{10^{0.4\Delta}} = A^4 = \bar{\delta}^{4}\ . \tag{9}$$

Dividing equations (4) by π_1, and forming the means of the squares, we find

$$k^2\overline{\tau'^2} = \sigma^2 A^4 \overline{\epsilon^2}\ .$$

From this and equation (8) we obtain

$$A^2 = \frac{\tau'^2\,\theta^2}{\tau'^2_m\,\overline{\epsilon^2}}\ . \tag{10}$$

Here for $\overline{\epsilon^2}$ we may use the mean-square peculiar radial velocity.

When the proper motions themselves are small, the values of τ_m and τ'_m in equations (7) and (8) are systematically affected by the errors in the measurements. To correct them, I have used the formulae

$$\frac{\text{Corr. }\tau_m}{\tau_m} = \frac{\text{Corr. }\tau'_m}{\tau'_m} = \sqrt{1 - \frac{\eta^2}{\tau^2_m}}\ ,$$

where η is the average error, assumed to be ±0″003, in a component of the proper motion.

To increase the accuracy, the proper motions have been corrected for the systematic errors in right ascension as given in Boss's *Catalogue*, page xxviii. To the proper motions in declination, Raymond's corrections[1] were applied. Further, use was made not only of the τ-components, but also of the components of proper motion in right ascension and declination, corrected for parallactic motion with the aid of π_1 as an approximate value of the parallax. The formulae used are

$$\tau_\alpha=\mu_1-B_1\pi_1\ ;\qquad \tau_\delta=\mu_2-B_2\pi_1$$
$$kB_1=x_0\sin\alpha-y_0\cos\alpha$$
$$kB_2=x_0\cos\alpha\sin\delta+y_0\sin\alpha\sin\delta-z_0\cos\delta\ ,$$

where x_0, y_0, and z_0 are the equatorial components of the sun's motion. This motion has been assumed throughout to have the co-ordinates $\alpha=270^\circ$, $\delta=+30^\circ$, $v=20$ km/sec. Although the solar motion as derived from the radial velocities of the M stars has a value of about 23 km/sec., this difference has no appreciable effect upon the mean peculiar motions. In the computation of A^2, only the actual τ-components were used. As long as S and σ are small, there is no systematic difference between the results from the τ-components and from τ_α and τ_δ.

The quantity A and the corresponding dispersion can be computed from equations (10) and (6) only for fairly large groups. If the dispersion thus found is assumed to hold also for the smaller groups, individual determination of σ can be made for these groups.

The three quantities σ, σ_1, and σ_2 represent the factors by which the provisional spectroscopic parallaxes π_1 must be multiplied in using them to obtain the most probable absolute magnitudes, the mean parallaxes, and the mean linear tangential motions. The corresponding corrections to M_1 are S, S_1, and S_2, defined by the equations

$$S=5\log\sigma\ ,\qquad S_1=5\log\sigma_1\ ,\qquad S_2=5\log\sigma_2\ .$$

The data computed by these formulae are collected in Table I. The third and the last row may be regarded as representative for

---

[1] *Astronomical Journal*, **36**, 129, 1926.

TABLE I

Sp.	M_1	No.	$\bar{\pi}_1$	θ km/sec.	S	S_1	S_2	r	$\dot{M}_1$	M_1+S	S'	S'_1	S'_2
Mo–M2. . .	≤ -1.0	24	0″.00428	16.17	+0.34	+0.25	+0.54	±0.63	−2.16	−1.82	−0.16	−0.25	+0.04
M3–M5. . .	≤ -1.0	20	.00558	17.60	.69	.61	.90	.63	−1.25	−0.56	+ .19	+ .11	+ .40
Mo–M5. . .	≤ -1.10	44	.00487	16.82	.52	.42	.72	.63	−1.75	−1.23	+ .02	− .08	+ .22
Mo–M2. . .	$-0.9 - -0.5$	49	.00620	17.38	.36	.27	.46	.45	−0.64	−0.28	− .02	− .10	+ .09
Mo–M2. . .	≥ -0.4	93	.00749	17.93	.32	.34	.42	.45	− .15	+ .17	+ .01	+ .02	+ .11
Mo–M2. . .	$\geq +0.1$	19	.00899	16.2	.14	.27	.25	.45	+ .22	+ .36	− .13	− .01	− .03
M3–M5. . .	≥ -0.9	70	.00673	17.35	.27	.34	.37	.45	− .48	− .21	− .09	− .01	+ .01
Mo–M7. . .	≥ -0.9	223	0.00686	17.86	+0.27	+0.30	+0.37	±0.45	−0.39	−0.12	−0.08	−0.05	+0.03

the supergiants and the ordinary giants, respectively, although no sharp dividing limit can be given. The quantity r is the probable error in the spectroscopic absolute magnitude for a single star, and is simply the dispersion q converted into probable error. An important feature is the small variation in θ, which is derived from the radial velocities for the same stars whose proper motions are used.

Figure 1 shows the relationship between $\overline{M}_1$ and the computed mean absolute magnitude $\overline{M}$, which is equal to $\overline{M}_1+S$. The line drawn was used in deriving the systematic corrections to the system, and the residuals are denoted by S', S_1', and S_2'. These quantities may be regarded as the residual systematic corrections to the absolute magnitudes, as published by Adams, Joy, and Humason, which are to be applied according as it is desired to find absolute magnitudes, mean parallaxes, or mean tangential motions. They are all smaller than their mean errors and can well be neglected.

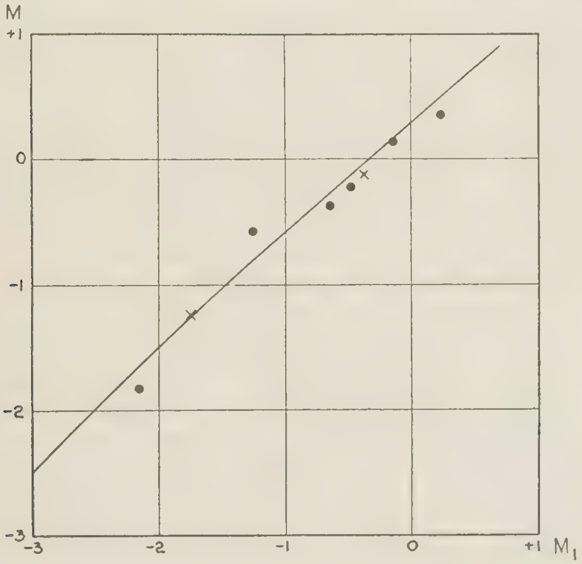

FIG. 1.—Correlation between absolute magnitudes M_1, derived from line intensities by using a provisional system of reduction curves, and the absolute magnitudes M derived from peculiar motions.

Appreciably different reduction curves have been used for the different spectral subdivisions. In *Contribution* No. 199, on the other hand, the same reduction curves were used for all spectral subdivisions. Although the line intensities vary considerably, the new reduction curves make the ordinary giants of all spectral subdivisions of nearly the same visual absolute magnitude. The small dispersion in absolute magnitude for these stars is quite remarkable. This cannot be due to a failure of the spectral criteria, for, as seen by the diagram, the variation of M with respect to $\overline{M}_1$ is practically linear throughout the entire range of absolute magnitude. If we compute the dispersion in absolute magnitude among the supergiants and ordinary giants separately by assuming the absolute magnitude to be constant, we find by formula (10), (where τ' now is equal to $\tau\, 10^{0.2m}$), $q=1.17$ and 0.70 mag., respectively, corresponding to the probable errors of ±0.79 and ±0.47 mag. This means that the dispersion in the ordinary giants is so small that, if we could separate them from the supergiants, which have a much larger dispersion, we should attain nearly the same accuracy by giving them all the same absolute magnitude.

Part of the error in the absolute magnitude arises from error in the measurement of the line-intensities. If we estimate the probable error from this source to be ±0.2, a somewhat larger amount must be due to a lack of correspondence between the spectral criteria and the absolute magnitudes.

The most important question, however, concerns the reliability of the systematic corrections. To determine the corrections, parallactic motions have also been used, but the results are very uncertain, mainly because of the large dispersion in velocity. The solar motion as computed from a small number of radial velocities has little weight, and, similarly, the group motion for a small number of objects may differ greatly from that derived from very large groups. Further, the underlying assumption is quite different from that used in dealing with peculiar motions. The assumption usually made is that the linear group motion is known and that the sum of the squares of the peculiar angular motions is a minimum. When the dispersion in linear motion is large, the result must be very uncertain, and may even be systematically affected. Systematic errors in the proper motions are also very serious, since the motions themselves are very small. Further, in using peculiar motions, all stars have the same weight, which is not at all the case when the parallactic motions are employed.

In the present case, we find that the absolute magnitudes computed from parallactic motion, with a solar motion of 23 km/sec., would be brighter by 1.02 for the supergiants and 0.49 for the ordinary giants. A similar discrepancy was found for the long-period variables.[1]

The adopted value of the average error in the proper-motion components, which was supposed to be ±0".003, may be too small. If we assume an error of ±0".008, the effect on the magnitudes of the two classes of stars would be to make them 0.12 and 0.05 mag. brighter, respectively, than the published values. The uncertainty from this cause is therefore not serious.

The trigonometric parallaxes are very small and not numerous enough to determine the mean absolute magnitude with the same accuracy as can be derived from the peculiar motions. Using the parallaxes compiled by Schlesinger, we find the systematic correction to the provisional system to be +0.24 mag., which is in good agreement with the results from peculiar motion. For an assumed probable error of ±0".007 in the trigonometric parallaxes, the corresponding probable error in the absolute magnitudes is ±0.3. A larger probable error in the trigonometric parallaxes would make the probable error in the absolute magnitudes even smaller. But all results from the trigonometric parallaxes are rather uncertain, and it seems better to reverse the process and determine the errors in the trigonometric parallaxes from the spectroscopic values.

Although the cause of the systematic difference between the results based upon peculiar and parallactic motion is still obscure, there can be little doubt about the small dispersion in the visual absolute magnitudes. Moreover, a systematic correction as large as 0.5 mag. cannot be applied to the absolute magnitudes without producing a serious discrepancy between the dispersion in tangential and radial velocities, which is of special importance when the parallaxes are used for computing space velocities.

MOUNT WILSON OBSERVATORY
December 1926

---

[1] *Mt. Wilson Contr.*, No. 267; *Astrophysical Journal*, 59, 97, 1924.

Contributions from the Mount Wilson Observatory, No. 328
Reprinted from the *Astrophysical Journal*, Vol. LXV, pp. 140–162, 1927
Printed in the U.S.A.

A STUDY OF THE INFRA-RED SOLAR SPECTRUM WITH THE INTERFEROMETER

By HAROLD D. BABCOCK

ABSTRACT

Solar wave-lengths in the infra-red.—The solar spectrum in the interval λ 6868–λ 8980 has been photographed on plates sensitized with *neocyanin* through interferometers crossed with a concave grating. The *methods* and *apparatus* used are described, and also some of the precautions taken to avoid instrumental errors. The *wave-lengths* of 507 lines (Table II) were measured in terms of oxygen band lines due to terrestrial absorption, and are expressed on the *neon scale.*

Identification of solar lines.—Of the 507 *lines measured*, 176 are of solar origin; most of the remainder are probably lines of terrestrial water vapor. The measurements have been used for a revision of the identification of solar lines, but refined laboratory wave-lengths are much needed for further work. The more prominent solar lines still awaiting identification are listed in Table IV.

Differences between solar and terrestrial wave-lengths.—In the absence of precise laboratory data for vacuum spectra in the infra-red, the new solar wave-lengths are compared with interferometer measurements on the spectrum of a short iron arc at atmospheric pressure. This brings out clearly the correlation of multiplet grouping, excitation potential, and behavior under increased excitation with the combined influence of pressure displacement and pole effect. The data, though not definitive, are consistent with the gravitational displacement predicted by Einstein.

INTRODUCTION

The photographic difficulties which have somewhat retarded the progress of spectroscopy in the near infra-red have recently been markedly reduced. A new sensitizing material, neocyanin, makes it easy to obtain photographs which with dicyanin are troublesome and unsatisfactory. This is particularly important in investigations involving precise measurements, where instrumental changes and variations of observing conditions become a serious drawback, if the exposures are greatly prolonged. This paper presents the results obtained from a series of photographs of the solar spectrum covering the region λ 6868–λ 8980, neocyanin being used for wave-lengths greater than λ 7300.

The plates, which were prepared by Mr. C. E. K. Mees at the Research Laboratory of the Eastman Kodak Company, require a brief treatment with ammonia to make them ready for use. They keep indefinitely before this treatment and for at least two months afterward. Their maximum sensitivity is at λ 8300; their absolute speed is far higher than that of plates prepared with dicyanin; and, in addition, the negatives are free from fog and brilliant in contrast.

Although it has been found that terrestrial absorption lines dominate the infra-red solar spectrum, both in number and in average intensity, the several hundred recognized solar lines offer valuable opportunity for study. Some prominent unidentified solar lines call for new data from the laboratory, and accuracy of a comparatively high order is required in both solar and laboratory wave-lengths for fixing their origin. But beside the possibility of bringing to light elements hitherto unrecognized in the sun, it is perhaps more important to examine in greater detail the application of the fruitful theory of ionization to astrophysical problems, and to add to the impressive mass of data bearing on the existence of the Einstein effect the results of a study of that part of the spectrum in some ways peculiarly suitable for a test.

Grating measurements of the solar spectrum λ 6500–λ 9000 have been published by W. F. Meggers,[1] and F. S. Brackett[2] has studied the region λ 8900–λ 9850, but the methods employed were not sufficiently refined to yield wave-lengths accurate enough for any but the obvious identifications of solar lines. These papers are very useful for distinguishing between solar and terrestrial absorption lines and in providing wave-lengths sufficiently approximate for the reduction of observations made with the interferometer. The work of K. Burns[3] gives no wave-lengths in the infra-red region. No measurements made by the interference method in this part of the solar spectrum appear to have been published. It is hoped that the data now made available will be confirmed by other observers and that interpolation by the grating method will promptly be undertaken.

The observations presented here are part of a study of the whole solar spectrum photographically accessible, which has long been in progress at this Observatory. Results for the visible region, based on extensive measurements with gratings of high dispersion and with interferometers, will soon be published.

---

[1] *Publications Allegheny Observatory*, **6**, No. 3, 1919.

[2] *Mt. Wilson Contr.*, No. 197; *Astrophysical Journal*, **53**, 121, 1921.

[3] *Lick Observatory Bulletins*, **10**, 64 (No. 327), 1920.

METHOD

The Fabry-Perot interferometer with concave grating for auxiliary dispersion, which forms part of the equipment of the Pasadena Laboratory, has already been described.[1] This apparatus, so effective for the study of emission spectra, has proved suitable for extensive work on the solar spectrum as well. For this purpose, a coelostat was built in the instrument shop of the Observatory and mounted on the roof of the laboratory, where a second flat mirror directs the light vertically downward into the building upon a third mirror, which reflects it horizontally to the spectrograph. Space is lacking for the installation of a long-focus objective which would provide a large image of the sun. Instead, a lens of about 1-m focal length is used, and the measurements are made upon the spectrum of integrated sunlight. The lens, a visually corrected achromat of 9.5-cm clear aperture, produces a small image of the sun in focus on the etalon. The latter is so placed with respect to the concave mirror which projects the interference pattern on the slit that a real image of the sun 5 cm in diameter is formed on the ruled surface of the concave grating.

The integration of light over the whole disk necessarily produces spectral lines wider than those obtained from a restricted area of the disk. This disadvantage is not serious, however, since the lines in this part of the spectrum are inherently wide and the additional width is not relatively large. Quite apart from this effect, which is due primarily to the rotation of the sun, is the question of the comparability of wave-lengths derived from the center of the disk and from the entire disk. The well-known limb effect, although made somewhat less effective by the darkening at the limb, might be expected to produce slightly longer wave-lengths when integrated sunlight is used than when light is isolated from the center of the disk. An examination of the data available indicates that for the visible spectrum this difference can hardly exceed 0.001 A, a result confirmed by direct spectroscopic comparison. Data are lacking for such a comparison in the infra-red, but it is improbable that the wave-lengths of integrated sunlight can exceed those from the center of the disk by more than 0.002 or 0.003 A at λ 9000, which is near the limit of accuracy obtainable in that region.

---

[1] *Mt. Wilson Contr.*, No. 137; *Astrophysical Journal*, 46, 138, 1917.

The grating now in use was ruled in the instrument shop of the Observatory by Mr. Jacomini. It has 66,100 lines, spaced 600 to the millimeter, and the area of the ruled surface is 110 sq. cm. It gives exceptional brightness in the infra-red of one first-order spectrum, with some false light due to imperfection in the ruling. With the use of filters excellent contrast is obtained on photographs extending to λ 8980, which is the limit set by the space available for turning the camera.

Various filters were used, such as cobalt glass, Prussian blue in gelatin, and aqueous solutions of malachite green, with an ordinary red screen added for removing the short wave-lengths which they transmit. Occasionally the solution of malachite green was made dense enough to require no auxiliary screen. My thanks are due to Mr. Pettit for examining with a thermocouple the transmission of several screens over a wide range of wave-length. His observations, which will be published when completed, indicate that between λ 7000 and λ 9000 the cobalt glass Corning G585M, 3.5 mm thick, is the most efficient of the screens tested for the special purposes of this investigation.

The extent of spectrum to be photographed at one time and the curve of sensitivity of the emulsions to be used, together impose conditions on the properties of the screen which can be only approximately fulfilled. With some combinations of screens it was necessary to reduce the exposure of one part of the plate by means of a light shutter in front of the plateholder. In some instances a portion of one photograph was permitted to overexpose, and was subsequently reduced with potassium ferricyanide. For a few plates a region of under-exposure was copied twice by contact printing on emulsions of strong contrast, in order to make more lines available for measurement. In such cases the measurements on the original negative were carefully compared with those of the same lines on the copy in order to allow for any possible change of scale. Fifteen or twenty lines, inaccessible on certain original plates but measurable on others, were thus made to yield accordant results.

In the description of the spectrograph to which reference has been made, it was stated that flat plates 10 inches long were used. Since that was written, the plateholder has been changed to accommodate plates 16 inches long. The radius of curvature of the focal surface is readily calculated from the elementary theory of the concave grating, details of which need not be repeated here. It turns out to be nearly 131 cm. Attention is directed to this point because in one description of this type of spectrograph it is erroneously stated that "the grating focused the spectra in a circle with its center at the grating and radius equal to the focal length of the grating."

A very satisfactory procedure consists in using three flat plates, each 5 inches long, held tangent to a form having the correct curvature. The residual errors in focal position of the plates are entirely negligible under these conditions, and the reduction of the measurements is facilitated.

The method of reduction developed and described in a previous paper[1] has been slightly modified to adapt it to the increased range of spectrum covered by each plate. The plate constant is now a constant only for the central section of the photograph; for the end sections it must be slightly increased, because the magnification of the spectrograph is slightly less at the ends of the plateholder than in the center. This variation is represented for each photograph by three straight lines on a diagram having wave-lengths for abscissae and values of the "constant" (or its four-place logarithm) as ordinates. From the radius of curvature of the focal surface the symmetrical relation between these lines is calculated once for all, so that it requires only a moment to construct the diagram after a value of the ordinate for any point is determined. From a large number of measurements corresponding to known focal settings of the spectrograph, an instrumental constant has been found by means of which the ordinate for the central section of the plate can be calculated with higher precision than it can be measured for a single plate. No measurements are required except those of the ring diameters themselves.

Etalons of 2.5, 5.0, 7.5, and 10.0 mm thickness have been used in this investigation, with four pairs of planes—two of fused quartz, one of crystalline quartz, and one of glass. Most of the observations have been made with films of gold sputtered on the quartz planes, two different thicknesses of metal being used. Silver films were used for two photographs, and copper films were tried, but these gave a distinctly lower ratio of reflecting power to transmission coefficient than gold. The results are based entirely on photographs made with gold and silver.

---

[1] *Mt. Wilson Contr.*, No. 202; *Astrophysical Journal*, 53, 43, 1921.

The correction for change of phase has been found in the usual way by the use of etalons of different thickness having the same metallic films. For a 10-mm etalon with gold films the correction amounts to only −0.001 A for wave-lengths observed at λ 7700 in terms of standards at λ 6900, and it is a linear function of the wave-length. I am indebted to Mr. Pettit for thermocouple measurements of the transmission of one of my thinner gold films. He finds that the light transmitted falls uniformly from 27 per cent at λ 7000 to 15 per cent at λ 9000. Evidently no marked variation in the optical constants of gold occurs within this region, and no great phase change is to be expected.

The phase correction given above is in excellent agreement with a previous determination for a different pair of films, which were studied in the region λ 6000–λ 7438. It would appear that sputtered films of gold, like those of silver, are highly reproducible, at least with respect to the properties which determine the so-called "phase change." In fact, for silver, it has been found that the amount of the correction is the same for films two years old as for those a few hours old; for thick films as for thin ones; for those sputtered in one laboratory as for those made elsewhere. In all probability the same is true for gold.

During the course of the investigation the entire optical system was purposely displaced and readjusted with extreme care. The concave mirror used for projecting the interference pattern on the slit was replaced by another of nearly the same focal length, and every detail of the operation of the apparatus was thoroughly examined.

Diaphragms were used to prevent all useless light from reaching the etalon, and a water cell was usually inserted in the beam of light. The effect of exposing the etalon continuously to the solar image under conditions distinctly less favorable than those regularly employed was tested by using the very fine line λ 6292, due to terrestrial oxygen, for a series of visual measurements of the thickness of the etalon. Seven sets of readings made at ten-minute intervals showed a steady increase in thickness, amounting to one part in one-and-a-half million at the end of an hour. The sunlight was then cut off, and a half-hour later a trial showed that the thickness had continued to increase at about the same rate. In making photographs of the infra-red spectrum, the total energy incident on the etalon was less than one-half of what it was in this test. The lines on long exposures appear as sharp, and give the same wave-lengths, as on the short ones.

The well-known difficulties of securing reliable comparison spectra for precise measurements of wave-length are no less troublesome in the infra-red region, where exposures are sometimes necessarily prolonged. Neither the method of simultaneous exposures nor that of successive exposures is satisfactory for use with the interferometer in this part of the spectrum; and the overlapping higher-order spectra are not available, because interferometers economical of infra-red light generally have too little reflecting power to produce good fringes in violet light.

Instead of employing directly either the primary standard or any of the adopted secondaries, it was decided to refer all measurements to the wave-lengths of selected absorption lines of terrestrial oxygen which have been well determined from secondary standards in the spectrum of neon. These oxygen lines offer definite advantages, since they are automatically present on photographs of the solar spectrum, under conditions of illumination identical with those obtaining for the solar lines. Furthermore, many of them are very sharp, and a thorough examination has shown[1] that they are constant in position within the errors of established methods of observation. The use made of them here confirms the reliability of both oxygen and water vapor lines, at least for solar altitudes greater than about 40°.

The work was done between June 9 and October 28, 1926, at different hours between 9:00 A.M. and 4:00 P.M. No evidence of variability in position is shown by any of the observed wave-lengths, except that due to the motion of the apparatus with respect to the sun. Corrections for this motion ranging from −0.013 to +0.015 A were applied to the observed wave-lengths of all solar lines, and it is an indication of the accuracy of the results that the application of these corrections always increased the accordance of the data. In fact, one may readily distinguish between solar and terrestrial lines without using the rotation of the sun, by taking interferometer plates at such hour angles and longitudes of the sun as to make use of the variation in the earth's motion with respect to the sun.

---

[1] *Mt. Wilson Contr.*. No. 223; *Astrophysical Journal*, 55, 321, 1922.

TABLE I

Wave-Lengths of Oxygen Lines Used as Standards; Neon Scale

α-Band	*B*-Band		*A*-Band
6276.609	6868.915	6893.309	7676.563
6276.818	6869.093	6896.037	7677.618
6278.878	6870.946	6896.965	7682.756
6279.100	6871.285	6899.954	7683.800
6279.896	6872.247	6900.868	7689.177
6280.393	6872.843	6904.117	7690.217
6281.178*	6873.798	6905.023	7695.837
6281.956*	6874.653	6908.534	7696.868
6283.795*	6875.590	6909.431	
6287.747	6876.715	6913.200	
6289.397	6877.637	6914.090	
6290.222	6879.041	6918.122*	
6292.162*	6879.928*	6919.002*	
6292.957*	6883.832*	6923.302*	
6295.178*	6886.743	6924.172*	
6295.961*	6888.948		
6302.001	6889.903		
6305.810	6892.369		

With the exception of three short gaps of about 200 A each, atmospheric lines suitable for use as secondary standards of wave-length are distributed over the entire region λ 6900–λ 9000. In contrast with the solar lines in this part of the spectrum, the atmospheric lines are notable for their great sharpness and blackness. They will undoubtedly prove of material assistance in further work.

In Table I are given the wave-lengths of some oxygen band lines which have been found particularly useful as working standards. Attention is specially directed to the fact that all the wave-lengths communicated in this paper are independent of the adopted system of secondary standards in the iron-arc spectrum. It is now fully recognized that a slight revision of that system is necessary in order to make it accordant with the primary standard and with the adopted secondaries in the spectrum of neon. The latter, however, have shown no appreciable errors under the most critical scrutiny, and the adopted wave-lengths may be accepted with confidence. For this reason the data given in Tables I and II have been marked "neon scale," and it is hoped that they are free from systematic errors. New measurements of the wave-lengths of iron-arc lines have now been completed at this Observatory for the region λ 3400–λ 6750, which will soon be ready for publication.

The data given in Table I for lines in the a-band were derived from thirteen plates made with the interferometer and an equal number of grating plates. For each kind of exposure two entirely different instruments were used, one on Mount Wilson and one in the Pasadena Laboratory. In some cases the neon standards were used, while in others the revised values of the iron standards furnished the reference system. The agreement among the separate determinations is excellent, and the wave-lengths are probably reliable to the nearest 0.001 A. Lines marked with an asterisk are of slightly higher weight than the remainder.

The *B*-band lines of Table I were measured in terms of the best lines in the a-band on from six to thirteen interferometer plates. These plates also were made with two different instruments, as in the case of the a-band plates. The *B*-band lines were arranged in two groups corresponding to the two branches of the band, and the vacuum wave numbers were examined by taking first and second differences consecutively. The second differences are very accordant, the most probable value being 0.518 cm^{-1} with a probable error of ±0.002. On the wave-length scale this corresponds to an uncertainty of about ±0.001 A in the relative values, which is nearly the same as the uncertainty in the absolute values of the wave-lengths.

The relative values of the best lines in the *B*-band have been further studied by using these lines as standards for determining the thicknesses of the etalons in the regular course of reduction of the infra-red photographs. When the thickness is found from ten or twelve such lines, the probable error in the mean value is somewhat less than one part in ten million, and no systematic deviations are shown by the individual lines.

The *A*-band lines given in Table I were measured in terms of the *B*-band on twelve excellent interferometer plates made with four different lengths of etalons and three different pairs of films, both gold and silver. The variety of instrumental equipment used and the accordance of the results inspire confidence in the reliability of these working standards. Measurements made in terms of these *A*-band lines are in excellent agreement with those which are referred directly to the *B*-band.

Much of the measurement represented in this paper has been done under my direction by Mr. W. P. Hoge, and it is a pleasure to acknowledge my appreciation of his interested co-operation. Part of the photographs have been measured in duplicate and others solely by myself. The accordance of the measurements is closer than the nature of the lines would lead one to expect, even the wide solar lines showing accidental errors of only a few thousandths of an angstrom. As examples, the results from individual photographs are given below for the atmospheric line λ 8329 and for two solar iron lines λ 8085 and λ 8515. These lines were not specially selected and are typical of the material in Table II. For lines observed on ten plates, the average wave-lengths generally have probable errors somewhat less than ±0.001 A, so that the probable error of a single determination may be taken as ±0.003 or 0.004 A as a rule.

λ 8329.685	λ 8085.183	λ 8515.124
8329.681	8085.185	8515.122
8329.685	8085.173	8515.117
8329.678	8085.174	8515.123
8329.678	8085.174	8515.123
8329.679	8085.168	8515.117
8329.673	8085.171	8515.124
8329.681	8085.164	8515.116
8329.683	8085.175	8515.132
8329.688	8085.177	8515.120
8329.689	8085.176	8515.115

Table II, to which reference has already been made, gives in

TABLE II

Solar Spectrum Wave-Lengths; Neon Scale

λ	Int.	Substance	No. Obs.	λ	Int.	Substance	No. Obs.
6868.915	7	A	4	7011.323	2	A	7
6869.093	6	A	4	7016.442	3	Fe, A	5
6870.946	8	A	4	7022.958	2	Fe	5
6871.285	10	A	4	7023.503	2	A	5
6872.247	11	A	8	7027.477	2	⊙, A	4
6872.843	12	A	8	7034.910	2N	⊙	4
6873.798	12	A	8	7039.793	1N	A	8
6874.653	13	A	8	7050.853	0	A	8
6875.590	13	A	8	7052.776	1	A	6
6876.715	13	A	8	7057.005	0N	A	2
6877.637	12	A	8	7065.647	1	A	3
6879.041	12	A	9	7068.423	2	Fe	2
6879.928	6	A	13	7084.975	2N	Co	4
6883.832	10	A	13	7088.153	00N	A	1
6885.754	11	A, Fe	9	7090.390	2	Fe	7
6886.743	12	A	9	7122.207	4	Co, Ni	8
6888.948	13	A	9	7130.925	3	Fe	8
6889.903	14	A	7	7132.983	1	Fe	3
6892.369	14	A	7	7148.149	3N	Ca	8
6893.309	15	A	8	7158.775	0N	A	1
6896.037	14	A	8	7162.041	00N	A	1
6896.965	15	A	8	7164.415	2	Fe, A	2
6899.954	14	A	8	7167.904	4N	A	6
6900.868	15	A	8	7172.713	1	A	1
6904.117	14	A	8	7181.509	2	A	1
6905.023	14	A	8	7184.526	4	A	1
6908.534	13	A	8	7191.493	6N	A	2
6909.431	13	A	8	7195.044	2	A	3
6913.200	11	A	7	7195.794	0N	A	1
6914.090	11	A	7	7197.865	1N	A	1
6914.564	4	Ni	12	7198.437	2	A	1
6916.677	2	Fe	8	7201.201	4	A	1
6918.122	9	A	12	7202.206	1N	Ca	1
6919.002	9	A	12	7204.306	5	A	3
6923.302	9	A	12	7206.420	6	A	3
6924.172	9	A	12	7207.396	1	Fe	2
6928.728	4	A	2	7209.504	3	Ti, A	8
6929.598	4	A	1	7211.202	1	A	2
6934.421	2	A	1	7216.527	2	A	7
6935.283	2	A	1	7223.636	3	A, Fe	6
6937.702	2N	A	4	7227.493	3	A	8
6943.801	3	A	6	7232.256	1	A	2
6945.210	4	Fe	7	7232.901	3	A	4
6947.543	5	Fe, A	6	7236.136	1	A	10
6959.453	3	A	8	7239.838	1	A, Fe	2
6961.261	4	A	8	7243.700	2	A	1
6977.469	3	Fe, A	1	7245.676	2	A	9
6978.861	2	Fe	4	7247.210	1N	A	5
6986.578	3N	A	9	7248.922	0N	A	3
6988.987	3	A	9	7250.216	1N	A	3
6993.521	2	A	4	7252.378	2N	A	1
6998.962	2	A	1	7253.723	2	A	1
7005.903	1	⊙	1	7257.371	00	A	3

TABLE II—*Continued*

λ	Int.	Substance	No. Obs.
7257.933	1N	A	1
7260.731	0	A	4
7261.457	00N	A, Fe	2
7262.973	0	A	3
7265.594	5	A	4
7269.752	00N	A	3
7272.973	5N	A	9
7275.398	2N	A	5
7277.391	2N	A	1
7282.299	1N	A, Fe	2
7287.378	2N	A	7
7288.119	1	A	1
7290.414	3N	A	4
7303.197	2	A	4
7304.173	3N	A	5
7308.760	1	A	2
7309.518	2N	A	6
7312.618	1	A	2
7315.516	0	A	4
7318.688	1	A	2
7323.972	1	A	4
7326.164	0	Ca	3
7327.370	1	A	1
7330.857	1N	A	5
7333.683	1	A	5
7335.334	1	A	4
7343.950	0	A	1
7344.767	0	A	1
7349.490	0	A	1
7355.893	1	Cr	1
7360.346	1	A	1
7369.208	1	A	2
7383.722	1	A	2
7389.391	2	Fe	6
7393.610	2	Ni	7
7400.184	1	Cr	3
7405.790	1	Si	4
7409.355	1	Ni	1
7411.158	1	Fe	6
7414.512	1	Ni	5
7415.957	1	Si	3
7418.674	0	Fe	1
7422.286	1	Ni	4
7423.509	1	Si	4
7440.915	1	Fe?	1
7445.755	2	Fe	4
7462.342	2	Cr, Fe+?	4
7491.652	1	Fe	6
7495.076	2	Fe	5
7507.276	1	Fe	2
7511.030	2	Fe	4
7522.782	1	Ni	4
7525.115	1	Ni	5
7531.152	2	Fe	5
7555.608	2	Ni	8
7568.906	1	Fe	9
7574.046	1	Ni	8
7583.796	1	Fe	10
7586.025	2	Fe	7
7593.699	3	A	4
7593.851	0	A	1
7593.990	3	A	2
7594.293	0	A	1
7594.503	6	A	3
7594.974	4	A	1
7595.780	5	A	2
7597.433	16	A	1
7598.004	0	A	1
7612.054	23	A	1
7613.181	19	A	1
7615.038	17d?	A	2
7616.134	10	A	2
7616.977	2	Ni	2
7619.212	1	Ni	4
7620.987	15d?	A	1
7623.288	22d?	A	1
7624.486	23d?	A	1
7625.350	0	A	1
7627.045	24	A	1
7628.227	25	A	1
7630.237	0	A	2
7631.019	24	A	1
7632.163	25	A	1
7634.166	0	A	2
7635.189	24	A	1
7636.310	25	A	1
7637.174	0	A	1
7638.302	0	A	5
7639.577	22	A	1
7640.693	23	A	1
7642.644	0	A	4
7644.195	18	A	1
7645.310	19	A	1
7647.191	0	A	3
7649.032	15	A	1
7649.583	0	A	1
7650.126	16	A	1
7654.076	12	A	2
7655.178	13	A	2
7657.605	2	Mg	4
7659.350	9	A	2
7659.898	0	⊙	1
7660.440	10	A	3
7661.196	1	Fe	2
7664.297	1	Fe	4
7664.880	6	A, K	1
7665.938	6	A	3
7670.600	5	A	5

TABLE II—*Continued*

λ	Int.	Substance	No. Obs.	λ	Int.	Substance	No. Obs.
7671.664	5	A	5	7937.149	3	Fe	10
7676.563	4	A	11	7941.096	1	Fe	4
7677.618	4	A	11	7944.001	2	⊙	8
7680.267	1	Mn	7	7945.857	2	Fe	11
7682.756	3	A	12	7958.491	1	A	7
7683.800	3	A	12	7960.734	1	A	6
7689.177	2	A	12	7968.122	0	A	4
7690.217	2	A	12	7971.520	0	A	4
7691.562	2	⊙	10	7984.343	1	A	5
7695.837	0	A	11	7994.488	1	Fe, Ni	3
7696.868	0	A	11	7998.952	2	Fe	4
7698.977	5	K	14	8000.303	2	A	4
7702.736	0	A	2	8007.470	1d?	Co? A	3
7703.754	0	A	2	8012.940	1	A	5
7710.367	1	Fe	4	8028.327	1	Fe, Ni	1
7711.737	1	Fe+	1	8028.542	1	A	1
7714.309	3	Ni	11	8034.293	1	A	3
7715.577	1	Ni	1	8036.459	1	A	3
7723.211	1	Fe	3	8039.598	1	A	3
7727.616	3	Ni	11	8045.532	1	A	1
7742.722	2	Fe	8	8046.056	2	Fe	10
7748.284	2	Fe	7	8047.626	1	Fe	4
7748.894	2	Ni	7	8075.161	0	Fe	3
7751.117	0	Fe	3	8085.175	2	Fe	11
7771.954	2	O	5	8090.464	00N	⊙	2
7774.177	2	O	4	8093.236	0	Si?	2
7775.394	1	O	3	8094.269	00	A	2
7780.567	3	Fe	11	8096.584	1	A	2
7788.933	2	Ni	11	8096.876	0	Fe	2
7797.587	2	Ni	10	8103.169	0	A	1
7799.995	0	⊙	3	8107.841	1	A	7
7807.915	1	Fe	10	8110.570	0	A	2
7832.207	2	Fe	10	8112.400	0	A	2
7836.139	0	⊙	1	8113.638	0	A	2
7849.984	1	⊙	4	8113.948	1	A	2
7855.392	0	Fe	3	8118.912	1	A	2
7866.070	0	A	1	8120.662	1	A	2
7872.789	1	A	1	8121.500	1	A	2
7880.709	1	A	1	8122.580	2	A	2
7887.117	1	A	6	8125.444	1	A	7
7889.340	0	A	2	8126.854	1	A	7
7891.900	1	A	4	8130.016	1	A	2
7893.511	2	A	7	8130.234	00	A	2
7895.515	2	A	4	8130.459	2	A	3
7896.035	2	A	4	8131.214	1	A	2
7901.780	3	A	9	8133.208	0	A	2
7908.750	2	A, Co?	7	8133.560	0	A	2
7912.869	1	Fe	5	8133.774	5	A	3
7915.633	2	A	2	8135.047	5	A	5
7918.383	1	Si	7	8136.208	1	A	2
7920.664	1	A	6	8136.528	2	A	2
7924.348	2	A	4	8139.718	2	A	6
7928.617	2	A	8	8140.668	5	A	4
7932.351	2	Si?—	9	8141.936	4	A	5

TABLE II—*Continued*

λ	Int.	Substance	No. Obs.	λ	Int.	Substance	No. Obs.
8143.794	1	A	7	8233.905	5	A	10
8144.193	0	A	2	8234.627	1	A	3
8146.214	2	A	7	8237.341	3	A	8
8147.185	2	A	3	8239.139	0	Fe	1
8148.084	0	A	2	8239.925	3	A	5
8148.387	3	A	5	8243.136	0	A	2
8149.273	1	A	2	8243.481	5	A	5
8149.692	3	A	2	8248.140	0	Fe	3
8149.876	1	A	1	8248.801	0	⊙	3
8152.498	4	A	4	8252.727	2	A	11
8153.702	2	A	2	8256.514	8	A	8
8154.405	1	A	1	8259.692	4	A	11
8154.662	5	A	2	8203.446	3	A	11
8158.019	6	A	8	8272.041	4	A	12
8161.436	8	A	5	8274.353	8	Fe? $\underline{A}$	6
8161.977	3	A	1	8276.519	4	A	1
8162.349	8	A	3	8276.676	4	A	1
8164.530	10	A	4	8279.600	5	A	11
8165.334	1	A	2	8282.022	8	A	8
8168.825	4	A	1	8287.944	8	A	5
8169.386	2	A	2	8289.533	4	A	9
8169.990	8	A	2	8293.526	00	Fe	2
8174.678	1	A	1	8294.164	4	A	2
8176.976	10	A	6	8294.536	2	A	2
8177.934	4	A	2	8295.292	0	A	2
8178.494	2	A	2	8300.406	3	A	11
8179.046	4	Fe? $\underline{A}$	1	8304.302	1	A	8
8181.847	6	A	7	8305.092	5	A	4
8183.274	3	Na	2	8311.955	2	A	4
8186.371	5	A	9	8313.874	0	A	4
8189.271	8	A	7	8316.224	1	A	10
8193.113	7	Co? $\underline{A}$	7	8318.139	2	A	11
8194.835	2	Na	12	8321.247	2	A	2
8197.702	8	A	7	8321.564	4	A	2
8198.995	1	A	3	8327.060	2	Fe	10
8199.988	2	A	3	8329.682	3	A	11
8200.695	3	A	6	8331.927	1	Fe	2
8204.807	1	A	3	8332.141	1	A	1
8207.747	1	Fe	3	8333.584	2	A	8
8209.560	2	A	3	8335.178	00	⊙	2
8210.321	2	A	3	8335.506	1	A	3
8212.132	4	A	10	8339.035	2	A	3
8213.037	3	⊙	2	8339.403	0	Fe	1
8218.112	5	A	11	8342.289	1	A	7
8200.393	2	Fe	7	8346.131	0N	⊙	3
8221.553	4	A	8	8349.150	1	A	1
8223.990	5	A	11	8349.385	0	A	1
8224.462	1	A	2	8353.643	1	A	6
8225.690	2	A	3	8357.041	1	A	10
8226.963	10	A	4	8357.447	0	A	1
8228.738	4	A	1	8362.003	0	A	1
8229.761	3	A	5.	8362.296	0	A	2
8231.303	6	A	1	8365.640	1	Fe	6
8231.683	4	A	1	8367.333	2	A	10

TABLE II—*Continued*

λ	Int.	Substance	No. Obs.	λ	Int.	Substance	No. Obs.
8373.712.......	1	A	7	8710.393.......	0	Fe	3
8376.384.......	1	A	2	8712.679.......	00	⊙	1
8387.783.......	3	Fe	11	8713.214.......	00	Fe	1
8394.014.......	0	A	1	8717.832.......	0	⊙	4
8397.154.......	0	A	2	8728.022.......	0	⊙	4
8405.390.......	00N	A	1	8736.043.......	1	⊙	5
8408.759.......	0	A	2	8742.466.......	1	—, Si	4
8412.356.......	0	Ti	1	8752.024.......	1	Si	4
8415.438.......	0	A	3	8757.195.......	1	Fe	3
8426.518.......	0	Ti	4	8763.974.......	1	Fe	4
8434.969.......	1	Ti	5	8772.878.......	0	⊙	3
8435.656.......	1	Ti	4	8773.909.......	0	⊙	3
8439.583.......	0	Fe	9	8790.456.......	1	Fe	2
8460.252.......	0	A	1	8793.346.......	1	Fe	2
8468.420.......	2	Fe, Ti	10	8804.641.......	0	Fe	2
8471.733.......	00	Fe	1	8806.768.......	4	Mg	3
8497.003.......	0	Fe	1	8824.233.......	2	Fe	4
8498.061.......	12	Ca+	4	8838.442.......	1	Fe	2
8514.081.......	1	Fe	9	8846.748.......	00	Fe	1
8515.121.......	0	Fe	11	8862.564.......	0	Ni	1
8526.674.......	0	Fe	8	8866.937.......	1	Fe	2
8542.131.......	16	Ca+	6	8868.444.......	0	⊙	1
8556.795.......	1	Si?	9	8879.321.......	1	A	2
8582.271.......	1	Fe	8	8892.714.......	0	A?	2
8592.968.......	00	Fe	2	8912.100.......	0	⊙	2
8595.967.......	00	⊙	1	8917.517.......	0	A	1
8598.832.......	00	Fe	2	8920.028.......	0	Fe? A?	1
8611.813.......	1	Fe	8	8923.548.......	00	⊙	1
8613.943.......	00	⊙	1	8927.388.......	00	⊙	2
8616.277.......	0	Fe,—	3	8929.062.......	1	A, Fe?	1
8621.619.......	1	Fe	9	8930.260.......	0	A	1
8648.472.......	2	⊙	8	8934.100.......	1	A	2
8662.175.......	15	Fe, Ca+	4	8940.216.......	0	A	2
8674.756.......	1	Fe	8	8952.172.......	0	A	1
8679.652.......	00	⊙	1	8958.399.......	1	A	2
8686.370.......	00	⊙	2	8971.567.......	3	A	1
8688.642.......	2	Fe	6	8980.519.......	4	A	1
8699.459.......	1	Fe	5				

the first column the wave-length on the neon scale; in the second column, the intensity; in the third, the identification; and in the fourth, the number of plates on which the line was observed. When two substances are given for the same line, the symbol of the predominant one is sometimes underlined. Solar lines of unknown origin are indicated by the symbol ⊙. The intensities are from Rowland's table as far as λ 7330, and from the table of Meggers[1] thereafter. In the case of those atmospheric lines for which Meggers gives a variable intensity, only his greatest value has been entered, since the variations on my plates were not particularly noticeable. With some changes which are discussed below, the identifications have been taken from Meggers.

---

[1] *Loc. cit.*

As noted above, corrections for motion in the line of sight have been applied to all solar wave-lengths in Table II. Corrections for atmospheric dispersion were found to be negligible throughout the investigation.

DISCUSSION

Comparison of the wave-lengths in Table II with those in Rowland's table shows a systematic difference in good agreement with that to be expected. The corrections required to transform the Rowland system into the international system range from −0.247 A at λ 6900 to −0.300 A at λ 7330, with evidence of numerous accidental errors much greater than those in the region of shorter wave-lengths. These are naturally to be expected when the difficulties which were faced by Professor Rowland in photographing the deep red are recalled. A more complete study of the differences between the Rowland and international systems, covering the entire Rowland table, is in progress at this Observatory and will soon be ready for publication.

The paper of Meggers to which reference has already been made furnishes the only other wave-lengths available for extended comparison with the data gathered here. The agreement turns out to be only approximate—a natural result, no doubt, of the method which he used. From λ 6900 to λ 8000 his wave-lengths are systematically longer than mine by an average of about 0.025 A, but within these limits the correction curve has six maxima. The irregularity of the corrections is further indicated by the following average values:

λ	Correction
7350	−0.065 A
7850	− .060
8050–8200	.000
8290	+ .045
8420	.000
8670	+ .070
8780	+ .035
8950	+0.075

Superposed on these systematic errors are accidental errors amounting frequently to ±0.02 A.

The correction curve was plotted and used for a revision of the identification of solar lines, the first results being collected in Table III. All the solar lines in Meggers' table not given in Table II of this paper were revised by the curve and compared with the available laboratory data. The first column of Table III gives the revised value of Meggers' wave-length; the second states the intensity which he assigned; and the third, his identification; while in the fourth column suggested changes are indicated.

TABLE III

Suggested Changes in Published Identifications of Solar Lines

λ	Int.	Identification	Revision
6920.13	00	....	Cu?
6922.25	00	Co? A	Co, A
6933.02	00	....	Fe
7011.22	000	Fe	....
7011.33	2	A	Fe, A
7024.64	0	Fe, Ni?	Fe
7024.86	0	....	Ni?
7028.62	000	Ni	....
7037.21	0	A, Ni?	A, Ni
7141.54	000	Ni?	Ni
7164.43	3	Fe, A?	Fe? A?
7181.96	0	Fe? Ni	Fe, Ni?
7191.65	000	Fe?	Fe
7222.39	00	....	Fe+
7224.46	00	....	Fe+
7285.28	0	....	Co
7285.37	000	Co?	....
7291.44	0	Ni	Ni?
7295.03	0–1	A, Fe?	A, Fe
7301.55	000	....	Fe+
7308.05	000	....	Fe+
7310.18	00–0	A	A, Fe+
7320.67	0	Fe	Fe, Fe+
7363.97	000N	Ti	Ti?
7447.91	00	Mn?	Mn
7449.34	00	....	Fe+
7462.33	2	Cr	Cr, Fe+?
7515.85	00	....	Fe+, Mn?
7533.39	00	—Co?	Fe+
7551.12	000	....	Mn?
7578.77	000	....	Zn
7655.44	00N	A	A, Fe+
7711.74	1	....	Fe+
7764.58	000	Mn	....
7877.05	000	....	Mg+?
7877.46	000	....	Co
7896.40	00	....	Mg+?
7908.75	0–2	A, Co?	A, Co
7949.15	000	Ti? A	Ti, A
8085.44	000	A?	A? Co?
8112.15	00	....	Co
8179.05	2–4	Fe? A	Fe, A
8395.10	000	A? Fe?	A? Fe
8417.23	000	A, Ni?	A, Ni
8468.42	2	Fe	Fe, Ti
8710.39	0	Fe	Fe?
8929.04	1	A, Fe?	A, Fe

At this point it is well to remark on the need for improved laboratory data in the infra-red region. The existing tables of arc spectra show discrepancies which frequently amount to 0.05 A, and in some cases to nearly 0.1 A. Even with accurate data on the solar spectrum available, the difficulties of identification are considerable when the basis of terrestrial wave-lengths is so insecure. Relative intensities of lines, and especially relative excitation potentials or multiplet groupings, assume first importance in the solution of this problem; but such information is too often lacking. In addition it may be noted that very little has been published on the infra-red spectra of ionized atoms which are of astrophysical importance.

In Table IV are collected all the stronger unidentified solar lines between λ 6900 and λ 9000. Wave-lengths found by the interference method are given to the third decimal; for other lines the revision of Meggers' value is given. An attempt has been made to examine the behavior of these lines in the spectra of sun-spots, but for most of them definite results have not yet been found. A few lines are clearly much weakened in the spot spectrum, which indicates that they should be sought among the spectra of ionized elements or among the high-temperature lines of arc spectra.

TABLE IV

STRONGER UNIDENTIFIED SOLAR LINES BETWEEN λ 6900 AND λ 9000

λ	Int.	λ	Int.	λ	Int.
6911.50	0	7588.32	0	8248.801	0
6976.52	0	7659.14	1	8335.178	00
7005.903	1	7659.91	0	8346.131	0N
7012.61	0	7669.66	0	8502.23	0
7017.35	0	7691.561	2	8536.16	0
7017.66	0	7719.06	0	8648.472	2
7032.32	0	7799.995	0	8717.832	0
7034.910	2	7835.31	0	8728.022	0
7127.54	0	7836.139	0	8736.043	1
7165.55	0	7849.984	1	8772.878	0
7207.11	2	7930.82	0N	8773.909	0
7282.82	0	7944.001	2	8868.444	0
7351.11	0	8035.62	0	8912.100	0
7387.69	1N	8098.71	0N	8974.77	1
7440.88	1	8213.037	0–3		

In Table V the solar wave-lengths from Table II are compared, as far as possible, with the iron-arc wave-lengths obtained with the interferometer by Meggers and Kiess.[1] The third column of the table shows the differences, sun *minus* arc; the fourth and fifth columns give the excitation potential[2] and the multiplet designation,[3] respectively; while the sixth indicates the behavior of the lines in an arc carrying over 1000 amp., as observed by King.[1] Here S means that even under this extreme excitation the line remains sharp; u_4 indicates great widening toward the side of longer wave-length, without reversal; ru_4 means partially reversed, with great dissymmetry, the long-wave side being stronger; w_2 means small widening without dissymmetry. As King's data for iron do not at present extend beyond λ 8400, only two members of the D–H multiplet are referred to in the sixth column.

---

[1] *Scientific Papers of the Bureau of Standards,* **19,** 273 (No. 479), 1924.

[2] Unpublished results of Professor Russell and Miss Moore.

[3] Meggers, *Astrophysical Journal,* **60,** 60, 1924; Laporte, *Proceedings Nat. Acad. of Sciences,* **12,** 496, 1926.

In examining this comparison it should be remembered that the arc used by Meggers and Kiess was operated at atmospheric pressure with a current of 6 amp. and an arc length of 6 mm. The light was partially integrated by the method of projection. Under such conditions the wave-lengths of all sensitive lines exhibit a large amount of pole effect,[2] causing displacements from their normal positions amounting to several hundredths of an angstrom, toward the red for groups c_5 and d, toward the violet for group e. No lines belonging to group e occur in Table V. This group has not yet been definitely recognized in the infra-red spectrum of iron, and it may here be ignored.

The evidence of low pressure in the solar atmosphere may now be considered conclusive. Saha,[3] St. John,[4] Russell,[5] Stewart,[6] and St. John and Babcock[7] have shown, both from theoretical considerations and from several kinds of observational data, that the pressure in the sun has a negligible influence on the positions of Fraunhofer lines.

Two causes evidently operate to make the wave-lengths of the arc lines in Table V appear too great with respect to their values in the sun, namely, the higher pressure existing in the arc and the pole effect. These causes will be effective to varying degrees with different types of lines, but in general they will rise and fall together.

[1] *Mt. Wilson Contr.*, No. 298; *Astrophysical Journal*, **62**, 299, 1925.

[2] *Mt. Wilson Contr.*, No. 106; *Astrophysical Journal*, **42**, 1, 1915.

[3] *Philosophical Magazine*, **40**, 809, 1920.

[4] *Contributions of the Jefferson Physical Laboratory*, **15**, 1921.

[5] *Mt. Wilson Contr.*, No. 225; *Astrophysical Journal*, **55**, 134, 1922.

[6] *Physical Review*, **22**, 324, 1923.

[7] *Mt. Wilson Contr.*, No. 278; *Astrophysical Journal*, **60**, 399, 1924.

The correlation shown between the last four columns of Table V is emphasized by the rearrangement of the data in Table VI, where mean values of the differences sun *minus* arc and the excitation

TABLE V

Comparison of Solar and Arc Wave-Lengths from Interferometer Measurements

λ I.A.		Sun *minus* Arc	E.P. Volts	Multiplet	High-Current Arc
Table II	Arc; Meggers and Kiess				
6916.677	.709	−0.032 A	4.136	J–f	u_4
6945.210	.211	− .001	....	....	S
6978.861	.857	+ .004	....	....	S
7022.958	.976	− .018	4.173	J–U	u_4
7068.423	.418	+ .005	....	....	S
7090.390	.410	− .020	4.212	J–U	u_4
7130.925	.946	− .021	4.199	J–U	u_4
7207.396	.422	− .026	4.136	J–U	u_4
7389.391*	.423	− .032	4.283	K–U	u_4
7411.158	.184	− .026	4.265	K–U	u_4
7418.674†	.676	− .002	....	....	S
7445.755	.778	− .023	4.238	K–U	u_4
7491.652	.678	− .026	4.283	K–U	u_4
7495.076	.092	− .016	4.202	K–U	u_4
7507.276	.300	− .024	4.396	L–f	u_4
7511.030	.047	− .017	4.160	K–U	ru_4
7531.152	.178	− .026	4.353	L–f	u_4
7568.906	.931	− .025	4.265	K–U	u_4
7583.796	.801	− .005	....	....	S
7586.025	.050	− .025	4.294	L–f	u_4
7661.196	.230	− .034	4.238	K–U	u_4
7664.297	.306	− .009	....	....	S
7710.367	.397	− .030	4.202	K–U	u_4
7748.284	.282	+ .002	....	....	S
7780.567	.594	− .027	4.454	M–f	u_4
7832.207	.233	− .026	4.416	M–f	u_4
7937.149	.172	− .023	4.294	L–U	u_4
7945.857	.882	− .025	4.368	M–f	u_4
7998.952	.980	− .028	4.353	L–U	u_4
8046.056	.084	− .028	4.396	L–U	u_4
8085.175	.207	− .032	4.426	L–U	u_4
8220.393	.413	− .020	4.302	L–U	u_4
8327.060	.069	− .009	2.188	D–H	w_2
8331.927	.956	− .029	4.368	M–U	u_4
8387.783	.787	− .004	2.167	D–H	w_2
8468.420	.422	− .002	2.213	D–H	....
8514.081	.088	− .007	2.188	D–H	....
8688.642	.641	+ .001	2.167	D–H	....
8824.233	.238	−0.005	2.188	D–H	....

* Solar λ poor.

† Only one solar plate.

potentials are shown. It is clear that these arc wave-lengths exhibit a combined pole effect and pressure displacement, which increases with the excitation potential in a manner analogous to what has been found in the visible region, and that the lines in Table V which are not yet assigned to multiplets must be characterized by an excitation potential not much in excess of 2 volts.

On the basis of experience in using such an arc as that described by Meggers and Kiess, from measurements of the pole effect made by St. John and Babcock,[1] and from unpublished determinations of the pressure shift under conditions practically free from pole effect, an estimate may be made of the amounts which should be subtracted from the iron-arc wave-lengths of Meggers and Kiess to reduce them to what they would have been if a vacuum arc had been used. For iron lines arising from combinations of J, K, L, and M terms with a U term or an *f* term, the data indicate a deduction of about 0.04 A, while for the D–H multiplet about 0.02 A would suffice. The application of these changes to the arc wave-lengths would result in a consistent series of sun *minus* arc differences averaging +0.015 A.

The gravitational displacement predicted by Einstein averages +0.017 A in the region discussed here, and it may reasonably be expected to appear when vacuum-arc measurements of high accuracy become available.

The sun *minus* arc differences in Table V, when grouped according to solar intensity and behavior in high-current arc, show that the more intense solar lines are slightly displaced toward longer wave-lengths as compared to weaker lines of the same multiplets. The data are too meager to justify any conclusion, but it is interesting to note that such effects are well established in the region of shorter wave-lengths, and have been discussed at length by St. John.[2]

Table V also indicates that neither the arc wave-lengths of Meggers and Kiess nor the new solar wave-lengths now presented are affected by serious accidental errors. Were such errors present with random distribution, the chances are that at least one would appear in Table V, whereas none are found to exceed 0.006 A. It is also very unlikely that systematic errors independent of the source of light exceeding a few thousandths of an angstrom occur in either list of lines. Inasmuch as the range of wave-length is 1800 A, the existence of such errors would obscure the relation between excitation potential and difference between solar and arc wave-length shown in Table VI.

---

[1] *Loc. cit.*

[2] *Proceedings of the National Academy of Sciences*, 12, 65, 1926.

So much has been said about the differences in structure and behavior of various types of lines when studied in artificial sources that it may be well to recall some related facts in regard to the solar spectrum. For example, Fabry and Buisson,[1] after describing the peculiarities of some iron-arc lines, go on to say:

TABLE VI

UNCORRECTED SUN—ARC DISPLACEMENT COMPARED WITH EXCITATION POTENTIAL

Multiplet	No. Lines	Mean E.P. Volts	Mean Difference Sun *minus* Arc	High-Current Arc
D–H.........	6	2.185	−0.004 A	w_2
J–f	1	4.136	.032	u_4
J–U..........	4	4.180	.021	u_4
K–U.........	9	4.237	.026	u_4
L–f..........	3	4.348	.025	u_4
L–U.........	5	4.354	.026	u_4
M–U.........	1	4.368	.029	u_4
M–f	3	4.413	.026	u_4
?............	7	?	.001	S

> Dans le spectre solaire, ces différences d'aspect ne se manifestent aucunement. On n'aperçoit aucune dissymétrie dans l'absorption; les raies différent uniquement par leur intensité, ou, ce qui revient au même, par leur largeur. Certaines raies qui, dans l'arc à la pression atmosphérique, sont nettement diffuses et se distinguent des autres au premier coup d'œil, ne présentent rien de particulier dans le spectre solaire. On peut citer, comme exemple frappant de ce fait, les raies 5410.92, 5415.22, 5424.09.

St. John and Ware also noted[2] that iron lines of groups *d* and *e* are as sharp in the solar spectrum as those of groups *a* and *b*.

It is interesting to note that the remarks of Fabry and Buisson

---

[1] *Astrophysical Journal*, **31**, 112, 1910.

[2] *Mt. Wilson Contr.*, No. 61; *Astrophysical Journal*, **36**, 235, 1912.

PLATE I

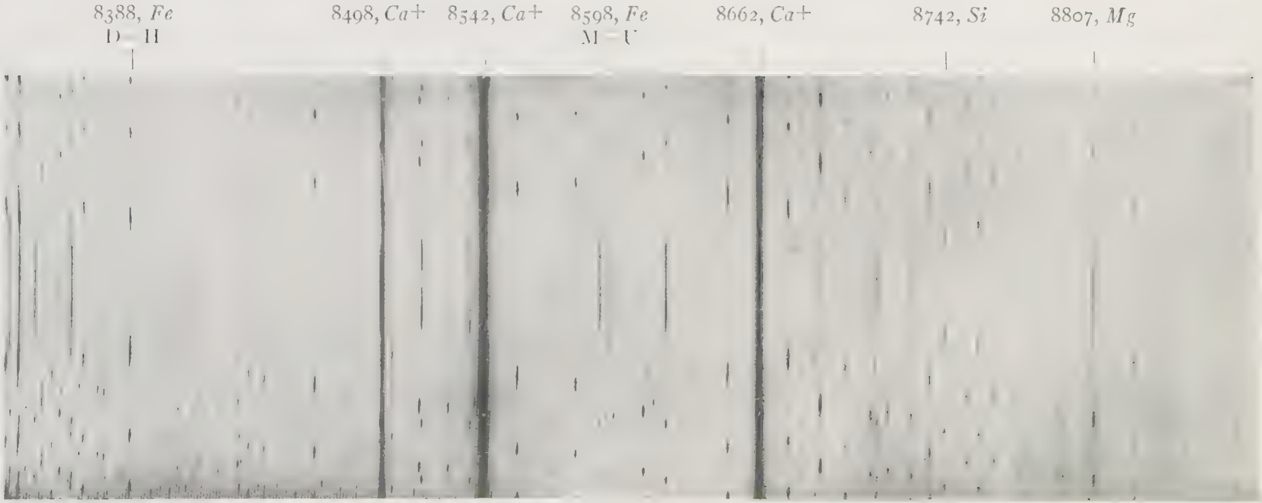

SPECTRUM OF INTEGRATED SUNLIGHT
Order of Interference at λ8600 is 6000

apply accurately to the infra-red region of the solar spectrum, since our photographs show that here, as well as in the visible region, lines, which in the arc are extremely diffuse and unsymmetrical, are symmetrical and sharp in the solar spectrum.

Plate I shows a small part of the spectrum in which solar lines predominate. This illustration is an enlargement of 1.5 times from a negative made with a 2.5-mm etalon having gold films. The original exposure was thirty-one minutes. A few lines are marked, among which may be found members of both the M–U and D–H multiplets. The photograph also illustrates the foregoing remarks on the appearance of the solar lines.

My cordial thanks are due to Miss Moore for access to unpublished data which she and Professor Russell are preparing, and to Mrs. Thome, née Keener, for assistance in measuring some of the grating plates of the α-band of oxygen.

Mount Wilson Observatory
December 1926

Contributions from the Mount Wilson Observatory, No. 329
Reprinted from the *Astrophysical Journal*, Vol. LXV, pp. 1–22, 1927
Printed in the U.S.A.

MEASUREMENT OF THE VELOCITY OF LIGHT BETWEEN MOUNT WILSON AND MOUNT SAN ANTONIO

By A. A. MICHELSON
Research Associate of the Carnegie Institution

Assisted by F. Pearson

ABSTRACT

The following is a continuation of the experiments described in the *Astrophysical Journal*, **60**, 256, 1924. The arrangement of apparatus differs slightly from that of the former investigation, allowing a more nearly normal incidence on the facets of the revolving mirror, and providing greater symmetry as well as increase in illumination.

Five independent series of measurements made with different revolving mirrors (one of steel having the form of a prism with eight facets, and another with twelve, and three of glass with eight, twelve, and sixteen facets) gave results showing a remarkable agreement.

The final result for the velocity of light *in vacuo* is 299,796 km per second.

The increasing appreciation of the importance of this fundamental constant of nature and the anticipation of the possibility of attaining a considerable increase in accuracy in its measurement justified the acceptance of the generous invitation of Dr. G. E. Hale, then director of the Mount Wilson Observatory, to make use of the facilities there available. It is with sincere appreciation that I take this opportunity of extending my acknowledgment of the many courtesies received and of the cordial co-operation of Dr. Hale and subsequently of Dr. Adams and the entire staff of the Observatory.

The result of the preliminary experiments described in a previous article[1] gave for the final value of the velocity of light in air 299,735 km per second.

---

[1] *Astrophysical Journal*, **60**, 256, 1924.

The correction[1] to *vacuum* is given by

$$n-1=(n_0-1)\frac{d}{d_0}=(n_0-1)\frac{p}{p_0}\frac{T_0}{T}$$

$$\frac{p}{p_0}=.822$$

and

$$\frac{T_0}{T}=.932\ ,$$

whence

$$n-1=.000294\times .765$$

or

$$n=1.000225\ ,$$

giving 67 km for the correction.[2]

Accordingly, for the preliminary determination

$$V=299{,}735+67$$

or

$$V=299{,}802\ .$$

A second series of observations with the glass octagon was begun in July of 1925, the arrangement of apparatus being essentially the same as in the preliminary work, except that instead of driving the electric fork ($N=132$) by make and break between platinum points, the fork ($N=528$) was driven by a vacuum-tube circuit, giving a rate far more nearly constant.

This rate was measured by comparison with a free pendulum furnished by the United States Coast and Geodetic Survey, as in the previous work; but with an important improvement in the stroboscopic method. This consists in allowing the light from a very narrow slit to fall on a mirror attached to the pendulum, forming, by means of a good achromatic lens, an image of the slit in the plane of an edge of the fork, where it is observed by an eyepiece.

---

[1] The correction should be applied to the individual observations; but the result is not appreciably altered by taking the mean values given above.

[2] This was erroneously given as 85 km in the article cited.

This method of making the stroboscopic comparison was found to be far more convenient and accurate than that described in the work of last year.

As before, the octagonal mirror making 528 turns per second rotates through one-eighth of a turn during the time of passage of light from the revolving mirror to the distant station and return, thus presenting the succeeding face of the mirror to the returning beam at (very nearly) the same angle as at rest.

The observations consist, then, in increasing the speed of the revolving mirror until the stroboscopic image between fork and mirror is stationary, at which instant the measurement is taken of the small angle α_1 by which the displacement of the image differs from 90°. The direction of rotation is then reversed, and a similar series of observations furnishes the angle α_2. If $\alpha=\alpha_1+\alpha_2$, then the angle through which the mirror rotates during the time required for light to travel through the distance $2D$ will be $\pi/4-\alpha/4$, and the velocity is given by $V=(16ND)/(1-\alpha/\pi)$.

If $1/n$ is the period of the (optical) beats between the fork and the pendulum and $1/\nu$ that of the coincidences between the C.G.S. pendulum and the true seconds, and if N is the nearest whole number (in the present instance 528), then, as both α and ν are small,

$$V=\frac{16D}{1-\nu}(N+n)\left(1+\frac{\alpha}{\pi}\right),$$

or, since α and n are small,

$$V=\frac{16\times 35425.15\times 528}{1-.00051}\left(1+\frac{\alpha}{\pi}+\frac{n}{N}\right) \qquad D=35425.1$$

$$V=299{,}425\left(1+\frac{\alpha}{\pi}+\frac{n}{N}\right).$$

Table I gives the results of ten series of observations with the glass octagon.

These results, as well as those previously published,[1] are to be regarded as preliminary. The definitive measurements were begun in June, 1926, and continued until the middle of September.

---

[1] *Astrophysical Journal*, **60**, 256, 1924.

TABLE I

TEN SERIES OF OBSERVATIONS

	a/π	n/N	V_a
I	0.00077	0.00013	299,695
II	.00057	.00015	299,651
III	.00044	.00038	299,671
IV	.00037	.00047	299,677
V	.00054	.00045	299,722
VI	.00047	.00043	299,695
VII	.00032	.00068	299,725
VIII	.00017	.00070	299,686
IX	.00018	.00076	299,707
X	0.00021	0.00058	299,662
Mean velocity in air			299,689
Correction			+67
V in vacuo			299,756

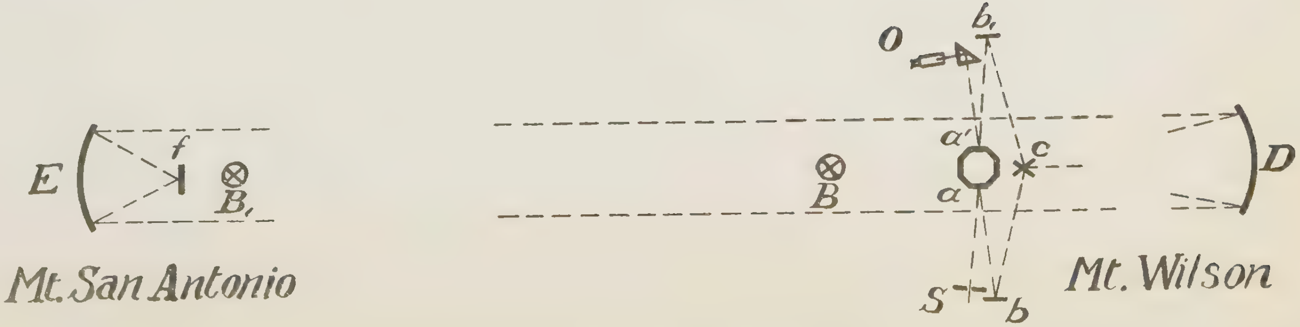

FIG. 1.—Arrangement of apparatus

The arrangement of apparatus at the home station was slightly different, as shown in Figure 1, the advantage being an increase in intensity in consequence of greater effective width of the light beam falling on the revolving mirror at nearly normal incidence, as well as greater symmetry.

With this layout a series of observations with the same small glass octagon gave the results recorded in Table II. The numbers given are the means of three series of observations, each series containing six (double) observations.

TABLE II

	a	*b*	*c*	*V*	Wt.
I	0.00059	0.00028	0.00072	299,747	2
II	.00046	.00040	.00073	299,747	2
III	.00045	.00038	.00073	299,738	3
IV	.00057	.00036	.00072	299,762	3
V	.00047	.00033	.00073	299,729	3
VI	.00052	.00038	.00073	299,759	3
VII	.00061	.00041	.00073	299,792	1
VIII	.00048	.00038	.00072	299,744	4
IX	.00049	.00036	.00072	299,741	4
X	.00047	.00040	.00072	299,747	4
XI	.00044	.00042	.00072	299,744	4
XII	0.00042	0.00042	0.00073	299,741	4
Weighted mean				299,746	
Correction				+67	
Velocity *in vacuo*				299,813	

On account of the small values of $a = \alpha/\pi$, $b = n/N$, and $c = \nu$, the formula for the velocity may be written

$$V = 16DN(1+a+b+c) .$$

With $D = 35{,}425$ and $N = 528$, this gives

$$V = 299270 + V(a+b+c) .$$

The results with the glass octagon are shown in Table II.

Giving these three results the weights 1, 2, and 5, respectively, the weighted mean of all the observations with the glass octagon is $V = 299{,}797$.

DEFINITIVE MEASUREMENTS

Toward the close of the work of the summer of 1925 an attempt was made to attain a speed of rotation of 528 turns per second with a glass octagon nearly twice as large as that used in the experiments just described. Owing probably to some defect in the glass, it burst at a speed of 400, thus terminating the work. In order to provide against a repetition of such an accident four mirrors were constructed. Two of these were of glass, of about the same construction, but twice as large as the small octagon, a photograph of which is given in Figure 2. The first of these had twelve facets and the second sixteen, the diameters being $6\frac{1}{4}$ and $7\frac{1}{2}$ cm, respectively, and the speed of rotations 350 and 264. The flat end of the steel axle on which the glass mirrors are mounted rests on a steel flat with a small aperture for oil, under pressure a trifle less than that which would lift it from its bearing. The driving power is furnished by an air blast issuing through two nozzles and impinging on the vanes of a paddle wheel.

Regulation of the speed was obtained by a counterblast controlled by a valve by means of which the speed could be kept constant for several seconds (as indicated by the immobility of the stroboscopic image), quite sufficient for the measurement of the corresponding small displacement of the image.

The other two mirrors were of nickel steel and furnished by Mr. Elmer A. Sperry. A photograph of the first, an octagon, is shown in Figure 3.

The driving power is furnished by an air blast from four nozzles impinging on the buckets attached to the axle.[1] The flat end of the latter rests on a single ball-bearing.

All four mirrors gave excellent results notwithstanding the fact that time was insufficient for the attainment of very great accuracy in the surfaces. This was particularly noticeable in the steel mirrors, the lack of homogeneity making the process of polishing and figuring much more difficult than in the case of the glass mirrors.[2]

---

[1] The mirrors actually employed were provided with duplicate bucket wheels and nozzles, allowing of reversal of the direction of rotation.

[2] All are now in process of refiguring in preparation for a resumption of operations during the winter, when atmospheric conditions are likely to be more favorable.

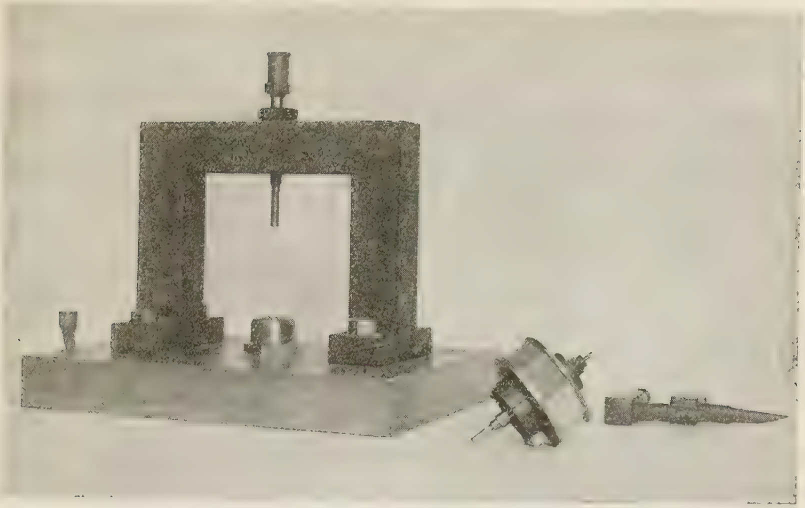

FIG. 2*a*.—The small octagon detached from its mounting

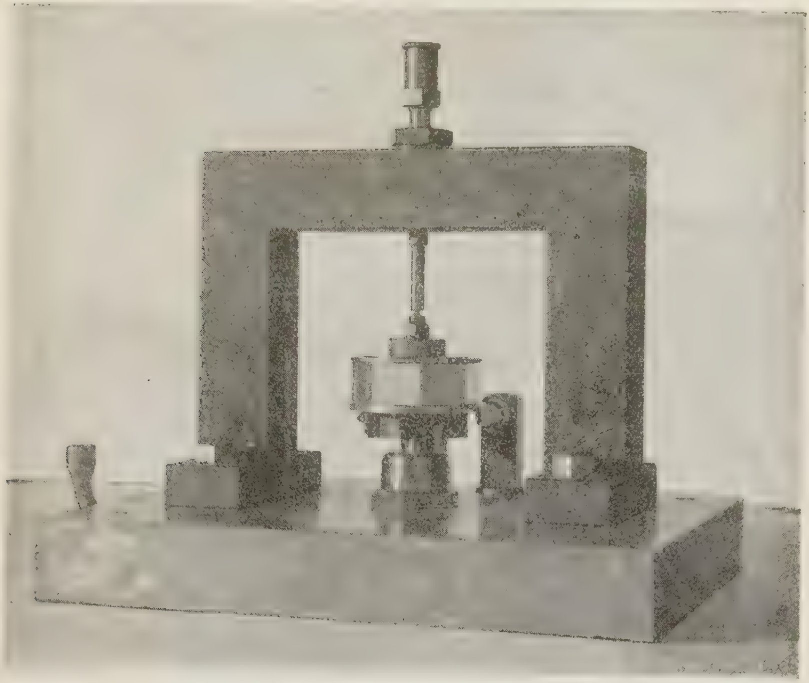

FIG. 2*b*.—The small octagon in its mounting

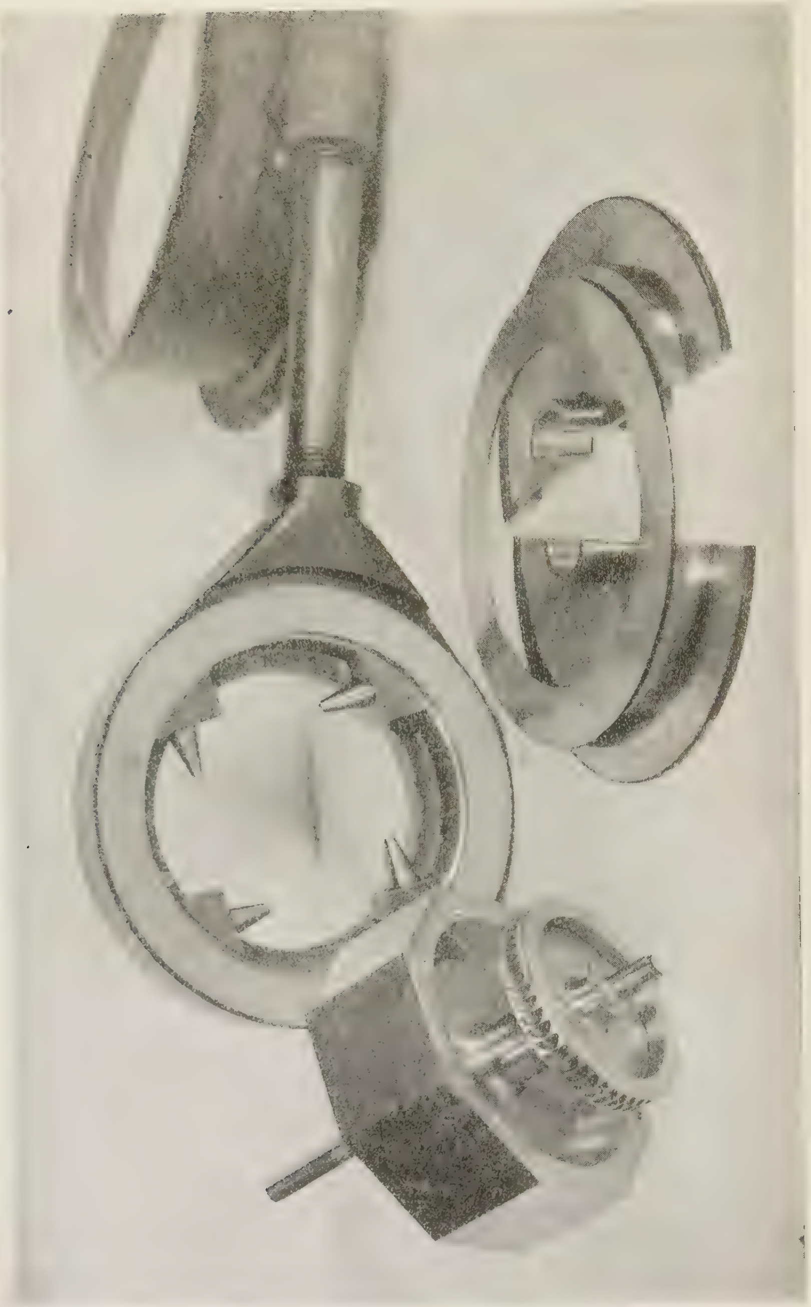

Fig. 3.—The octagon of nickel steel furnished by Mr. Sperry

With a twelve-facet glass mirror and the layout of apparatus and method of procedure essentially the same as in last year's work, the following results were obtained:

$$V=\frac{24DN}{1-\nu}(N+n)\left(1+\frac{3\alpha}{2\pi}\right)$$

or if

$$\frac{3\alpha}{2\pi}=a\quad \frac{n}{N}=b$$

and

$$-\nu=c\qquad D=35424.5$$

$$r=53\text{ cm}$$

$$V=299{,}265+3(a+b+c)\ .$$

The results obtained are shown in Table III.

TABLE III

TWELVE-FACET GLASS MIRROR

	a	b	c	VS	V	Wt.
I	−0.00018	0.00100	0.00075	471	299,736	1
II	.00047	.00040	.00073	480	299,745	3
III	.00058	.00026	.00073	471	299,733	3
IV	.00022	.00061	.00072	465	299,730	3
V	.00012	.00062	.00071	435	299,700	1
VI	− .00007	.00088	.00073	462	299,727	5
VII	.00020	.00098	.00073	453	299,718	5
VIII	.00004	.00085	.00073	462	299,727	5
IX	.00009	.00100	.00073	492	299,757	1
X	− .00021	.00114	.00074	501	299,766	2
XI	.00050	.00037	.00074	483	299,748	2
XII	.00071	.00009	.00073	459	299,724	5
XIII	.00052	.00034	.00073	477	299,742	5
XIV	.00003	.00073	.00075	453	299,718	5
XV	0.00004	0.00071	0.00075	450	299,715	5
Weighted mean					299,729	
Correction					+67	
Velocity *in vacuo*					299,796	

A series of measurements with the sixteen-facet glass mirror, the formula for which is

$$V=\frac{32DN}{1+2\,\alpha/\pi},\qquad D=35424.5$$

$$\gamma=55\text{ cm}$$

gave the results shown in Table IV.

TABLE IV

	a	*b*	*c*	*VS*	*V*	Wt.
I_{I}	0.00159	−0.00089	0.00076	438	299,703	.....
I_{II}	.00115	− .00033	.00076	474	299,739	
I	$(2\times I_{II}+I_{I})/3$	....	....	.....	299,727	1
II	.00051	.00045	.00071	501	299,766	2
III	.00038	.00052	.00071	483	299,748	2
IV_{I}	.00006	.00073	.00071	450	299,715	.....
IV_{II}	.00079	− .00006	.00073	438	299,703	
IV	$(2\times IV_{II}+IV_{I})/3$	....	....	.....	299,707	5
V	.00090	− .00009	.00073	462	299,727	5
VI_{I}	.00111	− .00029	.00072	462	299,727	.....
VI_{II}	.00074	.00013	.00072	477	299,742	
VI	$(2\times VI_{II}+VI_{I})/3$	....	....	.....	299,737	4
VII	.00085	.00011	.00072	504	299,769	3
VIII	.00097	− .00013	.00069	459	299,724	2
IX	.00104	.00008	.00070	498	299,763	2
X	.00081	.00002	.00071	450	299,715	4
XI	.00091	.00007	.00071	465	299,730	4
XII	.00112	.00027	.00069	462	299,727	2
XIII	.00117	.00027	.00069	477	299,742	2
XIV	.00098	.00009	.00070	477	299,742	3
XV	0.00104	−0.00009	0.00070	495	299,760	3
Weighted mean	....	....	....	.....	299,736	.....
Correction	....	....	....	.....	+67	.....
Velocity *in vacuo*	....	....	....	.....	299,803	.....

A second series with the sixteen-facet glass mirror gave the results summarized in Table V.

TABLE V

	a	*b*	*c*	*VS*	*V*	Wt
I	0.00067	0.00029	0.00071	501	299,766	1
II	.00019	.00060	.00073	456	299,721	5
III	.00020	.00061	.00073	462	299,727	5
IV	.00053	.00029	.00074	468	299,733	1
V	.00039	.00034	.00075	444	299,709	5
VI	.00049	.00029	.00075	459	299,724	5
VII	.00066	.00009	.00073	444	299,709	2
VIII	.00064	.00010	.00073	441	299,706	2
IX	.00078	.00006	.00074	474	299,739	3
X	.00102	− .00015	.00072	477	299,742	3
XI	.00053	.00025	.00073	453	299,718	3
XII	.00059	.00018	.00072	447	299,712	1
XIII	0.00071	0.00023	0.00072	498	299,763	1
Weighted mean	....	....	....	....	299,722	....
Correction	....	....	....	....	+67	....
Velocity *in vacuo*	....	....	....	....	299,789	....

A series of measurements with the twelve-facet steel mirror gave the results shown in Table VI.

TABLE VI

	a	*b*	*c*	*VS*	*V*	Wt
I_{I}	0.00063	0.00016	0.00072	453	299,718	
I_{II}	.00030	.00046	.00072	444	299,709	
I	$(2\times\mathrm{I}_{\mathrm{II}}+\mathrm{I}_{\mathrm{I}})/3$				299,712	2
II	.00040	.00043	.00072	465	299,730	4
III	.00051	.00032	.00072	465	299,730	4
IV	.00052	.00030	.00072	462	299,727	5
V	.00052	.00031	.00072	465	299,730	5
VI	.00055	.00031	.00072	474	299,739	5
VII	.00001	.00078	.00072	453	299.718	2
VIII	.00054	.00027	.00073	462	299,727	2
IX	.00056	.000315	.000736	483	299,748	3
X	.00052	.00027	.00074	459	299,724	3
XI	0.00054	0.00023	0.00074	453	299,718	3
Weighted mean					299,729	
Correction					+67	
Velocity *in vacuo*					299,796	

Table VII gives the results obtained with the steel octagon.

TABLE VII

	a	*b*	*c*	*VS*	*V*	Wt.
I	0.00027	0.00057	0.00071	465	299,730	3
II	.00032	.00049	.00071	456	299,721	3
III	.00059	.00028	.00069	468	299,733	3
IV	.00057	.00025	.00069	453	299,718	5
V_{I}	.00008	.00072	.00072	456	299,712	
V_{II}	.00054	.00030	.00072	468	299,733	
$\mathrm{V}_{\mathrm{III}}$	.00076	.00005	.00072	459	299,724	
V	Mean of 3				299,723	3
VI_{I}	.00065	.00027	.00072	492	299,757	3
$\mathrm{VI}_{\mathrm{II}}$	.00081	.00005	.00072	474	299,739	
VI	$(2\times\mathrm{VI}_{\mathrm{II}}+\mathrm{VI}_{\mathrm{I}})/3$				299,744	3
VII	.00035	.00049	.00072	468	299,733	3
VIII	.00059	.00024	.00072	465	299,730	5
IX	.00055	.00026	.00072	459	299,724	5
X	.00056	.00025	.00072	459	299,724	5
XI	0.00058	0.00025	0.00072	465	299,730	5
Weighted mean					299,728	
Correction					+67	
Velocity *in vacuo*					299,795	

These results are collected in Table VIII.

TABLE VIII

Mirror	Year	*N*	*n*	*V*	Wt.
Glass 8	1925	528	150	299,802	1
Glass 8	1925	528	200	299,756	1
Glass 8	1926	528	216	299,813	3
Steel 8	1926	528	195	299,795	5
Glass 12	1926	352	270	299,796	3
Steel 12	1926	352	218	299,796	5
Glass 16	1926	264	270	299,803	5
Glass 16	1926	264	234	299,789	5
Weighted mean				299,796±4	

When grouped in series of observations with the five mirrors the results show a much more striking agreement, as follows:

Glass 8	299,797
Steel 8	299,795
Glass 12	299,796
Steel 12	299,796
Glass 16	299,796

The ready success of the measurements at the distance of twenty-two miles, the majority of which were made under conditions not the most favorable (haze and smoke from forest fires; imperfections of surfaces of the revolving mirrors), would seem to indicate the feasibility of a measurement at a considerably greater distance. A convenient location for the distant mirror (diameter, 40 in.) was found at Mount San Jacinto, eighty-two miles distant. In a preliminary trial, light was returned, but so enfeebled by smoke that measurements were quite impracticable.

It is hoped that during the winter season the rains will clear the atmosphere sufficiently for accurate measurement, and accordingly work will begin again toward the end of December, 1926.

I take this opportunity to express my appreciation of the generous gift of $10,000 by Mr. Martin A. Ryerson which made this investigation possible.

APPENDIX I

Measurement of the length $2D$ of the light-path.

The light-path as shown in Figure 1 is from the surface *a* of the revolving mirror to $b\ c\ D\ E\ f\ E\ D\ c\ b_1\ a_1$.

The measurements of the separate elements are as follows:

Distance between bench marks $B\ B_1$, as furnished by U.S. Coast and Geodetic Survey, 35,385.5 m

	Meters
$BD=$	11.57
$Dc=$	8.00
$bc=b_1c=$	0.40
$ab=$	0.34
$B_1f=$	0.11
$fE=$	9.30

The D of the formula will be

$$D=ab+bc+cD+DB_1+B_1f+2fE=35,424.5\text{ m}\ .$$

APPENDIX II (JULY 1)

Comparison between C.G.S. pendulum[1] and standard observatory clock:

Period of Coincidences	Temperature
23^m46^s	24°0
23 44	24.1
23 24	24.1
23 40	24.2
24 00	24.4
1423	

N = number of (double) swings per second = 1.00070 at 24°2.

Another comparison gave 1.00074 at 17°.

Whence the temperature correction is − .0000055 per degree.

The clock gains one second per day by comparison with time signals from Washington; giving

$$T=1.00075 \text{ at } 17^\circ\ .$$

Another comparison taken August 13 gave the following results:

Period of Coincidences	Temperature
22^m41^s	19°0
23 15	19.2
23 07	19.4
22 58	19.7
22 50	20.1
23 48	21.0
23 20	21.5

from which $N=1.00072$ at 19.9°.

---

[1] The pendulum case was evacuated to a residual pressure of about 1 cm, for which the pressure correction is inappreciable. The amplitude correction was also negligible.

The rate of the standard clock was $+0^{s}.5$ per day, giving

$$N_2 = 1.000726 \text{ at } 19.9^\circ$$

and

$$N = 1.00074 \text{ at } 17^\circ.$$

APPENDIX III. MEASUREMENT OF LENGTH OF LINE USED IN DETERMINATION OF VELOCITY OF LIGHT

By WILLIAM BOWIE[1]

As a result of several conferences between Professor A. A. Michelson and the writer on the question of the determination, with high accuracy, of the distance between a point on Mount Wilson and one on San Antonio Peak, California, to be used as a base line in the determination of the velocity of light, Professor Michelson made a request on May 1, 1920, upon the director of the United States Coast and Geodetic Survey, Colonel E. Lester Jones, that the work be done. The director, realizing that the determination of the velocity of light with great accuracy might lead to the determination of distance in terms of the velocity of light and thus might furnish a means of measuring base lines in mountainous regions or on archipelagoes, agreed to measure the distance between the two peaks in question.

Professor Michelson requested that the distance be measured with an accuracy of 1 part in 200,000 but with greater accuracy if possible. In a letter to the director, dated March 23, 1922, Professor Michelson made the statement:

> In my conversations and correspondence with Major William Bowie, I was given to understand that the measurement [of the distance between Mt. Wilson and San Antonio Peak] could be made to an order of accuracy of one in a million which would be highly desirable, if possible, but an order of accuracy of one in 100,000 or 200,000 would be sufficient.

In a letter dated March 14, 1922, Professor George E. Hale, director of the Mount Wilson Observatory, requested the director of the United States Coast and Geodetic Survey to determine by triangulation the distance between Mount Wilson and San Antonio Peak for Professor Michelson's use in his redetermination of the velocity of light. The director of the Coast and Geodetic Survey replied to Dr. Hale, expressing his deep interest in the work on the velocity of light, and made the statement that the field measurements would be undertaken later in the year.

---

[1] Chief, Division of Geodesy, U.S. Coast and Geodetic Survey, Washington, D.C.

It was realized that to obtain an accuracy in the determination of the length of a line of triangulation as great as 1 in 200,000 or more would necessitate some modifications and refinements in the methods that are usually employed in what is known as first-order triangulation. It is rather difficult to estimate just what is the accuracy of a line of triangulation carried from a base through a series of triangles or quadrilaterals, but it has generally been supposed that the order of accuracy is about 1 part in 100,000.

Ordinarily, the quadrilaterals used in a chain of triangulation approach the square in shape, that being the most satisfactory shape, if both accuracy and rapid progress are desired. For the Michelson length it was believed best not to depend on a triangulation extended from the Los Angeles base, which had been measured in 1888–1889. There was the possibility that this base had changed its length during the interval since its measurement, and, besides, it was believed that even though the angles of the triangles extending from the Los Angeles base to the Michelson line were remeasured with the greatest care, the lengths carried through the triangles would not have an accuracy of 1 part in 200,000. After careful consideration of the problem, it was decided to measure a base line in the San Gabriel Valley, parallel to the line between Mount Wilson and San Antonio Peak, and to have the base line as close to the foothills as possible in order that the angles involved in transferring the length of the base to the line between the peaks might be of such size as to give the strongest possible connection.

An inspection of the topographic maps of the United States Geological Survey indicated that it was feasible to measure a base of the desired length in this locality. The methods to be employed in the field work were carefully planned at the office of the United States Coast and Geodetic Survey by the members of the Division of Geodesy. The field work was placed in charge of Clem L. Garner, one of the field engineers of the United States Coast and Geodetic Survey who had had a number of years of experience on first-order triangulation and in the measurement of first-order base lines. In his party were a number of engineers of the Survey who had also had experience in the most accurate geodetic work. They were J. S. Bilby, F. W. Hough, and E. O. Heaton.

The computation of the precise levels on the base line was in charge of H. G. Avers. The computations of the measured lengths were made under the direction of W. D. Sutcliffe. Unusual care was employed to take into account all refinements in computation that could affect the final results. The computation and adjustment of the triangulation to carry the length from the bases to the required line extending from the station Michelson on Mount Wilson to the station Antonio on San Antonio Peak were made under the direction of O. S. Adams. Extra computations were made for the deflection of the vertical, and extreme care was employed at all stages of the work. Other mathematicians engaged upon the work, either directly or in consultation, were W. D. Lambert, C. H. Swick, C. A. Mourhess, Sarah Beall, and W. F. Reynolds.

By a field reconnaissance the ends of the base were located where they could be made intervisible by the erection of observing towers of moderate height and where the two peaks at the ends of the Michelson line were visible from each end of the base. It was found, however, that a straight base from end to end could not be measured, owing to the character of the terrain and to the presence of orange groves and other obstructions. Correspondence between the office and the field resulted in the adoption of a plan to measure a broken base, with the various sections located where the measurements could be most easily made.

The methods adopted for the field measurements and the office computations were such as to assure the attainment of an accuracy, for the straight-line distance between Mount Wilson and San Antonio Peak, corresponding to a probable error of about 1 part in 2,000,000, derived from field measurements and observations alone, and to an actual error surely less than 1 part in 300,000. It is the feeling of those who have been engaged in the work that the actual error is somewhere between 1 part in 500,000 and 1 part in 1,000,000.

It was decided to make the distance between the peaks depend on more than one base. This was accomplished by dividing the total base into three parts. The length of each part was obtained during the measurement of the whole base line, as the subsidiary stations were placed along the base itself.

The base was measured in forty-six sections, owing to the character of the terrain, to the presence of obstructions, and to the fact that the base cut the property lines at an angle. Each section of the base was measured at least four times, with 50-m invar tapes which were standardized with extreme accuracy at the Bureau of Standards, Washington, D.C., just before and just after the measurements in the field. The maximum number of measurements of any one section was six. Eight tapes were used in the measurement of the base, and on each section the different measures were made with different tapes.

Along a portion of the line, wooden stakes were set into the ground to support the tapes during the measurements. The length of the tape was transferred by a marker to metal strips nailed to the tops of the stakes at the tape ends. Where the measurement was over a paved highway, special portable tripods made of iron were used. These were set over points which had previously been selected and marked with small iron bolts cemented in drill holes in the pavement. Five supports were used for all the measurements over stakes, and three supports for the measurements over portable tripods and towers. If possible, the intermediate supports were placed in line between the tops of the end supports.

When stakes were used, accurate levels were run over them to determine the difference in elevation of consecutive tape ends. The leveling was done in both directions in order to have a check. Necessarily, where stakes were used, the same grade corrections would be applied to each tape length as measured by each of the four or more tapes. On the other hand, when the movable tripods were used, the distance of the tripod head above the mark on the road was obtained during the measurement with each tape. Later, when levels were run over these parts of the base to give the differences in elevation of the marked points, these differences were combined with the heights of the tripods to give the data from which to compute the corrections for grade for each tape. Necessarily, the grade corrections were slightly different for the different measurements, owing to the fact that the tripods could not be set exactly at the same heights for the different measurements.

At places where the line had to be lifted above orange groves, the tapes were supported on towers. Towers were also used to avoid steep grades where measurements were made across rather sharp depressions in the ground. One of the large uncertainties in base measurements, where the ground is very steep, is in the determination of the grade corrections. In order to avoid this uncertainty, the slope for any tape length was seldom allowed to be greater than 10 per cent.

In computing the base, the lengths of the forty-six sections were projected on to straight lines joining the ends of the three main divisions of the base mentioned above. In general, the difference in direction of a section and the line on which it was projected was only a few degrees, and in only one case did it exceed the limit of 14° specified in the instructions, the deflection angle in this instance being 18°.

The uncertainty in the measured length of a base is due to the following causes: errors in the standardization of the tapes, use of erroneous tension on the tapes during the measurements, effect of wind on the tapes, constant and systematic errors in transferring the ends of the tape to the metal strips on the end supports of the tape, errors in leveling from which the grade corrections are computed, uncertainty in the coefficient of expansion of the tape, and errors in the reduction to sea-level from uncertainty in the average elevation of the base line.

The differences in the lengths of the tapes, as derived from the two standardizations at the Bureau of Standards, one before the measurements in the field and the other shortly afterward, are given in Table I.

The effect of the wind on the tape may be considered as having been negligible, for the measurements were made only when there was a very light wind or during spells of calm weather. The use of five-point supports whenever possible also lessened the effect of the wind on the tape.

The errors in transferring the ends of the tape to the metal strips were undoubtedly small, for the observers doing the marking changed positions between the forward and backward measurements, thus eliminating the systematic effect of any tendency to mark ahead or behind the graduation on the tape. The accidental errors in the marking were very small, owing to the care with which the line on the tape was transferred to the metal strip. The marking was done only when the tape had come to rest after the tension had been applied.

Seven different spring balances were used to apply the tension to the tapes. Each balance was tested twice on every day it was used with a standard 15-kg weight. The balance was placed in a horizontal position during the test, and a small wire led from the tongue of the balance to the weight over a pulley which was practically frictionless. The balances were also tested at the Bureau of Standards after the field work was completed, and the effect of changes in temperature on the springs of the balances was determined. No attempt was made to set the indexes of the balances to make the dials give correct readings, but in the office computations corrections were applied to the measured lengths to account for the errors of the balances as disclosed by the daily tests and for the effects on the springs of any temperature variations.

TABLE I

Tape Nos.	Differences in Length Millimeters
914	+0.17
918	.18
921	.04
925	.03
927	.19
928*	......
929	.20
933	+0.04

* Owing to a misunderstanding when this tape was sent to the Bureau of Standards, its length was not redetermined. The second standardization gave a shorter length for each of the tapes used.

Extreme care was used in determining the elevation of the tape supports. Levels were run in both directions over the base and, wherever the two runnings failed to agree within a certain amount, a third running was made as a check. The elevations of the ends of the different sections of the base were determined by first-order leveling, and the elevations, as carried through the differences of elevation of the tape ends, were checked with the elevations determined by the first-order levels. It may be assumed, therefore, that the corrections for grade had exceedingly small errors.

The temperature range during the measurements of the base was from 5° to 25° C. The tapes were standardized at 26° and 28° C. The coefficient of expansion of each tape had been determined at the Bureau of Standards with such accuracy that it is believed that any error in the length of the base, due to erroneous temperature corrections, is exceedingly small.

The elevation of the base above sea-level was determined by checked first-order leveling from a nearby bench mark of known elevation, so it is reasonably certain that no error was involved in the sea-level correction.

The agreement of the several measurements of each section indicates that the accidental and systematic errors were largely eliminated by the methods employed. As was mentioned earlier, each section was measured at least four times, each time with a different tape. The average residual of a single measure from the mean of all measurements on a section was 1.1 mm. Only three measures were rejected, and in only thirty-two measures of the remaining total of two hundred eight was the residual more than 2 mm. The average size of the probable error of the sections was 0.5 mm, with no probable errors greater than 1 mm. The maximum probable error of a section was 0.9 mm.

The probable error of the length of the base from field measurements and observations alone was 3.45 mm, or 1 part in 11,600,000. The Bureau of Standards certified that the lengths of the tapes were correct within 1 part in 300,000 and that the probable error did not exceed 1 part in 2,000,000.

During the measurement of the base, observations were made for horizontal directions at four points along the base line, including the two ends, and at San Antonio Peak and Mount Wilson. These observations were made with high-grade direction theodolites. The observations were repeated a number of times in order to eliminate, as far as practicable, the effect of the accidental errors, and they were made on each of several nights in order that any systematic errors resulting from atmospheric conditions might be largely eliminated.

The deflection of the vertical was determined at each of the stations in order that corrections could be applied to the observed directions to eliminate the effect of any tilting of the geoidal surface with respect to the spheroidal surface. The mountain masses to the north of the base line evidently deflect the plumb line to a marked degree. The determination of the astronomic latitudes was made at each of the angle stations except at station Joaquin, which is within a mile of Pasadena west base, and at station Michelson, where it had already been determined. It was assumed that the deflection in the meridian at Joaquin would be approximately the same as at Pasadena west base.

The effect of the deflection of the vertical is to tilt the horizontal plate of the theodolite with respect to the spheroid and, therefore, to cause the measured angles to vary somewhat from the true spherical angles. The astronomic longitude had been determined at Mount Wilson some years before. A comparison of it with the geodetic longitude furnished a deflection of the vertical in the prime vertical at that point, thus making it possible to correct the astronomic azimuth at Mount Wilson for the deflection of the vertical. In the adjustment of the triangulation the true azimuth obtained at Mount Wilson was held fixed. This made it possible to determine the approximate deflection of the vertical in the prime vertical at each of the other stations by a comparison of the astronomic azimuth and the geodetic azimuth at each of them.

The results of the computations showed clearly that it was a wise move to determine the deflections at each of the stations, for the maximum correction to a direction was nearly $1''.5$. A number of directions were only slightly affected, but on the whole the application of corrections for the deflections resulted in appreciably greater accuracy in the determination of the length of the Michelson line.

Owing to the fact that the lines from the base stations to the mountain peaks have inclinations as great as 8° to the horizontal plane, it was necessary to read the stride level of the theodolite whenever pointings were made over the steep lines, in order that corrections might be applied for any tilting of the horizontal axis of the telescope during the observations. This is a refinement in angle measurements that has never been applied in the regular triangulation of the country. In fact, the inclination of a line of triangulation is seldom greater than 1° or 2°, and the error from this source is ordinarily negligible.

The heights of the stations on Mount Wilson and on San Antonio Peak were determined from the base stations by trigonometric leveling. These elevations were required for the purpose of determining the air-line distance between the stations on the two peaks.

The average closing error of the triangles involved in the triangulation was $0\overset{''}{.}55$. There were only two triangles with closing errors greater than $1''$, while the maximum closing error was $1\overset{''}{.}57$.

The average correction to a direction, resulting from the least-squares adjustment, was $0\overset{''}{.}24$; and the maximum correction was $0\overset{''}{.}83$.

The distance, reduced to sea-level, between the triangulation stations Michelson on Mount Wilson and Antonio on San Antonio Peak, resulting from the adjustment, is 35373.21 m. The air-line distance between these two stations is 35385.53 m. No correction was applied to the distance to allow for normal curvature of the line of light between the two stations on account of refraction. A computation was made which showed that this correction is only one part in several million.

The probable error of the straight-line distance from Mount Wilson to San Antonio Peak is 1 part in 6,800,000 from field measurements and observations alone. It is believed that the length of this line has been determined with greater accuracy than that of any other line of triangulation in this or any other country.

Contributions from the Mount Wilson Observatory, No. 330
Reprinted from the *Astrophysical Journal*, Vol. LXV, pp. 124–129, 1927
Printed in the U.S.A.

THE SHORT-PERIOD VARIABLE STAR RV CANUM VENATICORUM

By J. SCHILT

ABSTRACT

Light-curve.—From ninety-one plates the light-curve of RV Canum Venaticorum is found to be of the type of W Ursae Majoris, with a period of 0.269572 day. This makes it highly probable that the star is a dwarf eclipsing binary, instead of a variable of the cluster type, as stated by Graff.

Spectrum and range in light.—The spectrum is F8; the photographic range is 0.75 mag. and apparently does not exceed the visual range.

The variability of this star, which is 25′ from the center of the globular cluster M3, was first detected by J. Larink,[1] who found a period of 0.134786 day. A photometric visual light-curve has been published by K. Graff,[2] who calls attention to many irregularities. The reality of these irregularities seems doubtful. I have combined Graff's observations into groups of three. The dispersion of the deviations of such normal points from a symmetrical smooth curve is ±0.062±0.019 mag. (mean error). Graff gives a mean error of ±0.06 mag. for his individual observations, which, if the latter are independent, amounts to ±0.036 mag. for the normal points. The difference between the observed dispersion and the value given is 0.026±0.019 mag. Whether this is accidental or a consequence of some systematic error in Graff's observations cannot be settled. It will be seen, however, that the present observations do not corroborate the alleged irregularities.

To determine the photographic light-curve, ninety-six plates, each with eight minutes' exposure, were taken, mainly during four nights, with the 60-inch reflecting telescope. The plates used are Eastman 40, size 4 by 5 inches, so that the center of the globular cluster M3 is just on the following edge of the plates. Ninety-one of these plates have been measured with the thermopile microphotometer. The magnitudes of the comparison stars were derived from the comparison plates SS 145, 146, and 147, which have the following exposures and zenith distances:

---

[1] *Astronomische Nachrichten*, 214, 71, 1921.

[2] *Ibid.*, 217, 310, 1923.

Plate	First Exposure		Second Exposure	
SS 145	Selected Area 57,	15°	RV Can. Ven.,	12°
146	RV Can. Ven.,	13	Selected Area 57,	8
147	Selected Area 57,	5	RV Can. Ven.	4

Because of the small zenith distances, no correction for differential extinction is required. The magnitudes, on the international scale, of the stars of the Selected Area were kindly supplied by Mr. Seares, and the resulting magnitudes of the comparison stars, together with their rectangular co-ordinates, are entered in Table I.

TABLE I

Variable and Comparison Stars

Star	X	Y	Pg. Mag.	
			Provis.	Adopted
RV Can. Ven.	0″	0″	....	....
a	+358	+35	15.74	15.78
b	320	41	15.33	15.38
c	+274	30	14.72	14.59
d	−279	37	16.20	16.16
e	−417	+ 8	14.62	14.71

The provisional values were derived directly from the three comparison plates, whereas the adopted magnitudes are the smoothed values found by using measurements from all the plates. The comparison stars *c* and *e* happen to be the same as Graff's stars *f* (vis. mag., 13.41) and *a* (vis. mag., 13.66), respectively.

The observational data are entered in Table II. The observations have been combined into groups of four in order of phase. The normal points thus obtained are given in Table III, and are shown graphically in Figure 1. The computed minimum is at phase 0.185 P. The mean magnitude at maximum from the eighteen observations between phases $0.685 \pm 0.100P$ is 14.897 ± 0.014 mag. (mean error); from the eleven observations between the narrower limits 0.685 ± 0.050 it is 14.883 ± 0.017 mag. (mean error). The adopted maximum light is 14.88 mag. The magnitude at minimum is estimated to be 15.63 ± 0.04 mag., from which the photographic range is 0.75 ± 0.04 mag.

TABLE II

THE OBSERVATIONS

Plate	J.D. Hel. G.M.T. 2424000+	Epoch and Phase	Mag.	Plate	J.D. Hel. G.M.T. 2424000+	Epoch and Phase	Mag.
SS 64..	564.9255	0.000*P*	15.33	SS 128..	620.9386	415.571*P*	14.85
65..	.9330	.055	15.38	129..	.9455	.622	14.87
66..	.9400	.106	15.56	130..	.9524	.673	14.83
67..	.9469	.158	15.69	131..	.9593	.724	14.90
68..	.9538	.209	15.70	132..	.9766	.853	14.94
69..	.9608	.261	15.61	138..	621.7003	421.222	15.55
70..	.9677	.312	15.38	139..	.7072	.273	15.44
72..	.9816	.415	15.23	140..	.7142	.325	15.10
73..	.9885	.467	15.06	141..	.7211	.376	15.02
74..	.9954	.518	15.11	142..	.7280	.427	14.94
75..	565.0024	.569	15.15	143..	.7349	.470	14.82
76..	.0093	.621	14.89	144..	.7418	.530	14.90
77..	.0163	.672	14.95	145..	.7883	.875	14.86
78..	.0232	.723	14.93	146..	.7953	.927	15.06
79..	.0301	.775	14.95	147..	.8243	422.142	15.60
80..	.0371	.826	14.78*	149..	.8804	.558	14.93
81..	.0440	.878	15.03	150..	.8874	.610	15.04
82..	.0510	.930	15.02	151..	.8943	.661	14.98
83..	.0579	0.981	15.06	152..	.9012	.712	14.87*
98..	619.9025	407.884	15.02	153..	.9082	.764	14.91
99..	.9140	.969	14.90	154..	.9151	.816	14.94
102..	620.7307	414.029	15.25	155..	.9220	.867	14.97
103..	.7377	.080	15.34	156..	.9289	.918	15.10
104..	.7446	.131	15.58	157..	.9358	.969	15.13
105..	.7515	.182	15.67	158..	.9428	423.021	15.18
106..	.7585	.234	15.58	159..	.9497	.072	15.20
107..	.7654	.286	15.36	171..	642.6838	576.902	14.86
108..	.7724	.338	15.24	172..	.6908	.954	15.07
109..	.7793	.389	15.13	173..	.6977	577.005	15.19
110..	.7862	.440	15.03	174..	.7046	.056	15.19
111..	.7932	.492	14.94	175..	.7115	.108	15.31
112..	.8001	.543	14.89	176..	.7184	.159	15.39
113..	.8070	.594	14.86	177..	.7253	.210	15.55
114..	.8140	.646	14.82	178..	.7323	.262	15.28
115..	.8209	.697	14.86	179..	.7392	.313	15.18
116..	.8278	.749	14.83	180..	.7461	.364	15.10
117..	.8347	.800	14.84	181..	.7530	.415	15.00
118..	.8416	.851	14.95	182..	.7600	.467	14.98
119..	.8486	.903	14.88	183..	.7669	.518	14.95
120..	.8555	.954	15.10	184..	.7738	.570	14.94
122..	.8971	415.263	15.28	185..	.7807	.621	14.91
123..	.9040	.314	14.95	186..	.7877	.673	14.84
124..	.9110	.366	15.11	187..	.7946	.724	14.90
125..	.9179	.417	15.04	188..	.8113	.848	14.89
126..	.9248	.468	14.97	190..	642.8535	578.161	15.50
127..	.9317	.520	15.01				

* Taken through the glass.

The observations by Graff have been plotted as crosses in Figure 1, each cross representing the mean of three successive observations. In order to make the ordinates correspond to the photographic light-curve, a constant, +1.35 mag., has been applied to Graff's visual observations. The magnitudes at maximum, 13.48±0.03 mag., and at minimum, 14.29±0.05 mag., give a visual range on Graff's scale of 0.81±0.06 mag. The difference between the photographic and visual amplitudes is thus −0.06±0.075 mag., from which we may conclude that, on the basis of the adopted scales, the photographic amplitude does not exceed the visual range.

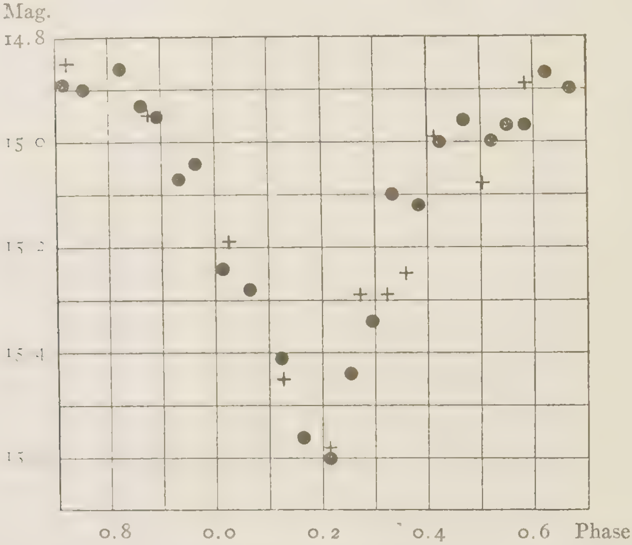

FIG. 1.—Observations of RV Canum Venaticorum in groups of four (dots) plotted according to phase as calculated from Larink's period (half-period). Crosses represent means of three consecutive observations by Graff, reduced to the zero point of the Mount Wilson measures.

It is evident from the measures that the light-curve is of the type of W Ursae Majoris, and this conclusion is not contradicted by Graff's observations.

The spectrum obtained with a slitless spectrograph at the 60-inch reflector is F8. The lines seem to be diffuse, though there is some uncertainty on account of the low dispersion used.

The data so far obtained indicate that RV Canum Venaticorum is a very faint representative of the W Ursae Majoris class of stars, and presumably a dwarf. As it is an eclipsing binary, Larink's period must be doubled. New normal points for the complete period of revolution are entered in Table IV, where the phase is now counted from the primary minimum.[1] The light-curve for the double period,

TABLE III

NORMAL POINTS

Phase	Mag.	Phase	Mag.
0.014*P*	15.24	0.550*P*	14.97
.066	15.28	.586	14.97
.122	15.41	.628	14.87
.165	15.56	.670	14.90
.212	15.60*	.714	14.89
.255	15.44	.753	14.90
.296	15.34	.822	14.86
.335	15.10	.862	14.93
.386	15.12	.892	14.95
.425	15.00	.932	15.07
.470	14.96	0.968	15.04
0.512	15.00		

* Mean of three observations.

TABLE IV

NORMAL POINTS FOR REVOLUTION PERIOD

Phase	Mag.	Phase	Mag.
0.006*P*	15.61	0.514*P*	15.40
.057	15.40	.553	15.21
.122	15.11	.586	15.08
.172	14.97	.624	14.99
.206	14.98	.656	14.94
.242	14.90	.694	14.90
.276	14.88	.744	14.86
.310	14.88	.820	14.90
.344	14.95	.871	14.99*
.370	15.02	.928	15.32
.396	15.11	0.974	15.61
0.440	15.22		

* Mean of three observations.

---

[1] It is suspected that the comparison star *e* may be variable. The magnitudes were therefore determined a second time without using star *e*. The average difference, without regard to sign, between the two sets of values is 0.02 mag. The results of the first reduction have been retained.

shown in Figure 2, has slightly different minima and an asymmetry which, even if real, need cause no surprise, since it is quite comparable with asymmetries found in other stars of this class.

The heliocentric time of principal minimum derived from the present observations is J.D. (Greenwich Mean Time) 2424642.5863, while that of the minimum observed by Graff is 2422811.5540. Since the period is known only with an accuracy of one second,[1] the interval between the two epochs is, unfortunately, too large to determine the number of intervening revolutions. The revised elements are:

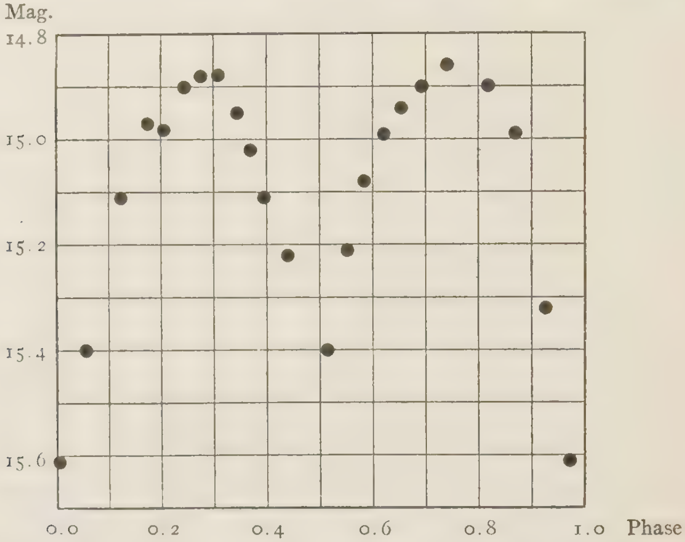

FIG. 2.—Normal points for RV Canum Venaticorum corresponding to complete period of revolution.

Min. (J.D. Hel. G.M.T.) = $2424642.5863 \pm 0.269572E$
$\pm .0020 \pm 0.000023$ (m.e.)
Maximum light........ 14.88 ± 0.02 mag. (m.e.)
Primary minimum...... 15.65 ± 0.10
Secondary minimum.... 15.48 ± 0.10

where the period is Larink's value doubled.

MOUNT WILSON OBSERVATORY
August 1926

---

[1] J. Larink, *loc. cit.*

Contributions from the Mount Wilson Observatory, No. 331
Reprinted from the *Astrophysical Journal*, Vol. LXV, pp. 163–199, 1927
Printed in the U.S.A.

INTERSTELLAR CALCIUM

BY OTTO STRUVE

ABSTRACT

Intensities of detached calcium lines.—Estimates have been made for 321 stars of spectral type not later than B3. Some of these were from spectrograms in the collections of the Mount Wilson, Victoria, Lick, and Yerkes observatories; others from plates taken by me with the 60-inch reflector at Mount Wilson. *The mean intensity of detached lines increases* from 1.6 to 3.6 units between 1 and 7 mag. The *probable error* of a single estimate is 0.5 unit. One unit corresponds to a difference of about 0.1 mag. between the intensity of the continuous spectrum at λ 3933 and the center of the K line. The increase in intensity for the fainter stars is probably an *effect of distance*, the space around the sun out to 150 or 200 parsecs being unfavorable for the appearance of strong detached lines. The strongest lines occur at a distance of 500 or 600 parsecs, beyond which conditions are perhaps again less favorable for the production of strong lines. *Regional effects* seem to be the most important factor in defining the intensity of detached K. In Cepheus (36 stars) the mean intensity is more than 5 units, while in Orion (24 stars) it is only 2 units. *B3 stars have*, on the average, *weaker lines* than the earlier spectral subdivisions. Detached lines seem *not to occur in types later than B3*. The lines appear to be slightly *stronger* in a belt of 20° along *the plane of the Milky Way*.

The components of visual *double stars have identical intensities*, without respect to differences in brightness or spectral type. The spectroscopic binary *2 Lacertae*, type B3, *shows a detached calcium line* between two stellar components, at or near the time of passage through the node.

Calcium cloud in Cepheus.—The residual velocities from detached K lines of 36 stars in the Cepheus region are *systematically smaller* than those from the stellar lines, and effects of group motion may be present. The intensity of K in these stars is slightly smaller in regions where dark nebulae are present. It is estimated that the *distance* of the beginning of the *calcium cloud* is *250 parsecs*. The *dark nebula* is found, from star-counts, to be at a distance of about 350 parsecs. The region of strong calcium lines in Cepheus extends into portions of the Milky Way where the distribution of stars is normal, whence it is believed that *calcium clouds are transparent.*

INTRODUCTION

Although twenty-two years have elapsed since Hartmann discovered "stationary" calcium lines in the spectrum of the binary δ Orionis, our knowledge concerning the origin of these lines has advanced but little.[1] The most important observational investigation made in recent years is that of J. S. Plaskett.[2] From this we now know that the peculiar lines of calcium and sodium are not confined to spectroscopic binaries alone, but occur in nearly all stars of spectral type not later than B3. Since the calcium lines in stars of constant velocity have exactly the same properties as the so-called "stationary lines" in spectroscopic binaries, I am following a suggestion by P. W. Merrill[1] in using the word "detached" throughout this paper. This term includes all lines that behave differently from ordinary stellar lines with respect to Doppler shift, intensity, width, and general appearance.

---

[1] For a more detailed summary of earlier work on detached calcium lines see my paper in *Popular Astronomy*, **33**, 639, 1925; **34**, 1, 1926.

[2] *Publications of the Dominion Astrophysical Observatory, Victoria*, **2**, 335, 1924; *Monthly Notices of the Royal Astronomical Society*, **84**, 80, 1924.

Plaskett has shown that the radial velocities derived from detached lines do not agree with those from ordinary lines, and that the difference is frequently so large that it cannot be explained by abnormalities in wave-length or in the structure of stellar absorption lines. Furthermore, the velocities from the detached lines have a tendency to agree very closely with the radial component of the solar motion, indicating that, referred to our stellar system, the peculiar velocities of the gases responsible for the appearance of these lines are small.

In explaining the origin of detached lines Plaskett modified the original hypothesis of Hartmann. He suggested that the detached lines are produced by absorption in a "widely distributed tenuous cloud of matter," enveloping the stars so that its calcium atoms will be ionized in the neighborhood of the hottest stars. This would account for the occurrence of the detached lines in spectral types O and B only.

For details of other investigations concerning the detached calcium lines the reader is referred to the original papers by R. K. Young,[2] G. Strömberg,[3] H. Kienle,[4] H. Vogt,[5] H. Ludendorff,[6] J. Woltjer,[7] F. Henroteau,[8] M. N. Saha,[9] B. P. Gerasimovič,[10] and others. My previous work, of which the present paper is a continuation, will be found in several short articles.[1] Of particular importance is A. S. Eddington's recent discussion on "Diffuse Matter in Interstellar Space."[2] From theoretical considerations Eddington concludes that it is impossible to assume that the detached-line absorption, although occurring in an interstellar cloud, is controlled by the hot stars, stellar radiation being required to alter the constitution of the calcium and to produce the peculiar lines in stellar spectra. From certain assumptions he finds that "proximity to a very hot star would decrease the amount of $Ca+$ by causing more double ionization." Eddington suggests that absorption occurs evenly all along the path of the light, and that diffuse matter of calcium and other elements is present everywhere in sufficient quantity to produce appreciable monochromatic absorption, but in insufficient quantity to affect to any measurable amount the brightnesses or the colors of the stars.

---

[1] *Publications of the Astronomical Society of the Pacific*, **38**, 211, 1926.

[2] *Publications of the Dominion Astrophysical Observatory, Victoria*, **1**, 219, 1920; *Journal of the Royal Astronomical Society of Canada*, **19**, 46, 1925.

[3] *Mt. Wilson Contr.*, No. 293, p. 10; *Astrophysical Journal*, **61**, 372, 1925.

[4] *Probleme der Astronomie; Festschrift für H. v. Seeliger*, p. 38, 1924; *Monthly Notices of the Royal Astronomical Society*, **84**, 583, 1924.

[5] *Astronomische Nachrichten*, **224**, 16, 1925.

[6] *Ibid.*, **212**, 3, 1920.

[7] *Bulletin of the Astronomical Institutes of the Netherlands*, **2**, 195, 1925.

[8] *Journal of the Royal Astronomical Society of Canada*, **14**, 234, 1920; **15**, 62, 109, 1921.

[9] *Nature*, **110**, 488, 1921.

[10] *Ibid.*, **113**, 458, 1924.

The present contribution gives additional observational material concerning detached calcium lines and an interpretation of this material from the point of view of the two hypotheses—that of Eddington and that of Plaskett.

Preliminary work on spectrograms taken at the Yerkes Observatory showed that certain deductions could be made from the intensities of the detached lines. If the detached lines do not originate in the atmospheres of the stars, their intensities must be functions, not only of stellar temperature, but also of the properties of the clouds, and interesting revelations may be expected from a study of such intensities.

Plaskett's list of radial velocities determined from detached lines includes 40 stars. Because of the excellence of the Victoria equipment and the special care taken by Dr. Plaskett, these velocities are undoubtedly the best available at present. About 70 calcium velocities were made accessible by the publication of the velocities of 368 helium stars observed at the Yerkes Observatory.[3] It seemed desirable, however, to obtain more radial velocities, in order to strengthen Plaskett's results and to permit the investigation of systematic motions of separate calcium clouds.

---

[1] *Popular Astronomy*, **33**, 639, 1925; **34**, 1, 158, 1926; *Astronomische Nachrichten* **227**, 377, 1926; *Publications of the Astronomical Society of the Pacific*, **38**, 211, 1926.

[2] *Proceedings of the Royal Society of London*, A, **111**, 424, 1926.

[3] *Astrophysical Journal*, **64**, 1, 1926.

The material on line intensities, on which the first part of this paper is based, was obtained by me during the summer of 1926, at the Mount Wilson, Victoria, and Lick Observatories. Through the courtesy of the directors, Dr. W. S. Adams, Dr. J. S. Plaskett, and Dr. R. G. Aitken, I was permitted to look over a large number of spectrograms of early-type stars and to make estimates of the intensities of the calcium line K. Although not complete for stars of every given apparent magnitude, these estimates are ample for an independent discussion, including the determination of systematic and probable errors.

The second part of the investigation—that concerning the radial velocities and intensities from the detached calcium lines in a limited region of the sky—was made during a stay of three months at the Mount Wilson Observatory. Most of the necessary spectrograms were obtained with the 60-inch reflector. Two plates were taken by Mr. A. H. Joy with the 100-inch telescope, and several earlier plates by various observers at Mount Wilson were also utilized. For the brighter stars, I used the material available at the Yerkes Observatory, which was published in part in the paper on 368 helium stars. Several additional plates were taken by Professor S. B. Barrett and Mr. C. T. Elvey with the Bruce spectrograph attached to the 40-inch refractor.

Each of the three spectrographs was equipped with one prism. The cameras are of different focal lengths, and the linear dispersions are not the same. The Yerkes plates have the largest scale, about 30 A to the millimeter at λ 4500. The Mount Wilson plates taken with the 60-inch telescope are on a slightly smaller scale, about 45 A to the millimeter, while the scale of the spectrograph attached to the 100-inch is only about 80 A to the millimeter. The quality of the plates is nearly uniform in all three cases.

The special region selected for study was that in Cepheus, in which I had previously suspected the existence of abnormally strong detached lines. Furthermore this region is interesting because of the comparatively large positive values of the color-excess for a considerable number of stars.[1] The stars observed were selected from the *Draper Catalogue* between α 21^{h}0^m and 22^{h}20^m and δ +50°0′ and +70°0′. An attempt was made to observe the 36 stars within the foregoing limits for which this *Catalogue* gives the spectral type as not later than B3. Two of these had to be excluded because of faintness. In their place I included two other stars, situated somewhat farther to the south. While selecting these it was noticed that the number of objects of spectral type earlier than B5 situated in the dense galactic star cloud between α 21^{h}50^m and 22^{h}15^m and δ +40° and 50° is unexpectedly small—only 3 in an area of 43 square degrees, while in an approximately equal area, adjoining on the north, the number is 22. The 36 stars of the final observing program are divided nearly equally between areas where the stellar distribution seems to be normal and where there are striking obscuring nebulae. Several stars are in the large bright nebula in Cepheus, around α 21^{h}35^m, δ +57°, which was discovered by E. E. Barnard and frequently photographed both by him and by Dr. Max Wolf, of Heidelberg. Because of this distribution it was possible to investigate the relation between calcium clouds and obscuring or bright galactic nebulae.

I. DISCUSSION OF THE INTENSITIES

Material.—In estimating the intensity of the K line of calcium I have followed the method previously used for the Yerkes spectrograms.[2] The plate was put under a microscope or a low-power eyepiece, and the intensity of the center of the K line with respect to the adjoining portion of the continuous spectrum was estimated on an arbitrary scale. If no line could be seen, the intensity was called "0." If a line was suspected but not definitely seen, it was called "1." A very faint line, the reality of which seemed certain, was denoted by "2." A faint line seen without difficulty was indicated by "3." Fairly strong lines were indicated by "4" and "5." A line corresponding in intensity to the K line in Vega was denoted by "10." In the majority of cases the detached lines are fainter than this value, but for a few stars they are somewhat stronger than 10.

---

[1] *Astronomische Nachrichten*, **227**, 377, 1926.

[2] *Popular Astronomy*, **33**, 651, 1925; **34**, 4, 1926.

Precision of the intensity estimates.—The intensities of the detached K line had previously been estimated for 152 stars observed at Yerkes. To determine the accuracy of the estimates I determined the intensities of the K line for a large number of stars on spectrograms available at the Victoria, Lick, and Mount Wilson Observatories. As a result, determinations of intensity from more than one observatory are available for 94 stars. Since the various estimates were made independently, at different observatories, and on plates obtained with different instruments, they afford material for deriving systematic and probable errors, and thus provide a test of the accuracy of the whole method. My own Mount Wilson observations were treated in this comparison as an independent series of estimates. The residuals from the mean intensity for each star lead to the systematic and probable errors shown in Table I.

TABLE I

SYSTEMATIC AND PROBABLE ERRORS OF INTENSITY ESTIMATES

	OBSERVATORY				
	Yerkes	Victoria	Lick	Mt. Wilson	Mt. Wilson, Struve
Number of stars	67	63	7	51	20
Systematic error	+ 0.22	− 0.02	− 0.17	− 0.03	− 0.12
Probable error of one estimate	± 0.55	± 0.51	± 0.25	± 0.50	± 0.61

The systematic errors are in all cases very small, and can safely be neglected. Since in the following discussion all groups of stars include estimates from different observatories, it is obvious that systematic errors of more than 0.1 unit will not occur, which is about the limit of accuracy to be expected. The probable errors are also small, ±0.5 unit on the average. This means that, in the majority of cases, a single estimate is accurate within 1 unit. The small values of both the systematic and probable errors are reassuring, and give confidence in the results obtained from the estimates.

Effect of unaer-exposure.—In my earlier investigation,[1] based wholly on spectrograms obtained at the Yerkes Observatory, the limiting magnitude was 6.0. It was found[1] that the intensity of the

---

[1] *Publications of the Astronomical Society of the Pacific*, **38**, 220, 1926.

K line increased for the fainter stars, and it was inferred that under-exposure did not vitiate the results. This conclusion is now confirmed by a much larger amount of material. At Victoria and Mount Wilson stars of apparent magnitude 6.0 can be photographed in a few minutes, and the limiting magnitude lies close to 9.0. The new material, therefore, extends the list to much fainter stars; nevertheless, the general run of average intensity with apparent magnitude remains essentially the same as for the Yerkes spectrograms alone, thus indicating that the earlier data were not affected by under-exposure.

TABLE II

EFFECT OF UNDER-EXPOSURE

Star	Plate	Limiting λ Cont. Sp.	Intensity of K	Remarks
Boss 5642.........	γ 12224	λ 3920	3	
	γ 12110	λ 3920	4	
	γ 12013	λ 3889	4	
	γ 12283	λ 3889	6	
	γ 12205	λ 3889	5	
Boss 5535.........	γ 6205	λ 3957	....	Invisible
	γ 5932	λ 3900	4	
	γ 3748	λ 3841	4	
H.D. 209339......	γ 1924	λ 3928	4	
	γ 2566	λ 3860	4	
B.D.+57°2309....	C 2792	λ 3889	9	
	C 2325	λ 3879	10	
	C 2435	λ 3860	10	
	C 2429	λ 3860	8	
χ^2 Orionis.........	C 2641	λ 3879	11	
	C 899	λ 3860	8	
	γ 10765	λ 3841	8	
	γ 12404	λ 3841	10	

To obtain an independent test of the effects of under-exposure, I selected from the Mount Wilson collection spectrograms of several stars for which weak and strong plates were available and such that detached lines of both strong and average intensity were represented. On these plates I estimated the intensity of the detached K line and also noted the approximate wave-length in the violet to which the continuous spectrum extended. The results are shown in Table II, in which the plates are arranged in the order of increasing density.

The first star shows a slightly greater intensity, of the order of

1.5 units, for the stronger plates; but for the others the effect is completely absent. We conclude that if a plate is strong enough to show the continuous spectrum to about λ 3900, the estimated intensity may be regarded as reliable; but on weak plates extending only to λ 3920 there is some danger of making too low an estimate.

In most of my estimates, I made no record of the limiting wavelength. It is therefore not possible to check the number of plates on which the continuous spectrum extends only to λ 3920. Stars of apparent magnitude 7 or brighter can safely be regarded as being free from effects of under-exposure. For the fainter stars caution must be exercised in the interpretation of the results. For the brightest stars estimates were made only on plates of normal density, and effects of over-exposure need not be considered.

Calibration of intensity scale.—The spectra of a few bright stars were photographed on the same plate with varying exposure times, and the photographic density of the center of the K line, obtained with a long exposure, was matched up with the density of the continuous spectrum, obtained from a short exposure. The ratios of exposure times were then converted into intensities by means of Schwarzschild's formula. The method was first applied to Arcturus and the sun, with the result that the strongest lines appeared to be about 2 mag. fainter than the continuous spectrum. For several A-type stars the values for the magnesium line at λ 4481 ranged from 0.3 to 1.8 mag. These results are in general agreement with those of Bottlinger,[1] who found that in stars such as α Cygni and Sirius λ 4481 had an intensity 1.0–1.2 mag. below that of the background.

The same method was later applied to the calcium line K in several stars,[2] with the following results:

Star	Intensity of *Ca*K on Arbitrary Scale	Mag. Diff. Line and Cont. Spectrum
α Lyrae....................	10	1.8
γ Orionis..................	4	0.8
β Tauri....................	2	0.6

---

[1] *Astronomische Nachrichten*, **195**, 119, 1913.

[2] *Popular Astronomy*, **33**, 652, 1925

These results are very uncertain because of the inaccuracy of the method used. In a recent paper by Cecilia H. Payne and Harlow Shapley,[1] the intensity of the K line in Vega is given as 0.23 mag. This value was obtained from microphotometer tracings and, as far as the photometric method is concerned, is certainly reliable. Even a casual glance at our plates, however, shows that the difference between the continuous spectrum and the center of the line is much greater than the value obtained at Harvard. The problem may be compared to that of estimating stellar magnitudes on direct photographs, where under the best conditions a difference in photographic density corresponding to 0.1 mag. can be detected. The faintest visible spectral lines should therefore correspond to a similar difference in density. If the plates are over- or under-exposed or influenced by the Eberhard effect, or if the width of monochromatic absorption is small in comparison to the theoretical line-width of the spectrograph, then the limiting difference in intensity for which a line is detectable will be rather more than 0.1 mag. For the particular line λ 3933, it is also necessary to take into consideration the relation between contrast and wave-length. F. E. Ross has shown[2] that under ordinary conditions and for simple blue-sensitive plates the contrast factor gamma decreases for the shorter wave-lengths. From his experiments I find that for λ 3900, gamma = 0.5, while for λ 4800, where the continuous spectrum is strongest, gamma = 1.2. Such a large difference in contrast tends to increase the limiting difference in intensity detectable with the eye. It would probably be more nearly correct to assume that the faintest K line discernible with certainty has an intensity about 0.2 mag. lower than the background of continuous spectrum.

If in the case of Vega we imagine that we are dealing, not with spectra, but with star-images, one of the density of the continuous spectrum at λ 3930, the other of the density of the center of the K line, we should estimate the difference in density to be of the order of 1 or 2 mag. This value roughly confirms that obtained from scale plates.

---

[1] *Proceedings of the American Academy of Arts and Sciences*, **61**, 459, 1926; *Harvard Reprint*, No. 28.

[2] *Physics of the Developed Photographic Image*, p. 74, 1924.

In order to determine entirely independent values of the intensity, I obtained tracings from some of the plates with the registering thermoelectric microphotometer of the Mount Wilson Observatory. Photographed upon the plates was a photometric scale by means of which it was possible to read off the intensities corresponding to various densities on the plate. Scale and spectrum were given the same treatment, except that the wedge was exposed to the light of an ordinary electric lamp, of effective wave-length near λ 4800. Since the K line has a wave-length of 3933 A, it is necessary to introduce corrections for change of contrast with change of wavelength. According to Ross, the value of gamma at K, as previously stated, is only about one-half of that which would apply to the wedge. As a check on this effect of contrast, I used a number of exposures of the wedge made with the same electric lamp and battery as were used for the spectrograms. These exposures, for which I am indebted to Dr. E. Pettit, were made, some without filter and others with a combination of Wood's U.V. filter with Corning heat-absorbing glass 124J, which has a maximum transmission at λ 3750. A comparison of the plates shows clearly less contrast for the exposures made through the screen, but the corrections are somewhat smaller than those derived from Ross's values of gamma. In view of this slight discordance, I have adopted averages from the corrections of Pettit and of Ross.

Intensities were determined with the microphotometer for eleven plates. Grouping these according to intensity and smoothing the results, I obtained the following approximate calibration for my estimates:

Estimate.....	0	1	2	3	4	5	6	7	8	9	10	11	12	13
Mag. diff.....	0.0	0.1	0.2	0.3	0.4	0.5	0.6	0.7	0.8	0.9	1.0	1.1	1.2	1.3

These values are somewhat smaller than those obtained from direct comparisons, but their order of magnitude is about the same. The relation between my arbitrary estimates and the magnitude difference is linear. One unit in the arbitrary scale corresponds to about 0.1 mag.

Regional effects.—Figure 1 represents the intensities of detached K lines, plotted on Aitoff's equal-area projection of the sphere.

Galactic co-ordinates as defined in *Harvard Annals*, **56**, were used. The average intensity of all individual estimates for every star was plotted according to its position in the sky. The total number of

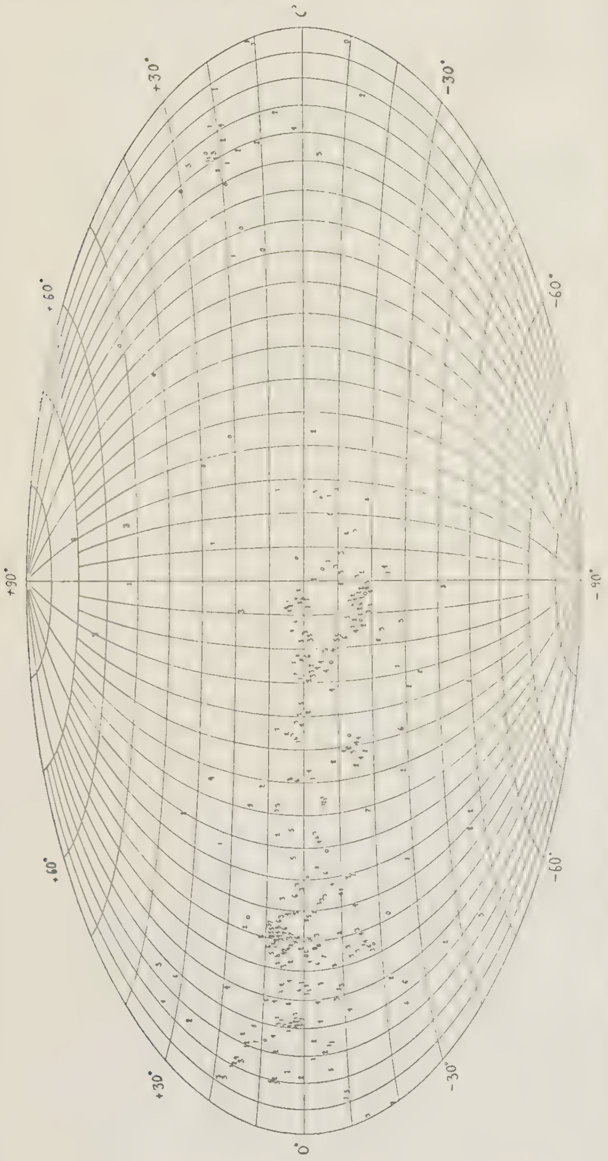

FIG. 1.—Distribution according to galactic co-ordinates of the intensities of the detached calcium line K in 321 stars of spectral types O–B3. Absence of K is denoted by 0; the strongest lines, corresponding to those of Vega, are called 10 = x.

stars is 321. Of these 155 were photographed at Yerkes, 131 at Victoria, 107 at Mount Wilson by various observers, 8 at the Lick Observatory, and 37 estimates were derived from my own plates taken at Mount Wilson with the 60-inch reflector.

The distribution of the stars along the Milky Way is not uniform. In a portion of the southern sky the estimates are completely lacking, while they are especially numerous in longitudes 70° and 170°. The first region falls in the constellation of Cepheus, while the second lies in Orion, where B and O stars are especially frequent.

The intensities of detached lines in these two regions show an unmistakable regional effect. In Cepheus strong lines are unusually numerous, while in Orion faint lines are the more abundant. For two circular areas of 8° radius, centered at galactic longitude 71°, latitude +3° for the Cepheus region and longitude 174°, latitude −14° for Orion, the intensities have the characteristics shown in Table III.

TABLE III

Intensities of Detached Lines in Cepheus and in Orion

	Cepheus	Orion
Number of stars	36	24
Mean intensity	5.1	2.2
Probable error of mean	± 0.15	± 0.06
Standard deviation	± 1.9	± 1.0
Range in intensity	0–15	0–6

The outstanding difference in mean intensity cannot be attributed to chance. Since the mean spectral type is the same for the two groups, B1, the effect cannot be due to differences in spectral type. The average apparent magnitude is 6.4 for the Cepheus region and 4.2 for Orion. The suspicion might therefore arise that the effect is one of distance, especially since such an effect actually exists for the mean of all stars. If, however, we use only the brightest stars in the Cepheus region, some 20 in number, the average intensity is even larger, which proves that in this case the effect is not due to greater distance. We are thus led to the conclusion that a certain portion of space—in the constellation Cepheus—favors the production of strong detached calcium lines, while another portion of space —in Orion—is more favorable for the production of weak lines.

Intensities of detached calcium lines as a function of distance.— Eddington was the first to suggest that the intensity of a detached line may be a function of distance.[1] Guided by this suggestion, I have attempted to find whether the estimates show such a relationship.

The number and the relative precision of trigonometric parallaxes for B and O stars are insufficient for an investigation of this kind. It was therefore necessary to use other criteria for distance, such as apparent magnitude. Accordingly, I have grouped all 321 stars according to brightness, as shown in Table IV.

TABLE IV

INTENSITY OF DETACHED K AS A FUNCTION OF APPARENT MAGNITUDE

Apparent Magnitude	Number of Stars	Mean Intensity of K
1.0–1.9	7	1.6
2.0–2.9	17	1.7
3.0–3.9	22	2.5
4.0–4.9	78	2.9
5.0–5.9	89	3.1
6.0–6.9	64	3.6
7.0–7.9	34	3.6
8.0–8.9	7	2.1
9.0–9.9	3	2.7

The mean intensity for all 321 stars is 3.03. The data, plotted in Figure 2, show a definite increase in intensity between magnitudes 1 and 7. For fainter stars the intensities are slightly smaller. In order to find whether the relationship is a consequence of systematic errors, I made separate tabulations for the different sets of plates; but the result remained essentially the same. Regional effects and those of spectral type were also looked into, without finding any evidence that would tend to discredit the results. Accordingly, we seem to be justified in assuming that the increase in intensity from magnitudes 1 to 7 is an essential property of detached calcium lines. The decline in intensity for magnitudes 8 and 9, although indicated by the figures in Table IV and supported by certain other evidence, should not be regarded as definitely established. It is based on a comparatively small number of stars, and may be influenced by regional effects. As we have seen, it is also possible that effects of under-exposure become sensible for stars fainter than magnitude 7.

---

[1] *Proceedings of the Royal Society of London*, A, **111**, 424, 1926.

At the suggestion of P. W. Merrill I have attempted to correlate intensity directly with distance. It is obvious that mixing stars of different absolute magnitudes increases the dispersion. To avoid this I computed the distances of the stars, in parsecs, from the formula

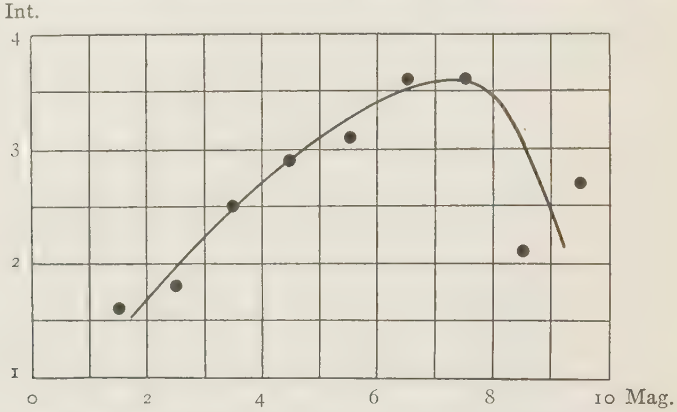

FIG. 2.—Intensity of the detached K line as function of apparent magnitude

$$\log D = \frac{m-M}{5} + 1 \ .$$

For the O Stars I used $M = -4.0$, which is the value found for them by J. S. Plaskett.[1] For the B stars I adopted the means of the values given by Adams and Joy:[2] B0, -3.1; B1, -2.5; B2, -1.8; B3, -1.2. The spectral types used were those given in the *Draper Catalogue*, except in a few cases where Mount Wilson determinations or my own estimates seemed to be more accurate. The average intensities, grouped according to distance, are shown in Table V.

The relation between intensity and distance is plain. The total range in intensity here is 2.5 units, while in Table IV it is 2.0 units.

---

[1] *Publications of the Dominion Astrophysical Observatory, Victoria*, **2**, 328, 1924.

[2] *Mt. Wilson Contr.*, No. 262; *Astrophysical Journal*, **57**, 294, 1923 (Table I).

In an earlier publication[1] I have suggested that the average intensity of detached lines may depend on spectral type, for the earlier spectral subdivisions exhibit somewhat stronger lines than the later ones. It appeared desirable, therefore, to investigate the run of intensities with apparent magnitude separately for each spectral subdivision. The O-type stars were so few in number that they were combined into one group. Subdivisions B0, B1, B2, and B3 were examined separately. Table VI gives the numerical results, and Figure 3, a graphical representation of intensity as a function of apparent magnitude.

TABLE V

INTENSITY OF DETACHED K AS A FUNCTION OF DISTANCE

Distance in Parsecs	No. of Stars	Intensity of K
0–100	22	2.1
100–200	101	2.2
200–300	62	3.1
300–400	47	3.3
400–600	30	4.2
600–800	26	4.6
800–3900	33	3.9

TABLE VI

INTENSITY OF K FOR DIFFERENT SPECTRAL TYPES

APP. MAG.	O		B0		B1		B2		B3	
	No.	Av. Int.	No.	Av. Int.	No.	Av. Int.	No.	Av. Int.	No.	Av. Int.
1.0–1.9	.....	.....	2	2.2	2	1.5	2	1.8	1	0.3
2.0–2.9	2	1.8	6	1.4	4	2.2	2	1.5	3	2.0
3.0–3.9	1	5.5	2	3.6	3	1.0	6	2.4	10	2.6
4.0–4.9	3	5.3	6	3.6	8	3.4	11	4.3	50	2.3
5.0–5.9	8	4.7	9	5.1	4	5.4	10	4.3	58	2.2
6.0–6.9	6	4.2	8	4.3	2	4.2	8	4.5	39	3.1
7.0–7.9	4	3.4	5	4.1	3	3.5	9	4.2	14	3.3
8.0–8.9	1	1.0	4	2.2	1	3.0	1	15.0	.....	.....
9.0–9.9	1	3.0	1	2.0	.....	.....	.....	.....	1	3.0

The curves in Figure 3 are based on very few stars, and it is therefore necessary to be cautious in their interpretation. In all five curves, however, the lowest intensities have a tendency to occur among the brightest apparent magnitudes. In all cases a maximum appears somewhere in the middle, followed by a small decline for the faintest stars. A progression in the maxima of the five curves from about magnitude 4 for type O to magnitude 7 for B3 seems also to be indicated. The inclined line in Figure 3 illustrates this progression. It is remarkable that this change in the position of maximum intensity corresponds almost exactly to the change in absolute magnitude. Indeed, if we read from the curves the points of maximum intensity and subtract the absolute magnitudes, we obtain:

---

[1] *Popular Astronomy*, **34**, 7, 1926.

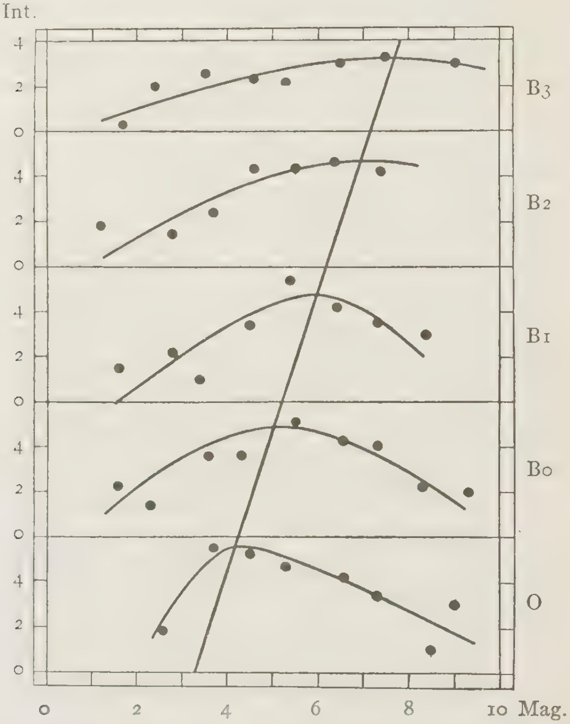

FIG. 3.—Intensity of detached K line as function of apparent magnitude, for separate spectral types. One star was omitted in type B2. The inclined straight line joins the maxima of the curves.

Spectral Type	
O	4.2+4.0=8.2
B0	5.0+3.1=8.1
B1	6.0+2.5=8.5
B2	6.7+1.8=8.5
B3	7.5+1.2=8.7
Mean	8.4

These values would indicate that for a star of absolute magnitude 0.0, maximum intensity occurs at apparent magnitude 8.4, which corresponds, roughly, to a distance of 500 parsecs. This result is in fair agreement with the general run of the intensities for all stars. It means that the detached calcium lines are very faint in the neighborhood of the sun, that they increase in intensity for regions farther away from us, and that the strongest lines are favored by a spherical shell at a distance of about 500 parsecs from the sun. Beyond this distance conditions may be less favorable for the production of strong detached lines. It is necessary, at this point, again to call attention to the small number of stars fainter than the seventh magnitude. It is possible, therefore, that the decline in intensity for distances greater than 500 parsecs is not real.

Nevertheless, it is interesting to note that the distance of 500 parsecs, where our figures indicate maximum intensity for the detached K line, corresponds closely to the dimensions of the local cluster of B stars, as outlined by Charlier and later by Shapley.[1] One feels tempted, therefore, to suggest that the regions most favorable for the production of strong detached lines of calcium lie near the outer boundaries of the local cluster of helium stars. The results of E. S. King[2] also lead to the assumption of an absorbing medium in the local cluster which produces reddening of the more distant stars. Since strong detached calcium lines seem frequently to be associated with positive color-excess, it seems possible that King's absorbing medium and the local cloud of calcium are identical.

---

[1] *Proceedings of the American Academy of Arts and Sciences*, **59**, 22, 1924; *Harvard Reprint*, No. 6. However, Professor B. Gerasimovič informs me that he has recently obtained for the size of the local system a value twice as large.

[2] *Popular Astronomy*, **34**, 557, 1926.

The progression of the maxima in Figure 3 seems to support the decline in intensity for distances greater than about 500 parsecs; but, in view of the possibility that effects of under-exposure become appreciable for faint stars, and also because of the small number of stars used, this result should be regarded as tentative. The gradual increase in mean intensity of detached K for distances up to 500 parsecs may, however, be regarded as certain.

O-type stars.—The results concerning the progression of the maxima in Figure 3 are based in part on the very asymmetric curve for O-type stars. It is for this same group of stars, however, that J. S. Plaskett found a large dispersion in absolute magnitude. More recent work by R. E. Wilson[1] tends to throw some doubt on the assumption that in O-type stars apparent magnitude is an indication of relative distance. His tables seem to indicate that the distance of all O stars is about the same, and that apparent magnitude is linearly correlated with luminosity. If this is correct, the curve for O stars cannot be interpreted as the result of varying distance, and the decline in intensity for the fainter stars, if real, must be attributed to a decline in luminosity.

Brightest stars.—In Table VII are listed all stars brighter than magnitude 3.0 for which the intensity of the detached K lines was estimated. Of these 24 stars only 3 have intensities that exceed 3.0—the mean for all 321 stars. The strongest line, 4.2, occurs in 44 ζ Persei. For 13 stars the intensities are between 0 and 2, which means that K was either absent entirely or was only suspected as a very faint line in the spectra of these stars.

Twenty-three of these stars are within 130 parsecs from the sun, and only one is at a distance as great as 250 parsecs. It seems, therefore, that the space around the sun out to 100 or 200 parsecs in all directions is not favorable for the production of strong detached lines of calcium.

Intensity and spectral type.—Grouping all the stars according to spectral type, but without respect to apparent magnitude, we find the mean intensities given in the third column of Table VIII.

With the exception of B2, the intensity declines smoothly toward the later types, agreeing well with preliminary results from

[1] *Astronomical Journal*, **36**, 1, 1924.

Yerkes plates.[1] Perhaps more representative are the maximum values from the five curves in Figure 3, which are given in the last column of Table VIII.

TABLE VII

List of 24 Brightest Stars

Star	α 1900	δ 1900	Mag.	Sp.	Distance in Parsecs	Int. of K
88 γ Pegasi	$0^{h}\ 8^{m}1$	+14° 38′	2.7	B2	80	2.0
27 γ Cassiop.	0 50.7	+60 11	2.0	B0p	100	0.0
44 ζ Persei	3 47.8	+31 35	2.9	B1	120	4.2
45 ε Persei	3 51.1	+39 43	2.7	B1	110	1.7
24 γ Orionis	5 19.8	+ 6 16	1.5	B2	45	3.5
34 δ Orionis	5 26.9	− 0 22	2.2	B0	110	2.2
44 ι Orionis	5 30.5	− 5 59	2.9	Oe5	240	2.0
46 ε Orionis	5 31.1	− 1 16	1.5	B0	83	3.0
123 ζ Tauri	5 31.7	+21 05	2.8	B3p	63	3.5
50 ζ Orionis br.	5 35.7	− 2 00	1.8	B0	95	1.5
53 κ Orionis	5 43.0	− 9 42	2.0	B0	100	2.0
2 β Can. Maj.	6 18.3	−17 54	1.8	B1	72	2.0
21 ε Can. Maj.	6 54.7	−28 50	1.4	B1	60	1.0
ζ Puppis	8 0.1	−39 43	2.3	Od	130	1.5
67 α Virginis	13 19.9	−10 38	1.0	B2	36	0.2
85 η Urs. Maj.	13 43.6	+49 49	1.7	B3	38	0.3
η Centauri	14 29.2	−41 43	2.5	B3p	55	0.5
6 π Scorpii	15 52.8	−25 50	2.8	B2	83	1.0
7 δ Scorpii	15 54.4	−22 20	2.3	B0	120	1.0
8 β Scorpii	15 59.6	−19 32	2.7	B1	110	1.3
20 σ Scorpii	16 15.1	−25 21	2.9	B1	120	1.5
23 τ Scorpii	16 29.7	−28 01	2.7	B0	140	2.0
13 ζ Ophiuchi	16 31.7	−10 22	2.5	B0	130	1.3
34 σ Sagittarii	18 49.1	−26 25	2.0	B3	43	2.0

TABLE VIII

Intensity of Detached K as a Function of Spectral Type

Sp. Type	No. of Stars	Average Intensity	Maximum Intensity from Fig. 3
O	26	4.05	5.5
B0	43	3.56	5.1
B1	27	3.17	5.4
B2	49	4.08	4.3
B3	175	2.53	3.3

The general character of the relation with spectral type is the same whether we consider maximum or mean intensity. The strongest lines occur in O-type stars and the weakest in subdivision B3. The decline per one-tenth of a spectral class from O to B2 is comparatively small, while from B2 to B3 it is very pronounced.

---

[1] *Popular Astronomy*, **34**, 7, 1926.

The dispersion in intensity within each spectral subdivision is considerable. Although there can be no doubt of the reality of progression with spectral type, it is evident that regional effects are the most powerful factors in determining the intensity of detached K. It is probably for this reason that the strongest individual lines do not occur in spectral type O. The four stars having the strongest detached lines known to me (intensity 9 or more) are given in Table IX.

The first star is of spectral type B0; the others are B2. The great intensity of the K line in H.D. 212455 at a distance of about 1000 parsecs might perhaps tend to shake the suggestion made above, that the lines grow fainter for distances greater than 500 parsecs. Too much weight should not be attached to this single star, however, particularly because of the regional effects, but also because of the uncertainty in spectral type. Mr. Joy suggests that the type is more nearly B3, which would reduce the distance to about 750 parsecs. Uncertainty in the adopted absolute magnitude of −1.2 may easily bring this value down to 500 parsecs.

TABLE IX

STARS WITH EXCEPTIONALLY STRONG DETACHED LINES

Star	α 1900	δ 1900	Mag.	Sp.	Dist.	Int.
9 Camelop.	$4^h 44^m.1$	+66° 10′	4.1	B0	270	9.3
62 χ^2 Orionis	5 58.1	20 08	4.5	B2p	180	13.0
9 Cephei	21 35.2	61 38	4.7	B2p	200	9.0
H.D. 212455	22 19.3	+54 47	8.2	B2	1000	15.0

The relation between spectral type and intensity can be interpreted only as a real effect of stellar radiation or temperature. It cannot be due to the greater average distance of the more luminous early-type stars, since the same relation exists for the maximum intensities of each spectral subdivision. As we have seen before, these maximum intensities refer in all cases to very nearly the same distance, 500 parsecs. We are justified, therefore, in assuming that the figures in the last column of Table VIII are free from any effects due to distance, and their progression with spectral type must be due to the stars themselves.

Calcium lines in later spectral subdivisions of spectral type B.—Eddington[1] has attached some importance to the spectroscopic binary 66 Eridani,[2] of type B9, which at maximum separation of the two components should show a stationary detached line. No such line having an intensity more than 0.2 mag. below the continuous spectrum has been observed on any of our plates, a result verified by means of tracings obtained with the thermoelectric photometer.

Other spectroscopic binaries of types B5–A0, with large orbital velocities, have been observed by J. S. Plaskett.[3] The K line was measured in most of these stars, but no such abnormality as the appearance of an undisplaced line was recorded. Some of these stars are faint eclipsing variables at distances of the order of 300 parsecs or more. These results support the view that the detached lines disappear rather abruptly at subdivision B3—another argument in favor of the idea that the radiation of the stars influences the intensity of detached lines.

In type B3, however, some stars (like 16 Lacertae[4]) have detached lines, while others (like π^5 Orionis[5]) have stellar lines only. Various observers have suspected that in some stars detached lines and stellar lines occur simultaneously. The most reliable cases of this nature are σ Aquilae[6] and H.R. 8803,[7] both of type B3.

In order to find whether detached and stellar lines may coexist in stars of spectral type B5, I obtained a number of spectrograms with the Bruce spectrograph of the binary 2 Lacertae, the orbit of which was worked out by R. H. Baker[8] without reference to the calcium lines. The semi-amplitude of the velocity variation is 80.3 km/sec. for the first component and 98.8 km/sec. for the other. On only one of my plates are the two components sufficiently separated, and on that plate the detached line is easily visible between the two stellar components. The spectral type, however, appears to be B3 rather than B5. *He* λ 4121 is appreciably stronger than *Si* II λ 4128 and λ 4131. *He* λ 4471 is about twice as strong as *Mg* λ 4481. According to the specifications of Joy,[1] such a star should be classified as B3.

---

[1] *Loc. cit.*

[2] E. B. Frost and O. Struve, *Astrophysical Journal*, **60**, 313, 1924.

[3] *Publications of the Dominion Astrophysical Observatory, Victoria*, **1**, 138, 141, 145, 1919; **2**, 142, 1922.

[4] O. Struve and N. Bobrovnikoff, *Astrophysical Journal*, **62**, 139, 1925.

[5] This results from Mr. Lee's original measures. See *Astrophysical Journal*, **64**, 20, 1926 (Remark 98).

[6] F. C. Jordan, *Publications of the Allegheny Observatory*, **3**, 189, 1916.

[7] S. L. Boothroyd, *Publications of the Dominion Astrophysical Observatory, Victoria*, **1**, 281, 1921.

[8] *Publications of the Allegheny Observatory*, **1**, 98, 1909.

The case of 2 Lacertae seems thus to prove that detached and stellar lines may coexist in stars of type B3. In later subdivisions, only stellar lines occur.

TABLE X

INTENSITY OF K AND GALACTIC LATITUDE

GAL. LAT.	O			B0			B1			B2			B3		
	Mag.	No.	Int.	Mag.	No.	Int.	Mag.	No.	Int.	Mag.	No.	Int.	Mag.	No.	Int.
± (0°–10°).........	5.8	18	4.3	6.0	27	3.6	5.0	15	4.1	5.7	30	5.3	5.1	94	2.6
(10 –20).........	4.5	8	3.4	3.5	13	3.9	2.9	8	2.1	3.7	11	2.5	4.8	48	2.5
(20 –30).........	....	....	....	2.0	2	1.0	3.3	3	1.0	3.3	3	1.3	4.5	21	2.3
(30 –40).........	....	....	....	....	....	....	....	....	....	6.0	1	4.0	5.1	7	2.7
(40 –50).........	....	....	....	....	....	....	4.0	1	3.0	2.0	1	2.0	5.0	3	1.7
(50 –60).........	....	....	....	3.0	1	3.0	....	....	....	1.5	2	0.5	5.0	1	1.0
(60 –70).........	....	....	....	....	....	....	....	....	....	....	....	....	2.3	2	1.5
± (70 –80).........	....	....	....	....	....	....	....	....	....	....	....	....	5.0	1	2.0

Intensity and galactic latitude.—In order to investigate effects of galactic concentration I have taken the mean intensities for belts of 10° width in galactic latitude. Table X shows the results for all stars subdivided according to spectral type.

To make the data more homogeneous I have applied corrections to the mean intensities which reduce them to the same apparent magnitude, 5.0. The corrections were taken from the smooth curve in Figure 2, the average apparent magnitudes being given in Table X. On account of the scantiness of the data it seemed desirable to combine the different spectral subdivisions. I reduced all intensities to subdivision B0 by applying the following corrections for spectral type: O, −0.2; B0, 0.0; B1, +0.4; B2, +1.0; B3, +1.7.

It should be noted that the corrections for magnitude and spectral type were derived from all stars, without respect to galactic latitude. But since nearly 85 per cent of our stars lie within 20° from the Milky Way, possible effects of galactic latitude upon the corrections can here be neglected.

---

[1] A. H. Joy, "Selected Physical Properties of Stars and Nebulae," *International Critical Tables*, 1, 384, 1926.

The final results, reduced to apparent magnitude 5.0 and to spectral type B0, are shown in Table XI.

The values indicate that the lines are strongest in a belt of 20° along the galactic circle and that they are somewhat fainter in high latitudes. This would correspond to a slight galactic concentration of the calcium clouds.

Since the inclination between the galactic plane and the central plane of the local cluster of helium stars is well marked in Figure 1, I have constructed another diagram, assuming the central plane to be inclined by 14°, the co-ordinates of the pole in the new system being α 11^h40^m, δ $+27°$. The effects due to galactic concentration remain essentially the same. Regional effects may influence these results. The Cepheus and Orion regions both fall within 20° of the galactic circle, and their effects will partially balance each other. The data are not sufficient to investigate the existence of other regions of abnormal intensity.

TABLE XI

INTENSITY AND GALACTIC LATITUDE FOR ALL STARS

Gal. Lat.	No.	Mean Intensity
±(0°–10°)..........	184	4.5
(10 –20)..........	88	3.9
(20 –30)..........	29	3.7
(30 –50)..........	13	4.2
±(50 –90)..........	7	3.4

Intensities of detached calcium lines in double stars.—If regional effects are the most important factors in defining the intensity of a detached line, we should expect that the components of physically connected double stars, observed separately, would show similar intensities. With this end in view I selected all stars earlier than B5 which are either known as double stars or may reasonably be supposed to be relatively near each other in space.

Table XII shows that the intensities of the components of double stars are practically identical. This holds for a range in intensity of from about 0 (for 50 ζ Orionis) to 6 (for λ and ϕ' Orionis). It will also be seen that neither a difference of 3.6 mag. in the brightness of the components nor a difference of 0.3 spectral class has the least influence upon the intensity of detached K. This probably means that in double stars the two components act as one body with respect to the calcium gas. In other words, absorption takes place within a sphere the radius of which is large compared with the distance of the two components. Obviously, this result does not permit discrimination between the hypotheses of Eddington and of Plaskett; but it fixes a lower limit for the distance at which the radiation of an early-type star can produce absorption of the detached type. In the case of the two components of λ Orionis, for example, the angular separation is nearly 5″. The distance of this star from the sun, computed from spectral type and spectroscopic absolute magnitude, is 250 parsecs. The separation of the two components is, accordingly, of the order of 1000 astronomical units. We

TABLE XII

INTENSITY OF DETACHED K IN DOUBLE STARS

Star	α 1900	δ 1900	Sp.	Mag.	Int.
H.D. 25638	$3^{h}59^{m}.1$	+62° 04′	B0	6.8	3
H.D. 25639	3 59.1	+62 04	B0	6.8	3
37 φ^1 Orionis	5 29.3	+ 9 25	B0	4.5	5
39 λ Orionis br.	5 29.6	+ 9 52	O8	3.7	6
39 λ Orionis ft.	5 29.6	+ 9 52	B1	5.3	6
θ^2 Orionis prec.	5 30.4	− 5 27	O	6.8	1
43 θ^2 Orionis	5 30.5	− 5 28	O8	5.2	2
41 θ^1 Orionis	5 30.4	− 5 27	O7	5.4	2
44 ι Orionis	5 30.5	− 5 59	O8	2.9	2
50 ζ Orionis br.	5 35.7	− 2 00	B0	2.0	1
50 ζ Orionis ft.	5 35.7	− 2 00	B0	4.0	0
8 β Scorpii br.	15 59.6	−19 32	B1	2.7	2
8 β Scorpii ft.	15 59.6	−19 32	B1	4.8	2
H.D. 170051	18 22.4	+26 23	B3	6.7	4
H.D. 170111	18 22.7	+26 23	B3	6.2	3

may tentatively assume that the effective reach of stellar radiation in producing detached absorption lines is at least ten times larger—of the order of 10,000 astronomical units, or one-twentieth of a parsec.

II. A CALCIUM CLOUD IN CEPHEUS

Radial velocities.—Table XIII gives the radial velocities separately for each plate for the 36 stars in the Cepheus region. The velocities from stellar and detached calcium lines are given in separate columns. The results are summarized in Table XIV, which, in addition to the mean velocities derived from the data in Table XIII, also gives the radial components of the solar motion computed from $\alpha = 270°$, $\delta = +30°$, $V = 20.0$ km/sec. No correction was made for a K-term. The ninth and tenth columns of Table XIV give the residual radial velocities for the stars and the calcium cloud. The eleventh indicates the intensity of the detached K line, as determined at Mount Wilson and Yerkes Observatories.

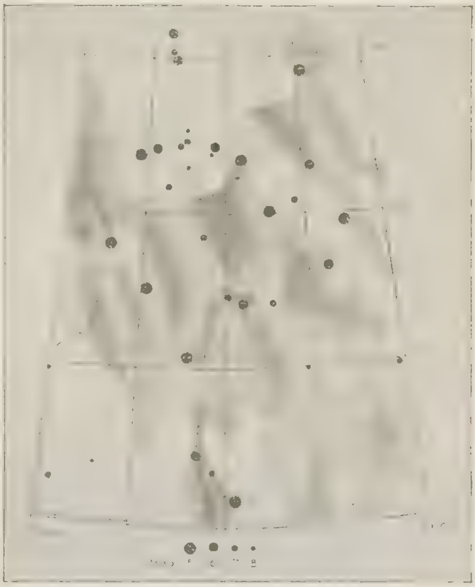

FIG. 4.—Map of region in Cepheus. The dots indicate the positions of all stars earlier than B5 which have been observed at Mount Wilson. The shaded areas indicate regions of obscuration of greater or less density. The broken lines show the two regions in which star counts have been made.

The number of spectrograms per star is admittedly too small to permit of a complete discussion. The probable error of one Yerkes plate is ±9 km/sec. The Mount Wilson plates were all measured twice, and their probable error is estimated to be about ±3 km/sec. In view of the scantiness of the material on velocities, nothing more than suggestions can be made concerning systematic motions.

TABLE XIII

RADIAL VELOCITIES OF 36 STARS IN CEPHEUS REGION

STAR	MEAS. BY	DATE	RADIAL VELOCITY		QUAL.	REMARKS
			Star	*Ca*		
H.D. 200857....	S	1926 June 29.260	− 35.4	....	v.p.	* Few, fair; *Ca* v. poor, faint
	S	1926 Sept. 15.209	− 31.2	−24.6	g	
Boss 5453.......	YO	1904 Apr. 15.906	− 14.8	− 2.7	v.g.	* Many v.g.; *Ca* fair
	YO	1904 Nov. 25.494	− 20.1	....	v p.	
	YO	1905 Apr. 7.931	− 14.7	....	v.p.	
	YO	1918 July 1.777	− 10.0	....	f	
	S	1926 June 28.299	− 7.4	− 8.0	g	
H.D. 203025....	MtW	....	− 17.2	−19.4	......	* Good; *Ca* v.g.; sp. triple; orbit: Sanford (*ASP*, **38**, 262, 1926)
H.D. 203374....	S	1921 Nov. 19.667	− 6.8	−25.3	g	* V. few; *Ca* fairly strong; hydrogen lines show emission in β and γ; Hδ and $H\epsilon$ are absent; *Mg* 4481 is indistinct; absence of $H\epsilon$ makes *Ca*H stand out very distinctly
	S	1926 June 28.338	+ 18.3	−14.1	g	
6 Cephei.......	YO	1905 May 8.854	− 14.9	....	p	* Few poor; *Ca* poor; sp. bin.
	YO	1924 Aug. 9.662	− 25.0	....	g	Bright lines give −9.2
	YO	1924 Aug. 11.680	− 41.1	....	g	Bright lines give +2.0
	S	1926 June 30.248	− 48.5	−37.0	g	
H.D. 204116....	S	1926 June 29.444	− 5.0	− 8.1	p	* Many fair; *Ca* weak; probably sp. bin.
	S	1926 Aug. 23.558	− 40.2	−23.8	g	
H.D. 204150....	S	1926 Aug. 23.199	− 36.7	− 8.4	g	* Few fair; *Ca* faint
β Cephei.......	YO	....	− 9.1	....	......	* Many v. g.; *Ca* absent or extremely faint; sp. bin.; velocity of system from many Yerkes plates
	S	1926 July 24.337	+ 12.0	....	......	
Boss 5535......	S	1914 Oct. 4.736	− 16.5	(− 1.6)	f	* Many fair; *Ca* fair
	MtW	1917 July 4.963	− 9.9	....	g	
	MtW	1917 Sept. 7.891	− 4.5	....	f	
	S	1926 June 30.267	− 18.0	−16.2	g	
H.D. 205196....	S	1926 June 30.322	− 20.4	(−81.6)	f	* Many good; *Ca* v. faint or absent
	S	1926 July 22.244	− 21.5	(−39.3)	g	
9 Cephei.......	YO	1909 Aug. 6.894	− 19.2	(− 0.7)	v.g	* Many good; *Ca* good
	YO	1909 Aug. 16.715	− 16.5	....	p	
	YO	1909 Sept. 10.657	− 17.2	....	p	
	YO	1909 Oct. 25.633	− 9.0	(+10.8)	g	
	S	1926 June 30.433	− 16.2	−21.9	g	
	S	1926 July 10.292	− 5.0	....	p	
	S	1926 July 16.131	− 8.6	−29.3	f	
	S	1926 July 23.384	− 12.9	−21.0	g	
Boss 5565.......	YO	1906 Sept. 24.676	− 24.1	....	p	* Few poor; *Ca* v.g.; sp. bin.; velocity of system, according to J. S. Plaskett, is −1.0 km/sec.; *Ca* gives −18.5 km/sec.
	S	1926 June 30.457	−113.6	−19.0	g	
H.D. 206327....	S	1926 Aug. 21.426	− 37.1	(−62.9)	g	* Many good; *Ca* faint

TABLE XIII—*Continued*

STAR	MEAS. BY	DATE	RADIAL VELOCITY		QUAL.	REMARKS
			Star	*Ca*		
80 π^2 Cygni.....	YO	1903 July 11.750	− 8.1	....	g	* Few fair; *Ca* fair; sp. bin.
	YO	1903 Aug. 8.710	− 7.4	....	f	
	YO	1903 Sept. 18.601	− 7.7	....	g	
	YO	1906 Sept. 10.707	− 17.6	....	g	
	YO	1911 Aug. 18.684	− 25.1	−25.6	v.g.	
	YO	1911 Aug. 28.658	− 31.2	−38.2	g	
H.D. 206773....	S	1921 Sept. 22.752	− 1.0	....	f	* Few v. poor; *Ca* v. faint and diffuse
	S	1924 June 10.965	− 3.6	−16.1	g	
	S	1926 June 28.404	− 40.7	− 9.4	g	
	S	1926 July 23.219	− 24.6	−26.0	g	
H.D. 207198....	S	1926 June 30.488	− 24.0	− 9.8	g	* Many good; *Ca* v.g.
H.D. 207308....	S	1926 July 22.367	− 25.8	−28.0	g	* Few v. poor; *Ca* v. broad
H.D. 207329....	S	1926 July 24.403	− 66.0	−21.6	f	* Few fair; *Ca* fair
H.D. 207538....	S	1926 July 23.457	− 12.6	−13.2	g	* Many good; *Ca* fair
	S	1926 Sept. 16.396	− 14.2	−26.4	g	
H.D. 207793....	S	1926 June 30.394	− 57.8	−16.4	g	* Few v. poor; *Ca* v.g.
H.D. 208095....	YO	1913 Aug. 1.752	+ 80.2	....	f	* Few fair; *Ca* absent; sp. bin.; sp. type B5
	YO	1924 Dec. 9.628	+ 1.1	....	g	
	YO	1924 Dec. 22.594	− 4.6	....	p	
	S	1926 July 23.169	− 33.6	....	g	
H.D. 208106....	S	1926 Aug. 23.397	− 23.7	−10.2	g	* Few poor; *Ca* good
H.D. 208185....	S	1926 Aug. 22.349	− 16.0	(−36.8)	f	* Many good; *Ca* poor
H.D. 208218....	S	1926 Aug. 22.156	− 22.1	− 9.4	g	* Many good; *Ca* v. faint
H.D. 208392....	S	1926 Aug. 22.484	− 14.2	− 8.8	g	* Few v. poor; *Ca* v.g.
	S	1926 Sept. 16.158	− 31.1	−12.2	g	
Boss 5642......	S	1922 Aug. 5.900	−113.5	(−22.7)	g	* Few poor; *Ca* v.g.; sp. bin.; on Aug. 5, 1922, a second component was measured at +49.2 km/sec.; mean velocity as measured by Plaskett, −16.5 km/sec. *Ca* −17.0 km/sec.
	MtW	1923 Aug. 18.812	+ 73.8	....	g	
	MtW	1923 Sept. 20.799	+ 12.4	....	g	
	MtW	1923 Oct. 22.640	+ 18.1	(−30.0)	g	
	MtW	1923 Nov. 20.696	− 27.0	(+ 8.0)	g	
	S	1926 July 22.455	− 21.2	− 7.6	g	
	S	1926 Sept. 15.123	− 28.8	− 9.0	g	
H.D. 208904....	S	1926 July 23.359	− 17.1	−20.7	g	* Few fair; *Ca* good but faint
H.D. 208905....	S	1926 Aug. 22.218	− 10.4	(+38.3)	g	* Few fair; *Ca* v. faint
H.D. 208947....	S	1926 July 23.275	− 17.6	−19.6	g	* Few fair; *Ca* good
H.D. 209339....	MtW	1912 Aug. 4.908	− 16.9	....	f	* Few fair; *Ca* good
	MtW	1912 Dec. 18.610	− 19.0	....	g	
	MtW	1913 Aug. 12.988	− 28.7	(−42.2)	g	
	S	1919 Aug. 16.848	− 4.3	−12.5	f	
	S	1926 July 24.490	− 23.4	− 7.6	f	
14 Cephei......	S	1922 June 16.765	+ 10.3	−12.9	v.g.	* Few v. poor; *Ca* v.g.
	S	1922 July 3.794	− 16.4	(−42.6)	f	
	S	1926 June 24.267	+ 22.9	....	p	
	S	1926 Aug. 8.385	+ 22.7	(− 5.6)	f	
H.D. 209961....	S	1926 Sept. 16.240	− 11.6	− 1.8	g	* Few good; *Ca* good; sp. bin.; velocity of system, according to R. K. Young, is −17.8 km/sec. *Ca*, +1.5 km/sec.

TABLE XIII—*Continued*

Star	Meas. By	Date	Radial Velocity		Qual.	Remarks
			Star	*Ca*		
19 Cephei......	YO	1913 June 27.869	− 15.0	....	g	* Many fair; *Ca* good; sp. bin.; Plaskett gives for radial velocity −10.9 km/sec. *Ca*, −12.8 km/sce.
	YO	1913 July 9.853	+ 7.6	....	p	
	YO	1913 Sept. 1.808	− 19.1	....	p	
	YO	1920 June 25.844	− 43.0	....	f	
	YO	1920 July 23.801	− 30.9	....	f	
	S	1923 Aug. 19.729	+ 13.1	− 5.2	g	
	S	1923 Aug. 19.729	+ 13.1	− 5.2	g	
H.D. 210809....	S	1926 Sept. 15.362	− 81.4	−20.7	g	* Many good; *Ca* good
λ Cephei.......	YO	1904 Oct. 28.606	− 51.1	....	g	* Few v. poor; *Ca* good; Plaskett gives for radial velocity −73.6 km/sec. *Ca*, −14.4 km/sec.
	YO	1904 Nov. 1.683	− 93.5	....	g	
	YO	1908 Aug. 24.733	− 62.3	....	g	
	YO	1918 Sept. 13.625	− 74.4	−12.1	f	
H.D. 212044....	S	1921 Nov. 20.663	− 3.1	−14.6	g	* Few poor; *Ca* good
	S	1924 July 17.970	+ 1.9	−14.0	g	
H.D. 212222....	S	1926 Sept. 16.300	− 24.6	−14.4	g	* Few good; *Ca* good
H.D. 212455....	S	1926 Aug. 23.427	− 54.7	−13.5	g	* Few poor; *Ca* v.g.

NOTE TO TABLE XIII

In the second column my own measures are indicated by the letter "S"; "MtW" denotes measures by various Mount Wilson observers, and "YO" stands for earlier Yerkes measures. The date is given in Greenwich Civil Time, except for plates taken before January 1, 1925, for which Greenwich Mean Time is given. The velocities from the calcium lines were not used in forming the mean velocity of the star. Measures which for any reason seemed to be unreliable are in parentheses and were not used in the discussion. Remarks in the last column concern the character of stellar (*) and calcium (*Ca*) lines.

The velocities of the stars in the Cepheus region do not exhibit any very striking systematic effects (Fig. 5). It is quite possible that some of these stars are in reality spectroscopic binaries. It need not surprise us, therefore, that the two stars H.D. 207329 and H.D. 207793 show large negative velocities. Remarks are added to Table XIII concerning a few stars, definitely known or suspected to be spectroscopic binaries.

The calcium velocities differ in many cases very considerably from the stellar velocities. In general, the residual velocities from the calcium lines are small. This supports Plaskett's earlier result that the calcium clouds have small velocities with respect to the stellar system. Between declinations +50° and +60°, negative values predominate, the mean residual velocity being −4.0 km/sec., with a probable error of ±0.8 km/sec. North of declination +60°, positive values are more frequent, while in the same region the stellar residual velocities are mostly negative.

Intensities of the detached K line in the Cepheus region.—The intensities plotted in Figure 7 show, as previously mentioned, that the calcium lines are unusually strong in practically the whole Cepheus region. This suggests at once that no direct relation can exist between calcium cloud and obscuring nebula. By grouping the stars into three classes, I find for 19 stars situated in regions where the stellar distribution is normal a mean intensity of 5.1 units; for 11 stars in obscured regions, a mean intensity of 4.8; and for 8 stars in regions where the obscuring nebulae are especially dense, a mean of

TABLE XIV

SUMMARY OF RADIAL VELOCITIES

STAR	α 1900	δ 1900	SP.	MAG.	RADIAL VEL.		SUN	VEL. RESIDUAL		INTENSITY
					Star	*Ca*		Star	*Ca*	
H.D. 200857	$21^{h}\ 1^{m}0$	+45°51′	B2	7.0	−33.3	−24.6	+15.0	−18.3	− 9.6	3
Boss 5453.......	21 9.3	+59 35	B2	5.5	−13.4	− 5.4	+14.5	+ 1.1	+ 9.1	5
H.D. 203025.....	21 14.6	+58 10	B3	6.2	−17.2	−19.4	+14.4	− 2.8	− 5.0	8
H.D. 203374.....	21 16.7	+61 25	Bop	6.4	+ 5.8	−19.7	+14.2	+20.0	− 5.5	6
6 Cephei........	21 17.3	+64 27	B3p	5.0	−32.4	−37.0	+13.8	−18.6	−23.2	2
H.D. 204116.....	21 21.4	+54 57	Bo	7.7	−22.6	−16.0	+14.3	− 8.3	− 1.7	2
H.D. 204150.....	21 21.6	+60 23	B3	7.4	−36.7	− 8.4	+14.1	−22.6	+ 5.7	2
β Cephei........	21 27.4	+70 7	B1	3.1	− 9.1	....	+13.0	+ 3.9	....	0
Boss 5535.......	21 28.3	+60 1	Bo	5.3	−12.2	−16.2	+14.0	+ 1.8	− 2.2	6
H.D. 205196.....	21 28.6	+57 4	Bo	7.1	−21.0	....	+14.0	− 7.0	....	4
9 Cephei........	21 35.2	+61 38	B2p	4.7	−13.1	−24.1	+13.7	+ 0.6	−10.4	9
Boss 5565.......	21 35.9	+57 2	Oe5	5.6	− 1.0	−19.0	+14.2	+13.2	− 4.8	7
H.D. 206327.....	21 36.3	+61 6	Oe5	8.5	−37.1	....	+13.7	−23.4	....	1
80 π^1 Cygni.....	21 38.6	+50 44	B3	4.6	−16.2	−31.9	+14.0	− 2.2	−17.9	4
H.D. 206773.....	21 39.3	+57 17	Bop	6.7	−17.5	−17.2	+13.6	− 3.9	− 3.6	4
H.D. 207198.....	21 42.2	+61 59	B2	5.8	−24.0	− 9.8	+13.4	−10.6	+ 3.6	8
H.D. 207308.....	21 42.9	+61 50	B2	7.7	−25.8	−28.0	+13.4	−12.4	−14.6	4
H.D. 207329.....	21 43.1	+51 39	B2	7.3	−66.0	−21.6	+13.9	−52.1	− 7.7	0
H.D. 207538.....	21 44.6	+59 14	B3	6.9	−13.4	−19.8	+13.3	− 0.1	− 6.5	2
H.D. 207793.....	21 46.5	+52 14	B2	6.4	−57.8	−16.4	+13.7	−44.1	− 2.7	6
H.D. 208095.....	21 48.8	+55 20	B5	5.4	+10.8	....	+13.5	+24.3	....	......
H.D. 208106.....	21 48.9	+61 27	B3	7.9	−23.7	−10.2	+13.3	−10.4	+ 3.1	7
H.D. 208185.....	21 49.5	+62 38	B3	7.5	−16.0	....	+13.1	− 2.9	....	4
H.D. 208218.....	21 49.7	+62 13	B1	6.5	−22.1	− 9.4	+13.1	− 9.0	+ 3.7	5
H.D. 208392.....	21 50.9	+62 8	B3	6.9	−22.6	−10.5	+13.0	− 9.6	+ 2.5	8
Boss 5642.......	21 52.9	+64 52	B2	5.7	−12.3	− 8.3	+12.7	+ 0.4	+ 4.4	5
H.D. 208904.....	21 54.3	+65 9	B3	7.4	−17.1	−20.7	+12.7	− 4.4	− 8.0	3
H.D. 208905.....	21 54.3	+60 49	B3	6.7	−10.4	....	+13.0	+ 2.6	....	3
H.D. 208947.....	21 54.7	+65 41	B3	6.1	−17.6	−19.6	+12.7	− 4.9	− 6.9	7
H.D. 209339.....	21 57.6	+62 0	Bo	6.2	−18.5	−10.0	+12.8	− 5.7	+ 2.8	6
14 Cephei.......	21 58.7	+57 31	Bo	5.3	+ 9.9	−12.9	+13.0	+22.9	+ 0.1	7
H.D. 209961.....	22 2.0	+47 45	B3	6.0	−17.8	− 1.8	+12.9	− 4.9	+11.1	7
19 Cephei.......	22 2.1	+61 48	Oe5	5.2	−14.6	− 5.2	+12.7	− 1.9	+ 7.9	7
H.D. 210809.....	22 7.9	+51 56	B2	7.5	−81.4	−20.7	+12.6	−68.8	− 8.1	8
λ Cephei........	22 8.1	+58 56	Od	5.2	−70.3	−12.1	+12.5	−57.8	+ 0.4	6
H.D. 212044.....	22 16.4	+51 21	B2p	6.9	− 0.6	−14.3	+12.4	+11.8	− 1.9	6
H.D. 212222.....	22 17.6	+41 36	B3	6.1	−24.6	−14.4	+12.2	−12.4	− 2.2	3
H.D. 212455.....	22 19.3	+54 44	B2	8.2	−54.7	−13.5	+12.2	−42.5	− 1.3	15

NOTE TO TABLE XIV

For four spectroscopic binaries with determined orbits I have given the velocity of the system, as shown in Table XIII. The other radial velocities are the means of the observations listed in Table XIII.

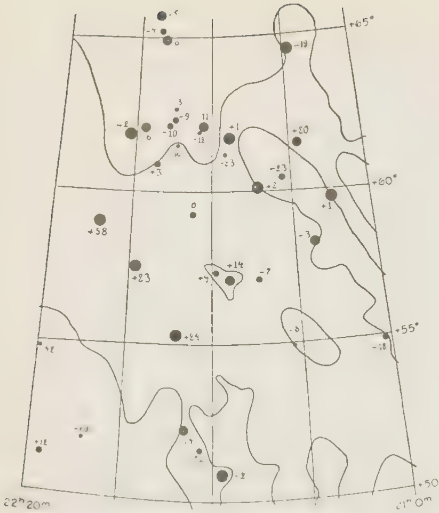

FIG. 5.—Map of region in Cepheus showing the residual radial velocities of stars of spectral type earlier than B5.

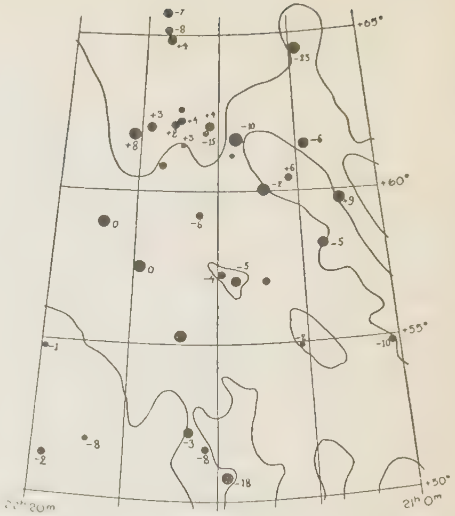

FIG. 6.—Map of region in Cepheus showing residual radial velocities from detached calcium lines.

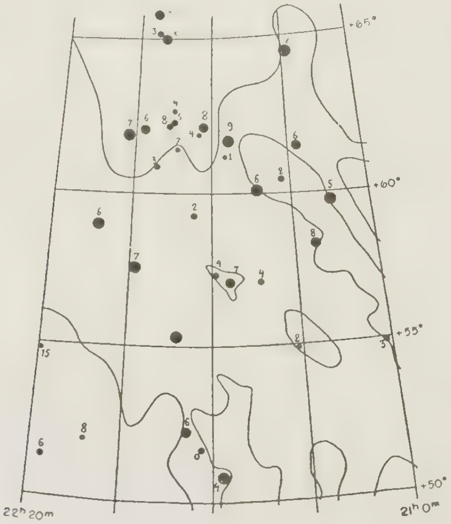

FIG. 7.—Map of region in Cepheus showing the intensities of detached calcium lines. One star was found to be of spectral type later than B3 and the corresponding intensity was omitted.

4.0. If there is any relationship at all, the obscured regions are correlated with relatively weak detached lines.[1]

Grouping the stars according to apparent magnitude makes it possible roughly to establish the distance at which the calcium lines appear particularly strong. Table XV gives the mean intensities.

The comparatively large value in the last line is due to H.D. 212455, which has an unusually strong K line (intensity 15). If this star were excluded, the last value would be 3.2. The lines appear to be strongest, on the average, for apparent magnitude 5, which corresponds to a distance of about 250 parsecs. The figures indicate a small decline in intensity for the fainter stars. In any case, we are justified in assuming that the calcium cloud in Cepheus begins at a distance of about 250 parsecs.

TABLE XV

INTENSITY AND APPARENT MAGNITUDE IN CEPHEUS REGION

App. Mag.	No. of Stars	Mean Int.
3–4	1	0.5
4–5	2	6.5
5–6	11	5.5
6–7	13	5.4
7–9	12	4.4

The obscuring nebula.—Although no very definite relation exists between the intensities of detached lines and the location of stars with respect to regions of obscuration, I have tried to estimate the distance of the dark nebula, for comparison with the distance found above for the calcium cloud.

For this purpose I have made star-counts in two regions; one of 16.5 square degrees is situated in the galactic star cloud around

---

[1] I have since made similar determinations for two other regions photographed by Professor F. E. Ross with long exposures. The results are as follows:

Region	Orion		Perseus	
	Av. Int.	No. Stars	Av. Int.	No. Stars
Normal	2.5	9	2.8	6
Obscured	2.2	3	....	....
Br. Nebula	2.2	17	3.2	7

α 22^h10^m, δ $+52°$, while the other, including 19.8 square degrees, lies in a region of obscuration, around α 21^h55^m, δ $+58°$ (see Fig. 4). The counts were made separately for each spectral type, with the aid of the *Draper Catalogue*. For counting stars fainter than the eighth magnitude, I obtained a number of plates with different exposure times, using a wide-angle 2-inch lens and the 10-inch Cooke photographic telescope of the Mount Wilson Observatory. The limiting magnitudes were determined from similar exposures on Selected Area 18, the photographic magnitudes of the comparison stars having been supplied by Mr. Seares, and independently checked by means of Harvard magnitudes.[1] Systematic differences between Mount Wilson and Harvard magnitudes can be neglected for the present purpose. On each plate I counted all stars down to the limiting magnitude, within the areas described. Table XVI gives the total number of stars per square degree brighter than each given magnitude, as counted from the *Draper Catalogue*.

TABLE XVI

NUMBER OF STARS PER SQUARE DEGREE DOWN TO EVERY GIVEN MAGNITUDE

APP. MAG.	O, B		A		F		G		K, M	
	I*	II*	I	II	I	II	I	II	I	II
1.5	......	......	......	......	......	......	......	......	......	......
2.5	......	......	......	......	......	......	......	......	......	......
3.5	......	......	......	......	......	......	......	......	......	......
4.5	......	......	......	......	......	......	......	......	......	......
5.5	......	0.15	......	0.05	......	0.05	......	......	......	0.05
6.5	0.12	.30	0.06	.10	......	.10	......	......	0.06	.05
7.5	.24	.50	0.24	0.40	......	.15	......	0.05	.06	.10
8.5	.71	.80	1.24	1.21	0.29	.45	......	.05	0.41	.25
9.5	.89	.85	3.30	1.97	.70	.65	0.18	.30	1.11	.60
10.5	.89	.85	3.48	1.97	.76	.65	.18	.50	1.34	.95
11.5	0.95	0.85	3.48	1.97	0.76	0.65	0.18	0.50	1.46	0.95

* Region I is situated in the galactic star cloud, while Region II lies in an area of obscuration.

For types O, B, and A the effect of obscuration begins to be noticeable at apparent magnitude 8, while for F stars it begins at magnitude 9. For the later types the effect lies below the limit for which the *Draper Catalogue* is complete. From the estimates made for types B, A, and F it appears that the distance of the nearer edge of the dark nebula is about 400 parsecs.

---

[1] *Annals of the Harvard College Observatory*, **101**, 1918.

From the star-counts made without respect to spectral type, I find numbers of stars (per square degree) brighter than each given apparent magnitude as shown in Table XVII.

The values of log B_m are plotted in Figure 8. For the star cloud my values agree fairly well with those of Seares, Van Rhijn, Joyner, and Richmond.[1] In the obscured region the number of bright stars is greater than normal. Table XVI shows that this is due almost entirely to the large number of B-type stars in this region. The effect of the cloud begins to be noticeable at about apparent magnitude 9.5 and reaches its full value at magnitude 11. Between magnitudes 11 and 15 the two curves run parallel, with a displacement of about 1 mag.

TABLE XVII

NUMBER OF STARS PER SQUARE DEGREE

App. Mag.	Region in Milky Way			Region of Obscuration			Method
	B_m	log B_m	Resid.*	B_m	log B_m	Resid.*	
5.5	0.00	−1.	+0.12	0.30	−0.52	+0.60	*H.D. Cat.*
6.3	0.18	−0.75	+ .01	0.35	−0.46	+ .30	2-inch
6.5	0.24	−0.62	+ .05	0.55	−0.26	+ .41	*H.D. Cat.*
7.4	0.24	−0.62	− .36	0.66	−0.18	+ .08	2-inch
7.5	0.54	−0.27	− .05	1.20	+0.08	+ .30	*H.D. Cat.*
8.3	0.70	−0.15	− .29	1.67	+0.22	+ .08	2-inch
8.5	2.65	+0.42	+ .19	2.71	+0.43	+ .20	*H.D. Cat.*
9.5	1.82	+0.26	− .41	3.70	+0.57	− .10	2-inch
10.6	14.1	+1.15	.00	8.3	+0.92	− .23	2-inch
12.0	64.5	+1.81	+ .07	27.5	+1.44	− .30	10-inch
12.3	110.	+2.04	+ .17	59.0	+1.77	− .10	2-inch
12.6	117.	+2.07	+ .07	65.8	+1.82	− .18	10-inch
13.7	210.	+2.32	− .13	95.4	+1.98	− .47	10-inch
14.8	514.	+2.71	− .17	260.	+2.42	− .46	10-inch
15.7	1110.	+3.05	−0.17	508.	+2.71	−0.51	10-inch

* The residuals give the differences between my values of log B_m and those of Seares, Van Rhijn, Joyner, and Richmond (*Mt. Wilson Contr.*, No. 301; *Astrophysical Journal*, 62, 362, 1925 [Table XVII]; gal. lat., 0°).

Assuming with Seares[2] that the mean parallax of stars of apparent magnitude 9.5 is about 0".003, I find the distance at which the obscuring nebula begins is 330 parsecs.

---

[1] *Mt. Wilson Contr.*, No. 301; *Astrophysical Journal*, 62, 362, 1925 (Table XVII).

[2] *Mt. Wilson Contr.*, No. 281; *Astrophysical Journal*, 60, 59, 1924.

A greater distance, of 500–600 parsecs, is obtained from a Russell diagram of stars belonging to the open cluster around Boss 5565 (α 21^h36^m, δ $+57°$). Lundmark[1] places this object at a distance of about 1000 parsecs. It is possible, however, that the magnitudes of the stars involved in the bright nebula are affected by obscuration.

In any case, it seems certain that the obscuring masses lie farther away than the beginning of the calcium cloud. The existence of strong detached lines in Boss 5565 and in other stars at distances of at least 500 parsecs suggests that the calcium cloud merges into the obscuring nebula.

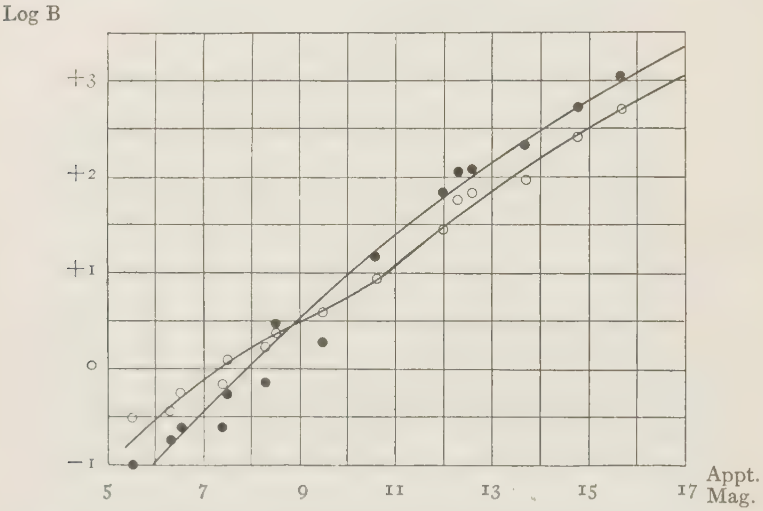

FIG. 8.—Logarithm of the number of stars brighter than apparent magnitude m in the galactic star cloud (dots) and in the region of obscuration (open circles).

Since the region of strong calcium lines also extends over portions of the Milky Way where the distribution of stars is normal, we conclude that the calcium cloud is transparent, except, of course, for monochromatic radiation.

It is perhaps significant that in Orion, as well as in Cepheus, the presence of nebulous matter seems to favor comparatively weak detached lines; the strongest lines occur in regions devoid of nebulous matter. In both cases the calcium cloud merges into the nebula, and in Orion it partly coincides in space with the nebula.

---

[1] *Meddelanden från Astronomiska Observatorium, Upsala,* No. 12, 1926; *Populär Astronomisk Tidskrift,* Häfte 1, 1926.

III. CONCLUSIONS

The results given in this paper support the hypothesis that detached lines originate in interstellar clouds of calcium matter. This is evidenced by the radial velocities from the detached lines, which have no relation to the velocities of the stars; also by the increase in intensity for the hottest stars, which is contrary to the expected behavior of stellar lines of ionized calcium. The existence of regional effects, as well as of effects due to distance, also supports this hypothesis.

The increase of intensity with distance was predicted by Eddington's hypothesis, and found to exist for distances up to 500 parsecs from the sun. Quantitatively, the observed increase in intensity depends upon the calibration of the arbitrary scale. The lines nearly double in strength for a doubling of the distance. This is in fair agreement with Eddington's deductions.

On the other hand, the decrease in intensity for distances greater than 600 parsecs, if real, would be contrary to Eddington's hypothesis. It will be interesting to obtain a larger amount of material for stars fainter than the seventh magnitude, which would settle this point definitely.

In favor of Eddington is the fact that the detached lines occur in the vast majority of stars of spectral type not later than B3. Table V shows that in the galactic plane interstellar calcium may be observed at distances of over 1000 parsecs. In galactic latitudes greater than 30° the calcium lines appear to be a little fainter. Spectroscopic parallaxes of the stars included in the last five lines of Table X show that in such directions interstellar calcium exists at distances of at least 150 parsecs. Since in the higher galactic latitudes B stars of distances greater than 150 parsecs are very infrequent, we have no information concerning the distribution of interstellar calcium beyond this distance. The possibility that the calcium clouds are distributed in an oblate spheroid is, therefore, not excluded.[1] Nevertheless, the existence of detached lines in stars situated far from the Milky Way and at distances of the order of over 150 parsecs suggests that the distribution of the calcium clouds in our stellar system differs essentially from the distribution of all other known types of nebulae.

---

[1] I am indebted for this suggestion to Professor F. H. Seares.

The sudden disappearance of the detached lines beyond spectral type B3 seems to me, however, to be fatal to Eddington's hypothesis in its present form. All the information available at present indicates that detached K does not exist in subdivisions later than B3. The sudden drop in intensity begins at about B2, and seems to show that stellar radiation is a factor in determining the intensity of detached K. Perhaps Eddington's hypothesis could be modified in such a way as to account for this effect.

On the other hand, my results are not contrary to the original hypothesis of Plaskett. If absorption occurs only in the vicinity of hot stars enveloped in calcium clouds, the effect of spectral type is at once explained. The effect of distance requires only that we assume a greater concentration of calcium clouds near the boundaries of the local cluster of helium stars. Under such conditions the probability of a star being enveloped in a dense cloud increases with distance. The same thing is probably true for dark and bright galactic nebulae, and therefore need not surprise us. Neither would it be surprising if the clouds should be less dense beyond the boundaries of the local cluster. Stars situated at distances greater than 600 parsecs would again have a small chance of being enveloped in a calcium cloud—and the mean intensity will thus be smaller. This hinges, of course, on the assumption that ionization and absorption are limited to a shell around the star and that all other intervening calcium masses are left in a state in which they do not appreciably absorb the light of the star.

Present observational material does not make it possible to accept definitely either hypothesis. It is therefore advisable to accept the effects due to distance, spectral type, region in the sky, etc., as properties of the calcium clouds without, at present, attempting to specify the physical explanation.

I am greatly indebted to Director W. S. Adams for his kindness in granting me the use of the 60-inch reflector and other instruments of the Mount Wilson Observatory. To him, as well as to Directors E. B. Frost, J. S. Plaskett, and R. G. Aitken, I am also indebted for generous permission to use earlier spectrograms taken by themselves or by their associates. Grateful acknowledgment is likewise made to members of the staff of the Mount Wilson Observatory for material and helpful suggestions relating to the investigation. The reductions were made in part by Miss M. Wiberg and Miss M. Fretz at Mount Wilson, and by Miss L. D. Cable and Madame L. Struve at the Yerkes Observatory. The investigation was carried out under a grant from the International Education Board of New York.

YERKES OBSERVATORY
January 1927

NOTE ADDED APRIL 14

Since this paper was written Miss Payne and Mr. Hogg at the Harvard College Observatory have undertaken the determination of the intensity of K on a spectrogram of Sirius taken at the Yerkes Observatory. Their value is about 0.6 mag., while my estimate would be about 8 units or 0.8 mag. Similarly, their value for Vega would be 0.75 mag., while I have used 1.0 mag. The differences are not large and are fully discussed by Miss Payne and Mr. Hogg (*Harvard College Observatory Circular*, No. 304, in press). The authors also discuss the difference in the results between slit spectrographs and objective-prism instruments, for narrow lines. For further details the reader is referred to the original publication. I have the impression that the order of magnitude of my estimates is correct, but it is possible that they should be reduced by something like 20 or 25 per cent. I am obliged to Miss Payne for having communicated to me her results in advance of publication.

175591

Contributions from the Mount Wilson Observatory, No. 332
Reprinted from the *Astrophysical Journal*, Vol. LXV, pp. 238–265, 1927
Printed in the U.S.A.

THE MOTIONS OF GIANT M STARS

By GUSTAF STRÖMBERG

ABSTRACT

The *velocities* of 278 giant M stars have been computed from the proper motions, radial velocities, and spectroscopic parallaxes, and projected on three fundamental axes, x, y, and z. The x-axis is the axis of preferential motion, and the y-axis is the axis of asymmetry; the z-axis is nearly perpendicular to the galactic plane. The velocities are referred to the sun as origin.

Formulae for computing the *effect of errors* in absolute magnitude, proper motion, and radial velocity upon the velocity distribution are derived (par. 3). These formulae are applicable to any form of continuous distribution function for the velocities, provided the errors are small.

The distribution of the *apparent velocity components* (i.e., computed without regard to errors) n_o, for intervals of 5 km/sec., is shown in Table I. The *computed* numbers n_c are derived by integration from analytical distribution functions for the true velocities, to the results of which the effect of the errors is added.

The *distribution* of the *x-components* (par. 4) is well represented by a normal error-curve. It has much larger dispersion than the distribution of the y- and *z-components*, but, nevertheless, shows *no trace* of Kapteyn's *two streams*. The true axis of preferential motion for these stars is *perpendicular* to the *axis of asymmetry*. The *distribution* of the *y-components* (par. 5) can be well represented by a function of the type: $A \exp[-a|y-c|-p(y-c)]$. The value for the *asymmetry constant*, $p=+0.0206$ sec./km, is in good agreement with that found for cosmical objects in general, as is also the value of the constant $c=-9.0$ km/sec. No trace of any *discontinuity* can be found in this distribution. The *distribution* of the *z-components* (par. 6) is represented by an error function with a large *positive excess*. Graphical representations of the apparent distribution curves and of the effects of errors are shown in Figs. 1, 2, and 3 by full-drawn curves. For comparison the diagrams also show the observed numbers of velocities within uniform intervals. The dotted curves are representations of the same data based upon distribution functions computed by the *method of moments*. This method gives a poor representation for the y- and z-components.

The *two-dimensional distribution* (par. 7) in the galactic plane can be well represented by a product of the distributions along the x- and y-axes. This representation is shown in Table II, where the upper figures are computed numbers and the lower figures observed numbers. No trace of any discontinuity is indicated; in particular, the high velocities are as well represented as the low velocities. A similar representation is possible for the velocities in the xz- and yz-planes, respectively, which indicates that the velocity components projected on the principal axes are independent of one another.

The velocity components for the "limiting center" are given in par. 8, and the sun's velocity relative to the group of stars studied in par. 9.

Some points in connection with the nature of the general asymmetry in stellar motions are discussed (par. 10); in particular, *the continuous nature of the asymmetry* is emphasized, in contradistinction to another representation of the same phenomenon advocated by Oort. The possible *physical nature* of the asymmetry as suggested by the writer, by Oort, and by Lindblad, is briefly discussed.

1. Different classes of stellar objects show differences both in group motion and velocity dispersion, and it is for this reason important to study the motions of homogeneous groups of objects. In

particular, it is of importance to study groups of objects which are not selected on any basis directly correlated with motion. Stars selected on the basis of large proper motion are often included in studies of radial velocities, and, since the dispersion in linear tangential motion and in radial velocity are correlated, the dispersion in the radial velocity is affected by the selection. The effect is even larger and more complicated when three-dimensional motions are studied. In the determination of the asymmetry in stellar motions it is of particular interest to study a homogeneous group of objects having comparatively large velocity dispersion, and the giant M stars seem to be particularly suited to this purpose.

2. In *Mount Wilson Contribution* No. 319,[1] Adams, Joy, and Humason have published absolute magnitudes of practically all known M stars brighter than apparent magnitude 6.0 and north of declination −30°. All of these stars are giants, and were selected on the basis of spectral type and apparent brightness alone. The writer has derived the reduction curves for these stars and also the probable errors in the absolute magnitudes.[2] A large number of the radial velocities have been determined at the Lick Observatory and the rest at the Mount Wilson Observatory. The three velocity components of these stars have been computed from the radial velocities, parallaxes, and proper motions, the latter being taken from Boss's *Catalogue*. The result of this study is given in the following pages.

The formulae used for computing space velocities have been published in *Contribution* No. 245.[3] The absolute magnitudes were taken without any correction from *Contribution* No. 319. The proper motions have been corrected for the systematic errors in right ascension as given in Boss's *Catalogue*, page xxviii. To the proper motions in declination, H. Raymond's[4] corrections were applied. One of the principal objects being to study the asymmetry in the velocity distribution, the velocities were projected on three axes, one of which was parallel to the asymmetry axis as determined in *Contribution* No. 293,[5] while the others were in a plane perpendicular to this axis with the x-axis in the galactic plane. The right ascension and declination (α, δ), and the galactic longitude and latitude (l, b), of the three axes are:

---

[1] *Astrophysical Journal*, **64**, 225, 1926.

[2] *Mt. Wilson Contr.*, No. 327; *Astrophysical Journal*, **65**, 108, 1927.

[3] *Astrophysical Journal*, **56**, 265, 1922.

[4] *Astronomical Journal*, **36**, 129, 1926.

[5] *Astrophysical Journal*, **61**, 379, 1925.

Axis	α	δ	l	b
x..........	265°7	−24°9	331°5	0°0
y..........	309.8	+57.1	61.5	+ 9.0
z..........	185.4	+20.0	241.5	+81.0

The y-axis is the axis of asymmetry; the x-axis is nearly parallel to the direction of stream motion; and the z-axis is nearly perpendicular to the galactic plane. The longitudes and latitudes are referred to the standard galaxy, the pole of which has the co-ordinates $\alpha = 190°$, $\delta = +28°$.

3. The computed velocities are affected by errors in the absolute magnitudes, proper motions, and radial velocities. The effect of errors in the absolute magnitudes has been studied by J. H. Oort[1] on the assumption that the true velocity distribution is a normal error function. In the present case we need expressions for the effect of all three classes of errors, without making any particular assumption as to the form of the true frequency function of the velocities; and we also need expressions for the effect of errors integrated over arbitrary intervals.

We will assume that the errors Δ in the adopted absolute magnitudes M are distributed according to a normal error-curve around a zero value. The same will be assumed for the errors ϵ and ν in the proper-motion components μ and the radial velocities V. Denoting true values by subscripts, we have

$$M_1 = M + \Delta \; ; \qquad \mu_1 = \mu + \epsilon \; ; \qquad V_1 = V + \nu \; . \tag{1}$$

For the parallaxes p we have

$$\left. \begin{aligned} p_1 &= p10^{0.2\Delta} = pe^{q\Delta} \\ q &= \frac{0.2}{\text{Mod}} = 0.4605 \; . \end{aligned} \right\} \tag{2}$$

---

[1] *Groningen Publications*, No. 40, p. 17, 1926.

Projecting the proper motions upon an arbitrary axis x perpendicular to the line of sight, we have for the linear motion along this axis the expression

$$x_1 = \frac{k\mu_1}{p_1} = \frac{k(\mu+\epsilon)}{p} e^{-q\Delta} = (x+\epsilon')e^{-q\Delta} \,, \tag{3}$$

where $k = 4.738$ km×year/sec., and ϵ' is the error in the proper-motion component converted into km/sec. The distribution function of the errors Δ and ϵ are supposed to have the moduli h and h_1. Let $F_1(x_1)$ be the frequency function of the true velocities projected on a certain axis. The frequency function $F(x)$ of the apparent tangential velocity components (i.e., computed without regard to the effect of errors) is then found from the equation

$$F(x)dx = \frac{h\,h_1}{\pi} \iint_{\Delta,\,\epsilon=-\infty}^{+\infty} F_1(x_1) e^{-h^2\Delta^2 - h_1^2\epsilon^2} d\Delta\, d\epsilon\, dx_1 \,, \tag{4}$$

where x_1 has the value given in equation (3). We have

$$d\Delta\, d\epsilon\, dx_1 = e^{-q\Delta} d\Delta\, d\epsilon\, dx \,.$$

Putting

$$h\Delta = z$$

and

$$\frac{q}{2h} = \beta \,,$$

we find

$$F(x)dx = \frac{dx\, h_1}{\pi} e^{\beta^2} \iint_{-\infty}^{+\infty} e^{-(z+\beta)^2 - h_1^2\epsilon^2} F_1[(x+\epsilon')e^{-2\beta z}] dz\, d\epsilon \,. \tag{5}$$

As will appear later, the quantities β and ϵ', the latter being expressed in units equal to the dispersion in x, are small quantities, and we can develop the function F_1 under the integration sign in a power series, limiting ourselves to quantities of the second order in β and ϵ'. We derive thus

$$\left.\begin{aligned} F_1[(x+\epsilon')e^{-2\beta z}] = F_1(x) &+ \epsilon'\frac{dF_1}{dx_1} - 2\beta z x\frac{dF_1}{dx_1} + \frac{\epsilon'^2}{2}\frac{d^2F_1}{dx_1^2} - 2\beta\epsilon' z\frac{dF_1}{dx_1} \\ &- 2\beta z\epsilon' x\frac{d^2F_1}{dx_1} + 2\beta^2 z^2\left[x^2\frac{d^2F_1}{dx_1^2} + x\frac{dF_1}{dx_1}\right] . \end{aligned}\right\} \tag{6}$$

From equation (5) we now find

$$F(x)=F_1(x)+\beta^2\left[F_1(x)+3x\frac{dF_1}{dx_1}+x^2\frac{d^2F_1}{dx_1^2}\right]+\frac{k^2\overline{\epsilon^2}}{2\overline{p_1^2}}\frac{d^2F_1}{dx_1^2}\,. \qquad (7)$$

The quantity β is connected with the dispersion r in the absolute magnitudes by the equation

$$\beta=\frac{qr}{\sqrt{2}}\,.$$

For the particular case that $F_1(x)$ is a normal error function and $\overline{\epsilon^2}=0$, we may derive Oort's expression from equation (7).

The effect of the errors ν in the radial velocities can be found in exactly the same way as in the case of ϵ'. If we assume that the dispersion in the errors is small as compared with that in the velocities, we find the effect of these errors to be

$$E'(x)dx=\frac{\overline{\nu^2}}{2}\frac{d^2F_1}{dx_1^2}\,. \qquad (8)$$

The errors in the velocities projected on a fixed axis x are the combined effect of errors in tangential and radial motions. For a uniform distribution of the stars over the sky, or over one hemisphere, we can find the total effect by multiplying equations (7) and (8) by 2:3 and 1:3, respectively. The total effect of the errors in absolute magnitude, proper motion, and radial velocity is thus

$$\left.\begin{aligned}E(x)dx=\left[\alpha\left\{F_1(x)+3x\frac{dF_1}{dx_1}+x^2\frac{d^2F_1}{dx_1^2}\right\}+\frac{T^2}{2}\frac{d^2F_1}{dx_1^2}\right]dx\\ \alpha=\frac{q^2r^2}{3}\,;\quad T^2=\frac{2}{3}\frac{k^2\epsilon^2}{\overline{p_1^2}}+\frac{\overline{\nu^2}}{3}\,.\end{aligned}\right\} \qquad (9)$$

In this equation we may replace $\overline{p_1^2}$ by the mean of the squares of the assumed parallaxes. The velocities x must here be referred to the sun as origin.

The function $F(x)dx=F_1(x)dx+E(x)dx$ can be integrated over finite intervals and compared with the observed distribution. Such expressions will later be derived for three types of distribution functions. In the case of a normal error-curve the last term in the expression for $E(x)$ in equation (9) may be dropped and replaced by an increase in the square of the dispersion by an amount equal to T^2. Although this rule is also applicable to more complex forms of distribution functions, the dispersion will not in these cases be used as one of the constants of the distribution law.

The value used for the mean error r in the absolute magnitudes is ± 0.75, based upon a probable error ± 0.5 derived in *Contribution* No. 327. This may be regarded as a mean value for the giants and supergiants. We have thus $\alpha = 0.0398$. The mean error in the proper-motion components has been assumed to be $\pm 0''.005$, and that in the radial velocities ± 3.0 km/sec. The value found for the square root of $\overline{p^2}$ is $0''.0071$. We have thus $T = 3.22$ km/sec., which is small compared to the dispersion in velocity; the expansion is consequently valid.

4. A total number of 278 stars was studied. No difference could be found in the motions of the giants and supergiants, and they were consequently studied together.

The distribution of the velocities projected on the x-axis showed, when plotted, a great resemblance to a normal error-curve. The apparent distribution was first represented with the aid of the method of moments. This method has been developed and extensively used by Charlier and his co-workers at the Lund Observatory. Analytically it is very beautiful, but has the disadvantage of giving stars of high velocity much higher weight than those of the smaller velocities. Although the distribution function represents the moments exactly, it does not follow that it is the best representation for the actual distribution which can be obtained with the same number of parameters. The formulae used in this method are given below.

The distribution is represented by the function

$$\left. F(\xi) = \phi + \beta_3 \frac{d^3\phi}{d\xi^3} + \beta_4 \frac{d^4\phi}{d\xi^4}\,, \qquad \phi = \frac{1}{\sqrt{2\pi}} e^{-\xi^2/2}\,, \qquad \xi = \frac{x-c}{\sigma} \right\} \qquad (10)$$

The dispersion is here represented by σ and the mean by c. It is customary to limit one's self to moments of the fourth order. Denoting the moments of order n by v_n, the moments are defined by the expression

$$v_n = \sigma^n \int_{-\infty}^{+\infty} \xi^n F(\xi) d\xi\ ,$$

which is the analytical expression for the mean of the nth power of the differences $x-c$. In the numerical computation of the moments, we use the expression

$$v_n=\overline{(x-c)^n}\ .$$

It is obvious that the moments of high order are extremely uncertain, being greatly affected by a few large values. The coefficients β_3 and β_4 represent the skewness and the excess of the distribution, respectively, and are connected with the moments of third and fourth order by the expressions

$$\beta_3=-\frac{v_3}{6\sigma^3}\ ;\qquad \beta_4=\frac{1}{24}\left(\frac{v_4}{\sigma^4}-3\right)\ . \tag{11}$$

The skewness S and the excess E are defined by the equations

$$S=3\beta_3\ ;\qquad E=3\beta_4\ . \tag{12}$$

Tables for $\phi(\xi)$, $d^3\phi/d\xi^3$, and $d^4\phi/d\xi^4$ have been published by C. V. L. Charlier,[1] which greatly facilitate the computation of the distribution from the constants.

For the distribution of the apparent velocities projected on the x-axis, I find from the moments

$$\left.\begin{array}{ll} c=-\ \ 9.19\text{ km/sec.} & S=+0.028 \\ \sigma=\ \ 31.34\text{ km/sec.} & E=+0.202 \end{array}\right\} \tag{13}$$

Figure 1 shows the frequency curve based on these constants as a dotted curve, together with the observed numbers of velocities in intervals of 5 km/sec. The representation by the use of moments is in this case very good.

Since the positive excess thus found might possibly be entirely due to the errors in the velocities, an attempt was made to represent the true distribution by a normal error-curve. For this the constants were determined from the distribution itself according to a method similar to that used in *Contribution* No. 245,[2] which involves the determination of approximate values of the constants, subsequently corrected by means of the differences between computed and observed numbers of velocities between different limits. The intervals, ten in number, were so chosen that they included approximately equal numbers of velocities, the equations of condition then being given equal weights.

---

[1] *Vorlesungen über die Grundzüge der Mathematischen Statistik.* Lund, Verlag Scientia, 1920.

[2] *Astrophysical Journal*, **56**, 265, 1922.

The assumed frequency function for the apparent velocities is

$$F(x)dx=\frac{Nh}{\sqrt{\pi}}e^{-h^2(x-c)^2}dx+E(x)dx\ , \tag{14}$$

where N is the number of stars and $E(x)$ has the value given in equation (9).

Integrating between the limits x_1 and x_2, we find

$$\left.\begin{array}{ll}
n_c=\int_{x_1}^{x_2}F(x)dx=\frac{N\Theta}{2}+\frac{N}{\sqrt{\pi}}[b_0\psi_0+b_1\psi_1+b_2\psi_2+b_3\psi_3] & \\
\Theta=\frac{2}{\sqrt{\pi}}\int_{t_1}^{t_2}e^{-t^2}dt\ ;\quad t_1=h(x_1-c)\ ;\quad t_2=h(x_2-c) & \\
\psi_n=t_1^n e^{-t_1^2}-t_2^n e^{-t_2^2} & \\
b_0=-a\,hc\ ; & b_2=4a\,hc \\
b_1=a(-1+2h^2c^2)+T^2h^2\ ; & b_3=2a
\end{array}\right\} \tag{15}$$

The expressions for the derivatives are

$$\frac{dn_c}{dh}=-\frac{N}{h\sqrt{\pi}}\psi_1\ ;\qquad \frac{dn_c}{dc}=\frac{Nh}{\sqrt{\pi}}\psi_0\ , \tag{16}$$

and the equations of condition for the correction of the constants are

$$\Delta h\frac{dn_c}{dh}+\Delta c\frac{dn_c}{dc}=n_0-n_c\ ,$$

where n_0 and n_c are the observed and computed numbers of velocities, respectively, lying between the limits x_1 and x_2.

The following values and probable errors for the mean c and the dispersion σ for the true velocity distribution were thus derived:

$$\left.\begin{array}{r}
c=-8.78\pm0.68\ \text{km/sec.} \\
\sigma=\frac{1}{\sqrt{2h}}=\ 27.58\pm0.55\ \text{km/sec.}
\end{array}\right\} \tag{17}$$

TABLE I

VELOCITY KM/SEC.	x−AXIS					y−AXIS					z−AXIS				
	$\int F_1(x)dx$	$\int E(x)dx$	n_c	n_o	O−C	$\int F_1(y)dy$	$\int E(y)dy$	n_c	n_o	O−C	$\int F_1(z)dz$	$\int E(z)dz$	n_c	n_o	O−C
−∞															
−110	0.03	+0.29	0.32	1	+0.7	1.16	+1.13	2.29	0	−2.3	0.00	0.00	0.00	0	0.0
−105	0.04	+0.19	0.23	0	−0.2	0.33	+0.18	0.51	0	−0.5					
−100	0.06	+0.27	0.33	1	+0.7	0.42	+0.20	0.62	1.5	+0.9					
−95	0.13	+0.38	0.51	0	−0.5	0.56	+0.23	0.79	1.5	+0.7				1	+1.0
−90	0.19	+0.52	0.71	1	+0.3	0.68	+0.23	0.91	0	−0.9				0	0.0
−85	0.35	+0.63	0.98	1	0.0	0.88	+0.25	1.13	0	−1.1				0	0.0
−80	0.57	+0.74	1.31	2	+0.7	1.13	+0.25	1.38	1.5	+0.1				0.5	+0.5
−75	0.92	+0.79	1.71	1	−0.7	1.46	+0.27	1.73	1	−0.7				0.5	+0.5
−70	1.39	+0.74	2.13	3	+0.9	1.86	+0.25	2.11	1.5	−0.6				0	0.0
−65	2.10	+0.59	2.69	3	+0.3	2.38	+0.24	2.62	3	+0.4		+0.01	0.01	1	+1.0
−60	3.03	+0.31	3.34	2	−1.3	3.06	+0.19	3.25	4	+0.8		+0.04	0.04	0	0.0
−55	4.24	−0.08	4.16	3.5	−0.7	3.91	+0.15	4.06	4.5	+0.4	0.02	+0.19	0.21	1	+0.8
−50	5.73	−0.53	5.20	4.5	−0.7	5.00	+0.04	5.04	3.5	−1.5	0.07	+0.59	0.66	0.5	−0.2
−45	7.52	−0.95	6.57	7	+0.4	6.42	−0.04	6.38	7	+0.6	0.33	+1.26	1.59	2.5	+0.9
−40	9.54	−1.28	8.26	8	−0.3	8.21	−0.22	7.99	8.5	+0.5	1.21	+2.32	3.53	1.5	−2.0
−35	11.68	−1.42	10.26	11	+0.7	10.52	−0.32	10.20	10	−0.2	2.49	+0.77	3.26	3	−0.3
−30	13.89	−1.34	12.55	14	+1.4	13.47	−0.49	12.98	16.5	+3.5	5.56	−0.39	5.17	4.5	−0.7
−25	15.96	−1.05	14.91	14.5	−0.4	17.25	−0.62	16.63	17	+0.4	9.51	−1.70	7.81	5.5	−2.3
−20	17.75	−0.60	17.15	15	−2.2	22.10	−0.68	21.42	25.5	+4.1	14.04	−1.29	12.75	14	+1.2
−15	19.10	−0.09	19.01	19	0.0	28.31	−0.58	27.73	28.5	+0.8	19.40	−0.52	18.88	18	−0.9
−10	19.90	+0.34	20.24	17.5	−2.7	36.27	−0.21	36.06	30	−6.1	26.41	−0.80	25.61	21	−4.6
−5	20.06	+0.62	20.68	22	+1.3	37.25	(+2.52)	(39.77)	40	(+0.2)	34.00	−0.84	33.16	42.5	+9.3
0	19.57	+0.69	20.26	23	+2.7	24.05	(+5.39)	(29.44)	26.5	(−2.9)	38.28	−0.15	38.13	38	−0.1

TABLE I—*Continued*

Velocity km/sec.	x—Axis					y—Axis					z—Axis				
	$\int F_1(x)dx$	$\int E(x)dx$	n_c	n_o	O−C	$\int F_1(y)dy$	$\int E(y)dy$	n_c	n_o	O−C	$\int F_1(z)dz$	$\int E(z)dz$	n_c	n_o	O−C
0															
+ 5	18.47	+0.54	19.01	18.5	−0.5	15.28	+0.91	16.19	14.5	−1.7	36.17	−0.03	36.14	29.5	−6.6
+ 10	16.87	+0.24	17.11	21	+3.9	9.71	+0.21	9.92	15.5	+5.6	29.23	−0.30	28.93	29.5	+0.6
+ 15	14.91	−0.12	14.79	13	−1.8	6.18	0.00	6.18	4.5	−1.7	21.73	−0.27	21.46	23.5	+2.0
+ 20	12.77	−0.44	12.33	14	+1.7	3.91	−0.02	3.89	4	+0.1	15.82	−0.75	15.07	17.5	+2.4
+ 25	10.58	−0.64	9.94	8.5	−1.4	2.52	+0.01	2.53	1.5	−1.0	11.09	−1.50	9.59	9	−0.6
+ 30	8.47	−0.70	7.77	5	−2.8	1.56	+0.05	1.61	3.5	+1.9	6.90	−0.99	5.91	4.5	−1.4
+ 35	6.57	−0.61	5.96	3.5	−2.5	1.01	+0.07	1.08	1	−0.1	3.57	+0.53	4.10	6.5	+2.4
+ 40	4.93	−0.42	4.51	6.5	+2.0	0.64	+0.09	0.73	0	−0.7	1.50	+1.44	2.94	0	−2.9
+ 45	3.57	−0.19	3.38	4	+0.6	0.40	+0.08	0.48	0	−0.5	0.49	+1.28	1.77	1	−0.8
+ 50	2.52	+0.04	2.56	2	−0.6	0.26	+0.08	0.34	0	−0.3	0.14	+0.71	0.85	1	+0.2
+ 55	1.71	+0.22	1.93	1.5	−0.4	0.17	+0.08	0.25	1.5	+1.2	0.03	+0.28	0.31	0	−0.3
+ 60	1.14	+0.34	1.48	2	+0.5	0.10	+0.05	0.15	0.5	+0.4	0.00	+0.06	0.06	1	+0.9
+ 65	0.71	+0.38	1.09	1.5	+0.4	0.07	+0.05	0.12	0	−0.1	0.00	+0.02	0.02	0	0.0
+ 70	0.44	+0.37	0.81	0	−0.8	0.03	+0.02	0.05	0	0.0		0.00	0.00	0	0.0
+ 75	0.26	+0.34	0.60	1	+0.4	0.03	+0.03	0.06	0	−0.1					
+ 80	0.15	+0.27	0.42	0	−0.4	0.02	+0.02	0.04	0	0.0					
+ 85	0.08	+0.20	0.28	1	+0.7	0.01	+0.02	0.03	0	0.0					
+ 90	0.06	+0.16	0.22	0	−0.2	0.02	+0.04	0.06	0	−0.1					
+ 95	0.01	+0.10	0.11	0	−0.1										
+100	0.01	+0.06	0.07	0	−0.1										
+ ∞	0.01	+0.09	0.10	1	+0.9										

The apparent distribution, that is, the true distribution plus the effect of the errors, is shown as a continuous curve in Figure 1. The effect of the errors is shown as another continuous curve near the axis of the abscissae. The numerical values are given in Table I.

The representation of the observed data is perfectly satisfactory, and no excess is now found for the true distribution. In fact, the excess for the true distribution was actually computed by a method explained later in connection with the z-components, and, as measured by the quantity γ_4, was found to be $+0.002 \pm 0.044$, which means that no excess is present after the distribution has been corrected for the effect of errors of observation.

An attempt was also made to determine the mean error in the absolute magnitudes by assuming that the true distribution is a normal error function. The result is $r = \pm 0.75 \pm 0.28$, in exact agreement with the adopted value, but with a fairly large uncertainty.

The x-axis is nearly in the direction of preferential motion as ordinarily given. Thus the direction of the latter as found by A. S. Eddington[1] from the proper motions of the Boss stars analyzed on the basis of the two-stream theory is toward galactic longitude 347°, whereas the x-axis has a longitude of 332°, both axes having zero galactic latitudes. From Eddington's data, I have computed the position of the centers of the two streams in the frequency curve and found that the first stream has its center at the point -15.7 km/sec. and the second stream at $+23.5$ km/sec. Allowing for the slight inclination between the two axes, we should expect the center of the first stream at the point -15.2 and of the second stream at $+22.7$. These points are marked with Roman numerals in Figure 1. No trace of any division into two streams is noticeable, although the "stream" motion is very pronounced among these stars, as shown by a comparison of the dispersions along the three axes. For the giant M stars the evidence is thus all in favor of the ellipsoidal hypothesis.

The direction of the axis of preferential motion for the "central group" among the A stars, for the giant stars of spectral classes K and M, and also for the dwarf stars of the latter types, has been determined by the writer[1] to be toward longitude 330°, differing appreciably from the direction found for other spectral classes, which is about 357°. The reason for this difference is probably that we have eliminated from the first-mentioned objects the effect of moving groups, in particular the generalized Taurus group and the Ursa Major group, and any existing traces of Kapteyn's two streams. A direct computation from the present data, using the method devised in *Contribution* No. 245, gives $332\overset{\circ}{.}0 \pm 2\overset{\circ}{.}1$ for the galactic longitude of the axis of preferential motion, in exact agreement with the direction used. For the stars studied the axis of preferential motion is thus perpendicular to the axis of asymmetry, at least within the uncertainty of the directions involved.

---

[1] *Stellar Movements*, pp. 101, 102. Macmillan, 1914.

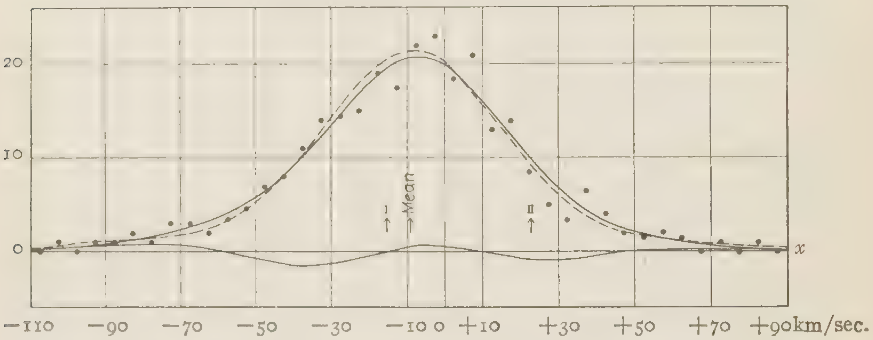

FIG. 1.—Distribution of velocities projected on the axis of preferential motion. The dots represent observed numbers of velocities between limits of 5 km/sec. The dotted curve is a representation determined by the method of moments; the full-drawn curve is based upon an analytical distribution function to which the effect of errors has been added. The curve near the axis of abscissae represents the effect of errors in the absolute magnitudes, proper motions, and radial velocities.

5. The y-axis is the axis of asymmetry as determined in *Contribution* No. 293. The observed frequency function was first represented by the method of moments, values for the mean, dispersion, skewness, and excess being found as follows:

$$\left.\begin{array}{ll} c=-17.43 \text{ km/sec.} & S=+0.356 \\ \sigma=22.59 \text{ km/sec.} & E=+0.369 \end{array}\right\} \qquad (18)$$

---

[1] *Mt. Wilson Contr.*, Nos. 245, 257; *Astrophysical Journal*, **56**, 265, 1922; **57**, 77, 1923.

The representation of the distribution with the aid of these constants is shown as a dotted curve in Figure 2. The representation is very poor because the actual distribution differs greatly from a normal error-curve. A slightly better representation could perhaps be obtained by omitting a few of the higher velocities; but such omissions are of a rather arbitrary nature, and one of the specific purposes of this study was to find if it were possible to represent the whole distribution by a simple function.

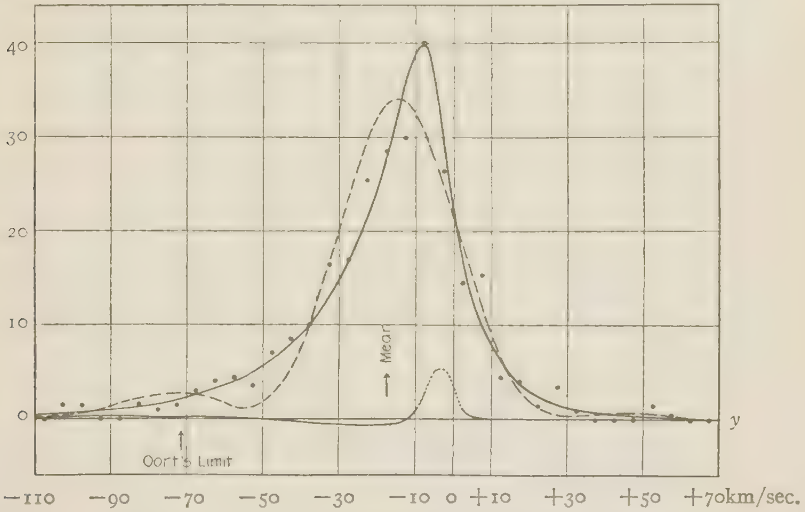

FIG. 2.—Same as Fig. 1, but the velocities are here projected on the axis of asymmetry.

Contributions Nos. 275 and 293 give evidence that the aggregate of practically all cosmical objects has a velocity distribution which is symmetrical for the x- and z-components and asymmetrical for the y-components. The velocity distribution for the y-axis was represented by a function of the form

$$F(y)dy = e^{-p(y-c)}\, S[(y-c)^2]dy\,, \tag{19}$$

where S indicates a distribution function symmetrical around the value $y=c$, and p is a quantity which produces the asymmetry and may be referred to as the "asymmetry constant"; in reality it is a vector directed toward the negative y-axis. In the papers cited, S was represented by a sum of concentric normal error-curves, which was a natural representation on account of the heterogeneous mixture of objects used. If S is a normal error-curve, the effect of the asymmetry constant is to shift the center of this error-curve in the direction of the asymmetry vector by an amount which is a quadratic function of the dispersion.

An attempt was made to represent the true distribution by a function of the form given in equation (19). The difficulty was to find an analytical form for the function S. After several trials with error-curves having different kinds of excess, a very simple form was found which represents the true distribution remarkably well.

The form used was

$$S \sim e^{-a|y-c|}, \tag{20}$$

where the absolute value of $(y-c)$ is used in the exponent. This function has a singularity at the point $y=c$, which will be discussed later.

The observed distribution was thus represented by the function

$$F(y)dy = \frac{N(a^2-p^2)}{2a} e^{-a|y-c|-p(y-c)} dy + E(y)dy , \tag{21}$$

where $E(y)dy$, as before, is the effect of errors.

Integrating the function $F(y)dy$ between the limits $-\infty$ and y for $y \leq c$, and between y and $+\infty$ for $y \geq c$, we obtain

$$\left.\begin{aligned} n'_c &= \int_{-\infty}^{y} F(y)dy = \frac{N(a+p)}{2a} e^{(a-p)(y-c)} \Big[1 + a\{(a-p)y + (a-p)^2 y^2\} \\ &\qquad + \frac{T^2}{2}(a-p)^2 \Big] , \\ n''_c &= \int_{y}^{+\infty} F(y)dy = \frac{N(a-p)}{2a} e^{-(a+p)(y-c)} \Big[1 - a\{(a+p)y \\ &\qquad - (a+p)^2 y^2\} + \frac{T^2}{2}(a+p)^2 \Big] . \end{aligned}\right\} \tag{22}$$

The expressions for the derivatives are

$$\left.\begin{aligned}
&\left.\begin{aligned}
\frac{dn'_c}{da}&=\frac{N}{2a}\,e^{(a-p)(y-c)}\left[-\frac{p}{a}+(a+p)(y-c)\right]\\
\frac{dn'_c}{dp}&=\frac{N}{2a}\,e^{(a-p)(y-c)}\left[1-(a+p)(y-c)\right]\\
\frac{dn'_c}{dc}&=-\frac{N}{2a}\,(a^2-p^2)e^{(a-p)(y-c)}
\end{aligned}\right\}(y\leq c)\\
&\left.\begin{aligned}
\frac{dn''_c}{da}&=\frac{N}{2a}\,e^{-(a+p)(y-c)}\left[\frac{p}{a}-(a-p)(y-c)\right]\\
\frac{dn''_c}{dp}&=\frac{N}{2a}\,e^{-(a+p)(y-c)}\left[-1-(a-p)(y-c)\right]\\
\frac{dn''_c}{dc}&=\frac{N}{2a}\,(a^2-p^2)e^{-(a+p)(y-c)}\ .
\end{aligned}\right\}(y\geq c)
\end{aligned}\right\}\qquad(23)$$

I have employed the method used in the case of the x-coordinates and determined corrections to provisional values of the constants a, p, and c from the differences between observed and computed numbers of velocities in different intervals. These intervals, ten in number, were so chosen that they include approximately equal numbers of velocities.

The expression for $E(y)dy$ is derived on the assumption that the first and second derivatives of the frequency function are continuous. In the present case these derivatives are discontinuous for the value $y=c$. Consequently, we must imagine some kind of continuous transition in these derivatives in the neighborhood of this point. The computation was carried out to the singularity at $y=c$, but the computed value of $\int E(y)dy$ in the region around this point was regarded as uncertain, and the corresponding equation of condition was omitted in the least-squares solution.

The following constants were found:

$$\left.\begin{aligned}
a&=+0.0701\pm 0.0041\ \text{sec./km}\\
p&=+0.0206\pm 0.0041\ \text{sec./km}\\
c&=-9.02\quad\ \pm 1.03\quad\ \text{km/sec.}
\end{aligned}\right\}\qquad(24)$$

The apparent distribution function based upon these constants and integrated over intervals of 5 km/sec. is shown graphically as a full-drawn curve in Figure 2, and the numerical data are given in Table I. The effect of the errors is also shown in the diagram, but the computed effect near the singularity is not exact. The above constants are, however, independent of the errors in this region of the distribution curve.

The representation by means of the foregoing constants is seen to fit the observed data remarkably well throughout the range. The values of p and c are in good agreement with those found in *Contribution* No. 293 for the asymmetry constant and the "limiting center" from cosmical objects in general. The values previously derived are

$$\left.\begin{array}{lll} p=+0.0192 & \pm 0.0020 & \text{sec./km} \\ c=-10.0 & \pm 1.0 & \text{km/sec.} \end{array}\right\} \qquad (25)$$

In fact, we might have adopted these values and obtained a representation practically identical with the one given, by the use of only one constant (a), the others (p, c, α, and T) being derived from other objects or by other means.

6. The velocity distribution along the z-axis is shown in Table I and Figure 3. This axis is nearly perpendicular to the galactic plane. Using again the method of moments, we find the following constants for the apparent distribution

$$\left.\begin{array}{ll} c=-\ 2.33 \text{ km/sec.}\ ; & S=+0.419 \\ \sigma=\ 18.64 \text{ km/sec.}\ ; & E=+0.445 \end{array}\right\} \qquad (26)$$

The dispersion is slightly smaller than that found for the y-axis, but the skewness and excess are very large. The representation by these constants is shown by a dotted curve in Figure 3 and is rather poor. When the excess or the skewness becomes large, pronounced inflections occur and the frequency function may even become negative. To avoid these inflections, which do not appear in the observed distribution, a function of the following form was used:

$$F_1(z)dz=\frac{Nh}{\gamma\sqrt{\pi}}e^{-h^2(z-c)^2}\left[1+\gamma_4 h^4(z-c)^4\right]dz\,;\ \gamma=1+\frac{3}{4}\gamma_4\,. \qquad (27)$$

This function gradually becomes zero and is always positive when γ_4 is positive. It must be emphasized that h is not here a measure of the actual dispersion.

The apparent distribution is thus

$$F(z)dz = F_1(z)dz + E(z)dz \, .$$

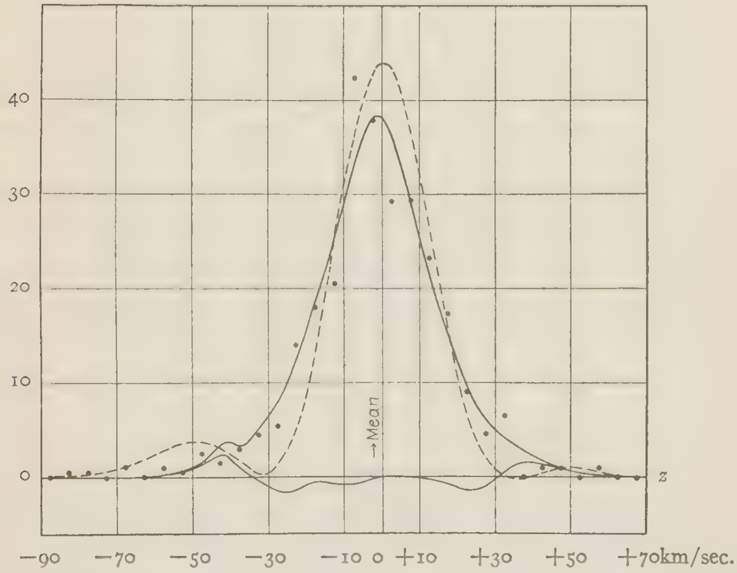

FIG. 3.—Same as Fig. 1, the velocities being projected on an axis nearly perpendicular to the galactic plane.

Integrating this function between the limits z_1 and z_2 we find

$$\left.\begin{array}{ll} \multicolumn{2}{l}{n_c = \int_{z_1}^{z_2} F(z)dz = \frac{N\Theta}{2} + \frac{N\gamma_4}{4\gamma\sqrt{\pi}}(3\psi_1 + 2\psi_3) + \frac{N}{\gamma\sqrt{\pi}} \sum_{n=0}^{n=7} b_n\psi_n} \\ b_0 = -ahc & b_4 = -9ahc\gamma_4 \\ b_1 = a(-1 + 2h^2c^2) + T^2h^2 & b_5 = a\gamma_4(-5 + 2h^2c^2) + T^2h^2\gamma_4 \\ b_2 = 4ahc & b_6 = 4ahc\gamma_4 \\ b_3 = a(2 - 4h^2c^2\gamma_4) - 2T^2h^2\gamma_4 & b_7 = 2a\gamma_4 \end{array}\right\} \quad (28)$$

The functions Θ and ψ_n are defined by equations (15).

The expressions for the derivatives are

$$\begin{aligned} \frac{dn_c}{dh} &= -\frac{N}{h\sqrt{\pi\gamma}}(\psi_1+\gamma_4\psi_5) \\ \frac{dn_c}{dc} &= \frac{Nh}{\sqrt{\pi\gamma}}(\psi_0+\gamma_4\psi_4) \\ \frac{dn_c}{d\gamma_4} &= \frac{N}{2\sqrt{\pi\gamma^2}}\left(\frac{3}{2}\psi_1+\psi_3\right) \end{aligned} \tag{29}$$

The following values for the constants were found:

$$\left.\begin{aligned} c &= -\ 1.61\ \pm 0.61 \text{ km/sec.} \\ \sigma' = \frac{1}{\sqrt{2h}} &= \ 11.54\ \pm 1.36 \text{ km/sec.} \\ \gamma_4 &= +\ 0.322 \pm 0.191\ . \end{aligned}\right\} \tag{30}$$

The true dispersion σ can be found from the equation

$$\sigma^2 = \frac{\sigma'^2}{\gamma}\left(1+\frac{15}{4}\gamma_4\right) ,$$

and we find thus

$$\sigma = 15.39 \text{ km/sec.}$$

The representation with these constants is shown in Figure 3 by a full-drawn curve, and may be regarded as fairly satisfactory. The effect of the errors is shown as before by a full-drawn curve near the line of abscissae. The hump in the distribution at $z = -40$ km/sec. is due to the errors in the absolute magnitudes, as may be seen from the curve representing the effect of the errors.

The true distribution function is slightly asymmetric, and an attempt was made to represent the asymmetry by a factor $e^{-p(z-c)}$, as in the case of the y-components. The slight asymmetry which exists is, however, not of a type that can be represented in this way, and is probably not a general phenomenon.

7. Even if the velocity distributions for the three principal axes are known, it does not necessarily follow that the three-dimensional distribution can be represented by a product of the three functions. It is only when the velocity components are independent that the simple product may be used. In case, for instance, of a mixture of

two classes of objects having different velocity dispersions but the same group motion, there would be a positive correlation between the velocity components, numerically small and large velocity components on one axis being statistically associated with small and large components, respectively, on another axis, a condition[1] which may be expressed by inequalities of the type $\overline{x^2y^2} > \overline{x^2}\,\overline{y^2}$.

TABLE II

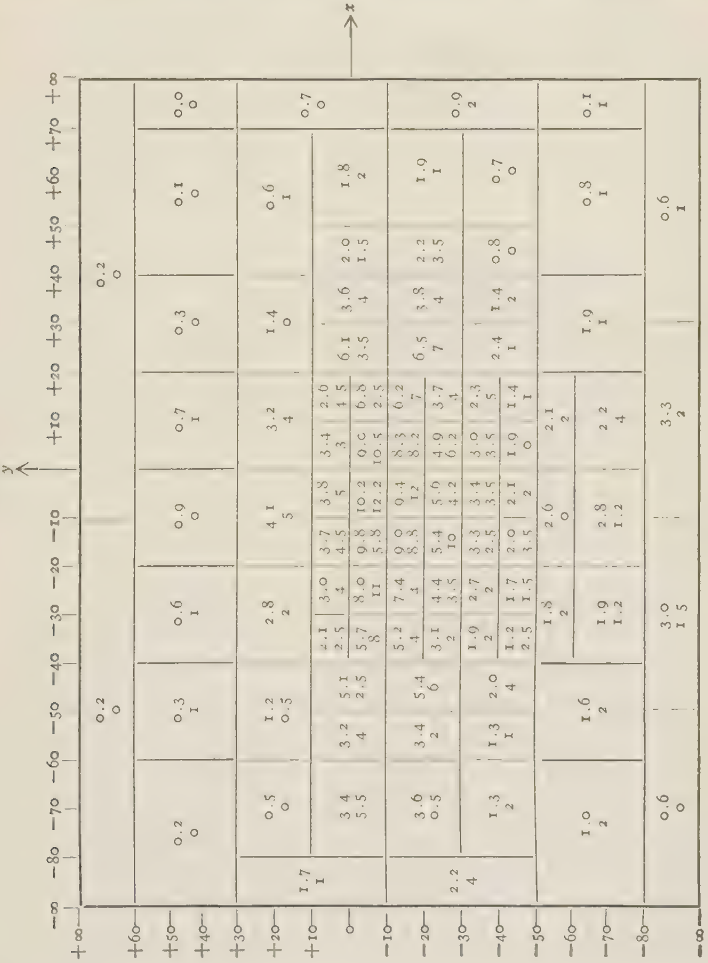
x
y
+∞
+70
+60
+50
+40
+30
+20
+10
0
−10
−20
−30
−40
−50
−60
−70
−80
−∞

---

[1] A slight correlation of the type mentioned above would be introduced by the fact that the errors in the absolute magnitudes are the same for the three velocity components.

In the present case the data are hardly sufficient for a three-dimensional subdivision, and we will limit ourselves to a study of the motions in the xy-plane. If we multiply the apparent distribution functions for the x- and y-axes and divide the result by the total number of objects N, we may test the possibility of representing the velocity distribution in the galactic plane by this product. Table II gives the results of such a study. The elements of area are necessarily increased as the density decreases, in order to obtain enough stars in each element. The upper figure in each rectangle is the computed number of velocity vectors terminating within the corresponding element of the xy-plane, while the lower figure is the observed number. On account of the use of even kilometers in the individual velocity components, the observed numbers often include fractions of a star. In view of the comparatively small number of stars in the different elements, the agreement between computed and observed values is all that can be expected.

It was of particular interest to ascertain whether the high velocities show any evidence of discontinuity. A little below the x-axis there is an excess of four or five stars with velocities beyond -80 and $+70$ km/sec., but the opposite occurs for the $y < -80$. No appreciable correlation could be found between the x- and y-components.[1] As a whole, the representation is valid for the whole range in x and y and shows no discontinuities. No definite trace of any moving groups could be found from the velocity diagram.

A similar study was made of the velocities projected on the xz- and yz-planes. It was found in all cases that no dependence existed between the velocity components, apart from a slight correlation due to the fact that the errors in the absolute magnitudes are the same for all directions. In general, the high velocities are as well represented as the smaller velocities, and no discontinuity could be found.

8. The values found for the centers of the three symmetrical functions may be compared with the values of α', β', and γ' derived in *Contribution* No. 293, page 20, from the radial velocities of the stars in general.

---

[1] The absence of a linear correlation ($\overline{xy}=\bar{x}\bar{y}$) simply means that the velocities are projected on the principal axes.

We have

$$\alpha' = -10.1 \pm 0.5 \text{ km/sec.} ; \qquad c_x = -8.8 \pm 0.7 \text{ km/sec.}$$
$$\beta' = -10.0 \pm 1.0 \text{ km/sec.} ; \qquad c_y = -9.0 \pm 1.0 \text{ km/sec.}$$
$$\gamma' = -\ \ 4.1 \pm 0.3 \text{ km/sec.} ; \qquad c_z = -1.6 \pm 0.6 \text{ km/sec.}$$

Except for the value of c_z, which, as may be seen from Figure 3, is difficult to determine, the agreement is satisfactory, but there is a systematic difference which will be discussed in connection with the solar motion. The asymmetry constant here determined may be regarded as a vector starting at this point (the "limiting center") and directed toward the negative y-axis ($\alpha = 130°$, $\delta = -57°$) and has a length of 0.0206 sec./km. We may also use the inverse value, 48.5 km/sec., as a measure of the asymmetry vector. This is to be compared with the value 52.1 km/sec. corresponding to $p = 0.0192$ found in *Contribution* No. 293. This is probably the best method of expressing the asymmetry vector.

9. We will now consider the solar motion as derived from the giant M stars. On account of the asymmetry in the velocity distributions, the group motion loses some of its usual meaning; we shall retain the expression, however, supposing it to represent the arithmetical mean of the velocity components, while the solar motion will be the opposite vector. Since there is no appreciable asymmetry along the x- and z-axes, we may identify the mean for these axes with the center of the distribution. Comparing the means for the apparent and true distributions, we see that for the x- and z-components the effect of the accidental errors of observation upon the mean values is very small. The computation of the true mean for the y-components is complicated by the fact that the computed effect of the errors near the maximum of the distribution-curve is not correct on account of the discontinuity in the derivatives. But, without appreciable error, we may regard the mean of the apparent distribution for the y-components also as representing the mean of the true distribution.[1] The three means are thus

$$\bar{x} = -9.2 \pm 1.3 ; \quad \bar{y} = -17.4 \pm 0.9 ; \quad \bar{z} = -2.3 \pm 0.8 \text{ km/sec.}$$

---

[1] Assuming the frequency function to be valid up to the singular point, we find for the true mean $\bar{y} = -18.20$ km/sec.

The opposite vector, referred to equatorial co-ordinates, gives the following value for the sun's motion referred to the giant M stars:

$$A_0 = 281\overset{\circ}{.}7\ ;\quad D_0 = +35\overset{\circ}{.}5\ ;\quad V_0 = 19.8 \pm 1.0 \text{ km/sec.}$$

From the radial velocities of 307 M stars brighter than apparent magnitude 6.5, the following elements were derived for the solar motion:

$$A_0 = 279\overset{\circ}{.}1\ ;\quad D_0 = +35\overset{\circ}{.}2\ ;\quad V_0 = 23.4 \pm 1.6 \text{ km/sec.}$$

Although the two apices agree well, there is an appreciable difference in the sun's velocity. This difference is intimately connected with the fact mentioned in *Contribution* No. 327[1] that the parallactic motions give a smaller value for the mean parallaxes, and thus a brighter mean absolute magnitude than the peculiar motions, provided we use the higher value for the sun's velocity.

The ratio of the two values for the sun's velocity would indicate that the absolute magnitudes need a systematic correction of $\Delta M = -0.57$. Such a correction is difficult to reconcile with the result of the comparison between angular and linear peculiar motions. Systematic errors in the proper motions may be partly responsible for this difference. A small excess of stars of high radial velocity in the southern hemisphere would account for part, or even the whole, of the effect. It must be noted, however, that a correction $\Delta M = -0.57$ would not appreciably modify the shape of the three distribution-curves here given. The only effect would be to change the scale of the velocities, counted from the sun as origin, by the factor $23.4/19.8 = 1.18$. All quantities expressed in km/sec. would be multiplied by this factor; quantities expressed by pure numbers (S, E, γ_4) would remain unaffected.

10. There has been some discussion about the nature of the asymmetry, and a few remarks may remove some misconceptions. Oort[2] has studied practically the same stars as those discussed in

---

[1] *Astrophysical Journal*, 65, 108, 1927.

[2] *Bulletin of the Astronomical Institutes of the Netherlands*, No. 23, 1922, and *Groningen Publications*, No. 40, 1926.

Contributions Nos. 245, 275, and 293,[1] and arrived at the conclusion that the asymmetry exists only for stars having a peculiar velocity greater than a certain fixed limit, which he places at 63 km/sec. Stars with peculiar velocities smaller than this limit are supposed to show no asymmetry. This asymmetry extends over a whole hemisphere, but no provision is made for effecting the transition to the other hemisphere, or for expressing the change in the limit as the axis of preferential motion is approached. No analytical expression for the velocity distribution of the high-velocity stars has been given, apart from the statement that they must lie outside a certain sphere in velocity space. This, however, would be of less importance, if any fixed discontinuity could actually be found. But the distribution curve in Figure 2 gives no trace of any such discontinuity at Oort's limit, or at any other limit. In the two-dimensional distribution, Table II, there is no indication of any discontinuity separating the high-velocity stars from those of smaller velocity. From both the one- and the two-dimensional velocity distributions we may conclude that the asymmetry is a phenomenon which affects the velocity distribution of the giant M stars as a whole.

In *The Observatory*, October, 1926, Oort writes, ". . . . after inspection of the figures on page 4 of *Groningen Publications*, No. 40, most astronomers, Strömberg also, will agree that there is a pronounced *change* in the velocity distribution near 62 km/sec." To this I would say that the stars there studied are very heterogeneous as regards motion and for such a mixture we should expect a change even on the basis of the present theory. If we mix, say, Cepheids of long and short period, we should certainly find a pronounced discontinuity and, if the two classes of objects are in nearly the same proportion, also an additional maximum in the velocity distribution. The same applies, although to a lesser extent, if we mix together stars selected on the basis of apparent brightness and large proper motion. Since large radial velocities are correlated with large linear tangential motions (at least in a heterogeneous mixture), we obtain, in studying the radial motions, the equivalent of two or more different velocity ellipsoids, as in *Contribution* No. 293; and the transition between these velocity ellipsoids, or error-curves in the one-dimensional case, may easily show at least a break in the continuous run. The F stars of large reduced proper motion and of large radial velocity, for instance, probably will produce a change in the distribution somewhere around Oort's limit. For this reason my more homogeneous data in *The Observatory*, September, 1926, are more satisfactory as a test of the existence of the fixed discontinuity than Oort's larger numbers, which were also previously studied by me. It is also for this reason that the giant M stars are well suited to test this question.

---

[1] *Astrophysical Journal*, **56**, 265, 1922; **59**, 228, 1924; **61**, 379, 1925.

Some doubts have been expressed by Oort upon the general validity of the quadratic relationship between group motion and velocity dispersion, but although there is some scattering of the points on my parabola in *Contribution* No. 293 the general tendency is unmistakable. In fact, the M stars fit the parabola rather poorly; but we now find, when the three-dimensional motions are studied, that the asymmetry is the same as for the stars in general. The division into several velocity groups made in *Contribution* No. 293 does not mean, as has been conjectured, that there is no asymmetry within the individual groups; in fact, the asymmetry may be rather pronounced within the component groups, the dissection serving merely as an artifice to determine the asymmetry vector. The separation into velocity groups could have been used in the present case for the distribution of the y-components, in which case the distribution would have been represented by at least two error-curves with quite different dispersions, one having its center at about -10 and the other at about -70 km/sec. But such a representation would have been rather artificial, and, in the present case, in view of the non-existence of any correlation between x and y, without any justification. Using Oort's method, we would have expressed the same distribution by an error-curve and, in addition, an extremely asymmetrical distribution starting rather abruptly at a fixed point. It must be borne in mind, however, that Oort's representation refers primarily to the three-dimensional distribution; but as seen in Table II there is no justification for introducing any discontinuity or separation into two velocity groups of more or less complex nature. The problem would have been somewhat different were there dynamical reasons for expecting a strictly Maxwellian distribution of stellar velocities; then we should have to invent special causes to explain the excess of high velocities.

The asymmetry vector seems to be the same for all known cosmical objects, although there is some doubt about the spiral nebulae, principally on account of the large K-term. The phenomenon is complicated by the existence of moving groups, like the Taurus and the Ursa Major groups, which probably must be treated as individual stars. The B stars show a decided discrepancy, but we have reason to believe that the bright B stars form a separate system (the "secondary galaxy," or the "local system" of Shapley), and may be comparable to a moving cluster. Several of the groups in *Contribution* No. 293 selected on the basis of small reduced proper motions (i.e., high intrinsic brightness) seem to include a large percentage of stars belonging to this local B-star system.

From a comparison of mean parallaxes computed from the luminosity and density functions with those derived from parallactic motions, Seares[1] has concluded that the sun's velocity is larger for intrinsically faint stars than for stars of higher luminosity. This result has been objected to by van Rhijn,[2] Oort and N. W. Doorn,[3] and P. van de Kamp.[4] There may be some connection between the phenomenon found by Seares and the general asymmetry in stellar motions. My own results indicate not a direct dependence of solar motion upon absolute magnitude but rather upon velocity dispersion, and this can well be reconciled with Oort's and Doorn's data. Van de Kamp finds that the radial velocities of stars of apparent magnitudes 9–10 give not only the same solar motion, but also about the same velocity dispersion as the brighter stars of the same spectra. Although seldom explicitly stated, everybody seems to have found a larger dispersion and larger solar motion for the giant K stars than for A, F, and G stars.

On account of the correlation between mean peculiar motion and absolute magnitude, we should expect a correlation such as

---

[1] *Mt. Wilson Contr.*, No. 281; *Astrophysical Journal*, **60**, 50, 1924.

[2] *Groningen Publications*, No. 37, p. 11, 1925.

[3] *Bulletin of the Astronomical Institutes of the Netherlands*, No. 89, 1925.

[4] *Ibid.*, No. 112, 1926; *Lick Observatory Bulletin*, **12**, 88 (No. 374), 1926.

Seares finds. The apparent contradictions can, however, all be reconciled by making the assumption that the sun's velocity varies with the velocity dispersion (or, in Oort's terminology, with the percentage of high-velocity stars), and it is only when there is a marked correlation between this dispersion (relative percentage) and the absolute magnitude that we may expect any correlation between absolute magnitude and solar motion. The determination of the latter correlation requires, however, a large amount of observational data, in particular for dwarf stars, which form such a large percentage when dealing with the stars as a whole, as Seares has done.

The "limiting center" was defined as an unattainable limit for the group motion of a class of objects as its velocity dispersion approaches zero. When using the distribution function in equation (19), this name becomes somewhat inadequate; but if we use equation (12) in *Contribution* No. 293, we see that this limit is the center of one of the two symmetrical functions composing the general distribution function, the other center defining the "world-frame."

It has been objected that the "velocity restriction[1] in a universal world-frame" which can be deduced from, but may not be a necessary consequence of, the form of the general distribution law can hardly be expected to have any effect when the velocities are as small as those found in stellar motions. But we must consider that a star is not a simple object, but is composed of electrons and atomic nuclei, and that the electrons within the stars may have velocities nearly equal to that of light. If the mass of an electron were a function of its velocity relative to the world-frame, and if the classical theory of compounding velocities were used, we should expect such a restriction. Further, we are here dealing with effects accumulated during the whole lifetime of a star, and the slightest lack of symmetry in the impulses would produce an appreciable effect. Although it is simplest to think of an ether in the classical sense as the cause of the velocity restriction, this conception is probably too mechanistic, and must be replaced by something which can serve as a substratum for electro-magnetic and inertio-gravitational phenomena. The general tendency is to regard the material universe not as an ensemble of cosmical objects but rather as a single entity with physical properties and singularities (atomic nuclei and electrons).

---

[1] The word "damping" has been suggested to me by several physicists, but as this term implies a physical rather than a statistical property the original term has been retained.

The simplest way to explain the connection and coincidence between the inertial and optical frame, on the one hand, and the stellar frame, on the other, seems to be to assume such a velocity restriction for transverse motions; and it was considerations of this kind which led me to try the new type of distribution law.[1] Meanwhile, many new data have been added, and detailed studies have been made of the velocity distribution. The form suggested for the velocity distribution has been found to represent the general distribution with a much higher accuracy than was ever anticipated.

The physical basis of Oort's theory is that certain stars have velocities higher than that of escape, which of course is perfectly reasonable. The reason, however, that these velocities are not distributed equally in all directions, at least in the galactic plane, is that these stars are interlopers belonging to a larger system, relative to which our local system has a high velocity. The larger system with which they are connected is supposed to be the system of globular clusters. We should then expect that these high-velocity stars would form a system statistically at rest, relative to the larger system, and that the sun's motion, relative to the system of high-velocity stars, would be around 250 or 300 km/sec. This, however, is not at all the case. According to Oort, a clustering seems to prevail outside a fixed limit in velocity space, and for higher velocities the number of stars decreases rapidly, only a very few attaining velocities equal to that of the system of globular clusters.

Since it is definitely proved that the high-velocity stars do not have the same group motion as the globular-cluster system, they can hardly be regarded as interlopers belonging to this system. Nevertheless, there is a connection, and this connection may be expressed formally by introducing a constant asymmetry vector, and physically, or rather conceptually, by a velocity restriction in a universal world-frame; and the introduction of this vector makes it possible to express the velocity distribution of practically all cosmical objects in a very simple form.

---

[1] *Mt. Wilson Communication*, No. 84; *Proceedings of the National Academy of Sciences*, **9**, 312, 1923.

Another physical explanation of the asymmetry has been put forward by B. Lindblad.[1] According to his theory, a number of different classes of objects occupy the same space, forming subsystems having their common center of mass at a distance of about 18,000 parsecs in the direction of galactic longitude 325°. The period of rotation is different for the different subsystems, the system of globular clusters, to which the galactic clouds are supposed to belong, having only a small or zero rotation; the different speeds of rotation are in the same order as the sequence of velocity ellipsoids in *Contribution* No. 293. Such a system, according to Lindblad, may remain stable for a very long time, as the encounters of the stars have very little influence on their motions. The difficulty with this theory, as the writer sees it, is that it introduces hypotheses about the motions and distribution of cosmical objects which can hardly be tested by comparison with present observational data. As far as known at present, the center of the galactic stellar system is at a distance of only 1000–2000 parsecs. Further, it is very difficult to understand how such a system of intermingled subsystems can ever have evolved from a primordial mass of gas or dust, and the actual cause of the asymmetry remains unexplained. Nevertheless, it seems to require a distribution law of velocities practically identical with the one used here.

After all, hardly anything is known of the ultimate reason for the fact that objects of different spectral types, and even of different periods of light variation, have quite different velocities. Certain important factors seem to be missing from our theories of stellar motions; and if we look carefully enough we may even find that space itself has properties—in addition to those which we ordinarily include among inertio-gravitational and electro-magnetic phenomena—which are essential for an understanding of the problem.

CARNEGIE INSTITUTION OF WASHINGTON
MOUNT WILSON OBSERVATORY
March 1927

---

[1] *Arkiv för Matematik, Astronomi och Fysik*, **19*A***, Nos. 21, 27, and 35; **19*B***, No. 7, 1925–1926.

Contributions from the Mount Wilson Observatory, No. 333
Reprinted from the *Astrophysical Journal*, Vol. LXV, pp. 295–299, 1927
Printed in the U.S.A.

SPECTROGRAPHIC ORBITS OF THE TWO COMPONENTS OF BOSS 5683

By ROSCOE F. SANFORD

ABSTRACT

Spectrum.—Star B of the visual system Σ 2873 is a *spectroscopic binary* in which two spectra of about class G4 are at times distinguishable and measurable.

Orbit.—The spectroscopic orbit of the primary and the semi-amplitude of velocity variation for the secondary have been found from thirty-eight spectrograms (Table I) made with the 60-inch reflector. The *orbit is circular*, with a period of 1.1522019 days; the semi-amplitudes of velocity variation for primary and secondary are 105.5 and 112.4 km/sec., respectively, and the velocity of the system −17.0 km/sec. A velocity diagram is shown in Fig. 1. The elements give $(a_1+a_2)\sin i=3,470,000$ km; $m_1\sin^3 i=0.65\odot$; and $m_2\sin^3 i=0.61\odot$ (Table II). The velocity of the system here found is 5 km/sec. greater, algebraically, than that derived for star A, a difference hardly too large to attribute to the respective probable errors, although part of it may find a legitimate explanation in the orbital motion of the components of the visual system. Attention is called to the possibility of variability by eclipse.

This is star B of the visual system Σ 2873[1] (1900, α $22^{h}1^{m}.9$, $\delta+82^{\circ}23'$, mag. 7.3, G4p). Both A (Boss 5682) and B have been found to have the same proper motion, but during the fifty years that the stars have been observed no certain evidence of orbital motion has been noted. Five spectrograms of star A made at this observatory gave the apparently constant radial velocity −22.7 km/sec.[2] Its spectral class is F6, apparent magnitude 7.1, and absolute magnitude 3.5.[3] The obvious conclusion that star B has a still fainter absolute magnitude has been borne out by the evidence of its spectrum, for this gives $M=4.8$.[3] In addition, it was soon noticed that the radial velocities from the different plates were certainly unlike, and it was later announced[4] as a spectroscopic binary which at times shows the spectral lines of both components.

The variation in radial velocity of the two components was at first taken as evidence of a period of several days. As no such period could be found which would predict the phases for very long, an effort was finally made to obtain two spectrograms on the same night. This was accomplished on August 16, 1926, the two plates having mid-exposures that differ by a little more than six hours (Table I). The first of these shows a spectrum of double lines, and the second, one of single lines. The results from these two plates, in combination with the velocity found from that of August 17, taken

---

[1] H.D. 209943; βGC. (11514).

[2] *Mt. Wilson Contr.*, No. 258, p. 25; *Astrophysical Journal*, **57**, 173, 1923.

[3] *Mt. Wilson Contr.*, No. 199, p. 76; *Astrophysical Journal*, **53**, 88, 1921.

[4] *Publications of the Astronomical Society of the Pacific*, **31**, 42, 1919.

TABLE I

OBSERVATIONS OF BOSS 5683

PLATE NO.	DATE	G.M.T.	PHASE	VELOCITY		O−C PRIM.	WT.
				Prim.	Sec.		
			days	km/sec.	km/sec.	km/sec.	
γ 5238	1916 Nov. 9	15^h41^m	0.252	− 30.8	....	−34	0.5
6081	1917 July 8	23 26	0.765	− 11.2	....	+59	0.5
6141	Aug. 31	22 38	0.576	−123.5	....	− 1	0.5
6267	Oct. 5	19 30	0.878	− 7.0	....	+ 2	1.0
6450	Dec. 5	17 00	0.707	−104.1	....	− 7	1.0
6520	1918 Jan. 2	16 12	1.021	+ 43.1	− 97.7	−20	1.0
7497	Oct. 23	18 30	0.150	+ 66.6	−111.2	+11	1.0
9489	1920 Aug. 28	17 15	1.052	+ 79.6	− 92.1	+ 6	0.5
9498	Aug. 29	16 54	0.885	− 13.0	....	− 8	1.0
9520	Sept. 1	23 43	0.713	− 79.9	+ 94.8	+15	0.5
10201	1921 June 14	21 51	0.886	− 26.6	....	−22	0.5
10252	July 11	20 13	0.165	+ 57.1	− 76.4	+ 9	1.0
10256	July 12	19 39	1.141	+111.0	−112.1	+22	1.0
10265	July 13	20 42	1.032	+ 49.4	− 64.8	−17	0.5
11097	1922 June 7	23 18	0.608	−131.0	+ 87.8	−10	0.5
11101	June 8	22 52	0.438	− 94.6	....	− 1	0.25
11121	July 2	20 59	0.161	+ 55.3	....	+ 5	0.5
11127	July 3	20 22	1.136	+ 83.3	−126.8	− 5	0.5
11133	July 4	20 46	1.000	+ 52.5	− 78.1	− 2	0.5
11226	Aug. 5	23 24	0.849	− 18.5	....	+ 7	1.0
11296	Sept. 2	22 36	1.151	+ 68.6	....	−20	0.5
11303	Sept. 3	21 49	0.979	+ 37.0	....	− 8	0.5
12330	1923 Dec. 16	16 6	0.789	− 44.6	....	+14	1.0
12337	Dec. 17	16 24	0.648	−118.8	+110.2	− 4	1.0
13519	1925 July 5	20 00	1.061	+ 74.8	−114.4	− 1	1.0
13525	July 6	20 00	0.909	+ 13.2	....	+ 5	1.0
13532	July 7	19 15	0.726	− 88.6	+ 43.3	+ 1	1.0
13538	July 8	19 58	0.603	−128.5	+102.4	− 7	1.0
13544	July 9	20 39	0.479	−124.6	+ 88.4	−16	1.0
13628	Aug. 6	23 24	0.950	+ 32.0	....	+ 1	1.0
13629	Aug. 7	16 20	0.496	−107.8	+ 96.6	+ 5	1.0
13630	Aug. 8	18 02	0.414	− 82.0	+ 64.7	+ 2	1.0
13641	Aug. 10	17 30	0.087	+ 76.4	− 93.1	0	0.25
13653	Aug. 12	16 37	0.898	− 9.2	....	−12	1.0
13943	Dec. 29	15 58	0.452	−112.2	+ 99.6	−13	0.5
14427	1926 Aug. 16	16 35	0.035	+ 88.6	−118.0	+ 2	1.0
14430	Aug. 16	23 19	0.316	− 23.0	....	+10	1.0
14431	Aug. 17	16 27	1.030	+ 69.2	−104.2	+ 3	1.0

eighteen hours later, showed that the period could not be much greater than one day. Indeed this clue led finally to 1.1522019 days as the period best suited to assemble the velocities derived from the thirty-eight spectrograms made between November, 1916, and August, 1926.

All the plates were obtained with the 60-inch reflector and a one-prism spectrograph. The observational data are in Table I, which has two columns for the radial velocities. If the spectra are blended, a velocity appears only in the column for the primary. In some cases, although the two spectra were separated, only that of the primary could be measured. When two spectra of types as late as these are blended, difficulties arise which often diminish the accuracy of the velocities for the two components and sometimes prevent the measurement of the weaker component entirely. All these difficulties have been encountered in this case.

Careful consideration of the freehand velocity-curves drawn through the assembled observations resulted in the assumption of circular orbits. Furthermore, since the curve for the primary seemed much more accurate than that for the secondary, it was decided to determine all the elements, except the semi-amplitude of velocity-variation for the secondary, from the curve for the primary alone. The preliminary elements for the assumed circular orbit were therefore P, the period; T, the time when the primary attains maximum positive velocity; K_1, the semi-amplitude of velocity-variation for the primary; and, finally, γ, that value of the velocity which divides the radial-velocity diagram into equal areas.

The first two values of the radial velocity in Table I gave large residuals which could have been considerably diminished by slightly increasing the period; but other considerations seemed to favor the adopted period, and the final correction of this element was left to the least-squares solution. For this the weights assigned are based upon the various characteristics of the individual plates which may affect the accuracy of the measures. The least-squares solution resulted in sensible corrections only to K_1 and P; but the application of these corrections reduced $[pvv]$ 40 per cent, the effect, in large measure, of the change in P upon the residuals for the first two plates. A second solution based on all but the first two velocities also gave sensible corrections only in the case of K_1 and P, and of the same sign as before. Since these elements do not materially better the representation of the thirty-six values of the velocity employed, and are quite inferior to the first set in representing the first two velocities, the results of the original solution are adopted.

A value of K_2, the semi-amplitude of velocity-variation of the secondary, has been derived from the measures of velocity by a least-squares solution of the equation

$$C_2 = \gamma - K_2 \cos M \ ,$$

where C_2 is the measured velocity of the secondary, $\gamma = -17$ km/sec., the velocity of the system, and M the phase as reckoned for the primary, the weights being the same as appear in Table I. The resulting value, $K_2 = 112.4$ km/sec., seems, however, to be somewhat too small, because of the use of some values of C_2 that are unduly small but whose rejection would be an arbitrary procedure. Furthermore, the near equality of K_1 and K_2 does not seem compatible with the very considerable difference in the intensity of the two spectra when seen separated. Nevertheless, the value obtained above is retained.

The preliminary elements, corrections, and final elements, together with their probable errors and the functions of mean distance and mass, are:

Preliminary Elements	Corrections	Final Elements
P 1.1522019 days	+0.0000124 day	1.1522143 ± 0.0000003 day
γ −16.0 km/sec.	−1.0 km/sec.	−17.0 km/sec.
T J.D. 2423213.380	−0.017 day	J.D. 2423213.363 ± 0.003 day
K_1 112 km/sec.	−6.4 km/sec.	105.6 ± 2.0 km/sec.
K_2		112.4 km/sec.
$(a_1+a_2) \sin i$		3,470,000 km
$m_1 \sin^3 i$		0.65 ☉
$m_2 \sin^3 i$		0.61 ☉

The last column in Table I gives the residuals for the primary as computed from the adopted elements.

Velocity-curves are given in Figure 1 for both components, although the elements upon which they are based, with the exception of K_2, are derived solely from the primary. The smaller circles indicate velocities for the primary; larger circles, those for the secondary.

The interval covered by the observations here represented includes 2886 revolutions in the orbits.

It is worthy of note that the velocity of this system (B of the visual pair) is −17.0 km/sec., whereas that for A, as mentioned in the beginning, is −22.7 km/sec. Attention should also be called to the fact that the velocities for the secondary would be better represented if its curve were raised somewhat; in other words, if its γ were algebraically larger. No explanation for this discordance in the γ-value for the two components is offered, except in so far as the fault may be traceable to the relative inaccuracy of the velocities for the secondary. Any weight that the secondary of the spectroscopic binary may have in determining the center-of-mass velocity for the system B can only accentuate the difference in velocity already shown to exist between stars A and B. The respective probable errors of the two velocities and the possibility of orbital motion in the visual binary would, however, suffice to explain this difference.

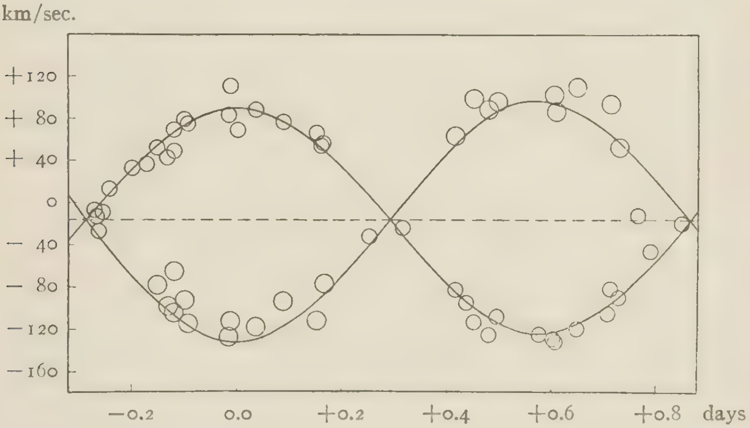

FIG. 1.—Velocity-curves for the spectroscopic binary Boss 5683 (Σ 2873 B)

It would be of interest to observe this spectroscopic binary photometrically at appropriate epochs in order to test for a decrease in brightness produced by eclipse. The spectroscopic data are quite consistent with such a possibility.

CARNEGIE INSTITUTION OF WASHINGTON
MOUNT WILSON OBSERVATORY
March 1927

Contributions from the Mount Wilson Observatory, No. 334
Reprinted from the *Astrophysical Journal*, Vol. LXV, pp. 286–294, 1927
Printed in the U.S.A.

STARS WHOSE SPECTRA HAVE BRIGHT IRON LINES

By PAUL W. MERRILL

ABSTRACT

Classification of stellar spectra having bright iron lines.—These spectra may be classified in the following groups: (1) long-period variables; (2) peculiar stars of classes G, K, and M; (3*a*) class Be normal; (3*b*) class Be peculiar; (4) novae. Available information concerning these stars is summarized, and a few unpublished observations are recorded.

Lists of stars in groups 2, 3*a*, and 3*b* are given, with references to published descriptions. New data are recorded for Z Canis Majoris (H.D. 53179), and B.D.+14°3887. It seems possible that stars of group 3*b* (with outstanding bright lines and other peculiarities) have fainter absolute magnitudes than those of 3*a*.

Lines of the ionized atom are of more frequent occurrence than those of the neutral atom. This fact is briefly discussed.

Hydrogen stands by itself among the chemical elements in the frequency with which its emission lines are found in stellar spectra. Iron comes next and helium third, unless we count long-period variables at phases other than maximum, in which case magnesium and silicon might outrank helium. The properties of bright hydrogen lines in stellar spectra are fairly well known, as these lines have been extensively investigated, and many data concerning them have been published.

Bright iron lines appear in quite different types of stars, and references to them are widely scattered through astronomical literature. The present paper attempts to summarize the available information concerning the occurrence of these lines, and in addition records a few unpublished observations.

Stars in whose spectra bright iron lines have been found may be classified as follows:

1. Long-period variables. Examples, *o* Ceti and R Cygni
2. Peculiar stars of classes G, K, and M. Examples, T Tauri, W Cephei, and VV Cephei (Boss 5650)
3. Class Be
   a) Normal. Examples, γ Cassiopeiae and β Monocerotis (brightest component)
   b) Peculiar. Examples, η Carinae and XX Ophiuchi (H.D. 161114)
4. Novae

Recent progress in the analysis of spectra has emphasized the importance of distinguishing between lines of the neutral and of the ionized atom. The difference in behavior in stellar spectra of various lines arising from the same chemical element has, of course, impressed itself upon observers for many years, and has been a most important factor in hastening the interpretation of line spectra in terms of the structure of the atom.

The fact that in various types of stars having bright iron lines we are dealing chiefly with enhanced lines (i.e., those of the ionized atom) is thus of considerable interest. Long-period variables are the only stars in which bright lines of the neutral iron atom appear in any strength, and in these stars enhanced lines also are present. We now proceed to a brief description of the characteristics of the iron lines in the various groups of the foregoing classification.

I. LONG-PERIOD VARIABLES

The neutral and ionized lines occur under different circumstances and must be discussed separately.

Lines of the neutral atom. Fe I.—During the time of decreasing light, the spectra of variables of classes Me and Se exhibit a number of unusual bright lines, among which are the extreme low-temperature lines of iron. In the spectral region λ 4200–λ 4500, King's list of persistent low-temperature lines[1] is so consistently represented in the variables[2] as to leave very little doubt concerning the identification.

Two of the most conspicuous bright lines present during the time of decreasing light[3] lie near the positions of the iron lines λ 4202.03 and λ 4307.91. These lines are believed by several observers actually to be iron lines, and, in addition to the agreement of the laboratory and stellar wave-lengths, the careful discussion of identifications in *o* Ceti by Joy[4] has brought out several indirect but plausible arguments in favor of this view. Nevertheless, some doubt may remain[1] until these lines are shown by laboratory experiments to be outstanding under special circumstances, or until the presence in emission of certain related iron lines is recorded in the variables.

---

[1] *Mt. Wilson Contr.*, No. 247; *Astrophysical Journal*, **56**, 318, Table V, 1922.

[2] *Mt. Wilson Contr.*, Nos. 311 and 325; *Astrophysical Journal*, **63**, 281, 1926, and **65**, 23, 1927.

[3] *Mt. Wilson Contr.*, Nos. 200, 265, 311, 325; *Astrophysical Journal*, **53**, 185, 1921; **58**, 195, 1923; **63**, 281, 1926; **65**, 23, 1927.

[4] *Mt. Wilson Contr.*, No. 311; *Astrophysical Journal*, **63**, 281, 1926.

Enhanced (ionized atom) lines. Fe II.—According to Joy,[2] the identification of several bright lines in the spectrum of *o* Ceti near maximum, with ionized iron, "may be considered as entirely probable." This may apply to numerous other Me variables as well, although I think that the lines in question are less prominent in some of them. In the spectra of Se variables, on the other hand, the bright iron lines are decidedly more conspicuous, several of them, in particular λλ 4583, 4924, and 5018, being present on numerous spectrograms of these stars.[3] They are especially prominent in S Cassiopeiae and R Cygni. In several variables, the bright enhanced iron lines seem strongest near maximum, as would be expected, but in R Cygni they persist throughout a considerable portion of the light-cycle.

2. PECULIAR STARS OF CLASSES G, K, AND M

Stars of these classes which are known to exhibit bright iron lines are listed in Table I. The iron lines are those of the ionized atom, including λλ 4179, 4233, 4549, 4584, 4924, 5018, as well as other weaker lines. The hydrogen lines are bright, as are also numerous lines of unknown origin. Concerning VV Cephei (Boss 5650), W Cephei, and H.D. 42474, Adams, Joy, and Humason[4] say, "There can be little doubt that the spectrum of these stars is closely allied to that of the well-known southern variable, η Carinae. A comparison of the results with those published by Moore and Sanford for the latter star[5] shows all of these bright lines to be present in much the same relative intensity." Many of the same lines are found also in the spectra of H.D. 45677[6] and other peculiar stars of class Be.

---

[1] Baxandall, *Observatory*, **46**, 82, 1923.

[2] *Loc. cit.*

[3] *Mt. Wilson Contr.*, No. 325; *Astrophysical Journal*, **65**, 23, 1927.

[4] *Publications of the Astronomical Society of the Pacific*, **34**, 176, 1922.

[5] *Lick Observatory Bulletins*, **8**, 55 (No. 252), 1913.

[6] *Publications of the Astronomical Society of the Pacific*, **37**, 163, 1925.

3. CLASS Be

Many spectra of class B show bright hydrogen lines, and in about one-eighth of these, bright iron lines also have been observed. We may, for convenience, divide the stars with bright iron lines into two groups according to the appearance of the bright lines. In the first group the bright hydrogen lines are of the "normal," symmetrical, or nearly symmetrical type described as S, D?, or D in *Contribution* No. 294.[1] The iron lines have about the same structure as the hydrogen lines, but are much weaker and usually exhibit small contrast with the continuous spectrum. This group includes γ Cassiopeiae, φ Persei, β Monocerotis, μ Centauri (prior to 1904), and other bright and well-known stars of class Be. Stars of this kind are listed in Table II.

TABLE I

STARS OF CLASSES G, K, M, WITH BRIGHT IRON LINES

Star	No.	R.A. 1900	Dec. 1900	Mag.	Type	Notes
T Tauri	N.G.C. 1555	$4^{\mathrm{h}}16^{\mathrm{m}}1$	+19° 17′	(10)	Gpe	1
....	H.D. 42474	6 5.8	+23 14	7.4	M3ep	2
Boss 1985	H.D. 60414, 5	7 29.2	−14 18	5.1	M3ep	3
R Cor. Austr.	N.G.C. 6729	18 55.2	−37 5	10–13	Gpe	4
Boss 5481	H.D. 203338, 9	21 16.5	+58 12	5.8	(M1+B)e	3
VV Cephei	H.D. 208816	21 53.8	+63 9	5.4	M2ep	2, 5
W Cephei	H.D. 214369	22 32.6	+57 54	8.6–9.3	K5e	2

NOTES TO TABLE I

1. *Publications of the Astronomical Society of the Pacific*, **32**, 59, 1920.
2. *Ibid.*, **34**, 175, 1922.
3. *Ibid.*, **37**, 161, 1925.
4. *Mt. Wilson Contr.*, No. 241; *Astrophysical Journal*, **56**, 181, 1922.
5. *Publications of the Astronomical Society of the Pacific*, **33**, 263, 1921.

The list will doubtless be extended by future work, as many bright-line B-type stars probably remain to be discovered. Moreover, not all known Be stars have been observed in such a way as to bring out the broad, weak iron lines here considered. This would require widened spectrograms on emulsions of considerable contrast.

---

[1] *Astrophysical Journal*, **61**, 416, 1925. See also *Transactions of the International Astronomical Union*, **1**, 100, 1922.

The identification of iron lines in this type of spectrum was apparently first made by N. Lockyer and F. E. Baxandall in the stars μ Centauri and γ Cassiopeiae.[1] A spectrogram of μ Centauri obtained at Mount Wilson in June, 1924, shows that the recent disappearance of the bright hydrogen lines, noted by several observers, was accompanied by the disappearance of the bright iron lines.

TABLE II

NORMAL BE STARS WITH BRIGHT IRON LINES

Star	H.D.	R.A. 1900	Dec. 1900	Mag.	Type	Notes
γ Cass...........	5394	$0^{h}\,50^{m}.7$	+60° 11′	2.2	Boe	1, 2, 3
φ Persei..........	10516	1 37.4	+50 11	4.2	Boe	2, 3
....	20336	3 11.2	+65 17	4.8	B3e	2, 3
....	21212	3 20.3	+62 9	8.7	B2e	4
ψ Persei..........	22192	3 29.4	+47 51	4.3	B5e	2, 3
11 Camelop........	32343	4 57.4	+58 50	5.3	B3e	2
....	35345	5 19.0	+35 33	8.4	B2e	4
25 Orionis.........	35439	5 19.6	+ 1 45	4.7	B3e	3
ζ Tauri..........	37202	5 31.7	+21 5	3.0	B3e	3
....	41335	5 59.4	− 6 42	5.1	B2e	2
β Mono. (pre.)....	45725	6 24.0	− 6 58	4.7	B2e	2
ω Can. Maj.......	56139	7 10.7	−26 35	3.8	B3e	2
....	65875	7 55.8	− 2 36	6.4	B3e	4
r Puppis.........	68980	8 9.7	−35 35	4.8	B3e	2
μ Centauri.......	120324	13 43.6	−41 59	3.3	B2(e)	1, 3
χ Ophiuchi.......	148184	16 21.2	−18 14	4.8	B3e	2
....	190944	20 2.3	+46 24	8.8	B2e	4
π Aquarii.........	212571	22 20.2	+ 0 52	4.6	B1e	3
β Piscium........	217891	22 58.8	+ 3 17	4.6	B5e	2
....	225095	23 58.3	+55 0	7.6	B1e	4

NOTES TO TABLE II

1. *Proceedings of the Royal Society of London*, A, **74**, 548, 1905.
2. *Lick Observatory Bulletins*, **7**, 177 (No. 237), 1913.
3. *Monthly Notices, R.A.S.*, **85**, 594, 1925.
4. Unpublished observations at Mount Wilson.

The spectra of the second group of B-type stars with bright iron lines show a more pronounced departure from ordinary B-type spectra than do those of the first group. The bright lines are more outstanding, and peculiarities, such as those of the type of P Cygni, are often present. Stars of this kind are listed in Table III.

---

[1] *Proceedings of the Royal Society of London*, A, **74**, 548, 1905.

TABLE III

Peculiar Be Stars with Bright Iron Lines

Star	No.	R.A. 1900	Dec. 1900	Mag.	Notes
Comp. *o* Ceti	....	$2^{h}14^{m}.3$	− 3° 26′	10–11	1
....	H.D. 45677	6 23.7	−13 0	7.5	2
....	H.D. 45910	6 25.2	+ 5 57	6.7	3
R Mono	N.G.C. 2261	6 33.7	+ 8 49	(13)	4
....	H.D. 51480	6 52.4	−10 41	7.0	5
Z Can. Maj	53179	6 59.0	−11 24	(9.1)	11
η Carinae	93308	10 41.2	−59 10	7–8	6
XX Ophiuchi	161114	17 38.6	− 6 14	9.6–10.7	7
DM. −27° 11944	....	17 41.9	−27 59	9.0	5
B.D. +14° 3887	....	19 17.0	+14 42	9.5	12
B.D. +11° 4673	207757	21 46.2	+12 9	(7.6)	8
Z Androm.	221650	23 28.8	+48 16	8.3–11.4	9
Comp. R Aquarii	....	23 38.6	−15 50	9–10	10

NOTES TO TABLE III

1. *Mt. Wilson Contr.*, No. 311; *Astrophysical Journal*, **63**, 337, 1926.

2. *Publications of the Astronomical Society of the Pacific*, **37**, 163, 1925.

3. *Ibid.*, **35**, 145 and 303, 1923.

4. *Lowell Observatory Bulletins*, **3**, 63 (No. 81), 1918.

5. *Mt. Wilson Contr.*, No. 295; *Astrophysical Journal*, **61**, 418, 1925.

6. *Lick Observatory Bulletins*, **8**, 55 (No. 252), 1913.

7. *Publications of the Astronomical Society of the Pacific*, **36**, 225, 1924, and **38**, 45, 1926.

8. *Publications of the Astronomical Observatory of the University of Michigan*, **2**, 71, 1916.

9. The presence of bright iron lines in this spectrum was mentioned by J. S. Plaskett at the Pasadena meeting of the American Astronomical Society in September, 1923. A paper by H. H. Plaskett on this spectrum will appear in Volume IV of the *Publications of the Dominion Astrophysical Observatory.*

10. *Publications of the Astronomical Society of the Pacific*, **39**, 48, 1927.

11. *Z Canis Majoris, B.D.−11°1760.*—Miss Cannon's discovery of the bright lines $H\beta$ and $H\gamma$ was announced in *Harvard Circular*, No. 178. The following remark is found in the *Henry Draper Catalogue:* "The lines $H\beta$ and $H\gamma$ are bright. The dark lines are very faint, but helium lines are certainly present. The line K is very strong for Class B." In *Harvard Circular*, No. 225, it is stated that this star is an irregular variable and that its light-curve bears some resemblance to that of R Coronae Borealis.

Spectrograms were obtained at Mount Wilson on October 30, 1925, and January 18, 1927. A one-prism spectrograph with 10-inch camera was employed. The magnitude of the star on both dates was about 9.

On the first plate, the hydrogen lines and several enhanced iron lines are bright, with broad dark components on their violet sides. The bright iron lines include λλ 4173, 4179, 4233, 4352, 4385, 4417?, 4451, 4490 (blend), 4508, 4515, 4521 (blend), 4549, 4556?, 4584, 4629, 4924, 5018. The absorption components are not seen in all cases. Feeble bright lines are seen in the positions of the following strong lines in the enhanced titanium spectrum: λλ 4395, 4444, 4469. They probably have the same structure as the iron lines.

On the second plate, the bright lines, especially those of iron, are less intense, while the absorption lines of titanium are stronger, twelve or more being measurable. The behavior of this spectrum thus in a measure resembles that of the "iron star" XX Ophiuchi (H.D. 161114).[1]

The apparent radial velocity corresponding to the displacements of the bright portions of the hydrogen lines is +67 km/sec. From about ten iron lines, it is +45 on the first plate, and +75 on the second. The difference probably reflects the relative increase in strength of the dark components. It is not certain that any of these results represents the actual velocity of the star.

The dark lines are considerably displaced toward the violet. The measured differences between the effective centers of the emission and absorption components of the hydrogen lines are as follows: $H\delta$, 4.0 A; $H\gamma$, 4.3 A; $H\beta$, 6.1 A. The iron lines, being less intense, give smaller differences. A smooth curve drawn through the scattering points plotted from the measured separations of ten iron lines has the following co-ordinates: λ 4200, 2.7 A; λ 4600, 3.2 A; λ 5000, 4.2 A. For both hydrogen and iron, the separations are represented approximately by a function varying as the square of the wave-length.

The apparent position of this star is quite near that of the somewhat similar star H.D. 51480,[2] and not far from H.D. 45677, but this may be a coincidence, as the three objects lie close to the central line of the Milky Way. In some respects the spectrum of Z Canis Majoris (H.D. 53179) is intermediate between that of H.D. 51480 and of Cordoba DM. −27°11944.[2]

12. *B.D.+14°3887*.—The bright $H\alpha$ line in this spectrum was discovered at Mount Wilson from objective-prism photographs.[3] Observations with a one-prism slit-spectrograph and 18-inch camera have been obtained on the following dates: September 20, 1921; July 4, 1923; July 5, 1925. They show only the usual photographic region. The spectra are narrow and somewhat under-exposed.

The bright hydrogen lines are strong, narrow, and apparently symmetrical. Dark components are not distinctly visible. Eight or ten bright enhanced lines of iron are present. Most of them are weak and appear as uncertain condensations in the narrow continuous spectrum. On better photographs, such as those usually obtained for brighter stars, the iron lines would doubtless be rather conspicuous.

The hydrogen lines, as well as those due to iron, are narrower and stronger than in the stars of the normal Be group (Table II). The spectrum is probably the same at the times of the three photographs.

The measured displacements of the bright $H\beta$ and $H\gamma$ lines give, in the mean, +33 km/sec. for the radial motion. The bright iron lines give +27 km/sec. These values doubtless agree within the errors of determination.

It is difficult to define precisely the distinction between the "normal" and "peculiar" Be spectra listed in Tables II and III, respectively. There may or may not be a fundamental difference between the two groups. The normal Be stars are much more closely related to ordinary dark-line B-type stars than are those of the other group. This is evidenced not only by the general appearance of the spectra, but by the fact that some of them, e.g., Pleione and μ Centauri, have changed into ordinary dark-line spectra by the fading of the bright lines. This seems to have occurred without notable changes in other features of the spectrum or appreciable variation of the total light. A number of spectra in the peculiar group also have shown variations, but of a different and more complex nature, which seem, in several instances, to have accompanied changes in the integrated brightness.

---

[1] *Publications of the Astronomical Society of the Pacific*, **38**, 45, 1926.

[2] *Mt. Wilson Contr.*, No. 295; *Astrophysical Journal*, **61**, 418, 1925.

[3] *Mt. Wilson Contr.*, No. 294; *Astrophysical Journal*, **61**, 389, 1925.

It is possible that the stars of the second group have a considerably lower mean absolute magnitude than those of the first. The apparent magnitudes in Table III average considerably fainter than those in Table II. The greater ease of detection of very strong bright lines may be partly responsible for this, but the absence of apparently bright stars from Table III, as compared with Table II, suggests a lower intrinsic brightness. Two of the stars in Table III are associated with long-period variables whose absolute magnitude at maximum is probably about zero. Joy,[1] and Merrill and Strömberg[2] have pointed out that the peculiar bright-line companion of o Ceti appears to have an absolute magnitude about +6. Similarly, the bright-line star closely associated with R Aquarii[3] is several magnitudes fainter than the variable star at maximum.

4. NOVAE

The occurrence of bright lines of ionized iron in the spectra of novae is well known. The lines are broad but apparently occupy their normal positions. At an early stage they are accompanied by dark lines on their violet edges. For a description of the complicated changes which these lines undergo, the original memoirs on novae spectra must be consulted.[4]

---

[1] *Mt. Wilson Contr.*, No. 311; *Astrophysical Journal*, **63**, 339, 1926.

[2] *Mt. Wilson Contr.*, No. 267; *Astrophysical Journal*, **59**, 106, 1924.

[3] *Publications of the Astronomical Society of the Pacific*, **39**, 48, 1927.

[4] For example, Nova Geminorum: Stratton, *Annals of the Solar Physics Observatory, Cambridge*, **4**, 1, 1920; Wright, *Publications of the Lick Observatory*, **14**, 27, 1926.

It is rather curious that the stronger arc lines of iron do not occur more frequently in emission in stellar spectra. They are, of course, prominent in absorption in the spectra of classes F, G, K, M, N, and S, and one might expect them to show in emission more frequently than any other iron lines. This is, however, decidedly not the case. Two or three of the strongest lines were faintly present in emission in the spectrum of XX Ophiuchi (H.D. 161114) when the enhanced lines were very strong.[1] This and the well-known cases of λ 4202 and λ 4308 in long-period variables are the only observations which come to mind. In the outer atmospheres of most stars in which conditions favor bright lines, the iron vapor is probably too thoroughly ionized to permit neutral lines to show in emission. In other cases, the low density of the stellar atmosphere may tend to suppress the ordinary arc lines, as in King's observations of the high-current arc in vacuum.[2]

Bright lines of the ionized iron atom occur in novae and in stars of classes B, G, K, M, and S. They are very rare[3] except in stars near the extremes of the temperature sequence. Their presence is probably an indication of high temperature or low density. In all stars in which they have been found, the hydrogen lines also are bright.

CARNEGIE INSTITUTION OF WASHINGTON
MOUNT WILSON OBSERVATORY
February 1927

NOTE ADDED TO PROOF.—Since this paper was written, Mr. Joy has discovered the existence of bright iron lines in the spectrum of the short-period variable W Serpentis (R.A. $19^{h}\ 4^{m}.1$, Dec. $-15^{\circ}\ 34'$), at the time of minimum light.

---

[1] *Publications of the Astronomical Society of the Pacific*, **36**, 225, 1924.

[2] *Ibid.*, **38**, 235, 1926.

[3] Rare, that is, in the integrated light. Doubtless they are freely emitted in certain portions of many stars as, for example, in the solar chromosphere. If conditions were such as to make the light of the chromosphere sufficiently important in the total radiation between certain wave-lengths, the sun would then be a bright-iron-line star.

Contributions from the Mount Wilson Observatory, No. 335
Reprinted from the *Astrophysical Journal*, Vol. LXVI, pp. 59–63, 1927
Printed in the U.S.A.

THE NEBULOUS ENVELOPE AROUND NOVA AQUILAE NO. 3

BY EDWIN HUBBLE AND JOHN CHARLES DUNCAN

ABSTRACT

Expanding envelope of Nova Aquilae No. 3 (1918).—Photographs made with the 100-inch reflector at Mount Wilson show a *nebulous disk* around the nova, which *expanded* perceptibly *during the interval of eleven months* covered by the observations. *Measures at four epochs* give a *mean diameter* of 16″.4 corresponding to the mean epoch, September 21, 1926.

This indicates an *angular increase in the radius* of the expanding disk or shell of nebulosity of 1″.0 per year, which is consistent with the earlier micrometric measures of the visual envelope. A *comparison* with the *linear rate* of expansion, 1700 km/sec. as derived from early spectrograms, leads to a *distance* of 360 parsecs; $\pi = 0''.0028$.

Slitless spectrograms show a strong *image of the disk* at λ 4686, slightly weaker images at $H\beta$, $H\gamma$, and $H\delta$, and traces at N_1 and λ 4363.

The outburst of Nova Aquilae No. 3 (1918) was first observed early in June, 1918. By October of the same year, Barnard had detected and measured a bright nebulous envelope about two-thirds of a second of arc in diameter, symmetrically distributed around the star. This envelope expanded steadily and gradually faded until it could no longer be observed with visual refractors. Both Barnard[1] and Aitken[2] measured the diameter as long as this could be done with confidence. The last-published value is that of Aitken,[2] 5″.0, on July 7, 1921, some three years after the outburst.

Photographs with the 100-inch reflector at Mount Wilson in the early summer of 1926 brought the envelope once more under direct observation. It had continued to expand (and probably to grow fainter)[3] until, at that time, its diameter was about 16″. The envelope photographs as a uniform disk with a sharp and sensibly circular edge. The star is central, as nearly as can be determined. The object has the appearance of a planetary nebula in which the central star is unusually bright.

---

[1] *Astrophysical Journal*, **49**, 199, 1918; *Publications of the Astronomical Society of the Pacific*, **32**, 222, 1920.

[2] *Publications of the Astronomical Society of the Pacific*, **31**, 283, 1919; **32**, 231, 1920; **33**, 219, 1921.

[3] In July, 1926, the envelope was invisible under favorable conditions at the primary focus of the 100-inch reflector.

Exposures on Eastman 40 plates, ranging from a few seconds up to sixty-five minutes, indicate that a limiting exposure of about two minutes is necessary to register a trace of the envelope; but that once impressed, its diameter does not materially increase with increasing exposure. On the short exposures there is a slight brightening at the rim, consistent with the theory that the envelope is a shell of material thrown off from the star at the time of the outburst. The limiting exposure corresponds to a surface brightness of the order of 19.5 in photographic magnitudes per square second of arc.[1] This, combined with the area, leads to a total magnitude of the order of 13.8. The central star was estimated as about 10.5.

The measures of the diameter of the envelope are given below. Each value represents the mean of two plates and has a probable error of the order of 0″.2.

May 17, 1926	15″.7
July 13, 1926	15.9
Sept. 4, 1926	16.4
April 25, 1927	17.6
Mean (Sept. 21, 1926)	16.4

On the assumption that the expansion has proceeded at a uniform rate since the initial outburst, the rate of increase in the radius is approximately 1″.0 per year. The early visual measures of Barnard and of Aitken, with the exception of the last one by Aitken, are consistent with this interpretation. The discordant measure was made in July, 1921, and hence, for a rate of 1″.0 annually, should have given a diameter of about 6″.1. It was in fact about 5″.0.

Since it is improbable that the velocity of expansion has been accelerated since 1921, it seems easier to account for the discrepancy as due either to the faintness of the object or to differences in the size of the visual and photographic images. In 1920, for instance, the light appears to have been largely concentrated in the N_1 and N_2 images, while in 1926 these were inconspicuous, and most of the light came from the Balmer lines of hydrogen and λ 4686. Slitless spectrograms made in August, 1926, at the primary focus of the 100-inch

---

[1] Seares has determined the limiting surface brightness which will register in an exposure of one minute on Seed 30 plates with a reflector of focal ratio 1:5, as 18.8 ± 0.3 pg. mag. per square second.

PLATE II

NOVA AQUILAE NO. 3 (1918)

Direct photograph with 100-inch reflector, April 25, 1927. Exposure 45 min. on an Eastman 40 plate. Scale 1 mm = 2.″1.

Slitless spectrogram with 100-inch reflector, August 2, 1926. Exposure 3 hrs. on an Eastman 40 plate. Two prisms and 3-inch camera.

reflector, with the use of two prisms and a 3-inch camera, show four distinct images of the envelope. λ 4686 is the strongest and is perhaps twice as strong as the equally dense images in $H\beta$, $H\gamma$, and $H\delta$. Faint traces of images appear in the region of N_1 and of λ 4363.

A velocity of expansion of 1″.0 per year corresponds to a distance, in parsecs, of

$$D=0.211r\ ,$$

where r is the radial velocity, in kilometers per second, of the expanding shell relative to the central star. The radial velocity cannot be accurately measured on spectrograms obtainable at present, but reasonable values may be derived from the many high-dispersion spectra accumulated during the five or six months immediately following the outburst. The measures at Mount Wilson indicate that, after the systematic changes during the first month, the radial velocity, as derived from the displacements of metallic absorption lines, settled down to a fairly constant value of 1650 km/sec.[1] This velocity was maintained from July to November, 1918—as long, in fact, as the object could be followed with high dispersion. By the end of this period the envelope had already been detected and measured by Barnard.

The Balmer lines of hydrogen appeared as broad emission bands, the widths remaining approximately constant at least as late as March, 1919.[2] The velocities of approach and recession, as represented by the violet and the red ends of the bands, were about 1750 km/sec.,[3] and hence of the same order as those derived from the absorption lines. Adams has suggested that the emission bands represent the expanding envelope and that the absorption lines arise from that portion directly in front of the star.[3]

---

[1] This result is derived from unpublished measures made at the Mount Wilson Observatory. See, in this connection, *Proceedings of the National Academy of Sciences*, 4, 355, 1918.

[2] The Mount Wilson measures have not been published in detail, but, as a sample, those for the emission bands in February and March, 1919, may be found in *Publications of the Astronomical Society of the Pacific*, 31, 183, 1919.

[3] *Mt. Wilson Communications*, No. 55; *Proceedings of the National Academy of Sciences*, 4, 355, 1918; *Mt. Wilson Contr.*, No. 179; *Astrophysical Journal*, 51, 121, 1920.

On this assumption, the radial velocity could be taken from either source. The larger values derived from the emission bands are more germane to the present problem, but the uncertainties involved in the measures suggest that the smaller but more precise values represented by the absorption lines may be a closer approximation to the actual conditions. The mean of the two, however, is a round number, 1700 km/sec., with an uncertainty of the order of 3 per cent, and this is sufficient for the purpose.

The corresponding distance[1] of Nova Aquilae No. 3, as derived from the formula given above, is

$$D = 360 \text{ parsecs},$$
$$\pi = 0\overset{''}{.}0028,$$
$$m - M = 7.8 \text{ mag.}$$

The apparent magnitude of the star was about 10.5 before the outburst, and −1.4 at maximum. Hence, from an absolute magnitude of +2.7, it flared up to −9.2 and then slowly faded to its original luminosity. The diameter of the envelope is now about 6000 astronomical units, and is increasing at the rate of 360 units per year.

The results are consistent with the fact that the mean of the various trigonometric parallaxes, as determined by the photographic method, is small and negative. This indicates that the distance is very probably greater than 200 parsecs and hence that the linear velocity of expansion is greater than say 1000 km/sec.

Carnegie Institution of Washington
Mount Wilson Observatory
April 1927

ADDENDUM

While the foregoing account of Nova Aquilae was in press, a 20-minute exposure on a fast plate, made by Milton Humason with the 100-inch reflector on July 20, 1922, came to our attention. No definite indications of a disk could be seen, but the size of the image relative to that of the diffraction pattern, when compared with other stars on the plate, suggested the possibility of a disk concealed by over-exposure. When the plate was reduced by ferrocyanide, the supposition was confirmed; a sharp uniform disk was revealed about the central star.

---

[1] Lundmark, in 1922, stated that he had determined the parallax of Nova Aquilae No. 3 by this method, and that the result, 0.006, agreed exactly both with the mean of the three photographic parallaxes then available and with the value derived from the upsilon component of the proper motion (*Publications of the Astronomical Society of the Pacific*, **34**, 210, 1922). He gives no further details.

The measured diameter of the original image, 8″8, is probably too large because of the over-exposure. The diameter after the reduction, 7″6, is believed to be too small because the narrow fringe of fainter nebulosity, apparent on the recent plates, was wiped out in the reduction. Although a nice accuracy in this matter is scarcely possible, it is significant that, on the obvious hypothesis of uniform expansion, the recent observations indicate a diameter for July, 1922, of 8″2, which is exactly midway between the extreme values representing measures before and after the reduction.

Humason's plate, therefore, is believed to be the earliest direct photograph on which the image is definitely recorded; and the diameter at that date was of the order of eight seconds of arc.

Contributions from the Mount Wilson Observatory, No. 336
Reprinted from the *Astrophysical Journal*, Vol. LXVI, pp. 43–58, 1927
Printed in the U.S.A.

TRANSMISSION PROPERTIES OF SOME FILTERS

By EDISON PETTIT

ABSTRACT

Determination of transmissions.—The determinations between λ 0.23 and 0.45 μ were made photographically with a 1-m concave grating spectrograph; those to the red of λ 0.45 μ were made with a monochromatic illuminator and vacuum thermocouple.

Standards of wave-length in the infra-red.—A table of wave-lengths of easily recognized features of *absorption spectra* is given for the region λ 0.74 to 2.1 μ, which may be used where accuracy greater than 0.01 μ is not required.

Transmission data.—The transmission curves of 44 filters are given from λ 0.23 to 2.3 μ, and in several cases to greater wave-lengths in the infra-red.

Photochemical effects.—The effect of sunlight on green celluloid, glass, silver, and gold films has been studied. Solarized green celluloid is a valuable filter transmitting the infra-red with an efficiency of 80–90 per cent, has a sharp cut-off at λ 0.7 μ, and transmits nothing from this point to λ 0.23 μ.

During several years past the writer has had occasion to test the properties of transmission of a number of filters in connection with measurements of radiation. These have been collected and are given here in the form of plotted curves. Gibson[1] has recently compiled a list of such curves, a few of which were re-determined and are included in this collection, since the present results extend much farther into the infra-red. As the curves extend from λ 0.2 to 2.3 μ and beyond, they should be of some interest to those engaged in photography and spectroscopy, in either ultra violet or infra red.

DETERMINATIONS IN THE ULTRA-VIOLET

The determination of transmissions to the violet of λ 0.45 μ was made photographically with a 1-m concave grating ruled by Jacomini with shallow lines. This was mounted in Littrow form and was used in the first order, giving a dispersion of 17.4 A per millimeter. The plateholder was so arranged that fifteen exposures could be put on each plate. Cramer contrast plates were used, as the time-intensity coefficient is nearly unity.

The image of an iron arc was projected upon the slit by a quartz lens. Exposures of 50 and 20 seconds were made through the filter, and exposures of 20 to 1 seconds by steps of 2 seconds were made without the filter. The former were cut off the plate and the line intensities compared under a magnifier with those of the latter. Transmissions from λ 0.45 to 0.23 μ were thus obtained with ease. In one or two cases a spark between silver electrodes was used to extend the transmission curve to the violet of λ 0.23 μ.

---

[1] *Journal of the Optical Society of America*, 13, 267, 1926.

For very low transmissions, such as are found in metallic films, non-adjustable sectors having factors of 0.10 and 0.05 were used to reduce the free exposures. These sectors were 15 inches in diameter and were driven at a considerable speed. The geometric and photometric factors were found to be practically identical.

DETERMINATIONS IN THE VISUAL AND INFRA-RED REGIONS

Most of the measurements for wave-lengths greater than 0.45 μ were made with a Hilger constant-deviation spectroscope arranged as a monochromatic illuminator. The source of radiation was a nitrogen lamp of the straight-filament street-lighting type, run with 30 per cent overload, an image of the filament being formed on the first slit by a lens. The radiation from the second slit was focused upon one junction of a compensated vacuum-thermocouple by means of a convex lens of 1-inch focal length. This arrangement is more efficient than a thermopile placed immediately behind the second slit, but is somewhat slower. A moving-coil galvanometer was used, an image of a filament being projected on a scale, the deflections being kept near 100 mm.

The widths of the slits were kept the same, being approximately 0.0015 ×μ at λ 0.5 μ, 0.0045 ×μ at λ 1.0 μ, 0.008 ×μ at λ 1.5 μ, and 0.020 ×μ at λ 2.0 μ where μ indicates the wave-length. For wave-lengths greater than 2.5 μ a rocksalt monochromatic illuminator was used with concave mirrors throughout. A six-junction thermopile was employed with this instrument, and the source of radiation was a heated platinum strip or Nernst glower.

In both instruments the filter was placed either in front of the first slit or behind the second, the change in focus being of no importance; hence collimation of the light passing through the filter was unnecessary.

DISPERSION IN THE INFRA RED

The dispersion curve of the Hilger instrument could not be computed, as the properties of the glass were unknown, hence standards were sought in the infra red. For a first approximation the atmospheric absorption bands and sodium emission lines were used. After smoothing by a number of determinations, the transmission-curves for benzol 1 cm and glycerine 1 cm were run and compared with the curves obtained by Coblentz.[1]

TABLE I

WAVE-LENGTHS OF THE PRINCIPAL FEATURES OF ABSORPTION SPECTRA

λ	Substance	Thickness in Millimeters	Feature	Transmission	Figure	Curve
0.740μ	Didymium	8.8	Min.	0.05	2	4
0.740	Neodymium	5	Min.	.03	2	3
0.770	Didymium, Neodymium	....	Max.	.58, .80	......	......
0.800	Neodymium	....	Min.	.03	......	......
0.805	Didymium	....	Min.	.01	......	......
0.830	Neodymium	....	Max.	.85	......	......
0.845	Didymium	....	Max.	.63	......	......
0.865	Neodymium	....	Min.	.16	......	......
0.880	Didymium	....	Min.	.18	......	......
0.940	H_2O	10	V slope	.70	3	5
0.975	H_2O	10	Min.	.55	......	......
1.000	H_2O	10	R slope	.62	......	......
1.065	Didymium	8.8	Min.	.53	......	......
1.110	Benzol	10	V slope	.60	1	1
1.130	H_2O	10	V slope	.50	......	......
1.135	Benzol	10	Min.	.20	......	......
1.160	Benzol	10	R slope	.60	......	......
1.225	Didymium	8.8	Min.	.54	......	......
1.350	H_2O	10	V slope	.09	......	......
1.350	H_2O	5	V slope	.28	2	3
1.430	Benzol	10	Min.	.61	......	......
1.520	Didymium	8.8	Min.	.26	......	......
1.610	Benzol	10	V slope	.50	......	......
1.680	Benzol	10	Min.	.03	......	......
1.700	Didymium	8.8	Max.	.62	......	......
1.800	Benzol	10	R slope	.26	......	......
1.920	Didymium	8.8	Min.	.31	......	......
1.970	Benzol	10	Max.	.42	......	......
2.100	Benzol	10	V slope	0.23	......	......

Figure 1 shows how these curves agree, the dotted curves being due to Coblentz. An interesting feature of the curve for benzol is the sharp absorption band at λ 1.135 μ. As the crosses indicate, the observations of Coblentz were made on the edges of the band, which was therefore drawn much too shallow. This band serves as a convenient standard of wave-length.

---

[1] *Scientific Papers of the Bureau of Standards*, 17, 267, 1922.

Aside from narrow absorption bands, the edges of wide bands with steep sides may be used for calibration purposes. A list of standards available in the absorption spectra observed in the course of the present work is listed in Table I. The point referred to is indicated on the corresponding curve by the letter *S*. The data in the table will be useful in securing dispersion curves in the infra red where accuracy greater than about 0.01 μ is not desired.

THE TRANSMISSION CURVES

The curves of similar transmission features have been grouped in Figures 1–9. Data concerning each curve appear opposite its symbol in the margin of each plot. In the case of solutions of salts, the mass of crystalline salt per square centimeter in the optical path is given, since the water plays little part in the form of the curve to the violet of 1 μ, and the form to the red of this is the typical (OH) absorption.

Table II is a key to the various curves and will assist in identification.

PHOTO-CHEMICAL EFFECTS

The transmission curve of green celluloid is shown in Figure 4, curve 10. This screen, on exposure to sunlight for a period of two months, turns nearly black, transmitting only a dull-red light. The transmission curve for this solarized green celluloid is practically identical with that of ordinary green celluloid in the infra-red from λ 0.7 to 2.0 μ, the transmission bands in the green λ 0.50 μ and ultra-violet λ 0.36 μ being completely suppressed.[1] This solarized celluloid forms the only screen, to the writer's knowledge, which has a sharp cut-off at λ 0.7 μ, transmits no radiation from this point to λ 0.23 μ, and transmits the infra-red beyond λ 0.7 μ with an efficiency of 80–90 per cent. This should be of interest to those working in spectroscopy and photography in the infra red.

---

[1] *Publications of the Astronomical Society of the Pacific*, **39**, 170, 1927.

TABLE II

Filter	Thickness in Millimeters	Cell	Wall Thickness in Millimeters	Figure	Curve
Acetic acid, glacial	10	Quartz	5	9	37
Alum, crystal	1.65			7 9	34 47
Asphalt (Abbot)		Glass		7	26
Asphalt	0.090	Glass	0.6	7	30
Benzol	10	Quartz	5	1	1
Bottle glass	4			7	29
Bottle glass solarized	4			7 9	28 49
Celluloid, green	0.25			4	10
Copper ammonium sulphate*	8	Glass	2	3	9
Corning G 24 (red)	6			4	14
G 38 (noviol)	3.93			4	13
124 J (heat absorbing)	1.17			6	20
124 J (heat absorbing)	4.85			6	21
G 555 Q (didymium)	8.8			2	4
G 585 M (blue-purple ultra)	3.52			5	16
G 980 A (ultra-violet clear)	4.10			9	46
G 984 B (green)	3.95			4	15
G 985 B (ultra-violet)	4.97			5	17
Uviol	4.25			7 9	27 39
Glycerine	10	Quartz	5	1	2
Gold film	Thin	Quartz	5	6	23
Gold film	Thick	Quartz	1	6	24
Gold	2 Thick films	Quartz	1	6	25
Iceland spar	1.67			8 9	36 48
Malachite green†	30	Glass	5	3	8
Microscope cover-glass	0.165			8 9	35 45
Neodymium chloride‡	5	Glass	2	2	3
Photographic plate, Clear		Glass		7	31
Photographic plate, Fogged		Glass		7	33
Photographic plate, Ratio Fogged/Clear		Glass		7	32
Plate glass	6.5			9	40
Pulkowa B 67	3.52			4	11
Pulkowa B 68	3.55			4	12
Quinine sulphate§	10	Quartz	5	9	38
Silver film	Thin			9	41
Silver film	Thick			9	42
Silver film	2 Thick films			9	43
Spencer (heat absorbing) 4110	2.85			6	22
Vitaglass	2.56			9	44
Water	10	Quartz	5	3	5
Water (old)	10	Glass	0.165	3	6
Water	10	Glass	0.165	3	7
Wratten W 13	4.26			5	19
Wood's filter glass	1.72			5	18

* Mass per cm² = 17 mg. † Mass per cm² = 0.4 mg. ‡ Mass per cm² = 43 mg. § Mass per cm² = 3 mg.

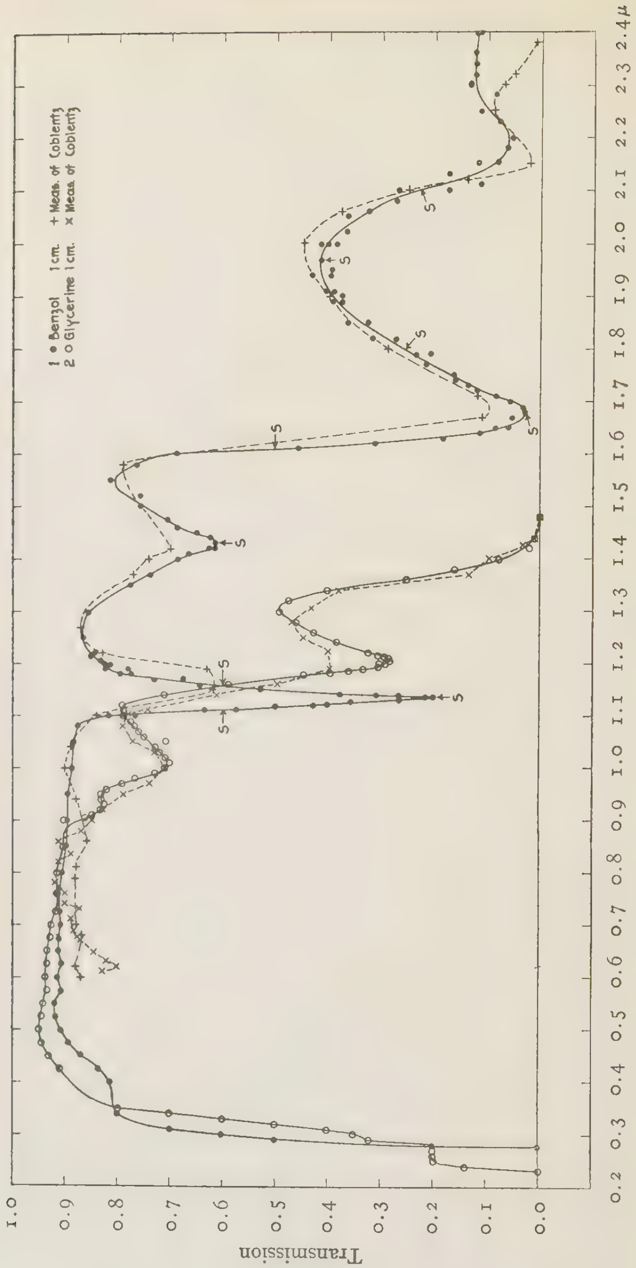
1 ● Benzol 1 cm. + Meas. of Coblentz
2 ○ Glycerine 1 cm. × Meas. of Coblentz
S
Transmission
0.0
0.1
0.2
0.3
0.4
0.5
0.6
0.7
0.8
0.9
1.0
0.2
0.3
0.4
0.5
0.6
0.7
0.8
0.9
1.0
1.1
1.2
1.3
1.4
1.5
1.6
1.7
1.8
1.9
2.0
2.1
2.2
2.3
2.4 μ

Fig. 1

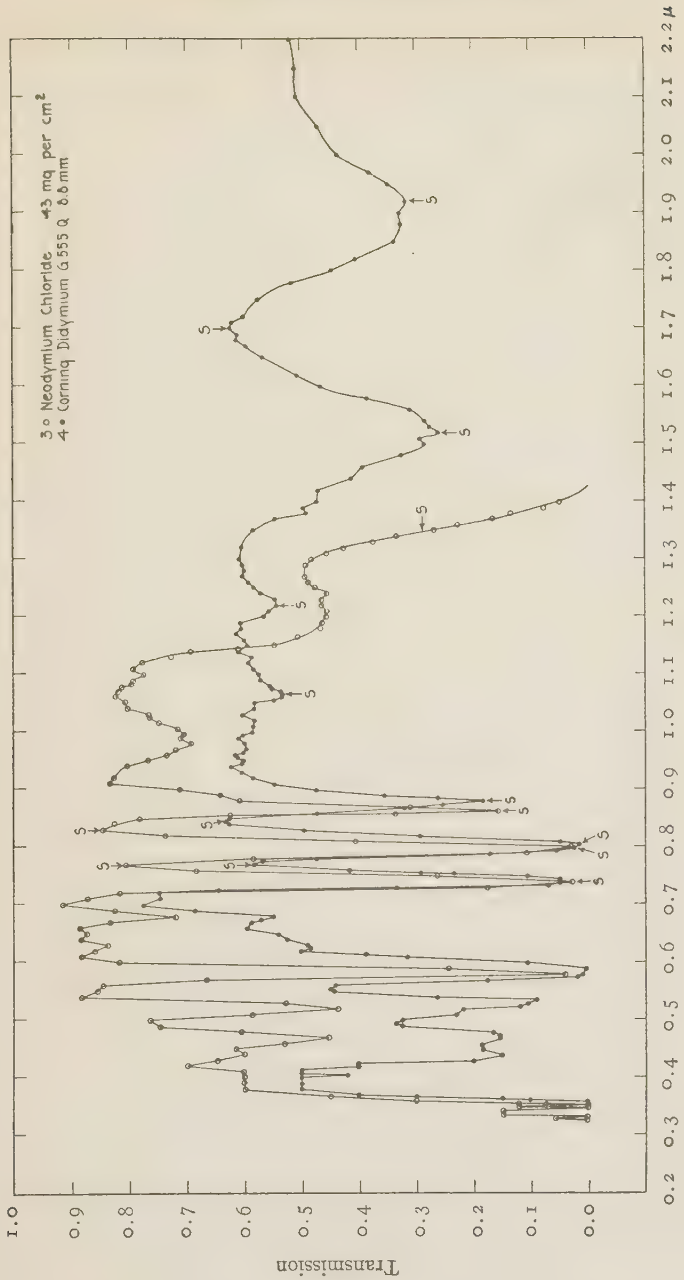
3 ○ Neodymium Chloride 43 mg per cm²
4 ● Corning Didymium G555 Q 8.8 mm
5
Transmission
1.0
0.9
0.8
0.7
0.6
0.5
0.4
0.3
0.2
0.1
0.0
0.2
0.3
0.4
0.5
0.6
0.7
0.8
0.9
1.0
1.1
1.2
1.3
1.4
1.5
1.6
1.7
1.8
1.9
2.0
2.1
2.2μ

FIG. 2

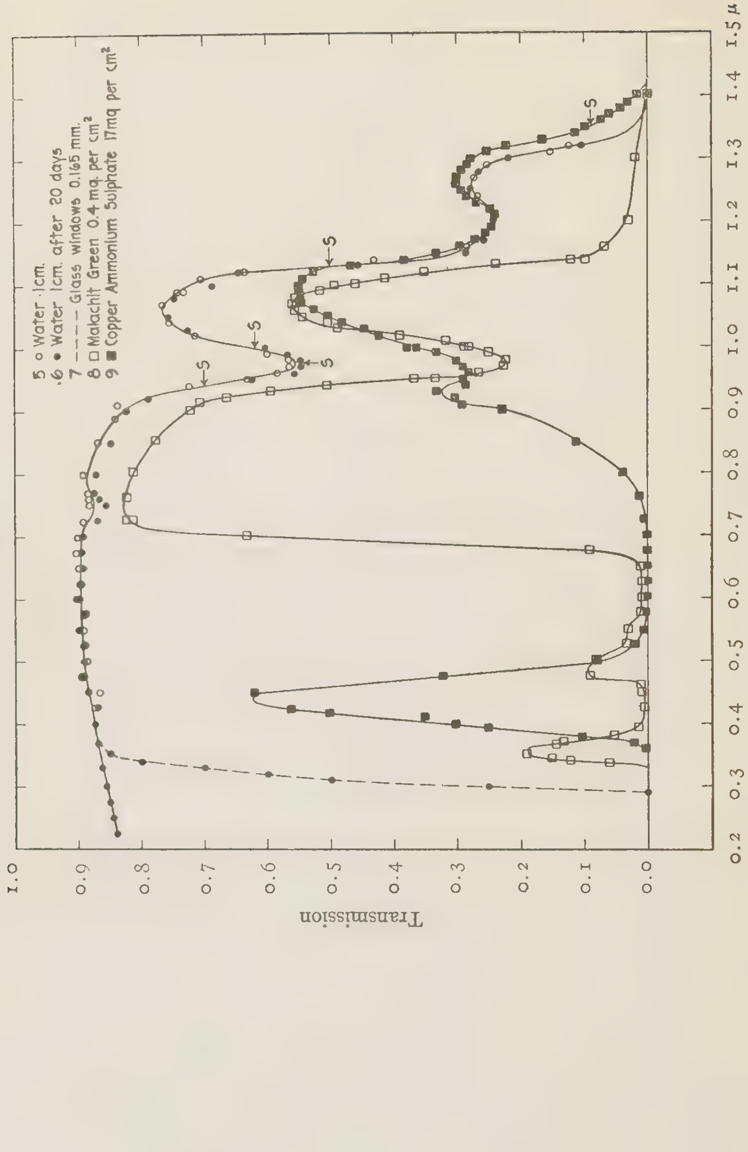
5 ○ Water ·1cm.
6 ● Water 1cm. after 20 days
7 – – – – Glass windows 0.165 mm.
8 □ Malachit Green 0.4 mg. per cm²
9 ■ Copper Ammonium Sulphate 17mg per cm²
5
5
5
5
5
Transmission
1.0
0.9
0.8
0.7
0.6
0.5
0.4
0.3
0.2
0.1
0.0
0.2
0.3
0.4
0.5
0.6
0.7
0.8
0.9
1.0
1.1
1.2
1.3
1.4
1.5 μ

FIG. 3

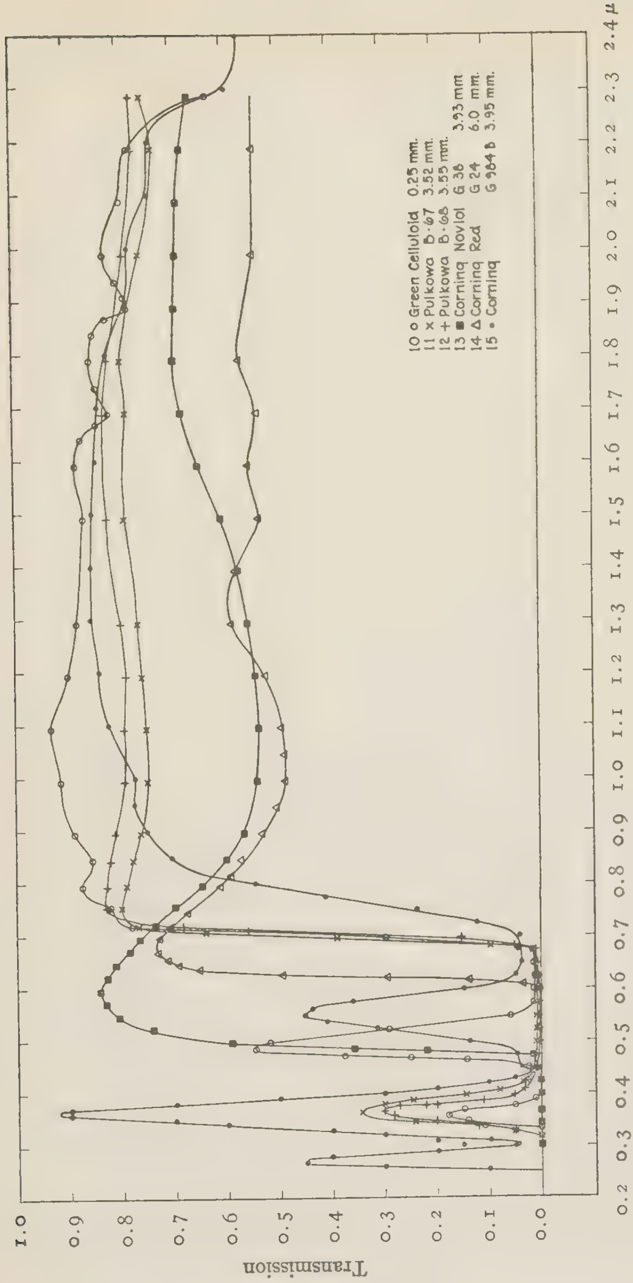
Transmission
1.0
0.9
0.8
0.7
0.6
0.5
0.4
0.3
0.2
0.1
0.0
0.2
0.3
0.4
0.5
0.6
0.7
0.8
0.9
1.0
1.1
1.2
1.3
1.4
1.5
1.6
1.7
1.8
1.9
2.0
2.1
2.2
2.3
2.4 μ
10 ○ Green Celluloid 0.25 mm.
11 × Pulkowa B·67 3.52 mm.
12 + Pulkowa B·68 3.55 mm.
13 ■ Corning Noviol G 38 3.93 mm
14 △ Corning Red G 24 6.0 mm.
15 • Corning G 984 B 3.95 mm.

Fig. 4

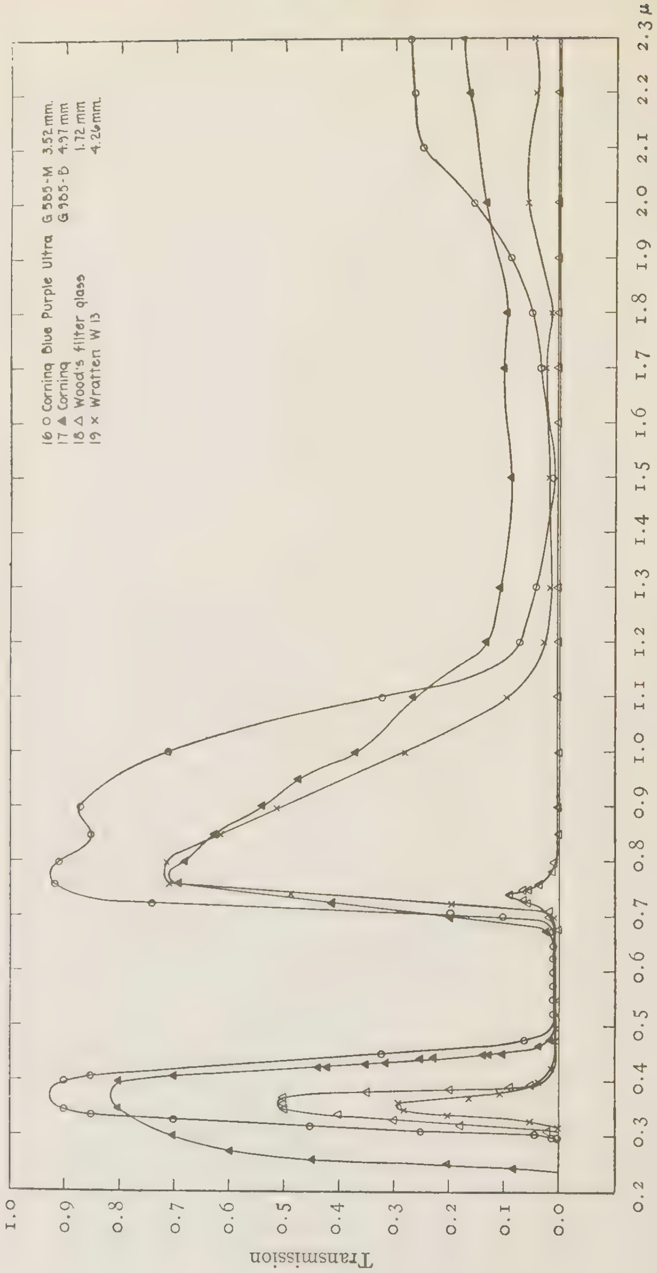
16 ○ Corning Blue Purple Ultra G 585-M 3.52 mm.
17 ▲ Corning G 965-B 4.97 mm
18 △ Wood's filter glass 1.72 mm
19 × Wratten W 13 4.26 mm.
Transmission
1.0
0.9
0.8
0.7
0.6
0.5
0.4
0.3
0.2
0.1
0.0
0.2
0.3
0.4
0.5
0.6
0.7
0.8
0.9
1.0
1.1
1.2
1.3
1.4
1.5
1.6
1.7
1.8
1.9
2.0
2.1
2.2
2.3 μ

FIG. 5

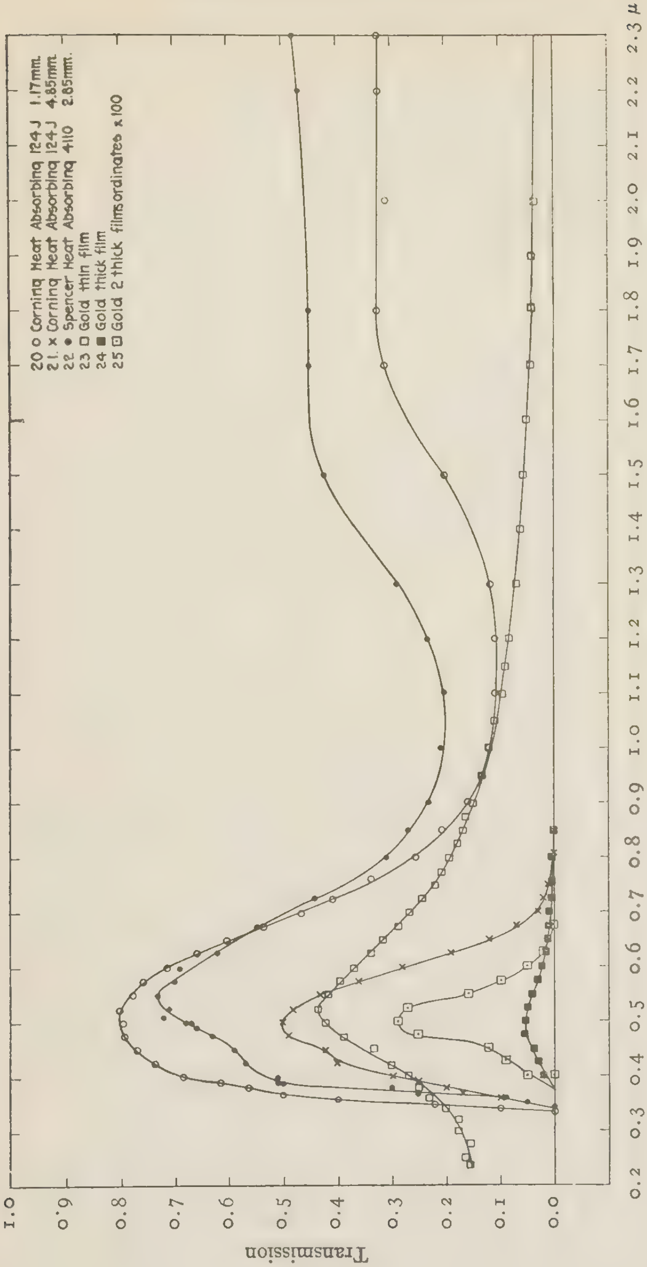
20 ○ Corning Heat Absorbing 124 J 1.17mm.
21 × Corning Heat Absorbing 124 J 4.85mm.
22 ● Spencer Heat Absorbing 4110 2.85mm.
23 □ Gold thin film
24 ■ Gold thick film
25 ⊡ Gold 2 thick films ordinates x 100
Transmission
1.0
0.9
0.8
0.7
0.6
0.5
0.4
0.3
0.2
0.1
0.0
0.2
0.3
0.4
0.5
0.6
0.7
0.8
0.9
1.0
1.1
1.2
1.3
1.4
1.5
1.6
1.7
1.8
1.9
2.0
2.1
2.2
2.3 μ

FIG. 6

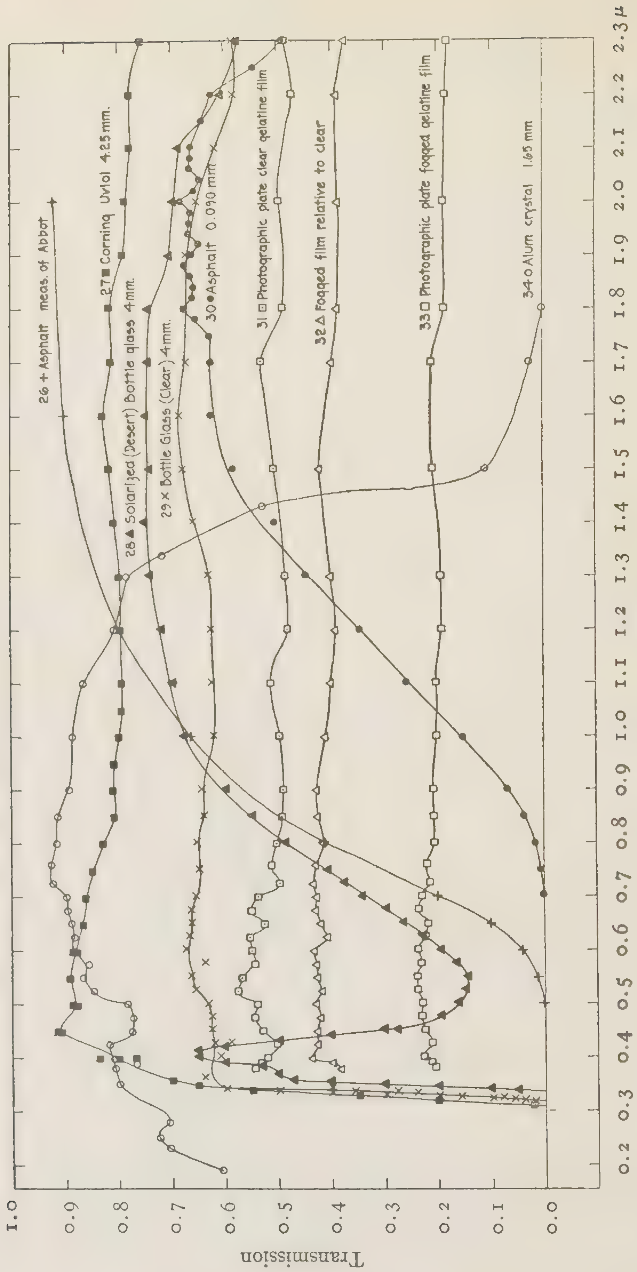
26 + Asphalt meas. of Abbot
27 ■ Corning Uviol 4.25 mm.
28 ▲ Solarized (Desert) Bottle glass 4 mm.
29 × Bottle Glass (Clear) 4 mm.
30 ● Asphalt 0.090 mm
31 ⊡ Photographic plate clear gelatine film
32 △ Fogged film relative to clear
33 □ Photographic plate fogged gelatine film
34 ○ Alum crystal 1.65 mm
Transmission
1.0
0.9
0.8
0.7
0.6
0.5
0.4
0.3
0.2
0.1
0.0
0.2
0.3
0.4
0.5
0.6
0.7
0.8
0.9
1.0
1.1
1.2
1.3
1.4
1.5
1.6
1.7
1.8
1.9
2.0
2.1
2.2
2.3 μ

FIG. 7

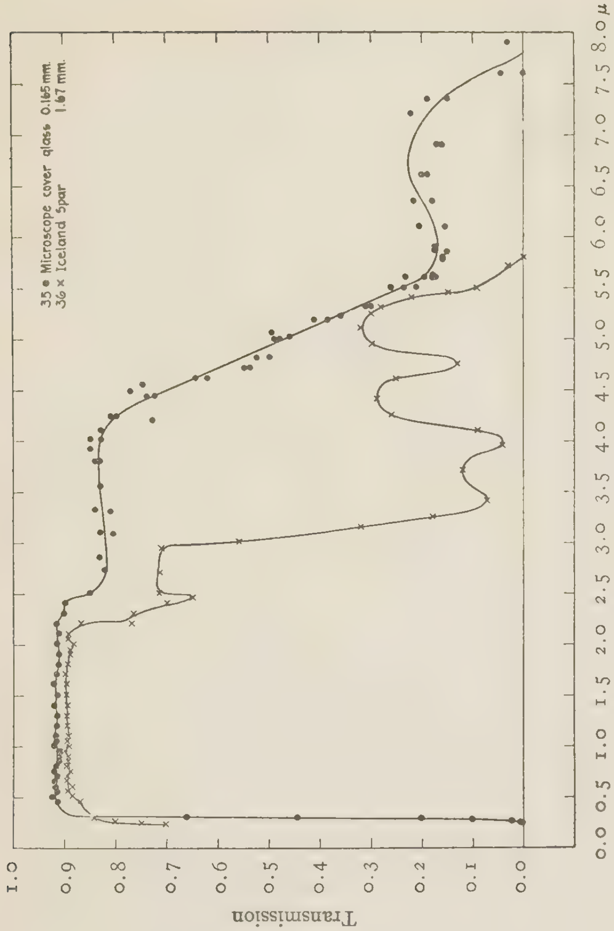
35 ● Microscope cover glass 0.165 mm.
36 × Iceland Spar 1.67 mm.
Transmission
0.0
0.1
0.2
0.3
0.4
0.5
0.6
0.7
0.8
0.9
1.0
0.0
0.5
1.0
1.5
2.0
2.5
3.0
3.5
4.0
4.5
5.0
5.5
6.0
6.5
7.0
7.5
8.0 μ

Fig. 8

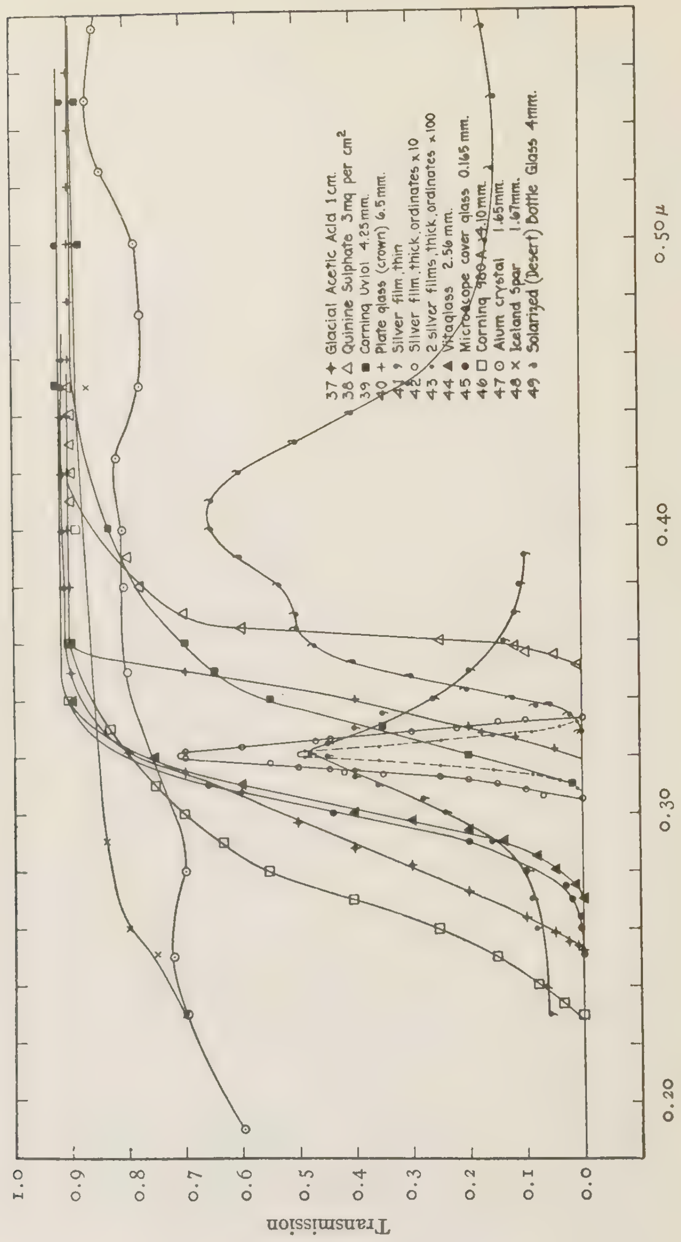
37 ✦ Glacial Acetic Acid 1 cm.
38 △ Quinine Sulphate 3 mg per cm²
39 ■ Corning Uviol 4.25 mm.
40 + Plate glass (crown) 6.5 mm.
41 • Silver film, thin
42 ○ Silver film, thick, ordinates x 10
43 • 2 silver films, thick, ordinates x 100
44 ▲ Vitaglass 2.56 mm.
45 ● Microscope cover glass 0.165 mm.
46 □ Corning 980-A 4.10 mm.
47 ⊙ Alum crystal 1.65 mm.
48 × Iceland Spar 1.67 mm.
49 • Solarized (Desert) Bottle Glass 4 mm.
Transmission
1.0
0.9
0.8
0.7
0.6
0.5
0.4
0.3
0.2
0.1
0.0
0.20
0.30
0.40
0.50 μ

Fig. 9

Photo-chemical effects of sunlight on glass are especially important in the study of solar radiation. Curve 29, Figure 7, is the transmission of an ordinary colorless bottle, and curve 28, Figure 7, is the transmission of a bottle picked up at the New Dale mining camp in the Mojave Desert. The bottle had turned a dark-violet tint, and its age may be judged from the fact that this mining camp has been abandoned for eleven years. The wave-length of the radiation producing this violet tint must be greater than 0.33 μ approximately, since this and a number of other such bottles examined by the writer are almost uniformly colored throughout, showing only a slightly deeper tint on the side exposed to the sun. It is probable that the effect is practically confined to the region λ 0.33 to 0.45 μ, where the transmission is high.

Pieces of window-glass found at the same place showed no tendency to color; and no specimen of window, plate, or optical glass showing this tint has been brought to the writer's attention. It is probable that the violet tint produced by sunlight is due to the manganese dioxide used to decolorize bottle glass, and does not appear in glass not treated with this substance. Such objectives as the Yerkes 40-inch, and those in the tower telescopes, which are much exposed to sunlight, show no trace of color due to solarization.

That the transmissions of the gold and silver films used in the ultra-violet solar radiometer are not affected by sunlight has already been pointed out.[1] These films are on the inside of the lens cells and protected from the air. After a period of more than two-and-a-half years these films show no change in transmission between the exposed portions and that behind the diaphragm, and no trace of tarnish. A case of tarnish on silver, apparently due to photochemical effects, was observed, however, in the coelostat of the Snow telescope. A 12-inch diaphragm was put on the 30-inch coelostat mirror after freshly silvering. After a few days the exposed area of the mirror became tarnished a brown color, while the remainder of the mirror was unaffected. The 24-inch fixed flat, which had no diaphragm, also showed tarnish over an area 12 inches in diameter where a spot of light from the coelostat was received. This tarnish was probably due to insufficient cleaning of the silver film after being deposited, and is not ordinarily seen in mirrors used for solar investigations.

---

[1] *Proceedings of the National Academy of Sciences*, **13**, 380, 1927.

There is a current opinion that a silver film through which the sky can be easily seen transmits nearly 100 per cent at λ 0.32 μ. Such films of chemically deposited and sputtered silver were tested and found to transmit only 8 per cent. Curve 41, Figure 9, is for a chemically deposited film, so thin that it is nearly colorless, and that not only the sky but objects at a distance are easily distinguishable. Its transmission at λ 0.32 μ is only 48 per cent. There appears to be little difference in this respect between chemically deposited and sputtered films.

Visual-light values can be obtained with radiometric apparatus by passing the source of light through a combination of green celluloid and Corning 124 J, about 4 mm thick. The efficiency of this screen is only 25–30 per cent, but it may prove useful under certain circumstances.

The writer is indebted to Mr. Nicholson for assistance in obtaining curves 35 and 36, and to Miss Richmond and Miss Ware for assistance in the computation of transmissions.

Carnegie Institution of Washington
Mount Wilson Observatory
May 1927

Contributions from the Mount Wilson Observatory, No. 337
Reprinted from the *Astrophysical Journal*, Vol. LXVI, pp. 13–42, 1927
Printed in the U.S.A.

ON THE SPECTRA OF DOUBLY AND TREBLY IONIZED TITANIUM (*Ti* III AND *Ti* IV)

By HENRY NORRIS RUSSELL[1] AND R. J. LANG

ABSTRACT

The lines of trebly ionized titanium (*Ti* IV) are *peculiar to the spectrum of the vacuum spark.* Those of *Ti* III appear in the ordinary spark, but are *much enhanced in the vacuum source.*

31 *lines* of *Ti* IV and 90 *lines* of *Ti* III have been *identified.* All of the former and most of the latter are *new. Tables* of wave-lengths and intensities based on plates obtained at Mount Wilson and Edmonton are given. The wave-lengths range from 5492 to 423 A. All the lines of *Ti* IV and all but four of *Ti* III have been *classified.*

The spectrum of Ti IV is very *regular* and consists entirely of *doublets,* arranged in series conforming to the Ritz formula. Twelve lines, of types ranging from S to H, have been identified and are tabulated. The 3D term is the lowest, and the *ionization potential* is 43.06 volts. The *doublet separations* are in excellent agreement with Landé's formula.

The spectrum of Ti III includes *triplet* and *singlet terms* and is closely analogous to that of *Sc* II. Nineteen terms, of types ranging from S to G, have been identified. The lowest term is of type ^3F, followed by ^1D, ^3P, and ^1G. The observed terms are in perfect agreement with Hund's theory, arising from the electron configurations $(3d)^2$, $3d \cdot 4s$, $3d \cdot 4p$, $3d \cdot 4d$, and $4s \cdot 4p$. The estimated *ionization potential* is 27.6 volts, with an uncertainty not exceeding 1 volt. The *term separations* are again in general agreement with Landé's formula.

The spectrum of Sc III is also briefly discussed. One new term is added (5S). All the strong lines of the spectrum which have not been observed must lie in the visible region. Their predicted positions are given.

Comparisons are made between the series spectra, *K* I, *Ca* II, *Sc* III, and *Ti* IV, and also *Ca* I, *Sc* II, and *Ti* III. *Moseley's law* as extended to the optical region is fully verified—the differences in $\sqrt{\nu/R}$ being practically constant for similar terms, from one spectrum to the next. The identifications of certain doubtful terms are thus confirmed.

The senior author of this paper has for some time been engaged in an analysis of the spectrum of titanium, with the aid of material furnished by his colleagues at the Mount Wilson Observatory. During the course of this work, it became evident that certain lines must belong to multiply ionized atoms, and a number of multiplets of *Ti* III were identified. A full analysis of these spectra, however, is not possible without observations in the extreme ultra violet; and these have been furnished by the work of the junior author. The present communication is therefore based upon observations made at Mount Wilson by Mr. Anderson and Miss Carter, and at the University of Alberta by Mr. Lang, while Mr. Russell is responsible for the analysis and discussion.

---

[1] Research Associate of the Mount Wilson Observatory, Carnegie Institution of Washington.

I. THE OBSERVATIONS

The first definite evidence of the existence of lines of titanium corresponding to higher stages of ionization than the first was found by Miss Carter, in the spectrum of the discharge of a large condenser, such as is used in "exploding" fine wires, between electrodes of metallic titanium *in vacuo*. The spectrum was photographed with a concave grating of 1-m radius, and extends from the green to λ 2100. The ordinary spark and arc spectra were taken on the same film for comparison.

Most of the lines in the "hot-spark" spectrum agree with those of the ordinary spark (*Ti* II). The stronger arc lines show faintly, but are much weaker than in the ordinary spark. Certain lines, however, which appear in the latter spectrum—many of them strongly—are greatly enhanced in the hot-spark. These lines are completely absent from the arc spectrum, in which practically all the lines of *Ti* II are present; and they appear distinctly "polar" in the ordinary spark. All these properties indicate that these are lines of *Ti* III, which is confirmed by the fact that the strongest ones obviously come in three's, as should be expected in this spectrum. Besides these lines, however, the hot-spark shows others, some of them very strong, which are absent from the ordinary spark, and form conspicuous pairs. These must belong to *Ti* IV.

These lines are illustrated in Plate III, which shows the third order near λ 2500 with the overlapping second order near λ 3750. The principal lines of the metal in its four stages of ionization are marked on the margins. The differences in their behavior are very conspicuous and show how definitely the separation of the successive spectra can be made. Another photograph of the hot-spark spectrum taken by Dr. Anderson shows lines of *Ti* III and *Ti* IV down to λ 1905.

This overlaps the region observed at Edmonton with the vacuum spectrograph. This instrument has been fully described elsewhere,[1] and it may suffice to say that the concave grating has a radius of

---

[1] *Journal of the Optical Society of America*, **12**, 523, 1926.

PLATE III

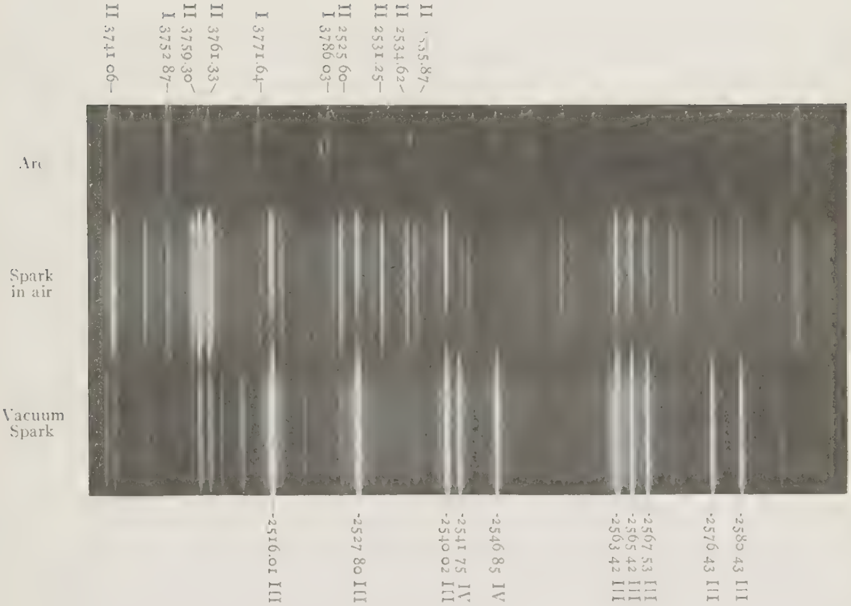

Arc, Spark, and Vacuum-Spark Spectra of Titanium
Photographed at Pasadena by Miss Carter

PLATE IV

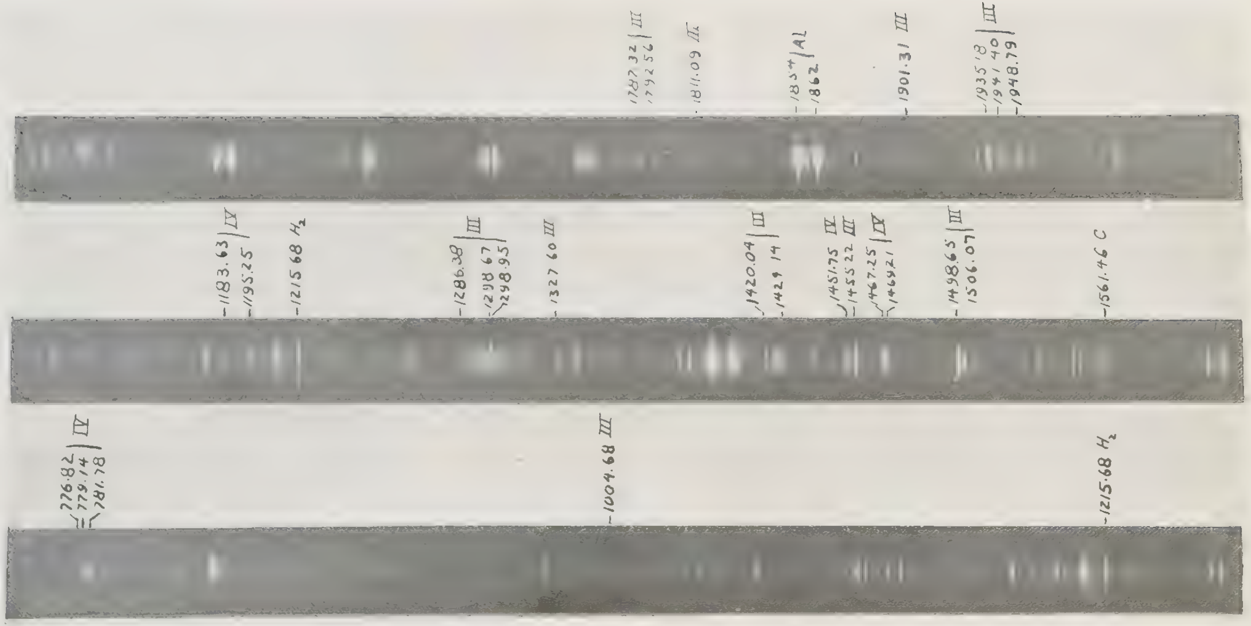

Vacuum-Spark Spectrum of Titanium

Photographed at Edmonton by R. J. Lang. The principal lines of titanium are marked, and also a few of those due to impurities, of which the most conspicuous belong to silicon and aluminum.

6 feet and 30,000 lines to the inch. The spectra obtained from the vacuum spark between electrodes of the best metallic titanium available showed the lines of silicon more strongly than those of the metal; but the former have been eliminated by comparison with the spectrum of the silicon spark, and other impurities were similarly eliminated. The remaining lines may be ascribed with some confidence to titanium. The strongest of them have been identified as belonging to *Ti* III or *Ti* IV; but the majority of the lines remain unclassified, and it is probable that most of these belong to *Ti* V, which, like *Ca* III, should be a very complex spectrum resembling that of argon. This spectrum is illustrated in Plate IV.

The measures on the Edmonton spectrograms were made by Lang, using the standards recently determined by Smith and Lang.[1] From the agreement of the observed frequency differences with those derived from the analysis of the spectrum, it appears that the probable error of a measured wave-length is approximately ±0.02 A (see below). For the longer wave-lengths, Exner and Haschek's measures are available for many lines of *Ti* III, which appear in the ordinary spark. Some of these lines have been remeasured; and many new lines of *Ti* III and *Ti* IV have been measured for the first time, by Mr. Russell on positive enlargements of the Mount Wilson films. The probable error of the resulting wave-lengths appears to be about ±0.01 A.

2. THE SPECTRUM OF THE TREBLY IONIZED ATOM (*Ti* IV)

In discussing the results, it is well to begin with the simplest spectrum, which is that corresponding to the highest degree of ionization. From theoretical considerations, this should be of the "stripped-atom" type. All the terms should be doublets, and should be arranged in normal series, closely following the Ritz formula.

The lowest terms in this spectrum were discovered by Gibbs and White.[2] The base level is a ^{2}D term, and the next a ^{1}S term, both of which combine with a higher ^{2}P term. The lines of the corresponding groups are conspicuous on the Edmonton photographs, as are also two other groups which evidently arise from combinations between the ^2P term and higher-lying ^2S and ^2D terms. The strong pair shown on the Mount Wilson photograph in Plate III have proved to arise from a transition from the new ^2D term to a ^2F term, and other combinations revealed the existence of several higher levels. Three S terms, two P's, four D's, one F, one G, and two H's were finally identified. Most of the new lines are in the region accessible with ordinary instruments; but the important pair, $3D-4F$, are in the extreme ultra violet. Their computed positions, which can be very accurately found by the aid of other combinations, are at λλ 424.18, 423.50. Lines have been observed at λ 424.28 and λ 423.58, and these are evidently the pair in question, the systematic discordance of 0.09 A being explicable by the lack of good standards in the region. This pair, and also the groups $4P-5S$ and $4P-4D$, were independently identified by Mr. Stanley Smith, to whom we are indebted for the measures of these two lines.

---

[1] *Physical Review*, 28, 36, 1926.

[2] *Proceedings of the National Academy of Sciences*, 12, 600, 1926.

The S terms are exactly represented by the Ritz formula

$$mS=16R/\{m-1.38265-2.55\times10^{-7}(mS)\}^2\ ,$$

where $m=4$, 5, 6. The term values referred to the limit of this series, with the Rydberg denominators, n^*, are given in Table I.

TABLE I

SERIES TERMS FOR *Ti* IV

		n^*			n^*			n^*
$4S_1$.....	268439.2	2.5568	$3D_3$....	348433.5	2.2442	$4F_4$....	112685.3	3.9463
				384.3	*.00119*		*7.2*	*.00012*
$5S_1$.....	136422.0	3.5866	$3D_2$....	348817.8	2.2430	$4F_3$....	112692.5	3.9462
$6S_1$.....	82982.0	4.5986	$4D_3$....	151937.3	3.3985	5G....	70316.7	4.9956
				85.7	*.00095*			
$4P_2$.....	220086.9	2.8238	$4D_2$....	152023.0	3.3975	6H....	48805.3	5.9964
	818.4	*.00534*						
$4P_1$.....	220905.3	2.8185	$5D_3$....	89951.1	4.4179	7H....	25844.3	6.9970
				39.5	*.00097*			
$5P_2$.....	117904.4	3.8580	$5D_2$....	89990.6	4.4169			
	315.8	*.00522*						
$5P_1$.....	118220.2	3.8528						

The spectrum is extremely regular in its structure. The differences of the denominator n^* for the successive pairs of terms of the same series are very nearly equal, as they should be, and the quantum defects for the "hydrogenic" G and H terms are very small. The terms 6H and 7H are each determined from only a single

TABLE II

MULTIPLETS OF *Ti* IV

	$4P_2$	$4P_1$	$5P_2$	$5P_1$	$4F_4$	$4F_3$	6H	7H
$4S_1$	(15) 48352.2 52.3	(10) 47534.1 33.9	(140535)	(140219)				
$5S_1$	(5) 83664.5 64.9	(5) 84485.9 83.3	(8) 18517.6 17.6	(6) 18201.8 01.8				
$6S_1$	(0) ?137100.9 04.9	(137923)	(1*n*) 34922.2 22.4	(0*n*) 35238.4 38.2				
$3D_3$	(20) 128346.6 46.6		(230527)		(4) 235694 748	(235741)		
$3D_2$	(10) 128730.0 30.9	(20) 127913.3 12.3	(230913)	(230597)		(3) 236083 125		
$4D_3$	(30) 68150.0 49.6		(5) 34032.4 32.9		(12) 39252.4 52 0	(3) 39245.5 45.1		
$4D_2$	(15) 68063.7 63.9	(30) 68882.3 82.3	(1) 34118.1 18.6	(4) 33802.5 02 6		(8) 39331.1 30.5		
$5D_3$	(130155)		(4) 27952.8 53.3		(2) 22734.5 34.2	(22741.4)		
$5D_2$	(130096)	(130915)	(27913 8)	(3) 28229.1 29.6		(2) 22702.6 01.9		
5G					(5) 42368.7 68.7	(5) 42375.9) 75.9	(3) 21511.4 11.4	(0) 34472.4 72.4

line, but their excellent agreement with the values which are to be anticipated is sufficient evidence of their reality.

All the series are nearly Ritzian. The expression $0.4443-3.00\times 10^{-7}$ (mD) has the values 0.3398, 0.3987, 0.4173, for the three D terms, so that the limit found from the last two, ignoring the first term, would agree very closely with that given by the S series. The normal state, 3D, is at a considerably lower level than the formula derived from the rest of the series would indicate, as happens often in other similar series. It is evident that all the series have the same limit, which should be determined with a probable uncertainty of only about 20 frequency units. The normal state of the trebly

TABLE III

IDENTIFIED LINES OF *Ti* IV

λ I.A.	Int.	ν	Designation
Air			
5492.43	(6)	18201.8	$5S_1-5P_1$
5398.82	(8)	18517.6	$5S_1-5P_2$
4647.40	(3)	21511.4	$5G-6H$
4403.54	(2)	22702.6	$4F_3-5D_2$
4397.37	(2)	22734.5	$4F_4-5D_3$
3576.44	(4)	27952.8	$5P_2-5D_3$
3541.44	(3)	28229.1	$5P_1-5D_2$
2957.50	(4)	33802.5	$4D_2-5P_1$
2937.52	(5)	34032.4	$4D_3-5P_2$
2930.14	(1)	34118.1	$4D_2-5P_2$
2900.02	(0)	34472.4	$5G-7H$
2862.67	(1*n*)	34922.2	$5P_2-6S_1$
2836.98	(0*n*)	35238.4	$5P_1-6S_1$
2547.30	(3)	39245.5	$4D_3-4F_3$
2546.85	(12)	39252.4	$4D_3-4F_4$
2541.75	(8)	39331.1	$4D_2-4F_3$
2359.51	(5)	42368.7	$4F_4-5G$
2359.11	(5)	42375.9	$4F_3-5G$
Vacuum			
2103.75	(10)	47534.1	$4S_1-4P_1$
2068.16	(15)	48352.2	$4S_1-4P_2$
1469.21	(15)	68063.7	$4P_2-4D_2$
1467.25	(30)	68150.0	$4P_2-4D_3$
1451.75	(30)	68882.3	$4P_1-4D_2$
1195.25	(5)	83664.5	$4P_2-5S_1$
1183.63	(5)	84485.9	$4P_1-5S_1$
781.78	(20)	127913.3	$3D_2-4P_1$
779.14	(20)	128346.6	$3D_3-4P_2$
776.82	(10)	128730.0	$3D_2-4P_2$
729.39	(0)	137100.9	$4P_2-6S_1$
424.28	(3)	235694	$3D_3-4F_4$
423.58	(4)	236083	$3D_3-4F_3$

ionized atom corresponds to the 3^2D_2 term, and the ionization potential is 43.06 volts.

The observed combinations between these terms are listed in Table II, which gives the wave-numbers alone, as the wave-lengths are found in Table III. The intensity of each line is given in parentheses above the observed wave-number, while the last three figures of the wave-number, computed from the data of Table I, are given below it. The computed wave-numbers of a few lines which have not been observed are given in parentheses.

It is noteworthy that no long series have been found. Only the leading member of the series which corresponds to transitions between a given level and the higher levels is strong; the next, if observable, is weak. This is a well-known characteristic of the vacuum spark.

A complete list of the lines which have been identified by their series relations as belonging to *Ti* IV is given in Table III. Certain other lines which appear in the hot-spark and may belong to this spectrum, but cannot be definitely identified, are listed in Table X.

3. A NOTE ON *Sc* III

The ultimate lines of *Sc* III have been detected by Gibbs and White,[1] and additional lines have been found by Stanley Smith[2] on plates taken by one of us. His identification of the group near λ 2000 as $4P-4D$ rather than $4P-5S$ appears to be correct. The term values which he gives are derived on the assumption that $4F=62,570$, corresponding to the Rydberg denominator 3.9720. The corresponding denominators for *K* I, *Ca* II, and *Ti* IV are 3.9930, 3.9801, and 3.9463. Smith's value was obtained by extrapolation from the first two of these; now that the last is known, interpolation gives the presumably more accurate value 3.9640, whence $4F=62,822$, so that all his term values may be increased by 250, a hardly significant correction. The resulting term values and Rydberg denominators are entered in Table IV, and also the values for other terms not yet observed, but predicted as follows. The denominators n^* for *K* I, *Ca* II, and *Ti* IV are accurately known, and hence the differences of the fractional part of their values for the successive terms of the same series (which depend upon the "Ritz correction"). These differences are small and run smoothly so that they can be interpolated for *Sc* III with considerable confidence, as shown below where the estimated values are in parentheses.

---

[1] *Proceedings of National Academy of Sciences*, **12**, 598, 1926.

[2] *Ibid.*, **13**, 66, 1927.

	K I	*Ca* II	*Sc* III	*Ti* IV
$5S-4S$	+0.0309	+0.0322	+0.0304	+0.0204
$6S-5S$	.0090	.0126	(.013)	.0120
$5P_2-4P_2$	.0313	.0362	(.037)	.0342
$6P_2-5P_2$	+ .0095	.0126	(.014)	....
$4D_3-3D_3$	− .0570	.0461	.1362	.1543
$5D_3-4D_3$	.0280	.0071	(.022)	+0.0194
$6D_3-5D_3$	.0130	+ .0031	(+ .011)	....
$5F_4-4F_4$	−0.0028	−0.0035	(−0.005)	....

In this way it was predicted that the value of n^* for 5S should be 3.420±0.002 and the term itself 84,900±100. This leads to the identification of $4P_2-5S$ as λ 1912.48 (intensity 2) for which $n=52,288$, making $5S=84,829$.

There is also a line of intensity 2 on the scandium plates at λ 1895.33 ($n=52761.3$), which appears with equal intensity in the spectrum of silicon, and faintly in that of titanium. It is in exactly the right place for $4P_1-5S$, and is probably a blend of a scandium line with some impurity.

We then have the results shown in Table IV.

TABLE IV

OBSERVED AND PREDICTED TERMS OF *Sc* III

	Observed	n^*		Predicted	n^*
4S	174156.3	2.3808	6S	50440	4.424
5S	84829.2	3.4112	$5P_2$	71330	3.720
$4P_2$	137117.1	2.6831	$5P_1$	71510	3.715
	473.7	*.0046*	$5D_3$	51410	4.382
$4P_1$	137590.8	2.6785	$5D_2$	51430	4.381+
$3D_3$	199495.5	2.2244	5F	40140	4.959
	197.5	*.00110*	5G	39560	4.995
$3D_2$	199693.0	2.2233			
$4D_3$	87393.8	3.3601			
	45.0	*.00086*			
$4D_2$	87438.8	3.3592			
4F	62822.0	3.9640			

The combinations of the predicted terms with the low terms give lines in the far ultra-violet, which, from the well-known properties of the vacuum spark, might be expected to be very faint. They have not been found. Judged by the analogy of *Ti* IV, the lines in the visible region should be much stronger. Those which might be expected to appear are, in the order of their probable intensity,

5S−5P	7406, 7506
4D−5P	6223, 6276, 6206
4F−5G	4298 (close double)
5P−5D	5018, 4978, 5023
4F−5D	8762, 8777

It is noteworthy that all these lines lie in the visible region, and about half of them in the red.

4. COMPARISON OF *K* I, *Ca* II, *Sc* III, *Ti* IV, ETC.

It is well known that the term values in atomic systems which contain the same number of electrons exhibit marked regularities.

The values of $\sqrt{\nu/R}$ (where R is the Rydberg constant, and ν any given spectroscopic term, referred to the limit of the series to which it belongs) form an arithmetical progression for successive atoms in order of atomic number.

The constant difference in this progression is nearly the same for all terms involving an electron of the same total quantum number; whence it follows that the wave-numbers of lines corresponding to transitions of an electron between two orbits of the same total quantum number will themselves be in arithmetical progression with increasing atomic number (which is the irregular doublet law).

A thorough test of these relations can be made by comparison of terms from successive spectra *K* I[1], *Ca* II[2], *Sc* III, and *Ti* IV. The values of $\sqrt{\nu/R}$ for such terms as have been identified in *Ti* IV are given in Table V with the differences Δ between each spectrum and the next.

The terms are arranged in order of their total quantum numbers, according to Bohr's theory of atomic structure, and the means of the two components of the double terms are taken.

---

[1] Fowler, *Report on Series in Line Spectra* (London, 1922).

[2] Saunders and Russell, *Astrophysical Journal*, 62, 1, 1925.

Certain values of ν which have not been observed, but can be rather accurately estimated (including those in *Sc* III, discussed above), are given in parentheses in the table, as are the differences involving them. The differences in $\sqrt{\nu/R}$ are not constant, but run very smoothly. For *V* V, for which the data given by Gibbs and White suffice only to determine the differences of the terms 3D, 4S, 4P, the mean value of the last-named term has been derived on the assumption that the difference of $\sqrt{\nu/R}$ was the same as the mean value for the two preceding difference columns. This gives $4P_2=318{,}567$, $4P_1=319{,}833$, $4S=378{,}113$, $4D_3=525{,}613$ $5D_2=526{,}250$. The differences of $\sqrt{\nu/R}$ for 3D and 4S can then be determined, and fit smoothly into the scheme. The identification of further terms in this spectrum is much to be desired.

TABLE V

VALUES OF $\sqrt{\nu/R}$

Term	*K* I	Diff.	*Ca* II	Diff.	*Sc* III	Diff.	*Ti* IV	Diff.	*V* V
3D	0.350	0.535	0.865	0.484	1.349	0.434	1.783	0.407	2.190
4S	.565	.369	.934	.326	1.260	.305	1.565	.292	1.857
4P	.448	.353	.801	.319	1.120	.298	1.418	(0.288)	1.706
4D	.263	.334	.597	.296	0.893	.284	1.177	....	....
4F	.250	.252	.502	.255	.757	.257	1.014	....	....
5S	.357	.273	.630	.250	.880	.235	1.115	....	....
5P	.306	.260	.566	(.242)	(.808)	(.229)	1.037	....	....
5D	.210	.248	.458	.227	(.685)	(.220)	0.905	....	....
5F	.200	.202	.402	....	....	....	....	....	....
5G	.200	.200	(.400)	(.200)	(.600)	(.201)	.801	....	....
6S	.263	.204	.467	(0.210)	(0.677)	(0.193)	.870	....	....
6P	.234	.200	.430	....	....	....	....	....	....
6D	.174	.198	.372	....	....	....	....	....	....
6F	.167	0.167	.334	....	....	....	....	....	....
6G	....	....	0.333	....	....	....	....	....	....
6H	0.166	....	....	....	....	....	0.667	....	....

The pairs 4S−4P have been identified by Gibbs and White[1] for *Cr* VI and *Mn* VII. On taking the mean of the two lines (as above) and estimating the values of $\sqrt{\nu/R}$ for 4P as 1.996 and 2.286, by adding the difference 0.290 twice more, the resulting values for 4S are found to be 2.149 and 2.442, giving two new horizontal differences of 292 and 293, which fit perfectly into the scheme. This means, however, only that the irregular doublet law is closely followed, as Gibbs and White have already pointed out.

---

[1] *Proceedings of the National Academy of Sciences*, 12, 676, 1926.

For the separation $\Delta\nu$ of the components of a doublet term, two formulae have been given. The first is the "regular doublet law," extended to the optical region by Millikan and Bowen.[1] According to this $\Delta\nu = K(Z-s)^4$, where K has the value 0.0456 for 4P terms, 0.0234 for 5P, 0.036 for 3D, 0.0152 for 4D, and 0.0076 for 4F, and s is a screening constant, which may be expected to be roughly constant, decreasing slowly along any given series of "stripped atoms."

Gibbs and White have given the values of s for the 4P terms, and those computed from the formulae for other terms are added here:

	K I	*Ca* II	*Sc* III	*Ti* IV	*V* V	*Cr* VI	*Mn* VII
4P	13.04	11.64	10.91	10.43	10.09	9.85	9.75
5P	13.68	12.40	(11.62)	11.22	. . . .	. . . .	. . . .
3D	16.04	13.59	12.40	11.84	11.48	. . . .	. . . .
4D	. . . .	15.13	13.61	13.32	. . . .	. . . .	. . . .
4F	. . . .	. . . .	. . . .	12.13	. . . .	. . . .	. . . .

The screening numbers s are of the same order of magnitude, but the differences among them are considerable, and correspond to very much greater proportional differences in the values of $\Delta\nu$.

The second law of separation is that suggested by Landé, and since then found to be deducible from the theory of the spinning electron. It may be written

$$\Delta\nu = \frac{R\alpha^2 Z_a^2 Z_i^2}{K(K+1)n^{*3}} ,$$

where R and α have their usual meanings, $K=1$ for P terms, 2 for D terms, etc., n^* is the Rydberg denominator, Z_a is the effective nuclear charge for the outer part of the electron orbit, and is 1 for the neutral atom, 2 for the singly ionized atom, etc., and Z_i is the effective charge for the inner part of the orbit (which may be written in the form $Z-s$, where s is a new screening constant). The corresponding differences in the Rydberg denominator are given by the much simpler formula

$$\Delta n = \frac{\alpha^2 Z_i^2}{2K(K+1)} ,$$

($\alpha^2 = 5.31 \times 10^{-5}$). This difference should therefore be constant.

---

[1] *Physical Review*, **24**, 209–233, 1924.

The values of Δn are actually nearly constant for each series in *K* I, *Ca* II, and *Ti* IV, so far as they have been observed. For the other stripped atoms of this series only the values for the leading terms are known, and therefore the values for these terms alone are tabulated below, with the resulting values of *s*.

In determining Δn for the last three spectra, the values of $\sqrt{\nu/R}$ derived above have been used.

TABLE VI

DOUBLET SEPARATIONS

	K I	*Ca* II	*Sc* III	*Ti* IV	*V* V	*Cr* VI	*Mn* VII
4P:							
$\Delta\nu$	57.5	222.8	473.8	818.4	1265	1822	2465
$10^5\,\Delta n$	295	392	486	524	560	592	618
Z_i	14.9	17.2	19.1	19.9	20.6	21.1	21.6
s	4.1	2.8	1.9	2.1	2.4	2.9	3.4
3D:							
$\Delta\nu$	2.74	60.8	197	384.5	637	....	....
$10^5\,\Delta n$	29	86	113	119	135	....	....
Z_i	8.1	11.7	16.0	16.4	17.4	....	....
s	10.9	8.3	5.0	5.6	5.6	....	....
4F:							
$\Delta\nu$	....	....	....	7.3	....	....	....
$10^5\,\Delta n$	....	....	....	12	....	....	....
Z_i	....	....	....	7.4	....	....	....
s	....	....	....	14.6	....	....	....

For the P terms the values of *s* are remarkably steady and run very smoothly. In this case, the tabulated numbers are the differences of two rather large quantities, and the inequality of their values corresponds to far less percentage difference in the doublet separations than in the case of the other formula. When it is further considered that Landé has shown[1] that his formula represents all the doublets in the arc and spark spectra of alkali-like structure from *Li* to Ra^+, with values of *s* ranging only from 2 to about 8, it is evident that it gives really a remarkable approximation to the truth.

Why it is better than the "relativity doublet" formula becomes clear when it is considered that the latter is derived on the assumption that the electron moves throughout its orbit in a Coulomb field of intensity corresponding to the nuclear charge $Z-s$, while Landé's formula is based on the assumption of an effective charge of different amounts Z_i and Z_o in the inner and outer parts of the orbit. As several simplifying assumptions were made in deriving it, it is not to be expected that s should come out exactly the same in all cases.

---

[1] *Zeitschrift für Physik*, 25, 46, 1924.

For the D terms the values of s are greater, which might be expected, as the d orbits do not penetrate so deeply into the atomic structure. The screening appears to be exceptionally great in the case of potassium, giving a very narrow doublet. This may well be connected with the small quantum defect and the nearly hydrogenic character of the 3d orbit in this atom. The screening for the 4F term, in the single case where this is known, is still greater.

5. THE SPECTRUM OF DOUBLY IONIZED TITANIUM (*Ti* III)

The conspicuous groups near λ 2500, two of which are shown in Plate III, are evidently due to *Ti* III. The stronger lines are given by Exner and Haschek; a number of weaker ones were added from the Mount Wilson plates. With the aid of these, multiplets were found corresponding to transitions from a ^3D term to a triad of terms ^3P, $^3D'$, ^3F. The strong isolated line at λ 2985 was identified as a $^1D-{}^1D'$ combination, and a few faint intersystem combinations were located.

On theoretical grounds, there was reason to anticipate the existence of $^3P'$ and $^3F'$ terms, lower than the ^3D, and combining with the P, D′, F triad. The corresponding multiplets were easily found in the list of lines measured at Edmonton. Two of the three strongest lines of the group $^3F'-{}^3D'$ are too close to resolve even in the second order, and the third falls just upon the strongest line of a multiplet of silicon (which shows strongly as an impurity in the titanium). Comparisons with the spectrum of pure silicon, however, show that the line in question is considerably strengthened when titanium is present.

This completes the list of easily recognizable multiplets; but further progress was made by comparison with the very similar spectrum of *Sc* II,[1] aided by the values of $\sqrt{\nu/R}$ for this spectrum and for *Ca* I. In this way a considerable group of lines lying between λ 1700 and λ 1960 was assorted into multiplets corresponding to transitions from the ^{3}P, ^{3}D′, ^{3}F triad, to a higher-lying "pentad" of terms ^{3}S, ^{3}P′, ^{3}D, ^{3}F′, ^{3}G, while a group of faint lines near λ 1000 was identified as a ^{3}D – ^{3}P multiplet like that near λ 2500 in *Sc* II. In addition to these, a few lines which could not be identified by the combination principle have been classified with the aid of the values of $\sqrt{\nu/R}$. In most cases this identification is practically certain. In a few, where it is more doubtful, the corresponding terms are marked with a colon in the list. The arguments in favor of these identifications are given in section 7.

---

[1] Russell and Meggers, *Scientific Papers of the Bureau of Standards* (in press).

Table VII gives a list of all the terms which have thus been identified, and shows with what other terms they have been observed to combine. The term values are counted *upward* from the lowest-known level, $^3F'_2$, which is doubtless the lowest for the atom in this state of ionization.

The multiplets resulting from the combinations of these terms are given in Table VIII, which is arranged like Table II. In some cases a line which is believed to be a blend is listed in more than one place.

The multiplets arising from combinations between the low terms and the middle triad are strong, and all the predicted lines of importance are observed, except for some blends too close to be resolvable. The groups arising from transitions from the middle triad to the higher levels are faint and incomplete—so much so, indeed, that, if nothing but the data of Table VIII were available, the reality of the term b^{3}D would be very doubtful. Strong confirmation of the arrangement given above is found, however, by comparison with an exactly similar group of multiplets in *Sc* II, which are much stronger, and substantially complete, so that their interpretation cannot be doubted.

The energy levels of the leading components of the five terms involved, relative to $^3G_5$ as origin, and the separations of the components of the terms, are as follows:

Term	^{3}G	^{3}F′	^{3}D	^{3}P′	^{3}S
Level *Sc* II	0	3072	−454	4250	616
Level *Ti* III	0	3901	547	6251	3371
Separation *Sc* II	108.8, 81.3	83.3, 70.5	72.4, 54.4	59.1, 31.2	....
Separation *Ti* III	216.7, 159.7	164.0, 143.5	145.6, ...	121.7, 58.9	....

The relative levels of the five terms oscillate in just the same way, while the component separations are in all cases very nearly twice as great for *Ti* III as for *Sc* II. The similarity of the two sets of terms would therefore appear to be beyond question. The faint multiplet a^3D-b^3P was found by means of the differences in $\sqrt{\nu/R}$ from corresponding terms in *Sc* II and *Ca* I.

TABLE VII

TERMS OF *Ti* III

Desig.	Level	Combinations
$a^3F'_2$	0.0	a^3D', a^3F
	183.7	
$a^3F'_3$	183.7	
	238.2	
$a^3F'_4$	421.9	
a^1D_2	8472.6	a^1P, a^1D', a^1F a^3D'
$a^3P'_0$	10536.4	a^3P, a^3D', a^3F
	67.1	
$a^3P'_1$	10603.5	
	117.6	
$a^3P'_2$	10721.1	
a^1S_0	14052.7?	a^1P, a^3P?
a^1G_4	14398.5	a^1F
a^3D_1	38063.50	a^3P, b^3P, a^3D' a^3F, a^1D'
	134.48	
a^3D_2	38197.98	
	227.21	
a^3D_3	38425.19	
b^1D	41703.65	a^1P, a^1D', a^1F a^3P, a^3D', a^3F
a^1D'	75197.43	a^1D, b^1D, a^3D
$a^3D'_1$	76999.70	a^3P', b^3P', a^3D, b^3D, a^3F', b^3F'
	166.95	
$a^3D'_2$	77166.65	a^1D, b^1D
	257.55	
$a^3D'_3$	77424.20	
a^3F_2	77421.48	a^3P', a^3D, a^3F' b^3F', a^3G, b^1D
	324.70	
a^3F_3	77746.18	
	412.53	
a^3F_4	78158.71	
a^3P_0	80943.95	a^3S, a^3P', b^3P' a^3D, b^1D
	−5.93	
a^3P_1	80938.02	
	85.58	
a^3P_2	81023.60	
a^1F_3	83116.58	a^1D
a^1P_1	83795.70	a^1D
a^3G_3	129096.3	a^3F
	159.7	
a^3G_4	129256.0	
	216.6	
a^3G^5	129472.6	
b^3D_1	....	a^3D'
b^3D_2	129873.9	
	145.6	
b^3D_3	130019.5	
a^3S_2	132854.6	a^3P
$b^3F'_2$	133067.2	a^3D', a^3F
	142.5	
$b^3F'_3$	133209.7	
	164.0	
$b^3F'_4$	133373.7	
$b^3P'_0$	135543.8	a^3P, a^3D'
	58.6	
$b^3P'_1$	135602.4	
	121.7	
$b^3P'_2$	135724.1	
b^3P_0	137262	a^3D
	228	
b^3P_1	137490	
	481	
b^3P_2	137971	

TABLE VIII

MULTIPLETS OF *Ti* III

	a^3F_4	a^3F_3	a^3F_2	$a^3D'_3$	$a^3D'_2$	$a^3D'_1$	a^3P_2	a^3P_1	a^3P_0
$a^3F'_4$	(40) 77737.5 37.0	(30) 77323.9 24.5	...	(50) 77001.9 02.5	...	...	...	...	...
$a^3F'_3$	(3) 77973.3 75.0	(30) 77560.2 62.5	(50) 77239.8 37.8	(50) 77239.8 40.5	(40) 76985.3 83.0	...	...	...	...
$a^3F'_2$	...	... (77746.2) ...	(20) 77420.0 21.5	...	(30) 77168.3 66.7	(50) 77001.9 999.4	...	...	...
a^1D_2	...	...	...	(2) 68951.8 51.6	...	...	...	...	...
$a^3P'_2$	...	(5) 67025.0 25.1	...	(20) 66703.5 03.1	5d 66449.2 45.6	...	(25) 70303.2 02.5	(20) 70216.8 16.9	...
$a^3P'_1$	...	...	(1) 66819.0 18.0	...	(10) 66561.9 63.2	(10) 66398.0 96.2	(15) 70420.5 20.1	(20) 70338.8 34.9	(20) 70338.8 40.4
$a^3P'_0$	...	...	...	...	...	(10) 66463.3 63.3	...	(15) 70401.7 01.6	...
a^3D_3	(20) 39733.52 33.52	(1) 39320.95 20.99	...	(15) 38998.73 99.01	(5) 38741.64 41.66	...	(6) 42598.52 98.41	...	...
a^3D_2	...	(15) 39548.20 8.20	(1) 39224.08 3.50	(1) 39226.23 26.22	(8) 38968.31 8.67	(5) 38801.79 1.72	(3) 42825.71 25.62	(5) 42740.02 40.04	...
a^3D_1	...	...	(15) 39357.96 7.98	...	(1) 39103.03 03.15	(8) 38936.28 36.20	(1) 42959.85 60.10	(3) 42874.55 74.52	(3) 42880.45 80.45

TABLE VIII—*Continued*

	a^3F_4	a^3F_3	a^3F_2	$a^3D'_3$	$a^3D'_2$	$a^3D'_1$	a^3P_2	a^3P_1	a^3P_0
b^1D_2		(1) 36041.90 42.53	(1) 35717.65 17.83	(0) 35719.97 20.65	(1) 35462.90 63 00			(0) 39234.35 34.37	
a^3G_5	(5) 51313.9 13.9								
a^3G_4	(1) 51098.1 97.3	(4) 51509.2 09.8							
a^3G_3		(51300)	(3) 51674.8 74.8						
$b^3F'_4$	(2) 55215.5 15.0	(1) 55627.0 27.5		(2) 55949.7 49.5					
$b^3F'_3$	(55051.0)	(55463.5)	(55788.2)	(2) 55786.1 85.5	(1) 56042.5 43.0				
$b^3F'_2$		(55321.0)	(0) 55645.2 45.7		(1) 55901.5 00 5	(1) 56067.0 67.3			
b^3D_3	(51860.8)	(52273.3)		(3) 52595.3 95.3	(52852.9)		(48995.9)		
b^3D_2		(52127.7)	(52452.5)	(52449.7)	(0) 52707.3 07.3	(52874.2)	(48800.3)	(48935.9)	
b^3D_1									

TABLE VIII—*Continued*

	a^3F_4	a^3F_3	a^3F_2	$a^3D'_3$	$a^3D'_2$	$a^3D'_1$	a^3P_2	a^3P_1	a^3P_0
$b^3P'_2$				(00) 58300.8 299.9	(58557.5)		(1) 54700.4 00.5	(0) 54785.5 86.1	
$b^3P'_1$					(58435.8)	(58602.7)	(0) 54578.8 78.8	(0) 54662.1 64.0	(0) 54662.1 58.5
$b^3P'_0$						(58544.1)		(0) 54605.8 05.8	
a^3S_1							(1) 51831.2 31.0	(00) 51916.3 16.6	(51910.4)

TABLE VIII—*Continued*

	b^3P_2	b^3P_1	b^3P_0
a^3D_3	(2) 99534 536		
a^3D_2	(00) 99777 773	(1) 99290 292	
a^3D_1		(0) 99428 427	(0) 99198 198

	a^1P_1	$a^1D'_2$	a^1F_3
a^1D_2	(15) 75321.7 23.1	(30) 66726.7 24.8	(2) 74642.5 44.0
b^1D_2	(6) 42092.05 92.05	(10) 33493.78 93.78	(15) 41412.93 12.93
a^1G_4			(40) 68718.1 18.1
a^3D_3		(0) 36772.22 72.24	
a^3D_2		(3) 36909.36 99.47	
a^3D_1		(3) 37134.03 33.93	

Of the singlet terms, b^1D and a^1D' are confirmed by several intercombinations. There should be ^1P and ^1F terms to complete the triad, and, by analogy with *Sc* II, these should combine with b^1D and give strong lines not far from λ 2400. Two strong lines of *Ti* III occur at λ 2414 and λ 2375, and nothing else remains unaccounted for in this part of the spectrum. There is a second ^1D term in *Sc* II, intermediate in level between the $^3F'$ and $^3P'$ terms, and related to them. The corresponding term in *Ti* III should be much lower than that already found, and should combine with a^1P more strongly than with a^1F. After some searching, this was found. It combines with a^1P, a^1D', a^1F, and a^3D_2'. The first combination gives a strong line at λ 1327.61, which was accidentally omitted from the original list, but is clearly due to titanium, as is confirmed by the close agreement of the observed and calculated positions.

A ^1G term appears in *Sc* II, at a little higher level than a^3P' which combines with the ^1F term to give a very strong line. The strong unclassified line of *Ti* at λ 1455 probably represents the same combination in *Ti* III. Though no other combinations with this level have been found, its reality is confirmed by the test depending on $\sqrt{\nu/R}$ (see below). A low ^1S term is also present in *Sc* II, combining with a^1P and a^3P, to give rather faint lines. Two lines at λ 1495 and λ 1433 show the right frequency difference, and about the right relative intensity. They have been inserted in the table, but are marked with a question, for the agreement may be accidental, and the resulting term value lies higher than might be expected.

All the stronger vacuum-spark lines of titanium have now been accounted for as belonging to *Ti* III or *Ti* IV. About 120 additional lines have been observed, of which only 11 have estimated intensities greater than 4. The three strongest are of intensity 10. Most, if not all, of these lines are probably due to *Ti* V.

Table IX gives all the lines which are known to belong to *Ti* III, including a few not appearing in the foregoing analysis, which are identified by their behavior in the spark and hot-spark. The wave-lengths shorter than λ 2000 are from measures by the authors (almost all by Mr. Lang) on the Edmonton plates. For the longer wave-lengths, those marked (**) have been measured for the first time on the Mount Wilson plates, and those marked (*) remeas-

TABLE IX

LINES OF TITANIUM III

λ I.A.	Int.	ν	Designation
Air			
**4215.55	5	23715.04	....
**4207.54	3	23760.18	....
**4204.95	2	23774.82	....
**4200.11	2	23802.21	....
2984.76	10	33493.78	$b^1D_2-a^1D'_2$
*2819.02	1	35462.90	$b^1D_2-a^3D'_2$
*2798.95	1	35717.65	$b^1D_2-a^3F_2$
**2798.73	0	35719.97	$b^1D_2-a^3D'_3$
*2773.73	1	36041.90	$b^1D_2-a^3F_3$
**2718.64	0	36772.22	$a^3D_3-a^1D'_2$
2701.95	1	36999.36	$a^3D_2-a^1D'_2$
2692.15	1	37134.03	$a^3D_1-a^1D'_2$
2580.43	5	38741.64	$a^3D_3-a^3D'_2$
2576.43	5	38801.79	$a^3D_2-a^3D'_1$
2567.53	8	38936.28	$a^3D_1-a^3D'_1$
2565.42	8	38968.31	$a^3D_2-a^3D'_2$
2563.42	15	38998.73	$a^3D_3-a^3D'_3$
**2556.58	1	39103.03	$a^3D_1-a^3D'_2$
**2548.69	1	39224.08	$a^3D_2-a^3F_2$
**2548.55	1	39226.23	$a^3D_2-a^3D'_3$
**2547.98	0	39234.35	$b^1D_2-a^3P_1$
*2542.41	1	39320.95	$a^3D_3-a^3F_3$
2540.02	15	39357.96	$a^3D_1-a^3F_2$
*2527.80	15	39548.20	$a^3D_2-a^3F_3$
2516.01	20	39733.52	$a^3D_3-a^3F_4$
2413.97	15	41412.93	$b^1D_2-a^1F_3$
2375.02	6	42092.05	$b^1D_2-a^1P_1$
2346.78	6	42598.52	$a^3D_3-a^3P_2$
2339.01	5	42740.02	$a^3D_2-a^3P_1$
2334.33	3	42825.71	$a^3D_2-a^3P_2$
2331.67	3	42874.55	$a^3D_1-a^3P_1$
2331.35	3	42880.45	$a^3D_1-a^3P_0$
2327.04	1	42959.85	$a^3D_1-a^3P_2$
2237.82	1	44672.43	....
2199.30	1	45454.79	....
Vacuum			
1957.02	00	51098.1	$a^3F_4-a^3G_4$
1948.79	5	51313.9	$a^3F_4-a^3G_5$
1941.40	4	51509.2	$a^3F_3-a^3G_4$
1935.18	3	51674.8	$a^3F_2-a^3G_3$
1929.34	1	51831.2	$a^3P_2-a^3S_1$
1926.18	00	51916.3	$a^3P_1-a^3S_1$
1901.31	3	52595.3	$a^3D'_3-b^3D_3$
1897.27	0	52707.3	$a^3D'_2-b^3D_2$
1832.21	0	54578.8	$a^3P_2-b^3P'_1$
1831.31	0	54605.8	$a^3P_1-b^3P'_0$
1829.42	0	54662.1	$\left\{\begin{array}{l} a^3P_1-b^3P'_1 \\ a^3P_0-b^3P'_1 \end{array}\right.$
1828.14	1	54700.4	$a^3P_2-b^3P'_2$
1825.30	0	54785.5	$a^3P_1-b^3P'_2$

TABLE IX—*Continued*

λ I.A.	Int.	ν	Designation
Vacuum			
1811.09	2	55215.4	$a^3F_4-b^3F'_4$
1797.69	1	55627.0	$a^3F_3-b^3F'_4$
1797.10	0	55645.2	$a^3F_2-b^3F'_2$
1792.56	2	55786.1	$a^3D'_3-b^3F'_3$ $a^3F_2-b^3D_2$
1788.86	1	55901.5	$a^3D'_2-b^3F'_2$
1787.32	2	55949.7	$a^3D'_3-b^3F'_4$
1784.36	1	56042.5	$a^3D'_2-b^3F'_3$
1783.58	1	56067.0	$a^3D'_1-b^3F'_2$
1715.24	00	58300.8	$a^3D'_3-b^3P'_2$
1506.07	10	66398.0	$a^3P'_1-a^3D'_1$
1504.91	5D	66449.2	$a^3P'_2-a^3D'_2$
1504.59	10	66463.3	$a^3P'_0-a^3D'_1$
1502.36	10	66561.9	$a^3P'_1-a^3D'_2$
1499.17	20	66703.5	$a^3P'_2-a^3D'_3$
1498.65	30	66726.7	$a^1D_2-a^1D'_2$
1496.59	1	66819.0	$a^3P'_1-a^3F_2$
1495.08	1	66886.0	$a^1S_0-a^3P_1$?
1491.98	5	67025.0	$a^3P'_2-a^3F_3$
1455.22	40	68718.1	$a^1G_4-a^1F_3$
1450.29	2	68951.8	$a^1D_2-a^3D'_3$
1433.85	2	69742.3	$a^1S_0-a^1P_1$
1424.14	20	70216.8	$a^3P'_2-a^3P_1$
1422.41	25	70303.2	$a^3P'_2-a^3P_2$
1421.69	20	70338.8	$a^3P'_1-a^3P_1$ $a^3P'_1-a^3P_0$
1420.42	15	70401.7	$a^3P'_0-a^3P_1$
1420.04	15	70420.5	$a^3P'_1-a^3P_2$
1339.72	2	74642.5	$a^1D_2-a^1F_3$
1327.60	15	75321.7	$a^1D_2-a^1P_1$
1298.95	40	76985.3	$a^3F'_3-a^3D'_2$
1298.67	50	77001.9	$a^3F'_4-a^3D'_3$ $a^3F'_2-a^3D'_1$
1295.91	30	77168.3	$a^3F'_2-a^3D'_2$
1294.67	50	77239.8	$a^3F'_3-a^3D'_3$ $a^3F'_3-a^3F_2$
1293.26	30	77323.9	$a^3F'_4-a^3F_3$
1291.64	20	77420.0	$a^3F'_2-a^3F_2$
1289.32	30	77560.2	$a^3F'_3-a^3F_3$
1286.38	40	77737.5	$a^3F'_4-a^3F_4$
1282.49	3	77973.3	$a^3F'_3-a^3F_4$
1008.08	0	99198	$a^3D_1-b^3P_0$
1007.15	1	99290	$a^3D_2-b^3P_1$
1005.75	0	99428	$a^3D_1-b^3P_1$
1004.68	2	99534	$a^3D_3-b^3P_2$
1002.23	00	99777	$a^3D_2-b^3P_2$

ured there. The rest are Exner and Haschek's, reduced to the international scale.

A good test of the accuracy of the vacuum wave-lengths is afforded by the constant differences in the multiplets, since a number of these are determined with high precision by means of the multiplets in the region of longer wave-length. The average residual O−C for all the lines involving the low terms a^3F', a^3P', and a^1D is ±1.17 frequency units, which corresponds to ±0.020 A. The largest residual, 0.08 A, belongs to an unresolved double line; no other exceeds 0.05 A. Since, on the average, these residuals correspond to differences from the mean of 3.5 quantities, the probable error of the measured wave-lengths would also be ±0.02 A, provided that all the errors arose from this source. They may actually be a little less. For the groups near λ 2500, involving the terms a^3D and b^1D, the average residual for 27 lines is 0.009 A, giving a probable error rather less than ±0.01 A.

A few lines of longer wave-length, which appear in the spectrum of the Mount Wilson hot-spark between titanium electrodes and may belong to *Ti* III or *Ti* IV, but have not been classified, are given in Table X. None of these lines is visible in the ordinary spark.

TABLE X

LINES PROBABLY BELONGING TO *Ti* III OR *Ti* IV

λ I.A.	Int.	ν	λ I.A.	Int.	ν
6292.43	2	15887.72	5812.01	4	17200.99
6246.56	2	16004.39	5801.27	6	17232.84
6243.47	2	16012.30	5722.72	2	17439.67
6234.46	0	16035.42	5695.97	10	17551.41
6231.10	0	16044.05	5306.80	5	18838.52
5889.69	2*h*	16974.13	5301.19	5	18858.45
5885.91	6	16985.03	5278.16	7	18940.74
5877.75	4	17008.60			

6. THEORETICAL INTERPRETATION OF THE SPECTRUM OF *Ti* III

The doubly ionized atom of titanium has two electrons outside the complete "argon shell," and these alone are effective in producing the optical spectrum. These electrons may occupy orbits of types 4s, 4p, 3d, 4f, or others with higher total quantum numbers.[1] In *Ti* IV, where there is but one active electron, each orbit corresponds to a single spectroscopic term of the same name, 4S, 4P, 3D, etc. It is evident from the term values that, in this case, the 3d electron is the most closely bound, next 4s, then 4p, 4d, etc.

---

[1] The word "orbit" is here used for convenience, to describe the corresponding feature of the atomic structure, with full recognition of the possibility of more complete interpretations in other terms. The notation 4s, 4p, and 3d is, by definition, exactly equivalent to Bohr's 4_1, 4_2, 3_3, ... , s, p, d, f, being substituted for the subscripts 1, 2, 3, 4.

We may therefore expect that the normal state of lowest energy in *Ti* III will be one in which both electrons are in 3d orbits, which we may denote by $(3d)^2$. The spectroscopic terms which correspond to this atomic configuration are given by Hund's theory[1] as $^3P'$, $^3F'$, ^1S, ^1D, ^1G, and of those the $^3F'$ should lie the lowest.[2] The lowest term is actually of this type, a^3F'. The terms a^3P' and a^1D evidently arise also from this configuration, while the probable term a^1G and the suspected a^1S complete the group.

Next lowest in energy, but considerably higher, should be the configuration 3d·4s, which should give rise to a ^3D and a ^1D term. These are evidently a^3D and b^1D.

None of the terms so far mentioned should combine with another to produce spectral lines, since such a transition would demand the shift of an electron from an s to a d orbit; but they should all combine (as far as their inner-quantum numbers permit) with the terms arising from the atomic configuration 3d·4p, which can be reached from $(3d)^2$ or 3d·4s by "permissible" changes of an s orbit or a d orbit to a p orbit. This last configuration should give terms of the types ^3P, $^3D'$, ^3F, ^1P, $^1D'$, ^1F. The terms called aP, aD′, and aF in the triplet and singlet systems satisfy these conditions perfectly. The configuration 4s·4p should give terms ^3P, ^1P. These should combine strongly with those coming from 4s·3d, and much less strongly with those of origin $(3d)^2$, for in the latter case one electron would have to jump from a d to an s orbit and the other from a d to a p, and such changes, though not impossible, are relatively unlikely.

The term b^3P meets these requirements. The corresponding singlet term has not been found.

The configuration 3d·4d should give high-lying terms which combine with the P, D′, F, triads, at the middle level, but not with the low terms. Here Pauli's restriction is not operative, and we should expect S, P′, D, F′, G terms in both singlets and triplets. The full set of triplet terms has been found—a^3S, b^3P', b^3D, b^3F', a^3G. The singlets should be much harder to identify and have not been detected.

---

[1] *Zeitschrift für Physik*, **33**, 345–371, 1925.

[2] The assignment of the accents follows Heisenberg's rule (*ibid.*, **32**, 859, 1925).

All the observed terms in *Ti* III have now been interpreted. They are found to arise from just those atomic configurations which might be expected to give the stronger lines, and their relative energy levels are exactly what might be expected.

The configurations which should theoretically come next in importance are $3d \cdot 5s$ and $(4p)^2$, the former giving ^3D and ^1D terms, and the latter $^3P'$, ^1S, ^1D. Three of these five terms have been identified in *Sc* II, and some of them may yet be found in *Ti* III.

The terms of origin $(3d)^2$ and $3d \cdot 4d$ represent the first two members of a series; but, as is shown by the analogy of *Sc* II, or, for that matter, of *Ti* IV, the Rydberg formula cannot safely be applied to them, for the binding energy of the low 3d electron is abnormally great, and the application of this formula leads to too high a limit for the series, while the series involving changes in an s electron gives a much better value.

The application of the simple Rydberg formula to the 3D and 4D terms in *Ti* IV leads to an ionization potential of 45.7 volts, 2.7 volts too high.

Similar treatment of the series in *Sc* II, beginning with the $^3F'$, $^3P'$, and ^1D terms of the $(3d)^2$ configuration, gives ionization potentials of 13.7, 13.5, and 13.5 volts, as against 12.8 given by the more trustworthy series.

The uncorrected Rydberg formula therefore gives a result which is too high by 6 per cent for *Ti* IV and for *Sc* II also. If applied to the terms a^3F', b^3F' and a^3P', b^3P' of *Ti* III, it indicates that the limits of the series to which these terms belong, which is 3^2D_3 in *Ti* IV, lie at heights of 241,277 and 240,170 frequency units above the lowest level, $^3F'_2$ in *Ti* III. The corresponding ionization potentials are 29.79 and 29.65 volts. On the assumption that the mean of these values is again 6 per cent too high, the true value of the ionization potential may be estimated as 28 volts, which is probably right within a volt or so.

7. COMPARISON OF *Ca* I, *Sc* II AND *Ti* III

The spectra of atoms comprising two or more spectroscopically active electrons may be compared as in section 4 by tabulating the values of $\sqrt{\nu/R}$. One precaution is necessary here, however, for which no need arose in the simpler case discussed in section 4. In that instance all the series converge toward a single limit, representing the normal energy state of the atom stripped down to the argon shell. In the general case the series fall into groups having different limits, corresponding to different states of the atom in the next higher degree of ionization. For example, starting with the configuration 3d·4p of *Ti* III, the p electron may be shifted to 5p, 6p, etc., orbits, while the other is unchanged, giving a series with the term 3^2D of *Ti* IV as limit; or the d electron may be shifted, giving a quite different series, with the 4^2P term as limit.

Every term of *Ti* III (and of all other similar spectra) therefore belongs to two series, which have different limits—with the exception of terms arising from configurations such as $(3d)^2$.

In general, it is advantageous to measure the value of ν from the lower of these two limits; but, even so, this limit will not be the same in all cases. For example, for the 3d·4p configurations of *Ti* III, it will be 3^2D of *Ti* IV, for 4p·4s, 4^2S; and for $(4p)^2$, 4^2P. The ionization potential is usually measured from the state of lowest energy in one spectrum to that of lowest energy in the next—e.g., from $^1S_0$ in *Ca* I to $^2S_1$ in *Ca* II, from $^3D_1$ in *Sc* II to $^2D_2$ in *Sc* III, and from $^3F_2$ in *Ti* III to $^2D_2$ in *Ti* IV. The corresponding changes in electron configuration are from $(4s)^2$ to 4s in *Ca*, 4s·3d to 3d in *Sc*, and $(3d)^2$ to 3d in *Ti*. Care is therefore necessary in comparing different spectra to make sure that the values of ν are actually measured from the proper limits.

For example, adopting the approximate value 28 volts derived above for the ionization potential of *Ti* III, it follows that the 3^2D_2 term of *Ti* IV lies higher than the base level a^3F_2 of *Ti* III by 226,800 frequency units. For any term of *Ti* III arising from the configuration $(3d)^2$, 3d·4s, or 3d·4p, the value of ν may be found by subtracting the tabular energy level from this quantity. But for terms arising from 4s·4p the limit is 4^2S of *Ti* IV, which lies higher by 80,388 units; hence for these terms the tabular level must be subtracted from 307,188. If, as is usually desirable, we take the component of greatest inner-quantum number in each term, we must also take the similar component of the limit, which makes the lower limit 3^2D_3 or 227,184. In view of the uncertainty of the estimate of the ionization potential, these figures will be rounded off in what follows to 227,000 and 307,000, corresponding to a principal ionization potential of 27.98 volts. For the term a^3P, for example, which arises from the configuration 3d·4p, the value of ν is 227,000 − 81,024, or 145,976, while for b^3P, which arises from 4s·4p, it is 307,000 − 137,971 or 169,029.

TABLE XI

COMPARISON OF *Ca* I, *Sc* II, AND *Ti* III

CONFIGURATION	ELECTRON REMOVED	TERM	VALUES OF $\sqrt{\nu/R}$				
			Ca I	Diff.	*Sc* II	Diff.	*Ti* III
$(3d)^2$............	3d	$^3F'_4$	....	....	0.951	0.487	1.438
		$^3P'_2$	0.363	0.551	.914	.490	1.404
		$^1G_4$	....	....	.905	.487	1.392
		$^1D_2$	.372	.554	.926	.486	1.412
		$^1S_0$	....	....	0.919	.475?	1.394?
3d·4s...........	3d	$^3D_3$	.514	.573	1.087	.478	1.565
		$^1D_1$	.500	.577	1.077	.479	1.556
3d·4s...........	4s	$^3D_3$	.623	.351	0.974	.337	1.311
		$^1D_1$	.612	.351	.963	.337	1.300
3d·4p...........	4p	$^3F_4$	.497	.337	.834	.331	1.165
		$^3D'_3$	.475	.358	.833	.335	1.168
		$^3P_2$	.465	.359	.824	.330	1.154
		$^1F_3$	.453	.357	.810	.335	1.145
		$^1D'_2$	.498	.345	.843	.333	1.176
		$^1P_1$	....	....	.818	.325	1.143
3d·4d...........	4d	$^3G_5$	....	....	.631	.312	0.943
		$^3F'_4$	....	....	.607	.317	.924
		$^3D_3$	.323	.312	.635	.305	.940
		$^3P'_2$	.282	.318	.600	.312	.912
		$^3S_1$	.325	.301	.626	.300	0.926
4s·4p...........	4p	$^3P_2$	.557	.338	.895	0.346	1.241
		$^1P_2$	.483	....	....	....	....
$(4p)^2$............	4p	$^3P'_2$	0.574	0.331	0.905	....	....

In this way the values of $\sqrt{\nu/R}$ given in Table XI have been derived. The terms are grouped according to the configuration from which they arise and the character of the electron which is removed in passing to the limit. The data for *Sc* II are from Russell and Meggers,[1] those for *Ca* I from Russell and Saunders.[2] The differences in $\sqrt{\nu/R}$ are very nearly the same for all the terms corresponding to the same electronic configuration. The reality of the low ^{1}G term in *Ti* III is thus satisfactorily confirmed. For the suspected ^{1}S term the difference is discordant, making its reality very doubtful. It is evident that a rather accurate prediction of the terms and principal lines in *V* IV could be made by extension of this scheme. Indeed, the value of the term b^3P in *Ti* III, arising from the configuration 4s·4p, was predicted in this way, and the multiplet which depends upon it found near the predicted position.

The mean differences in $\sqrt{\nu/R}$ for the related groups of terms are nearly the same as those for the corresponding terms for the one-electron systems, given in Table IV. Confining our attention to the terms produced by adding a given electron orbit to the normal state of the more highly ionized atom, we find:

Added Electron	Two-Electron Systems			One-Electron Systems		
	Ca I	*Sc* II	*Ti* III	*K* I	*Ca* II	*Sc* III
3d..............		0.551	0.487		0.535	0.470
4s..............		.351	.337		.369	.326
4p..............		.351	.332		.353	.319
4d..............		0.310	0.306		0.334	0.296

On the whole, the rate of diminution of the differences from the first column to the second is smaller for the two-electron systems. This may indicate that the assumed ionization potential for *Ti* III is a little too high. If it should be diminished by 0.5 volt, the mean differences in $\sqrt{\nu/R}$ between *Sc* II and *Ti* III would become 0.474, 0.323, 0.316, and 0.285, respectively. The value 27.6 volts would give the best agreement.

The triplet separations remain to be considered. Landé has shown that his formulae for the doublets are applicable to the triplets as well, provided that the extreme separation of the outer components is taken. Slater[1] has shown that there is good reason to expect it to hold for terms arising from any configuration composed

---

[1] *Loc. cit.*

[2] *Astrophysical Journal*, 61, 1, 1925. Later work shows that the term there called 1p′ is the ^{3}P′ term arising from the configuration $(4p)^2$; 2p′ comes from $(3d)^2$, and 3p′ from 3d·4d, while the term there called q_2 is the ^{3}S term from the same configuration,′ and q_1 a component of the ^{3}D term of similar origin.

TABLE XII

Triplet Separations

Configuration and Terms		$\Delta\nu$	n^*	$10^5\,\Delta n$	Mean	Z_i	s
	Terms Involving a 4p Electron						
4s·4p	*Ca* I	158	1.796	419	....	17.7	2.3
^{3}p	*Sc* II	343	2.239	440	....	18.2	2.8
	Ti III	709	2.396	461	....	18.6	3.4
(4p)^2	*Ca* I	134	1.739	323	....	15.6	4.3
^{3}P′	*Sc* II	346	2.206	417	....	17.7	3.3
3d·4p	*Ca* I	6.7	2.011	25	....	....	....
^{3}P	....	66.7	2.105	284	356	16.4	3.6
^{3}D′	....	166.3	2.152	759	....	....	....
^{3}F	*Sc* II	87	2.397	139	....	....	....
		243	2.402	384	403	17.4	3.6
		397	2.471	686	....	....	....
	Ti III	80	2.576	62	....	....	....
		425	2.569	365	360	16.4	5.6
		737	2.600	653	....	....	....
	Terms Involving a 3d Electron						
4d·3d	*Ca* I	35.3	1.947	119	....	16.4	3.6
^{3}D	*Sc* II	168	1.842	120	....	16.5	4.5
	Ti III	362	1.917	129	....	17.1	4.9
4p·3d	*Ca* I	6.7	1.445	9	....	....	....
^{3}P	....	66.7	1.479	98	121	16.5	3.5
^{3}D′	....	166.3	1.495	255	....	....	....
^{3}F	*Sc* II	87	1.777	56	....	....	....
		243	1.779	156	157	18.8	2.2
		397	1.790	260	....	....	....
	Ti III	80	2.077	36	....	....	....
		425	2.074	192	189	20.7	1.3
		737	2.090	340	....	....	....
(3d)^2	*Ca* I	39.5	2.755	378	....	....	....
^{3}P′	....	....	....	....	....	....	....
^{3}F′	*Sc* II	80.1	2.193	100	151	18.5	2.5
		185	2.124	202			
	Ti III	185	2.122	90	142	17.9	4:1
		422	2.088	195			

---

[1] *Physical Review*, **28**, 311, 1926.

only of s electrons, and electrons of any *one* other kind (e.g., 3d or 4p), except that the extreme separations for P, D, F, ... terms arising from the same configuration should be proportional to certain integers, which he takes as 1, 2, 3, ... , so that the mean of the separations for a triad such as P, D′, F, should be equal to that for the D′ term. For configurations involving electron orbits, other than s orbits, of two different sorts, his formulae are much more complicated.

The results derived in this way from the three spectra now under consideration are given in Table XII. The 3d·4p configuration is here presented in a double rôle, as arising from the addition of a 4p electron to a previously existing 3d state, and vice versa. The values of n^* are of course quite different in the two cases. The individual values of Δn are rather ragged, but if the mean is taken for the triad, and this is treated as if it arose from a single electron of the type which has been supposed to be added in forming the configuration, the resulting mean values of Δn, and those of s derived from them, are in surprisingly good agreement with the others. This, however, means little more than that the mean separations of the terms arising from the simpler and more complex configurations are of about the same size. The $^3F'$ and $^3P'$ terms of origin $(3d)^2$ have been treated in the same way. The irregularity of the individual values is so great as to make it evident that a great deal more work must be done before a satisfactory theory of the term separations in such cases can be reached.

In conclusion, we take much pleasure in expressing once more our thanks to Dr. Anderson and Miss Carter for the observational material upon which much of the present investigation has been based.

PRINCETON UNIVERSITY OBSERVATORY
UNIVERSITY OF ALBERTA
April 1927

Contributions from the Mount Wilson Observatory, No. 338
Reprinted from the *Astrophysical Journal*, Vol. LXVI, pp. 89–112, 1927
Printed in the U.S.A.

INVESTIGATIONS ON PROPER MOTION

TWELFTH PAPER: THE PROPER MOTIONS AND INTERNAL MOTIONS OF MESSIER 2, 13, AND 56

By ADRIAAN VAN MAANEN

ABSTRACT

Proper motions and internal motions of globular clusters.—Three pairs of photographs of M 13 and two each of M 56 and 2 have been measured with the stereocomparator in order to determine the proper motions and internal motions of these clusters. Part of the plates were taken at the 80-foot focus, part at the 25-foot focus of the 60-inch reflector; the interval between the old and new exposures ranges from nine to fifteen years.

The probable errors of an individual μ_α or μ_δ for the 80-foot- and 25-foot-focus plates is found to be $0''.030$ and $0''.064$, respectively, divided by the interval in years.

The absolute proper motions of the clusters have been derived by correcting the comparison stars for parallactic motion. The results are:

M 13	$\mu_\alpha = +0''.0005$	$\mu_\delta = +0''.0008$
M 56	$\mu_\alpha = -0.0013$	$\mu_\delta = +0.0066$
M 2	$\mu_\alpha = +0.0082$	$\mu_\delta = +0.0026$

The internal motions were analyzed into components parallel to and at right angles to the "galactic planes" of the clusters. The dispersion of the motions in these two directions is sensibly the same, which indicates that there is no pronounced rotational motion parallel to the galactic planes.

The internal motions were further analyzed into radial and tangential components. There is a small preponderance of outward motion, but it is too small to permit any definite conclusions.

The tangential component was found to be exactly zero for the 80-foot-focus plates and $0''.003$ in the direction N-W-S-E for the 25-foot-focus plates. The tangential component found for the spiral nebulae was in the mean $0''.014$ and $0''.018^5$ for the 80-foot- and 25-foot-focus plates, respectively, and is therefore of a different order of magnitude.

No correlation was found between the tangential components and the magnitudes of the stars, although the range in the case of the 25-foot-focus plates was more than 6 magnitudes.

In *Mount Wilson Contribution*, No. 284, it was shown from photographs taken at the 80-foot focus of the 60-inch reflector that the total motion of the globular cluster M 13, as well as its internal motion, is extremely small, of the order of a few thousandths of a second of arc per year only. As a check on the displacements found in spiral nebulae, which amount to a few hundredths of a second of arc per year, it was deemed worth while to investigate a few more globular clusters, especially at the 25-foot focus at which most of the spirals were photographed, as soon as material for the derivation of the proper motions should be available.

The present paper discusses the results from two pairs of plates of M 56 and one pair of M 2, taken at the 80-foot focus of the 60-inch reflector, and from one pair of plates each of M 13 and M 2, taken at the 25-foot focus of the same instrument. Further, the measures communicated in *Contribution* No. 284 have been re-reduced. The material for these plates is assembled in Table I.

TABLE I

Object	Plate Number	Exposure Time	Date	Quality	Observer
M 13	π 5*	30^{m}	1913, May 26	g	van Maanen
M 13	π 119†	30	1914, April 18	g	van Maanen
M 13	π 3728†	30	1923, June 8	g	van Maanen
M 13	π 3878*	31½	1924, May 30	fg	van Maanen
M 13	P 133§	300	1912, June 15	fg	Pease
M 13	B 242§	300	1926, July 3–5	fg	Humason
M 56	π 153*	30	1914, July 26	fg	van Maanen
M 56	π 160†	30	1914, July 27	fg	van Maanen
M 56	π 3754*	30	1923, July 7	fg	van Maanen
M 56	π 4151†	30	1925, Aug. 24	g	van Maanen
M 2	π 239*	15	1914, Sept. 14	g	van Maanen
M 2	π 4154*	20	1925, Aug. 24	g	van Maanen
M 2	P 5†	100	1911, July 2	fg	Pease
M 2	B 248†	100	1926, July 6	fg	Humason

The plates marked π were taken with the Cassegrain arrangement of the 60-inch reflector (equivalent focal length, 80 feet); those marked P or B, at the Newtonian focus (25 feet) of the same instrument. All plates were measured differentially in pairs with the stereocomparator. The grouping of these plates is indicated by the signs *, †, and §, following the plate numbers.

The usual methods of measurement and reduction were followed, the plates being measured in four positions each, with east, west, north, and south in the direction of the increasing readings of the micrometer. For the reduction, the two series of measures in right ascension, as well as those in declination, were combined into single series. The quantities so derived were then reduced to seconds of arc per year by multiplying by the factor:

$$q=\frac{\text{No. seconds of arc per mm on plate}}{\text{No. revolutions of micrometer screw per mm}\times\text{interval in years}}\cdot$$

The resulting quantities, m, were used as the second members of the equations of condition (1) from which the final proper motions were derived.

$$\left.\begin{array}{l}\mu_\alpha+a+bx+cy+dx+exy+fy=m_\alpha\\ \mu_\delta+a'+b'x+c'y+d'x^2+e'xy+f'y^2=m_\delta\end{array}\right\}\qquad(1)$$

Here a, b, c, ... e', f', are the plate constants; x and y, the coordinates of the stars measured; and μ_α and μ_δ, the resulting annual motions relative to the mean motion of the comparison stars. The plate constants were derived by least-squares solutions from equations (1) for the comparison stars, and were then substituted into the equations of condition for all the stars measured.

In the case of M 13, Shapley had indicated which stars might be members of the cluster and which not. The comparison stars were selected from the latter, the selection being based on distance from the center, magnitude, and color-index. For M 2 and 56 no such data were available. Accordingly, a limiting distance was adopted outside of which it was assumed that no stars were members of the cluster. The cluster stars were chosen well within these limits. It is, however, still possible that some of the comparison stars may belong to the cluster, and that some of the cluster stars are in reality foreground or background stars; but the number in either case will probably be small and cannot disturb the mean motions very seriously.

In *Contribution* No. 284, dealing with the motion of M 13, fifty stars were used for comparison purposes. It was found that the star s had a proper motion of 0″.110 in declination, while p had a motion of 0″.054 in the same co-ordinate. It would therefore have been better had these two stars been excluded from the derivation of the plate constants. Furthermore, on the long-exposure plates taken at the 25-foot focus, stars 831 and 1019, being located in the denser part of the cluster, could not be measured; and, as it was desirable to use the same set of comparison stars for the pairs of plates taken at both the 80- and 25-foot foci, a re-reduction of the measures in *Contribution* No. 284 was made, excluding these four stars. Accordingly, for M 13, forty-six comparison stars were used, while sixty-two cluster stars were measured at the 80-foot focus, and seventy-three at the 25-foot focus, the latter including some of the very faintest stars measurable on the plates of five-hour exposure. For these twenty-two faint stars no magnitudes are available, but they are estimated to be between the eighteenth and nineteenth magnitudes. In Table III their magnitudes are given as *ff*.

For M 56, sixty-five comparison stars were selected and fifty cluster stars. Six of the cluster stars are, however, considerably brighter (12.7–13.6 mag.) than the other cluster stars (14.4–16.3 mag.) and it is possible that they may be foreground stars. These stars, numbered 101, 105, 125, 131, 144, and 149, have accordingly been excluded from the derivation of the mean motion of the cluster, as well as from the discussion of the internal motions.

TABLE II

PROBABLE ERROR OF MEASURES

Object	P.E. in μ_α	P.E. in μ_δ	Interval in Years between Plates	Focal Length in Feet
M 13	0″.0038	0″.0036	11	80
	0.0031	0.0028	9	80
	0.0050	0.0037	14	25
M 56	0.0031	0.0035	9	80
	0.0023	0.0037	11	80
M 2	0.0017	0.0023	11	80
	0.0052	0.0036	15	25

For M 2 the same set of thirty-eight comparison stars was used for both the 80-foot- and the 25-foot-focus plates. For the former, seventy-six cluster stars were chosen, of which three, Nos. 164, 175, and 176, were later rejected as too bright and too far from the center, while for the 25-foot-focus plates the number of cluster stars was seventy-six. Numbers 175 and 176 were also excluded from the discussion of the motion of the cluster.

In the case of M 13, twenty of the cluster stars were measured on all sets of plates; in the case of M 2, twenty-eight.

As stated before, the magnitudes for the stars of M 13 are due to Dr. Shapley, those for M 56 were derived by Dr. Pannekoek from Mount Wilson plates, while those for M 2 are by Mr. J. A. Brown, to all of whom I wish to express my sincere thanks for their kind co-operation.

TABLE III

Co-ordinates and Annual Displacements in M 13

(The Motions Are Given in 0″.001 as a Unit)

No.	Pg. Mag.	x	y	80-Foot Focus		25-Foot Focus	
				μ_α	μ_δ	μ_α	μ_δ
Comparison Stars							
a	13.06	−9′.7	−4′.8	− 5	+ 9	− 7	+ 14
c	13.40	−8.2	−6.7	+ 5	0	+ 3	− 3
b	14.96	−8.0	+3.0	+11	+ 3	+10	− 4
e	14.52	−6.9	−2.4	+ 5	0	+ 2	− 5
d	14.52	−6.8	+5.8	+ 5	− 19	+ 8	− 21
1	14.85	−6.5	+2.5	+ 8	− 1	+ 6	+ 2
f	14.52	−6.1	−6.2	+ 4	0	+ 8	− 5
10	15.14	−5.6	+1.3	+ 2	+ 3	− 5	+ 2
13	15.50	−5.4	+2.8	+ 3	+ 2	− 8	− 2
15	13.06	−5.2	+5.6	−25	+ 19	−17	+ 21
19	15.91	−5.0	+3.2	+ 2	− 4	+ 1	− 5
36	16.13	−4.3	+1.9	− 6	− 7	+10	− 7
g	13.30	−4.3	−6.6	− 6	0	+ 1	− 3
43	14.52	−4.2	−3.2	+ 2	− 2	− 1	+ 10
47	15.89	−4.0	−3.8	+ 2	+ 2	− 3	+ 2
h	14.95	−2.9	−8.5	− 6	− 4	−11	+ 1
90	16.22	−2.8	−1.8	−18	− 20	− 8	+ 3
99	16.03	−2.6	−1.5	− 2	+ 15	− 8	− 14
1120	16.17	−2.3	+0.6	− 8	− 13	+11	+ 11
234	16.16	−1.3	+3.7	+ 1	− 2	− 7	+ 1
i	15.00	−0.8	+8.4	0	+ 7	+ 8	+ 9
331	16.13	−0.8	−4.2	+ 6	0	− 1	− 2
j	15.17	−0.1	+8.0	+ 1	+ 2	− 1	+ 1
505	16.16	0.0	+4.4	+ 1	+ 5	+ 4	− 1
557	15.11	+0.2	+6.3	+ 4	− 1	− 3	+ 7
599	16.17	+0.3	+4.4	+ 1	− 1	−11	− 5
k	13.82	+0.4	−8.1	+ 5	− 1	− 3	− 4
687	13.76	+0.7	−5.3	− 3	0	− 2	− 5
762	15.95	+1.0	+4.0	+ 1	− 1	+ 2	− 12
814	16.20	+1.2	+2.4	+ 6	+ 1	+11	− 3
831*	16.06	+1.3	−2.9	+ 4	− 7	....	....
1015	16.14	+2.7	−4.2	+ 4	+ 2	+10	+ 5
1019*	12.98	+2.7	−1.4	+ 5	− 13	....	....
l	14.34	+3.4	−6.1	+ 2	− 1	+ 1	− 2
1057	15.86	+3.5	−2.3	− 4	+ 6	0	+ 1
1075	15.79	+4.1	−3.9	+ 1	+ 2	+10	+ 2
1087	13.14	+4.4	+3.9	− 6	+ 16	−17	+ 4
m	14.88	+5.3	+7.6	+ 4	0	+ 5	− 5
1111	16.10	+5.7	+3.0	− 4	− 14	+ 2	+ 11
1114	14.63	+5.8	−5.5	+ 3	− 5	+ 7	+ 7
1115	15.71	+5.9	+6.0	+ 3	+ 6	− 2	+ 3
n	13.90	+7.2	−3.0	+ 5	− 1	+ 7	+ 3
*p**	13.14	+7.3	−8.0	−42	+ 31	−41	+ 36
o	14.88	+7.7	+1.2	− 5	− 3	−10	− 5
r	14.09	+8.0	−1.0	+ 2	+ 10	+ 6	+ 2
q	14.33	+8.2	+6.2	+ 6	− 24	− 5	− 18

* Rejected in deriving the plate constants.

TABLE III—*Continued*

No.	Pg. Mag.	*x*	*y*	80-Foot Focus		25-Foot Focus	
				μ_α	μ_δ	μ_α	μ_δ
Comparison Stars							
*s**	14.88	+8′.4	−6′.7	−15	−132	− 8	−135
t	15.77	+9.2	+6.5	− 2	+ 6	+10	+ 8
u	15.50	+9.3	−0.4	− 2	+ 11	− 1	+ 3
v	15.28	+9.8	−3.0	− 2	− 3	−12	− 6
Cluster Stars							
2	14.96	−6′.5	+2′.3	+11	− 3	− 5	+ 3
7	15.04	−6.1	+6.4	+ 5	− 2	+10	+ 4
17	14.86	−5.1	−4.6	+ 2	− 1	− 4	− 3
21	16.01	−4.9	+4.4	....	....	0	+ 5
25	15.06	−4.8	+1.8	+ 3	+ 1	+ 4	+ 1
46	15.57	−4.0	−1.9	− 9	+ 1	− 9	− 4
49*a*	*ff*	−4.0	−0.4	....	....	+14	− 2
49	14.83	−3.9	−0.2	+ 4	− 3	− 1	+ 2
51	16.63	−3.9	+0.8	....	....	+ 2	+ 2
51*a*	*ff*	−3.8	+0.7	....	....	+ 8	+ 1
54	16.20	−3.8	+2.9	....	....	− 1	− 5
59*a*	*ff*	−3.8	+3.3	....	....	+ 6	+ 1
59	15.08	−3.7	+3.2	+ 7	− 5	− 1	+ 1
70	13.45	−3.4	+2.4	− 5	+ 1	− 1	+ 2
70*a*	*ff*	−3.2	+2.6	....	....	+ 6	− 7
71	16.21	−3.3	+0.8	....	....	− 1	+ 2
71*a*	*ff*	−3.3	+0.9	....	....	+ 5	− 2
72	13.74	−3.3	−2.3	− 6	− 1	− 4	− 4
76	16.04	−3.2	−1.7	....	....	− 7	+ 1
82*a*	*ff*	−3.1	+2.7	....	....	+ 9	− 7
82	16.10	−3.0	+2.6	....	....	− 2	− 13
96	13.70	−2.7	+0.2	− 3	− 1	−10	+ 2
113	16.22	−2.4	−5.0	....	....	+11	− 4
113*a*	*ff*	−2.3	−4.9	....	....	+14	− 1
118	15.03	−2.4	−0.9	+ 4	− 3	....	....
155	16.56	−2.0	−4.8	....	....	+ 7	+ 2
158	13.86	−2.0	+1.9	− 2	− 3	+ 4	− 10
159	16.09	−2.0	−5.6	....	....	0	− 7
222	12.54	−1.4	−1.7	− 4	+ 1	....	....
236	16.63	−1.3	+2.8	....	....	− 8	+ 5
246	15.49	−1.2	−1.6	− 3	+ 4	....	....
252	13.84	−1.2	+2.4	+ 2	+ 1	....	....
275	16.24	−1.1	+3.9	....	....	+ 1	+ 1
275*a*	*ff*	−0.9	+4.1	....	....	+ 7	− 6
275*b*	*ff*	−0.8	+4.2	....	....	+ 5	+ 3
283	16.26	−1.0	+3.7	....	....	+ 5	− 17
299	15.31	−0.9	+0.4	0	+ 2	....	....
306	var.	−0.9	0.0	− 3	+ 1	....	....
310	15.30	−0.9	−1.9	+ 2	+ 2	....	....
311	15.50	−0.9	+0.5	− 9	− 3	....	....
313	15.42	−0.8	+1.6	0	+ 3	....	....

---

* Rejected in deriving the plate constants.

TABLE III—*Continued*

No.	Pg. Mag.	x	y	80-Foot Focus		25-Foot Focus	
				μ_α	μ_δ	μ_α	μ_δ
Cluster Stars							
323	15.42	−0′8	−1′0	−6	+2	....	....
325	15.31	−0.8	−0.4	−2	−4	....	....
326	13.76	−0.8	+3.0	+4	+1	−10	+12
326*a*	*ff*	−0.7	+3.1	....	....	−4	+3
363	15.18	−0.6	−4.0	0	+4	....	....
365	16.04	−0.6	−4.9	....	....	+10	−6
406	15.20	−0.4	−1.4	+2	−2	....	....
418	15.46	−0.4	−2.8	−3	+2	....	....
500	15.44	0.0	+2.2	+4	0	....	....
523	15.31	0.0	+0.7	+1	−3	....	....
559	15.20	+0.2	+0.9	−2	−1	....	....
590	16.20	+0.3	−5.2	....	....	+4	−4
627	16.15	+0.4	+5.0	....	....	−2	−1
641	15.14	+0.5	+3.6	+2	+1	−2	+7
641*a*	*ff*	+0.6	+3.6	....	....	+8	+2
653	15.18	+0.5	+3.2	0	+5	....	....
686	15.42	+0.7	−2.2	0	+1	....	....
690	15.26	+0.7	+0.9	0	0	....	....
712	15.36	+0.8	−1.2	−2	−2	....	....
737	15.20	+0.9	−1.2	+4	−1	....	....
749	16.03	+1.0	+3.5	....	....	+1	+8
775	14.91	+1.0	−2.6	+2	−1	....	....
784	15.31	+1.1	+0.7	+2	−6	....	....
790	16.17	+1.1	−5.6	....	....	+2	+2
791	16.10	+1.1	−4.8	....	....	+6	+1
791*a*	*ff*	+1.2	−5.0	....	....	+15	+4
796	14.93	+1.1	−2.1	+5	0	....	....
804	15.20	+1.2	+0.4	−1	0	....	....
808	15.30	+1.2	+4.2	+8	+4	−11	−3
813	16.22	+1.2	−4.2	....	....	+11	−4
816	var.	+1.2	−0.4	−3	+6	....	....
822*a*	*ff*	+1.2	+5.4	....	....	+4	+5
822	15.09	+1.2	+5.4	+2	+4	+1	+3
829	15.20	+1.3	+0.1	0	+6	....	....
835	13.23	+1.3	−1.9	−4	+2	....	....
837	15.42	+1.3	−1.3	+7	+5	....	....
840	15.50	+1.3	−0.6	+4	−1	....	....
851	15.30	+1.4	−0.3	−1	0	....	....
852	15.17	+1.4	−2.2	+2	−4	....	....
861	14.86	+1.5	−2.4	−1	+1	....	....
873	15.09	+1.6	+1.9	+4	−2	....	....
879	16.20	+1.6	−4.1	....	....	+5	−7
879*a*	*ff*	+1.7	−4.2	....	....	+1	−1
899	15.14	+1.7	+1.8	+2	−2	−4	−2
915	16.58	+1.7	−5.3	....	....	+6	+3
922*a*	*ff*	+1.7	+4.2	....	....	+11	+10
922	16.03	+1.8	+4.2	....	....	+1	+9
925	15.07	+1.8	−2.0	+5	0	....	....
935	14.50	+1.9	+1.2	+4	+3	....	....

TABLE III—*Continued*

No.	Pg. Mag.	x	y	80-Foot Focus		25-Foot Focus	
				μ_α	μ_δ	μ_α	μ_δ
Cluster Stars							
953	15.20	+2′.0	+1′.1	+ 4	+ 2	....	....
978	15.04	+2.2	−0.6	0	− 3	....	....
989	15.60	+2.3	−1.6	− 1	+ 1	....	....
1010	16.26	+2.6	+2.7	....	....	− 1	+ 5
1031	16.07	+2.9	−2.9	....	....	+ 8	+ 5
1034	16.23	+3.0	−5.0	....	....	+ 7	− 6
1034*a*	*ff*	+3.1	−5.1	....	....	+ 4	+ 2
1037*a*	*ff*	+2.9	+3.4	....	....	− 1	+ 5
1037	16.74	+3.0	+3.4	....	....	+11	+ 1
1038*β*	15.07	+3.0	+1.1	+ 3	+ 3	....	....
1042	15.09	+3.0	−0.1	− 2	0	....	....
1063	15.08	+3.7	+1.5	+ 2	+ 4	−18	− 4
1069*a*	*ff*	+3.8	+1.4	....	....	− 1	+ 3
1069	16.26	+4.0	+1.4	....	....	− 1	+ 5
1076	16.27	+4.1	+5.6	....	....	− 1	+ 7
1079	15.14	+4.2	+5.8	+ 3	0	− 2	+ 2
1083*a*	*ff*	+4.2	−2.6	....	....	+12	+ 1
1083	16.10	+4.3	−2.6	....	....	+10	+ 8
1090	16.28	+4.4	+0.8	....	....	+ 3	+ 8
1090*a*	*ff*	+4.6	+0.8	....	....	+11	+ 8
1102	16.06	+5.0	+3.7	....	....	0	− 1
1106*a*	*ff*	+5.2	−4.4	....	....	+22	+ 14
1106	15.18	+5.4	−4.4	− 1	+ 2	+15	+ 2
1106*b*	*ff*	+5.5	−4.4	....	....	+20	+ 8
1113	15.26	+5.8	+3.5	+ 6	+ 7	−10	− 5

As will be seen later, the internal motions for all three clusters are very small indeed; accordingly, the deviations from the mean motion of a cluster may be used to gain an idea of the accuracy of the measures. This will be an upper limit, since the internal motions, while small, may still amount to a few thousandths of a second of arc, and further, since some stars may have been included which are not members of the clusters. The results for the probable error of an individual μ_α or μ_δ so derived are collected in Table II.

We may conclude from this table that the probable errors in an individual μ_α or μ_δ as derived from plates taken at the 80-foot and 25-foot foci of the 60-inch reflector are, respectively, 0″.030 and 0″.064, divided by the interval in years between the two exposures.

The remaining tables contain the results of the measures. The third and fourth columns in Tables III, V, and VI give the co-ordinates of the stars from the center of the clusters. Table III gives first, in the fifth and sixth columns, the results of the re-reduction of the mean motions derived in *Contribution* No. 284. It is interesting to note that the exclusion of two stars having considerable proper motion has changed the results but slightly, 0″.0015 in each co-ordinate, on the average, for the motion of the cluster stars.

The *ff* stars may be identified by their co-ordinates relative to neighboring stars, which are given in Table IV.

TABLE IV

POSITIONS OF THE *ff* STARS

No.	Position	No.	Position
49*a*........	2″.5 W, 10″.5 S of 49	791*a*.......	5″.7 E, 11″.1 S of 791
51*a*........	6.8 E, 3.8 S of 51	822*a*.......	4.9 W, 4.1 N of 822
59*a*........	6.8 W, 4.9 N of 59	879*a*.......	7.2 E, 5.2 S of 879
70*a*........	6.8 E, 5.3 N of 70	922*a*.......	4.9 W, 1.7 S of 922
71*a*........	3.4 E, 6.4 N of 71	1034*a*.......	7.1 E, 6.8 S of 1034
82*a*........	1.7 W, 4.5 N of 82	1037*a*.......	3.5 W, 0.4 S of 1037
113*a*........	6.6 E, 8.7 N of 113	1069*a*.......	6.8 W, 3.6 N of 1069
275*a*........	11.2 E, 11.9 N of 275	1083*a*.......	10.0 W, 2.6 S of 1083
275*b*........	19.5 E, 15.6 N of 275	1090*a*.......	7.8 E, 1.6 S of 1090
326*a*........	5.4 E, 7.3 N of 326	1106*a*.......	8.2 W, 0.5 S of 1106
641*a*........	6.9 E, 3.1 S of 641	1106*b*.......	10.0 E, 4.3 S of 1106

Table V gives the results for M 56. The fifth and sixth columns contain the results of the measures of the two pairs of plates in right ascension; the seventh and eighth columns, those in declination; while the last two columns give the means of the measures in the two co-ordinates. The comparison stars are numbered 1 . . . . 65; the cluster stars, 101 . . . . 150.

TABLE V

Co-ordinates and Annual Displacements in M 56

(The Motions Are Given in 0″.001 as a Unit)

No.	Pg. Mag.	x	y	$\mu_{1\alpha}$	$\mu_{2\alpha}$	$\mu_{1\delta}$	$\mu_{2\delta}$	μ_{α}	μ_{δ}
Comparison Stars									
1......	14.0	−6′.0	+3′.5	+ 3	− 4	+ 7	+ 2	0	+ 4
2......	14.9	−5.9	+0.1	+ 5	0	0	+ 6	+ 2	+ 3
3......	15.0	−5.7	−1.6	+ 6	+ 7	+ 3	+ 1	+ 6	+ 2
4......	14.1	−5.6	−0.8	+ 1	− 3	+ 1	− 1	− 1	0
5......	15.2	−5.2	−3.1	− 2	+ 3	−10	0	0	− 5
6......	13.8	−4.4	+1.1	+ 1	+ 4	− 1	− 5	+ 2	− 3
7......	14.5	−4.2	+5.0	− 4	− 4	−16	−17	− 4	−16
8......	15.1	−3.8	−1.6	− 1	− 2	− 2	− 4	− 2	− 3
9......	14.0	−3.7	−0.6	+ 9	+ 5	−25	−25	+ 7	−25
10......	14.4	−3.6	−4.1	+ 2	+ 1	+ 1	+ 4	+ 2	+ 2
11......	15.5	−3.5	−0.6	− 2	+ 3	+ 1	− 4	0	− 2
12......	14.9	−3.6	+5.6	+ 2	+ 2	+35	+32	+ 2	+34
13......	13.3	−3.4	+0.7	0	0	− 1	− 3	0	− 2
14......	14.3	−3.4	−4.8	− 1	0	+ 5	+ 7	0	+ 6
15......	15.6	−3.4	−0.5	− 4	− 4	− 1	+ 1	− 4	0
16......	15.0	−3.2	−1.5	− 7	+ 3	+ 8	+ 8	− 2	+ 8
17......	14.6	−3.1	−3.7	+ 3	0	− 7	−10	+ 2	− 8
18......	13.9	−3.0	+3.1	−10	−11	−16	−16	−10	−16
19......	14.6	−2.8	+1.0	− 6	+ 1	+14	+13	− 2	+14
20......	<12	−2.8	+0.2	− 3	− 3	0	+10	− 3	+ 5
21......	15.0	−2.7	+0.3	− 6	− 1	+ 2	+ 3	− 4	+ 2
22......	14.8	−2.4	−1.9	+ 5	+ 5	− 2	0	+ 5	− 1
23......	14.7	−2.3	+4.0	− 3	− 1	− 2	− 6	− 2	− 4
24......	15.2	−2.2	+1.9	+ 1	− 4	− 1	+ 3	− 2	+ 1
25......	13.6	−2.0	+3.8	− 1	− 1	− 5	0	− 1	− 2
26......	13.9	−1.7	−6.5	− 2	0	+11	+ 3	− 1	+ 7
27......	13.5	−1.5	−2.5	− 3	+ 1	+ 7	+ 6	− 1	+ 6
28......	15.7	−1.3	−5.0	− 1	− 8	+ 6	+ 4	− 4	+ 5
29......	13.5	−1.1	+6.2	+23	+13	− 3	− 1	+18	− 2
30......	15.3	−1.2	−3.0	0	+ 6	+ 6	+ 3	+ 3	+ 4
31......	15.0	−1.0	−5.6	− 3	− 3	− 4	− 4	− 3	− 4
32......	14.9	−0.1	+4.0	+ 1	− 1	− 1	− 1	0	− 1
33......	14.8	+0.1	−3.2	+ 1	− 4	+ 2	− 1	− 2	0
34......	15.0	+0.2	+3.2	− 7	− 4	−16	−17	− 6	−16
35......	14.0	+0.5	−2.9	− 9	− 5	+10	+ 2	− 7	+ 6
36......	15.2	+0.5	−4.6	+ 4	− 3	+ 7	+ 5	0	+ 6
37......	14.2	+0.8	−4.6	+ 3	+ 2	−15	−18	+ 2	−16
38......	15.5	+1.1	−4.4	+ 5	− 3	+ 7	+ 6	+ 1	+ 6
39......	12.5	+1.5	+2.6	− 7	− 1	+ 4	+ 8	− 4	+ 6
40......	15.1	+1.5	+4.9	− 8	0	−11	−18	− 4	−14
41......	14.8	+1.6	+6.0	− 2	+ 2	+ 5	0	0	+ 2
42......	14.0	+2.1	+4.8	+ 2	+ 4	+ 1	+ 5	+ 3	+ 3
43......	14.1	+2.4	+4.8	+ 2	+11	−10	+14	+ 6	+ 2
44......	15.9	+2.1	−3.1	0	− 2	− 9	+ 6	− 1	− 2
45......	15.7	+2.3	−5.3	−12	− 2	−22	− 8	− 7	−15
46......	14.9	+2.7	−0.3	− 1	0	+12	+10	0	+11
47......	15.4	+2.8	−0.5	− 1	− 2	+ 4	+ 9	− 2	+ 6
48......	13.6	+3.1	−3.6	+ 2	− 1	+15	+ 4	0	+10

TABLE V—*Continued*

No.	Pg. Mag.	x	y	$\mu_{1\alpha}$	$\mu_{2\alpha}$	$\mu_{1\delta}$	$\mu_{2\delta}$	μ_{α}	μ_{δ}
Comparison Stars									
49.....	15.4	+3′.1	+0′.9	+ 4	− 3	+11	+12	0	+12
50.....	15.6	+3.3	−1.7	+21	+21	− 2	− 4	+21	− 3
51.....	15.9	+3.4	−1.6	+ 7	+ 3	+ 2	− 2	+ 5	0
52.....	15.2	+3.6	+4.6	− 3	− 8	− 6	− 7	− 6	− 6
53.....	15.7	+3.8	+3.4	− 3	0	+ 7	+ 5	− 2	+ 6
54.....	15.8	+3.8	−0.1	+ 9	0	0	−11	+ 4	− 6
55.....	16.0	+4.4	+0.4	− 3	− 3	+ 1	+ 1	− 3	+ 1
56.....	13.7	+4.3	−1.8	− 7	− 5	− 3	− 2	− 6	− 2
57.....	15.5	+4.5	−1.8	+ 6	+ 8	− 8	− 7	+ 7	− 8
58.....	15.3	+4.6	+0.5	+ 5	+ 6	− 6	− 6	+ 6	− 6
59.....	14.6	+4.6	−0.5	+ 2	0	0	+ 1	+ 1	0
60.....	13.8	+4.6	+1.4	− 9	− 3	+ 3	+ 6	− 6	+ 4
61.....	15.0	+5.3	+4.6	0	− 4	+ 4	0	− 2	+ 2
62.....	15.8	+4.8	−5.0	− 2	+ 2	− 2	− 1	0	− 2
63.....	15.4	+5.8	+4.6	− 8	− 6	+ 2	− 5	− 7	− 2
64.....	15.2	+5.4	+3.4	+ 7	− 1	+ 1	+ 3	+ 3	+ 2
65.....	15.5	+5.4	−2.1	− 6	− 4	− 2	+ 3	− 5	0
Cluster Stars									
101.....	13.6	−1′.5	+1′.7	− 1	0	+ 7	+ 8	0	+ 8
102.....	15.1	−1.4	+0.9	− 2	− 5	+ 5	+ 6	− 4	+ 6
103.....	15.6	−1.4	−0.3	− 3	− 2	+12	+ 5	− 2	+ 8
104.....	15.1	−1.3	+0.7	+ 1	− 1	+ 9	+ 5	0	+ 7
105.....	13.0	−1.0	+1.9	+ 5	+ 6	− 5	− 1	+ 6	− 3
106.....	15.7	−1.0	−0.3	− 2	− 5	+ 9	+ 9	− 4	+ 9
107.....	15.9	−1.0	+0.8	− 4	− 9	− 4	+11	− 6	+ 4
108.....	15.9	−0.9	+0.6	0	+ 1	+ 8	+ 8	0	+ 8
109.....	15.6	−0.9	+0.5	0	− 2	+ 9	+12	− 1	+10
110.....	15.0	−0.9	−1.3	0	− 4	+ 3	+ 5	− 2	+ 4
111.....	15.1	−0.7	+0.3	− 5	+ 4	+ 9	+ 9	0	+ 9
112.....	15.8	−0.9	−1.3	− 1	− 3	+ 2	+ 7	− 2	+ 4
113.....	16.3	−0.7	−1.5	+ 5	− 5	+14	+ 6	0	+10
114.....	15.1	−0.6	−0.1	0	+ 5	+ 9	+ 7	+ 2	+ 8
115.....	15.4	−0.6	+0.8	− 8	− 4	+ 9	+12	− 6	+10
116.....	14.4	−0.6	−0.5	+ 6	+ 2	+ 5	+ 8	+ 4	+ 6
117.....	15.2	−0.5	−0.5	− 8	− 3	+11	+12	− 6	+12
118.....	15.9	−0.4	−0.8	− 5	0	+10	+ 9	− 2	+10
119.....	16.2	−0.5	−1.3	−10	− 3	+ 6	+11	− 6	+ 8
120.....	15.2	−0.3	+1.3	− 4	− 3	+ 3	+10	− 4	+ 6
121.....	15.1	−0.3	−0.3	− 2	+ 2	+14	+ 4	0	+ 9
122.....	15.6	−0.3	−0.3	0	+ 2	+ 4	+ 1	+ 1	+ 2
123.....	15.6	−0.3	−0.3	− 8	− 3	+11	+ 9	− 6	+10
124.....	16.2	+0.1	−0.8	+ 2	+ 2	+ 3	+ 4	+ 2	+ 4
125.....	13.1	0.0	+0.5	0	+ 2	+10	+12	+ 1	+11
126.....	15.8	0.0	+0.6	− 8	− 7	− 2	+ 5	− 8	+ 2
127.....	15.4	+0.1	+0.2	− 8	− 4	−12	−10	− 6	−11
128.....	15.0	+0.1	+0.1	+ 2	− 2	+ 3	+10	0	+ 6
129.....	16.0	+0.2	−0.4	− 3	+10	+ 6	+ 4	+ 4	+ 5
130.....	15.8	+0.1	−1.1	0	− 2	+ 4	+ 2	− 1	+ 3

TABLE V—*Continued*

No.	Pg. Mag.	x	y	$\mu_{1\alpha}$	$\mu_{2\alpha}$	$\mu_{1\delta}$	$\mu_{2\delta}$	μ_{α}	μ_{δ}
Cluster Stars									
131.....	13.2	+0′.2	−1′.5	+4	0	+7	+10	+2	+8
132.....	14.5	+0.1	−2.3	+2	0	+15	+8	+1	+12
133.....	15.5	+0.3	−0.3	+3	−3	+7	+14	0	+10
134.....	15.5	+0.3	−0.1	+3	+4	+6	+10	+4	+8
135.....	16.5	+0.3	+0.7	−8	−7	+7	−6	−8	0
136.....	15.4	+0.3	+0.5	−2	−3	+4	+11	−2	+8
137.....	14.5	+0.4	+1.5	+2	−2	+9	+9	0	+9
138.....	15.4	+0.5	+2.3	−5	−6	+4	+10	−6	+7
139.....	15.8	+0.5	+0.1	−4	−1	+2	+11	−2	+6
140.....	15.3	+0.5	−0.2	−9	−2	+12	+4	−6	+8
141.....	15.9	+0.7	−0.1	+1	−2	+7	+13	0	+10
142.....	15.2	+0.7	+1.7	−3	−1	−3	−3	−2	−3
143.....	16.2	+0.9	+0.3	−10	−1	+6	+15	−6	+10
144.....	12.7	+0.9	−1.4	−2	−1	+11	+2	−2	+6
145.....	15.9	+1.0	−1.2	+4	−1	+6	+4	+2	+5
146.....	15.9	+1.1	−0.7	−3	−3	+5	+2	−3	+4
147.....	14.8	+1.2	+1.7	−2	0	+9	+18	−1	+14
148.....	15.5	+1.4	+1.7	−2	−1	+6	−2	−2	+2
149.....	13.3	+1.7	−0.5	−4	−5	−11	−7	−4	−9
150.....	16.2	+1.9	−0.3	+11	+1	+14	+12	+6	+13

Table VI shows the results for M 2. The fifth and sixth columns give the results for the 80-foot-focus plates; the last two columns, those for the 25-foot-focus plates. The comparison stars are numbered 1 . . . . 39, but star 17 was excluded from the derivation of the plate constants, as it has a considerable proper motion. The cluster stars are numbered 101 . . . . 224.

TABLE VI

Co-ordinates and Annual Displacements in M 2

(The motions are given in 0″.001 as a unit)

No.	Pg. Mag.	x	y	80-Foot Focus		25-Foot Focus	
				μ_α	μ_δ	μ_α	μ_δ
Comparison Stars							
1......	10.6	−9′.4	−3′.7	+10	+6	−3	+6
2......	15.2	−8.4	+1.9	−7	−2	−4	+3
3......	14.9	−8.3	−4.6	+5	+5	+6	+1
4......	15.1	−7.9	−4.8	−8	−3	−2	−1
5......	13.3	−7.7	−5.4	−7	−3	−12	−12
6......	13.4	−7.1	+0.1	+4	−21	0	−15
7......	15.1	−6.7	+2.9	−5	−12	+2	−12
8......	14.4	−6.2	+6.8	−5	+3	−3	+11
9......	16.3	−4.4	−2.7	−13	−3	+8	−1
10......	15.2	−5.2	+5.0	+7	+24	+3	+14
11......	14.8	−4.5	+8.6	−4	−1	−4	−6
12......	13.7	−3.4	−8.7	+2	−6	+9	+7
13......	15.3	−3.3	−4.5	+8	+10	+6	+3
14......	15.0	−3.4	+9.6	+9	+19	+11	+11
15......	15.1	−1.2	+8.4	+1	−6	−4	−4
16......	15.4	−0.8	−6.0	+4	+12	−1	+6
17*.....	13.8	−0.7	−7.1	−129	−35	−144	−41
18......	13.7	−0.3	−8.3	+16	0	+9	−2
19......	14.3	+0.4	−8.6	+2	+2	−12	+4
20......	14.8	−1.5	+10.0	+3	−6	+5	−1
21......	15.2	+1.0	−5.6	+8	+8	+14	+9
22......	15.3	+1.4	−9.2	−13	+3	−7	−4
23......	14.9	+1.8	−4.2	+6	+12	+6	+12
24......	14.8	+1.9	+8.6	+9	−4	+4	−9
25......	15.1	+2.3	+5.6	−5	0	−10	−2
26......	10.3	+2.7	+3.5	+9	−2	+6	+6
27......	15.2	+2.9	−5.6	+11	+4	+6	+8
28......	13.6	+3.1	+6.7	−11	−17	−14	−21
29......	15.9	+4.6	+3.3	−18	−13	−19	−8
30......	15.6	+4.9	−6.1	−33	−27	−26	−23
31......	14.7	+6.0	−1.8	+5	+8	+2	+1
32......	16.1†	+6.3	+1.5	+4	+3	+24	+5
33......	14.9	+6.2	−2.4	+3	−1	+4	−2
34......	12.7	+6.4	−2.3	−10	+6	−9	+3
35......	11.8	+7.3	+7.7	+1	−14	+1	−7
36......	13.0	+7.7	+6.4	+1	+17	−6	+18
37......	11.7	+7.6	−7.9	+2	−5	+2	+2
38......	14.0	+10.5	−4.1	+12	+2	+4	−6
39......	13.5	+10.7	+5.2	0	+7	+7	+7
Cluster Stars							
101......	15.4	−3′.0	+0′.7	+3	+12	+2	+6
102......	15.2	−3.0	−0.5	+3	+4	+3	+8
103......	15.1	−2.4	+1.1	+7	+5	0	+2
104......	15.1	−2.3	+1.9	+8	+8	+2	+4

TABLE VI—*Continued*

No.	Pg. Mag.	x	y	80-Foot Focus		25-Foot Focus	
				μ_a	μ_δ	μ_a	μ_δ
Cluster Stars							
105......	15.2	−2′.3	+1′.1	+8	+6	−7	+6
106......	15.4	−2.2	−2.6	+9	+2	+7	+6
107......	15.3	−2.0	+0.8	+8	+1	−1	−3
108......	15.4	−1.9	−1.6	+6	+9	+8	+6
109......	15.4	−1.6	−1.4	+6	−5	+9	+10
110......	15.1	−1.5	−1.1	+4	+2	....	....
111......	15.2	−1.2	+1.0	+1	+9	....	....
112......	14.8	−1.0	−1.0	+3	+3	....	....
113......	14.2	−0.8	+0.1	+4	+4	....	....
114......	14.5	−0.8	+1.1	+5	+9	....	....
115......	14.4	−0.7	−0.2	+1	+6	....	....
116......	14.8†	−0.7	−0.3	+6	+8	....	....
117......	14.2†	−0.7	+0.1	+6	+6	....	....
118......	14.2	−0.5	+0.5	+2	+2	....	....
119......	14.2	−0.4	+0.5	+7	+1	....	....
120......	15.0	−0.7	−1.5	+4	+8	....	....
121......	15.1	−0.5	−1.0	+2	+10	....	....
122......	15.1	−0.5	−1.3	+2	+4	....	....
123......	14.3†	−0.5	−0.5	+6	+2	....	....
124......	14.3	−0.4	−0.3	+5	+5	....	....
125......	13.7	−0.3	+0.4	+8	+1	....	....
126......	15.1	−0.5	−1.1	+8	+9	....	....
127......	15.1†	−0.4	−1.1	+4	−1	....	....
128......	15.1	−0.5	−1.2	+2	+8	....	....
129......	15.5	−0.4	−2.4	−1	−1	+3	+2
130......	15.2	−0.4	−2.9	+3	+1	+6	+7
131......	15.2	−0.4	−3.5	+2	+12	+9	+9
132......	15.1	−0.3	+4.1	+5	+4	−1	+5
133......	15.0†	−0.4	+2.3	+2	+6	+4	+1
134......	14.8	−0.4	+1.8	+6	+3	−2	+2
135......	14.8	−0.1	+1.4	+5	+7	....	....
136......	13.8	−0.1	+0.4	+8	+4	....	....
137......	13.1†	+0.1	−0.5	+6	+11	....	....
138......	14.0	0.0	−0.5	+6	+8	....	....
139......	14.2†	−0.1	−0.7	+1	+4	....	....
140......	14.7	−0.1	−1.1	+1	+7	....	....
141......	15.1	−0.1	−1.5	+3	+3	....	....
142......	15.1	+0.1	−1.4	+6	+2	....	....
143......	14.7	+0.1	−0.8	+2	+7	....	....
144......	13.9	+0.1	−0.6	+4	+3	....	....
145......	14.7†	+0.1	−0.4	+7	+3	....	....
146......	14.1†	+0.3	−0.3	+5	+9	....	....
147......	13.3†	+0.4	−0.3	+4	+6	....	....
148......	14.4	+0.3	+0.7	+5	+10	....	....
149......	14.5	+0.3	+0.8	+3	+5	....	....
150......	14.5	+0.3	+1.5	+3	−2	....	....
151......	14.6	+0.5	+1.4	+5	+5	....	....
152......	15.0	+0.7	+3.5	+6	+5	+2	+1
153......	14.0†	+0.5	−0.1	+3	+9	....	....

TABLE VI—*Continued*

No.	Pg. Mag.	x	y	80-Foot Focus		25-Foot Focus	
				μ_α	μ_δ	μ_α	μ_δ
Cluster Stars							
154......	13.6	+ 0′.6	− 0′.3	+ 5	+ 6	....	....
155......	13.9†	+ 0.7	− 0.4	+ 5	+ 6	....	....
156......	14.9	+ 0.6	− 1.5	+ 4	+ 5	....	....
157......	15.1	+ 0.8	− 0.2	− 1	+ 6	....	....
158......	14.5	+ 0.8	+ 0.3	+ 3	+ 4	....	....
159......	14.8	+ 0.7	+ 0.5	+ 9	+ 3	....	....
160......	14.0	+ 1.2	+ 3.1	+ 4	+ 4	0	+ 1
161......	15.3	+ 1.0	− 2.9	+ 6	+11	+ 11	+ 3
162......	14.8	+ 1.2	− 0.7	+ 1	+ 6	....	....
163......	15.0	+ 1.4	− 0.4	+ 4	+ 2	....	....
164......	12.7	+ 1.4	+ 0.3	+ 5	+ 2	....	....
165......	15.4	+ 1.6	+ 1.4	+ 10	+ 7	+ 7	+ 8
166......	14.9	+ 1.6	− 1.0	+ 6	+ 8	....	....
167......	15.1	+ 1.6	− 1.4	+ 9	+ 4	....	....
168......	15.2	+ 1.8	− 2.0	+ 2	+ 6	+ 3	+ 7
169......	14.9	+ 1.9	+ 1.4	+ 6	+ 4	+ 1	+ 8
170......	14.7	+ 2.0	+ 3.3	+ 9	+ 4	− 2	+ 8
171......	15.2	+ 2.0	+ 3.7	+ 7	+ 2	+ 3	+ 7
172......	14.9	+ 2.2	0.0	+ 3	+ 7	+ 5	+ 3
173......	15.0	+ 2.4	− 1.8	+ 3	+ 9	+ 6	+10
174......	15.2	+ 2.9	− 1.1	+ 6	0	+ 5	+ 9
175......	13.2	+ 2.9	− 2.9	+ 17	+ 6	+ 9	+ 1
176......	13.1	+ 3.7	− 2.3	+ 1	+ 6	− 5	+ 3
177......	16.2	− 1.6	− 1.6	....	....	+ 12	+ 2
178......	16.7	− 1.5	− 2.3	....	....	+ 11	− 2
179......	16.0	− 1.4	− 2.4	....	....	+ 12	+ 3
180......	16.2	− 1.3	− 3.3	....	....	+ 8	+ 3
181......	16.2	− 1.0	− 2.9	....	....	+ 12	0
182......	16.0	− 1.2	− 1.7	....	....	+ 9	+ 7
183......	16.0	− 1.5	+ 2.4	....	....	+ 12	+ 1
184......	16.1	− 1.3	+ 2.2	....	....	+ 11	+ 3
185......	16.0	− 1.3	+ 2.4	....	....	+ 12	+ 3
186......	15.6	− 0.8	+ 3.2	....	....	+ 1	+ 4
187......	17.0	− 0.7	+ 3.3	....	....	+ 14	+ 3
188......	15.8	− 0.6	+ 3.5	....	....	+ 10	+ 5
189......	>17	− 0.8	+ 4.7	....	....	+ 19	+ 3
190......	>17	− 0.7	+ 4.6	....	....	+ 16	+11
191......	>17	− 1.2	− 4.2	....	....	+ 14	− 1
192......	16.8	− 1.0	− 4.5	....	....	+ 20	− 7
193......	16.3	− 1.0	− 4.7	....	....	+ 14	− 1
194......	>17	− 0.8	− 4.7	....	....	+ 17	− 7
195......	17.0	− 0.3	− 3.6	....	....	+ 19	− 3
196......	16.3	0.0	+ 2.3	....	....	+ 9	− 3
197......	16.2	0.0	+ 2.5	....	....	+ 6	+ 8
198......	16.0	0.0	+ 2.7	....	....	+ 7	+ 3
199......	16.7	+ 1.5	− 4.8	....	....	+ 23	− 6
200......	16.8	+ 2.0	− 3.7	....	....	+ 18	0
201......	16.2	+ 2.2	− 3.6	....	....	+ 14	− 2
202......	16.7	+ 2.3	− 4.9	....	....	+ 10	−22

TABLE VI—*Continued*

No.	Pg. Mag.	x	y	80-Foot Focus μ_α	80-Foot Focus μ_δ	25-Foot Focus μ_α	25-Foot Focus μ_δ
Cluster Stars							
203......	16.6	+2′3	−5′2	....	....	+19	+5
204......	17.0	+2.7	−4.8	....	....	+34	−8
205......	17.0	+2.2	−3.0	....	....	+27	−3
206......	16.6	+2.5	−3.0	....	....	+18	+1
207......	16.6	+1.9	+4.1	....	....	+1	+7
208......	>17	+2.1	+3.8	....	....	+21	−2
209......	>17	+0.2	+4.2	....	....	+4	0
210......	16.7	+0.3	+4.1	....	....	+2	+3
211......	16.6	+0.6	+4.3	....	....	+11	+11
212......	16.4	+0.7	+5.5	....	....	+14	+7
213......	>17	+0.8	+5.4	....	....	+2	−1
214......	15.7	+1.3	+4.9	....	....	+1	+4
215......	>17	+1.1	+6.4	....	....	−6	−3
216......	16.8	+1.6	+6.4	....	....	+8	+7
217......	16.9	+1.4	+5.8	....	....	+3	+6
218......	16.8	−2.4	+4.1	....	....	+9	+2
219......	16.9	−2.5	+3.8	....	....	+12	+3
220......	17.0	−3.4	+1.7	....	....	+9	−4
221......	16.6	−3.5	+1.6	....	....	+13	+3
222......	16.9†	−2.6	+3.5	....	....	+8	−2
223......	>17	+4.7	+0.7	....	....	+16	+9
224......	17.0	+5.1	+0.8	....	....	+26	+7

* Rejected in determining the plate constants.

† Magnitude uncertain.

The next step is the derivation of the total motions of the clusters. Because of the nearly symmetrical distribution of the stars around the center, we may take the straight mean of the motions. In this way we find the results given in Table VII. The agreement between

TABLE VII

RELATIVE PROPER MOTIONS OF CLUSTERS

Object	Plates, with Focus in Feet	μ_α	μ_δ
M 13..........	Two pairs 80	+0″0008	+0″0004
	One pair 25	+0.0028	+0.0008
M 56..........	Two pairs 80	−0.0018	+0.0066
M 2..........	One pair 80	+0.0046	+0.0050
	One pair 25	+0.0091	+0.0027

the values derived from the 80-foot- and 25-foot-focus plates is satisfactory. Taking into account the weights of the different sets of plates, we adopt the mean relative motions:

M 13............	$\mu_\alpha = +0''0015$	$\mu_\delta = +0''0005$
M 56............	$\mu_\alpha = -0.0018$	$\mu_\delta = +0.0066$
M 2.............	$\mu_\alpha = +0.0061$	$\mu_\delta = +0.0042$

These motions are referred to the mean of the comparison stars. With the help of Table 26 of *Groningen Publications*, No. 29, we can compute the mean parallactic motions of the comparison stars used. For the three clusters, M 13, 56, and 2, they are 0″0010 in $\chi = 286°$, 0″0005 in $\chi = 94°$, and 0″0027 in $\chi = 127°$, respectively. The final absolute motions of the clusters may therefore be taken as:

M 13...........	$\mu_\alpha = +0''0005$	$\mu_\delta = +0''0008$
M 56...........	-0.0013	$+0.0066$
M 2............	$+0.0082$	$+0.0026$

Although the number of clusters is but three, it seems worth while to derive from these motions an indication of their mean parallax by the use of the formula:

$$\bar{\pi} = \frac{4.74}{V} \cdot \frac{\bar{\mu}}{\sqrt{2}} .$$

Using Strömberg's recent value, $V = 329$ km/sec.,[1] we find $\bar{\pi} = 0''000061$, which compares favorably with the mean of the three parallaxes found by Shapley, viz., 0″000065.

Subtracting the values of the mean motions given in Table VII from the proper motions in Tables III, V, and VI, we derive the internal motions of the clusters given in the second and third columns of Tables VIII, IX, and X. The unit for the motions is again 0″001.

---

[1] *Mt. Wilson Contr.*, No. 292; *Astrophysical Journal*, **61**, 353, 1925.

TABLE VIII

INTERNAL MOTION IN M 13

No.	μ_α	μ_δ	$\mu_{\text{rad.}}$	$\mu_{\text{tang.}}$	No.	μ_α	μ_δ	$\mu_{\text{rad.}}$	$\mu_{\text{tang.}}$
80-Foot-Focus Plates									
2	+10	−3	−10	+2	686	−1	+1	−1	+1
7	+4	−2	−4	+2	690	−1	0	0	−1
17	+1	−1	0	−1	712	−3	−2	0	+4
25	+2	+1	−1	+2	737	+3	−1	+3	−2
46	−10	+1	+9	+4	775	+1	−1	+1	0
49	+3	−3	−3	−3	784	+1	−6	−4	+5
59	+6	−5	−8	+1	796	+4	0	+2	−4
70	−6	+1	+5	−3	804	−2	0	−2	−1
72	−7	−1	+7	+3	808	+7	+4	+5	+6
96	−4	−1	+4	−1	816	−4	+6	−4	−6
118	+3	−3	−3	−3	822	+1	+4	+4	+1
158	−3	−3	0	−4	829	−1	+6	+1	−6
222	−5	+1	+3	+4	835	−5	+2	−4	+3
246	−4	+4	+1	+5	837	+6	+5	+1	−8
252	+1	+1	0	+1	840	+3	−1	+3	0
299	−1	+2	+2	+1	851	−2	0	−2	0
306	−4	+1	+4	0	852	+1	−4	+4	+1
310	+1	+2	−2	+1	861	−2	+1	−2	+1
311	−10	−3	+6	−8	873	+3	−2	0	+4
313	−1	+3	+3	+1	899	+1	−2	−1	+2
323	−7	+2	+5	+6	925	+4	0	+3	−3
325	−3	−4	+3	−4	935	+3	+3	+4	0
326	+3	+1	0	+3	953	+3	+2	+3	+1
363	−1	+4	−4	+2	978	−1	−3	−1	+3
406	+1	−2	+1	−2	989	−2	+1	−2	0
418	−4	+2	−1	+4	1038β	+2	+3	+3	−2
500	+3	0	0	+3	1042	−3	0	−3	0
523	0	−3	−3	−1	1063	+1	+4	+3	−3
559	−3	−1	−1	−3	1079	+2	0	+1	+2
641	+1	+1	+1	+1	1106	−2	+2	−3	0
653	−1	+5	+5	−1	1113	+5	+7	+8	−3
25-Foot-Focus Plates									
2	−8	+2	+8	−1	71	−4	+1	+4	0
7	+7	+3	−3	+7	71*a*	+2	−3	−3	−2
17	−7	−4	+8	+1	72	−7	−5	+9	0
21	−3	+4	+5	+1	76	−10	0	+9	+4
25	+1	0	−1	0	82*a*	+6	−8	−10	−1
46	−12	−5	+13	0	82	−5	−14	−5	−14
49*a*	+11	−3	−11	−3	96	−13	+1	+13	−1
49	−4	+1	+4	+1	113	+8	−5	0	−9
51	−1	+1	+1	+1	113*a*	+11	−2	−4	−10
51*a*	+5	0	−5	+1	155	+4	+1	−2	−3
54	−4	−6	−1	−7	158	+1	−11	−8	−7
59*a*	+3	0	−2	+2	159	−3	−8	+8	−1
59	−4	0	+3	−3	236	−11	+4	+7	−9
70	−4	+1	+4	−2	275	−2	0	0	−2
70*a*	+3	−8	−7	−4	275*a*	+4	−7	−7	+3

TABLE VIII—*Continued*

No.	μ_α	μ_δ	$\mu_{\text{rad.}}$	$\mu_{\text{tang.}}$	No.	μ_α	μ_δ	$\mu_{\text{rad.}}$	$\mu_{\text{tang.}}$
25-Foot-Focus Plates									
275*b*	+2	+2	+2	+2	922	−2	+8	+6	−5
283	+2	−18	−18	−3	1010	−4	+4	+1	−6
326	−13	+11	+14	−10	1031	+5	+4	+1	−6
326*a*	−7	+2	+3	−6	1034	+4	−7	+8	0
365	+7	−7	+6	−8	1034*a*	+1	+1	0	−1
590	+1	−5	+5	−1	1037*a*	−4	+4	+1	−6
627	−5	−2	−2	−5	1037	+8	0	+5	+6
641	−5	+6	+6	−5	1063	−21	−5	−21	−6
641*a*	+5	+1	+2	+5	1069*a*	−4	+2	−3	−3
749	−2	+7	+6	−4	1069	−4	+4	−2	−5
790	−1	+1	−1	+1	1076	−4	+6	+2	−7
791	+3	0	+1	−3	1079	−5	+1	−2	−5
791*a*	+12	+3	0	−12	1083	+9	0	+8	−4
808	−14	−4	−7	−13	1083*a*	+7	+7	+2	−10
813	+8	−5	+6	−7	1090	0	+7	+2	−7
822*a*	+1	+4	+4	0	1090*a*	+8	+7	+9	−5
822	−2	+2	+2	−2	1102	−3	−2	−3	−1
879	+2	−8	+8	+1	1106*a*	+19	+13	+6	−22
879*a*	−2	−2	+2	+2	1106	+12	+1	+9	−8
899	−7	−3	−6	−4	1106*b*	+17	+7	+9	−16
915	+3	+2	−1	−3	1113	−13	−6	−14	−2
922*a*	+8	+9	+11	+4					

The resulting values have been used for different purposes: (*a*) They were utilized to derive an upper limit of the probable errors; the results have been given on page 4. (*b*) In *Contribution* No. 129,[1] Pease and Shapley have called attention to the asymmetry found in several globular clusters. While this asymmetry is extremely small, if not negligible, for M 56, they were able to derive "galactic planes" for both M 13 and 2. From the flattening of several of the clusters, as well as for theoretical reasons, we might expect the stars in the clusters to be moving in orbits parallel to the galactic planes, around the center of gravity; but according to Russell such motions should be less than 0.″001 per year even in the nearest of clusters. The internal motions for the two clusters, M 13 and 2, were analyzed into components, parallel to and at right angles to these planes. In both cases the positive sign was used for motion in the direction southeast and away from the "galactic plane," respectively. The results are:

---

[1] *Astrophysical Journal*, **45**, 225, 1917.

M 13

$$\text{Two pairs of plates, 80-foot focus}\left\{\begin{array}{l}\bar{\mu}\parallel = -0\overset{''}{.}0004 \pm 0\overset{''}{.}0003 \\ \bar{\mu}\perp = +0.0005 \pm 0.0003\end{array}\right.$$

$$\text{One pair of plates, 25-foot focus}\left\{\begin{array}{l}\bar{\mu}\parallel = -0.0001 \pm 0.0005 \\ \bar{\mu}\perp = -0.0008 \pm 0.0005\end{array}\right.$$

M 2

$$\text{One pair of plates, 80-foot focus}\left\{\begin{array}{l}\bar{\mu}\parallel = -0.0003 \pm 0.0002 \\ \bar{\mu}\perp = +0.0002 \pm 0.0002\end{array}\right.$$

$$\text{One pair of plates, 25-foot focus}\left\{\begin{array}{l}\bar{\mu}\parallel = +0.0004 \pm 0.0006 \\ \bar{\mu}\perp = -0.0004 \pm 0.0005\end{array}\right.$$

The dispersion of the motions in the direction parallel to and at right angles to the "galactic plane" is practically the same; this indicates that there is no pronounced motion parallel to the galactic planes. (*c*) The internal motions for all three clusters were finally resolved

TABLE IX

INTERNAL MOTION IN M 56

No.	μ_α	μ_δ	$\mu_{\text{rad.}}$	$\mu_{\text{tang.}}$	No.	μ_α	μ_δ	$\mu_{\text{rad.}}$	$\mu_{\text{tang.}}$
101	+2	+ 1	0	+2	126	−6	− 5	− 7	− 4
102	−2	− 1	+ 1	−2	127	−4	−18	−17	+ 7
103	0	+ 1	0	+1	128	+2	− 1	+ 1	+ 2
104	+2	0	− 1	+2	129	+6	− 2	+ 6	+ 2
105	+8	−10	−12	+4	130	+1	− 4	+ 4	0
106	−2	+ 2	+ 2	+2	131	+4	+ 1	− 1	− 4
107	−4	− 3	0	−5	132	+3	+ 5	− 4	− 4
108	+2	+ 1	− 1	+2	133	+2	+ 3	+ 2	− 3
109	+1	+ 3	+ 1	+3	134	+6	+ 1	+ 6	+ 1
110	0	− 3	+ 2	−2	135	−6	− 7	− 9	− 2
111	+2	+ 2	0	+3	136	0	+ 1	+ 1	0
112	0	− 3	+ 2	−2	137	+2	+ 2	+ 3	+ 1
113	+2	+ 3	− 4	−1	138	−4	0	− 1	− 4
114	+4	+ 1	− 3	+3	139	0	− 1	− 1	+ 1
115	−4	+ 3	+ 4	−3	140	−4	+ 1	− 4	− 1
116	+6	− 1	− 3	−5	141	+2	+ 3	+ 3	− 2
117	−4	+ 5	− 1	+6	142	0	−10	− 9	+ 4
118	0	+ 3	− 3	+1	143	−4	+ 3	− 1	− 5
119	−4	+ 1	0	+4	144	0	− 1	+ 1	+ 1
120	−2	− 1	− 1	−2	145	+4	− 2	+ 4	− 1
121	+2	+ 2	− 1	+3	146	−1	− 3	0	+ 3
122	+3	− 5	− 2	−5	147	+1	+ 7	+ 6	− 3
123	−4	+ 3	+ 5	+1	148	0	− 5	− 4	+ 3
124	+4	− 3	+ 5	−2	149	−2	−16	+ 1	+16
125	+3	+ 4	+ 5	+2	150	+8	+ 6	+ 8	− 6

TABLE X

INTERNAL MOTION IN M 2

No.	μ_α	μ_δ	$\mu_{rad.}$	$\mu_{tang.}$	No.	μ_α	μ_δ	$\mu_{rad.}$	$\mu_{tang.}$
80-Foot-Focus Plates									
101	−2	+7	+3	+6	139	−4	−1	+1	+4
102	−2	−1	+2	−1	140	−4	+2	−1	+4
103	+2	0	−1	+1	141	−2	−2	+2	+2
104	+3	+3	0	+4	142	+1	−3	+3	−1
105	+3	+1	−3	+2	143	−3	+2	−2	+3
106	+4	−3	0	−5	144	−1	−2	+2	+1
107	+3	−4	−4	−3	145	+2	−2	+3	0
108	+1	+4	−4	+2	146	0	+4	−2	−3
109	+1	−10	+6	−8	147	−1	+1	−1	−1
110	−1	−3	+3	−1	148	0	+5	+4	−2
111	−4	+4	+6	+1	149	−2	0	−1	−2
112	−2	−2	+3	0	150	−2	−7	−7	−1
113	−1	−1	+1	−1	151	0	0	0	0
114	0	+4	+3	+2	152	+1	0	0	−1
115	−4	+1	+3	+2	153	−2	+4	−3	−3
116	+1	+3	−2	+3	154	0	+1	−1	−1
117	+1	+1	−1	+1	155	0	+1	−1	−1
118	−3	−3	−1	−4	156	−1	0	0	−1
119	+2	−4	−4	−2	157	−6	+1	−6	0
120	−1	+3	−2	+2	158	−2	−1	−2	−1
121	−3	+5	−3	+5	159	+4	−2	+3	+3
122	−3	−1	+2	+3	160	−1	−1	−1	0
123	+1	−3	+1	−3	161	+1	+6	−5	−4
124	0	0	0	0	162	−4	+1	−4	+1
125	+3	−4	−5	+1	163	−1	−3	0	+3
126	+3	+4	−5	−2	164	0	−3	−1	+3
127	−1	−6	+6	−1	165	+5	+2	+5	+2
128	−3	+3	−3	+3	166	+1	+3	0	−3
129	−6	−6	+7	+5	167	+4	−1	+4	−1
130	−2	−4	+4	+1	168	−3	+1	−2	+2
131	−3	+7	−7	+3	169	+1	−1	0	+1
132	0	−1	−1	0	170	+4	−1	+2	+4
133	−3	+1	+2	−2	171	+2	−3	−4	−1
134	+1	−2	−2	+1	172	−2	+2	−2	−1
135	0	+2	+2	0	173	−2	+4	−4	−2
136	+3	−1	−1	+3	174	+1	−5	+2	+5
137	+1	+6	−6	−2	175	+12	+1	+8	−9
138	+1	+3	−3	−1	176	−4	+1	−4	+1
25-Foot-Focus Plates									
101	−7	+3	+7	+1	109	0	+7	−4	+5
102	−6	+5	+5	+6	129	−6	+9	−7	+8
103	−9	−1	+8	−4	130	−3	+4	−3	+4
104	−7	+1	+6	−3	131	0	+6	−6	+1
105	−16	+3	+16	−4	132	−10	+2	+3	−10
106	−2	+3	−1	+3	133	−5	−2	−1	−5
107	−10	−6	+7	−9	134	−11	−1	+2	−11
108	−1	+3	−1	+3	152	−7	−2	−3	−7

TABLE X—*Continued*

No.	μ_α	μ_δ	$\mu_{\text{rad.}}$	$\mu_{\text{tang.}}$	No.	μ_α	μ_δ	$\mu_{\text{rad.}}$	$\mu_{\text{tang.}}$
25-Foot-Focus Plates									
160	−9	−2	−5	−8	195	+10	−6	+5	−11
161	+2	0	+1	−2	196	0	−6	−6	0
165	−2	+5	+2	−5	197	−3	+5	+5	−3
168	−6	+4	−7	+2	198	−2	0	0	−2
169	−8	+5	−4	−9	199	+14	−9	+13	−11
170	−11	+5	−2	−12	200	+9	−3	+7	−6
171	−6	+4	0	−7	201	+5	−5	+7	−2
172	−4	0	−4	0	202	+1	−25	+23	+9
173	−3	+7	−6	−4	203	+10	+2	+3	−10
174	−4	+6	−6	−4	204	+25	−11	+21	−17
175	0	−2	+2	+1	205	+18	−6	+15	−12
176	−14	0	−12	+7	206	+9	−2	+7	−6
177	+3	−1	−2	−3	207	−8	+4	0	−9
178	+2	−5	+3	−5	208	+12	−5	+2	+13
179	+3	0	−1	−3	209	−5	−3	−3	−5
180	−1	0	+1	0	210	−7	0	−7	+1
181	+3	−3	+2	−4	211	+2	+8	+8	+1
182	0	+4	−3	+2	212	+5	+4	+4	+5
183	+3	−2	−3	+2	213	+3	−4	−3	+4
184	+2	0	−1	+2	214	−8	+1	−1	−8
185	+3	0	−1	+3	215	−15	−6	−8	−14
186	−8	+1	+3	−8	216	−1	+4	+4	−2
187	+5	0	−1	+5	217	−6	+3	+2	−6
188	+1	+2	+2	+1	218	0	−1	−1	−1
189	+10	0	−2	+10	219	+3	0	−2	+2
190	+7	+8	+6	+9	220	0	−7	−3	−6
191	+5	−4	+2	−6	221	+4	0	−3	+2
192	+11	−10	+7	−13	222	−1	−5	−3	−4
193	+5	−4	+3	−6	223	+7	+6	+8	−5
194	+8	−10	+8	−10	224	+17	+4	+17	−2

into radial and tangential components, the positive signs being used for motion outward and in the direction N-E-S-W. The results are given in the fourth and fifth columns of Tables VIII, IX, and X, using again 0″.001 as a unit.

A radial motion might be expected if the clusters were either expanding or contracting. For M 13 we find from the 80-foot-focus plates the mean radial motion +0″.0006±0″.0003, and from the 25-foot-focus plates +0″.0013±0″.0005; for M 56 we find −0″.0002±0″.0005; for M 2 we find −0″.0004±0″.0003 from the 80-foot-focus plates and +0″.0019±0″.0005 from the 25-foot-focus plates. While there is slight preponderance of the positive sign, indicating an expansion of the clusters, the amount is too small to draw any definite conclusions.

From (*b*) it follows that the motions resulting from a possible rotation of the clusters are small. Tangential components of the motions were derived therefore only because evidence of such motions had been found in the measures of spiral nebulae. The results for the clusters are:

M 13.....	Two pairs of 80-foot-focus plates	$\mu_{\text{tang.}}=+0''.0001\pm0''.0003$
	One pair of 25-foot-focus plates	$\mu_{\text{tang.}}=-0.0034\pm0.0004$
M 56.....	Two pairs of 80-foot-focus plates	$\mu_{\text{tang.}}=-0.0002\pm0.0003$
M 2......	One pair of 80-foot-focus plates	$\mu_{\text{tang.}}=+0.0001\pm0.0002$
	One pair of 25-foot-focus plates	$\mu_{\text{tang.}}=-0.0026\pm0.0005$

In the mean, the tangential component for all the cluster plates taken at the 80-foot focus is exactly 0″.0000, while in the case of M 33, observed at that focus, an annual tangential component of 0″.0140 was found; for the cluster plates taken at the 25-foot focus the mean tangential component for M 13 and 2 is 0″.0030, while for seven spirals it is 0″.0184.

It has been thought that the large displacements in the spirals might be due to a difference in quality in the old and the new plates. In that case the annual motions derived would be smaller for pairs of plates with longer intervals, but the total displacements would be of the same order, and should be the same for both the clusters and the spirals. We find, however, that the total tangential displacement in the case of the 80-foot-focus plates is 0″.070 for the spirals, 0″.000 for the clusters, and, in the case of the 25-foot-focus plates, 0″.174 for the spirals and 0″.044 for the clusters.

The length of exposure, too, cannot have caused the displacements in the spirals; for all the 80-foot-focus plates, for M 33 as well as for the clusters, these were about a half-hour, except for M 2, where the exposure times were fifteen and twenty minutes. The exposures for the 25-foot-focus plates of the spirals ranged from one hour to eight hours, while for the clusters they were one hundred minutes and five hours, respectively.

Since the comparison stars for the spirals are brighter, on the whole, than the nebular points measured, it has been suggested that the rotational displacements found in the spirals might be due to some obscure magnitude error. It was for this reason that several faint objects were measured on the plates of the clusters taken at the 25-foot focus. While no stars fainter than magnitude 16.5 could be measured on the plates taken at the 80-foot focus, the range in magnitude for the 25-foot focus plates was from 12.5 to the eighteenth or nineteenth magnitude for M 13, and from 10.3 to well below the seventeenth magnitude for M 2. No correlation whatsoever seems to exist between magnitude and tangential component, as may be seen from Table XI, where the tangential components are given in thousandths of a second of arc, while the figures in parentheses indicate the number of stars used.

TABLE XI

Object	Magnitude							
	<12	13	14	15	16	17	18–19	
				80-Foot-Focus Plates				
M 13*....	....	0 (9)	+1 (13)	−1 (14)	−1 (12)	....	....	Comparison stars
		+1 (8)	−1 (7)	0 (45)	....	....	....	Cluster stars
M 56.....	....	−1 (12)	0 (21)	0 (32)	....	....	....	Comparison stars
		$+3^{5}$(6)†	−3 (4)	$+0^{5}$(33)	-1^{5}(7)	....	....	Cluster stars
M 2‡.....	+4(5)	−9 (7)	−2 (10)	+3 (14)	0 (2)	....	....	Comparison stars
	....	0 (7)	0 (32)	$+0^{5}$(34)	....	....	....	Cluster stars
				25-Foot Focus Plates				
M 13*....	....	-0^{5}(8)	$+0^{5}$(13)	0 (14)	−1 (11)	....	....	Comparison stars
		−4 (5)	0 (3)	−3 (12)	−3 (30)	....	-3^{5}(22)	Cluster stars
M 2‡.....	+2(5)	−8 (7)	+1 (10)	+1 (14)	-2^{5}(2)	....	....	Comparison stars
	....	....	−8 (5)	−2 (24)	−2 (30)	−3 (15)	....	Cluster stars

* The two variable stars, Nos. 306 and 816, and the two stars having considerable proper motion, *p* and *s*, were excluded.

† It is doubtful if these six stars, Nos. 101, 105, 125, 131, 144, and 149, are members of the cluster.

‡ Star No. 17 was excluded on account of its large proper motion; Nos. 164, 175, and 176, on account of the uncertainty as to their membership in the cluster.

In concluding I wish to express my thanks to Messrs. Pease and Humason for obtaining the 25-foot-focus plates, and to Mrs. Marsh, of the computing division, who has assisted in the numerous reductions involved.

Carnegie Institution of Washington
Mount Wilson Observatory
April 1917

Contributions from the Mount Wilson Observatory, No. 339
Reprinted from the *Astrophysical Journal*, Vol. LXVI, pp. 122–134, 1927
Printed in the U.S.A.

ON THE RELATIONS BETWEEN PERIOD, LUMINOSITY, AND SPECTRUM AMONG CEPHEIDS

By HENRY NORRIS RUSSELL[1]

ABSTRACT

If it is assumed that the median total luminosity of periodic variable stars follows the observed mass-luminosity law, and that the variation of any given type arises from a dynamical oscillation of some definite sort, it follows that the existence of a *relation between period and luminosity* demands one between *period and spectral class*, and vice versa. For the *normal Cepheids*, the observed *change in mean spectrum* with *period* is in *excellent agreement* with that computed from the *period-luminosity curve*. If *variability of long period* arises from a dynamical oscillation, the *relation* between *period* and *density* must be roughly the *same* as for the Cepheids. For the *cluster variables*, the *period* corresponding to a given density *must be shorter* than for the Cepheids, and the properties of the dynamical system must be rather peculiar.

Periodic variables decidedly fainter in absolute magnitude than the period-luminosity curve indicates should be *much redder* than Cepheids of the same period, if they owe their variability to *dynamical oscillations*. No cases of this sort are known among the galactic stars.

The existence of a very close correlation between mass and absolute magnitude is an established observational fact, the only exceptions being white dwarfs like the companion of Sirius. It is equally well established that, for stars of the same mass, the effective temperature (or spectral class) has a quite subordinate influence on the brightness.

We may therefore accept as a fact, independent of any theory, a relation of the form

$$L=F(M)T^m\ , \tag{1}$$

where L is the total radiation, M the mass, and T the effective temperature of the surface. The form of the function $F(M)$ over the whole observable range is close to that given in Eddington's theory.[2] For small luminosities it varies nearly as M^4, and for great luminosities about as M^2. As for the exponent m, the observational evidence shows only that it is small. Eddington makes it +4/5. We may, if we wish, write (1) in the form

---

[1] Research Associate of the Mount Wilson Observatory, Carnegie Institution of Washington.

[2] *Monthly Notices, R.A.S.*, 84, 310, 1924.

$$L = M^n T^m f(M) \; , \tag{2}$$

where, by suitable choice of n, $f(M)$ may be made nearly constant over a range of a few magnitudes in brightness. But we have always

$$L = 4\pi\sigma r^2 T^4 \qquad M = \tfrac{4}{3}\pi\rho r^3 \; ,$$

where σ is Stefan's constant, r the star's radius, and ρ its mean density. Eliminating M and r from (2) we find

$$L^{\frac{3}{2}n-1} f(M) = \text{Const.}\times\rho^{-n}T^{6n-m} \tag{3}$$

For the brighter stars the best value of n is about 2. This gives, according to Eddington's data, the following relative values of $f(M)$:

Abs. Mag......	+1	0	−1	−2	−3	−4	−5	−6
$f(M)$..........	0.64	0.83	1.00	1.13	1.16	1.09	0.97	0.82

Introducing $n = 2$ into (3), we have

$$L = \text{Const. } T^{6-\frac{1}{2}m}\rho^{-1}f^{-\frac{1}{2}} \; . \tag{4}$$

This equation is a transformation of that of the curve of mass and luminosity. It is applicable to any star whatever, provided that it is remembered that for absolutely faint stars, or for bright stars (if they exist) which do not follow Eddington's mass-luminosity curve, the values of f may differ seriously from unity. The great importance of the effective temperature in determining the brightness, and the relative insignificance of the imperfectly known constant m and of the correction term f are noteworthy.

We may now apply this equation to the case of Cepheid variables. There is a great deal of evidence that the immediate cause of the variation of all those stars whose variability is "punctually" periodic (as Miss Clerke put it) and not explicable by eclipses is a periodic variation in the effective temperature of the visible surface, accompanied perhaps by changes in size or shape, and that behind these changes there is some sort of dynamical oscillation within the system, taking place under gravity. The volume pulsations considered by Eddington and the changes of figure connected with rotational instability and fission considered by Jeans are examples of such oscillations. For any such dynamical oscillation of definite type, the period P and the mean density ρ should be related by an equation of the type

$$\rho = P^{-2} q(P) \, , \tag{5}$$

where q is a slowly varying function.

For similar systems, differing in density but not in physical constitution, q should be strictly constant. In an actual case, physical changes, such as that of the ratio of the specific heats in a pulsating star, or of the degree of internal condensation in a dividing mass, might cause it to vary gradually. For oscillations of different dynamical types, the values of q will be different; but it is well known that, except for higher harmonics, they are usually of the same order of magnitude.

There are, indeed, systems for which the relation between P and ρ is less simple, and depends on other parameters. For example, in an eclipsing pair it involves the radii of the two stars, in terms of that of the orbit. In such systems, however, one would expect that the form of the light-curve would depend upon these additional parameters, as it does for eclipsing variables. For the Cepheids, however, Hertzsprung[1] has given evidence that the remarkable differences in the forms of different light-curves are very closely correlated with the period, stars of the same period having very similar curves; and this is good prima facie evidence that no additional parameters are of fundamental importance, and thus equation (5) is applicable.

The radiation from an oscillating system will vary, and its mean value will presumably differ more or less from that which it would emit if the oscillation should be reduced to zero; but this difference may, in general, be expected to be of the second order with respect to the amplitude of the oscillation. It appears therefore safe to assume that the range of values of L during the oscillation will include the equilibrium value. Upon this assumption we may combine (4) and (5), introducing at the same time $m = 0.8$, which is abundantly accurate for our purpose, and write

---

[1] *Bulletin of the Astronomical Institutes of the Netherlands*, **3**, 115 (No. 96), 1926.

$$L = \text{Const.} \times \frac{T^{5.6} P^2}{q f^{\frac{1}{2}}} \; . \qquad (6)$$

With proper values of q and f, this equation should hold true for all oscillating systems.

It may next be remarked that there is nothing in these relations—or, indeed, in any relations derivable from the general nature of a dynamical oscillation—to give a period-luminosity curve. No general relation can pick out one distinctive value among the infinity of possible solutions of the dynamical problem for a given mass; such a relation must be based in some way upon the properties of atoms. The relation of mass and luminosity is a case in point; but, though it determines the radiation from a star of given mass and radius, it puts no restriction at all upon the radius of a star of given mass. The existence of a specific relation between period and luminosity, and hence between density and mass, indicates that the atomic (or quantum) properties of matter must again enter the physical problem. How and why they do so is not yet understood; but it is an immediate consequence of equation (6) that, if such a correlation between period and luminosity exists, there must also be an even closer correlation between period and effective temperature. Either one implies and demands the other.

This statement is not new; it is contained implicitly in the equations of Shapley[1] and the theoretical work of Eddington,[2] and Jeans[3] has recently shown how a period-luminosity curve follows, on his hypothesis, from the assumption of constant temperature. This assumption, however, really begs the question, from the standpoint of theory. We can at present give no definite reason why a rotating, or pulsating, star of given mass should find itself in a critical condition for some definite value of the mean density, although we may surmise that changes in ionization have something to do with the matter.[1] From this point, therefore, our procedure must be empirical. We take one of the two relations between period, luminosity, and effective temperature from observation, deduce what the other should be, and compare this with the facts.

---

[1] *Mt. Wilson Contr.*, No. 154; *Astrophysical Journal*, **49**, 24, 1919.

[2] *Monthly Notices, R.A.S.*, **79**, 2, 1918.

[3] *Ibid.*, **85**, 808, 1925

According to Shapley's latest period-luminosity curve[2] the visual absolute magnitude of a Cepheid increases from -1.30 to -3.13, for a change in log P from 0.5 to 1.5. The corresponding change in visual magnitude is probably about -2.2, and in bolometric magnitude about -2.5, so that approximately $L \propto P$. It follows from (6) that $\frac{T^{5.6}P}{qf^{\frac{1}{2}}} = \text{Const.}$ If we ignore the changes in f, which are probably quite negligible, and in q, which are likely to be small, we will have $T \propto P^{-0.18}$.

The observed datum is not the effective temperature but the spectral class. For the relation between them we may well adopt the values for giant stars deduced by the writer from various sources,[3] as follows:

Sp............	Ao	A5	Fo	F5	Go	G5	Ko
T.............	11,000°	8600°	7400°	6500°	5600°	4700°	4200°
Comp.........	10,500	8900	7600	6500	5600	4700	4000

The computed values are derived from the formula

$$\log T = 4.02 - 0.14\ (\mathrm{Sp} - \mathrm{Ao})\ ,$$

which is substantially identical with one used by Eddington,[4] Fo being taken as 1.0, etc. This is evidently a sufficient approximation for the present purpose. According to it we should expect to find the spectral class advancing by 0.18/0.14 or 1.3 divisions for an increase of 1.0 in log P. It is well to note that the Cepheids actually show an advance in spectral type of just about this amount.

Adams and Joy[5] have determined the spectral classes of more than fifty Cepheids, allowing for the variation during the period, and reducing to the median value for each star. A freehand curve drawn to represent these results gives the classes F4, G2, and G6 for log $P = 0.5$, 1.0, and 1.5, respectively. This close agreement encourages a more detailed test. By starting with Shapley's period-luminosity curve for photographic absolute magnitude A, the bolometric absolute magnitude, B, may be derived by applying E. S. King's color indices[1] and Eddington's corrections from visual to bolometric magnitude.[2] We have then from (6)

---

[1] Cf. Eddington, *The Internal Constitution of the Stars* (Cambridge, 1926), pp. 200–205; Russell, Dugan, Stewart, *Astronomy* (Boston, 1927), **2**, 921.

[2] *Harvard Circular*, No. 280, 1925.

[3] *Op. cit.*, p. 753.

[4] *Op. cit.*, p. 181.

[5] *Mt. Wilson Communications*, No. 100; *Proceedings of the National Academy of Sciences*, **13**, 391, 1927.

$$5.6 \log T = \text{Const.} + \log L - 2 \log P$$

or

$$\log T = 3.85 - \tfrac{1}{14} B - \tfrac{5}{14} \log P \,, \tag{7}$$

where the numerical constant has been determined so as to agree with the general mean of the spectroscopic data.

We thus find:

log P	A	B	log T	Spectrum
0.0	−0.51	−0.82	3.91	A8
0.4	1.14	1.56	3.82	F4
0.8	1.78	2.48	3.74	G0
1.2	2.48	3.6	3.68	G4
1.6	3.37	4.9	3.63	G8
2.0	−4.81	−6.5	3.60	K0

The observed spectra and those derived from equation (7) for the variables observed by Adams and Joy which have periods between one day and one hundred and thirty days are given in Table I and plotted in Fig. 1. Stars for which the variation is not of the normal Cepheid type are marked by asterisks, and cases in which but a single spectrogram has been obtained are marked by daggers.

The differences between the observed and computed spectra, which are given in tenths of a class in the last column, are usually very small. They are considerable for several of the stars at the end of the list, which, however, have not the typical Cepheid variation, but belong to the RV Tauri class, or are still more irregular. Of the stars of shorter period, RW Aquilae has a spectrum with hazy lines, very unlike a normal Cepheid, and RY Boötis shows no variations in radial velocity. The photometric data are poor in both cases. It appears justifiable, therefore, to exclude these stars from further discussion. The residuals for the excluded stars are placed in paren-

---

[1] *Harvard Annals*, **85**, 61 (No. 3), 1923.

[2] *Op. cit.*, p. 138.

TABLE I

Observed and Computed Spectra of Cepheids

Desig.	log *P*	Obs. Sp.	Comp. Sp.	O−C	Desig.	log *P*	Obs. Sp.	Comp. Sp.	O−C
SW Tau	0.20	F3†	F1	+2	SY Aur	1.00	G0	G2	−2
SU Cas	.28	F4	F3	+1	ζ Gem	1.00	G1	G2	−1
TU Cas	.33	F4	F4	0	Z Lac	1.04	G3	G2	+1
SZ Tau	.50	F7	F6	+1	VX Per	1.04	F7†	G3	−6
RT Aur	.57	F6	F6	0	SV Per	1.05	G2	G3	−1
SU Cyg	.58	F6	F7	−1	RX Aur	1.06	F8	G3	−5
Y Aur	.59	F9	F7	+2	SZ Cas	1.13	G1	G4	−3
α U Mi	.60	F7	F7	0	TT Aql	1.14	G2	G4	−2
ST Tau	.61	F8†	F7	+1	W Ser	1.15	G4	G4	0
T Vul	.64	G0	F8	+2	RW Cas	1.17	G5†	G4	+1
VZ Cyg	.69	G2	F8	+4	SZ Cyg	1.18	G6	G4	+2
V Lac	.70	F7†	F9	−2	SV Mon	1.18	G4	G4	0
AP Sgr	.71	G2	F9	+3	X Cyg	1.21	G4	G4	0
δ Cep	.72	F8	F9	−1	RW Cam	1.21	G4	G4	0
X Lac	.73	F9	F9	0	CD Cyg	1.23	G0†	G5	−5
Y Sgr	.76	G0	G0	0	SZ Aql	1.23	G3	G5	−2
RV Sco	.78	G5†	G0	+5	Y Oph	1.23	G3	G5	−2
X Vul	.80	G3	G0	+3	W Vir	1.23	G4	G5	−1
RR Lac	.81	G3	G0	+3	RS Cet	1.24	G0†	G5	−5
XX Sgr	.81	G0†	G0	0	RU Sct	1.29	G5†	G5	0
U Sgr	.83	F9	G0	−1	RY Sco	1.31	G5†	G5	0
U Aql	.84	F9	G0	−1	WZ Sgr	1.34	G8	G6	+2
X Sgr	.84	F7	G0	−3	X Pup	1.41	G7	G6	+1
η Aql	.85	F9	G0	−1	T Mon	1.43	G6	G7	−1
RS Ori	.88	G0	G1	−1	RS Pup	1.62	G4	G8	−4
W Sgr	.88	G0	G1	−1	SV Vul	1.65	G5	G8	−3
W Gem	.90	G1	G1	0	SS Gem*	1.65	G1†	G8	(−7)
RX Gem	.90	G0	G1	−1	UU Her*	1.66	G0	G8	(−8)
RW Aql	.90	F3n	G1	(−8)	S Vul*	1.82	G9	G9	(0)
U Vul	.90	G1	G1	0	V Vul*	1.88	K3	G9	(+4)
S Sge	.92	G0	G1	−1	R Sge*	1.89	G7	G9	(−2)
RY Boo	.95	F3	G1	(−8)	SX Her*	2.01	G3e	K0	(−7)
YZ Sgr	0.98	G0	G2	−2	RX Cep*	2.11	G7	K0	(−3)

* Not a normal Cepheid.

† Only one observation.

theses in the table. It is worthy of note that all but one are negative. Their average value is −0.4 class and the greatest is −0.8.

For the remaining fifty-seven stars, the average difference between the observed and computed spectra is only ±0.16 of a class. The eleven stars for which there is only one spectroscopic observation give ±0.25, and the forty-six others ±0.14.

The part of the discordance which arises from errors in the estimates of spectral class is small. For the forty-five stars for which more than one plate was obtained, the average deviation of a single estimate (corrected for periodic variation of spectrum) from the mean is ±0.094 class. By allowing for the fact that, on the average, a little more than three observations go to a mean, the actual average error of one estimate comes out at ±0.11 class, and that of an average mean value ±0.06 class. Correcting for this, we find the actual divergence from the computed curve to be ±0.13 class for the forty-five stars, corresponding to a probable error of distribution of ±0.11 class, or ±0.0154 in log T, which again corresponds to ±3.5 per cent in the temperature.

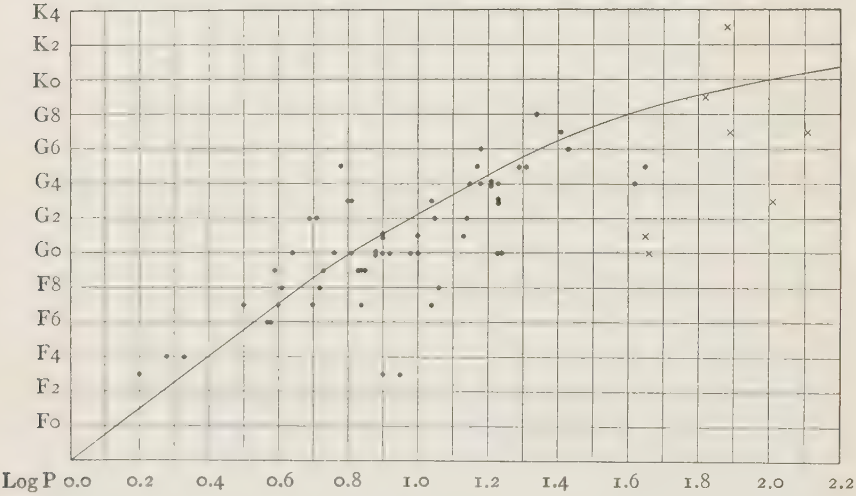

FIG. 1.—Relation between spectrum and period among Cepheid variables. The curve is that derived theoretically in this paper from Shapley's period-luminosity curve.

It may be concluded from this that the relation between period and spectral class among the typical Cepheids is very closely that which would exist if the stars were all similar dynamical systems, with densities inversely as the squares of their periods, and if their median magnitudes agreed exactly with Shapley's period-luminosity curve. If it is assumed that the quantities q and f in equation (6) are strictly constant, but that the deviations between the observed and computed spectral classes (and temperatures) are real, the mean deviation of ±0.13 class corresponds to one $0.14\times5.6\times2.5$, or 1.96 times as great in the absolute magnitude: that is, to ±0.25 mag.

The observed discordance is ±0.23 mag.,[1] but includes, however, the effect of several other factors. The greatest observed discordance for normal Cepheids, 0.6 class, corresponds to 1.2 mag. For the stars whose variation is abnormal, the largest discordance is −0.8 class, corresponding to −1.6 mag. (if the assumptions are to be trusted here, which is doubtful). It is noteworthy that all the considerable discordances indicate a higher temperature, and hence a brighter absolute magnitude than the normal curve. No observed discordance, for either a normal or an exceptional star, suggests that it is more than a magnitude fainter than the period-luminosity curve indicates. A small systematic error appears in the residuals, however, as shown by the following means:

log P	<0.6	0.6–0.8	0.8–1.0	1.0–1.2	1.2–1.3	>1.3
No. stars	7	10	14	12	8	6
Mean log P	0.44	0.69	0.87	1.09	1.23	1.46
Mean residual	+0.07	+0.12	−0.04	−0.13	−0.20	−0.08

These indicate a change in the residuals from about +0.1 to −0.1 class as log P increases by 1.0, which suggests that the factors q and f in (6) are not really constant. The latter is not likely to vary much; if the change is thrown on the former, it would appear that log q must decrease by about 0.16 as log P increases from 0.5 to 1.5, which, by (5), means that the density actually varies over this range, not as P^{-2}, but as $P^{-2.16}$.

Variation in the physical conditions might well account for such a change. The whole discordance could also be removed by the assumption that the actual difference in absolute magnitude between Cepheids of periods three and thirty days was greater by 0.4 mag. than Shapley's curve indicates; but this is beyond the bounds set by the observations.

---

[1] *Harvard Circular*, No. 280, p. 4.

This analysis affords strong evidence that a dynamical process, of a single definite type, lies behind the variation of the normal Cepheids. It does not, however, tell us anything more about the process—the hypotheses of pulsation, incipient fission, and probably many others would all meet this condition. Nor does it bear upon the vexed question of the zero-point of the period-luminosity curve. It does, however, afford strong evidence in favor of the existence of such a curve, and the close agreement of the luminosity of most Cepheids with it. It is worthy of special attention that all the considerable disagreements in spectrum are on the whiter side of the curve, indicating that the stars in question, if indeed they are similar dynamical systems, are brighter than the normal for their period. Stars which are fainter than indicated by the period-luminosity curve should be redder than normal, and no evidence of any serious deviation of this kind has been found for stars having periods from one to a hundred days. One or two variables of spectrum Me, which are obviously of the long-period type, though with periods slightly less than one hundred days, are not considered here.

Accepting this as an observational fact, we find it of interest to inquire under what other conditions a dynamically oscillating system could give rise to a variable star considerably fainter in absolute magnitude, but having a period and a surface temperature within the observed range. This can happen only if q or f is large compared with its values for the Cepheids.

Now, for stars which follow the mass-luminosity law, f is nearly constant for the brighter absolute magnitudes and decreases for the fainter ones, Eddington's data giving, on the same scale as above:

Abs. mag.........	0	2	4	6	8	10	12
f................	0.83	0.47	0.21	0.084	0.031	0.012	0.0045

If a variable is to be faint (for a given density and temperature), it must therefore emit very much more light than the mass-luminosity law allows. This seems at first paradoxical, but it is a simple consequence of the transformation of equation (2) into (4). No such stars are known, and there appears to be no way of escape in this direction. A larger value of q, by equation (5), signifies that the type of oscillation is such that the period is considerably longer for the same density than in the case of the typical Cepheids. This again seems improbable. For the pulsation of a spherical body, for example, the higher harmonics have shorter periods than the fundamental; and, in the case of rotation, there is no approach to instability for angular velocities much smaller than those which start fission. Periodic changes which depend on alterations of other physical conditions, however, may have far longer periods than those of gravitational oscillations; for example, the sun-spot period is of the order of fifty thousand times the length of a gravitational pulsation of the sun.

It is of interest to apply equation (7) to the periodic variables of other types. Take first the long-period variables. We have no accurate information regarding their bolometric magnitudes, but know that they are very bright. The visual absolute magnitude at maximum lies not far from 0 and the heat index is about four magnitudes. Taking a period of three hundred and thirty days (that of *o* Ceti), we find for $B=-4$, $T=1750°$; and for $B=-5$, $T=2050°$. The latter fits very well with Joy's estimates[1] of a temperature of 2300° at maximum and 1800° at minimum, thus indicating that, if long-period variation is due to a dynamical oscillation, the relation between period and density, in its case, may be much the same as for the Cepheids—which is far from saying that the oscillation is of the same type. The well-known advance of spectral type with increasing period among the long-period variables suggests the existence of a period-luminosity relation among them; but the observational data are not sufficient to test the matter at present.

The case of the variables of the cluster type is puzzling. Adams and Joy have determined the spectral class for thirty stars with periods less than a day. All but three of them are of classes between A4 and F5. The outstanding cases are TX Scorpii, $P=0^{d}.94$, Sp. A2n; SU Aurigae, $0^{d}.47$, G2; and RT Scuti, $0^{d}.50$, M2. The photometric data for all three stars are very weak, and it is doubtful whether any one of them is a normal variable of short period. Miss H. B. Sawyer[1] finds no evidence of variation of TX Scorpii on two hundred photographs. Pending further photometric observations, they may be removed from this list.

---

[1] *Mount Wilson Contr.*, No. 311; *Astrophysical Journal*, **63**, 281, 1926.

The remaining twenty-seven stars show no correlation between spectrum and period. The means for successive groups in order of period are

log P	9.52	9.66	9.70	9.78
Sp.	A7	A8	F0	A8
Stars	7	7	7	6

while the individual spectra are distributed as follows:

A4	A5	A6	A7	A8	A9	F0	F1	F2	F4	F5
1	4	1	7	1	3	3	2	3	1	1

and give an average deviation from the general mean of ±0.26 class, very little of which can be accounted for by the errors of observation.

For variables of the cluster type Shapley[2] finds a mean visual magnitude of -0.34, corresponding to a bolometric magnitude of -0.5. On the assumption that the constant q is the same for these stars as for the ordinary Cepheids, equation (7) then gives

log P	9.80	9.60	9.40
log T	3.96	4.03	4.10
Spectrum	A4	A0	(B8)

For the mean value of log P, 9.66, the computed value of log T is 4.01 and the spectrum A1, while the observed spectrum A9 corresponds to log $T = 3.89$. Not a single one of the stars is as white as the formula indicates, and the difference in period between the first and last of the groups given above should correspond to a difference in spectrum of fully 0.5 class, while the observed difference is zero.

It appears, then, that there must be some real difference between the dynamical processes which are behind variations of the Cepheid type and of the cluster type. (There is, of course, abundant evidence of important differences in the statistical properties of stars of the two groups.) If this difference is thrown on the value of q, it must be assumed that this quantity is, in the mean, 4.6 times greater for the Cepheids than for the cluster variables, or that the period corresponding to the same density is 2.1 times longer in the case of the Cepheids. Such a difference is probably not beyond the range of values which might be expected to result from varying physical conditions. The observed range in spectrum among (galactic) cluster variables of the same period would correspond to an average deviation from the mean absolute magnitude of ± 0.5 mag., which is not large, but much greater than the observed dispersion in globular clusters. The substantial identity of mean spectral class for a range of period in at least the ratio 2:1 indicates, by equation (6), that q must be correlated with the density, and least for the stars of shortest period; in other words, that it deviates more from the value holding good for the Cepheids, as the star is more dense, and indeed that q is proportional to the density. Stars of different densities would therefore have the same period of oscillation.

---

[1] *Harvard Bulletin*, No. 847, 10, 1927.

[2] *Mount Wilson Contr.*, No. 151; *Astrophysical Journal*, **48**, 89, 1918.

All this seems extraordinary and improbable; but, unless the mass-luminosity relation fails in this case, the similarity of absolute magnitude among the cluster variables indicates that this type of variation is confined to stars of a certain mass, which is still more remarkable. It is evident that a great deal is yet to be learned before we have any real understanding of the physical causes of variation of this sort, or, indeed, of any other real stellar variability.

It is a great pleasure to acknowledge the writer's indebtedness to his colleagues, Adams and Joy, who generously put all their observations at his disposal.

CARNEGIE INSTITUTION OF WASHINGTON
MOUNT WILSON OBSERVATORY
June 16, 1927

ADDENDUM.—By some mischance, Shapley's discussion of the same problem (*Harvard Circulars* 313, 314, 1927) did not come to the writer's attention until the present paper was in type. The two discussions are based on independent observational data. They proceed along similar lines, and reach entirely accordant conclusions. Each one, however, covers some points not included in the other.

Contributions from the Mount Wilson Observatory, No. 340
Reprinted from the *Astrophysical Journal*, Vol. LXVI, pp. 170–183, 1927
Printed in the U.S.A.

ON THE RADIAL VELOCITY AND SPECTRUM OF THE CEPHEID VARIABLE T MONOCEROTIS

BY ROSCOE F. SANFORD

ABSTRACT

Light-Curve.—The discovery and subsequent photometric observation of T Monocerotis are briefly discussed, and reasons are adduced for accepting the type of regular light-variation displayed by Wendell's curve, which has the maximum 5.61 mag., the minimum 6.77 mag., and an interval of seven days from minimum to maximum light. The maxima over the interval from 1874 to the present are best represented by

$$\text{Max} = \text{J.D. } 2410012.1956 + 27.003131E + 0.000025221E^2, \text{ G.M.T.}$$

which is Bemporad's formula with a somewhat larger value of the coefficient of E^2.

Radial-velocity curves.—Fifty values of radial velocity have been used to derive the general radial-velocity curve. Three of these were obtained by Frost at the Yerkes Observatory in 1905 and the remainder at Mount Wilson between 1917 and 1927 (Table II). The foregoing formula was found to be best suited to grouping all the radial velocities into a single cycle, and was used to derive the velocity-curve (top of Fig. 1).

Coincidence of maximum light and minimum velocity, and minimum light and maximum velocity, are brought out. Two contrasts between light-curve and velocity-curve are noted, one being the inflection in the latter about ten days after minimum velocity with no counterpart in the best light-curves, and the other, the blunt maximum of the velocity-curve as compared with the rather well-rounded minimum for the light-curve.

Maximum velocity, minimum velocity, and the velocity of the center of mass are +54, +4, and +32 km/sec., respectively.

There is evidence for greater amplitude of velocity variation in the lines whose chromospheric level in the sun averages 2700 km than in a contrasted group having a mean of about 550 km. On the other hand, $H\gamma$, chromospheric level 8000 km, has an amplitude no greater than that of the low-level lines.

The velocity-curve for $H\gamma$ is of special interest, for it seems to indicate a persistence of the maximum velocity of approach of its origin considerably beyond that of the other lines.

Spectrum and spectral changes.—The spectral class at median magnitude is about cG6, and has the small range cG4 to cG9 between maximum and minimum light.

The lines of hydrogen and those of the ionized atoms of certain elements attain their maximum intensity, relative to arc lines, at maximum light; but there is evidence that their minima precede minimum light, in some cases as much as ten days. The relation of relative intensity to phase for four pairs of lines is shown in Figure 2. Curves of photographic density for the spectral region λ 4325 to λ 4352 made with the Hartmann microphotometer from five plates for differing phases are given in Figure 3.

A variation in effective wave-length derived from the continuous spectrum at different phases agrees qualitatively with the evidence afforded by light-curves for different wave-length in that both show the star to be decidedly bluest at maximum light.

THE LIGHT-CURVE

This star, B.D. $+7^\circ 1273$, numbered 44990 in the new *Henry Draper Catalogue*, has the co-ordinates for 1900, $\alpha = 6^h 19^m.8$, $\delta = +7^\circ 8'$.

In 1872 Gould[1] announced that it was variable after he and his assistants at the Cordoba Observatory had noted that it was then about a magnitude fainter than it had been the year previous. A few years later Davis, one of these assistants, obtained the period $27^{d}.0054$ and an interval between minimum and maximum light ($M-m$) equal to 8.5 days. His observations showed that the light variations are akin to those of δ Cephei. The star was assigned the designation T Monocerotis and is of rather more than ordinary interest, because its period is one of the longest of the Cepheid variables.

Subsequent work by various other observers confirmed the Cepheid characteristics and agreed in general with Davis' results, although differences in detail exist. Among these may be mentioned differences in the values of $M-m$, an inflection in the light-curve about ten days after maximum light, different values for maxima and minima at different epochs, and increasing values for the period as later measures became available for comparison with the first observations.

Probably the most reliable light-curves are those from observations by E. C. Pickering[2] and O. C. Wendell,[3] respectively. The former made eighty-six observations with a meridian photometer in nine out of sixteen consecutive cycles (1896–1898), and the latter two hundred observations with polarizing photometers in each one of five consecutive cycles (1899–1900). Both light-curves, especially that of Wendell, are nearly regular in shape, and together include almost continuous observation over an interval of more than three years. They are strong evidence against an inflection at ten days after maximum light, give good agreement for repeated maxima and minima, and establish with considerable certainty the value for $M-m$. In consequence, the mean light-curve defined by Wendell's observations has been adopted here and appears in Figure 1. His maximum is 5.61 mag., minimum 6.77 mag., and the interval $M-m$ is seven days.

The question of the lengthening of the period has been studied by Bemporad,[4] who has collected representative maxima that have been satisfactorily determined in the interval 1874–1920 inclusive. To these may now be added a maximum determined by Gallisot,[1]

---

[1] *American Journal of Science* (3), **4**, 477, 1872.

[2] *Harvard Annals*, **46**, 122, 135, 145, 151, 155, 158, 160.

[3] *Ibid.*, **69**, 42.

[4] *Memorie della Società Astronomica Italiana* (Nuova Serie), **1**, 229, 1920.

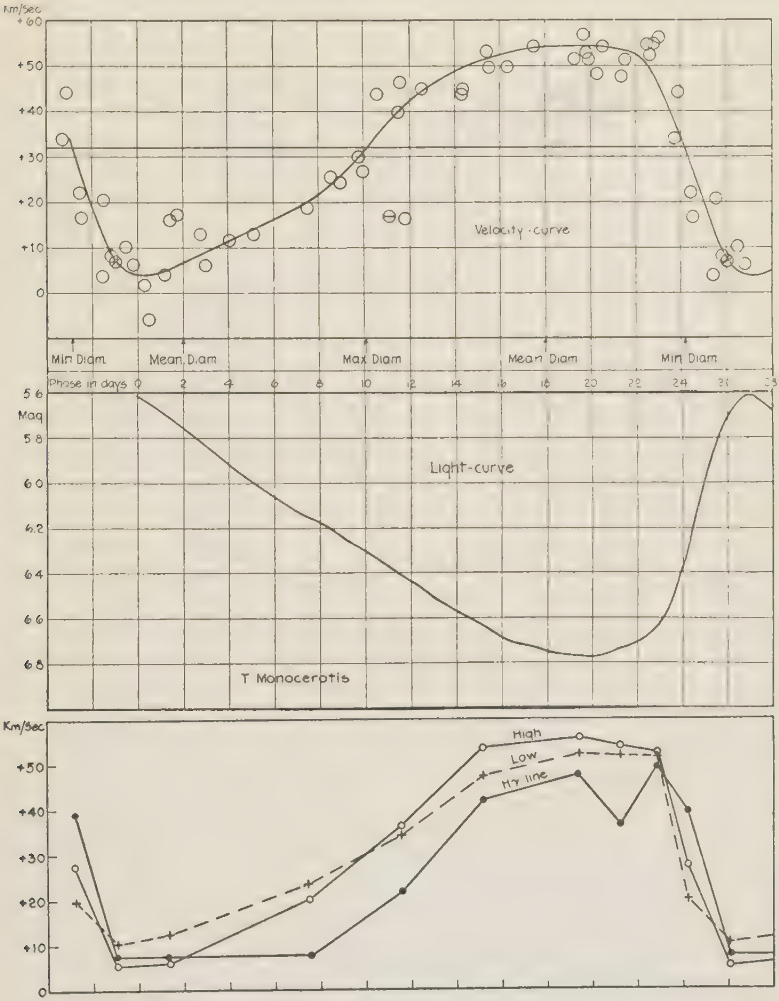

FIG. 1.—T Monocerotis. Top, velocity-curve. Middle, Wendell's light-curve. Bottom, velocity-curves from high- and low-level lines and from $H\gamma$.

and another from the radial velocities, by assuming coincidence of maximum light and minimum velocity.

---

[1] *Bulletin astronomique, mémoires et variétés*, 3, 207, 1923.

The first and second columns of Table I list the photometric observer and the maximum which he determined. The third, fourth, and fifth columns show the differences between observed maxima and maxima computed from the three formulae given at the foot of the table. The period used in formula I was found from the Mount Wilson radial velocities alone; formula II is that derived by Bemporad in the paper already cited; and formula III is identical with II except for a change in the coefficient of E^2. The first, typical of a formula with a constant period, evidently leaves something to be desired; II does very well except for the two maxima that I have added; and III gives no residual greater than $0^{d}9$. The last has been adopted. Whether this will continue to predict maxima in the future, or is merely an approximation to a portion of a periodic change in the period, can only be decided after the lapse of a considerable interval.

TABLE I

T MONOCEROTIS—REPRESENTATION OF MAXIMA

Observer	J.D. of Maximum	O−C		
		I	II	III
Davis	2405556.62	$+2^{d}26$	$-0^{d}61$	$-0^{d}74$
Sawyer	9040.13	0.56	+ .02	+ .02
Sawyer	2410012.19	0.00	.00	.00
Sawyer Yendell	2442.53	−1.20	− .12	− .26
Pickering	4144.25	1.56	+ .09	.01
Wendell	5089.60	1.81	.08	.07
Nijland	7628.83	2.20	+ .09	.26
Bemporad I	8412.10	2.42	− .09	.51
Bemporad II	2422357.00	2.03	+0.03	− .89
Gallisot	2737.03	0.25	1.72	+ .76
Sanford	3790.35	−0.58	+1.14	0.00

Formula I (Sanford) .... Max = J.D. $2410012.19 + 27.017149E$, G.M.T.

Formula II (Bemporad) .... Max = J.D. $2410012.1956 + 27.003131E + 0.000020841E^2$, G.M.T.

Formula III (Bemporad modified) .... Max = J.D. $2410012.1956 + 27.003131E + 0.000025221E^2$, G.M.T.

THE RADIAL-VELOCITY CURVES

Forty-seven slit spectrograms of T Monocerotis have been obtained with the 60-inch and 100-inch reflectors during the interval 1917–1927. Table II gives the data of these observations. The plate

TABLE II

OBSERVATIONS OF T MONOCEROTIS

Plate	Date	G.M.T.	Phase	Vel.	Remarks
				km/sec.	
γ 6373..	1917 Nov. 23	21^h57^m	$9^d.784$	+29.8	Very good
6384..	25	22 25	11.803	16.4	Very good
6434..	Dec. 3	23 40	10.855	53.0	Poor
6513..	30	20 49	19.712	56.8	Fair
6690..	1918 Feb. 1	17 49	25.562	20.7	Good
12334..	1923 Dec. 16	20 18	7.521	18.7	Good
12340..	17	20 30	8.530	25.6	Good
12350..	20	20 26	11.528	39.8	Poor
C 2592..	24	20 47	15.538	49.7	Good
γ 12406..	1924 Jan. 17	21 43	12.553	45.0	Fair
12416..	19	16 10	14.321	43.9	Poor
C 2642..	20	18 51	15.433	53.1	Fair
γ 12448..	26	17 28	21.376	47.6	Good (over-exposed)
12531..	Mar. 18	17 35	19.323	51.4	Poor
12538..	19	16 47	20.290	48.2	Poor
13029..	Oct. 16	0 42	14.385	44.9	Fair
13257..	1925 Feb. 9	18 54	23.026	56.3	Good
C 3197..	Mar. 11	15 10	25.842	8.2	Good (over-exposed)
C 3201..	12	15 01	26.836	6.3	Good (over-exposed)
γ 13365..	Apr. 11	15 38	2.811	12.8	Good
13822..	Oct. 7	23 30	19.950	51.4	Fair
13829..	9	0 33	20.994	53.4	Good (over-exposed)
C 3592..	Dec. 3	21 29	22.806	54.9	Poor
γ 13958..	1926 Jan. 2	20 05	25.717	16.4	Good density: poor focus
13980..	5	21 50	1.759	17.3	Good
14003..	26	18 34	22.623	52.3	Good (fogged)
14013..	27	20 21	22.697	34.0	Very good
14051..	Feb. 24	17 37	24.537	16.8	Good
14056..	25	15 17	25.430	3.8	Good
C 3713..	26	16 48	26.498	+10.3	Good
γ 14066..	27	16 57	0.496	− 5.7	Good
γ 14073..	28	15 53	1.449	+16.3	Fair
γ 14090..	Mar. 22	15 32	23.437	44.2	Good
γ 14098..	23	15 27	24.434	22.1	Good (over-exposed)
C 3999..	Sept. 15	0 16	10.587	43.8	Poor
C 4005..	16	0 25	11.594	46.4	Poor
C 4063..	Oct. 22	0 17	20.558	54.2	Good
γ 14627..	22	22 23	21.541	51.3	Good
14634..	24	0 27	22.565	54.7	Good
14684..	Nov. 13	20 15	16.359	49.7	Poor
14697..	14	23 52	17.510	54.2	Fair
14787..	1927 Jan. 17	21 25	0.314	1.9	7-inch camera;* very strong
14792..	18	18 54	1.210	4.0	7-inch camera;* very strong
14822..	Feb. 17	15 46	4.048	11.6	Good
14854..	Mar. 15	15 33	3.008	6.2	Very good
C 4230..	Apr. 17	15 41	8.983	24.3	Good
4237..	18	15 37	9.981	+26.7	Good stellar, poor comparison spectrum

* Dispersion about one-half that of the other plates.

numbers are in the first column, wherein the prefix C identifies spectrograms made with the 100-inch reflector and γ those taken with the 60-inch reflector. All but two noted in the table have an approximate dispersion of 36 A per millimeter at $H\gamma$.

Forty-seven lines between λ 4215 and λ 4571, together with the lines $H\delta$ and $H\beta$, have been used for deriving the radial velocities. These lines were chosen from those available within the spectral region in question so as to be as free as possible from troublesome blends, and yet be sufficiently numerous to furnish data regarding velocities derived separately from high-level, low-level, enhanced, and hydrogen lines. More will be said on this point later. The wave-lengths for the lines selected have been determined from measures upon eight plates whose velocities, as derived from tables used in our general radial-velocity work, are approximately midway between the maximum and minimum velocity for this variable. The fifth column in Table II gives the velocities measured with the use of these wave-lengths, exclusive of the hydrogen lines.

In addition to velocities in Table II, Frost[1] has published the three following values:

Date	G.M.T.	Phase	Vel.
			km/sec.
1905 Nov. 3........	21^h30^m	11.116	+17
24........	21 40	5.107	13
Dec. 15........	20 30	26.056	+ 7

We have, therefore, fifty values of the radial velocity extending from 1905 to 1927, from which to derive a radial-velocity curve. Efforts to combine the velocities into a single cycle by means of a period of constant length produce neither a smooth run of Mount Wilson observations nor a satisfactory utilization of the Yerkes velocities. Since the modified formula of Bemporad represents the observed light maxima so well, it was tried for grouping the radial velocities and found to improve the smoothness of the Mount Wilson observations and to harmonize the Yerkes values with these. This method of assembling the observations was therefore adopted, and the phases given for both Mount Wilson and Yerkes plates are so derived. The top of Figure 1 shows the individual observations plotted as circles (Mount Wilson) and barred circles (Yerkes). The freehand curve through them is deemed a fair approximation to the actual velocity-curve. Of the two very discrepant values of the radial velocity shown at slightly more than eleven days after minimum velocity, one is the first value given by Frost, which he remarked is the least accurate of his three; the other is derived from one of the best Mount Wilson plates, γ 6384, and its discordance remains unexplained.

---

[1] *Astrophysical Journal*, **23**, 266, 1906.

The coincidence of minimum velocity with zero phase is of course to be expected, since the modification of Bemporad's formula was largely to satisfy the epoch of observed minimum velocity (assumed to represent maximum light). The fact that such a formula brings all the radial velocities together into a satisfactory velocity-curve, although the first and last observations are separated by almost twenty-two years, seems to justify the assumption.

The radial-velocity curve may be compared with Wendell's light-curve, which is shown below the velocity-curve in Figure 1. The accordance of maximum light and minimum velocity has already been mentioned. The agreement of minimum light and maximum velocity is no less precise. Two differences, however, are to be noted: one, the contrast of a smooth progression in light-variation with what appears to be a well-marked inflection in the radial-velocity curve at about phase ten days; and the other, the well-rounded minimum of light as compared with the blunt maximum of the velocity-curve, followed as it is by a very rapid fall to minimum velocity. The inflection in the velocity-curve resembles that found in the curves for such Cepheids as W Sagitarii,[1] ζ Geminorum,[2] and η Aquilae,[3] and hence is not at all an abnormal feature. It also brings to mind the inflection found by some observers in the light-curve of T Monocerotis, although little dependence is to be placed on this because the most accurate observations do not show the inflection.

Around the times of both maximum and minimum velocity, especially the latter, the individual values of radial velocity show a considerable spread. To seek an explanation of this in the assumption that the velocity-curve is not always precisely the same seems hardly justified, for some of the differences in residuals for plates close together in the same cycle are about as large as any to be found between spectrograms made in different cycles. Large dispersion in radial velocity at maximum light is not, however, peculiar to this Cepheid, as may be verified by a glance at the radial-velocity curves for X Sagittarii,[1] Y Sagittarii,[2] and W Sagittarii,[3] for example.

---

[1] *Lick Observatory Bulletins*, **3**, 35, 1904.

[2] *Ibid.*, **12**, 148, 1926.

[3] *Ibid.*, p. 147, 1926.

The usual elements of elliptic motion have not been determined because (as evident at a glance) they could give only a crude approximation to the observations, and because such an interpretation of the curve is open to serious question. Maximum velocity, minimum velocity, and the center-of-mass velocity are +54, +4, and +32 km/sec., respectively, the last being that velocity which divides the velocity-curve into equal areas.

It is interesting to note the phases, indicated below the velocity diagram, for which, on the pulsation hypothesis, the star has its mean, maximum, and minimum diameters. Minimum diameter corresponds approximately to the phase of most rapid change in radial velocity on the downward slope, and maximum diameter is closely associated with the phase of most rapid change on the upward branch.

Furthermore, it may be noted incidentally that the curve can be resolved into two typical radial-velocity curves, each having a period equal to the photometric period. One curve would have a semi-amplitude of 20 km/sec. and a so-called periastron point at about twenty-four days after maximum light, and the other, a semi-amplitude of 8.5 km/sec. and periastron at about ten days after maximum light. It is merely pointed out that the curve may be so resolved, without inquiring whether such a procedure is legitimate, or, if legitimate, what the explanation may be.

From the foregoing paragraphs it may therefore be stated that the relation of the general velocity-curve to the mean light-curve for T Monocerotis is quite normal when compared with the results for numerous other Cepheid variables, for the most part of shorter period.

Various members of the staff of the Observatory of the University of Michigan have derived velocity-curves for certain Cepheids from different groups of lines, on the assumption that such treatment might possibly throw some light upon the pulsation theory of Cepheid variation. Adequate approach to this problem demands the highest practicable dispersion and resolving power, applied to the very brightest Cepheids. Nevertheless, it is probable that for some time, at least, the Mount Wilson observations here considered will be the only source from which to derive even qualitative results for T Monocerotis, whose rather long period makes it of considerable interest in this as in other respects. Such is the only justification for presenting the following discussion, which has been limited to deriving velocity-curves from (1) lines of high atmospheric level, (2) lines of low atmospheric level, and (3) the γ line of hydrogen.

---

[1] *Ibid.*, **5**, 113, 1909.

[2] *Ibid.*, p. 84, 1908.

[3] *Ibid.*, **3**, 35, 1904.

The lines have been chosen from the list of forty-seven lines according to heights assigned on the basis of Mitchell's[1] levels in the sun. The approximate mean level thus found for the first group (twenty-one lines) is about 2700 km; for the second group (nine lines), 550 km; and for $H\gamma$, 8000 km. $H\gamma$ alone was used since it is the only hydrogen line consistently measured at all phases. In order to minimize somewhat the accidental differences, the measures are grouped into nine normal places.

The velocity-curves defined by the normal places for each of the three classes of lines are shown at the bottom of Figure 1. Both high- and low-level curves resemble the general curve at the top of Figure 1, even after the drastic smoothing effected by the use of so small a number of normal places. The one point of interest seems to be a consistently smaller amplitude for the velocities from low-level lines as compared with those from high levels.

The velocity-curve derived from $H\gamma$ (and this is not essentially different when the data for $H\delta$ and $H\beta$ are considered), although it is representative of a still higher level, shows an amplitude at least not greater than that given by low-level lines. The three curves do not, therefore, show a steady progression in amplitude with increase in level.

By itself, the $H\gamma$ curve is of interest as pointing toward a lag after maximum velocity, as though the portion of the stellar atmosphere responsible for the $H\gamma$ line continued its most rapid approach to a much later phase than those portions associated with the other lines. About minimum light the deviations from the general curve are probably small. Although the two normal places just preceding the drop to minimum velocity both include several values which are fairly consistent, the reality of the depression which they show in the $H\gamma$ velocity-curve at phase twenty-one days is probably open to serious question.

---

[1] *Astrophysical Journal*, 38, 407, 1913.

A proper discussion of the radial-velocity variation shown by the enhanced lines undoubtedly requires a more elaborate classification than the number of lines here measured will warrant. All that can be said is that a group of titanium enhanced lines seems to give a velocity-curve differing little from the general curve, except perhaps in amplitude, which appears to be intermediate between that of the high- and the low-level curves, and probably somewhat nearer the value for the latter.

SPECTRUM AND SPECTRAL CHANGES

The spectral class of T Monocerotis is cG6 at median magnitude, with a variation from cG4 to cG9, according to the classification of Adams and his collaborators at Mount Wilson. As in other Cepheids, the enhanced lines of such elements as titanium, iron, strontium, scandium, etc., and the Balmer lines of hydrogen are conspicuous at all phases, but especially near maximum, when they attain maximum intensity.

In an attempt to fix the light-phases for maximum and minimum intensity of the absorption lines, measures have been made with the Hartmann microphotometer as arranged by Pettit for use with thermocouple and galvanometer. These measures have been made both visually and photographically by comparing galvanometer deflections for the sensitive lines with the deflections for certain arc lines. When these comparisons are plotted, the phase for maximum intensity seems to be fixed with considerable certainty at maximum light. On the other hand, the phases for which the sensitive enhanced and hydrogen lines are weakest, as compared with their arc standards, do not appear either to agree with one another or to approximate at all closely the phase of minimum light. In general, it may be said that minimum intensity is attained not later than minimum light, and in several cases seems to anticipate that phase, sometimes by as much as ten days.

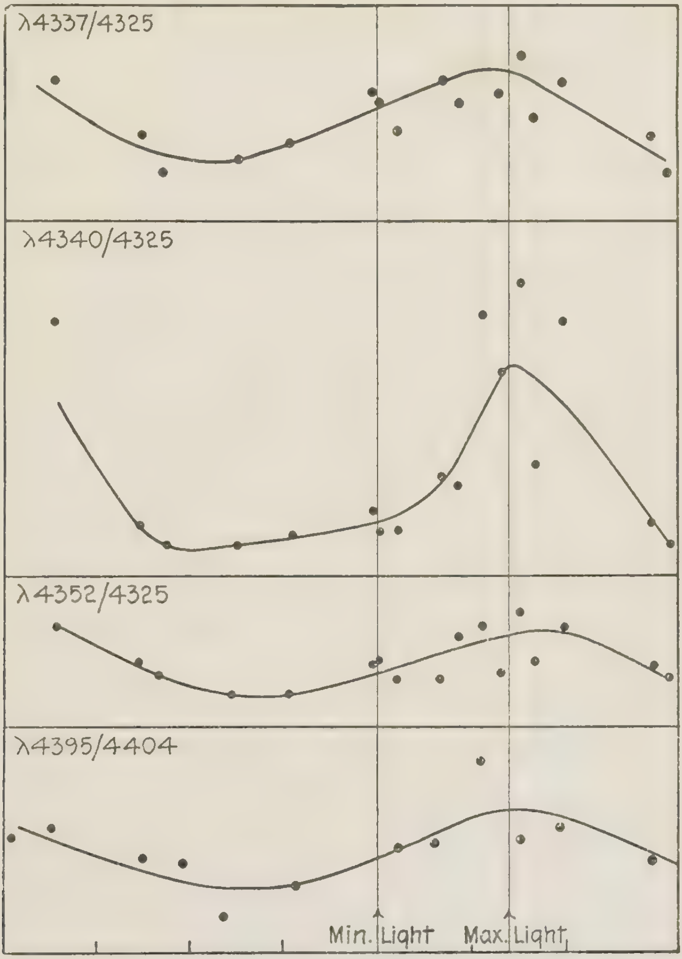

FIG. 2.—Changes of relative intensity with phase for four pairs of lines in the spectrum of T Monocerotis.

These relations of relative intensity to phase are shown qualitatively by the four curves in Figure 2, derived with the aid of the Hartmann microphotometer. The first three curves compare the strength of λ 4337 (Ti^+), λ 4340 ($H\gamma$), and λ 4352 (Ti^+), respectively, with that of λ 4325. In the last case λ 4395 (Ti^+) has been compared with λ 4404. Both λ 4325 and λ 4404 are strong lines from the neutral atom of iron. In the first three cases, the areas of the respective intensity-curves in terms of the area for λ 4325, photographically registered, have been plotted against phase. For the fourth case the visually observed galvanometer deflections of λ 4395, in terms of those of λ 4404, have likewise been plotted against phase. The points refer to single measures upon individual plates scattered over all phases and chosen for the general density best suited to the purpose. The maximum intensity in all four cases falls close to the phase of maximum light, but minimum intensity, for these four cases at least, seems to precede minimum light very considerably—by ten or eleven days in the case of $H\gamma$. $H\gamma$ then remains practically at minimum intensity until minimum light. Apparently, therefore, $H\gamma$ is more or less stable at minimum intensity for one-half the light-cycle, and then undergoes a rapid increase to maximum intensity at maximum light and a decrease to minimum, all in the other half of the light-cycle. For the three enhanced titanium lines a much steadier progression takes place, so that a fairly definite minimum is marked out seven or eight days before minimum light, after which the increase in relative intensity begins again. Other lines which were measured show the same trend, but these four have the most pronounced and most easily measurable changes with phase, and are reproduced for this reason. It should be kept in mind that these curves denote changes in relative intensity and are not necessarily to be interpreted as measures of the real changes, for they may be complicated by changes in the comparison lines.

Five different intensity-curves covering the spectral region λ 4325 to λ 4352 are illustrated in Figure 3, the last of the six curves being the same as the first. These have been traced from photographic intensity-curves made with the registering Hartmann microphotometer. A depression indicates an absorption line or a blend, and all such features fit for micrometric measurement, and several besides are consistently recorded. A number of lines of interest have been marked, and it is easy to trace several striking changes of relative intensity with phase. The most impressive change is, of course, in the $H\gamma$ line. These five curves, with those similarly obtained from fourteen other spectrograms, are the basis of the first three curves in Figure 2.

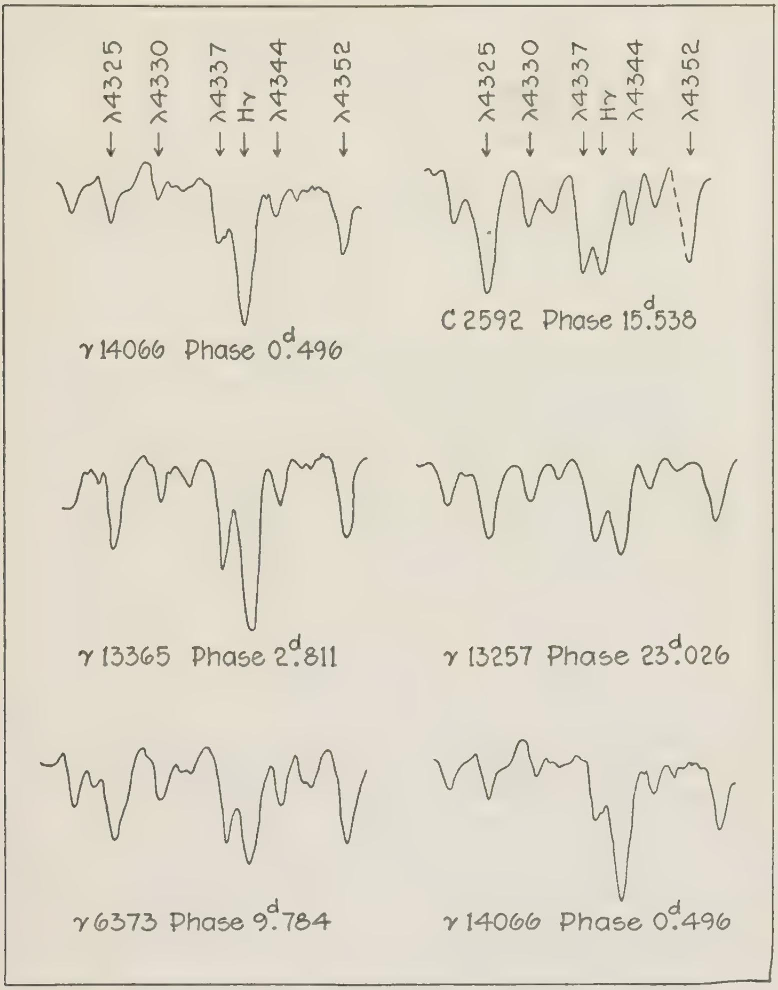

FIG. 3.—Microphotograms of the spectral region λ 4325 to λ 4352, inclusive, for different phases of the velocity variation in T Monocerotis.

In addition to the small change in spectral type and the change in the relative intensity of enhanced lines to arc lines (the two variations already treated), there is a definite change in effective wave-length with phase, so that the star is decidedly bluest at maximum light. Gallisot[1] measured this change with a Nordmann photometer, using three types of screens effective in giving measures of the star's brightness in each of three more or less isolated spectral regions, which are (*R*) from λ 5900 to the infra-red; (*V*) from λ 4900 to λ 5900; and (*B*) from λ 4900 to the ultra-violet. The light-curves thus derived gave amplitudes of 0.73, 1.00, and 1.28 mag., respectively, and hence show a marked difference in color at different phases—a well-established result for many Cepheids.

I have endeavored to estimate the wave-length at the violet end to which each spectrogram would be capable of wave-length measurement if the density at about λ 4600 had been ideal. Although it is recognized that many factors besides the effective wave-length of the star may modify this, the mean curve giving the relation of this wave-length to phase may still be of some value. It indicates that from about eight days after maximum to the phase of minimum light the star changes little in color, and that the extension to the violet limit on the basis outlined above is approximately 4250 A. From minimum, or very shortly after, the effective wave-length moves toward the violet, becomes somewhat less than $H\delta$ about maximum light, and then turns back to the value 4250 A at some eight days after maximum light. This result, crudely derived from the spectrograms, together with the shape of the light-curves which Gallisot obtained for different screens, leads to the remark that the star is "decidedly bluest at maximum light," rather than to the statement that it is "reddest at minimum light." The change in effective wave-length appears to bear some analogy to the anomalies found in both the velocity-curve and the relative intensity for $H\gamma$ shown in Figures 1 and 2, respectively.

Carnegie Institution of Washington
Mount Wilson Observatory
July 1927

---

[1] *Bulletin astronomique, mémoires et variétés*, **3**, 207, 1923.

Contributions from the Mount Wilson Observatory, No. 341
Reprinted from the *Astrophysical Journal*, Vol. LXVI, pp. 184–216, 1927
Printed in the U.S.A.

RELATED LINES IN THE SPECTRA OF THE ELEMENTS OF THE IRON GROUP

By HENRY NORRIS RUSSELL[1]

ABSTRACT

Homologous lines.—Recent theories of spectral structure suffice to identify those groups of homologous lines in the spectra of different elements which arise *from similar electronic transitions* within the atoms. Such groups have quite different spectroscopic names and multiplicities, but they show very *similar* physical and astrophysical *behavior.*

Tables are given of the *homologous terms* in the *arc spectra* from *K* to *Zn* and in the *spark spectra* from Ca^+ to Zn^+. The identifications of the lower terms follow Hund; those of many of the higher terms are new. The relations of the terms are illustrated graphically, thus clearing up certain doubtful questions.

Tables are also given of the *homologous lines* which arise from eight different electronic transitions in the neutral, and four in the ionized atom.

The transition from a 4p to a 4s orbit accounts for most of the strongest lines in both the arc and spark spectra. These lines shift steadily toward the ultra violet as the atomic number increases.

Transitions from a 5s to a 4p orbit give arc lines in the visible region, some of which are strong, while others make it possible to determine the ionization potential. Many other sets of homologous lines may be identified when the spectra have been more completely analyzed.

Relations between different spectra.—If the elements of the iron group are written as follows

K	*Ca*	*Sc*	*Ti*	*V*	*Cr*	*Mn*
Zn	*Cu*	*Ni*	*Co*	*Fe*	*Mn*	*Cr*

the spectrum of any element contains a large portion which is very similar to a corresponding portion of the element above or below, and one step to the right, and another portion similarly related to a part of that of the element above or below and to the left. Each spectrum also contains other portions peculiar to itself.

I. INTRODUCTION

It has long been recognized that the spectra of elements belonging in the same column of the periodic table are so similar that they can be correlated almost line by line. For example, the homology of *Ca* 4226, *Sr* 4607, *Ba* 5535, or of Ca^+ 3933, 3968, Sr^+ 4077, 4215, Ba^+ 4554, 4934, is a commonplace. The spectra of elements in the same row of the periodic table, however, present no apparent points of resemblance, nor did even their successful analysis, after the laws of multiplet structure were discovered, bring out much obvious similarity. The lowest spectroscopic term, corresponding to the normal state of the atom, may be of the types S, P, D, or F and belong to a system of any multiplicity from singlets to septets.

---

[1] Research Associate of the Mount Wilson Observatory, Carnegie Institution of Washington.

Order was recognized in the apparent chaos only when the work of several investigators, culminating in that of Hund,[1] traced the relation of these spectroscopic terms to the electronic configurations in the atom which produced them. It then became evident that our previous difficulties had arisen because we were seeking for similar spectroscopic terms, whereas we should have sought for lines produced by similar transitions within the atom. When once this is understood, very striking relations appear between spectra and between individual groups of lines which have previously seemed to be quite unconnected.

These new relations are especially well illustrated in the spectra of the elements in the earlier part of the first long period—from *K* to *Zn*—which are often called the "iron group."

2. SKETCH OF THE THEORY

In this group the complete inner shells include electron orbits[2] of types 1s, 2s, 2p, 3s, 3p, and the outer incomplete shell is formed, in the normal states of the neutral and ionized atoms, of electrons with 4s or 3d orbits—two of the former being first added in *K* and *Ca*, followed by ten of the latter from *Sc* to *Zn*. In the low metastable energy states, which are numerous in most of these atoms, only 4s and 3d electrons are present outside the completed shells. The corresponding terms are all "even" and do not combine with one another to give spectral lines; but they combine freely with higher "odd" terms arising from configurations including a 4p electron; and these again combine with still higher even terms coming from configurations in which one electron is in a 5s or 4d orbit. Few configurations involving higher orbits (6s, 5p, 5d, 4f, etc.) are known, except in the spectra in which series are prominent. Those including an odd number of p and f electrons (taken together) are "odd."

Configurations of this sort may be represented by symbols such as $(4s)^2(3d)^5(4p)$, in which the exponents denote the number of electrons of the given type which are present. We may abbreviate this for our present purpose into $s^2\, d^5\, p$, and denote configurations involving a more highly excited electron (where we shall have to consider only 5s and 4d) by expressions such as $s^2d^5\cdot s$, in full, $(4s)^2$-$(3d)^5(5s)$. Not more than two s electrons of the same total quantum number (e.g., 4s) can be present in any atom, but the number of similar d electrons may run up to ten. Six 4p electrons might be present—and actually are in *Kr;* but we shall not have to deal with more than two of them in the iron group. In a transition accompanied by the production of a spectral line, one electron must "jump" by one step—from s to p or p to d—and one other may sometimes simultaneously jump by two steps—from s to d, in this case. We may therefore arrange the configurations with which we have to deal in three groups as follows:

---

[1] For a full account see F. Hund, *Linienspektren und periodisches System der Elemente* (Berlin, 1927).

[2] This familiar nomenclature is used for convenience, without thought of opposition to the newer wave-mechanics.

I	II	III	
$d^{n-2}s^2$	$d^{n-2}sp$	$d^{n-2}s\cdot s$	$d^{n-1}\cdot s$
$d^{n-1}s$	$d^{n-1}p$	$d^{n-2}s\cdot d$	$d^{n-1}\cdot d$
d^n	$d^{n-1}f$	$d^{n-2}p^2$	

These represent the important configurations for an atom which, in its neutral state, has n outer electrons and the atomic number $n+18$. In the present paper "n" will be used in this sense throughout, so that the configurations I in the singly ionized atom will be denoted by $d^{n-3}s^2$, $d^{n-2}s$, d^{n-1}.

In general, the first group of configurations will give the even terms of lowest energy (since the 4s and 3d electrons are most firmly bound); those of the second will give "odd" terms at a middle level; and the third, high-lying "even" terms.

Spectral lines arise only from transitions between odd and even terms; for example, $d^{n-1}s-d^{n-1}p$ or $d^{n-2}s^2-d^{n-1}p$. The first of these transitions, which demands only the jumping of one electron from a p to an s orbit, is likely to give much stronger lines than the second, which involves the simultaneous jumping of two electrons, one from d to s and the other from p to s.

If now we vary n—that is, the atomic number—we shall have a series of transitions between states in successive elements of the periodic table in each of which the electron jump is essentially the same; and it is such transitions which produce the really homologous lines in the successive spectra.

These homologous configurations give rise, however, to apparently quite dissimilar spectroscopic terms. In accordance with Pauli's restriction, groups of 3d electrons produce the following terms:[1]

d^{10}	^1S	
d,d^9	^2D	
d^2,d^8	$^3F',^3P'$;	$^1G,^1D,^1S$
d^3,d^7	$^4F',^4P'$;	$^2H',^2G,^2F',^2D,^2P',^2D$
d^4,d^6	^5D ;	$^3H',^3G,^3F',^3D,^3P',^3F',^3P'$, etc.
d^5	^6S ;	$^4G,^4F',^4D,^4P'$ ...., etc.

Many terms of lower multiplicity, which do not now concern us, are omitted. The terms given in the first column, which are of the highest multiplicity present, lie lowest, and the F′ term lower than the P′, when both are present. In the next group, the G term is usually, though not always, the lowest, and the H′, D, and P′ terms (so many as are present) are not much higher.

The addition of other electrons to these configurations converts each "parent term," such as those tabulated, into a group of terms, usually of different multiplicity and name (letter). In general, the multiplicity is both increased and diminished by a unit for each added electron. Adding an s electron leaves the letters unchanged. Adding a p electron converts each parent term into a triad of closely related terms. Thus a D term goes into PD′F terms (but an S term into a P term only). Adding a d electron produces, in general, groups of five terms (pentads). Thus F gives PD′FG′H (but P gives PD′F and S, D alone). The terms which originate from the same parent term are closely related, and the combinations between them account for most of the strong lines of the spectrum. When two or more similar electrons are added, Pauli's restriction operates upon them too. Thus the addition of two 4s electrons leaves both the multiplicity and the letter unchanged; that of two 4p's is equivalent to combinations with the terms $^3P'^1S^1D$—the first changes the multiplicity by $+2, 0, -2$, and the others by 0, while the letters follow the previous rules.

3. PRINCIPAL TERMS IN SPECTRA OF THE IRON GROUP

With this brief summary of the theory, we proceed to tabulate the principal terms in the spectra which we have to consider. A complete tabulation of the terms which are theoretically to be expected, and which have actually been found, in almost perfect agreement with theory, in those spectra which have been fully analyzed, would occupy far too much space. We may content ourselves, in general, with listing those terms which arise from the lowest energy levels of the singly and doubly ionized atoms. Experience shows that, at least for the elements here considered, the term of lowest energy level always comes from the configuration d^{n-2} and is the one which is first listed for the corresponding number of electrons in the preceding section. How the resulting terms in the arc and spark spectra arise from it may be illustrated in the typical case of titanium (n = 4).

---

[1] Hund, *op. cit.*, p. 119.

The lowest energy state of *Ti* III is here a $^3F'$ term coming from the d^2 configuration. The results of adding s electrons are as follows:

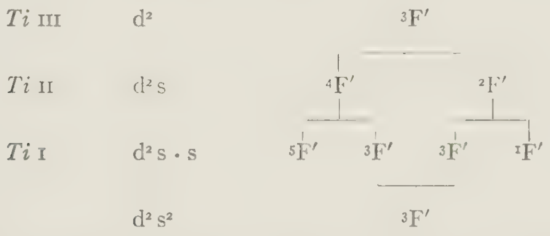

When the successive electrons which are added are unlike (4s and 5s), the original term splits up into four in *Ti* I; but when they are alike, Pauli's restriction abolishes the quintet and singlet terms and combines the triplet terms into one—which, however, is the leading member of both the series of $^3F'$ terms which may be obtained by adding 5s, 6s electrons (such series are actually known in several elements). On adding a p electron followed by a 4s electron or another p, we have

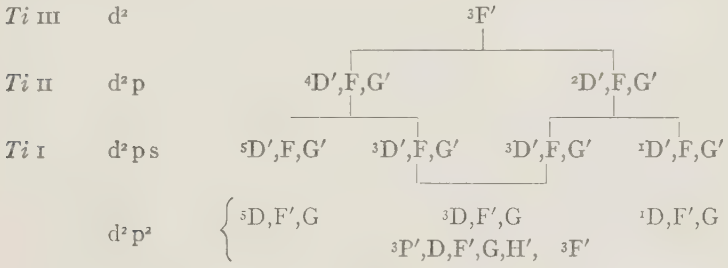

The addition of a 4d electron (unlike those already present) gives pentads:

Ti III	d^2	${}^3F'$			
Ti II	$d^2 \cdot d$	${}^4P', D, F', G, H'$		${}^2P', D, F', G, H'$	
Ti I	$d^2s \cdot d$	${}^5P', D, F', G, H'$	${}^3P', D, F', G, H'$	${}^3P', D, F', G, H'$	${}^1P', D, F', G, H'$

On adding a 3d electron Pauli's exclusion operates, and the list of terms from the d³ configurations must be consulted. The resulting terms in *Ti* II have no such simple relation to the parent terms of *Ti* III as in the previous case; but they show families of their own. We give here only the derivatives of the lowest term:

Ti II	d^3	${}^4F'$	
Ti I	d^3s	${}^5F'$	${}^3F'$
	d^3p	${}^5D', F, G'$	${}^3D', FG'$
	$d^3 \cdot d$	${}^5P', D, F,' G, H'$	${}^3P', D, F', G, H'$

All the members of most of these groups, and some members, at least, of almost all of them, have actually been identified in *Ti* I and *Ti* II, along with many others arising from other parent terms of the d² and d³ configurations. When an equally complete analysis has been made, the same will probably be true in all the other spectra.

Still another configuration, d⁴ (in general dⁿ), may exist in the neutral *Ti* atom; but this gives high-lying terms of little importance, which thus far are known in but a few cases.

The principal low-level terms in the spectra of the first three stages of ionization are related as follows:

$$\begin{tikzcd}
\mathrm{III} & & & d^{n-2} & & \\
\mathrm{II} & & d^{n-2}s \arrow[ur, "s"] & & d^{n-1} \arrow[ul, "d"'] & \\
\mathrm{I} & d^{n-2}\cdot s^2 \arrow[ur, "s"] & & d^{n-1}s \arrow[ul, "d"'] \arrow[ur, "s"] & & d^n \arrow[ul, "d"']
\end{tikzcd}$$

The arrows indicate the processes of ionization through which one state may be reached from another by removal of an electron. There are, therefore, two different ionization potentials for the spark spectra and four for the arc (three if the configuration d^n be neglected), and, of course, many more corresponding to transitions upward from other metastable terms, not here considered. In *K* and *Zn* the number of possible transitions is diminished by the limitation in the number of electrons as a complete group. The principal ionization potential is usually defined as the energy difference between the lowest (normal) states of the neutral and the ionized atom (and so on for higher ionizations). It should be especially remarked, however, that this quantity does not always correspond to the simple removal of one electron. Among the elements considered the normal state of the neutral atom belongs to $d^{n-2}\,s^2$, except for *K*, *Cr*, and *Cu;* in the ionized atom the state of lowest energy is $d^{n-2}\,s$ for *Ca*, *Sc*, *Ti*, *Mn*, and *Fe*, and d^{n-1} for the rest. In *V* and *Co*, therefore, the transition from one normal state to the other is from $d^{n-2}\,s^2$ to d^{n-1} and involves the removal of one electron and the shift of another.

4. TABLES OF THESE TERMS

The observed values of these principal terms in the arc and spark spectra of the elements from *K* to *Zn* are given in Tables I and II. The data have been collected from various sources,[1] and a few have been added by the writer, whose best thanks are due to his colleagues for generous permission to use valuable unpublished material. The values are counted upward from the lowest term of origin $d^{n-2}\,s^2$ in the arc (except for *K*, where there is no such term) or $d^{n-2}\,s$ in the spark. This unusual method has been adopted to make the regu-

---

[1] For papers up to 1926 see Hund, *op. cit.*, pp. 212–217; *Sc*, *Sc*$^+$, H. N. Russell and W. F. Meggers, *Scientific Papers of the Bureau of Standards*, **22**, 329 (No. 558), 1927; *Ti*, *Ti*$^+$, H. N. Russell, *Mt. Wilson Contr.*, Nos. 344, 345; *Astrophysical Journal*, **66**, 1927; *V*, *V*$^+$, W. F. Meggers, *Zeitschrift für Physik*, **39**, 114, 1926, and unpublished material; *Cr*, *Cr*$^+$, C. C. Kiess (unpublished); *Mn*, T. Dunham (unpublished); *Fe*, O. Laporte, *Proceedings of the National Academy of Sciences*, **12**, 496, 1926; *Fe*$^+$, H. N. Russell, *Mt. Wilson Contr.*, No. 318; *Astrophysical Journal*, **64**, 194, 1926; *Co*$^+$, W. F. Meggers (unpublished); *Ni*$^+$, A. G. Shenstone, *Physical Review*, **30**, 255, 1927; *Cu*, *Cu*$^+$, A. G. Shenstone, *Physical Review*, **28**, 449, 1926, and **29**, 380, 1927, and unpublished data.

TABLE I

OBSERVED TERMS AND ORIGINS, ARC SPECTRA

Configuration	n=1, *K*		n=2, *Ca*		n=3, *Sc*		n=4, *Ti*	
$d^{n-2}s^2$	.....	....	^1S	0.0	^2D	168.3	$^3F'$	386.9
							$^3P'$	8602.4
$d^{n-2}sp$	.....	....	^3P	15316.1	^4P	18571.4	$^5D'$	18695.2
					$^4D'$	16210.8	^5F	17215.4
					^4F	16026.5	$^5G'$	16458.7
					^2P	18855.8	$^3D'$	20126.1
					$^2D'$	16022.7	^3F	19574.0
					^2F	21085.8	$^3G'$	21739.7
			^1P	23652.4	^2P	24656.8	$^3D'$	25643.8
					$^2D'$	25014.2	^3F	25388.4
					^2F	25724.7	$^3G'$	30039.4
							$^1D'$	22081.2
							^1F	22404.7
							$^1G'$	24694.8
$d^{n-2}s \cdot s$	.....	....	^3S	31539.7	^4D	34567.1	$^5F'$	36351.4
			^1S	33316.6	^2D	35745.6	$^3F'$	37824.7
					^2D	....	$^3F'$	39785.9
							$^1F'$	41087.3
$d^{n-2}s \cdot d$	.....	....	^3D	37757.8	^4S	....	$^5P'$	42858.9
					$^4P'$	....	^5D	42184.7
					^4D	39799.9	$^5F'$	43330.1
			^1D	37298.5	$^4F'$	40670.9	^5G	42019.2
					^4G	40028.2	$^5H'$	42205.6
$d^{n-2}p^2$	.....	....	$^3P'$	38551.8	$^4P'$	....	^5D	49036.5
			^1S	40690.6	^4D	....	$^5F'$	48462.1
			^1D	40719.9	$^4F'$	45125.6	^5G	47446.8
$d^{n-2}sf$	.....	....	^3F	42170.9	^4P	....	$^5S'$	....
			^1F	42343.5	to	....	to	....
					^4H	....	$^5I'$	....
$d^{n-1}s$	^2S	0.0	^3D	20371.3	$^4F'$	11677.3	$^5F'$	6843.0
					$^4P'$	....	$^5P'$	14105.7
			^1D	21849.5	$^2F'$	15042.0	$^3F'$	11776.9
					$^2P'$	....	$^3P'$	18911.6
$d^{n-1}p$	^2P	12985.1	^3P	39340.5	$^4D'$	32751.5	$^5D'$	30060.3
			$^3D'$	38259.5	^4F	31350.8	^5F	28896.1
			^3F	35897.2	$^4G'$	29303.5	$^5G'$	26910.7
			^1P	36731.5	$^2D'$	33707.3	$^3D'$	29912.3
			$^1D'$	35835.7	^2F	33278.6	^3F	27025.7
			^1F	40537.8	$^2G'$	33151.4	$^3G'$	27750.2
$d^{n-1} \cdot s$	^2S	21025.6	^3D	46704.0:	$^4F'$	42085.0	$^5F'$	39412.8
			^1D	....	$^2F'$	....	$^3F'$	....
d^n	^2D	21535.6	$^3F'$	....	$^4F'$	33906.4	^5D	....
			$^3P'$	48563.7	$^4P'$	36572.7	.....	....
$d^{n-1} \cdot d$	^2D	27397.6	^3S	51571.3	$^4P'$	....	$^5P'$	....
			$^3P'$	54304.6	^4D	....	^5D	44381.2
			^3D	51396.3	$^4F'$	....	$^5F'$	....
			$^3F'$	....	^4G	....	^5G	45904.7
			^3G	....	$^4H'$	....	$^5H'$	44134.6

TABLE I—*Continued*

Configuration	n=5, *V*		n=6, *Cr*		n=7, *Mn*		n=8, *Fe*	
$d^{n-2}s^2$	$^4F'$	553.0	^5D	556.8	^6S	0.0	^5D	0.0
	$^4P'$	9824.6	.....	....	.....	....	.....	....
$d^{n-2}sp$	$^6D'$	18438.1	^7P	20184.6	^8P	18705.4	^7P	23711.5
	^6F	18680.5	$^7D'$	20074.5	.....	....	$^7D'$	19350.9
	$^6G'$	17136.4	^7F	18020.8	.....	....	^7F	22650.4
	$^4D'$	21032.4	^5P	22074.0	^6P	24802.2	^5P	29056.3
	^4F	23519.8	$^5D'$	26065.3	.....	....	$^5D'$	25900.0
	$^4G'$	22313.9	^5F	23529.3	.....	....	^5F	26874.6
	$^4D'$	34747.0	^5P	33292.7	^6P	35769.9	^5P	36767.0
	^4F	33155.4	$^5D'$	34031.5	.....	....	$^5D'$	39625.8
	$^4G'$	31937.0	^5F	33642.7	.....	....	^5F	40257.3
	$^2D'$	....	^3P	....	^4P	31001.0	^3P	33947.0
	^2F	....	$^3D'$	....	.....	....	$^3D'$	31322.6
	$^2G'$	....	^3F	....	.....	....	^3F	31307.3
$d^{n-2}s \cdot s$	$^6F'$	37931.3	^7D	39208.4	^8S	39431.4	^7D	42815.8
	$^4F'$	39596.9	^5D	41073.6	^6S	41404.0	^5D	44677.0
	$^4F'$	....	^5D	....	^6S	49415.3	^5D	51350.5
	$^2F'$	....	^3D	....	^4S	49591.4	^3D	53747.5
$d^{n-2}s \cdot d$	$^6P'$	....	^7S	....	^8D	46712.6	^7S	....
	^6D	....	$^7P'$	....	^6D	47207.3	$^7P'$	....
	$^6F'$	....	^7D	....	.....	....	^7D	....
	^6G	....	$^7F'$	....	^6D	....	$^7F'$	....
	$^6H'$	....	^7G	....	^4D	....	^7G	....
$d^{n-2}p^2$	^6D	....	$^7P'$	....	$^8P'$	57086.2	$^7P'$	....
	$^6F'$	....	^7D	....	.....	....	^7D	....
	^6G	....	$^7F'$	....	.....	....	$^7F'$	....
$d^{n-2}s\,f$	$^6S'$	....	^7P	....	^8F	52974.6	^7P	....
	to		to				to	
	$^6I'$	....	^7H	....	.....	....	^7H	....
$d^{n-1}s$	^6D	2424.9	^7S	−7750.7	^6D	17052.3	$^5F'$	6928.3
							$^5P'$	17550.2
							$^3F'$	11976.3
	^4D	8715.7	^5S	− 157.6	^4D	23296.7	$^3P'$	22838.3
$d^{n-1}p$	^6P	24838.6	^7P	15748.2	^6P	44993.9	$^5D'$	33096.0
	$^6D'$	26738.3	.....	....	$^6D'$	41789.5	^5F	33695.4
	^6F	25253.4	.....	....	^6F	43313.3	$^5G'$	34844.0
	^4P	25130.9	^5P	19036.6	^4P	46901.1	$^3D'$	38175.4
	$^4D'$	26480.3	.....	....	$^4D'$	45754.3	^3F	36686.2
	^4F	26172.0	.....	....	^4F	44288.8	$^3G'$	35379.2
$d^{n-1} \cdot s$	^6D	....	^7S	29145.1	^6D	56189.5	$^5F'$	47005.5
	^4D	....	^5S	30132.4	^4D	57305.7	$^3F'$	47960.9
d^n	^6S	....	^5D	....	$^4F'$	....	$^3F'$	....
					$^4P'$	....	$^3P'$	....
$d^{n-1} \cdot d$	^6S	....	^7D	34510.6	^6S	....	$^5P'$	....
	$^6P'$	....	.....	....	$^6P'$	....	^5D	....
	^6D	....	.....	....	^6D	....	$^5F'$	....
	$^6F'$	....	^5D	....	$^6F'$	....	^5G	....
	^6G	....	.....	....	^6G	....	$^5H'$	....

TABLE I—*Continued*

Configuration	n=9, *Co*		n=10, *Ni*		n=11, *Cu*		n=12, *Zn*	
$d^{n-2}s^2$	$^4F'$	0.0	$^3F'$	0.0	^2D	0.0	^1S	0.0
	$^4P'$	15184.0	$^3P'$	15609.8	.....	....	.....	....
$d^{n-2}sp$	$^6D'$	24627.8	$^5D'$	25753.6	^4P	27816.1	^3P	32890.5
	^6F	23611.7	^5F	28541.9	$^4D'$	32311.4	.....	....
	$^6G'$	25138.8	$^5G'$	27261.0	^4F	29706.6	.....	....
	$^4D'$	29294.5	$^3D'$	33500.8	^2P	34676.7	.....	....
	^4F	28345.8	^3F	32973.3	$^2D'$	35395.8	.....	....
	$^4G'$	28845.2	$^3G'$	30922.6	^2F	33760.7	.....	....
	$^4D'$	39649.0	$^3D'$	....	^2P	46746.7	^1P	46745.1
	^4F	41225.4	^3F	43258.7	$^2D'$	46916.8	.....	....
	$^4G'$	41528.3	$^3G'$	43089.5	^2F	44827.2	.....	....
	$^2D'$	33462.8	$^1D'$	36600.8	.....	....	.....	....
	^2F	31871.1	^1F	35639.1	.....	....	.....	....
	$^2G'$	31699.6	$^1G'$	33590.1	.....	....	.....	....
$d^{n-2}s{\cdot}s$	$^6F'$	45675.9	$^5F'$	48466.5	^4D	51200.7	^3S	53672.4
	$^4F'$	47524.4	$^3F'$	50466.1	^2D	53455.0	^1S	55788.1
	$^4F'$	....	$^3F'$	....	^2D	....	.....	....
	$^2F'$	....	$^1F'$	50832.0:	.....	....	.....	....
$d^{n-2}s{\cdot}d$	$^6P'$	....	$^5P'$	....	^4S	59650.8	^3D	62778.1
	^6D	....	^5D	....	$^4P'$	59975.6	.....	....
	$^6F'$	....	$^5F'$	....	^4D	60065.6	^1D	62458.2
	^6G	....	^5G	....	$^4F'$	60087.9	.....	....
	$^6H'$	....	$^5H'$	....	^4G	59928.1	.....	....
$d^{n-2}p^2$	^6D	....	^5D	....	$^4P'$	....	$^3P'$	80395.3
	$^6F'$	....	$^5F'$	....	^4D	....		....
	^6G	....	^5G	....	$^4F'$	....		....
$d^{n-2}sf$	$^6S'$	....	$^5S'$	....	^4P	....	^3F	68835.5
	to	....	to	....	to	....	.....	....
	$^6I'$	....	$^5I'$	....	^4H	....	^1F	....
$d^{n-1}s$	$^4F'$	3482.8	^3D	204.8	^2S	−11202.5	.....	....
	$^4P'$	13795.4	.....	....	.....	....	.....	....
	$^2F'$	7442.4	^1D	3410.0	.....	....	.....	....
	$^2P'$	16470.6:	.....	....	.....	....	.....	....
$d^{n-1}p$	$^4D'$	32027.4	^3P	28569.3	^2P	19581.1	.....	....
	^4F	32841.9	$^3D'$	29668.9	.....	....	.....	....
	$^4G'$	32430.6	^3F	29481.0	.....	....	.....	....
	$^2D'$	36092.4	^1P	32982.3	.....	....	.....	....
	^2F	35450.5	$^1D'$	31441.6	.....	....	.....	....
	$^2G'$	33439.6	^1F	31031.0	.....	....	.....	....
$d^{n-1}{\cdot}s$	$^4F'$	44782.0	^3D	42605.8	^2S	31934.4	.....	....
	$^2F'$	45924.8	^1D	44262.5	.....	....	.....	....
d^n	^2D	....	^1S	14728.9:	.....	....	.....	....
	.....	....	.....	....	.....	....	.....	....
$d^{n-1}{\cdot}d$	$^4P'$	....	^3S	....	.....	....	.....	....
	^4D	....	$^3P'$	....	.....	....	.....	....
	$^4F'$	....	^3D	....	^2D	38739.6	.....	....
	^4G	....	$^3F'$	....	.....	....	.....	....
	$^4H'$	....	^3G	....	.....	....	.....	....

TABLE II

OBSERVED TERMS AND ORIGINS, SPARK SPECTRA

Configuration	n=2, Ca^+		n=3, Sc^+		n=4, Ti^+		n=5, V^+	
$d^{n-2}s$	^2S	0.0	^3D	177.6	$^4F'$	393.2	$^5F'$	557.9
					$^4P'$	10024.7	$^5P'$	11136.5
			^1D	2541.0	$^2F'$	4897.6	$^3F'$	6492.6
					$^2P'$	16625.3	$^3P'$	....
d^{n-1}...........	^2D	13711.0	$^3F'$	4987.6	$^4F'$	1215.6	^5D	−2265.4
			$^3P'$	12154.3	$^4P'$	9518.0	.....	....
$d^{n-3}s^2$	.....	....	^1S	....	^2D	25193.0	$^3F'$	....
$d^{n-2}p$	^2P	25414.4	^3P	29823.9	$^4D'$	32767.0	$^5D'$	34925.9
			$^3D'$	28161.0	^4F	31300.9	^5F	34747.7
			^3F	27841.2	$^4G'$	30240.7	$^5G'$	32878.7
			^1P	30815.7	$^2D'$	32025.5	$^3D'$	34314.1
			$^1D'$	26081.3	^2F	31490.8	^3F	37824.8
			^1F	32350.0	$^2G'$	34748.5	$^3G'$	37007.7
$d^{n-3}sp$........	.....	....	^3P	39344.9	^4P	56325.9	$^5D'$	....
					$^4D'$	52631.1	^5F	....
					^4F	....	$^5G'$	....
			^1P	....	^2P	....	$^3D'$	....
					$^2D'$	69622.1	^3F	....
					^2F	70893.0	$^3G'$	....
$d^{n-2}\cdot s$.........	^2S	52167.0	^3D	57743.4	$^4F'$	62594.3	$^5F'$	....
			^1D	58251.9	$^2F'$	63444.8	$^3F'$	....
$d^{n-2}\cdot d$.........	^2D	56858.4	^3S	61071.1	$^4P'$	....	$^5P'$	....
			$^3P'$	64705.2	^4D	66996.7	^5D	....
			^3D	60001.6	$^4F'$	69081.4	$^5F'$	....
			$^3F'$	63527.7	^4G	65241.6	^5G	....
			^3G	60456.0	$^4H'$	65589.1	$^5H'$	....
			^1S	64942.8	$^2P'$	....	$^3P'$	....
			$^1P'$	60400.0	^2D	....	^3D	....
			^1D	64366.2	$^2F'$	65458.6	$^3F'$	....
			$^1F'$	59528.2	^2G	67820.9	^3G	....
			^1G	65235.8	$^2H'$	68582.3	$^3H'$	....
$d^{n-2}f$	^2F	68054.0	.....	....	.....	....	.....	....

TABLE II—*Continued*

Configuration	n=6, *Cr^+*		n=7, *Mn^+*		n=8, *Fe^+*		n=9, *Co^+*	
$d^{n-2}s$	^6D	0.0	^7S	0.0	^6D	0.0	$^5F'$	0.0
							$^5P'$	....
	^4D	7527.5	^5S	9472.9	^4D	7955.2	$^3F'$	....
							$^3P'$	....
d^{n-1}...........	^6S	−12498.3	^5D	14324.5	$^4F'$	1872.6	$^3F'$	(−3500)
					$^4P'$	13474.3	$^3P'$	....
$d^{n-3}s^2$	$^4F'$	....	^5D	....	^6S	23317.6	^5D	....
$d^{n-2}p$	^6P	36135.6	^7P	38806.5	^6P	42658.3	$^5D'$	42028.3
	$^6D'$	37341.8	.....	....	$^6D'$	38458.9	^5F	41847.4
	^6F	35255.1	.....	....	^6F	41968.1	$^5G'$	43728.0
	^4P	36855.0	^5P	43370.4	^4P	46967.3	$^3D'$	....
	$^4D'$	42287.9	.....	....	$^4D'$	44446.8	^3F	....
	^4F	39446.2	.....	....	^4F	44232.5	$^3G'$	....
$d^{n-3}sp$	$^6D'$	....	^7P	....	^8P	....	^7P	....
	^6F	....	$^7D'$	....	.....	....	$^7D'$	....
	$^6G'$	....	^7F	....	.....	....	^7F	....
	$^4D'$	....	^5P	....	^6P	....	^5P	....
	^4F	....	$^5D'$	....	.....	....	$^5D'$	....
	$^4G'$	....	^5F	....	.....	....	^5F	....
$d^{n-2}\cdot s$.........	^6D	....	^7S	74558.4	^6D	....	$^5F'$	....
	^4D	....	^5S	....	^4D	....	$^3F'$	....
$d^{n-2}\cdot d$.........	^6S	....	^7D	79568.4	^6S	....	$^5P'$	....
	$^6P'$	....	.....	....	$^6P'$	....	^5D	....
	^6D	....	.....	....	^6D	....	$^5F'$	....
	$^6F'$	....	.....	....	$^6F'$	....	^5G	....
	^6G	....	.....	....	^6G	....	$^5H'$	....
	^4S	....	^5D	....	^4S	....	$^3P'$	....
	$^4P'$	....	.....	....	$^4P'$	....	^3D	....
	^4D	....	.....	....	^4D	....	$^3F'$	....
	$^4F'$	....	.....	....	$^4F'$	....	^3G	....
	^4G	....	.....	....	^4G	....	$^3H'$	....
$d^{n-2}f$	.....	....	.....	....	.....	....	.....	....

TABLE II—*Continued*

Configuration	n=10, *Ni*$^+$		n=11, *Cu*$^+$		n=12, *Zn*$^+$	
$d^{n-2}s$	$^4F'$	0.0	^3D	0.0	^2S	0.0
	$^4P'$	16641.7	...	...	...	...
	$^2F'$	5156.2	^1D	4335.7	...	...
	$^2P'$	20676.5	...	...	...	...
d^{n-1}	^2D	(−8200)	^1S	−21925	...	...
	...	...	...	...	...	...
$d^{n-3}s^2$	$^4F'$	...	$^3F'$	...	^2D	62721.2
$d^{n-2}p$	$^4D'$	43164.0	^3P	44489.9	^2P	49353.7
	^4F	46163.2	$^3D'$	48912.5	...	...
	$^4G'$	45102.7	^3F	46802.1	...	...
	$^2D'$	49025.6	^1P	51667.1	...	...
	^2F	48686.2	$^1D'$	51424.3	...	...
	$^2G'$	46905.9	^1F	49991.3	...	...
$d^{n-3}sp$	$^6D'$	...	$^5D'$	...	$^4D'$	...
	^6F	...	^5F	...	^4F	...
	$^6G'$	...	$^5G'$	...	$^4G'$	...
	$^4D'$	...	$^3D'$	...	$^2D'$	...
	^4F	...	^3F	...	^2F	...
	$^4G'$	...	$^3G'$	...	$^2G'$	...
$d^{n-2}\cdot s$	$^4F'$	83404.4	^3D	86083.7	^2S	88435.8
	$^2F'$	85132.2	^1D	88435.0	...	...
$d^{n-2}\cdot d$	$^4P'$	...	^3S	...	^2D	96958.8
	^4D	...	$^3P'$	...	...	...
	$^4F'$	...	^3D	...	...	...
	^4G	...	$^3F'$	...	...	...
	$^4H'$	...	^3G	...	...	...
	$^2P'$	...	^1S	...	...	...
	^2D	...	$^1P'$	...	...	...
	$^2F'$	...	^1D	...	...	...
	^2G	...	$^1F'$	...	...	...
	$^2H'$	...	^1G	...	...	...
$d^{n-2}f$	...	...	...	...	^2F	117262.2

larities in arrangement of the various terms more apparent. Only the component of greatest inner-quantum number is tabulated. When the terms are "regular," this lies higher than the zero level, which corresponds to the smallest inner-quantum number. In a few of the spark spectra the lowest term has not yet been observed, but its position may be approximately found by means of series in the arc spectrum of the same element. These values are given in parentheses and in round numbers. Only the terms arising from those of highest multiplicity in the d^{n-2} or d^{n-1} configurations are tabulated, and the derivative terms arising from the P′ terms which accompany the F′ terms are omitted, because, where known, they give weaker lines. Even so, there are many blanks in the table, where terms remain to be found, and no attempt has been made to leave space for all the possible terms coming from $d^{n-2}\,s\cdot d$ or $d^{n-2}\,p^2$.

The assignment of the low terms to the various configurations follows Hund. That of the higher terms, in the cases of *Sc*, *Ti*, *Fe*, *Ni*, and *Cu*, is taken from the sources already listed. The remaining spectra have been reviewed by the writer for the present purpose. There is no room for full details here; but it may be said that the principles that the strongest combinations occur between related terms having the same parent term in the next higher spectrum, and that the terms of a triad or pentad usually lie at nearly the same level, generally suffice to identify the principal terms with reasonable security. Series relations identify most of the high even terms with certainty. A few terms for which the assignment to the given configuration is doubtful are marked with colons in the table.

5. REMARKS ON SPECTRAL STRUCTURE

Many striking regularities are shown in this table. The orderly change in the multiplicities and types of the terms is a direct consequence of Hund's theory, as is also the fact that, among the terms of similar origin, those of the higher multiplicity are almost always at the lower level.

The levels corresponding to excited configurations of the atom $d^{n-2}\,s\,p$, $d^{n-2}\,s\cdot s$, $d^{n-2}\,s\cdot d$, rise steadily, compared with $d^{n-2}\,s^2$, as the atomic number increases; and the same is true of $d^{n-1}\,p$, $d^{n-1}\cdot s$, $d^{n-1}\cdot d$ relative to $d^{n-1}\,s$. These relations are illustrated in Figures 1 and 2, in which, to avoid confusion, each triad or pentad is represented by a single point at the mean level of the known terms belonging to it.

The lines connect the points representing those terms which are related, not merely as regards the electron configurations, but also with respect to the multiplicity, and are found in the same column in Tables I and II. Some of these series of terms are longer than others, for the lower multiplicities do not always appear. Gaps where no observational data are at present available are bridged by dotted lines. Exactly the same relations (Fig. 3) hold good among the spark spectra.

The general upward trend of these lines is simply explained on the orbital theory of the atom. On passing up a series of homologous configurations, successive 3d electrons are built into the atoms, leaving the other orbits unaltered. In the group of

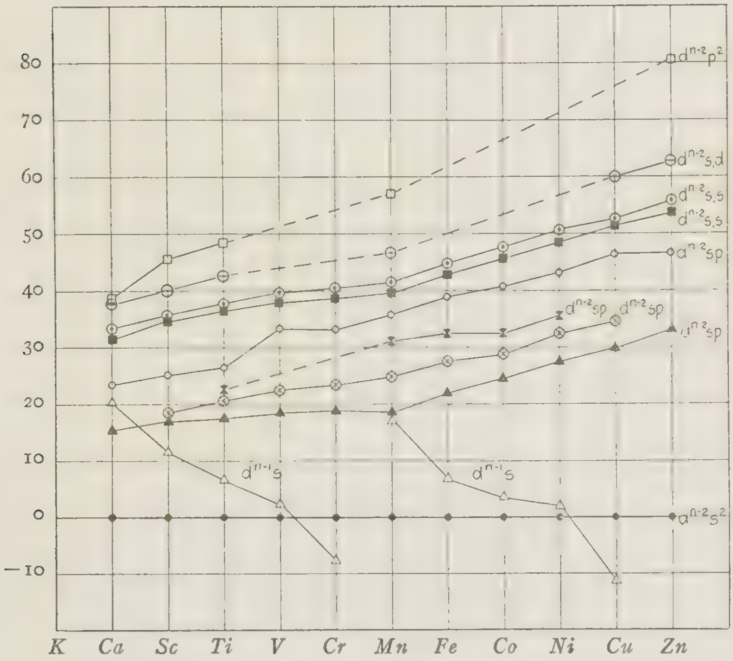

FIG. 1.—Energy levels relative to $d^{n-2}s^2$

configurations represented in Figure 2, for example, the only difference between the normal and excited states is that a single electron is shifted from a 4s to a 4p, 5s, or 5d orbit, and the difference of the spectroscopic terms represents the difference of the energy of binding of the electron to the atom in these orbits. For successive elements the nuclear charge increases. At a distance this increase is effectively neutralized by the influence of the additional 3d electrons; but for electrons such as are named above, all of which have orbits which at pericenter penetrate inside the 3d orbits, the "screening" of the additional central charge by the 3d electrons is incomplete. Every addition of such an electron, therefore, increases the average force with which the electron now specially considered is bound to the atom, and the energy of binding, which is directly shown by the increase in the ionization potential (discussed in a following paper).[1] This increase of binding energy is greater for the 4s electron than for the others; hence the difference of the spectroscopic terms increases with the atomic number.

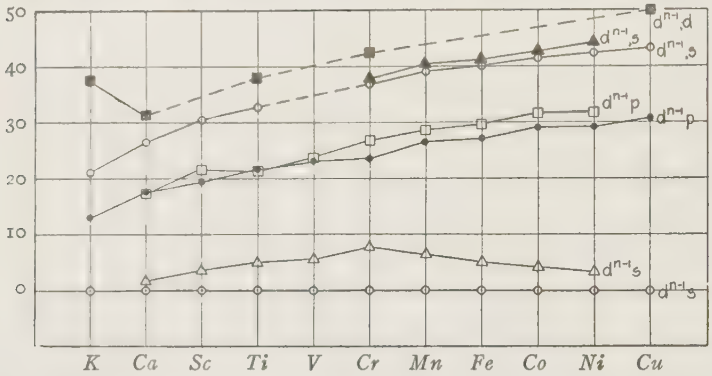

FIG. 2.—Energy levels relative to $d^{n-1}s$. The first point of the top curve should have been plotted with the ordinate 28.

This explanation, though conventional, is of course greatly oversimplified. What is really observed in the spectroscopic terms is the relative energy possessed by the atom as a whole, and not by any single electron in it, so that the "screening" should really take account of the combined influence of all the orbits. This is illustrated by the course of the differences between $d^{n-2}\,s^2$ and $d^{n-1}\,s$, or between $d^{n-2}\,s$ and d^{n-1} in the spark spectrum. Here the 3d electron appears to be bound with much more rapidly increasing energy than the 4s, until the shell of electrons is half-full in *Cr*, after which an abrupt change occurs in both the arc and spark spectra, and the energy differences nearly repeat themselves. Very similar relations appear in the second long period.[2] The break is associated with the change from increasing to decreasing multiplicity, and the appearance of inverted terms. It is easily explained by the reversal of the direction of spin of the added electron, which is demanded by Pauli's exclusion principle when a shell is more than half completed.

---

[1] *Mt. Wilson Contr.*, No. 342; *Astrophysical Journal*, **66**, 1927.

[2] O. Laporte, *Journal of the Optical Society of America*, **13**, 1, 1926. A similar discontinuity has been noticed for the shell of p electrons by McLennan and McLay, *Philosophical Magazine*, **4**, 407, 1927.

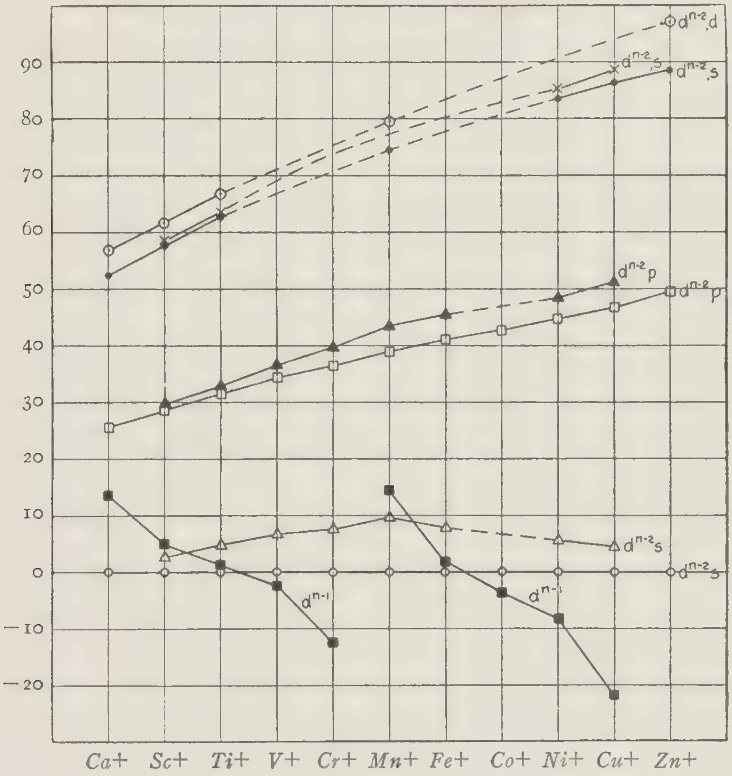

FIG. 3.—Energy levels relative to $d^{n-2}s$

Figures 1 and 2 bring out clearly many points of the spectral structure, some of which were previously puzzling. For example, the configuration $d^{n-2}sp$ gives rise in the arc spectra from *Sc* to *Cu* to two triads of the same multiplicity—doublets in *Sc*, triplets in *Ti*, and so on. In the spark spectra of the same elements, $d^{n-2}s$ gives rise to terms of the same name but different multiplicity, e.g., ^{3}D and ^{1}D in *Sc* II. It is evident that one of the arc triads, if the p electron were removed, step by step, would give rise to a series having as its limit the spark term of higher multiplicity, and the other to a series with the limit of lower multiplicity; but it is hardly practicable from inspection of a single spectrum to tell which belongs to which limit.[1] Figure 1 solves the problem, making it quite clear that the higher-lying of the two triads belongs to the sequence which begins with the ^{1}P term in *Ca* and ends with the similar term in *Zn*, while the lower-lying sequence has no correlatives in these spectra. In the spark spectra the d^{n-1} s terms of higher multiplicity form a sequence beginning with ^{2}S in *Ca*, ^{3}D in *Sc*, and ending with ^{2}S in *Zn*, while those of lower multiplicity begin with ^{1}D in *Sc* and end with the similar term in *Cu*. It is now evident that the higher set of triads must have the term of higher multiplicity as limit, which agrees with the fact that they give the stronger combinations. There are two other sequences of triads of origin d^{n-2} s p and of multiplicity higher and lower than those just considered, for example, quintets and singlets in *Ti* (the two being triplets). There can be no question about assigning these to the limits of high and low multiplicity, respectively, and it is now noteworthy that the terms of greater multiplicity always lie lower than those of smaller multiplicity arising from the same limit. This difference of level is much greater in the case of the terms with the limit of high multiplicity. Why this should be so is an excellent problem for the theorists.

6. TABLES OF HOMOLOGOUS LINES

The principal lines which result from combinations of the terms given in Tables I and II are listed in Tables III and IV. Each of the wide columns of the table gives data for a series of homologous lines, for which the electron jump is the same and the multiplicities are related as described above. Only the leading lines of the multiplets are given. The remainder may be found in most cases in the writer's "List of Ultimate and Penultimate Lines."[2] The letter *i* denotes that the predicted multiplet is in the infra-red. The intensities and temperature classes are taken from King's lists when available. Values derived from other sources are given in parentheses. The scale of intensities is not homogeneous throughout, nor even always for a single element. In certain cases, as in the combinations of a triad and a pentad of terms or in groups of intercombinations, only a few of the strongest multiplets are selected. It should be recalled once more that the list is very far from exhaustive, for only those terms

---

[1] Russell and Meggers, *Scientific Papers of the Bureau of Standards*, No. 558.

[2] *Mt. Wilson Contr.*, No. 286; *Astrophysical Journal*, **61**, 223–283, 1925.

TABLE III

Homologous Lines in Arc Spectra

Element	$d^{n-2}s^2-d^{n-2}sp$							
	Upper Triad			Lower Triad		Intersystem		
K.......	....	......	....	......	....	....	......	....
Ca......	$^1S-^1P$	4226.7	500 I	......	....	$^1S-^3P$	6572.8	8 I A
Sc......	$^2D-^2F$	3911.8	100 II	4779.4	20 I A	$^2D-^4F$	6413.4	50 I A
	$^2D'$	4023.7	100 II	6305.7	400 I A	$^4D'$	6259.0	100 I A
	^2P	4082.4	40 I	5349.7	15 II A	....	......	....
Ti......	$^3F'-^3G'$	3371.4	80 II	4681.9	30 I	$^3F'-^5G'$	6296.7	2 I A
	^3F	3998.6	100 II	5210.4	40 I	$^5D'$	5460.5	4 I A
	$^3D'$	3958.2	80 II	5064.6	25 I	$^1G'$	4112.7	20 II
V.......	$^4F'-^4G'$	3185.4	40 II	4594.1	60 I	$^4F'-^6D'$	5632.5	1 II A
	^4F	3066.4	125 II	4352.9	50 I	....	......	....
	$^4D'$	2923.6	70 II	4881.5	50 I	....	......	....
Cr......	$^5D-^5F$	3021.6	100 II	4351.8	60 I	$^5D-^7D'$	5122.1	4 I
	$^5D'$	2986.5	100 II	3919.2	35 II	^7P	5123.5	6 I
	^5P	3053.9	125 II	4646.2	40 I	....	......	....
Mn.....	$^6S-^6P$	2794.8	500 IV	4030.8	200 I	$^6S-^8P$	5394.7	10 I A
						^4P	3224.8	4 II
Fe......	$^5D-^5F$	2483.3	60 II	3719.9	250 I	$^5D-^7F$	4427.3	10 I
	$^5D'$	2522.9	40 II	3859.9	300 I	$^7D'$	5110.4	10 I
	^5P	2719.0	60 II	3440.6	150 I	^7P	4216.2	8 I
						^3P	2981.4	20 I
Co......	$^4F'-^4G'$	2407.3	(30 R)	3465.8	100 II	$^4F'-^6G'$	3909.9	15 I
	^4F	2425.0	(30 R)	3526.9	100 II	^6F	4190.7	20 I
	$^4D'$	2521.4	(30 R)	3412.6	80 II	$^2G'$	3237.0	8 II
Ni......	$^3F'-^3G'$	2320.0	(5 R)	3232.9	25 II	$^3F'-^5G'$	3624.7	15 II
	^3F	2311.0	(3 R)	3031.9	10 II	$^5D'$	3749.0	8 I
	$^3D'$	......	....	2984.1	12 II	^1F	2991.1	4 II
Cu......	$^2D-^2F$	2230.1	(6 R)	2961.2	(6)	$^2D-^4F$	3337.9	(6)
	$^2D'$	2130.8	(1)	2824.4	(8)	$^4D'$	3094.0	(6)
	^2P	2138.5	(1 R)	2883.0	(4)	^4P	3594.0	(2)
Zn......	$^1S-^1P$	2138.6	(8 R)	......	....	$^1S-^3P$	3075.9	(8 R)

TABLE III—*Continued*

ELEMENT	$d^{n-1}s-d^{n-1}p$								
	High Multiplicity			Low Multiplicity			Intersystem		
K....	$^{2}S-{}^{2}P$	7664.9	(10 R)	....	......	....	....	......	....
Ca....	$^{3}D-{}^{3}F$	6439.1	150 II	$^{1}D-{}^{1}F$	5349.5	25 III	$^{1}D-{}^{3}F$	7202.2	3 II
	$^{3}D'$	5588.7	80 III	$^{1}D'$	7148.1	10 II	....	......	....
	^{3}P	5270.3	60 III	^{1}P	6717.7	30 III	$^{3}D-{}^{1}D'$	6449.8	50 II
Sc....	$^{4}F'-{}^{4}G'$	5671.8	200 II	$^{2}F'-{}^{2}G'$	5520.5	100 III	$^{2}F'-{}^{4}G'$	......	....
	^{4}F	5081.6	125 II	^{2}F	5482.0	100 III	....	......	....
	$^{4}D'$	4743.8	40 III	$^{2}D'$	5356.1	60 III	$^{4}F'-{}^{2}G'$	......	....
Ti....	$^{5}F'-{}^{5}G'$	4981.8	60 II	$^{3}F'-{}^{3}G'$	6258.7	50 II	$^{3}F'-{}^{5}G'$	6666.6	(2)
	^{5}F	4533.3	80 II	^{3}F	6556.1	25 III	....	......	....
	$^{5}D'$	4305.9	60 II	$^{3}D'$	5512.5	25 II	$^{5}F'-{}^{3}G'$	4781.7	6 III A
V....	$^{6}D-{}^{6}F$	4379.2	150 II	$^{4}D-{}^{4}F$	5727.0	60 I	$^{4}D-{}^{6}F$	6128.3	2 III A
	$^{6}D'$	4111.8	100 I	$^{4}D'$	5627.6	30 I	....	......	....
	^{6}P	4460.3	50 I	^{4}P	6090.2	50 I	$^{6}D-{}^{4}F$	4209.9	20 I
Cr....	$^{7}S-{}^{7}P$	4254.3	500 II	$^{5}S-{}^{5}P$	5208.4	300 II	$^{5}S-{}^{7}P$	6330.1	25 I A
							$^{7}S-{}^{5}P$	3732.0	12 I
Mn...	$^{6}D-{}^{6}F$	3806.9	20 I	$^{4}D-{}^{4}F$	4762.4	30 III	$^{4}D-{}^{6}F$	4965.9	3 III
	$^{6}D'$	4041.4	50 I	$^{4}D'$	4451.6	15 II	....	......	....
	^{6}P	3577.9	40 II	^{4}P	4235.3	8 I	$^{6}D-{}^{4}F$	3670.5	3 III
Fe....	$^{5}F'-{}^{5}G'$	3581.2	250 I	$^{3}F'-{}^{3}G'$	4271.8	35 II	$^{3}F'-{}^{5}G'$	4383.5	45 II
	^{5}F	3734.9	300 II	^{3}F	4045.8	60 II	....	......	....
	$^{5}D'$	3820.4	250 II	$^{3}D'$	3815.8	100 II	$^{5}F'-{}^{3}G'$	3513.8	30 II
Co....	$^{4}F'-{}^{4}G'$	3453.5	200 II	$^{2}F'-{}^{2}G'$	3845.5	60 II	$^{2}F'-{}^{4}G'$	3995.3	60 II
	^{4}F	3405.1	150 II	^{2}F	3569.3	80 II	....	......	....
	$^{4}D'$	3502.3	100 II	$^{2}D'$	3489.4	60 II	$^{4}F'-{}^{2}G'$	3412.3	80 II
Ni...	$^{3}D-{}^{3}F$	3414.8	150 II	$^{1}D-{}^{1}F$	3619.4	150 II	$^{1}D-{}^{3}F$	3858.3	40 II
	$^{3}D'$	3393.0	100 II	$^{1}D'$	3566.4	100 II	....	......	....
	^{3}P	3524.5	200 II	^{1}P	3380.6	80 II	$^{3}D-{}^{1}F$	3243.1	25 I
Cu...	$^{2}S-{}^{2}P$	3247.5	(10 R)	....	......	....	....	......	....
Zn...	....	......	....	....	......	....	....	......	....

TABLE III—*Continued*

ELEMENT	$d^{n-1}s-d^{n-2}sp$					
	High Multiplicity			Low Multiplicity		
K..........	....	....	....	....	....	....
Ca..........	$^3D-^3P$	19771.1	....	$^1D-^1P$	*i*	....
Sc..........	$^4F'-^4F$	*i*	....	$^2F'-^2F$	*i*	....
	$^4D'$	*i*	....	$^2D'$	*i*	....
	^4P	*i*	....	^2P	*i*	....
Ti..........	$^5F'-^5G'$	*i*	....	$^3F'-^3G'$	5474.3	6 II
	^5F	9638.3	(2)	^3F	7344.7	4 IV
	$^5D'$	8435.6	(5)	$^3D'$	7209.4	20 III
V..........	$^6D-^6G'$	....	....	$^4D-^4G'$	....	....
	^6F	6150.1	15 I	^4F	6753.0	5 III A
	$^6D'$	6243.1	30 I	$^4D'$	8116.8	(5)
Cr..........	$^7S-^7F$	....	....	$^5S-^5F$	....	....
	$^7D'$	3615.7	4 II A	$^5D'$	3870.3	3 III
	^7P	3578.7	200 II	^5P	4496.9	25 I
Mn..........	$^6D-^6P$	12899.7	(8)	$^4D-^4P$	12975.9	(4)
	$^6D-^6P$	5341.1	20 III A	....	....	....
Fe..........	$^5F'-^5F$	5012.1	12 I	$^3F'-^3F$	5171.6	20 II
	$^5D'$	5269.5	60 I	$^3D'$	5167.5	40 II
	^5P			^3P	4765.5	(1)
Co..........	$^4F'-^4G'$	3941.7	20 II	$^2F'-^2G'$	4121.4	60 II
	^4F	4020.9	20 I	^2F	4092.4	25 I
	$^4D'$	3873.1	60 II	$^2D'$	3842.1	30 II
Ni	$^3D-^3G'$	3234.7	10 II	$^1D-^1G'$	....	....
	^3F	3050.8	100 II	^1F	3101.9	40 II
	$^3D'$	3002.5	100 II	$^1D'$	3012.0	75 II
Cu..........	$^2S-^2F$	....	....	....	....	....
	$^2D'$	2165.1	(1 R)	....	....	....
	^2P	2179.0	(1 R)	....	....	....
Zn..........	....	....	....	....	....	....

TABLE III—*Continued*

ELEMENT	$d^{n-2}s^2-d^{n-1}p$ (DOUBLE ELECTRON JUMP)					
				Intersystem		
K..........	....	....	....	....	....	....
Ca..........	$^1S-^1P$	2721.7	....	$^1S-^3F$	....	....
				$^3D'$	2617.6	(3)
				^3P	2541.4	(0)
Sc..........	$^2D-^2G'$	3039.8	(0) III A	$^2D-^4G'$	3455.9	(2) (II A)
	^2F	3019.3	10 II	^4F	3213.8	(0) (III A)
	$^2D'$	2980.7	(6)	$^4D'$	3073.3	(1) (III A)
Ti..........	$^3F'-^3G'$	3653.5	100 I	$^3F'-^5G'$	3788.8	2 III A
	^3F	3752.9	80 I	^5F	3506.6	8 I
	$^3D'$	3385.9	40 II	$^5D'$	3377.5	20 I
V..........	$^4F'-^4F$	3902.3	50 I	$^4F'-^6F$	4070.8	4 II
	$^4D'$	3855.9	60 I	$^6D'$	3817.9	8 I A
	^4P	4029.9	2 III A	^6P	....	....
Cr..........	$^5D-^5P$	5409.8	100 I	$^5D-^7P$	6630.0	4 I A
Mn..........	$^6S-^6F$	2296.9	(3)	$^6S-^4F$	....	....
	$^6D'$	2384.0	(2)	$^4D'$	2184.8	(1)
	^6P	2221.6	(9)	^4P	....	....
Fe..........	$^5D-^5G'$	2874.2	10 I	$^5D-^3G'$	2825.7	6 II
	^5F	2966.9	125 II	^3F	2690.1	2 III
	$^5D'$	3020.6	200 I	$^3D'$	2618.7	2 III
Co..........	$^4F'-^4G'$	3082.6	12 II	$^4F'-^2G'$	2989.6	15 II
	^4F	3044.0	30 II	^2F	2820.0	(2)
	$^4D'$	3121.4	10 II	$^2D'$	2833.9	(1)
Ni..........	$^3F'-^3F$	3391.1	50 II	$^3F'-^1F$	3366.2	20 II
	$^3D'$	3369.6	80 II	$^1D'$	3320.3	20 II
	^3P	3670.4	20 II	^1P	3249.4	6 I
Cu..........	$^2D-^2P$	5105.6	(8 R)	....	....	....
Zn..........	....	....	....	....	....	....

TABLE III—*Continued*

Element	$d^{n-2}sp-d^{n-2}s\cdot s$					
	High Multiplicity			Low Multiplicity		
K	....	....	....	....	....	....
Ca	$^{3}P-{}^{3}S$	6162.2	150 II	....	....	....
Sc	$^{4}F-{}^{4}D$	5392.1	30 III	$^{2}F-{}^{2}D$	6819.5	(20)
	$^{4}D'-{}^{4}D$	5446.2	20 III	$^{2}D'-{}^{2}D$	5068.9	2 III
	$^{4}P-{}^{4}D$	6250.0	15 IV	$^{2}P-{}^{2}D$	5919.2	tr IV A
Ti	$^{5}G'-{}^{5}F'$	5025.6	18 III	$^{3}G'-{}^{3}F'$	6215.2	20 III
	$^{5}F-{}^{5}F'$	5224.3	15 III	$^{3}F-{}^{3}F'$	5477.7	8 III
	$^{5}D'-{}^{5}F'$	5662.2	12 III	$^{3}D'-{}^{3}F'$	5648.6	5 IV
V	$^{6}G'-{}^{6}F'$	4807.5	25 III	$^{4}G'-{}^{4}F'$	5784.4	5 III
	$^{6}F-{}^{6}F'$	5193.0	7 III	$^{4}F-{}^{4}F'$	6218.3	3 IV
	$^{6}D'-{}^{6}F'$	5128.5	7 III	$^{4}D'-{}^{4}F'$	5385.1	3 III
Cr	$^{7}F-{}^{7}D$	4718.5	20 III	$^{5}F-{}^{5}D$	5698.3	20 III
	$^{7}D'-{}^{7}D$	5225.0	25 III	$^{5}D'-{}^{5}D$	6661.1	12 IV
	$^{7}P-{}^{7}D$	5255.1	15 IV	$^{5}P-{}^{5}D$	5261.8	6 IV
Mn	$^{8}P-{}^{8}S$	4823.5	50 I	$^{6}P-{}^{6}S$	6021.8	50 III
Fe	$^{7}F-{}^{7}D$	4957.6	60 III	$^{5}F-{}^{5}D$	5615.7	50 IV
	$^{7}D'-{}^{7}D$	4260.5	35 III	$^{5}D'-{}^{5}D$	5324.2	30 IV
	$^{7}P-{}^{7}D$	5232.9	40 III	$^{5}P-{}^{5}D$	6400.0	25 III
Co	$^{6}G'-{}^{6}F'$	4867.9	25 II	$^{4}G'-{}^{4}F'$	5352.0	20 III
	$^{6}F-{}^{6}F'$	4531.0	30 III	$^{4}F-{}^{4}F'$	5212.7	25 III
	$^{6}D'-{}^{6}F'$	4749.7	10 III	$^{4}D'-{}^{4}F'$	5484.0	10 V
Ni	$^{5}G'-{}^{5}F'$	4714.4	25 II	$^{3}G'-{}^{3}F'$	5115.4	8 V
	$^{5}F-{}^{5}F'$	5017.6	10 III?	$^{3}F-{}^{3}F'$	5715.1	6 V
	$^{5}D'-{}^{5}F'$	4401.6	30 III	$^{3}D'-{}^{3}F'$	5614.8	5 V
Cu	$^{4}F-{}^{4}D$	4651.1	(8)	$^{2}F-{}^{2}D$	5076.2	(3u)
	$^{4}D'-{}^{4}D$	5292.5	(4)	$^{2}D'-{}^{2}D$	5535.8	(3u)
	$^{4}P-{}^{4}D$	4275.1	(6)	$^{2}P-{}^{2}D$	....	....
Zn	$^{3}P-{}^{3}S$	4810.5	(10 R)	....	....	....

TABLE III—*Continued*

ELEMENT	$d^{n-1}p-d^{n-1}\cdot s$					
	High Multiplicity			Low Multiplicity		
K..........	${}^2P-{}^2S$	12523.0	....	....	....	....
Ca..........	${}^3F-{}^3D$	9250.8:	(2)	${}^1F-{}^1D$	....	....
	${}^3D'-{}^3D$	11840 :	(5)	${}^1D'-{}^1D$	....	....
	${}^3P-{}^3D$	....	....	${}^1P-{}^1D$	....	....
Sc..........	${}^4G'-{}^4F'$	7821.6	(6)	${}^2G'-{}^2F'$	....	....
	${}^4F-{}^4F'$	*i*	....	${}^2F-{}^2F'$	....	....
	${}^4D'-{}^4F'$	*i*	....	${}^2D'-{}^2F'$	....	....
Ti..........	${}^5G'-{}^5F'$	7996.5	(3)	${}^3G'-{}^3F'$	....	....
	${}^5F-{}^5F'$	*i*	....	${}^3F-{}^3F'$	....	....
	${}^5D'-{}^5F'$	*i*	....	${}^3D'-{}^3F'$	....	....
V..........	${}^6F-{}^6D$	*i*	....	${}^4F-{}^4D$	....	....
	${}^6D'-{}^6D$	*i*	....	${}^4D'-{}^4D$	....	....
	${}^6P-{}^6D$	*i*	....	${}^4P-{}^4D$	....	....
Cr..........	${}^7P-{}^7S$	7462.3	(10)	${}^5P-{}^5S$	9009.9	(6)
Mn..........	${}^6F-{}^6D$	7764.8	(5)	${}^4F-{}^4D$	7680.2	(5)
	${}^6D'-{}^6D$	6942.6	(5)	${}^4D'-{}^4D$	8654.6	(2)
	${}^6P-{}^6D$	8929.7	(1)	${}^4P-{}^4D$	*i*	....
Fe..........	${}^5G'-{}^5F'$	8220.4	(7)	${}^3G'-{}^3F'$	7945.9	(7)
	${}^5F-{}^5F'$	7511.1	(9)	${}^3F-{}^3F'$	8866.9	(3)
	${}^5D'-{}^5F'$	7187.4	5 V	${}^3D'-{}^3F'$	*i*	....
Co..........	${}^4G'-{}^4F'$	8094.0	8 III	${}^2G'-{}^2F'$	7027.9	6 V
	${}^4F-{}^4F'$	8372.8	(10)	${}^2F-{}^2F'$	7113.7	5 V
	${}^4D'-{}^4F'$	7838.2	3 V	${}^2D'-{}^2F'$	8022.2	(7)
Ni..........	${}^3F-{}^3D$	7617.0	5 III	${}^1F-{}^1D$	7555.7	5 III
	${}^3D'-{}^3D$	7727.7	3 IV	${}^1D'-{}^1D$	7797.7	3 V
	${}^3P-{}^3D$	7122.3	100 IV	${}^1P-{}^1D$	8862.6	(4)
Cu..........	${}^2P-{}^2S$	8092.7	(10)	....	....	....
Zn..........	....	....	....	....	....	....

TABLE III—*Continued*

ELEMENT	$d^{n-2}sp-d^{n-2}s\cdot d$			$d^{n-2}sp-d^{n-2}p^2$		
K..........	....	....	....	....	....	....
Ca..........	$^3P-^3D$	4454.8	80 I	$^3P-^3P'$	4302.5	60 I
Sc..........	$^4F-^4G$	4165.2	12 III	$^4F-^4F'$	3435.6	5 III A
	$^4D'-^4F'$	4087.2	8 III	$^4D'-^4F'$	3457.5	3 III A
	$^4P-^4D$	4709.3	5 III	....	....	....
Ti..........	$^5G'-^5H'$	3882.9	20n III?	$^5G'-^5G$	3226.1	12 III
	$^5F-^5G$	4030.5	25n III	$^5G'-^5F'$	3123.8	20n IV
	$^5D'-^5F'$	4058.2	7 IV	$^5F-^5D$	3141.7	10 IV
V..........	$^6G'-^6H'$	....	....	....	....	....
	$^6F-^6G$	....	....	....	....	....
	$^6D'-^6F'$	....	....	....	....	....
Cr..........	$^7F-^7G$	....	....	....	....	....
	$^7D'-^7F'$	....	....	....	....	....
	$^7P-^7D$	....	....	....	....	....
Mn..........	$^8P-^8D$	3569.5	60 III	$^8P-^8P'$	2584.3	(4)
Fe..........	$^7F-^7G$	....	....	....	....	....
	$^7D'-^7F'$	....	....	....	....	....
	$^7P-^7D$	....	....	....	....	....
Co..........	$^6G'-^6H'$	....	....	....	....	....
	$^6F-^6G$	....	....	....	....	....
	$^6D'-^6F'$	....	....	....	....	....
Ni..........	$^5G'-^5H'$	....	....	....	....	....
	$^5F-^5G$					
	$^5D'-^5F'$	....	....	....	....	....
Cu..........	$^4F-^4G$	3308.0	(8)	....	....	....
	$^4D'-^4F'$	3599.1	(6)	....	....	....
	$^4P-^4D$	3099.9	(4)	....	....	....
Zn..........	$^3P-^3D$	3344.9	(10 R)	$^3P-^3P'$	2096.9	(2)

TABLE IV

Related Lines in Spark Spectra

Element	$d^{n-2}s-d^{n-2}p$								
	High Multiplicity			Low Multiplicity			Intersystem		
Ca$^+$...	$^2S-^2P$	3933.7	400 II	....	......	....	....	......	....
Sc$^+$....	$^3D-^3F$	3613.8	30 II	$^1D-^1F$	3353.7	10 III	$^1D-^3F$	4014.5	5 IV
	$^3D'$	3572.5	20 II	$^1D'$	4246.8	75 III			
	^3P	3372.1	12 III	^1P	3535.7	6 III	$^3D-^1P$	3251.3	1 IV
Ti$^+$...	$^4F'-^4G'$	3349.4	40 II	$^2F'-^2G'$	3349.0	20 III	$^2F'-^4D'$	3596.0	10 V
	^4F	3234.5	60 III	^2F	3759.3	40 IV			
	$^4D'$	3088.0	60 III	$^2D'$	3685.2	40 IV	$^4F'-^2D'$	3143.8	10 IV
V$^+$....	$^5F'-^5G'$	3093.1	50 III	$^3F'-^3G'$	3276.1	20 V	$^3F'-^5D'$	3517.3	12 V
	^5F	2924.0	30 IV	^3F	3190.7	15 V			
	$^5D'$	2908.8	30 IV	$^3D'$	3593.3	12 V	$^5F'-^3D'$	2930.8	15 IV
Cr$^+$...	$^6D-^6F$	2835.6	40 V	$^4D-^4F$	3132.1	20 V	$^4D-^6P$	3511.8	6 V
	$^6D'$	2677.1	25 V	$^4D'$	2876.0	10 V			
	^6P	2766.6	30 V	^4P	3408.8	15 V	$^6D-^4P$	2698.4	10 V
Mn$^+$...	$^7S-^7P$	2576.2	(10 R)	$^5S-^5P$	2949.2	30 IV	$^5S-^7P$	3439.0	6 V
							$^7S-^5P$	2305.0	(2)
Fe$^+$...	$^6D-^6F$	2382.0	(10)	$^4D-^4F$	2755.7	(9)	$^4D-^6F$	2926.6	(6)
	$^6D'$	2599.4	(10)	$^4D'$	2739.6	(10)			
	^6P	2343.5	(7)	^4P	2562.5	(9)	$^6D-^4F$	2260.1	(3)
Co$^+$...	$^5F'-^5G'$	2286.2	(100)	$^3F'-^3G'$	......	....	$^3F'-^5G'$	......	....
	^5F	2388.9	(100)	^3F	......	....	....	......	....
	$^5D'$	2378.6	(100)	$^3D'$	......	....	$^5F'-^3G'$	......	....
Ni$^+$...	$^4F'-^4G'$	2216.5	(100 R)	$^2F'-^2G'$	2394.5	(50 R)	$^2F'-^4G'$	2510.9	(30)
	^4F	2165.6	(40 R)	^2F	2296.6	(30 R)			
	$^4D'$	2316.0	(80 R)	$^2D'$	2278.8	(30 R)	$^4F'-^2G'$	2131.3	(3)
Cu$^+$...	$^3D-^3F$	2136.0	(10)	$^1D-^1F$	2189.6	(6)	$^1D-^3F$	2369.9	(6)
	$^3D'$	2043.8	(8)	$^1D'$	2123.0	(5)			
	^3P	2247.0	(10)	^1P	2112.1	(5)	$^3D-^1F$	1999.7	(7)
Zn$^+$...	$^2S-^2P$	2061.9	....	....	......	....	....	......	....

TABLE IV—*Continued*

ELEMENT	$d^{n-1}-d^{n-2}p$			$d^{n-2}p-d^{n-2}\cdot s$			$d^{n-2}p-d^{n-2}\cdot d$		
Ca$^+$...	${}^2D-{}^2P$	8542.2	(10) V	${}^2P-{}^2S$	3736.9	12 V	${}^2P-{}^2D$	3179.3	15 V
Sc$^+$....	${}^3F'-{}^3F$	4374.5	60 III	${}^3F-{}^3D$	3343.3	1 III A	${}^3F-{}^3G$	3065.1	(30)
	${}^3D'$	4314.1	100 III	${}^3D'-{}^3D$	3379.4	(3)	${}^3D'-{}^3F'$	2826.7	(10)
	${}^3P$	......	....	${}^3P-{}^3D$	......	....	${}^3P-{}^3D$	3312.7	(5)
Ti$^+$...	${}^4F'-{}^4G'$	3444.3	15 III	${}^4G'-{}^4F'$	3090.0	(2n)	${}^4G'-{}^4H'$	2828.2	(7) V
	${}^4F$	3322.9	20 III	${}^4F-{}^4F'$	3194.5	(1)	${}^4F-{}^4G$	2945.5	(5)
	${}^4D'$	3168.5	30 III	${}^4D'-{}^4F'$	3351.7	(1)	${}^4D'-{}^4F'$	2752.9	(2)
V$^+$....	${}^5D-{}^5G'$	......	....	${}^5G'-{}^5F'$	......	....	....	......	....
	${}^5F$	2700.9	20 V	${}^5F-{}^5F'$	......	....	....	......	....
	${}^5D'$	2688.0	35 V	${}^5D'-{}^5F'$	......	....	....	......	....
Cr$^+$...	${}^6S-{}^6F$	......	....	${}^6F-{}^6D$	......	....	....	......	....
	${}^6D'$	......	....	${}^6D'-{}^6D$	......	....	....	......	....
	${}^6P$	2055.6	(5*u*)	${}^6P-{}^6D$	......	....	....	......	....
Mn$^+$...	${}^5D-{}^5P$	3442.0	30 V	${}^7P-{}^7S$	2796.2	(2)	${}^7P-{}^7D$	2452.5	(10)
Fe$^+$...	${}^4F'-{}^4F$	2360.0	(5)	${}^6F-{}^6D$	......	....	....	......	....
	${}^4D'$	2348.1	(6)	${}^6D'-{}^6D$	......	....	....	......	....
	${}^4P$	......	....	${}^6P-{}^6D$	......	....	....	......	....
Co$^+$...	${}^3F'-{}^3G'$	......	....	${}^5G'-{}^5F'$	......	....	....	......	....
	${}^3F$	......	....	${}^5F-{}^5F'$	......	....	....	......	....
	${}^3D'$	......	....	${}^5D'-{}^5F'$	......	....	....	......	....
Ni$^+$...	${}^2D-{}^2G'$	......	....	${}^4G'-{}^4F'$	2610.1	(25u)	....	......	....
	${}^2F$	......	....	${}^4F-{}^4F'$	2684.4	(20u)	....	......	....
	${}^2D'$	......	....	${}^4D'-{}^4F'$	2484.3	(10u)	....	......	....
Cu$^+$...	${}^1S-{}^1P$	1358.8	(12)	${}^3F-{}^3D$	2545.0	(10)	....	......	....
				${}^3D'-{}^3D$	2689.5	(7)	....	......	....
				${}^3P-{}^3D$	2403.5	(4)	....	......	....
Zn$^+$...	....	......	....	${}^2P-{}^2S$	2502.0	(7)	${}^2P-{}^2D$	2102.2	....

which are derived from the lowest of the numerous metastable terms in the d^{n-1} or d^{n-2} configurations of the singly or doubly ionized atom have been considered at all. A comparison of the lines resulting from other terms will be practicable in detail only when some of the spectra have been more completely analyzed. Even in the limited part of the spectrum here considered many gaps remain to be filled, and other sets of related lines are not tabulated because our present knowledge of them is fragmentary.

Many relations between the different spectra are now conspicuous. The most general is the tendency of the stronger lines to draw away into the ultra violet as the atomic number increases. These lines arise from transitions from the lower configurations including only 3d and 4s electrons to the middle configurations including a 4p electron, and the shift of the lines toward greater wave-numbers is the physical reality corresponding to the upward trend of the lines representing the middle configurations in Figures 1–3. It is therefore a direct result of the steady increase in the ionization potentials, and, by itself, provides sufficient qualitative evidence for such an increase —which may perhaps prove of value in the case of the rare earths. For the electron jump from 4p to 5s, the additional energy of binding in the neutral atoms is nearly the same for the two states, and the corresponding arc lines remain in the same region of the spectrum. Some of these transitions, for example that from the upper d^{n-2} s p triad to the d^{n-2} s·s terms of the same multiplicity, give lines which lie in the infra red, and are therefore known only for the few elements which have been investigated in this region.

For certain elements in the latter part of the first long period, notably for *As*, the two groups of lines corresponding to those just discussed have withdrawn completely into the ultra violet and the infra red, and the visible spectrum is completely empty.

The transition 4p – 4d gives terms which work slowly toward the violet, while that from (4s)(4p) to $(4p)^2$ gives, as might be expected, a very rapid shift to the shorter wave-lengths.

The transition d^{n-1} s – d^{n-2} s p, in which the electron jump is from 4p to 3d, gives lines shifting very rapidly to the violet, jumping back between *Cr* and *Mn*, and then going to the violet again, while for d^{n-2} s^2 – d^{n-1}p, which involves a double electron jump, the shift is toward the red, broken by a similar discontinuity. These are obvious consequences of the peculiar behavior of the relative levels discussed in the last section.

The individual sequences are noteworthy. Those which correspond to a transition 4s – 4p (d^{n-2} s^2 – d^{n-2}s p or d^{n-1} s – d^{n-1} p) include almost all the strongest lines in all the spectra.

The strongest multiplets in the sequence d^{n-2} s^2 – d^{n-2} s p have been tabulated by Gibbs and White,[1] who have pointed out the remarkably simple relations that exist between similar groups in spectra of several successive degrees of ionization.

---

[1] *Physical Review*, **29**, 661, 1927.

In the first case, the transitions to the upper triad, which has the limits of higher multiplicity, give stronger lines than those to the lower triad, as far as *Mn*. Beyond this the lines of the first sequence get so far into the ultra violet that they are at an observational disadvantage. It would be of much interest to investigate, preferably by absorption observations, whether they actually continue to be the stronger. The transition $d^{n-1}\,s - d^{n-1}\,p$ gives stronger lines than that to the lower triad, except in *Mn* where the lower level involved lies unusually high.

The 3d – 4p jump ($d^{n-1}\,s - d^{n-2}\,s\,p$) gives fainter lines than those previously mentioned. The double electron jump ($d^{n-2}\,s^2 - d^{n-1}\,p$) produces surprisingly strong lines. In both these cases the low term and the triad with which it combines are often out of step, so to speak, and one or more of the transitions involves a change of more than one unit in the apparent azimuthal quantum number L (which is 0 for an S term, 1 for a P, and so on). Many of the transitions for which $\Delta L = 2$ give observable lines, some of them of considerable strength.

The intersystem combinations between terms of the same origin but different multiplicity are of considerable interest. In these lists the multiplets containing the strongest lines have been tabulated. The general increase in the intensity of the intercombinations with increasing atomic number is obvious, and, as is well known, may be attributed to the same cause as the increase in multiplet separations. The sequence $d^{n-2}\,s^2 - d^{n-2}\,s\,p$, beginning with *Ca* λ 6572, contains a remarkable number of the lines which are greatly strengthened in sun-spots. In the sequence $d^{n-1}\,s - d^{n-1}\,p$ the intercombinations are remarkably strong, culminating in the great iron line λ 4383.

The *raies ultimes* and resonance lines of these elements, as given by Laporte and Meggers,[1] are shown in Table V.

For the spark spectra the *raies ultimes* and resonance lines are identical, and arise in all instances from the transition $d^{n-2}\cdot s - d^{n-2}\cdot p$. In the arc spectra the resonance lines are intersystem combinations of origin $d^{n-2}\,s^2 - d^{n-2}\,s\,p$, and are of considerably longer wave-length than the *raies ultimes*, except for *K* and *Cr*, where they are identical with the latter and come from $d^{n-1}s-d^{n-1}p$. The *raies ultimes* come from $d^{n-2}s^2-d^{n-2}sp$ in most of the other spectra. The fact that they shift from the upper to the lower triad with increasing atomic number may be largely or entirely due to observational preference for lines in the near, rather than the far, ultra violet. The persistence of the $^4F'-^4G'$ group as well as the $^2D-^2F$ in *Sc* is an example of the advantage of high *L* values discussed by Meggers.[1] The most remarkable case is *Ti*, in which the *raie ultime* involves a double electron jump. There is here no doubt about the correctness of the assignment of the electron configuration, for the intensities of the combinations are decisive. It is possible, however, that the $^3F'-^3G'$ line at λ 3371.4 may be actually as sensitive. The matter deserves further study.

---

[1] *Journal of the Optical Society of America*, **11**, 461, 1925, with unpublished corrections by Meggers. The resonance lines for *Co* and *Ni* are added from later work.

TABLE V

ELEMENT	RAIES ULTIMES				RESONANCE LINES	
	Arc		Spark		Arc	
	λ	Origin	λ	Origin	λ	Origin
K	7664	2			7664	2
Ca	4226	1*a*	3933	4	6572	1*c*
Sc	3911	1*a*	3613	4	6413	1*c*
Ti	3653	3	3349	4	6295	1*c*
V	3185	1*a*	3093	4	5632	1*c*
Cr	4254	2	2835	4	4254	2
Mn	4030	1*b*	2576	4	5394	1*c*
Fe	3719	1*b*	2382	4	5166	1*c*
Co	3453	2	2388	4	4134	1*c*
Ni	3414	2	2416	4	3624	1*c*

Under "Origin" 1*a* denotes $d^{n-2}s^2-d^{n-2}sp$ (high triad)
1*b* denotes $d^{n-2}s^2-d^{n-2}sp$ (low triad)
1*c* denotes $d^{n-2}s^2-d^{n-2}sp$ (intersystem)
2 denotes $d^{n-1}s-d^{n-1}p$
3 denotes $d^{n-2}s^2-d^{n-1}p$
4 denotes $d^{n-2}s-d^{n-2}p$

The transition $d^{n-2}sp-d^{n-2}s\cdot s$ (4p–5s) gives in the higher multiplicity a series of noteworthy lines, including some of the most conspicuous in the visible spectrum. They are usually high-temperature lines of class III, as might be expected from their relatively high level of origin. The same transition, in the lower multiplicity, produces fainter lines, by no means conspicuous among the others, but important as being those which are primarily concerned in the determination of the ionization potential. The similar transition $d^{n-1}p-d^{n-1}\cdot s$ gives lines in the deep red or infra red, which are also of importance in finding the ionization potential. The 4p−4d jump ($d^{n-2}sp-d^{n-2}s\cdot d$) gives strong multiplets, which are doubtless present in the spectra in which they have not yet been detected. Numerous iron lines, some of them of intensity as high as 25, occur in the region from λ 3300 to λ 3800, which arise from combinations between the $^7P^7D'^7F$ triad and a set of levels, not yet assorted into terms, which evidently belong to the pentad which is to be anticipated. The transition $d^{n-2}sp-d^{n-2}p^2$, which gives the well-known triplet PP′ group in calcium near λ 4300, is also presumably represented in all the spectra by lines identifiable upon close analysis.

---

[1] *Zeitschrift für Physik*, **39**, 122, 1926.

In the spark spectra, the lines shift toward the violet in all the sequences. For *Mn* and the following elements the strongest lines, belonging to the sequence $d^{n-2}s-d^{n-2}p$, pass into the region inaccessible to the astrophysicist, though all can readily be reached in the laboratory. The sequence $d^{n-1}-d^{n-2}p$ has a discontinuity in *Mn* similar to those already described. The high-excitation lines $d^{n-2}p-d^{n-2}\cdot s$ and $d^{n-2}p-d^{n-2}\cdot d$ are, in the spark spectra, of nearly the same wave-lengths as the easily excited lines $d^{n-2}s-d^{n-2}p$. Practically all the enhanced lines of these elements (except *Ca* and *Sc*) which are ordinarily observed in the stars arise from transitions between terms not given in Tables II and IV. These terms arise from the same configurations—$d^{n-2}s$ and d^{n-1}, but are metastable and lie at higher levels than those listed, so that the energy differences between them and the lower terms of origin $d^{n-1}p$ are small enough to put the lines in the observable region. Toward the end of the sequence, beyond *Fe*, even these lines shift, for the most part, out of reach, and the spark spectra are of little astrophysical importance.

7. THE MUTUAL RELATIONS OF THE DIFFERENT SPECTRA

In conclusion, reference may be made to a curious dual resemblance between parts of any given arc spectrum in the iron group and parts of two others. For example, it has long been familiar that a set of doublet series occurs in copper, very similar to those in potassium, and that series of singlets and triplets appear in zinc, closely resembling similar series in calcium. But in neither case does the likeness extend to the whole spectrum. Copper, for example, possesses another extensive system of doublets, with lowest term ^2D, and quartets, with the lowest terms ^4P, $^4D'$, ^4F. There is nothing at all like these in the potassium spectrum, but they may be very closely matched in that of scandium. Similarly, the calcium spectrum contains low ^3D and ^1D terms not found in zinc, and these combine with higher triads of PD′F terms, giving the system of "displaced" series, with the ^2D term of *Ca* II for limit. These terms can be matched with similar terms in nickel.

The reason for this is at once apparent on consulting the tables. The configurations d^x and d^{10-x} give exactly the same spectral terms —the main difference being that when the exponent is greater than 5 the terms are inverted and have much wider separations. It follows that in any spectrum the configuration $d^{n-2}s^2$, $d^{n-2}s\,p$, etc., may be closely matched by configurations $d^{n'-2}s^2$, etc., in another spectrum, if $n-2+n'-2=10$ or $n'=14-n$. Similarly the configurations $d^{n-1}s$, etc., may be matched if $n'=12-n$. This relation may be illustrated by writing the symbols for the elements as follows:

K	*Ca*	*Sc*	*Ti*	*V*	*Cr*	*Mn*
Zn	*Cu*	*Ni*	*Co*	*Fe*	*Mn*	*Cr*

The spectrum of any element in either row is related in structure to those of the elements in the other row and one step to the right or the left. A large portion of any one spectrum may be matched, line for line, with a similar portion of one of the related spectra, and another portion with a portion of the other. This correspondence extends beyond the terms and lines which have been listed in the tables to all the others which arise from the electronic configurations under consideration. Since, however, the terms are "regular" and of small separations for the first row, and inverted and of wide separation in the second, the spectra, even if reduced to the portions of essentially similar structure, would be somewhat dissimilar in appearance. At the end of the list, however, *Cu* and *Zn* show a "regular" multiplet separation, and the likeness to *K* and *Ca* is very conspicuous.

Two portions of spectra, consisting of septets, quintets, etc., in *Cr*, and octets, sextets, etc., in *Mn*, and including the strongest lines of each spectrum, correspond to themselves in the scheme and are unique. In these, too, series are conspicuous, as they are in *K*, *Ca*, *Cu*, and *Zn*. The reason for this is simple. These portions of the respective spectra, and these only, have for limits S terms of the spark spectrum. Under these conditions the triads and pentads of the excited states are reduced to isolated P and D terms, and the energy which would otherwise go into many multiplets is concentrated into one. Moreover, the various components of the terms go to a single limit, and the higher series members have narrow separations, which again makes the multiplets more conspicuous.

Series have been recognized, however, in all the other spectra, and, except in *V*, in both the principal parts of the spectrum.

Most of the spectra have many lines which do not belong to either of the portions already discussed—for example, those corresponding to the transitions $d^{n-2}s^2-d^{n-1}p$ and $d^{n-1}s-d^{n-2}sp$. These are the groups for which the progression in wave-length is broken by a discontinuity. They have no analogues in the spectra of any other element in the group, so that each spectrum, taken as a whole, has a definite individuality.

Among the spark spectra, the relations are somewhat simpler. The transitions $d^{n-2}s-d^{n-2}p$, etc., which give the strongest lines, produce portions of the spectrum which may be simply matched in pairs:

Ca^+ Sc^+ Ti^+ V^+ Cr^+ Mn^+
Zn^+ Cu^+ Ni^+ Co^+ Fe^+ Mn^+

each spectrum resembling that which is tabulated below or above it. The other portions of the spectra arising from the transitions $d^{n-1}-d^{n-2}p$ have no analogues.

The question of series and ionization potentials in these spectra, which is naturally associated with the matters here discussed, is taken up in the following paper.[1]

Carnegie Institution of Washington
Mount Wilson Observatory
June 15, 1927

---

[1] *Mt. Wilson Contr.*, No. 342; *Astrophysical Journal*, **66**, 233, 1927.

Contributions from the Mount Wilson Observatory, No. 342
Reprinted from the *Astrophysical Journal*, Vol. LXVI, pp. 233–255, 1927
Printed in the U.S.A.

SERIES AND IONIZATION POTENTIALS OF THE ELEMENTS OF THE IRON GROUP

By HENRY NORRIS RUSSELL[1]

ABSTRACT

Identification of series and calculation of ionization potentials.—The recognition of the electronic configurations corresponding to the terms of complex spectra has made it possible to *identify series* (usually of two members only) in all the arc spectra from K to Zn and in the majority of the spark spectra from Ca^+ to Zn^+. A Rydberg formula, applied to the first two terms, gives *approximate series limits*. These have been corrected by an empirical formula, which, in the fifteen cases where the test can be made, gives results differing from those of the more exact Ritz formula by an average of ±0.5 per cent. Values of the *first ionization potential* for all these elements, and of the *second* for all but V, Cr, Fe, and Co, have thus been obtained. Approximate values for the latter have been derived with the aid of Moseley's law.

For most of these elements, there are *four* important *modes of ionization* of the neutral atom, and *three* for the *second ionization*, corresponding to changes between various metastable states (and still others are possible). Tables of the values of these important ionization potentials are given.

The principal ionization potentials which measure the energy required for the change from the lowest energy state of the atom in one degree of ionization to the lowest energy state in the next are K, 4.32 volts; Ca, 6.09; Sc, 6.57; Ti, 6.80; V, 6.76; Cr, 6.74; Mn, 7.40; Fe, 7.83; Co, 7.81; Ni, 7.64; Cu, 7.69; Zn, 9.36; and for the *second* ionization, Ca^+, 11.82; Sc^+, 12.80; Ti^+, 13.60; V^+, (14.7); Cr^+, (16.6); Mn^+, 15.70; Fe^+, (16.5); Co^+, (17.2); Ni^+, 18.2; Cu^+, 20.34; Zn^+, 17.89.

These values should be accurate to 0.1 volt or better, except those in parentheses, which have been derived by Moseley's law, and may be in error by as much as 0.3 volt.

New terms in certain spectra.—New high terms, arising from configurations involving a 5s electron, have been identified in the spectra of V, Mn, Co, and Mn^+. *Tables* of these terms and of the multiplets involving them are given. The ionization potentials of V and Mn^+ have thus been determined for the first time.

I. INTRODUCTION

As appears from the data collected in the preceding communication,[2] series have now been detected in the arc spectra of all the elements of the iron group, and in the spark spectra of the majority. Most of the series consist of only two members, but even so they should suffice to give fairly good values of the ionization potential. As a number of these series have been detected in the examination of the spectra made for the purpose of the preceding paper, it may be appropriate to give details concerning them and to collect the resulting values for the ionization potentials.

---

[1] Research associate of the Mount Wilson Observatory, Carnegie Institution of Washington.

[2] *Mt. Wilson Contr.*, No. 341; *Astrophysical Journal*, **66**, 184, 1927.

Most of the atoms of this group can exist in many metastable states, and there are usually a great many ionization potentials, corresponding to transitions from each metastable state of the neutral atom, for example, to those states of the ionized atoms which would be obtained by removing one electron. We shall consider here, however, only those which involve the normal state of the atom or ion, or the lowest metastable states. These may be represented schematically as follows:

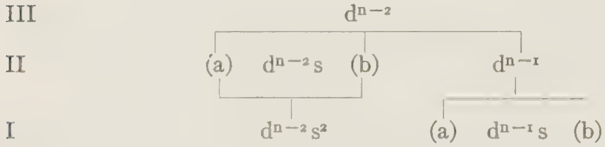

For an atom with n electrons outside the "argon-shell" and atomic number n+18, the normal state, when doubly ionized, corresponds to the configuration d^{n-2}, in which all the electrons are in 3d orbits. Only the lowest of the numerous terms arising from this configuration concerns us here. By the addition of a 4s electron we obtain the configuration $d^{n-2}s$ in the singly ionized atom, from which the lowest terms are two of the same name as the "parent-terms," but of multiplicities greater and less by a unit, here denoted by (a) and (b). On account of Pauli's restriction, addition of a second 4s electron gives rise to but a single low term for the configuration $d^{n-2}s^2$. Addition of a 3d electron to the original configuration gives d^{n-1}, for which the lowest term is usually of a different name, and is of multiplicity higher by a unit, unless n exceeds 6, when it is lower by a unit. Adding a 4s electron to this gives two terms of the same name, $d^{n-1}s$ (a) and (b). Details of the resulting states for all the elements of the iron group with term values are given in Tables I and II of the preceding paper.

As an example, we may indicate the terms in *Mn:*

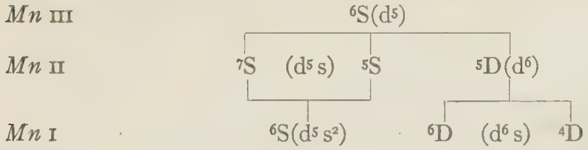

There are usually four principal processes of ionization for the neutral atom, represented by the vertical lines in the diagram. (Two others which take the $d^{n-1}s$ terms into $d^{n-2}s$ by removal of a d electron need not be considered here). In each of the four processes the 4s electron is removed by stages, 5s, 6s, and gives rise to a series of terms with one of the principal spark terms as limit, and one of the principal arc terms as a first member. The second members of some of these series are known in all the spectra, and all four of them have been identified in *Mn* (see below) and in *Fe*, where they were detected by Laporte[1]—the first instance of the kind.

For the singly ionized atom there are three principal types of ionization: two involving the removal of an s electron from $d^{n-2}s$, and the other, a d electron from d^{n-1}. Second members of some of these series are known in all the spark spectra except those of *V*, *Cr*, *Fe*, and *Co*, and those of all three series in *Sc* II and *Ti* II. The series involving changes in a d electron, is, however, not Ritzian, so that calculations of the ionization potential must depend on the other two.

For atoms near the beginning and end of the group the number of possible states and series is smaller, as is shown in detail in the table already mentioned.

2. NEW TERMS IN *V*, *Mn*, *Co*, Mn^+

For most of the data on which the series here discussed are based, reference may be made to the sources mentioned in the preceding paper. Certain terms, however, which were found by the writer in the course of preparation of the tables, may be given here, with the resulting multiplets. The notation needs no comment, except to say that the term values are always measured from the lowest level in the spectrum. The suggested new term in *Ca* is a mere fragment, and the only reason for believing in its reality is that it falls in just

---

[1] *Proceedings of the National Academy of Sciences*, 12, 496, 1926.

TABLE I

New Multiplets in Arc Spectra

Ca I

		x^3D_3 46704.0			
a^3F_4....	35897.2	9250.8 (2) 10807.3 (06.8)	...	...	...
$a^3D'_3$....	38259.5	11840.0 (5) 8443.6 (44.5)	...	...	...

V I

		$b^4F'_5$ 39596.94	$b^4F'_4$ 39391.75	$b^4F'_3$ 39241.25	$b^4F'_2$ 39126.92
$a^4G'_6$....	22313.92	5784.42(5 III) 17283.03 (3.02)	...	...	...
$a^4G'_5$....	22121.09	...	5788.58(3 III) 17270.62 (0.66)	...	...
$a^4G'_4$....	21963.40	...	...	5786.21(7 III) 17277.69 (7.85)	...
$a^4G'_3$....	21841.40	...	...	...	5783.59(2 III) 17285.52 (5.52)
$b^4D'_4$....	21032.44	5385.13(3 III 18564.50 (4.50)	...	...	...
$b^4D'_3$....	20828.49	...	... (18563.26) ...	...	...
$b^4D'_2$....	20687.80	...	...	5388.30(1 III) 18553.58 (3.45)	...
$b^4D'_1$....	20606.46	...	...	...	5397.93(1 IV) 18520.48 (0.46)
b^4F_5....	23519.84	6218.31(3 IV) 16077.10 (7.10)	6298.68(tr IV A) 15871.96 (1.91)	...	...
b^4F_4....	23353.06	...	6233.20 (12 I A)* 16038.95 (8.69)	...	...
b^4F_3....	23210.52	...	...	6236.28(1 IV) 16030.75 (0.73)	...
b^4F_2....	23088.04	...	...	...	6233.20(12 I A)* 16038.95 8.88

* Masks the expected line.

TABLE I—*Continued*

Mn I

		c^6D_5 56189.46	c^6D_4 56356.11	c^6D_3 56490.49	c^6D_2 56616.57
$a^6D'_5$....	41789.44	6942.57(5) 14399.92 (0.02)	6863.08(2) 14566.70 (6.67)	....	....
$a^6D'_4$....	41932.64	7012.22(2) 14256.88 (6.82)	6931.27(3) 14423.40 (3.47)	6867.18(2) 14558.00 (7.85)	....
$a^6D'_3$....	42053.70	....	6989.85(4) 14302.52 (2.41)	....	....
a^6F_6....	43314.23	7764.75(5) 12875.05 (5.23)	....	....	....
a^6F_5....	43428.56	7834.32(2) 12760.85 (0.90)	7733.23(4n) 12927.64 (7.55)	....	....
a^6F_4....	43524.09	....	7790.91(2) 12831.96 (2.02)	7710.21(5) 12966.23 (6.40)	....
a^6F_3....	43595.47	....	....	7752.78(3) 12895.05 (5.02)	7677.80(1) 13020.98 (1.10)
a^6F_2....	43644.46	....	....	....	7706.64(2) 12972.27 (2.11)
c^6P_4....	44993.89	8929.66(1) 11195.56 (5.57)	....	....	....

Co I†

		$c^4F'_5$ 44782.00	$c^4F'_4$ 45105.44	$c^4F'_3$ 45876.44	$c^4F'_2$ 46375.00
$a^4D'_4$....	29294.49	6455.03(10 III) 15487.53 (7.51)	6322.94(2) 15811.06 (0.95)	....	....
$a^4D'_3$....	29948.74	....	6595.91(9 V) 15156.73 (6.70)	6276.62(5)‡ 15927.75 (7.70)	....
$a^4D'_2$....	30443.56	....	....	6477.93(9 V) 15432.77 (2.88)	6275.16(4) 15931.45 (1.44)
$a^4D'_1$....	30742.55	....	....	....	6395.19(7 V) 15632.44 (2.45)

---

† The intensities are those tabulated by Meggers; King's temperature classification is added when available.

‡ Blend.

TABLE I—*Continued*

Co I—*Continued*

		$c^4F'_5$ 44782.00	$c^4F'_4$ 45105.44	$c^4F'_3$ 45876.44	$c^4F'_2$ 46375.00
a^4F_5....	28345.80	6082.49(10 III) 16436.10 (6.20)	5965.02(3) 16759.77 (9.64)		
a^4F_4....	28777.19	6246.42(2) 16004.75 (4.81)	6122.68(10 IV?) 16328.20 (8.25)	5846.57(3 V) 17099.31 (9.25)	
a^4F_3....	29216.32		6291.89(3) 15889.09 (9.12)	6000.70(8 I) 16660.11 (0.12)	5826.30(4) 17158.81 (8.68)
a^4F_2....	29563.05			6128.26(3) 16313.34 (3.39)	5946.51(7 III) 16811.94 (1.95)
$a^4G'_6$....	28845.16	6273.06(7 III?)§ 15936.79 (6.84)			
$a^4G'_5$....	29269.68	6444.75(6 V)‖ 15512.22 (2.32)	6313.07(6) 15835.79 (5.76)		
$a^4G'_4$....	29735.09	6643.78(3) 15047.62 (6.91)	6504.25(4) 15370.32 (0.35)	6193.58(6) 16141.29 (1.35)	
$a^4G'_3$....	30102.88		6663.68(2) 15002.59 (2.56)	6337.98(3) 15773.54 (3.56)	6143.78(4) 16272.13 (2.12)
$b^4D'_4$....	32027.42	7838.18(8 V) 12754.57 (4.58)			
$b^4D'_3$....	32654.45		8029 29(7) 12450.98 (0.99)	7561.08(4) 13221.99 (1.99)	
$b^4D'_2$....	33150.60			7855.88(7) 12725.82 (5.84)	7559.68(3) 13224.44 (4.40)
$b^4D'_1$....	33449.04				7734.25(6) 12925.95 (5.96)
b^4F_5....	32841.91	8372.82(10) 11940.14 (0.09)	8152.03(6) 12263.52 (3.53)		
b^4F_4....	33466.78	8835.22(8) 11315.23 (5.22)	8589.70(3) 11638.66 (8.66)	8056.03(8 V) 12409.65 (9.66)	
b^4F_3....	33945.81		8958.46(6) 11159.57 (9.63)	8379.54(3) 11930.56 (0.63)	8043.33(8 V) 12429.25 (9.19)
b^4F_2....	34196.11			8559.04(2) 11680.36 (0.33)	8208.67(8) 12178.91 (8.89)

§ Blend.

‖ Masks the expected line.

TABLE I—*Continued*

Co I—*Continued*

		$c^4F'_5$ 44782.00	$c^4F'_4$ 45105.44	$c^4F'_3$ 45876.44	$c^4F'_2$ 46375.00
$b^4G'_6$....	32430.56	8094.03(10 III) 12351.39 (1.44)	...	...	...
$b^4G'_5$....	32464.66	8116.43(7) 12317.31 (7.34)	7908.75(10 III?) 12640.25 (0.78)	...	...
$b^4G'_4$....	33173.30	...	8378.37(7) 11932.23 (2.14)	7869.92(6 V) 12703.12 (3.14)	...
$b^4G'_3$....	33674.32	...	...	8193.05(8) 12202.12 (2.12)	7871.43(6 V) 12700.68 (0.68)
$a^2D'_3$....	33462.80	...	8586.71(3) 11642.72 (2.64)	8053.50(1) 12413.55 (3.64)	...
$a^2D'_2$....	34352.38	...	...	8675.02(1) 11524.19 (4.06)	8315.32(2) 12022.70 (2.62)
a^2F_4....	31871.09	7743.27(5) 12910.89 (0.91)	7554.04(8 IV) 13234.31 (4.35)	...	...
a^2F_3....	32781.64	...	8112.13(1) 12323.84 (3.80)	7634.56(5) 13094.73 (4.80)	...
$a^2G'_5$....	31699.61	...	7457.43(8 V) 13405.77 (5.83)	...	...
$a^2G'_4$....	32732.99	8296.85(5) 12049.47 (9.01)	8080.23(5) 12372.49 (2.45)	7606.30(2 V)§ 13143.39 (3.45)	...
$b^2G'_5$....	33439.64	...	8569.72(2) 11665.79 (5.80)	...	...
$b^2G'_4$....	34133.50	...	...	8513.48(1) 11742.86 (2.94)	...

§ Blend.

TABLE I—*Continued*

Co I—*Continued*

		b^2F_4' 45924.82	b^2F_3' 46745.83
a^2D_3'..	....	8022.15(7) 12462.07 (2.02)	7526.32(1) 13283.06 (3.03)
a^2D_2'..	....	....	8066.50(7) 12293.55 (3.45)
a^2F_4..	....	7113.74(9 V) 14053.43 (3.73)	6720.97(2) 14874.71 (4.74)
a^2F_3..	....	7606.30(2 V)§ 13143.39 (3.18)	7159.23(8 V) 13964.14 (4.19)
a^2G_5'..	....	7027.86(8 V) 14225.17 (5.21)	....
a^2G_4'..	....	7578.34(1) 13191.88 (1.83)	7134.37(8 V) 14012.81 (2.84)
b^2F_4..	35450.51	9544.52(2) 10474.35 (4.31)	8850.74(10) 11295.39 (5.32)
b^2F_3..	36329.79	(9595.03)	9597.89(2) 10416.10 (6.04)
b^2G_5'..	....	8007.34(10 V) 12485.11 (5.18)	....
b^2G_4'..	....	8478.45(2) 11791.38 (1.32)	7926.59(8 V) 12612.30 (2.33)
a^4D_4'..	....	6011.43(3) 16630.38 (0.33)	....
a^4D_3'..	....	6257.56(10 III) 15976.28 (6.08)	5951.73(2) 16797.20 (7.09)
a^4D_2'..	....	....	6132.44(3) 16302.22 (2.27)
a^4F_5..	....	5686.96(3) 17579.22 (9.02)	....
a^4F_4..	....	5830.05(7 V) 17147.77 (7.63)	....
a^4F_3..	....	5983.36(3) 16708.39 (8.50)	5703.03(2) 17529.69 (9.51)
a^4F_2..	....	....	5818.09(2) 17183.02 (2.78)
a^4G_5'..	....	6002.48(3) 16655.18 (5.14)	....
a^4G_4'..	....	6175.08(2) 16189.65 (9.73)	....
a^4G_3'..	....	6318.55(4u) 15822.05 (1.94)	....
b^4D_4'..	....	7193.63(8 V) 13897.37 (7.40)	....
b^4D_3'..	....	7533.52(5 IV) 13270.35 (0.37)	7094.64(4 IV) 14091.27 (1.38)
b^4D_2'..	....	....	7353.48(2) 13595.26 (5.23)
b^4F_5..	....	7641.43(1) 13082.97 (2.91)	....
b^4F_4..	....	8024.75(4) 12458.03 (8.04)	....
b^4F_3..	....	8345.59(2) 11979.10 (9.01)	7810.39(1) 12799.95 (0.02)
b^4F_2..	....	....	7966.12(2) 12549.72 (9.72)
b^4G_4'..	....	7840.05(7) 12751.52 (1.52)	....
b^4G_3'..	....	8160.68(2) 12250.52 (0.50)	7648.19(4) 13071.39 (1.51)

§ Blend.

the right position, the limit of the series being known from other data. Further observations in the infra-red are desirable to confirm or disprove it.

The new multiplets in *V* are weak, in *Mn* fairly strong, though the intensities fall off so rapidly that the component of lowest inner-quantum number cannot be identified. Those in *Co* are remarkably strong, and account for almost all the heavy lines in the deep red. In all these cases the position of the high term was approximately predicted by means of the regularities discussed in the preceding paper, and the multiplets were then very easily found.

The resulting series in *V* I converge to the $^3F'$ term of the spark spectrum, thus giving the ionization potential which was previously unknown. Those in *Co* I also converge to a $^3F'$ term, which must be the lowest in the spark spectrum, which is very incompletely analyzed. The series in *Mn* I converges to the ^5D term in *Mn* II, as does also one involving a ^4D term, previously known. This gives a good approximation to the relative levels of the ^7S and ^5D terms in *Mn* II, and made it rather easy to find the intersystem combinations which fix these levels exactly.[1] Further search revealed an "inverted" triplet which locates a high ^7S term in series with the low one. These lines are given by Exner and Haschek, but have been remeasured on a plate kindly taken by Mr. King. They appear in the spark only, and are unsymmetrical and diffuse toward the red, differing widely in this respect from any other lines in the neighborhood—all of which characteristics are just what might be expected of lines arising from the transition to which they have been attributed. The frequency differences are also in very good agreement.

All of the lines of *Mn* II which thus far have been classified are given in Table II. This spectrum includes many other strong lines which probably arise from metastable terms not yet identified. The triplet of the quintet system, corresponding to that found in the septets, was sought for in vain and is probably faint.

3. THE SERIES LIMITS

By applying a simple Rydberg formula to the first two terms of any series, an approximate value of the limit and the ionization

---

[1] These combinations have been found independently by Black and Duffendack. *Science*, 66, 402, 1927.

TABLE II

Mn II*

		SEPTETS					QUINTETS				
		a^7P_4 38806.52	*263.58*	a^7P_3 38542.94	*176.91*	a^7P_2 38366.03	a^5P_3 43370.40	*114.08*	a^5P_2 43484.48	*72.45*	a^5P_1 43556.93
a^7S_3......	0.00	2576.12(30R) 38806.52 (6.52)		2593.73(15R) 38542.94 (2.94)		2605.70(10R) 38366.03 (6.03)	2305.02(2) 43370.2 (0.4)		2298.97(2) 43484.4 (4.5)		......
a^5S_2.....	9472.86	......		3438.99(3 V) 29070.00 (0.08)		3460.04(2) 28893.16 (3.17)	2949.21(30 IV) 33897.54 (7.54)		2939.32(20 V) 34011.62 (1.62)		2933.06(15 V) 34084.07 (4.07)
a^5D_4.....	14324.47 *269.29*	......		......		......	3442.00(30 V) 29045.93 (5.93)		......		......
a^5D_3.....	14593.76 *187.32*	......		......		......	3474.05(15 V) 28776.65 (6.64)		3460.33(20 V) 28890.71 (0.72)		......
a^5D_2.....	14781.08 *120.00*	......		......		......	3496.82(3 V) 28589.30 (9.32)		3482.92(12 V) 28703.37 (3.40)		3474.14(15 V) 28775.90 (5.85)
a^5D_1.....	14901.08 *58.59*	......		......		......	......		3497.54(6 V) 28583.37 (3.40)		3488.62(10 V) 28655.89 (5.85)
a^5D_0.....	14959.67	......		......		......	......		......		3495.84(7 V) 28597.26 (7.26)

* Intensities from Exner and Haschek (spark); temperature classes from King.

TABLE II—*Continued*

		SEPTETS					QUINTETS				
		a^7P_4 38806.52	*263.58*	a^7P_3 38542.94	*176.91*	a^7P_2 38366.03	a^5P_3 43370.40	*114.08*	a^5P_2 43484.48	*72.45*	a^5P_1 43556.93
a^7D_5.....	79568.4 *10.2*	2452.63(10) 40761.9 (1.9)									
a^7D_4.....	79558.2 *9.0*	2453.17(2) 40751.3 (1.7)		2437.45(5) 41015.7 (5.3)			2762.57(1) 36187.5 (7.8)				
a^7D_3.....	79549.2 *5.4*	2453.65(1) 40743.0 (2.7)		2437.92(3) 41006.1 (6.3)		2427.43(3) 41183.3 (3.2)	2763.19(1) 36179.5 (8.8)				
a^7D_2.....	79543.8 *3.7*			2438.22(3) 41001.1 (0.9)		2427.77(4) 41177.5 (7.8)					
a^7D_1.....	79540.1					2427.97(4) 41174.1 (4.1)					
b^7S_3.....	74558.69	2796.21(3hr) 35752.13 (2.17)		2775.75(2hr) 36015.70 (5.75)		2762.17(1hr) 36192.75 (2.66)					

potential can be obtained. Experience shows that this value is usually nearly correct when the series is produced by the removal of an s electron, since in such series the Ritz correction is almost always small. Series involving changes in a d electron are usually very regular, except for the lowest term, when this involves the binding of the electron as part of an incomplete shell. In this case the energy of binding is considerably increased, and the application of a simple Rydberg formula puts the limit a great deal too high.

Series involving a p electron, when d orbits are also present in the atom, are usually quite incapable of representation by a simple formula,[1] and the application of one to the first two terms would give wholly wild results.

In the iron group the majority of the series which can be identified are fortunately of the most favorable type for discussion with limited data. By applying the Rydberg formula to the data given in Tables I and II of the previous paper the results listed in Table III were obtained. For brevity the four types of series which may in general appear in the spectrum are here denoted as follows:

A	$d^{n-2}s^2$	to limit $d^{n-2}s$ (a)	(higher multiplicity)
B	$d^{n-2}s^2$	to limit $d^{n-2}s$ (b)	(lower multiplicity)
C	$d^{n-1}s$ (a)	to limit d^{n-1}	
D	$d^{n-1}s$ (b)	to limit d^{n-1}	

The series C and D should have the same limit, but the limits of A and B differ from this and from each other. When the differences between these limits (which are well-known terms of the spark spectrum) are found from analysis of that spectrum, a direct check upon the relative accuracy of the approximation involved in using the Rydberg formula is possible. Its absolute accuracy can be tested only when at least one series is known in which there are three or more terms, and when a Ritz formula can be employed. The other limits may then be found from that of this series by adding the differences of level which have been determined in the spark spectrum.

The first column of Table III gives the element and the second the designation of the series, as just explained. The third and fourth columns give the term values, from Table I of the preceding paper, for the configurations including a 4s and a 5s electron, and the next the limit (which is the energy level of the corresponding state of the spark spectrum referred to the standard energy level in the arc spectrum) as derived by a Rydberg formula. The sixth column gives the relative levels of these limits as determined from the analysis of the spark spectrum, and the next, the absolute levels determined by a Ritz formula when three or more members of some series are known.

---

[1] Cf. Fowler, *Report on Line Spectra* (London, 1922), p. 42.

The third member of the A series in *Fe* I suggested by Gieseler and Grotrian[1] has not been included. It is determined by a single multiplet of faint lines, a combination from the ^5P term. Most of the energy levels involved are clearly real, but they do not combine with the related $^5D'$ or ^5F terms, and it is therefore very improbable that they represent the $d^{n-2}s$ (6s) configuration. The term separations are also much smaller than those of the other two series members, or the limiting F term a^6D in *Fe* II. The doubts regarding this term expressed by Laporte[2] appear to be fully justified.

In the spark spectra we have two types of series:

C $d^{n-1}s$ (a) to limit d^{n-1}
D $d^{n-1}s$ (b) to limit d^{n-1}

The corresponding table (Table IV) is simple, since there is but a single limit.

The series in Tables III and IV refer in all cases to the leading component (of greatest inner-quantum number), and the limits give the leading components of the spark terms. The subtraction of the quantities given in Table III under the heading "Spark" suffices to reduce these to determinations of the relative position of the levels used as origins of measurement in the two cases. A similar correction cannot yet be made for the spark spectra, as the multiplet separations of the lowest terms in the third spectra are known only for *Sc* III and *Ti* III. This correction is, however, too small to be of practical importance.

The next to the last column of Tables III and IV gives the error in the limit determined from the first two members by a Rydberg formula, expressed as a percentage of the distance from the lowest term to the limit. It is positive, i.e., the first two members indicate too high a limit, for all the series but two, which happen to be about the least reliable of the lot. The rejected term in *Fe* also led to a negative error.

---

[1] *Zeitschrift für Physik*, **25**, 169, 1924.

[2] *Proceedings of the National Academy of Sciences*, **12**, 502, 1926.

TABLE III

SERIES LIMITS IN THE ARC SPECTRA OF THE IRON GROUP

Element	Type	4s	5s	Rydberg	Spark	Ritz	Percentage Error	Comp. Error
K......	C	0	21,026	35,439	0	35,006	+1.2	+1.6
Ca.....	A	0	33,317	51,438	0	49,305	+4.3	2.3
	C	20,371	46,704	62,841	13,711	63,016	−0.7	1.9
Sc.....	A	168	35,746	54,453	178	....	......	2.4
	C	11,677	42,085	59,414	4988	....	......	2.2
Ti.....	A	387	37,825	56,995	393	55,523	+2.7	2.6
	B	387	39,786	59,429	4898	60,028	−1.0	2.7
	C	6843	39,413	57,334	1216	56,346	+2.0	2.3
V......	A	553	39,597	59,154	558	....	......	2.7
Cr.....	A	557	41,074	60,980	0	59,388	2.6	2.7
	C	− 7751	29,145	48,182	−12,498	46,890	2.8	2.5
	D	− 158	30,132	47,428	−12,498	46,890	1.1	2.2
Mn....	A	0	41,404	61,515	0	59,937	2.6	2.7
	B	0	49,415	71,262	9473	69,410	2.7	3.2
	C	17,052	56,190	75,770	14,324	74,261	2.6	2.7
	D	23,297	57,306	75,607	14,324	74,261	2.6	2.4
Fe.....	A	0	44,677	65,523	0	....	......	2.9
	B	0	51,351	73,587	7955	....	......	3.3
	C	6928	47,006	66,808	1873	....	......	2.7
	D	11,976	47,961	66,743	1873	....	......	2.5
Co.....	A	0	47,524	68,979	0	....	......	3.1
	C	3483	44,782	64,371	−?	....	......	2.7
	D	7442	45,925	65,349	−?	....	......	2.6
Ni.....	A	0	50,466	72,526	0	....	......	3.3
	C	205	42,606	62,944	−?	....	......	2.8
	D	3410	44,263	64,247	−?	....	......	2.7
Cu.....	A	0	53,455	74,911	0	73,030	2.6	3.4
	C	−11,202	31,934	52,438	−21,925	51,105	2.2	2.8
Zn.....	A	0	55,788	78,883	0	75,767	+4.1	+3.6

For the rest of the series the percentage error is clearly a function of the length of the series itself. Dividing the terms for the spark spectrum by 4 to make them comparable with the others, and taking means by groups, we find:

Length of series	32,300	50,500	59,000	75,000
Percentage error	+1.5	+2.5	+2.6	+3.1
Number	3	4	6	3

These may be represented by the empirical formula

$$\text{Percentage error} = 4.5 \times 10^{-5} \times (\text{length of series}).$$

TABLE IV

SERIES LIMITS IN THE SPARK SPECTRA OF THE IRON GROUP

Element	Type	4s	5s	Rydberg	Ritz	Percentage Error	Comp. Error
Ca^{+}	C	0	52,167	97,060	95,748	+1.4	+1.1
Sc^{+}	C	178	57,743	105,046	...	...	1.2
	D	2541	58,252	104,745	...	...	1.2
Ti^{+}	C	393	62,594	111,874	...	...	1.3
	D	4898	63,445	111,174	...	...	1.2
Mn^{+}	C	0	74,558	128,715	...	...	1.5
Ni^{+}	C	0	83,404	140,772	...	...	1.6
	D	5156	85,132	141,284	...	...	1.6
Cu^{+}	C	0	86,084	144,388	...	...	1.6
	D	4336	88,435	146,048	...	...	1.6
Zn^{+}	C	0	88,436	147,548	144,890	+1.8	+1.6

The values computed by this formula are given in the last column of the tables. The average difference between the observed and computed errors is ±0.5 per cent (rejecting the two anomalous series already mentioned). It appears probable, therefore, that the application of these computed corrections, in the cases where only the Rydberg formula can be employed, will lead to rather accurate values for the limits. The resulting values are collected in Table V, which gives the distance of the lowest term of each of the series A, B, C, and D from its own proper limit, rounded off by omission of the last two figures, which in this case are quite uncertain.

The values have been adjusted to take account of the known

TABLE V

LIMITS FROM EMPIRICALLY CORRECTED RYDBERG FORMULAE

SERIES	Element	ν	Element	ν	$\sqrt{\nu/R}$		
					Arc	Spark	Diff.
C	*K*	34,800	Ca^+	96,000	0.619	0.936	0.317
A	*Ca*	50,300	Sc^+	....	....	....	....
C	*Ca*	43,700	Sc^+	103,700	.632	.973	.341
D	*Ca*	42,200	Sc^+	101,200	.622	0.961	.339
A	*Sc*	53,200	Ti^+	....	....	....	....
B	*Sc*	55,700	Ti^+	....	....	....	....
C	*Sc*	46,500	Ti^+	110,200	.652	1.003	.351
D	*Sc*	43,200	Ti^+	105,300	.628	0.980	.352
A	*Ti*	55,000	V^+	....	....	....	....
B	*Ti*	59,900	V^+	....	....	....	....
C	*Ti*	49,400	V^+	(116,000)	.672	(1.030)	(.358)
D	*Ti*	44,400	V^+	(109,000)	.637	(0.999)	(.362)
A	*V*	57,000	Cr^+	....	....	....	....
B	*V*	63,500	Cr^+	....	....	....	....
C	*V*	52,300	Cr^+	(122,000)	.692	(1.056)	(.364)
D	*V*	46,000	Cr^+	(114,000)	.649	(1.020)	(.371)
A	*Cr*	59,000	Mn^+	....	....	....	....
B	*Cr*	66,500	Mn^+	....	....	....	....
C	*Cr*	54,300	Mn^+	126,800	.705	1.076	.371
D	*Cr*	46,700	Mn^+	117,300	.654	1.035	.381
A	*Mn*	59,800	Fe^+	....	....	....	....
B	*Mn*	69,300	Fe^+	....	....	....	....
C	*Mn*	57,200	Fe^+	(133,000)	.723	(1.100)	(.377)
D	*Mn*	50,900	Fe^+	(124,000)	.682	(1.066)	(.384)
A	*Fe*	63,400	Co^+	....	....	....	....
B	*Fe*	71,400	Co^+	....	....	....	....
C	*Fe*	58,300	Co^+	(136,000)	.730	(1.112)	(.382)
D	*Fe*	53,300	Co^+	(129,000)	.698	(1.084)	(.386)
A	*Co*	66,800	Ni^+	....	....	....	....
B	*Co*	?	Ni^+	....	....	....	....
C	*Co*	59,800	Ni^+	138,800	.739	1.126	.387
D	*Co*	55,900	Ni^+	133,600	.714	1.103	.389
A	*Ni*	70,100	Cu^+	....	....	....	....
B	*Ni*	....	Cu^+	....	....	....	....
C	*Ni*	61,700	Cu^+	142,800	.750	1.141	.391
D	*Ni*	58,510	Cu^+	138,500	.732	1.124	.392
A	*Cu*	72,500	Zn^+	....	....	....	....
B	*Cu*	76,800	Zn^+	....	....	....	....
C	*Cu*	61,900	Zn^+	145,200	0.751	1.150	0.399
A	*Zn*	76,100	Ga^+	....	....	....	....

differences in level of the arc and spark terms. For example, for *Fe* I, subtracting from the values in the fifth column of Table III, which give the levels of the limits compared with the standard level in the arc as determined by the Rydberg formula, the corrections obtained by multiplying the distance of each term from its limit by the percentages given in the last column, we find for A, B, C, and D, to the nearest hundred, 63,600, 71,200, 65,200, 65,400. Subtracting from these again the spark levels given in the sixth column, we find 63,600, 63,200, 63,300, 63,500, which are four independent determinations of the difference between the lowest levels in the arc and spark. The mean, 63,400, is entered in Table V under "A" (where it belongs). The differences B, C, and D are then found by adding the level differences in the spark for their respective limits, and subtracting those in the arc. A considerable number of entries can thus be obtained for series in which only the first term and the limit are known.

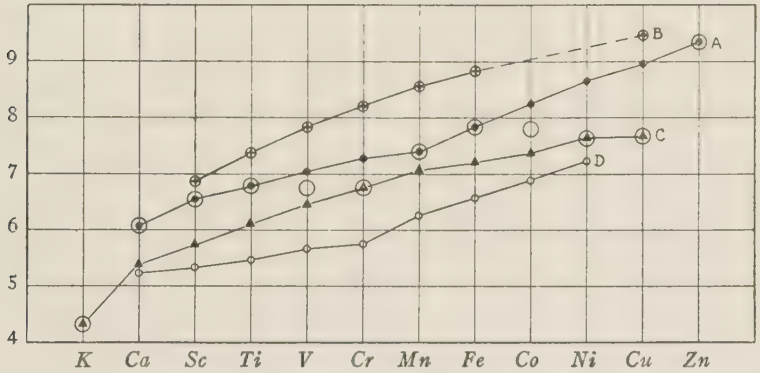

FIG. 1.—Ionization potentials of arc spectra. Large circles denote principal ionization potential.

The resulting limit-values, which represent the energy of homologous ionization processes in the successive spectra, run very smoothly, increasing steadily with the atomic number, so much so that it would probably be fairly accurate to fill in the missing values for the spark spectra by simple interpolation. It may be preferable, however, to apply Moseley's law. According to this, the differences of the quantities $\sqrt{\nu/R}$, where R is the Rydberg constant and ν the quantity which is given in Table V (i.e., the term value referred to its own limit), should be nearly constant for successive corresponding spectra. The values are given in the latter part of Table V, and run very smoothly, so far as known. When plotted, they show a break in the slope of the curve at the point of maximum multiplicity, *Cr* I and *Mn* II, such as is exhibited in several other cases in Figures 1, 2, and 3 of the preceding paper and Figure 1 here. Interpolating the values of this difference numerically across the gaps and calculating backward to the term values in those spark spectra for which they are unknown, we find the values given in parentheses in Table V. From the general run of the other curves, it seems probable that the error in the estimated differences of $V \nu/R$ does not much exceed 0.01, which would correspond to about 2300 wave-numbers in the estimated term values in the spark.

TABLE VI

IONIZATION POTENTIALS

ELEMENT	NEUTRAL ATOM					IONIZED ATOM			
	A	B	C	D	Principal	C	D	E	Principal
K......	....	....	4.30	....	**4.32**	....	....	....	....
Ca.....	6.21	....	5.39	5.22	**6.09**	11.83	....	10.13	**11.82**
Sc......	6.57	6.88	5.74	5.33	6.57	12.80	12.49	12.19	12.80
Ti......	6.79	7.39	6.10	5.48	**6.80**	13.60	12.99	13.45	13.60
V......	7.04	7.84	6.46	5.68	6.76	14.4	13.5	14.7	14.7
Cr......	7.28	8.21	6.70	5.76	**6.74**	15.1	14.1	16.6	16.6
Mn.....	7.38	8.55	7.06	6.28	**7.40**	15.70	14.52	13.80	15.70
Fe......	7.83	8.81	7.20	6.58	7.83	16.5	15.4	16.3	16.5
Co......	8.25	9.0	7.38	6.90	7.81	16.8	16.0	17.2	17.2
Ni......	8.65	9.30	7.62	7.22	7.64	17.15	16.50	18.2	18.2
Cu.....	8.95	9.48	7.63	....	**7.69**	17.62	17.09	20.34	20.34
Zn.....	9.40	....	....	....	**9.36**	17.93	....	....	**17.89**

From the data of Table V the various ionization potentials of the atoms can immediately be derived. These are collected in Table VI. For convenience the notation is repeated. The ionization denoted by

A is $d^{n-2}\,s^2$ to $d^{n-2}\,s$ (greater multiplicity)
B is $d^{n-2}\,s^2$ to $d^{n-2}\,s$ (smaller multiplicity)

$$\text{C is}\begin{cases} d^{n-1}\ s\ \text{(greater mult.) to } d^{n-1}\ \text{(arc)} \\ d^{n-2}\ s\ \text{(greater mult.) to } d^{n-2}\ \text{(spark)} \end{cases}$$

$$\text{D is}\begin{cases} d^{n-1}\ s\ \text{(smaller mult.) to } d^{n-1}\ \text{(arc)} \\ d^{n-2}\ s\ \text{(smaller mult.) to } d^{n-2}\ \text{(spark)} \end{cases}$$

E is d^{n-1} to d^{n-2} (spark)

The values listed under these headings are all derived from the first two members of the series by means of a Rydberg formula corrected as described above.

The "principal" ionization potentials represent the difference in energy between the normal states of the atoms in successive degrees of ionization. Those for *Ca*, *Sc*, *Ti*, *Mn*, *Fe*, and *Zn* correspond to a transition of type A; for *K*, *Cr*, and *Cu*, to type B (both involving the removal of a 4s electron); while for *V*, *Co*, and *Ni*, the transition involving the least energy change is from $d^{n-2}s^2$ to d^{n-1} and involves the simultaneous removal of one 4s electron and shift of another from 4s to 3d. In the spark spectra the principal ionization involves the removal of an s electron in *Ca*, *Sc*, *Ti*, *Mn*, *Fe*, and *Zn*, and of a d electron in *V*, *Cr*, *Co*, *Ni*, and *Cu*. The values given in heavy type are derived from longer series and are of course to be preferred. The average difference between these and the values

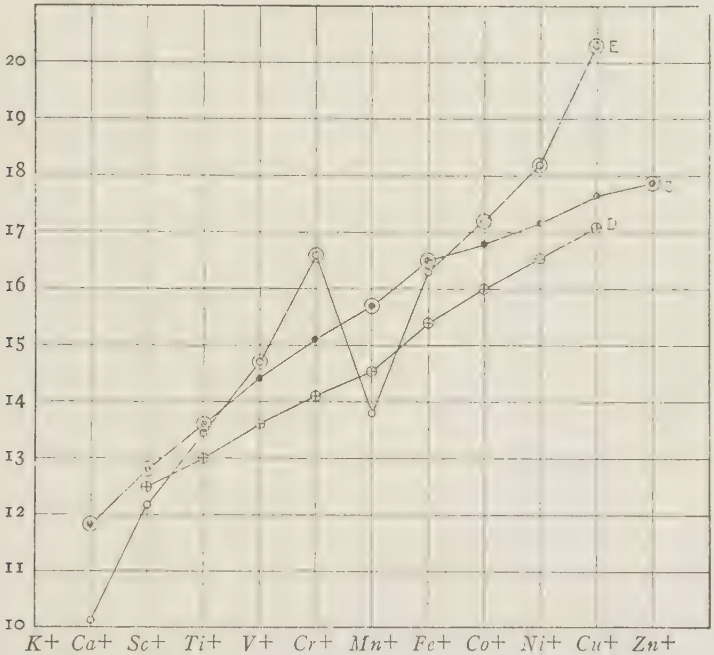

FIG. 2.—Ionization potentials of spark spectra. Large circles denote principal ionization potential.

given by the approximate formula is ±0.04 volt and the greatest, 0.12 volt for *Ca*, so that the approximation appears to be a good one.

For V^+, Cr^+, Fe^+, and Co^+, the ionization potentials have been derived from those of the neutral atoms: *Ti, V, Mn, Fe,* by the application of Moseley's law. These values are given to only one decimal place, and may be wrong by two- or three-tenths of a volt, but probably not more.

The ionization potentials are plotted in Figures 1 and 2. The smooth course of the values corresponding to the removal of a 4s electron under similar conditions contrasts strikingly with the ragged sequence of those for a 3d electron (Fig. 2). The principal ionization potentials are marked with large circles. The way in which the irregularity of their run arises from alternations between processes C and E in the spark spectra, or C and A in the arc, is now immediately comprehensible.

Much work remains to be done on many of these spectra, but the present summary may be of use, both in astrophysical and physical applications, and in suggesting profitable lines for fresh spectroscopic analysis.

Carnegie Institution of Washington
Mount Wilson Observatory
June 16, 1927

ADDENDUM

The differences between the ionization potentials A and B, or C and D, admit of a simple explanation. The reverse process for the transitions C and D, whether in the arc or the spark, consists of adding a 4s electron to a partially completed shell of 3d electrons. In case C, the multiplicity is increased; that is, the added electron is spinning in the same direction as the resultant spin of those already present. In case D, it is spinning in the opposite direction. Now, as Hund has pointed out, the magnetic interaction produces attraction in the first case, and repulsion in the second, so that the energy of binding is greater for C than for D.

The magnetic moment M of the group of d electrons increases from a single magneton in *Ca* and Sc^+ to five in *Cr* and Mn^+ and then diminishes to one unit in *Ni* and Cu^+. The differences C − D are actually nearly proportional to M, and greater in the spark than the arc spectrum. The differences $A-B$ in the arc spectrum are necessarily identical with $C-D$ in the spark.

The curious discontinuity in the run of the ionization potentials E is now intelligible. The reverse of this transaction involves the addition of a 3d electron to a group of similar electrons. From Ca^+ to Cr^+, the multiplicity is increased by the change; beyond this, owing to Pauli's restriction, it is diminished. The magnetic force should therefore change sign between Cr^+ and Mn^+, just where the observed discontinuity occurs. In the arc spectra the difference in energy between the configurations $d^{n-2}s^2$ and $d^{n-1}s$ should show a similar discontinuity between the same elements; and so it does.

The means of the values A and B, or C and D, should be uninfluenced by this effect of spin. They actually run much more smoothly than either series alone, increasing by almost uniform increments. This makes it possible to represent the ionization potentials approximately by means of very simple empirical equations as follows, Z being the atomic number, and M the magnetic moment defined above.

Arc Spectrum

$A=0.320Z-0.13M$
$B=\ .320Z+\ .13M$
$C=\ .262Z+\ .10M$
$D=0.262Z-0.10M$

Spark Spectrum

$C=0.601Z+0.13M$
$D=0.601Z-\ .13M$
$E=1.12Z\pm0.40M-12.00$

The values resulting from these formulae, and the residuals for the observational data, are as shown on page 22. (Residuals depending on terms not observed, but estimated as series limits, are given in parentheses.)

For the six types of ionization corresponding to the removal of a 4s electron, the agreement is remarkably good (except for *K* I, which is quite out of line with the others). The mean, regardless of sign, of the fifty residuals (rejecting *K* I and the less accurate values in parentheses) is ±0.066 volt. Only five disposable constants appear in the formulae which represent these fifty observed values so closely. It is evident, therefore, that the processes of ionization of the elements of the iron group are remarkably regular. The nine

	NEUTRAL ATOM								IONIZED ATOM					
	A	O—C	B	O—C	C	O—C	D	O—C	C	O—C	D	O—C	E	O—C
K........	....	....	....	....	5.02	−0.72								
Ca........	6.40	−0.19	....	....	5.38	+0.01	5.18	+0.04	12.02	−0.19	....	....	10.40	−0.27
Sc........	6.59	− .02	6.85	+0.03	5.74	.00	5.34	− .01	12.75	+ .05	12.49	0.00	11.92	+ .27
Ti........	6.78	+ .01	7.30	+ .09	6.11	− .01	5.51	− .03	13.48	+ .12	12.96	+ .03	13.44	+ .01
V........	6.97	+ .07	7.75	+ .09	6.47	− .01	5.67	+ .01	14.21	(+ .2)	13.43	(+ .1)	14.96	(− .3)
Cr........	7.16	+ .12	8.20	+ .01	6.83	− .13	5.83	− .07	14.94	(+ .2)	13.90	(+ .2)	16.48	(+ .1)
Mn........	7.35	+ .03	8.65	− .10	6.99	+ .07	6.19	+ .09	15.67	+ .03	14.37	+ .15	14.00	− .20
Fe........	7.80	+ .03	8.84	− .03	7.16	+ .04	6.56	+ .02	16.15	(+ .3)	15.11	(+ .3)	15.52	(+ .8)
Co........	8.25	.00	9.03	(.0)	7.32	+ .06	6.92	− .02	16.62	(+ .2)	15.84	(+ .2)	17.04	(+ .2)
Ni........	8.70	− .05	9.22	+ .08	7.48	+ .14	7.28	−0.06	17.09	+ .06	16.57	− .07	18.56	(− .4)
Cu........	9.15	− .20	9.41	+0.07	7.64	−0.01	....	....	17.56	+ .06	17.30	−0.21	20.08	(+0.2)
Zn........	9.60	−0.20	....	....	....	....	....	....	18.03	−0.10				

estimated values give an average residual of +0.20 volt (which perhaps indicates that the estimates are a little too high).

For the transition E, involving the removal of a 3d electron from a partially completed group, the constants of the formula are larger, and also the residuals, which average ±0.28 (including many estimated values). Though much more irregular, these are small enough to justify the explanation of the discontinuity given above.

PRINCETON
November 8, 1927

Contributions from the Mount Wilson Observatory, No. 343
Reprinted from the *Astrophysical Journal*, Vol. LXVI, pp. 256–282, 1927
Printed in the U.S.A.

SECONDARY STANDARDS OF WAVE-LENGTH; INTERFEROMETER MEASUREMENTS OF IRON AND NEON LINES

By HAROLD D. BABCOCK

ABSTRACT

After some discussion of the technique, standard wave-lengths are given for 286 iron lines, λ 3407–λ 6677, Table I, and for eleven neon lines, λ 5852–λ 6506, measured in terms of the primary standard, λ 6438.4696 of cadmium. The neon wave-lengths agree precisely with the values that have been adopted as secondary standards. Wave-lengths found for iron lines are systematically less than the adopted values, confirming results from other laboratories. From detailed comparisons it is concluded that the adopted system would be improved by a reduction of about 2 parts in 5,000,000 for wave-lengths less than λ 5506, and by a linear reduction in the red region amounting to 5 parts in 6,000,000 at λ 6200, and to 8 parts in 6,000,000 at λ 6600.

The systematic differences between the results of different observers are discussed and partially explained.

Table V gives a few additional wave-lengths obtained by the adjustment of earlier observations to the new scale. Table VI gives supplementary wave-lengths, λ 6213–λ 7586, for 63 iron lines observed under arc conditions somewhat different from those specified for the production of secondary standards.

I. INTRODUCTION

The development of the interference method of comparing wave-lengths by Fabry and Perot[1] and its subsequent extension and application by Fabry and Buisson,[2] Pfund,[3] Eversheim,[4] and others seemed to place the resulting system of secondary standards of wave-length[5] almost above criticism. Indeed, for fifteen years the most exacting tests have failed (except in the case of unstable lines), to reveal any errors as great as 2 parts in 1,000,000 in the adopted list of standard iron lines.

The observations of Meggers, Kiess, and Burns,[6] of Monk,[7] and the preliminary work of the writer[1] indicate, however, that a minute systematic adjustment would improve the adopted system of standards; and this is fully confirmed by the results now to be presented. The occasion for such an adjustment arises partly from the adoption[2] of new specifications for producing the iron spectrum, partly from improvements in the photography of the red part of the spectrum, and perhaps partly from the modern practice of transmitting the light of cadmium or of neon through the entire apparatus to the same plate which records the iron lines.

---

[1] *Astrophysical Journal*, **15**, 73, 1902.

[2] *Comptes Rendus*, **143**, 165, 1906; **144**, 1155, 1907; *Astrophysical Journal*, **28**, 169, 1908.

[3] *Ibid.*, p. 197, 1908.

[4] *Ibid.*, **26**, 172, 1907; *Zeitschrift für wissenschaftliche Photographie*, **5**, 152, 1907.

[5] *Transactions of the International Astronomical Union*, **1**, 41, 1922.

[6] *Scientific Papers of the Bureau of Standards*, **19**, 263 (No. 478), 1924.

[7] *Astrophysical Journal*, **62**, 375, 1925.

This paper describes details of the technique that has been followed and discusses a comparison of the results with those of other observers.

2. APPARATUS AND METHOD

The concave-grating spectrograph with interferometer attachment has previously been described,[3] but the grating itself and the plateholder were those to which reference has been made in a later paper.[4] A few plates were made with the aid of a small auxiliary spectrograph having a concave grating of 2-m radius mounted in parallel light. Seven pairs of planes were used in the etalons: some of fused quartz, some of glass, and one of crystalline quartz. Nine separators of either fused quartz or invar, ranging in thickness from 2.5 to 20 mm, served to keep the planes at fixed distances. Silver was usually sputtered on the planes to increase their reflecting power, but in a few cases gold was substituted.

Projection of an image of the source of light was accomplished by means of a concave mirror 40 cm in diameter and 46 cm in focal length, so arranged as to give about 7 diameters enlargement. Except for a vertical diametral strip 10 cm wide, the mirror was covered, since this reduces the radiation incident on the etalon to less than one-third of what it would be if the entire mirror were exposed, and still gives full illumination of the apparatus. A water-cell was generally placed before the etalon, and no radiation from the arc terminals was permitted to reach the etalon or its supports.

---

[1] *Physical Review*, Ser. 2, **25**, 716, 1925.

[2] *Transactions of the International Astronomical Union*, **1**, 36, 1922.

[3] *Mt. Wilson Contr.*, No. 137; *Astrophysical Journal*, **46**, 138, 1917.

[4] *Mt. Wilson Contr.*, No. 328; *Astrophysical Journal*, **65**, 140, 1927.

A distinct advantage is found in a strictly achromatic image of the source, accurately focused on the diaphragm of the etalon. This may be illustrated by comparison with the case of a quartz lens of 30-cm focal length used for projecting a fourfold magnified image of the arc on the interferometer. If such a lens is set to fulfil the foregoing condition for λ 5893, it is found that for λ 7200 the image is 6.3 cm from the interferometer, while for λ 3000 the image is 35 cm distant in the opposite direction. Further reference is made to this matter below.

It is customary to photograph lines of iron and of neon or cadmium on the same plate, by means of either divided or simultaneous exposures, or a combination of both. For example, ten photographs were made in the yellow-red region for which iron and neon spectra were simultaneous and cadmium was added by divided exposures. This was accomplished by projecting a real image of the neon lamp into the central region of the iron arc and again projecting the combined light by a concave mirror to the etalon. The concave mirror was mounted on a heavy iron table, capable of smooth rotation about a vertical axis and provided with a divided circle reading to one minute of arc. The cadmium lamp was situated symmetrically with respect to the combined iron and neon lamps, on the opposite side of the line joining etalon and concave mirror, so that nothing need be moved except the mirror, which required only a rotational displacement. Special care was taken to insure full illumination by each source separately.

In the case of other photographs the cadmium source was omitted, and the arrangement described above was used without moving the projecting mirror. Again, the neon and iron lamps were alternately projected on the etalon by rotation of the concave mirror, and in this case various schedules of exposure were followed, such as neon-iron-neon, iron-neon-iron, iron-neon-iron-neon- . . . ., etc. For all these cases the measurements showed no difference, a result dependent on the excellent stability of the apparatus and on the smallness of the variation in the etalons during the time of an exposure.

The iron arc was of the Pfund[1] type, and was used according to the latest specifications adopted by the International Astronomical

---

[1] *Astrophysical Journal*, **27**, 297, 1908.

Union[1] for the production of secondary standards of wave-length. The anode was below, consisting of a large bead of iron oxide supported on the hollowed upper end of a vertical cylinder of iron or copper 15–20 mm in diameter. The cathode was a rod of steel 6 mm in diameter, fitted with a large cooling cylinder of brass just above its lower extremity. The cooler permitted only 2 or 3 mm of the cathode to project, and was always massive enough to prevent the formation of a pendant drop of metal or oxide on the cathode. Commercial Bessemer steel rod was generally used for the cathode, since it was less inclined than wrought iron or cold rolled steel to form molten oxide, which causes unsteadiness of the arc. The line voltage was 250, the current 4.5 amp, and the length of arc 12–18 mm. Light was taken only from a horizontal central zone perpendicular to the axis of the arc, not exceeding $1\frac{1}{4}$ mm wide.

When this type of arc is clean and correctly adjusted, it operates, in a quiet atmosphere, at a length of 15–18 mm with remarkable steadiness and freedom from clouds of oxide. About once an hour it is necessary to remove the accumulated deposit of oxide from the cooling cylinder on the cathode and to readjust the amount of iron rod protruding. The results obtained in this investigation confirm much previous experience with this arc in showing that it is practically free from pole effect.

The primary standard was obtained from a fused quartz vacuum tube operated on a 10,000-volt transformer at about 20 milliamperes, except in the case of two exposures for which a vacuum arc lamp was substituted. As the wave-lengths showed no difference, the cadmium arc exposures have been included with the others. The vacuum cadmium arc was operated on a 250-volt circuit at about 1 amp, and the pressure was kept near to 1 cm of mercury.

The spectrum of neon was obtained from lamps supplied by Adam Hilger, which operate on direct current at 200–220 volts and at 0.010 to 0.015 amp. Such lamps have been in use in our laboratory for several years and have proved highly satisfactory for spectroscopic purposes. The light is concentrated, steady, and of high intrinsic brightness, while the lines are sharp and very accurately reproducible in position. The strong line λ 6402 is reversed in some lamps of this type, and occasionally λ 6143 also, but the other lines appear unreversed under the resolving powers usually employed in precise measurements of wave-length, i.e., up to orders of interference of at least 60,000.

---

[1] *Transactions of the International Astronomical Union*, 1, 36, 1922.

Photographic emulsions of various kinds were used for different parts of the spectrum. As the plates had to be cut into sections, each 12.5 cm long, in order to approximate to the focal surface, whose radius is 131 cm, it was customary to choose different emulsion for the various sections whenever the exposure could be shortened or simplified by their use. For the red, yellow, and green regions, Ilford Special Rapid Panchromatic plates were most frequently used, while for the blue and violet, Eastman Contrast Bromide plates were found most satisfactory. Color screens were frequently helpful in making the density of the photographs more uniform throughout their length.

The method of measurement and reduction of the photographs scarcely needs further description. Reference may be made to previous *Contributions*[1] for the details. Most of the results were obtained from photographs, each covering 2000 A, which were treated like those described in the last of these references.

Correction for change of phase was made by the method of two etalons of different thickness in which the same planes were mounted successively. Occasionally the two photographs obtained in this way were reduced by the difference method to a single set of wave-lengths without actually evaluating the amount of the correction. This method, described by Merrill,[2] consists in determining the two thicknesses from the standard cadmium line and dividing the difference of the thicknesses by the differences of the orders of interference for the individual iron lines. Such results obviously require no correction for change of phase.

Corrections for dispersion of the atmosphere were nearly always negligible, but when required were taken from the tables published for the purpose by the Bureau of Standards.

Most of the photographs were measured by one observer; a few of them by a second; and still others, with some duplication, by a third. The absence of appreciable personal equation in the results is shown by the accordance of the separate reductions of the same material.

---

[1] *Mt. Wilson Contr.*, Nos. 137, 202, 328; *Astrophysical Journal*, **46**, 138, 1917; **53**, 260, 1921; **65**, 140, 1927.

[2] *Scientific Papers of the Bureau of Standards*, **14**, 159 (No. 302), 1917.

In such delicate observations as those required for determining standards of wave-length, the greatest difficulty, in my experience, is the fulfilment, during an exposure, of certain optical conditions in the apparatus. In comparison, the difficulties of measurement and reduction are almost negligible, provided the interference pattern is properly photographed on a sufficiently large scale. For an illustration, I am indebted to my son Horace, a high-school student, who, during the first hour of his measurement of spectra, obtained results for typical iron and neon lines differing less than 0.001 A from those which had been obtained from the same plate by an experienced observer.

Some of the optical requirements are: (1) planeness and parallelism of the etalon plates; (2) coincidence of normal at center of etalon with optical axes of the projection systems which precede and follow it and also with that of the collimator of the spectrograph; (3) correct focus for each projection system and for the spectrograph throughout the whole extent of spectrum covered by each photograph; (4) projection, in focus on the grating, of a real image of the diaphragm which limits the etalon; (5) freedom from astigmatism and from variation of magnification over the whole field covered by the camera of the spectrograph; (6) reduction of total radiation incident on the etalon to a minimum by diaphragms and screens.

Throughout the investigation strict attention has been given to such conditions, and the correct position of each part of the system has been repeatedly verified. As noted above, seven pairs of planes have been used to make the etalons. These have always been adjusted to parallelism over a much larger aperture than is actually used for making a photograph. If left to themselves, they would remain in adjustment long after the completion of the photograph for which they were prepared.

The third condition, when a long range of spectrum is to be observed at one time, is not so easy to meet as might appear, and departure from it may introduce small systematic errors. If the image produced by the projection system is not in focus on the etalon, it is evident that some mixing of light from different parts of the source will occur, and in the case of the iron arc a departure from the specifications may result. In addition, the interference pattern may show a difference of brightness on opposite sides of the center, particularly in the red region where the arc is far more intense near the cathode than anywhere else.

Imperfect focus of the projector which puts the interference pattern on the slit may be an insidious source of small errors. For example, a certain spectrograph has a focal surface for dust lines which is closely represented by a circle of radius 131 cm. If an interference pattern is projected on its slit by a well-corrected triplet lens of 41-cm focal length adjusted for red light, the rings for λ 4000 will be in focus 2 mm behind the slit and the resultant focal surface for the rings will deviate by that amount from the true focal surface of the spectrograph. The use of concave mirrors throughout is a satisfactory solution of these difficulties.

The fourth condition, long ago pointed out by Fabry and Buisson,[1] appears often to have been overlooked. Yet it is essential for exact equivalence of the various ring segments of a given line. In this investigation the image of the diaphragm has always been made smaller than the ruled surface of the grating and sharply focused thereon, so that the portion of the etalon actually used is all of that defined by the diaphragm in front of the etalon, and is the same for every ring segment photographed. Disregard of this condition may easily lead to non-uniformity of intensity in the ring segments for each line, as well as to small differences of fractional order for inner and outer rings. Without more complete data regarding the apparatus used by other observers, it is impossible to determine the effect on their results of ignoring this detail; but from their published descriptions it would appear to be a possible explanation of some of the discrepancies noted below.

The fifth condition was examined in detail for my apparatus by measurements of photographs taken without the interferometer, but with a series of small apertures over the slit. No distortion was found on any part of the plate, although the tests would easily have shown its presence.

---

[1] *Journal de physique*, **7**, 169, 1908.

It is evidently desirable to reduce the time of exposure as much as possible for work of this exacting nature, in order to minimize the effects of earth tremors and inevitable small changes of temperature produced by exposing the etalon to the radiation of the arc. With a grating having remarkably high intensity in the red end of one first-order spectrum, the average time elapsing during a complete observation in the region λ 6200 was forty minutes, and for shorter wave-lengths it was still less. Comparison shows that in general other observers have required considerably longer intervals for the completion of an observation.

An important feature of the equipment used here is the concave mirror which projects the interference pattern on the slit. Highly perfect in figure, of 10-cm aperture, 63-cm focal length, and capable of precise adjustment, it provides accurate images of the rings for all wave-lengths on a large uniform scale. The aperture of the mirror actually used in the observations is of course determined by the size of the diaphragm on the etalon and the angular aperture of the projector which illuminates the etalon. An advantage resulting from the long focus of this mirror is the ease with which the maxima of the lines may be discerned on the photographs, with consequent freedom from systematic errors dependent on the width of the spectral lines. If all spectral lines were of equal width, no error would be introduced by measuring the geometrical centers instead of the maxima of the ring segments; but in the actual case appreciable differences may enter, which generally tend to make iron lines appear to have wave-lengths too long when they are compared with standards from neon and cadmium. Settings have always been made on the maxima of intensity of the lines, and thorough examination has failed to show any effects which depend on width or intensity. Furthermore, the differences in fractional order found from inner and outer rings are quite small and purely accidental in character.

The difficulty of maintaining high resolving power for violet light, without serious loss of intensity for red light, is an inherent limitation of the interferometer provided with silver films. For this reason not all the observed iron lines of wave-length less than λ 4271 were directly compared with the neon or cadmium standards; 18 of them were measured in terms of nearby iron lines, while 45 others were compared with both iron and neon standards. The lines so dealt with are referred to in a following paragraph.

3. RESULTS

The first column of Table I gives the wave-lengths which have been found for 286 iron lines. The second column indicates the number of plates on which each line was measured; the third gives the intensity assigned by Meggers, Kiess, and Burns[1] and also the pressure group of the Mount Wilson classification, revised in some cases with the aid of new data on the pressure effect. In the last column is found the multiplet designation, based on the papers of Walters,[2] Meggers,[3] and Laporte,[4] with additions from the unpublished list of term values prepared by Professor Russell and Miss Moore.

Wave-lengths marked with two asterisks were derived, not from the standards of neon and cadmium, but, for the reason indicated above, by comparison with nearby iron lines. The lines marked by a single asterisk were measured partly in this way and partly in terms of neon standards. For such lines no difference appeared between the results of the two procedures; and since the lines marked** occurred on photographs thus controlled, they have been included in Table I, and, in fact, are as well determined as the rest of the lines in the table.

The uniformity of the results from separate plates is illustrated in Table II, which gives for a few points in the spectrum the respective values for each plate measured. The corresponding average probable error of a mean wave-length is ±0.0002 A, and of a single determination, ±0.0008 A. The same order of accuracy is found throughout Table I, for lines of pressure groups *c* and *d* as well as for those of groups *a* and *b*. The probable error of any wave-length in Table I may therefore be found by dividing ±0.0008 A by the square root of the number of plates measured. For all lines except those measured on only one or two plates, the probable errors of the wave-lengths are evidently well under ±0.0005 A, and the fourth decimal place might have been retained with some justification. But the actual uncertainty is always greater than the probable error, and it appears better to omit the fourth place because of the probability of undetected systematic errors affecting this figure.

---

[1] *Loc. cit.*

[2] *Journal of the Optical Society of America*, **8**, 245, 1924.

[3] *Astrophysical Journal*, **60**, 60, 1924.

[4] *Proceedings of the National Academy of Sciences*, **12**, 496, 1926.

Eleven prominent neon lines between λ 5852 and λ 6506 were determined in terms of the primary standard from ten excellent photographs made with etalons ranging in thickness from 2.5 to 20 mm. The photographs were reduced by the method of differences referred to above, so that the wave-lengths are independent of any other observations. Except for two lines, the results are identical with the adopted wave-lengths of standard neon lines. For these exceptions my wave-lengths are 5852.487 and 6266.494, while the adopted values are 5852.488 and 6266.495, respectively. For the first of these Monk[1] found 5852.487. Since these photographs also show the iron-arc spectrum, exposed simultaneously with neon and referred in the same way to the primary standard, it seems reasonable to believe that the wave-lengths for the red iron lines are correctly determined. Moreover, wave-lengths for the same red iron lines, derived independently from neon standards on other plates, show no systematic difference from the results obtained from the ten plates referred to here.

4. DISCUSSION

A comparison of the wave-lengths in Table I with the system of secondary standards adopted by the International Astronomical Union[2] shows that the new values are systematically smaller. If unstable lines are omitted from the comparison, the differences, from the beginning of the table to λ 5506, are very uniform, averaging 0.0023 A for thirty-nine standards. A similar comparison with the "interpolated" wave-lengths[3] of the secondary standards gives the same average difference. For seventeen unstable secondary standards in this region of the spectrum the corresponding differences are 0.0094 and 0.0095 A, respectively, but if the new wave-lengths for these unstable lines are compared with the former Mount Wilson values[1] alone, instead of with the interpolated results, the mean difference becomes 0.0022 A, i.e., identical with the difference for stable lines. This clearly illustrates the reproducibility of the arc used at this Observatory, and indicates a mean pole effect of 0.007 A for these unstable secondary standards in the arcs which were originally used for producing them.

---

[1] *Loc. cit.*

[2] *Transactions of the International Astronomical Union*, **1**, 41, 1922.

[3] *Ibid.*

From the ultra-violet to the yellow the results in Table I are uniformly less than the adopted system of standards; an adjustment of 0.002 A will harmonize the two systems satisfactorily, if only stable lines are considered. For the spectral region λ 6065–λ 6750 the new values are also systematically less than the adopted system; but here, instead of being uniform, the difference increases with the wave-length. In fact, if the individual differences are plotted as ordinates against wave-lengths as abscissae (Fig. 1), the points lie throughout on a straight line with only one deviation as great as 0.001 A. The average amount of the difference is 0.0086 A.

A comparison of my measurements with those of Meggers, Kiess, and Burns,[2] the spectrum being divided into two parts as before, shows that for 80 lines, λ 3513–λ 5506, my wave-lengths are systematically shorter than theirs. The differences Babcock *minus* Meggers, Kiess, and Burns are positive for 2 lines, zero for 12, and negative for 66, with an average of -0.0013 A. From λ 6065 to λ 6677 there are 2 zero differences, 1 positive and 17 negative, with an average of -0.0022 A. Since for the red lines all the corrections usually become negligible and since these lines show the same consistency among individual measurements as lines of shorter wave-length, it is at first surprising to find a greater systematic difference in this part of the spectrum. Examination of the paper of Meggers, Kiess, and Burns shows, however, that although the title says clearly that their work was done with the new international arc, i.e., the arc specified by the International Astronomical Union in 1922, the description of the apparatus indicates that they did not use the specified arc. On page 264 they say: "Iron rods 7 mm in diameter were used as electrodes and the upper or positive pole was surrounded by a close fitting brass cylinder perforated with holes to serve as a radiator." In the Pfund arc, however, the negative pole and the attached cooling cylinder are above, while below is a massive rod of iron or copper, 10–15 mm thick, the actual anode being a bead of iron

---

[1] *Loc. cit.;* also *Mt. Wilson Contr.*, No. 202; *Astrophysical Journal*, **53**, 260, 1921.

[2] *Scientific Papers of the Bureau of Standards*, **19**, 263 (No. 478), 1924.

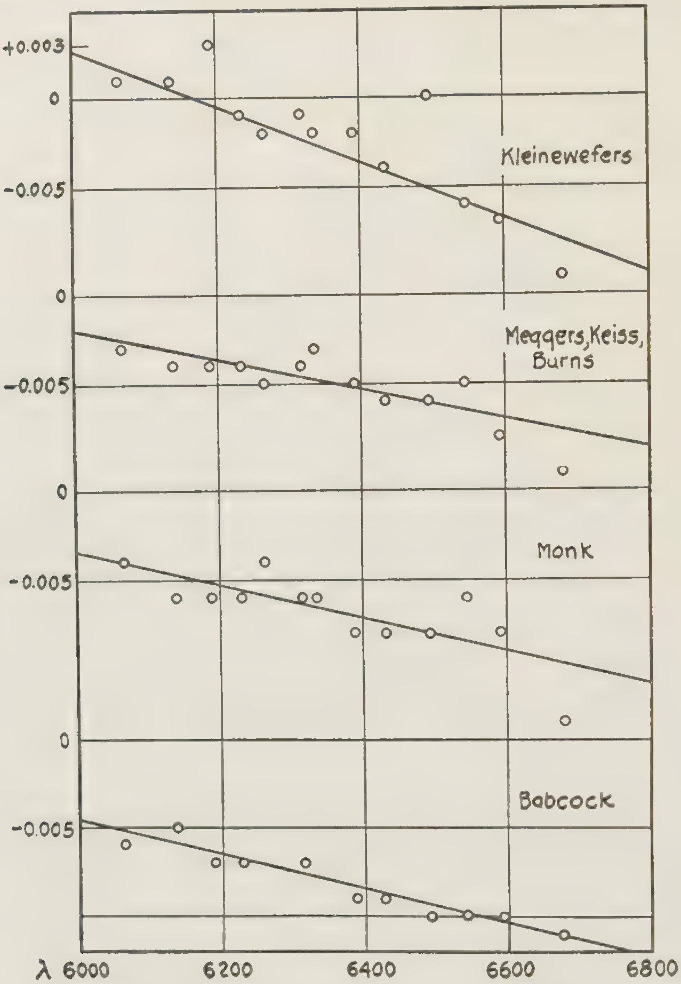

FIG. 1.—Comparison of recent measurements with adopted system of secondary standards in the red region. The horizontal line marked 0 above each observer's name represents the secondary standards. Small circles indicate the departures (unit = 1 A) for individual spectral lines.

oxide resting in the hollowed upper end. The differences indicated may appear slight, but they are in fact of real significance. Essential features of the Pfund type of arc are the polarity and the provisions made to prevent overheating of both terminals.

After discovering the systematic difference in the red region referred to above, I set up the same kind of arc as that described by Meggers, Kiess, and Burns and measured the red lines in exactly the same way as I had done previously with the specified arc. The results were confirmed on a second plate, and the means for 6 lines are on the average the same as the wave-lengths obtained by them.

Although it is not insisted that the entire systematic difference between my results and those of Meggers, Kiess, and Burns is caused by real differences in wave-length in the sources used, it would seem possible that such an explanation may account for part of the difference. This is confirmed by a comparison of our wave-lengths for 26 sensitive lines of groups *c* and *d*, which give a mean difference, Babcock *minus* Meggers, Kiess, and Burns, of −0.0023 A, instead of −0.0011 A, as for the stable lines. Here is found evidence that the arc used by them exhibits pole effect to the extent of about 0.001 A, and it might therefore be expected that the red *b* lines would show wave-lengths slightly too great when observed in their arc.

It may be remarked here that the observations of St. John and Babcock[1] on pole effect in the iron arc were made with arcs about 6 mm long. The measurements were differential, i.e., they showed the change in wave-length for each line when observed at the pole and at the center; but they failed to show the amount of pole effect still existing at the center of the arc. For the red *b* lines the measurements did indeed show slight apparent displacements toward the red at the negative pole, but of a magnitude too small to be distinguished from errors of observation. On this basis the lines were classed as stable, but later experience has shown them to be somewhat unstable, though far less so than nearby lines of group *d*. If in our early observations of pole effect we had compared negative pole and center of such an arc as the one now used for producing secondary standards, we probably would have found definite displacements of a few thousandths of an angstrom for the red *b* lines.

---

[1] *Mt. Wilson Contr.*, No. 106; *Astrophysical Journal*, **42**, 1, 1915.

Comparison of my wave-lengths with those of Monk[1] shows that the difference Babcock *minus* Monk is systematically negative. For 85 lines of all groups there are 7 positive, 18 zero, and 60 negative differences, the average being −0.0010 A. Practically no distinction appears between stable and unstable lines, nor between various spectral regions. Since the arc used by Monk was the same as mine, the slight systematic difference in our results is probably caused by some small difference in technique at present unrecognized. It appears unlikely that this should be connected with the correction for change of phase, for the difference is nearly uniform throughout a long range of spectrum, including that part where all corrections become zero.

The work of Wallerath[2] contains only 9 lines in common with Table I of this paper. For these the difference Babcock *minus* Wallerath is negative in every case, and the average is −0.0024 A. The lines compared are scattered over the region λ 3513–λ 5341 and are all stable. Kleinewefers,[3] working with practically the same apparatus as Wallerath, obtained wave-lengths for iron lines from λ 5167 to λ 6677, including 40 which are found in Table I. For an examination of the differences between his results and mine, the spectrum may be divided into two parts, λ 5167–λ 5658 and λ 6065–λ 6677. In the first part the differences Babcock *minus* Kleinewefers for 16 stable lines are all negative except two, one of which is zero, the other positive. The mean of these is −0.0021 A. Eleven lines of group *d*, however, all show negative differences averaging −0.0049 A, a definite indication of pole effect in the arc used by Kleinewefers. For 13 red *b* lines the differences, all negative, average −0.0057 A, but they range from −0.001 to −0.010 A in an irregular manner. In Figure 1, to which reference has already been made, the results, for the red *b* lines, of Meggers, Kiess, and Burns, Monk, Kleinewefers, and Babcock, are graphically compared with the adopted system of secondary standards.

The preceding paragraphs give comparisons of my results with those of other observers. It will be instructive to summarize for these observers the deviation of their wave-lengths from the inter-

---

[1] *Astrophysical Journal*, **62**, 375, 1925.

[2] *Annalen der Physik*, **75**, 37, 1924.

[3] *Zeitschrift für Physik*, **42**, 211, 1927.

TABLE I

Standard Wave-Lengths of Iron Arc Lines

λ	No. Plates	Intensity	Group	Multiplet
**3407.461	5	7	*d*	D–x
**3413.133	3	7	*d*	D–x
**3427.120	5	6	*d*	D–x
**3443.878	5	6	*a*	A–H
**3465.862	5	6R	*a*	A–H
**3476.704	5	5r	*a*	A–H
**3490.575	5	6	*a*	A–H
*3497.843	6	5r	*a*	A–H
*3513.819	6	5	*b*	B–M
*3521.264	6	5r	*b*	B–M
3541.087	1	6	....	....
3542.079	1	5	*d*	V–y
*3554.929	7	8	....	....
*3558.518	8	5r	*b*	B–M
3581.196	2	8R	*b*	B–L
3584.664	2	5	....	....
3585.321	8	6r	*b*	B–L
3586.114	2	5	....	....
3586.986	6	6	*b*	B–L
3589.108	2	4	*b*	B–L
3603.206	2	5	*d*	V′–U‴
3605.454	2	5	*d*	V′–U‴
*3606.682	6	5	*d*	V′–U‴
*3608.862	8	6R	*b*	B–L
3610.163	2	5	*d*	V–y ?
3617.788	2	6	*b*	....
*3618.769	6	6R	*b*	B–L
3621.464	2	6	....	....
3622.005	2	6	*d*	V′–U‴
*3631.465	5	6R	*b*	B–L
3638.301	2	6	*d*	V′–U‴
3640.391	2	6	*d*	V′–U‴
*3647.843	6	6R	*b*	B–L
3649.508	2	6	....	....
3651.470	2	6	*b*	....
3669.524	2	6	*b*	....
3677.630	2	6	....	....
*3679.915	13	5r	*a*	A–G
3683.056	2	4	*a*	A–G
3686.000	2	5	*e*	W–y
3687.459	10	6R	*b*	B–K
3689.460	2	6	....	....
3694.010	2	6	....	....
3695.053	1	3	*b*	....
3701.090	2	6	*d*	W–y

TABLE I—*Continued*

λ	No. Plates	Intensity	Group	Multiplet
3704.463.......	2	5	*b*	....
*3705.567.......	15	6R	*a*	A–G
3707.048.......	1	3	*d*	W–y
*3709.248.......	19	6	*b*	B–K
3716.447.......	2	6	....	....
**3719.937.......	3	8R	*a*	A–G
*3722.563.......	16	6R	*a*	A–G
*3727.621.......	18	6R	*b*	B–K
3732.398.......	2	6	*b*	....
*3733.318.......	13	6R	*a*	A–G
**3737.134.......	3	7R	*a*	A–G
3738.306.......	2	4	*b*	....
*3743.364.......	18	6	*b*	B–K
**3748.264.......	3	6R	*a*	A–G
**3749.487.......	3	8R	*b*	B–K
3753.612.......	2	6	*d*	D–S
*3758.234.......	4	7R	*b*	B–K
3760.050.......	2	5	*b*	....
*3763.791.......	10	6R	*b*	B–K
3765.541.......	2	6	*b*	....
*3767.193.......	18	6R	*b*	B–K
3787.882.......	13	6R	*b*	B–K
3790.095.......	2	4	*b*	B–K′
*3795.004.......	19	6r	*b*	B–K
3797.517.......	2	5	*b*	....
*3798.513.......	14	6r	*b*	B–K
*3799.549.......	15	6r	*b*	B–K
3805.344.......	2	6	*b*	....
3806.698.......	2	6	*d*	....
3807.538.......	2	4	*d*	D–S
*3812.966.......	15	6	*b*	B–K′
*3815.842.......	10	7R	*b*	C–P
**3820.428.......	3	8	*b*	B–J
3821.181.......	2	6	*d*	....
*3824.445.......	11	6R	*a*	A–F
**3825.884.......	3	8R	*b*	B–J
*3827.824.......	18	6R	*b*	C–P
3834.224.......	14	7R	*b*	B–J
3836.332.......	1	3	....	....
3839.258.......	2	5	....	....
3840.439.......	9	6R	*b*	B–J
3841.049.......	9	6R	*b*	C–P
3843.258.......	2	5	*b*	....
3846.802.......	2	5	*b*?	....
*3849.969.......	15	5	*b*	B–J

TABLE I—*Continued*

λ	No. Plates	Intensity	Group	Multiplet
3850.820	2	5	*b*	B–K′
3852.574	2	3	*d*	D–S
*3856.373	9	6R	*a*	A–F
3859.214	2	5	....	....
*3865.525	16	6R	*b*	B–J
3867.218	2	3	*b*	....
*3872.503	18	6r	*b*	B–J
3873.762	2	4	*b*	....
*3878.020	12	6r	*b*	B–J
3878.574	9	6R	*a*	A–F
3885.512	2	3	*b*	....
**3886.284	3	7R	*a*	A–F
*3887.050	12	6r	*b*	B–J
*3888.516	14	7	*b*	C–P
3893.391	2	4	....	....
*3895.658	19	5r	*a*	A–F
*3899.708	20	6r	*b*	A–F
3902.948	14	7r	*b*	C–P
*3906.481	9	5r	*a*	A–F
3907.937	1	3	*b*	....
3916.733	1	3	*b*	....
3917.184	2	5	*b*	B–J
*3920.259	19	6r	*a*	A–F
*3922.913	20	6R	*a*	A–F
*3927.921	18	6r	*a*	A–F
*3930.298	18	7R	*a*	A–F
3935.814	1	4	*b*	....
3940.880	2	4	*b*	B–J
3942.442	1	3	*b*	....
3948.778	2	4	*b*	....
3949.954	2	4	*d*	D–X′
3951.164	2	4	*b*	....
3952.606	1	4	*d*	V′–U′
3956.680	2	4	*d*	V′–U′
3966.064	2	7	*b*	C–P
3967.424	1	4	*b*	....
*3969.260	17	7r	*b*	C–N
3971.325	2	4	*d*	V′–x
3977.743	2	5	*d*	D–X′
3983.960	2	5	*d*	V′–x
3997.394	2	6	*d*	V′–U′
3998.054	2	5	*d*	V′–x
4005.244	12	7	*b*	C–N
4009.714	2	5	*d*	D–X′
4014.534	2	4	*b*	....

TABLE I—*Continued*

λ	No. Plates	Intensity	Group	Multiplet
4021.869	2	5	*d*	V′–U′
*4045.814	8	8R	*b*	C–N
4063.597	13	8	*b*	C–N
4071.741	12	7	*b*	C–N
**4132.061	4	7	*b*	C–N
**4143.871	5	7	*b*	C–N
**4202.032	5	7r	*b*	C–M
4233.608	5	6	*d*	E–X
4235.942	2	8	*d*	E–X
4238.816	3	4	*d*	....
4245.258	3	2	*b*	....
4247.432	1	5	*d*	....
*4250.790	6	8	*b*	C–M
*4260.480	5	10	*d*	E–X
4267.829	1	2	*b*	....
**4271.764	5	8r	*b*	C–M
4282.406	7	6	*a*	D–Y
4285.444	3	2	*b*	....
4291.466	1	1	*a*?	....
4294.128	6	6	*b*	C–L
4299.242	5	7	*d*	E–X
4305.455	3	2	*b*	....
4307.906	4	8r	*b*	C–M
4315.087	9	5	*a*	D–Y
4325.765	2	9r	*b*	C–M
4337.049	9	5	*b*	C–L
4352.737	8	4	*a*	D–Y
4369.774	6	3	*b*	....
4375.932	8	5	*a*	A–V
4383.548	3	10R	*b*	C–L
4390.956	2	3	*b*	....
4408.418	1	4	*c*	D–Q
4415.125	2	8r	*b*	C–L
4422.570	6	4	*b*	....
4427.311	8	5	*a*	A–V
4430.618	3	4	*c*	D–Q
4442.342	4	5	*c*	D–Q
4443.198	2	3	*b*	....
4447.721	5	5	*c*	D–Q
4454.383	4	3	*b*	....
4459.121	5	5	*c*	D–Q
4461.654	5	4	*a*	A–V
4466.554	9	5	*b*	....
4469.381	1	4	*d*	....
4476.021	8	7	*b*	....

TABLE I—*Continued*

λ	No. Plates	Intensity	Group	Multiplet
4484.227	1	3	d	H–T′
4489.740	4	3	a	A–V
4494.567	7	5	c	D–Q
4525.142	1	3	d ?	....
4528.618	5	7	c	D–Q
4531.152	9	5	b	C–K
4547.850	4	3	b	....
4592.655	5	4	b	C–K
4602.944	7	4	b	C–K
4611.285	1	4	d	....
4625.052	1	4	d	F–U
4647.436	6	4	b	....
4667.459	5	4	b ?	....
4678.851	4	5	b ?	....
4691.414	4	4	b ?	....
4707.280	5	5	d	F–U
4710.286	4	3	b	....
4733.595	4	3	b	C–J
4736.780	12	5	d	F–U
4745.805	1	3	b	....
4772.816	2	3	b	C–J
4786.809	2	3	b	....
4789.652	5	3	b	....
4859.747	9	5	d	V–X
4871.323	5	8	d	V–X
4872.144	5	6	d	V–X
4878.217	5	5	d	V–X
4891.496	2	9	d	V–X
4903.316	3	5	d	V–X
4918.999	7	8	d	V–X
4920.509	8	10	d	V–X
4957.603	1	10	d	V–X
4966.094	1	5	d	G–U
4994.133	1	3	a	B–G
5006.126	2	5	d	V–X
5012.071	11	4	a	B–G
5049.824	7	5	b	D′–P
5051.637	6	4	a	B–G
5083.342	2	4	a	B–G
5110.414	5	4	a	A–E
5167.490	9	8	a	C–Z
5168.899	1	3	a	A–E
5171.599	14	7	a	C–I
5192.350	9	8	d	W–X
5194.943	7	5	a	C–I

TABLE I—*Continued*

λ	No. Plates	Intensity	Group	Multiplet
5202.339	3	5	*b*	D–O
5216.276	6	5	*a*	C–I
5227.191	7	8	*a*	C–Z
5232.946	10	8	*d*	W–X
5266.562	10	8	*d*	W–X
5269.541	4	10	*a*	B–F
5270.359	8	8	*a*	C–Z
5281.796	2	5	*d*	W–X
5283.628	6	7	*d*	F–T
5302.307	2	5	*d*	F–T
5324.185	10	6	*d*	F–T
5328.042	5	4	*a*	B–F
5339.935	1	3	*d*	F–T
5341.025	20	5	*a*	C–Z
5364.874	1	3	*e*	L–λ
5367.470	2	3	*e*	L–L′
5369.965	3	4	*e*	L–L′
5371.493	9	7	*a*	B–F
5383.374	5	5	*e*	L–λ
5393.174	6	4	*d*	F–T
5397.130	17	6	*a*	B–F
5404.144	1	3	*e*	L–L′
5405.777	12	6	*a*	B–F
5410.913	2	3	*e*	....
5415.201	5	4	*e*	L–L′
5424.072	4	4	*e*	L–L′
5429.699	10	6	*a*	B–F
5434.526	22	6	*a*	B–F
5446.919	11	6	*a*	B–F
5455.613	15	6	*a*	B–F
5497.518	22	4	*a*	B–F
5501.468	17	4	*a*	B–F
5506.782	23	4	*a*	B–F
5554.895	2	3	*e*	....
5563.604	2	3	*d*	J–T′
5565.708	2	3	*e*	....
5569.624	2	5	*d*	G–T
5572.848	3	5	*d*	G–T
5586.761	4	6	*d*	G–T
5615.650	4	6	*d*	G–T
5624.548	2	5	*d*	G–T
5638.266	1	3	*d*	K–T′
5658.825	2	4	*d*	G–T
5662.524	2	3	*d*	K–T′
6065.486	25	4	*b*	c–N

TABLE I—*Continued*

λ	No. Plates	Intensity	Group	Multiplet
6136.618	26	4	*b*	v–M
6137.696	20	4	*b*	c–N
6191.561	26	5	*b*	v–M
6230.727	23	5	*b*	c–N
6252.559	16	4	*b*	v–M
6318.021	6	4	*b*	v–L
6393.603	19	5	*b*	v–L
6400.010	7	5	*d*	H–T
6421.354	10	4	*b*	D′–K′
6430.850	14	5	*b*	D–J
6494.983	20	5	*b*	v–L
6546.242	9	3	*b*	V′–N
6592.918	9	5	*b*	V′–N
6677.993	2	5	*b*	V′–N

polated[1] wave-lengths for stable lines in the range λ 3370–λ 5506, since a greater amount of material is thus available for comparison, and since the interpolated system is on the average identical with the adopted system of secondary standards. This is done in Table III.

The agreement of the last three means is probably as close as can be expected. They show systematic differences of only 1 part in 10,000,000, but little more than the probable errors of the observations. Taken together they seem to outweigh the first two for several reasons: (1) number of lines observed; (2) the last three are entirely independent results, while the first two depend on work done in the same laboratory with practically identical apparatus and technique; (3) results obtained with the same apparatus by Eversheim differ systematically from those of other observers, in the same direction[2] that those of Wallerath and Kleinewefers differ from the others in Table III.

The arithmetical mean of the five average differences is +0.0010 A; if the first two are combined and weights proportional to number of lines involved are assigned, the weighted mean is +0.0015 A; if the first two are omitted, the weighted mean is +0.0017 A. It appears safe to conclude that the adopted system of standards would be improved by a reduction of about 2 parts in 5,000,000 for wave-lengths less than λ 5506, and by a linear reduction in the red region amounting to about 5 parts in 6,000,000 at λ 6200 and about 8 parts in 6,000,000 at λ 6600.

---

[1] *Loc. cit.*

[2] Priest, *Physical Review*, Ser. 1, **31**, 602, 1910.

TABLE II

AGREEMENT OF SEPARATE DETERMINATIONS

	λ 3585	λ 4466	λ 5012	λ 5506	λ 6230	λ 6494
	.321	.553	.070	.780	.727	.982
	.321	.553	.070	.782	.726	.982
	.321	.555	.071	.783	.726	.982
	.320	.554	.070	.780	.726	.983
	.321	.554	.070	.780	.727	.983
	.321	.555	.074	.781	.724	.985
	.321	.556	.072	.780	.725	.982
	.320	.554	.072	.782	.725	.983
		.555	.071	.781	.729	.982
			.070	.782	.727	.982
			.071	.782	.729	.984
				.781	.728	.984
				.781	.728	.984
				.781	.728	.984
				.782	.728	.985
				.782	.728	.984
				.781	.728	
				.782	.726	
				.784	.729	
				.784		
				.782		
				.782		
				.782		
Means......	.321	.554	.071	.782	.727	.983

TABLE III

AVERAGE DIFFERENCES FOR STABLE LINES BETWEEN λ 3370–λ 5506

Comparison	Difference	No. Lines
Interpolated—Wallerath.................	+0.0000 A	30
Interpolated—Kleinewefers..............	.0002	17
Interpolated—Meggers, Kiess, Burns......	.0014	95
Interpolated—Monk....................	.0015	73
Interpolated—Babcock..................	+0.0019	187

It may be pointed out that Table I closely confirms the preliminary results[1] obtained with the same apparatus, and that the final wave-lengths given here for the red iron lines have been tested in actual use. Precise wave-lengths of oxygen absorption lines[1] have been derived in terms of these iron wave-lengths and independently from the neon standards. Both reference systems gave the same results for oxygen.

---

[1] *Ibid.*, Ser. 2, **25**, 716, 1925.

A summary of the features of this investigation which tend to reduce the number and magnitude of systematic errors would include: (1) reduced time of exposure; (2) photographs of large scale, both in the interference pattern and in the auxiliary dispersion; (3) reduced number of optical parts in the system; (4) large number of etalon plates successively employed; (5) variety of methods of exposing to the different sources; (6) achromatic projection throughout; (7) rigorous tests for correct adjustment of the entire optical system; (8) absence of systematic difference in fractional orders from inner and outer rings; (9) freedom from effects depending on width and intensity of the lines and on personal equation in the measurements; (10) freedom from pole effect in the iron arc.

During the progress of the work described here the same apparatus has been used for observations of wave-lengths from the vacuum iron arc, which will be discussed in a forthcoming paper. It is interesting to note that the dispersion among the results for the same line from individual plates is practically the same for the vacuum arc as for the open arc specified for producing secondary standards. There is no evidence of greater reproducibility or of higher attainable accuracy in the spectrum from the vacuum arc—a conclusion in agreement with that of Monk.[2]

For wave-lengths shorter than λ 5506, the work of St. John and Babcock[3] was done with the long Pfund arc under the same conditions as have been observed in obtaining the data of Table I. Lines measured by them but not included in Table I may readily be revised to the present scale by applying small corrections derived by comparing material common to the two lists. These corrections are summarized in Table IV. Since the corrections cover a range of only

[1] Dieke and Babcock, *Mt. Wilson Communications*, No. 102; *Proceedings of the National Academy of Sciences*, **13**, 670, 1927.

[2] *Loc. cit.*

[3] *Mt. Wilson Contr.*, No. 202; *Astrophysical Journal*, **53**, 260, 1921.

0.002 A throughout the region discussed, it appears that the wave-lengths relative to each other were determined almost as accurately in 1921 as they have been in the recent measurements. A few lines, chiefly secondary standards not included in Table I, have been reduced to the new scale by means of these average corrections and are listed in Table V.

TABLE IV

Corrections to Be Applied to Earlier Mount Wilson Wave-Lengths of Iron Lines

Region	No. Lines	Mean Correction
3407–3589	20	−0.0009 A
3603–3695	23	.0010
3701–3799	28	.0017
3805–3899	35	.0017
3902–3997	22	.0021
4005–4299	26	.0020
4305–4447	18	.0021
4454–4691	21	.0032
4707–4994	19	.0029
5001–5283	21	.0023
5302–5506	23	−0.0025

TABLE V

Corrected Wave-Lengths of Certain Iron Lines Measured in 1921

λ	No. Plates	Intensity	Group	Multiplet
3370.787	13	6	....	....
3399.336	20	6	*d*	D–x
3445.151	25	4	*d*	D–x
3485.341	14	6	*d*	D–a
3536.558	26	6	....	....
3565.381	39	6R	*b*	B–M
3676.313	29	6	....	....
3724.378	26	6	....	....
4095.975	17	3	*b*	....
4107.492	25	5	*b*	....
4118.549	37	6	*b*	....
4134.682	37	5	*b*	....
4147.674	40	4	*b*	C–M
4175.640	56	4	*b*	....
4184.895	52	4	*b*	....
4203.987	36	3	*b*	....

In addition to the new measurements and the revision of certain

TABLE VI

Supplementary Measurements; Probably Moderate Pole Effect

λ	No. Plates	Intensity	Group	Multiplet	Meggers and Kiess
6213.438	3	3	*b*	D–J	.435
6219.290	3	3	*b*	D–J	.286
6240.656	1	2	*b*	D–K	....
6254.262	2	3	*b*	D–K′	.262
6256.370	2	3	*b*	v–M	.366
6265.139	3	3	*b*	D–J	.140
6280.625	2	2	*a*	B–V	.621
6290.968	1	3	*e* ?	P–g	....
6297.800	2	3	*b*	D–J	.800
6322.693	3	3	*b*	c–N	.693
6335.338	2	4	*b*	D–J	.338
6336.835	2	4	*d*	H–T	.841
6344.154	2	2	*b*	v–M	.155
6355.038	2	3	*b*	c–P	.037
6358.692	2	3	*a*	B–V	....
6380.748	2	3	*b*	....	.748
6408.031	3	4	*d*	H–T	.034
6411.658	3	4	*d*	H–T	.666
6462.731	3	4	*a*	B–V	.732
6469.214	1	4	*b*	v–L ?	....
6475.632	2	3	*b*	c–M	.632
6481.878	3	3	*b*	D′–J	.878
6518.376	2	3	*b*	c–P	.375
6569.231	1	5	*d*	....	....
6575.022	2	3	*b*	c–M	.024
6593.878	2	3	*b*	v–L	.876
6609.116	2	4	*b*	c–M	.117
6663.444	2	4	*b*	....	.447
6705.117	1	3	....	....	....
6750.152	2	4	*b*	....	.157
6828.610	1	3	....	O–T′	.612
6841.349	1	4	....	O–T′	.355
6843.671	1	4	....	N–T′	.676
6855.176	1	4	....	O–T′	.179
6916.702	1	3	*d*	J–f	.709
6945.208	2	4	....	....	.211
6951.261	2	3	....	....	.271
6978.855	3	3	....	....	.857
6988.530	1	2	....	....	.531
6999.902	2	3	*d*	J–U	.912
7038.251	1	3	*d*	J–U	.255
7068.415	2	3	....	....	.418
7090.404	2	3	*d*	J–U	.410
7095.425	1	2	*d*	K′–U	....
7107.461	1	1	....	....	.464

TABLE VI—*Continued*

λ	No. Plates	Intensity	Group	Multiplet	Meggers and Kiess
7112.176	1	1	....	....	.178
7130.942	4	4	*d*	J–U	.946
7132.989	1	2	....	....	.996
7164.463	3	4	*d*	J–U	.472
7187.332	1	5	*d*	J–U	.341
7219.686	1	2	....	....	.690
7223.668	1	2	....	....	.670
7239.885	2	2	*d*	K′–U	.896
7288.760	1	3	*d*	K–U	.764
7293.068	1	3	*d*	K–U	.073
7311.101	1	2	*d*	K–U	.103
7389.414	4	4	*d*	K–U	.423
7411.174	4	3	*d*	K–U	.184
7445.769	3	3	*d*	K–U	.778
7495.084	4	3	*d*	K–U	.092
7511.042	4	4	*d*	K–U	.047
7531.162	1	2	*d*	L–f	.178
7586.048	1	3	*d*	L–f	.050

earlier ones, some supplementary results for the deep red are given in Table VI. These wave-lengths were obtained in terms of the neon standards, but from a Pfund arc shorter than the new international arc, and therefore presumably exhibit pole effect in some degree. They are given here because low intensity makes the measurement of such lines in the specified arc very difficult, and because the results are of some value for comparison with those of other observers. The last column of the table contains the wave-length found by Meggers and Kiess[1] in a 6-mm, 6-amp arc; the intensities are from their paper. The group designation for some of the lines has been deduced from unpublished observations which permit a reliable calculation of the pressure effect for many multiplets of iron.

For the lines marked *a* or *b* in Table VI there is no systematic difference between the wave-lengths in the first and last columns. For the *d* lines my results are systematically less than those of Meggers and Kiess, the mean difference being 0.007 A. For unclassified lines, some of which are known from other observations to belong to the stable groups, the difference is intermediate. Such a comparison illustrates the difference in the arcs from which the two lists of wave-lengths were obtained. If the arc which I used had conformed to the specifications adopted for producing secondary standards, the differences noted above would have been greater. This table emphasizes the unfortunate fact that most of the stronger infra-red iron lines are unsuitable for use as standards of wave-length.

---

[1] *Scientific Papers of the Bureau of Standards*, **19**, 273 (No. 479), 1924.

To Mrs. Thome, neé Keener, who measured a few of the photographs discussed in this paper, and to Mr. W. P. Hoge, who carried out nearly all the reductions as well as a large part of the measurement, my hearty thanks are extended. I am also indebted to Professor Russell and Miss Moore for access to unpublished data on the classification of iron lines.

Carnegie Institution of Washington
Mount Wilson Observatory
August 1927

Contributions from the Mount Wilson Observatory, No. 344
Reprinted from the *Astrophysical Journal* ,Vol. LXVI, pp. 283–328, 1927
Printed in the U.S.A.

THE ARC AND SPARK SPECTRA OF TITANIUM

PART I. THE SPARK SPECTRUM, *Ti* II

By HENRY NORRIS RUSSELL[1]

ABSTRACT FOR PART I

A detailed analysis of the titanium spectrum aided by much unpublished material generously supplied by colleagues has led to the classification of practically all the lines except the weakest.

The *spark spectrum* includes *doublet* and *quartet* terms; 33 doublet and 17 quartet terms have been identified. Their combinations give 164 multiplets, including 529 observed lines. The *lowest energy-level* belongs to a $^4F'$ term. A second $^4F'$ term is 0.1 volt higher, and a $^2F'$ term, 0.5 volt above this.

Tables of the terms are given and also of the classified lines, including the few lines of any strength which remain unclassified.

The *temperature classification* of the lines shows the usual close relation to their levels of origin.

The *Zeeman effect* is in good agreement with Landé's theory. *Tables* of the observed and computed patterns are given.

The *electronic configurations* in the atom which give rise to the various terms have been identified with the aid of Hund's theory. The *agreement* of theory and observation is *complete*. The *complexity* of the spectrum is explained by the numerous possible spatial orientations of the orbits of the three spectroscopically active electrons.

Three *series* of two members each have been identified. They indicate an *ionization potential of* 13.6 *volts.*

Comparison of the spectra of *Ti* II and *Sc* I shows that Moseley's law is closely satisfied and confirms the theoretical interpretation of both.

I. INTRODUCTION

The spectrum of titanium is typical of those of the heavier elements as regards its apparent complexity—the lines are very numerous in both the arc and spark spectra, and no conspicuous series exist.

The first analysis of the arc spectrum was published by Dr. and Mrs. Kiess,[2] who classified about four hundred lines in multiplets belonging to triplet and quintet systems and indicated the probable existence of a singlet system. Shortly afterward Frl. Gieseler and

---

[1] Research associate of the Mount Wilson Observatory, Carnegie Institution of Washington.

[2] C. C. and H. H. Kiess, *Proceedings of the Washington Academy of Sciences*, **13**, 270, 1923; *Journal of the Optical Society of America*, 8, 607, 1924.

Dr. Grotrian[1] published an account of independent investigations, which in general confirmed the results of the authors first named, and showed by absorption observations that the normal state of the atom corresponds to a ^3F term.

The work of the present writer was begun at about the same time as that of the other investigators, without knowledge of the work of either. When it was learned later that Dr. and Mrs. Kiess were also in the field, publication was deliberately delayed until after their results were presented and attention was given to making the present analysis as complete as possible.

A similar analysis of the spark spectrum, begun a little later, has likewise been carried approximately to completion. The only previous investigation known to the writer is a brief note by N. K. Sur.[2] Still later the analysis has been extended to higher degrees of ionization, *Ti* III and *Ti* IV. This has been a long task—particularly since experience has shown that the best road to success in the analysis of a complicated spectrum is to drop the work when no further immediate results are forthcoming and to take it up again after a month or two, when new terms have almost always been found. It is probable that, even now, more remains that could be unraveled, but since all the lines of any strength have been classified (except a few in the extreme ultra-violet), the two main purposes of the investigation have been met. These were to provide the data necessary for the astrophysical interpretation of the behavior of titanium lines in the spectra of the sun and stars and to determine how completely the methods of multiplet analysis on the principles introduced by Sommerfeld and Landé are able to account for these rich and complex spectra. During the progress of the work, the theory of spectral structure has been developed by Heisenberg, Pauli, and Hund, and may be applied to the results of the term analysis.

It may be said at once that the confirmation of theory by observation is extremely satisfactory. Practically all the titanium lines of any importance have been referred to transitions between definite energy-levels in the atom in one or the other of its states of ionization; these levels may be grouped into multiple terms satisfying the well-known rules; and Hund's theory gives a satisfactory account of the origin of these terms in electron configurations within the atom.

---

[1] *Zeitschrift für Physik*, **25**, 342, 1924.

[2] *Nature*, **114**, 611, 1924.

A few of the multiplets found in the writer's work upon *Ti* II have been published in detail,[1] and a summary account of the classification of 317 lines of *Ti* I and 121 of *Ti* II (including all the stronger ones with wave-lengths exceeding 3000 A) is found in his "List of Ultimate and Penultimate Lines."[2]

The analysis of *Ti* III and *Ti* IV has recently been published by the writer and Professor R. J. Lang.[3] The present communication, which gives full details for *Ti* I and *Ti* II, completes the presentation.

2. THE OBSERVATIONS

The observations of the arc and spark spectra upon which the present work is based have been derived from many sources. The main reliance for the wave-lengths was originally upon Kilby's[4] measures, extended toward the red by those of Kiess and Meggers[5] and supplemented as regards the fainter lines by the invaluable tables of Exner and Haschek.[6] The later precise measures of Crew[7] have also been utilized, and additional lines have been taken from observations of R. J. Lang[8] and other observers. The intensities and temperature classes determined by King[9] have been of fundamental importance in the analysis, as has also the observed behavior of the lines in the sun-spot spectrum. King's observations of the Zeeman effect[10] have also been freely employed.

In addition to these published data, much valuable material has been derived from unpublished sources. Measures of additional lines in the infra-red and ultra-violet made at the Bureau of Standards have been generously communicated by Dr. Kiess; and a plate of the spark spectrum in the extreme ultra-violet was taken for the writer by Professor Shenstone at Princeton with a large quartz spectrograph. The most valuable aid of all came from the writer's colleagues at this observatory.

---

[1] Meggers, Kiess, and Walters, *Journal of the Optical Society of America*, **9**, 363–364, 1924.

[2] *Mt. Wilson Contr.*, No. 286; *Astrophysical Journal*, **61**, 247–257, 1925.

[3] *Mt. Wilson Contr.*, No. 337; *Astrophysical Journal*, **66**, 13, 1927.

[4] *Astrophysical Journal*, **30**, 243, 1909.

[5] *Scientific Papers of the Bureau of Standards*, **16**, 54 (No. 372), 1920.

[6] Kayser, *Handbuch der Spectroscopie*, **6**, 655, 1912.

[7] *Astrophysical Journal*, **60**, 108, 1924.

[8] Private communication.

[9] *Mt. Wilson Contr.*, No. 76; *Astrophysical Journal*, **39**, 139, 1914; *Mt. Wilson Contr.*, No. 274; *Astrophysical Journal*, **59**, 155, 1924.

[10] *Publications of the Carnegie Institution of Washington*, No. 153, 35, 1912.

A series of contact prints and enlargements of the furnace, arc, and spark spectra of the metal, prepared for the writer by Mr. A. S. King, and covering the whole range from λ 8800 to λ 2150, have proved of very great aid throughout the work; and many new lines have been measured upon these, or upon King's original negatives. Unpublished measures of the Zeeman effect made by Mr. Babcock for the purpose have also been of much service.

Hearty acknowledgments are made to all those mentioned above for their generous aid; and likewise to Miss Charlotte E. Moore for very valuable help in preparing the material for publication.

3. STRUCTURE OF THE SPARK SPECTRUM, *Ti* II—LIST OF TERMS

It is of advantage to discuss the spark spectrum first, both because it is simpler and because a knowledge of it is necessary in interpreting certain features of the arc spectrum.

The most conspicuous spectral feature of the titanium spark is a great mass of strong lines in the near ultra-violet. Enhanced lines appear also in the visible region, though there are very few in the yellow and red. These are but faintly present in the arc, but many of the ultra-violet lines are strong lines there, and some appear in the furnace, even at moderate temperatures, and so fall into King's class III. These lines are numerous between λ 3000 and λ 3400. A pair at λλ 3759, 3761 and an isolated line at λ 3685 are also noteworthy. One line at λ 3349.41 is placed in class II and is the strongest *raie ultime* of the ionized atom. These persistent lines are heavily reversed in the spark, some symmetrically, while others are widened toward the red. The strongest of these are very conspicuous in the flash spectrum and rise to great heights in the chromosphere and even in the prominences.

On beginning the analysis it was found that the strongest symmetrically reversed lines, including the *raies ultimes*, belong to multiplets arising from transitions from a $^4F'$ term to a triad of D′, F, and G′ terms of the quartet system. A second $^4F'$ term, less than 1000 units higher, combines with the same triad, giving those lines which are unsymmetrically reversed in the spark. Two $^4P'$ terms close together were found later, which combine with the $^4D'$ term already mentioned to give multiplets in the violet, and with a new triad $^4S'$ ^4P $^4D'$, giving strong groups in the region λ 3100–λ 3300.

Numerous doublet terms are also present. A start in analyzing these was obtained by the Zeeman effect, which led to the identification of skew-symmetrical groups of types DD′, etc. It soon appeared that there is an important term with frequency separation 269.0, but the various combinations appeared to be inconsistent, some indicating that this was an F and others that it was a D term. The puzzle was solved by the recognition that there are two doublet terms with just this separation. The $^2F'$ term is the lowest in the doublet system and combines with a higher ^2F term to give the strong lines at λλ 3759, 3761. Its combination with the $^2D'$ term of identical separation (whose relative value was fixed by other combinations) led exactly to the very strong isolated line at λ 3685, which was thus found not to be a singlet, which would have no excuse for existence in a spectrum of even multiplicity, but an unresolvably close pair. The separation of this pair as calculated from the known separations of the terms involved can hardly exceed 0.002 A, and may be much less.

Many other doublet terms of all types from ^2S to ^2H were found, the combinations between these accounting for most of the outstanding strong lines. Numerous intercombinations between the doublet and quartet systems were also detected, and served to prove that the two $^4F'$ terms are the lowest in the whole scheme, and the $^2F'$ term the next.

A great many strong lines remaining in the region λ 3000–λ 2600 are hazy, but not reversed, in the spark, and appear faintly, if at all, in the arc. The most conspicuous of these were identified as combinations between the terms of the triad $^4D'$, ^4F, $^4G'$ and still higher terms of types ^4D, $^4F'$, ^4G, $^4H'$; and most of the rest, as similar combinations in the doublet system. Finally, several very high-

TABLE I

Ti II, Terms and Combinations

Type	Term	Combinations				
a^2S_1...	21338.00	a^2S'	a^2P	c^2P	a^4P	
		3	4	98	13	
$a^2P'_2$...	9975.92	a^2S'	a^2P	b^2P	a^2D'	b^2D'
	125.02	52	70	129	19	66
$a^2P'_1$...	9850.90	c^2D'	a^2F	b^2F	c^2F	a^4P
		124	17	75	140	101
		a^4D'	b^4D'			
		29	84			
$b^2P'_2$...	16625.25	a^2S'	a^2P	b^2P	c^2P	a^2D'
	109.46	14	33	64	136	2
$b^2P'_1$...	16515.79	b^2D'	c^2D'	d^2D'		
		31	58	139		
a^2D_3...	8744.27	a^2S'	a^2P	b^2P	a^2D'	b^2D'
	33.80	63	87	138	34	82
a^2D_2...	8710.47	c^2D'	d^2D'	a^2F	b^2F	c^2F
		135	157	28	92	143
		a^4S'	a^4P	b^4P	a^4D'	b^4D'
		94	112	161	37	99
		c^4D'	a^4F	a^4G'		
		154	25	15		
b^2D_3..	12758.15	a^2P	b^2P	a^2D'	b^2D'	c^2D'
	129.38	47	108	7	45	103
b^2D_2..	12628.77	d^2D'	a^2F	b^2F	c^2F	a^4D'
		152	5	50	122	10
		b^4D'				
		54				
c^2D_3...	25193.04	b^2P	c^2P	c^2D'	d^2D'	e^2D'
	231.70	11	56	9	59	156
c^2D_2...	24961.34	b^2F	c^2F	d^2F	e^2F	c^4D'
		1	26	118	158	49
$a^2F'_4$...	4897.60	a^2P	a^2D'	b^2D'	c^2D'	d^2D'
	268.99	125	48	120	150	163
$a^2F'_3$...	4628.61	a^2F	b^2F	a^2G'	b^2G'	a^4D'
		44	126	71	146	55
		b^4D'	c^4D'	a^4F	a^4G'	
		131	162	43	40	
$b^2F'_4$...	20891.88	b^2P	c^2D'	b^2F	c^2F	b^2G'
	−59.89	39	38	6	46	32
$b^2F'_3$...	20951.77					
$c^2F'_4$...	63444.76	a^2D'	a^2F	a^2G'		
	276.53	95	100	62		
$c^2F'_3$...	63168.23					
$d^2F'_4$...	65458.65	a^2D'	a^2F	a^4F		
	145.94	111	115	117		
$d^2F'_3$...	65312.71					

Type	Term	Combinations				
a^2G_5...	9118.15	a^2D'	b^2D'	a^2F	b^2F	a^2G'
	120.46	35	81	24	88	42
a^2G_4...	8997.69	b^2G'	a^2H	a^4F	a^4G'	
		121	137	23	12	
b^2G_5...	15257.53	b^2F	c^2F	d^2F	a^2G'	b^2G'
	−8.07	41	104	155	8	61
b^2G_4...	15265.60	a^2H				
		80				
c^2G_5...	67820.87	a^2F	a^2G'			
	216.67	132	110			
c^2G_4...	67604.20					
$a^2H'_6$...	12774.81	b^2F	a^2G'	b^2G'	a^2H	
	97.82	51	22	90	109	
$a^2H'_5$...	12676.99					
$b^2H'_6$..	68582.34	a^2G'				
	253.39	113				
$b^2H'_5$..	68328.95					
$a^4P'_3$...	9518.05	a^4S'	a^4P	b^4P	a^4D'	b^4D'
	122.29	83	107	160	36	93
$a^4P'_2$...	9395.76	a^4F	a^2S'	a^2P	b^2P	a^2D'
	32.05	18	57	78	134	27
$a^4P'_1$...	9363.71	b^2D'	c^2D'	a^2F		
		73	128	20		
$b^4P'_3$...	10024.74	a^4S'	a^4P	b^4P	a^4D'	b^4D'
	94.00	76	102	159	30	79
$b^4P'_2$...	9930.74	c^4D'	a^2S'	a^2P	a^2D'	b^2D'
	57.87	153	53	69	21	65
$b^4P'_1$...	9872.87	a^2F				
		16				
a^4D_4...	66996.67	a^4F				
	58.97	130				
a^4D_3...	66937.70					
	121.21					
a^4D_2...	66816.49					
	49.06					
a^4D_1...	66767.43?					
$a^4F'_5$...	393.22	a^4D'	b^4D'	c^4D'	a^4F	a^4G'
	167.75	106	151	164	85	68
$a^4F'_4$...	225.47	a^2D'	b^2D'	a^2F	b^2F	a^2G'
	131.53	97	147	89	149	119
$a^4F'_3$...	93.94					
	93.94					
$a^4F'_2$...	0.00					

TABLE I—*Continued*

Type	Term	Combinations				
$b^4F'_5$...	1215.58	a^4D'	b^4D'	a^4F	a^4G'	a^2D'
	128.37	96	148	74	60	86
$b^4F'_4$...	1087.21	b^2D'	a^2F	b^2F		
	103.41	142	77	144		
$b^4F'_3$...	983.80					
	75.84					
$b^4F'_2$...	907.96					
$c^4F'_5$...	62594.27	a^4D'	a^4F	a^4G'		
	184.69	72	91	105		
$c^4F'_4$...	62409.58					
	138.33					
$c^4F'_3$...	62271.25					
	91.23					
$c^4F'_2$...	62180.02					
$d^4F'_5$...	69081.35	a^4D'	b^4D'	a^4F	a^4G'	
	130.96	133	67	141	145	
$d^4F'_4$...	68950.39					
	105.25					
$d^4F'_3$...	68845.14					
	77.48					
$d^4F'_2$...	68767.66					
a^4G_6...	65241.60	a^4F	a^4G'			
	147.31	114	123			
a^4G_5...	65094.29					
	116.72					
a^4G_4...	64977.57					
	92.92					
a^4G_3...	64884.65					
$a^4H'_7$...	65589.10	a^4F	a^4G'			
	143.25	116	127			
$a^4H'_6$...	65445.85					
	138.40					
$a^4H'_5$...	65307.45					
	122.73					
$a^4H'_4$...	65184.72					
$a^2S'_1$...	37430.55	a^2S	a^2P'	b^2P'	a^2D	a^4P'
		3	52	14	63	57
		b^4P'				
		53				
a^2P_2...	39602.90	a^2S	a^2P'	b^2P'	a^2D	b^2D
	−71.74	4	70	33	87	47
a^2P_1...	39674.64	a^2F'	a^4P'	b^4P'		
		125	78	69		
b^2P_2...	45548.90	a^2P'	b^2P'	a^2D	b^2D	c^2D
	76.01	129	64	138	108	11
b^2P_1...	45472.89	b^2F'	a^4P'			
		39	134			
c^2P_2...	53128.17	a^2S	b^2P'	c^2D		
	6.69	98	136	56		
c^2P_1...	53121.48					
$a^2D'_3$...	32025.50	a^2P'	b^2P'	a^2D	b^2D	a^2F'
	269.00	19	2	34	7	48
$a^2D'_2$...	31756.50	c^2F'	d^2F'	a^2G	a^4P'	b^4P'
		95	111	35	27	21
		a^4F'	b^4F'			
		97	86			
$b^2D'_3$...	39476.87	a^2P'	b^2P'	a^2D	b^2D	a^2F'
	243.43	66	31	82	45	120
$b^2D'_2$...	39233.44	a^2G	a^4P'	b^4P'	a^4F'	b^4F'
		81	73	65	147	142
$c^2D'_3$...	44902.42	a^2P'	b^2P'	a^2D	b^2D	c^2D
	−12.38	124	58	135	103	9
$c^2D'_2$...	44914.80	a^2F'	b^2F'	a^4P'		
		150	38	128		
$d^2D'_3$...	53554.90	b^2P'	a^2D	b^2D	c^2D	a^2F'
	−41.80	139	157	152	59	163
$d^2D'_2$...	53596.70					
$e^2D'_3$...	69622.15	c^2D				
	294.83	156				
$e^2D'_2$...	69327.32					
a^2F_4...	31490.82	a^2P'	a^2D	b^2D	a^2F'	c^2F'
	283.38	17	28	5	44	100
a^2F_3...	31207.44	d^2F'	a^2G	c^2G	a^4P'	b^4P'
		115	24	132	20	16
		a^4F'	b^4F'			
		89	77			
b^2F_4...	40074.71	a^2P'	a^2D	b^2D	c^2D	a^2F'
	147.88	75	92	50	1	126
b^2F_3...	39926.83	b^2F'	a^2G	b^2G	a^2H'	a^4F'
		6	88	41	51	149
		b^4F'				
		144				
c^2F_4...	47466.80	a^2P'	a^2D	b^2D	c^2D	b^2F'
	−158.37	140	143	122	26	46
c^2F_3...	47625.17	b^2G				
		104				
d^2F_4...	59467.81	c^2D	b^2G			
	146.02	118	155			
d^2F_3...	59321.79					
e^2F_4...	70893.00	c^2D				
	286.65	158				
e^2F_3...	70606.35					

TABLE I—*Continued*

Type	Term	Combinations				
$a^2G'_5$...	34748.50	a^2F'	c^2F'	a^2G	b^2G	c^2G
	205.14	71	62	42	8	110
$a^2G'_4$...	34543.36	a^2H'	b^2H'	a^4F'		
		22	113	119		
$b^2G'_5$...	43780.99	a^2F'	b^2F'	a^2G	b^2G	a^2H'
	40.22	146	32	121	61	90
$b^2G'_4$...	43740.77					
a^2H_6...	45908.56	a^2G	b^2G	a^2H'		
	234.81	137	80	109		
a^2H_5...	45673.75					
$a^4S'_2$...	40027.28	a^4P'	b^4P'	a^2D		
		83	76	94		
a^4P_3...	42208.84	a^4P'	b^4P'	a^2S	a^2P'	a^2D
	139.99	107	102	13	101	112
a^4P_2...	42068.85					
	72.11					
a^4P_1...	41996.74					
b^4P_3...	56325.94	a^4P'	b^4P'	a^2D		
	76.83	160	159	161		
b^4P_2...	56249.11					
	25.98					
b^4P_1...	56223.13					
$a^4D'_4$...	32767.02	a^4P'	b^4P'	a^4F'	b^4F'	c^4F'
	69.08	36	30	106	96	72
$a^4D'_3$...	32697.94	d^4F'	a^2P'	a^2D	b^2D	a^2F'
	95.43	133	29	37	10	55
$a^4D'_2$...	32602.51					
	70.13					
$a^4D'_1$...	32532.38					
$b^4D'_4$...	40798.37	a^4P'	b^4P'	a^4F'	b^4F'	d^4F'
	216.57	93	79	151	148	67
$b^4D'_3$...	40581.80	a^2P'	a^2D	b^2D	a^2F'	
	156.00	84	99	54	131	
$b^4D'_2$...	40425.80					
	95.55					
$b^4D'_1$...	40330.25					
$c^4D'_4$...	52631.07	b^4P'	a^4F'	a^2D	c^2D	a^2F'
	159.59	153	164	154	49	162
$c^4D'_3$...	52471.48					
	12.50					
$c^4D'_2$...	52458.98					
	129.20					
$c^4D'_1$...	52329.78					
a^4F_5...	31300.92	a^4P'	a^4D	a^4F'	b^4F'	c^4F'
	187.31	18	130	85	74	91
a^4F_4...	31113.61	d^4F'	a^4G	a^4H'	a^2D	a^2F'
	154.91	141	114	116	25	43
a^4F_3...	30958.70	d^2F'	a^2G			
	122.18	117	23			
a^4F_2...	30836.52					
$a^4G'_6$...	30240.68	a^4F'	b^4F'	c^4F'	d^4F'	a^4G
	272.60	68	60	105	145	123
$a^4G'_5$...	29968.08	a^4H'	a^2D	a^2F'	a^2G	
	233.63	127	15	40	12	
$a^4G'_4$...	29734.45					
	190.08					
$a^4G'_3$...	29544.37					

lying terms were discovered, which combine with the low terms first mentioned to give multiplets occurring between λ 2450 and λ 1906, the shortest wave-length observed.

In all, 33 doublet terms and 17 quartet terms have been identified. They are listed in Table I. The term values are counted upward from the lowest energy-level, $a^4F'_2$, those of all the other terms being fixed by various combinations. The letters "a," "b," "c," are used simply to label the various terms of the same type and have no theoretical significance.

The combinations which have been observed between these terms are listed in Table I. They give rise in all to 87 multiplets belonging to the doublet system, 33 of the quartet system, and 44 intercombinations—164 in all. To facilitate reference, the numbers which have been assigned to the multiplets in Table II are inserted below the combinations in Table I; thus the combination a^2S-a^2S' gives multiplet number 3. It may be remarked that no less than 14 of these multiplets involve combinations between terms which differ by two units in the apparent azimuthal quantum number (Hund's L)—for example, a^2G-b^2D'. Such transitions are quite possible in the more complex spectra, but usually give faint lines. Figures 1 and 2 represent the relations of these terms. Owing to the complexity of the spectrum, the doublet and quartet terms are shown in separate diagrams. Those doublet terms, however, which combine with higher-lying quartet terms, are plotted on the quartet diagram, and vice versa, and the observed intercombinations are indicated by dotted lines.

4. TABLE OF LINES OF *Ti* II

To give all these multiplets in the conventional form would occupy far too much space, and it may suffice to list all the lines of *Ti* II in order of wave-length, and give the designations for those which have been classified. This is done in Table II. The first column indicates the source from which the wave-length is taken, the notation being explained at the end of the table; the second, the observed wave-length; and the third, the excess of this, in hundredths of an angstrom, above that computed from the term values of Table I. In the fourth and fifth columns are found the intensities of the lines in the arc and the condensed spark. As the previous data were very far from homogeneous, the intensities in the spark have been estimated anew on a uniform scale, upon original plates and enlargements of the spectrum of the condensed spark. Estimates of selected lines of all degrees of intensity, sufficient to fix the scale, were made by Mr. King, and, with these as standards, the remainder were observed by Miss Moore. These estimates represent the observable photographic intensity, and the values therefore tend to be low for the long and short wave-lengths. Lines barely visible on the plates are denoted by "tr." For lines which could not be seen there at all, the estimates of Exner and Haschek or, when necessary, of other observers, are entered in parentheses. The lines

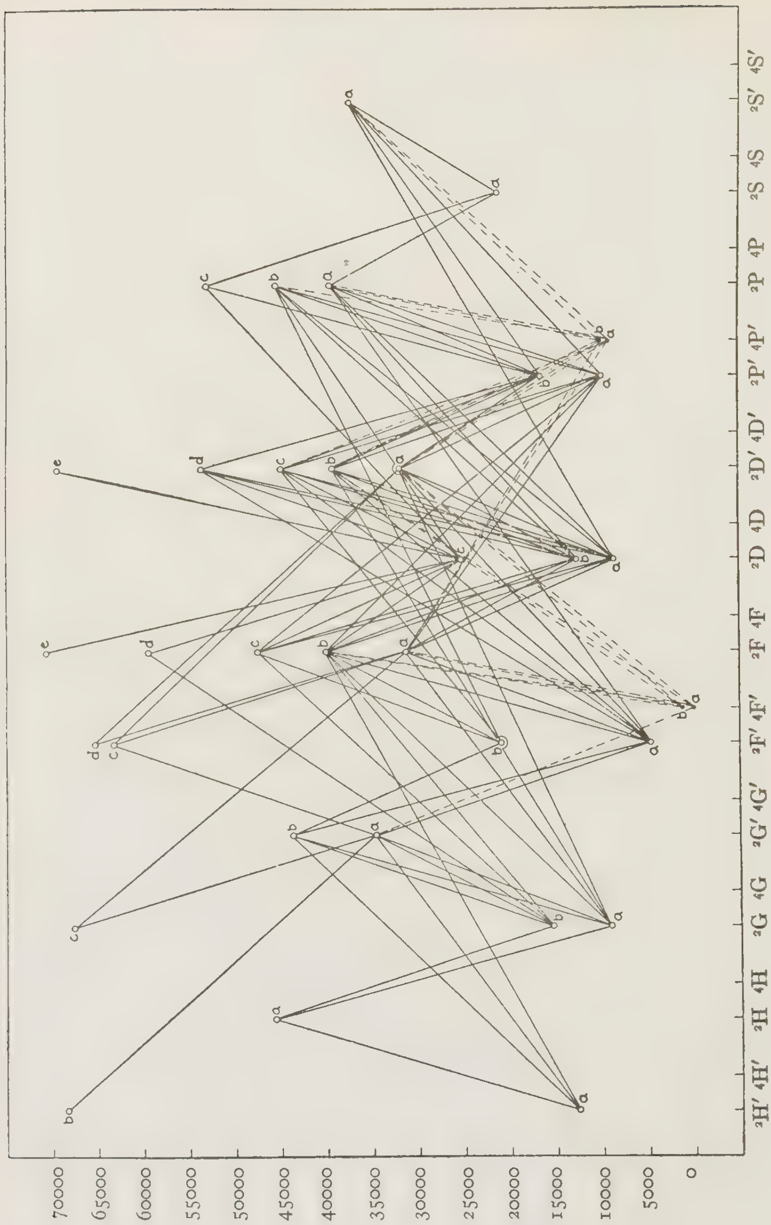

FIG. 1.—*Ti* II doublet combinations

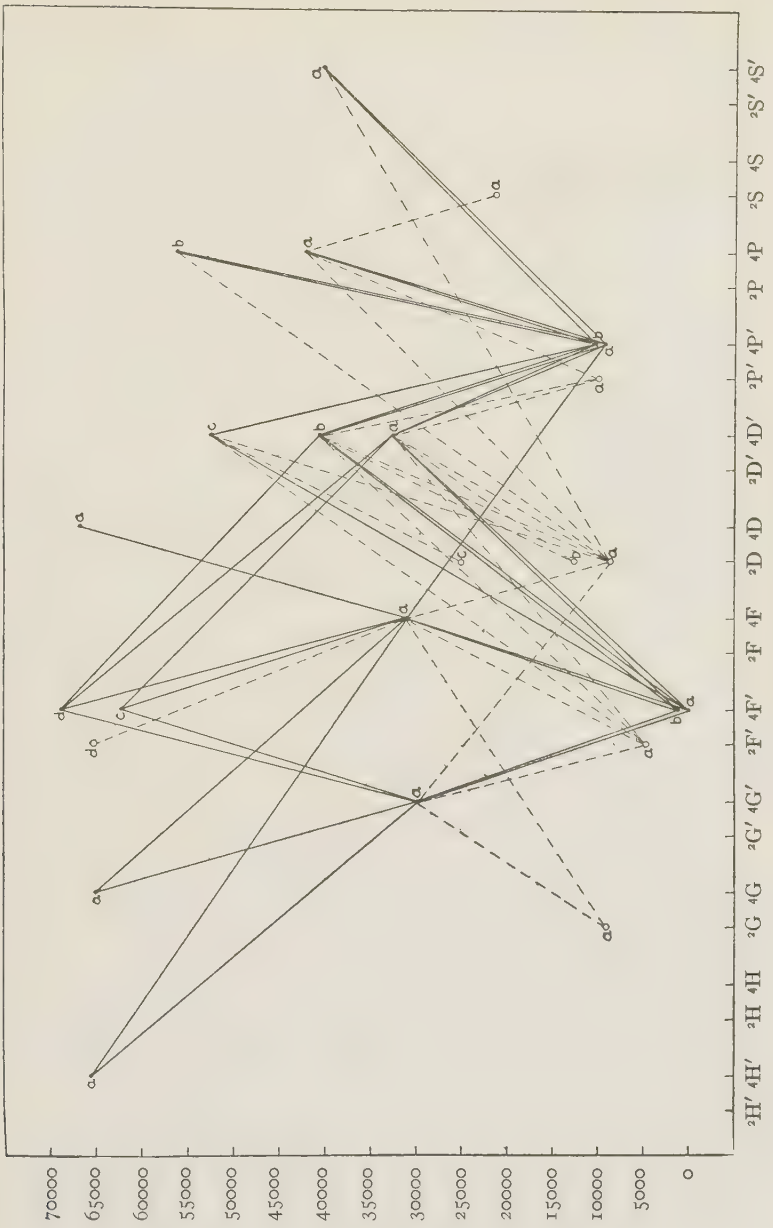

FIG. 2.—*Ti* II quartet combinations

for which the intensity is thus bracketed are faint, except for wavelengths less than 2400 A, for which the concave grating is at a disadvantage. The sixth column gives King's temperature classification, when available. The letter "r" denotes a line which is reversed in the spectrum of the condensed spark while "u" is added if the reversal is unsymmetrical. The seventh column contains the wave number *in vacuo*, ν, and the eighth, the identification of those lines which have been classified.

To facilitate identification of the various multiplets, the last column has been added. In this the multiplets are numbered in order of their position in the spectrum—that containing the first line on the list is numbered 1, and all other lines in this multiplet receive the same number, and so on.

All lines which are known to belong to the spectrum of *Ti* II and are of intensity greater than 3 on the scale here adopted, or 2 on Exner and Haschek's scale, are included in the table, and also all the fainter lines which have been classified. The unclassified lines are recognizable by the blanks in the last two columns. They number 31, and the strongest is of intensity 30, while the classified lines number 529, and run up to intensity 250.

There are many other faint unclassified lines which have been attributed to *Ti* II and in many cases probably belong to this spectrum. They may be found in tables in Kayser's *Handbuch.*

5. TEMPERATURE CLASSIFICATION

The relation between the temperature class and the level of origin is fully as conspicuous for enhanced lines as for the arc lines. This is very well illustrated by Table II.

Beginning with the lowest energy-level, a^4F', all the stronger lines which originate (in absorption) in this level are of temperature class IIIr (heavily reversed in the spark) and appear in the furnace at a temperature of about 2250°,[1] while the strongest line of all appears at 2000° and is of class II. Even the weakest lines in these multiplets, and many of the intersystem combinations originating in this level, appear in the furnace at 2600°, and are placed in class IV.

---

[1] A. S. King, *Mt. Wilson Contr.*, No. 274; *Astrophysical Journal*, **59**, 155, 1924.

TABLE II

Ti II, Identified Lines

Source	Obs. λ (I.A.)	Δλ O−C	Int. Arc	Int. Spark	Temp. Class	ν	Designation	Multiplet
4	6717.89	+ 7	......	(1u)	......	14881.52	$c^2D_3-b^2F_4$	1
2	6680.26	+ 6	......	(1)	......	14965.36	$c^2D_2-b^2F_3$	1
3	6559.58	+ 1	......	(1)	......	15240.68	$b^2P'_1-a^2D'_2$	2
3	6491.68	+ 7	......	(2)	......	15400.08	$b^2P'_2-a^2D'_3$	2
3	6212.29	− 3	......	(1)	......	16092.68	$a^2S_1-a^2S'_1$	3
1	5473.52	+ 6	......	(1)	......	18264.73	$a^2S_1-a^2P_2$	4
3	5452.02	− 3	......	(1)	......	18336.74	$a^2S_1-a^2P_1$	4
11	5418.77	+ 1	1	0	V	18449.26	$b^2D_3-a^2F_3$	5
3	5381.02	− 1	......	1	......	18578.69	$b^2D_2-a^2F_3$	5
11	5336.78	− 1	2	4	V	18732.70	$b^2D_3-a^2F_4$	5
3	5268.63	+ 1	......	1	......	18975.01	$b^2F'_3-b^2F_3$	6
3	5262.14	− 2	......	0	......	18998.41	$b^2D_3-a^2D'_2$	7
6	5226.56	0	3	5	V	19127.73	$b^2D_2-a^2D'_2$	7
3	5211.58	+ 3	......	0	......	19182.72	$b^2F'_4-b^2F_4$	6
6	5188.70	+ 1	4	6	V	19267.30	$b^2D_3-a^2D'_3$	7
11	5185.90	+ 2	......	2	......	19277.70	$b^2G_4-a^2G'_4$	8
3	5183.73	+ 1	......	tr	......	19285.78	$b^2G_5-a^2G'_4$	8
11	5154.07	− 1	......	0	......	19396.76	$b^2D_2-a^2D'_3$	7
11	5129.17	+ 1	......	1	......	19490.92	$b^2G_5-a^2G'_5$	8
11	5072.30	− 2	......	2	......	19709.44	$c^2D_3-c^2D'_3$	9
3	5069.12	− 1	......	tr	......	19721.81	$c^2D_3-c^2D'_2$	9
11	5013.69	− 2	......	tr	......	19939.85	$b^2D_3-a^4D'_3$	10
3	5010.21	− 6	......	tr	......	19953.70	$c^2D_2-c^2D'_2$	9
6	4911.19	− 3	......	0	......	20356.00	$c^2D_3-b^2P_2$	11
3	4873.95	+ 1	......	tr	......	20511.53	$c^2D_2-b^2P_1$	11
3	4865.62	+ 1	......	tr	......	20546.64	$a^2G_4-a^4G'_3$	12
3	4839.22	0	......	(1)	......	20658.74	$a^2S_1-a^4P_1$	13
6	4805.11	− 2	4	2	V	20805.38	$b^2P'_2-a^2S'_1$	14
3	4798.52	− 1	......	(2)	......	20833.96	$a^2D_2-a^4G'_3$	15
3	4779.99	+ 1	2	1	V	20914.71	$b^2P'_1-a^2S'_1$	14
3	4762.78	− 2	......	(1)	......	20990.29	$a^2D_3-a^4G'_4$	15
3	4719.51	− 1	......	(1)	......	21182.74	$b^4P'_3-a^2F_3$	16
3	4708.65	− 2	......	tr	......	21231.59	$a^2P'_2-a^2F_3$	17
11	4657.20	− 1	......	tr	......	21466.14	$b^4P'_3-a^2F_4$	16
3	4636.34	+ 5	......	(1)	......	21562.72	$a^4P'_2-a^4F_3$	18
6	4589.96	0	3	2	V	21780.60	$a^2P'_2-a^2D'_2$	19
3	4583.44	+ 2	......	(1)	......	21811.59	$a^4P'_2-a^2F_3$	20
3	4580.46	0	......	(1)	......	21825.78	$b^4P'_2-a^2D'_2$	21
6	4571.98	+ 2	15	50n	V	21866.26	$a^2H'_5-a^2G'_4$	22
3	4568.30	− 5	......	(1)	......	21883.87	$b^4P'_1-a^2D'_2$	21
6	4563.77	0	15	30	V	21905.60	$a^2P'_1-a^2D'_2$	19
6	4549.64	+ 1	25	60n	V	21973.64	$a^2H'_6-a^2G'_5$	22
3	4545.14	+ 2	......	tr	......	21995.38	$a^2G_5-a^4F_4$	23
3	4544.01	− 2	......	tr	......	22000.85	$b^4P'_3-a^2D'_3$	21
6	4533.97	0	20	30	V	22049.57	$a^2P'_2-a^2D'_3$	19
3	4529.46	− 1	1	1	V	22071.54	$a^2H'_5-a^2G'_5$	22
3	4524.72	+ 2	......	(1?)	......	22094.65	$b^4P'_2-a^2D'_3$	21
6	4501.27	0	25	40	V	22209.75	$a^2G_4-a^2F_3$	24
3	4493.52	+ 4	......	(1)	......	22248.05	$a^2D_2-a^4F_3$	25
6	4488.32	− 2	2	15	V	22273.84	$c^2D_3-c^2F_4$	26
6	4470.88	+ 1	2	tr	IV	22360.71	$a^4P'_2-a^2D'_2$	27
11	4469.15	− 1	1	tr	V	22369.37	$a^2D_3-a^4F_4$	25

TABLE II—*Continued*

Source	Obs. λ (I.A.)	Δλ O−C	Int. Arc	Int. Spark	Temp. Class	ν	Designation	Multiplet
6	4468.49	0	25	50	V	22372.67	$a^2G_5-a^2F_4$	24
6	4464.47	−1	2	1	V	22392.82	$a^4P'_1-a^2D'_2$	27
3	4456.62	−3	......	tr	....	22432.26	$c^2D_3-c^2F_3$	26
6	4450.49	0	4	10	V	22463.15	$a^2D_3-a^2F_3$	28
6‡	4444.56	0	1	1	V	22493.13	$a^2G_4-a^2F_4$	24
6	4443.80	0	25	50	V	22496.97	$a^2D_2-a^2F_3$	28
3	4432.1	+2	......	tr	....	22556.36	$a^2P'_2-a^4D'_1$	29
3	4421.95	+1	......	1	....	22608.14	$b^2P'_2-b^2D'_2$	31
11	4418.33	−1	1	1	V	22626.65	$a^2P'_2-a^4D'_2$	29
6	4417.71	+2	8	40	V	22629.84	$a^4P'_2-a^2D'_3$	27
3	4411.94	+2	......	(1)	....	22659.43	$b^4P'_1-a^4D'_1$	30
3	4411.10	+2	......	15	....	22663.75	$c^2D_2-c^2F_3$	26
3	4409.53	−1	......	tr	....	22671.82	$b^4P'_2-a^4D'_2$	30
5	4409.23	−3	......	tr	....	22673.36	$b^4P'_3-a^4D'_3$	30
6	4407.68	+3	......	1	....	22681.32	$a^2P'_1-a^4D'_1$	29
6	4399.77	−2	6	35	V	22722.10	$a^2P'_2-a^4D'_3$	29
3	4398.31	0	......	(1)	....	22729.65	$b^4P'_1-a^4D'_2$	30
6	4395.86	0	1	2	V	22742.30	$b^4P'_3-a^4D'_4$	30
6	4395.04	0	25	60	V	22746.55	$a^2D_3-a^2F_4$	28
11	4394.06	0	2	2	V	22751.63	$a^2P'_1-a^4D'_2$	29
11	4391.02	−4	......	tr	....	22767.39	$b^4P'_2-a^4D'_3$	30
11	4386.84	−1	......	10	....	22789.07	$b^2F'_3-b^2G'_4$	32
3	4374.82	−1	......	1	....	22851.68	$b^2P'_2-b^2D'_3$	31
11	4367.67	0	1	15	V	22889.09	$b^2F'_4-b^2G'_5$	32
11	4350.83	−1	......	1	....	22977.68	$b^2P'_2-a^2P_2$	33
6	4344.31	+1	3	2	V	23012.17	$a^2D_3-a^2D'_2$	34
6	4341.39	+3	2	1	V	23027.65	$a^2G_4-a^2D'_3$	35
6	4337.92	−1	10	50	V	23046.06	$a^2D_2-a^2D'_2$	34
3	4337.32	+3	......	(1)	....	23049.25	$b^2P'_2-a^2P_1$	33
11	4330.71	0	1	0	V	23084.44	$a^4P'_3-a^4D'_2$	36
3	4330.25	+4	......	0	....	23086.89	$b^2P'_1-a^2P_2$	33
6	4320.95	+1	1	1	V	23136.58	$a^4P'_2-a^4D'_1$	36
11	4316.80	+1	......	1	....	23158.81	$b^2P'_1-a^2P_1$	33
11	4314.98	+1	5	40	V	23168.59	$a^4P'_1-a^4D'_1$	36
6	4312.88	+1	7	35	V	23179.86	$a^4P'_3-a^4D'_3$	36
6	4307.89	+1	12	40	V	23206.72	$a^4P'_2-a^4D'_2$	36
6	4301.93	−1	5	15	V	23238.87	$a^4P'_1-a^4D'_2$	36
6	4300.05	−1	12	60	V	23249.02	$a^4P'_3-a^4D'_4$	36
6	4294.10	0	8	40	V	23281.24	$a^2D_3-a^2D'_3$	34
6	4290.23	−1	8	50	V	23302.24	$a^4P'_2-a^4D'_3$	36
11	4287.88	0	2	2	V	23315.01	$a^2D_2-a^2D'_3$	34
3	4190.29	+4	......	(1)	....	23858.01	$a^2D_3-a^4D'_2$	37
3	4184.33	+1	......	0	....	23891.98	$a^2D_2-a^4D'_2$	37
3	4173.55	0	3	1	V	23953.69	$a^2D_3-a^4D'_3$	37
6	4171.91	−1	5	30	V	23963.11	$b^2F'_3-c^2D'_2$	38
6	4163.65	−2	8	40	V	24010.64	$b^2F'_4-c^2D'_3$	38
3	4161.54	−1	2	1	V	24022.81	$a^2D_3-a^4D'_4$	37
3	4064.40	+3	......	(1)	....	24596.96	$b^2F'_3-b^2P_2$	39
3	4056.20	+1	......	(1)	....	24646.68	$a^2F'_4-a^4G'_3$	40
6	4053.84	+3	4	3	V	24661.03	$b^2G_4-b^2F_3$	41
6	4028.35	+2	5	7	V	24817.07	$b^2G_5-b^2F_4$	41
6	4025.13	−1	4	2	V	24836.93	$a^2F'_4-a^4G'_4$	40
6	4012.40	+1	10	4	V	24915.72	$a^2F'_3-a^4G'_3$	40
3	3982.01	0	......	tr	....	25105.87	$a^2F'_3-a^4G'_4$	40

TABLE II—*Continued*

Source	Obs. λ (I.A.)	Δλ O−C	Int. Arc	Int. Spark	Temp. Class	ν	Designation	Multi-plet
6	3932.02	+ 2	......	2	....	25425.05	$a^2G_5-a^2G'_4$	42
6	3913.45	− 1	18	60	V	25545.70	$a^2G_4-a^2G'_4$	42
6	3900.53	+ 1	20	70	V	25630.30	$a^2G_5-a^2G'_5$	42
6	3836.10	+ 5	1	1	V	26060.77	$a^2F'_4-a^4F_3$	43
3	3814.57	+ 1	......	4	....	26207.85	$a^2F'_3-a^4F_2$	43
6	3813.39	+ 1	2	2	IV?	26215.97	$a^2F'_4-a^4F_4$	43
3	3799.78	0	......	tr	....	26309.86	$a^2F'_4-a^2F_3$	44
3	3796.88	+ 2	......	2n	....	26329.96	$a^2F'_3-a^4F_3$	43
3	3776.04	0	......	6	....	26475.27	$b^2D_3-b^2D'_2$	45
3	3770.40	+ 2	......	(1)	....	26514.88	$b^2F'_3-c^2F_4$	46
3	3761.86	− 2	......	15	....	26575.07	$b^2F'_4-c^2F_4$	46
6	3761.33	0	40	200	IVr	26578.81	$a^2F'_3-a^2F_3$	44
6	3759.30	+ 1	40	200	IVr	26593.16	$a^2F'_4-a^2F_4$	44
6	3757.68	0	8	30	V	26604.64	$b^2D_2-b^2D'_2$	45
1	3748.01	+ 2	......	10	....	26673.27	$b^2F'_3-c^2F_3$	46
3	3741.63	0	8	50	Vru	26718.74	$b^2D_3-b^2D'_3$	45
3	3739.5	−10	......	tr	....	26733.97	$b^2F'_4-c^2F_3$	46
11	3724.08	+ 1	......	1	....	26844.66	$b^2D_3-a^2P_2$	47
3	3723.60	0	......	tr	....	26848.11	$b^2D_2-b^2D'_3$	45
6	3721.64	− 1	8	15	V	26862.26	$a^2F'_3-a^2F_4$	44
6	3706.22	+ 2	3	20	V	26974.02	$b^2D_2-a^2P_2$	47
3	3696.38	+ 1	......	(1)	....	27045.82	$b^2D_2-a^2P_1$	47
6*	3685.19	− 1 − 1	40	250	IVr	27127.94	$a^2F'_4-a^2D'_3$ $a^2F'_3-a^2D'_2$	48 48
9	3666.59	+ 5	......	(ou)	....	27265.56	$c^2D_3-c^4D'_2$	49
6	3662.22	0	4	40	V	27298.09	$b^2D_2-b^2F_3$	50
6	3659.75	+ 1	4	60	V	27316.50	$b^2D_3-b^2F_4$	50
9	3648.87	− 3	......	(0)	....	27397.97	$a^2H'_5-b^2F_4$	51
6	3641.33	− 1	10	100	V	27454.70	$a^2P'_2-a^2S'_1$	52
3	3627.70	− 2	......	(1)	....	27557.84	$b^4P'_1-a^2S'_1$	53
6	3624.84	+ 1	8	70	V	27579.59	$a^2P'_1-a^2S'_1$	52
3	3596.55	+ 7	......	tr	....	27796.52	$b^2D_2-b^4D'_2$	54
6	3596.05	− 1	10	60	V	27800.38	$a^2F'_4-a^4D'_3$	55
3	3593.11	+ 7	......	2	....	27823.13	$b^2D_3-b^4D'_3$	54
6	3587.13	− 1	4	12	V	27869.51	$a^2F'_4-a^4D'_4$	55
9	3578.70	0	......	(0)	....	27935.16	$c^2D_3-c^2P_2$	56
9	3576.37	− 4	......	(ou)	....	27953.35	$b^2D_2-b^4D'_3$	54
7	3573.72	− 2	6	20	V	27974.08	$a^2F'_3-a^4D'_2$	55
3	3566.00	+ 2	2	6	V	28034.64	$a^4P'_2-a^2S'_1$	57
3	3565.33	+ 4	......	3	....	28039.91	$b^2D_3-b^4D'_4$	54
3	3561.92	+ 1	1	1	V	28066.76	$a^4P'_1-a^2S'_1$	57
3	3561.59	0	2	3	V	28069.36	$a^2F'_3-a^4D'_3$	55
6	3535.40	− 1	10	40	V	28277.28	$b^2P'_2-c^2D'_3$	58
11	3533.85	− 2	......	2	....	28289.69	$b^2P'_2-c^2D'_2$	58
3	3524.85	− 1	......	tr	....	28361.92	$c^2D_3-d^2D'_3$	59
6	3520.25	0	8	20	V	28398.97	$b^2P'_1-c^2D'_2$	58
9	3513.08	+ 3	......	tr	....	28456.94	$b^4F'_4-a^4G'_3$	60
6	3510.84	+ 1	10	60	Vr	28475.09	$b^2G_4-b^2G'_4$	61
3	3509.85	+ 1	1	3	V	28483.13	$b^2G_5-b^2G'_4$	61
3	3505.91	+ 3	......	tr	....	28515.13	$b^2G_4-b^2G'_5$	61
6	3504.89	0	8	80	Vr	28523.43	$b^2G_5-b^2G'_5$	61
6	3500.33	0	4	2	IV	28560.59	$b^4F'_3-a^4G'_3$	60
3	3492.5	+ 3	......	3n	....	28624.62	$a^2G'_4-c^2F'_3$	62
6	3491.05	− 1	8	10	IIIru	28636.51	$b^4F'_2-a^4G'_3$	60

TABLE II—*Continued*

Source	Obs. λ (I.A.)	Δλ O−C	Int. Arc	Int. Spark	Temp. Class	ν	Designation	Multiplet
6	3489.74	0	4	2	IV	28647.26	$b^4F'_4-a^4G'_4$	60
3	3483.80	+2	......	4n	....	28696.09	$a^2G'_5-c^2F'_4$	62
6	3480.89	0	1	0	V	28720.09	$a^2D_2-a^2S'_1$	63
6	3477.18	−1	15	15	IIIru	28750.73	$b^4F'_3-a^4G'_4$	60
6	3476.99	+2	2	tr	V	28752.30	$b^4F'_5-a^4G'_5$	60
12	3465.58	+8	1	3	V	28846.97	$b^2P'_2-b^2P_1$	64
6	3461.50	−1	20	20	IIIru	28880.96	$b^4F'_4-a^4G'_5$	60
9	3459.01	−4	......	(0u)	....	28901.76	$a^2G'_4-c^2F'_4$	62
6	3456.40	+1	5	20	V	38923.58	$b^2P'_2-b^2P_2$	64
3	3452.42	+2	2	4	V	28956.92	$b^2P'_1-b^2P_1$	64
7	3444.31	0	15	30	IIIru	29025.10	$b^4F'_5-a^4G'_6$	60
3	3443.38	+2	......	1	....	29032.94	$b^2P'_1-b^2P_2$	64
3	3422.69	+3	......	(1)	....	29208.43	$b^4P'_3-b^2D'_2$	65
6	3416.95	0	3	2	IV	29257.50	$a^2P'_2-b^2D'_2$	66
9	3414.01	+3	......	(0)	....	29282.69	$b^4D'_4-d^4F'_5$	67
6	3409.80	+1	5	4	IV	29318.85	$a^4F'_4-a^4G'_3$	68
6	3407.20	0	4	3	IV	29341.23	$a^4F'_5-a^4G'_4$	68
3	3404.09	+3	......	(1)	....	29360.27	$b^4P'_1-b^2D'_2$	65
6	3402.42	+1	3	8	V	29382.44	$a^2P'_1-b^2D'_2$	66
6	3394.57	+1	15	40	IIIr	29450.38	$a^4F'_3-a^4G'_3$	68
6	3388.75	0	2	8	V	29500.97	$a^2P'_2-b^2D'_3$	66
6	3387.83	0	15	50	IIIr	29508.97	$a^4F'_4-a^4G'_4$	68
6	3383.76	−1	40	125	IIIr	29544.47	$a^4F'_2-a^4G'_3$	68
6	3380.28	0	15	30	IIIr	29574.88	$a^4F'_5-a^4G'_5$	68
11	3379.92	+1	......	1n	....	29578.03	$b^4P'_3-a^2P_2$	69
6	3374.34	0	2	8	V	29626.95	$a^2P'_2-a^2P_2$	70
6	3372.80	0	30	100	IIIr	29640.47	$a^4F'_3-a^4G'_4$	68
6	3372.20	0	5	10?	V	29645.74	$a^2F'_4-a^2G'_4$	71
12	3369.67	+8	......	0n	....	29668.00	$a^4D'_2-c^4F'_3$	72
6	3369.20	0	2	2	V	29672.14	$b^4P'_2-a^2P_2$	69
6†	3366.17	−1	5	8	III	29698.84	$a^2P'_2-a^2P_1$	70
3	3364.86	+14	......	1n	....	29710.41	$a^4D'_3-c^4F'_4$	72
3	3362.66	+2	......	1	....	29729.85	$b^4P'_1-a^2P_2$	69
6	3361.22	0	40	125	IIIr	29742.58	$a^4F'_4-a^4G'_5$	68
6	3352.06	−1	1	5	V	29823.86	$a^2P'_1-a^2P_1$	70
3	3351.66	−2	......	1n	....	29827.42	$a^4D'_4-c^4F'_5$	72
7†	3350.53	+2	......	1	....	29837.47	$a^4P'_2-b^2D'_2$	73
6	3349.41	0	40	125	IIr	29847.46	$a^4F'_5-a^4G'_6$	68
6	3349.02	0	20	75	IIIr	29850.93	$a^2F'_4-a^2G'_5$	71
6	3348.82	0	5	10?	III	29852.71	$b^4F'_3-a^4F_2$	74
6	3346.72	0	7	15	III	29871.45	$b^4F'_4-a^4F_3$	74
6	3343.76	+2	6	10	III	29897.88	$b^4F'_5-a^4F_4$	74
6†	3341.87	0	50	100	IIr	29914.79	$a^2F'_3-a^2G'_4$	71
6	3340.33	0	15	35	IIIru	29928.59	$b^4F'_2-a^4F_2$	74
3	3337.79	−5	2	2	V	29951.35	$a^2P'_2-b^2F_3$	75
3	3336.98	+2	......	tr	....	29958.63	$a^4P'_3-b^2D'_3$	73
6	3335.19	+2	20	40	IIIru	29974.71	$b^4F'_3-a^4F_3$	74
6	3332.10	0	8	30	Vr	30002.50	$b^4P'_3-a^4S'_2$	76
6	3329.45	0	20	70	IIIru	30026.39	$b^4F'_4-a^4F_4$	74
6	3326.76	+1	5	20	IIIru	30050.66	$b^4F'_2-a^4F_3$	74
6	3322.93	+1	20	75	IIIru	30085.29	$b^4F'_5-a^4F_5$	74
6	3321.70	+1	6	25	IVr	30096.44	$b^4P'_2-a^4S'_2$	76
3	3319.08	0	......	(1)	....	30120.19	$b^4F'_4-a^2F_3$	77
6	3318.01	−1	8	10	IIIru	30129.91	$b^4F'_3-a^4F_4$	74

TABLE II—*Continued*

Source	Obs. λ (I.A.)	Δλ O−C	Int. Arc	Int. Spark	Temp. Class	ν	Designation	Multiplet
6.......	3315.32	+1	4	10	V	30154.35	$b^4P_1'-a^4S_2'$	76
6.......	3308.79	−2	8	8	IIIru	30213.86	$b^4F_4'-a^4F_5$	74
3.......	3307.72	0	......	tr	....	30223.64	$b^4F_3'-a^2F_3$	77
3.......	3306.04	+2	......	tr	....	30238.98	$a^4P_1'-a^2P_2$	78
6.......	3302.09	+1	2	0	V	30275.16	$b^4F_5'-a^2F_4$	77
3.......	3298.20	+1	......	(1)	....	30310.87	$a^4P_1'-a^2P_1$	78
6.......	3288.58	0	3	5	IV	30399.53	$b^4P_2'-b^4D_1'$	79
6.......	3288.42	0	2	5	V	30401.02	$b^4P_3'-b^4D_2'$	79
6.......	3288.13	−1	3	on	IV	30403.71	$b^4F_4'-a^2F_4$	77
6.......	3287.64	−1	10	40	Vr	30408.24	$b^2G_4-a^2H_5$	80
3.......	3286.78	0	......	0..	....	30416.18	$b^2G_5-a^2H_5$	80
6.......	3282.32	−1	8	25	Vr	30457.51	$b^4P_1'-b^4D_1'$	79
6.......	3279.98	+1	3	4	V	30479.23	$a^2G_4-b^2D_3'$	81
6.......	3278.91	0	15	35	Vr	30489.18	$a^2D_3-b^2D_2'$	82
6.......	3278.28	0	10	30	Vr	30495.04	$b^4P_2'-b^4D_2'$	79
11.......	3276.98	−1	......	tr	....	30507.14	$b^4F_3'-a^2F_4$	77
6.......	3276.76	+1	4	5	V	30509.18	$a^4P_3'-a^4S_2'$	83
6.......	3275.28	0	2	3	V	30522.97	$a^2D_2-b^2D_2'$	82
6.......	3272.06	−1	10	25	Vr	30553.01	$b^4P_1'-b^4D_2'$	79
6.......	3271.63	0	10	25	Vr	30557.02	$b^4P_3'-b^4D_3'$	79
3.......	3269.75	+3	......	(1)	....	30574.59	$a^2P_1'-b^4D_2'$	84
3.......	3266.41	0	......	(1)	....	30605.85	$a^2P_2'-b^4D_3'$	84
6.......	3263.68	+1	2	4	V	30631.44	$a^4P_2'-a^4S_2'$	83
6*......	3261.59	−1 0	25	60	Vr	30651.09	$b^2G_5-a^2H_6$ $b^4P_2'-b^4D_3'$	80 79
6†......	3260.26	0	3	3	III	30663.59	$a^4P_1'-a^4S_2'$	83
6.......	3254.23	0	20	30	IIIr	30720.41	$a^4F_5'-a^4F_4$	85
6.......	3252.85	−2	25	40	IIIr	30733.43	$a^4F_4'-a^4F_3$	85
6.......	3251.89	+1	20	30	IIIr	30742.51	$a^4F_3'-a^4F_2$	85
6.......	3249.37	+1	2	2	V	30766.34	$a^2D_2-b^2D_3'$	82
6.......	3248.60	0	15	50	IIIr	30773.63	$b^4P_3'-b^4D_4'$	79
6.......	3241.97	−1	40	60	IIIr	30836.58	$a^4F_2'-a^4F_2$	85
3.......	3240.72	+1	......	1	....	30848.48	$b^4F_2'-a^2D_2'$	86
6.......	3239.65	0	8	30	Vr	30858.65	$a^2D_3-a^2P_2$	87
6.......	3239.03	+2	40	60	IIIr	30864.56	$a^4F_3'-a^4F_3$	85
6.......	3236.57	+1	50	70	IIIr	30888.02	$a^4F_4'-a^4F_4$	85
6.......	3236.10	−1	8	20	Vr	30892.50	$a^2D_2-a^2P_2$	87
6.......	3234.52	+1	60	75	IIIr	30907.60	$a^4F_5'-a^4F_5$	85
6.......	3232.26	−1	8	30	IVru	30929.21	$a^2G_4-b^2F_3$	88
6.......	3231.30	−1	6	4	III	30938.40	$b^4F_4'-a^2D_3'$	86
6.......	3229.40	0	10	35	Vru	30956.59	$a^2G_5-b^2F_4$	88
6.......	3229.18	0	15	40	IIIr	30958.70	$a^4F_2'-a^4F_3$	85
6.......	3228.59	−2	10	30	Vr	30964.37	$a^2D_2-a^2P_1$	87
6.......	3226.76	+1	5	2	IV	30981.92	$a^4F_4'-a^2F_3$	89
6.......	3224.23	−1	8	35	Vru	31006.23	$a^2H_6'-b^2G_5'$	90
6.......	3222.82	−1	15	35	IIIr	31019.79	$a^4F_3'-a^4F_4$	85
3.......	3220.48	−7	......	1	....	31042.34	$b^4F_3'-a^2D_3'$	86
6.......	3218.25	−1	8	25	IVru	31063.84	$a^2H_5'-b^2G_4'$	90
6.......	3217.04	−1	15	30	IIIr	31075.52	$a^4F_4'-a^4F_5$	85
6.......	3214.76	0	6	4	IV	31097.57	$a^4F_5'-a^2F_4$	89
3.......	3214.12	+2	......	1	....	31103.76	$a^2H_5'-b^2G_5'$	90
12.......	3213.59	−2	......	tr	....	31108.88	$a^4F_5-c^4F_4'$	91
6†......	3213.14	+3	8	1	III	31113.25	$a^4F_3'-a^2F_3$	89
3.......	3208.6	+4	......	1n	....	31157.27	$a^4F_4-c^4F_3'$	91

TABLE II—*Continued*

Source	Obs. λ (I.A.)	Δλ O−C	Int. Arc	Int. Spark	Temp. Class	ν	Designation	Multiplet
3	3206.00	0	......	1	....	31182.54	$a^2D_3-b^2F_3$	92
6	3203.42	− 2	4	3	IV	31207.65	$a^4F'_2-a^2F_3$	89
6	3202.52	− 1	12	40	Vr	31216.42	$a^2D_2-b^2F_3$	92
6	3197.51	0	4	2	IV	31265.32	$a^4F'_4-a^2F_4$	89
12	3195.99	+ 1	......	tr	....	31280.20	$a^4P'_3-b^4D'_4$	93
6	3195.71	+ 1	2	3	V	31282.93	$a^2D_3-a^4S'_2$	94
3	3194.77	......	......	6n?	....	31292.13	....	.....
3	3194.55	−10	......	8n?	....	31294.29	$a^4F_5-c^4F'_5$	91
3	3194.25	−13	......	5n?	....	31297.23	$a^4F_4-c^4F'_4$	91
3	3192.67	− 2	......	4n	....	31312.71	$a^4F_3-c^4F'_3$	91
12	3192.26	+ 1	......	2	....	31316.73	$a^2D_2-a^4S'_2$	94
6	3190.87	+ 1	20	30	IVr	31330.39	$a^2D_3-b^2F_4$	92
3	3189.52	− 1	......	5n	....	31343.64	$a^4F_2-c^4F'_2$	91
12	3184.09	− 2	......	2	....	31397.09	$a^4F'_3-a^2F_4$	89
3	3182.57	− 4	......	6n	....	31412.09	$a^2D'_2-c^2F'_3$	95
3	3181.82	− 2	......	8n	....	31419.50	$a^2D'_3-c^2F'_4$	95
3	3180.23	− 5	......	2n	....	31435.20	$a^4F_2-c^4F'_3$	91
3	3178.62	− 2	......	3n	....	31451.12	$a^4F_3-c^4F'_4$	91
3	3175.67	3	......	2n	....	31480.34	$a^4F_4-c^4F'_5$	91
3	3174.81	......	......	5	....	31488.86	....	.....
6	3168.52	+ 1	30	40	IIIru	31551.37	$b^4F'_5-a^4D'_4$	96
3	3164.89	......	......	8	....	31587.56	....	.....
6	3162.56	− 1	25	35	IIIru	31610.82	$b^4F'_4-a^4D'_3$	96
6	3161.76	− 1	20	30	IIIru	31618.83	$b^4F'_3-a^4D'_2$	96
6	3161.19	− 1	20	25	IIIru	31624.53	$b^4F'_2-a^4D'_1$	96
6	3157.39	0	2	2	IV	31662.59	$a^4F'_3-a^2D'_2$	97
6	3155.65	− 2	10	12	IVru	31680.05	$b^4F'_4-a^4D'_4$	96
6	3154.18	− 3	10	12	IVru	31694.81	$b^4F'_2-a^4D'_2$	96
6	3152.24	− 2	12	15	IVru	31714.31	$b^4F'_3-a^4D'_3$	96
6	3148.03	− 2	12	12	IV	31756.73	$a^4F'_2-a^2D'_2$	97
12	3145.38	0	......	0	(V)	31783.48	$a^2S_1-c^2P_1$	98
6	3144.72	0	2	1	V	31790.14	$a^2S_1-c^2P_2$	98
6	3143.75	+ 1	10	10	IV	31799.94	$a^4F'_4-a^2D'_3$	97
3	3136.75	+ 4	....	tr	....	31870.92	$a^2D_2-b^4D'_3$	99
7†	3130.81	+ 2	15?	15	IV	31931.39	$a^4F'_3-a^2D'_3$	97
6†	3128.64	+ 4	8	10n	IV	31953.53	$a^2F_4-c^2F'_4$	100
7†	3127.90	− 3	5	10n	IV	31961.09	$a^2F_3-c^2F'_3$	100
7	3122.10	+ 3	......	2	....	32020.47	$a^2P'_2-a^4P_1$	101
6	3121.60	− 1	2	1	V	32025.60	$a^4F'_2-a^2D'_3$	97
3	3119.80	0	5	15	V	32044.07	$b^4P'_3-a^4P_2$	102
3	3118.85	+ 3	......	2	....	32053.83	$a^2D_3-b^4D'_4$	99
6	3117.66	− 1	8	20	V	32066.07	$b^4P'_2-a^4P_1$	102
3	3115.09	+ 4	......	1	....	32092.52	$a^2P'_2-a^4P_2$	101
6	3112.05	0	3	10	V	32123.87	$b^4P'_1-a^4P_1$	102
7	3110.61	+ 4	4	20	IV	32138.74	$b^4P'_2-a^4P_2$	102
3	3110.11	+ 4	......	8	....	32143.90	$b^2D_3-c^2D'_3$	103
3	3108.93	+ 5	......	0	....	32156.10	$b^2D_3-c^2D'_2$	103
6	3106.23	0	10	35	Vr	32184.07	$b^4P'_3-a^4P_3$	102
6	3105.08	0	5	20	Vr	32195.97	$b^4P'_1-a^4P_2$	102
3	3104.60	+ 3	......	3	....	32200.94	$b^2G_4-c^2F_4$	104
6	3103.80	0	6	50	Vr	32209.25	$b^2G_5-c^2F_4$	104
3	3103.00	+ 4	......	2	....	32217.56	$a^2P'_1-a^4P_2$	101
3	3097.63	+ 2	......	1	....	32273.40	$b^2D_2-c^2D'_3$	103
6	3097.18	0	7	25	Vr	32278.09	$b^4P'_2-a^4P_3$	102

TABLE II—*Continued*

Source	Obs. λ (I.A.)	Δλ O−C	Int. Arc	Int. Spark	Temp. Class	ν	Designation	Multi-plet
3	3096.43	+1	......	2	....	32285.90	$b^2D_2-c^2D'_2$	103
12	3090.04	+7	......	8n	....	32352.82	$a^4G'_6-c^4F'_5$	105
6	3089.39	+1	6	15	Vr	32359.48	$b^2G_4-c^2F_3$	104
6	3088.03	+1	60	75	IIIr	32373.72	$a^4F'_5-a^4D'_4$	106
3	3081.58	0	......	5n	....	32441.48	$a^4G'_5-c^4F'_4$	105
6	3078.64	0	45	50	IIIr	32472.47	$a^4F'_4-a^4D'_3$	106
6	3075.22	0	40	40	IIIr	32508.58	$a^4F'_3-a^4D'_2$	106
6	3072.97	0	40	40	IIIr	32532.38	$a^4F'_2-a^4D'_1$	106
12	3072.54	−1	......	(on)	....	32536.93	$a^4G'_4-c^4F'_3$	105
6	3072.10	0	30	30	IIIr	32541.59	$a^4F'_4-a^4D'_4$	106
6	3071.23	0	4	15	V	32550.80	$a^4P'_3-a^4P_2$	107
6	3066.52	+2	3	3	IVr	32600.81	$a^4P'_2-a^4P_1$	107
6	3066.36	0	20	20	IVr	32602.50	$a^4F'_2-a^4D'_2$	106
6	3066.20	−2	30	30	IVr	32604.21	$a^4F'_3-a^4D'_3$	106
6	3063.48	−1	2	4	V	32633.16	$a^4P'_1-a^4P_1$	107
3	3063.26	+1	......	2	....	32635.50	$a^4G'_3-c^4F'_2$	105
6*	3059.73	0 −1	5	6 4	IV	32673.13	$a^4P'_2-a^4P_2$ $a^4F'_3-a^4D'_4$	107 106
6	3058.08	0	7	50	Vru	32690.77	$a^4P'_3-a^4P_3$	107
11	3057.43	+2	......	10	....	32697.73	$a^4F'_2-a^4D'_3$	106
6	3056.74	0	4	15	V	32705.10	$a^4P'_1-a^4P_2$	107
6	3048.77	+1	1	6	V	32790.61	$b^2D_3-b^2P_2$	108
6	3046.67	−1	5	30	V	32813.20	$a^4P'_2-a^4P_3$	107
3	3045.10	......	......	5n	....	32830.11	....	.....
6	3043.85	+5	1	5	V	32843.60	$b^2D_2-b^2P_1$	108
3	3038.71	−2	......	6	....	32899.15	$a^2H'_6-a^2H_5$	109
3	3036.78	+1	......	1	....	32920.04	$b^2D_2-b^2P_2$	108
6	3029.72	0	4	35	V	32996.77	$a^2H'_5-a^2H_5$	109
3	3023.88	+3	......	12	....	33060.49	$a^2G'_4-c^2G_4$	110
3	3022.83	+4	......	15	....	33071.97	$a^2G'_5-c^2G_5$	110
6	3017.18	−1	4	50	Vru	33133.91	$a^2H'_6-a^2H_6$	109
3	3008.33	+2	......	2	....	33231.38	$a^2H'_5-a^2H_6$	109
3†	2995.75	......	4	5	IV	33370.96	....	.....
3	2990.15	−2	......	10	....	33433.41	$a^2D'_3-d^2F'_4$	111
3	2987.38	+1	......	1	....	33464.41	$a^2D_3-a^4P_3$	112
3	2979.18	−3	......	10	....	33556.52	$a^2D'_2-d^2F'_3$	111
3	2977.78	......	......	7	....	33572.29	....	.....
3	2958.98	0	......	50	....	33785.59	$a^2G'_4-b^2H'_5$	113
3	2958.28	−2	......	2	....	33793.59	$a^4F_5-a^4G_5$	114
3	2954.76	0	......	60	....	33833.84	$a^2G'_5-b^2H'_6$	113
3	2952.10	−3	......	4	....	33864.32	$a^4F_4-a^4G_4$	114
3	2945.47	+1	......	50	....	33940.57	$a^4F_5-a^4G_6$	114
3	2943.12	2	......	12n	....	33967.65	$a^2F_4-d^2F'_4$	115
6§	2941.99	0	......	50	....	33980.69	$a^4F_4-a^4G_5$	114
3	2941.39	......	......	8n	....	33987.63	....	.....
3	2938.69	0	......	30	....	34018.84	$a^4F_3-a^4G_4$	114
3	2936.17	1	......	30	....	34048.05	$a^4F_2-a^4G_3$	114
3	2931.27	+3	......	40	....	34104.96	$a^2F_3-d^2F'_3$	115
3	2928.69	......	......	15	....	34135.01	....	.....
3	2927.87	3	......	2n	....	34144.57	$a^4F_5-a^4H'_6$	116
3	2926.75	1	......	10	....	34157.62	$a^4F_5-d^2F'_4$	117
6	2924.01	......	2	8	V	34189.63	....	.....
12	2923.65	0	......	tr	....	34193.83	$a^4F_4-a^4H'_5$	116
12	2920.79	−11	......	on	....	34227.32	$a^4F_3-a^4H'_4$	116

TABLE II—*Continued*

Source	Obs. λ (I.A.)	Δλ O−C	Int. Arc	Int. Spark	Temp. Class	ν	Designation	Multiplet
3	2918.77	+ 2	......	2n	....	34251.01	$a^2F_3-d^2F'_4$	115
3	2916.70	− 5	......	1	....	34275.31	$c^2D_3-d^2F_4$	118
3	2916.09	......	......	10	....	34282.48	....	......
3	2914.89	......	......	10	....	34305.78	....	......
3	2913.34	......	......	10	....	34314.85	....	......
10	2913.08	0	......	1	....	34317.91	$a^4F'_4-a^2G'_4$	119
3	2910.76	− 2	......	0n	....	34345.26	$a^4F_4-d^2F'_4$	117
6	2909.91	0	1	7	V	34355.29	$a^4F'_5-a^2G'_5$	119
3	2909.45	− 2	......	1n	....	34360.73	$c^2D_2-d^2F_3$	118
3	2908.14	......	......	4n	....	34376.21	....	......
3	2906.69	......	......	20	....	34393.34	....	......
3	2901.94	− 2	......	0	....	34449.63	$a^4F'_3-a^2G'_4$	119
3	2895.81	+ 4	......	tr	....	34522.56	$a^4F'_4-a^2G'_5$	119
6	2891.05	− 1	3	15	V	34579.40	$a^2F'_4-b^2D'_3$	120
3	2890.59	......	......	8n	....	34584.90	....	......
6	2888.92	− 1	2	15	V	34604.89	$a^2F'_3-b^2D'_2$	120
3	2888.62	......	......	10n	....	34608.48	....	......
6	2887.46	+ 2	1	2	V	34622.39	$a^2G_5-b^2G'_4$	121
6	2884.10	+ 1	7	70	V	34662.72	$a^2G_5-b^2G'_5$	121
3‡	2880.28	0	......	3	....	34708.70	$b^2D_3-c^2F_4$	122
6	2877.42	− 1	6	60	V	34743.18	$a^2G_4-b^2G'_4$	121
3	2875.79	......	......	10n	....	34762.88	....	......
3	2875.39	......	......	15n	....	34767.73	....	......
3‡	2874.08	− 2	......	2	....	34783.55	$a^2G_4-b^2G'_5$	121
3	2870.04	......	......	25n	....	34832.53	....	......
6	2868.73	− 1	2	15	V	34848.42	$a^2F'_3-b^2D'_3$	120
3	2868.29	− 1	......	0n	....	34853.78	$a^4G'_6-a^4G_5$	123
6	2862.31	− 1	4	30	V	34926.59	$a^2P'_2-c^2D'_3$	124
3	2861.99	......	......	20n	....	34930.49	....	......
6	2861.29	− 1	1	3	V	34939.04	$a^2P'_2-c^2D'_2$	124
3	2860.79	......	......	4n	....	34945.14	....	......
6	2858.40	0	1	8	V	34974.35	$a^2F'_3-a^2P_2$	125
3	2857.79	......	......	15	....	34981.82	....	......
3	2856.62	+ 2	......	2	....	34996.16	$b^2D_2-c^2F_3$	122
3	2856.24	+ 1	......	25	....	35000.81	$a^4G'_6-a^4G_6$	123
3	2855.49	− 4	......	1n	....	35010.00	$a^4G'_5-a^4G_4$	123
6	2853.92	0	2	10	V	35029.26	$a^2F'_4-b^2F_3$	126
6	2851.09	− 1	2	20	V	35064.02	$a^2P'_1-c^2D'_2$	124
3	2846.09	+ 5	......	15	....	35125.62	$a^4G'_5-a^4G_5$	123
3	2844.09	− 1	......	2n	....	35150.32	$a^4G'_4-a^4G_3$	123
6	2841.91	− 1	7	30	Vr	35177.28	$a^2F'_4-b^2F_4$	126
3‡	2839.70	+ 4	......	15	....	35204.67	$a^4G'_6-a^4H'_6$	127
3	2836.64	+ 4	......	15	....	35242.62	$a^4G'_4-a^4G_4$	123
3	2834.14	− 2	......	10	....	35273.73	$a^4G'_5-a^4G_6$	123
6	2832.16	− 1	5	20	V	35298.37	$a^2F'_3-b^2F_3$	126
3*	2828.89	+ 1 + 1	......	30n	....	35339.19	$a^4G'_3-a^4G_3$ $a^4G'_5-a^4H'_5$	123 127
6	2828.15	0	2	60	V	35348.42	$a^4G'_6-a^4H'_7$	127
3	2827.22	− 2	......	10	....	35360.06	$a^4G'_4-a^4G_5$	123
3	2821.41	+ 3	......	8	....	35432.87	$a^4G'_3-a^4G_4$	123
12	2820.36	......	1	4	V	35446.06	....	......
3	2819.99	− 4	......	8	....	35450.71	$a^4G'_4-a^4H'_4$	127
6	2817.84	0	(1)	60	....	35477.76	$a^4G'_5-a^4H'_6$	127
3	2815.57	+ 2	......	2	....	35506.35	$a^4P'_2-c^2D'_3$	128

TABLE II—*Continued*

Source	Obs. λ (I.A.)	Δλ O−C	Int. Arc	Int. Spark	Temp. Class	ν	Designation	Multiplet
3	2814.61	+ 5	......	tr	......	35518.46	$a^4P'_2-c^2D'_2$	128
3	2812.05	+ 2	......	1	......	35550.80	$a^4P'_1-c^2D'_2$	128
6	2810.28	− 2	1	50	V	35573.19	$a^4G'_4-a^4H'_5$	127
6	2806.41	− 2	1	5	V	35622.23	$a^2P'_1-b^2P_1$	129
3	2805.01	+ 3	(tr)	40	......	35640.01	$a^4G'_3-a^4H'_4$	127
3	2800.65	+ 2	......	30	......	35695.50	$a^4F_5-a^4D_4$	130
3	2790.62	+ 2	......	3n	......	35823.79	$a^4F_4-a^4D_3$	130
3	2788.00	+ 3	......	8	......	35857.46	$a^4F_3-a^4D_2$	130
3	2785.99	− 2	......	6n	......	35883.32	$a^4F_4-a^4D_4$	130
3	2784.67	+ 3	......	3	......	35900.32	$a^2F'_4-b^4D'_4$	131
3	2782.30	0	......	2n	......	35930.91	$a^4F_2-a^4D_1$	130
3	2780.55	− 2	......	5n	......	35953.51	$a^2F'_3-b^4D'_3$	131
3*	2778.48	− 3 − 10	......	2n	......	35980.31	$a^4F_2-a^4D_2$ $a^4F_3-a^4D_3$	130 130
3	2768.20	− 4	......	tr	......	36113.91	$a^2F_4-c^2G_4$	132
3	2765.65	0	......	0n	......	36147.21	$a^4D'_3-d^4F'_3$	133
3	2765.22	+ 2	......	0	......	36152.83	$a^4P'_2-b^2P_2$	134
3	2764.80	− 1	1	10	V	36158.33	$a^2D_3-c^2D'_3$	135
3	2764.3	+ 2	......	(1)	......	36164.87	$a^4D'_2-d^4F'_2$	133
3	2763.90	− 2	......	(1)	......	36170.08	$a^2F'_3-b^4D'_4$	131
12	2762.92	+ 3	......	(0n)	......	36182.92	$a^4D'_4-d^4F'_4$	133
3	2762.22	− 1	......	2	......	36192.11	$a^2D_2-c^2D'_3$	135
3	2761.29	0	(1)	7	......	36204.28	$a^2D_2-c^2D'_2$	135
3	2758.9	− 3	......	1n	......	36235.64	$a^4D'_1-d^4F'_2$	133
3	2758.35	− 2	......	2n	......	36242.87	$a^4D'_2-d^4F'_3$	133
12	2757.62	0	......	3n	......	36252.47	$a^4D'_3-d^4F'_4$	133
3	2752.85	− 7	......	4n	......	36315.27	$a^4D'_4-d^4F'_5$	133
3	2751.70	− 3	......	50n	......	36330.45	$a^2F_4-c^2G_5$	132
3	2746.70	+ 1	......	30n	......	36396.58	$a^2F_3-c^2G_4$	132
3†	2742.30	......	15	8n	III	36454.99	....	......
3	2738.7	0	......	3n	......	36502.90	$b^2P'_2-c^2P_2$	136
3*	2730.95	− 6	(tr)	6n?	......	36606.47	$b^2P'_1-c^2P_1$	136
3	2725.78	+ 1	(tr)	3	......	36675.91	$a^2G_4-a^2H_5$	137
3	2719.39	+ 2	(tr)	2	......	36762.09	$a^2D_2-b^2P_1$	138
3	2717.29	− 1	(tr)	3	......	36790.49	$a^2G_5-a^2H_6$	137
3	2716.20	− 5	(tr)	4	......	36805.24	$a^2D_3-b^2P_2$	138
3	2713.76	+ 1	......	(1)	......	36838.34	$a^2D_2-b^2P_2$	138
3	2707.05	0	......	0	......	36929.65	$b^2P'_2-d^2D'_3$	139
3	2698.52	......	......	30	......	37046.38	....	......
3	2695.97	− 4	......	0	......	37081.42	$b^2P'_1-d^2D'_2$	139
3*	2655.30	− 1 + 1	......	tr	......	37649.35	$a^2P'_2-c^2F_3$ $a^4F_5-d^4F'_4$	140 141
3	2646.08	− 1	......	50n	......	37780.52	$a^4F_5-d^4F'_5$	141
3	2642.15	0	(tr)	20n	......	37836.71	$a^4F_4-d^4F'_4$	141
3	2638.70	+ 2	......	10n	......	37886.18	$a^4F_3-d^4F'_3$	141
3	2635.60	+ 3	......	5n	......	37930.74	$a^4F_2-d^4F'_2$	141
3‖	2632.95	− 8	......	tr	......	37968.92	$a^4F_4-d^4F'_5$	141
3	2630.2	0	......	tr	......	38008.61	$a^4F_2-d^4F'_3$	141
3	2604.11	+ 2	......	(2)	......	38389.39	$b^4F'_4-b^2D'_3$	142
3	2581.73	+ 3	......	1	......	38722.15	$a^2D_3-c^2F_4$	143
3*	2573.91	− 1 − 1	......	tr	......	38839.79	$b^4F'_4-b^2F_3$ $a^4G'_6-d^4F'_5$	144 145
3	2573.72	+ 3	......	0	......	38842.65	$a^2F'_4-b^2G'_4$	146
7	2572.63	......	......	5	......	38859.11	....	......

TABLE II—*Continued*

Source	Obs. λ (I.A.)	Δλ O−C	Int. Arc	Int. Spark	Temp. Class	ν	Designation	Multiplet
7	2571.03	+1	(1)	20	......	38883.29	$a^2F'_4-b^2G'_5$	146
3	2568.98	+3	......	1	......	38914.31	$a^2D_2-c^2F_3$	143
3	2564.49	−1	......	1	......	38982.44	$a^4G'_5-d^4F'_4$	145
3	2555.98	0	(tr)	10	......	39112.22	$a^2F'_3-b^2G'_4$	146
3	2548.71	−3	......	tr	......	39223.77	$a^4G'_3-d^4F'_2$	145
3	2546.88	−4	......	tr	......	39251.96	$a^4F'_4-b^2D'_3$	147
7	2535.87	0	(1)	10	......	39422.36	$b^4F'_2-b^4D'_1$	148
7	2534.62	+1	(2)	20	......	39441.80	$b^4F'_3-b^4D'_2$	148
7	2531.25	+2	(2)	20	......	39494.31	$b^4F'_4-b^4D'_3$	148
3†	2529.86	+12	......	0	......	39516.00	$b^4F'_2-b^4D'_2$	148
3	2525.60	+1	(1)	30	......	39582.65	$b^4F'_5-b^4D'_4$	148
7	2524.63	+1	(tr)	8	......	39597.86	$b^4F'_3-b^4D'_3$	148
3	2519.79	−1	......	0	......	39673.92	$b^4F'_2-b^4D'_3$	148
3	2519.31	0	......	0	......	39681.48	$a^4F'_5-b^2F_4$	149
3	2518.06	+1	......	2	......	39701.17	$a^4F'_4-b^2F_3$	149
7	2517.43	0	......	2	......	39711.12	$b^4F'_4-b^4D'_4$	148
3	2510.90	+1	......	2	......	39814.38	$b^4F'_3-b^4D'_4$	148
3	2498.94	−1	......	(2)	......	40004.91	$a^2F'_4-c^2D'_3$	150
3	2481.49	0	......	(1)	......	40286.23	$a^2F'_3-c^2D'_2$	150
10	2478.77	−1	......	(1)	......	40330.41	$a^4F'_2-b^4D'_1$	151
3‖	2478.64	−4	(tr)	(5)	......	40332.52	$a^4F'_3-b^4D'_2$	151
3	2477.21	+3	......	(2)	......	40355.81	$a^4F'_4-b^4D'_3$	151
3	2474.22	+4	......	(2)	......	40404.58	$a^4F'_5-b^4D'_4$	151
3	2469.15	+2	......	(1)	......	40487.53	$a^4F'_3-b^4D'_3$	151
3	2464.00	+5	......	(1)	......	40572.15	$a^4F'_4-b^4D'_4$	151
12	2450.44	+1	(tr)	(6)	......	40796.64	$b^2D_3-d^2D'_3$	152
3	2447.92	−1	......	(2)	......	40838.64	$b^2D_3-d^2D'_2$	152
3	2442.67	−2	......	(2)	......	40926.39	$b^2D_2-d^2D'_3$	152
3	2440.21	+2	(tr)	(5)	......	40967.67	$b^2D_2-d^2D'_2$	152
3	2357.82	0	......	(2)	......	42399.07	$b^4P'_2-c^4D'_1$	153
3	2355.86	−1	......	(1)	......	42434.35	$b^4P'_3-c^4D'_2$	153
3	2355.17	0	......	(2)	......	42446.79	$b^4P'_3-c^4D'_3$	153
3	2354.61	0	......	(1)	......	42456.86	$b^4P'_1-c^4D'_1$	153
3	2354.12	......	......	(3)	......	42465.71	....	....
3	2350.67	+1	......	(2)	......	42528.04	$b^4P'_2-c^4D'_2$	153
3	2349.97	0	......	(3)	......	42540.69	$b^4P'_2-c^4D'_3$	153
3	2347.46	−1	......	(2)	......	42586.21	$b^4P'_1-c^4D'_2$	153
3	2346.35	0	......	(1)	......	42606.33	$b^4P'_3-c^4D'_4$	153
3	2342.31	......	......	(3)	......	42679.81	....	....
3	2341.23	......	......	(3)	......	42699.49	....	....
3	2334.54	......	......	(3)	......	42821.82	....	....
3	2291.85	0	......	(1)	......	43619.40	$a^2D_2-c^4D'_1$	154
3	2286.23	+3	......	(1)	......	43726.62	$a^2D_3-c^4D'_3$	154
3	2269.14	+1	......	(3)	......	44055.91	$b^2G_4-d^2F_3$	155
3	2265.13	+2	......	(1)	......	44133.90	$c^2D_3-e^2D'_2$	156
3	2261.64	+1	......	(1)	......	44201.98	$b^2G_4-d^2F_4$	155
3	2261.23	+1	......	(3)	......	44210.01	$b^2G_5-d^2F_4$	155
3	2253.26	−2	......	(2)	......	44366.37	$c^2D_2-e^2D'_2$	156
3	2250.09	+1	......	(2)	......	44428.85	$c^2D_3-e^2D'_3$	156
3	2238.39	−1	......	(1)	......	44661.07	$c^2D_2-e^2D'_3$	156
7	2231.04	......	......	(2)	......	44808.18	....	....
3	2230.95	+3	......	(1)	......	44809.98	$a^2D_3-d^2D'_3$	157
3	2229.25	+1	......	(1)	......	44844.18	$a^2D_2-d^2D'_3$	157
3	2228.85	+1	......	(1)	......	44852.21	$a^2D_3-d^2D'_2$	157

TABLE II—*Continued*

Source	Obs. λ (I.A.)	Δλ O−C	Int. Arc	Int. Spark	Temp. Class	ν	Designation	Multiplet
3	2227.14	−2	......	(2)	....	44886.64	$a^2D_2-d^2D_2'$	157
12	2201.31	0	......	(1)	....	45413.27	$c^2D_3-e^2F_3$	158
3	2190.13	0	......	(1)	....	45645.08	$c^2D_2-e^2F_3$	158
3	2187.50	0	......	(1)	....	45699.95	$c^2D_3-e^2F_4$	158
12	2162.68	0	......	(4)	....	46224.36	$b^4P_3'-b^4P_2$	159
12	2159.50	0	......	(3)	....	46292.42	$b^4P_2'-b^4P_1$	159
12	2159.09	0	......	(5)	....	46301.21	$b^4P_3'-b^4P_3$	159
12	2158.29	−1	......	(2)	....	46318.57	$b^4P_2'-b^4P_2$	159
12	2156.80	0	......	(1)	....	46350.36	$b^4P_1'-b^4P_1$	159
12	2155.58	−2	......	(4)	....	46376.59	$b^4P_1'-b^4P_2$	159
12	2154.70	−2	......	(4)	....	46395.53	$b^4P_2'-b^4P_3$	159
12	2139.25	+2	......	(0)	....	46730.57	$a^4P_3'-b^4P_2$	160
12	2135.73	+1	......	(1)	....	46807.57	$a^4P_3'-b^4P_3$	160
12	2134.84	+1	......	(0)	....	46827.09	$a^4P_2'-b^4P_1$	160
12	2133.63	−1	......	(00)	....	46853.64	$a^4P_2'-b^4P_2$	160
12	2133.36	−1	......	(0)	....	46859.57	$a^4P_1'-b^4P_1$	160
12	2132.20	+2	......	(0)	....	46885.06	$a^4P_1'-b^4P_2$	160
12	2130.15	0	......	(1)	....	46930.18	$a^4P_2'-b^4P_3$	160
12	2104.37	−2	......	(1)	....	47505.03	$a^2D_3-b^4P_2$	161
12	2101.28	0	......	(0)	....	47574.88	$a^2F_4'-c^4D_3'$	162
12	2054.54	+1	......	(3)	....	48657.04	$a^2F_4'-d^2D_3'$	163
12	2043.26	+3	......	tr	....	48925.62	$a^2F_3'-d^2D_3'$	163
12	2041.49	0	......	(3)	....	48968.03	$a^2F_3'-d^2D_2'$	163
8	1914.11	+9	......	(00)	....	52243.6	$a^4F_4'-c^4D_3'$	164
8	1911.01	+5	......	(0)	....	52328.4	$a^4F_2'-c^4D_1'$	164
8	1909.74	+11	......	(2)	....	52363.1	$a^4F_3'-c^4D_2'$	164
8	1909.33	+11	......	(2)	....	52374.4	$a^4F_3'-c^4D_3'$	164
8	1908.29	+10	......	(3)	....	52402.9	$a^4F_4'-c^4D_4'$	164
8	1906.30	+5	......	(3)	....	52457.7	$a^4F_2'-c^4D_2'$	164

NOTES TO TABLE II

Source

1. Crew, *Astrophysical Journal*, **60**, 108, 1924.
2. Eder und Valenta, in Kayser, *Handbuch der Spectroscopie*, **6**, 655, 1912.
3. Exner and Haschek, *ibid.*
4. Fiebig, *ibid.*
5. Hasselberg, *ibid.*
6. Kilby, *Astrophysical Journal*, **30**, 243, 1909.
7. King, *Mt. Wilson Contr.*, No. 274; *Astrophysical Journal*, **59**, 155, 1924, and unpublished material.
8. Lang, unpublished material.
9. Lohse, in Kayser, *Handbuch der Spectroscopie*, **6**, 655, 1912.
10. Miss Moore, unpublished material.
11. Rowland, in Kayser, *Handbuch der Spectroscopie*, **6**, 655, 1912.
12. Russell, unpublished material.

* Blend.

† Arc Blend.

‡ Error in λ corrected.

§ Strong reversed spark line coincides with arc line.

|| Displaced by blend.

TABLE IIa

LINES MASKING LINES OF *Ti* II

λ(I.A.)	Element	ν	Designation	Multiplet
4655.70	Ti	21473.06	$a^4P'_1-a^4F_2$	18
4629.34	Ti	21595.33	$a^4P'_3-a^4F_4$	18
4549.64	Ti^+	21973.64	$a^4P'_3-a^2F_4$	20
3491.05	Ti^+	28636.51	$c^2D_2-d^2D'_2$	59
3361.00	Ti	29744.53	$b^4P'_2-a^2P_1$	69
3354.64	Ti	29800.92	$b^4P'_1-a^2P_1$	69
3252.85	Ti^+	30733.43	$a^2D_3-b^2D'_3$	82
3248.60	Ti^+	30773.63	$b^4F'_3-a^2D'_2$	86
3234.52	Ti^+	30907.60	$a^4P'_3-b^4D'_2$	93
3218.25	Ti^+	31063.84	$a^4P'_3-b^4D'_3$	93
2810.28	Ti^+	35573.19	$a^2P'_2-b^2P_2$	129
2631.33	Fe^+	37992.27	$a^4F_3-d^4F'_4$	141
2555.98	Ti^+	39112.22	$a^4G'_4-d^4F'_3$	145

For the next level, b^4F', with excitation potential[1] 0.15 volt, the strongest lines are of class III and those of medium intensity often of class IV, and the faintest ones of class V—appearing in the arc but not in the furnace. For a^2F' (0.60 volt) the strong lines are of class IV and reversed in the spark, and the weaker ones of class V. Next come a^2D and a^2G (1.08 and 1.12 volts), for which the strongest lines are of class V; a few of them are reversed in the spark, while the weaker components of the multiplets appear in the spark alone. Substantially the same statement is true of all the following terms from a^4P' (1.18 volts) to b^2G (1.88), but the proportion of the fainter lines which appear in the arc at all tends to diminish. For b^2P' (2.05 volts) only the stronger lines appear in the arc, and the higher terms, b^2F' (2.58), a^2S (2.63), and c^2D (3.10) give very few lines which are not confined to the spark. Finally, the lines corresponding to transitions upward from the odd triad a^4D', a^4F, a^4G', and the corresponding doublet terms, for which the excitation potential ranges from 3.73 to 4.28 volts, though some of them are very strong in the spark, appear as mere traces, if at all, in heavy exposures to the arc.

---

[1] This term is to be understood here, as in the writer's "List of Ultimate and Penultimate Lines," as defining the energy required to raise an atom to the state in which it can absorb the lines in question. This is obviously the quantity which is of astrophysical importance. The excitation potential for emission of a line depends on the higher energy state involved and is much greater.

Temperature classification, therefore, is quite as important in analyzing a spark spectrum as it is for an arc spectrum. Additional stages in the classification—VI, VII, and so on—would be required to take care of the lines which appear feebly or not at all in the arc, and still further steps, based on a study of other sources, would lead up to more lines which appear only in the vacuum spark. The spectrum of titanium, which, in an easily observable region, contains lines of all degrees of difficulty of excitation up to the very refractory lines of *Ti* IV, would furnish excellent material for such an investigation.

6. ZEEMAN EFFECT

The magnetic resolutions of many titanium lines have been measured by King[1] and by Babcock (unpublished). A comparison of their results with the predictions of Landé's theory[2] is given in Table III. The first column gives the terms involved (without regard to which is at the higher energy-level); the second, the wave-length of the line; and the third and fourth, the observed displacements of the *p* and *n* components in the usual units. Babcock's values are distinguished by being given to three decimal places. When there are several *p* or *n* components, the strongest is printed in heavy type. The letters "w_1," "w_2," "w_3" denote numerically greater degrees of widening of an unresolved group of components.

The fifth and sixth columns give the theoretical pattern. When many close components are present, some of the intermediate ones are omitted, but the strongest ones are always given. The last two columns give the blended pattern which is likely to be observed when the group cannot be resolved. In deriving this, it has been assumed that the center of the unresolved group will appear to be one-fourth of the way from the strongest line toward the weakest. This rule closely approximates the results obtained by weighting the lines in proportion to their theoretical intensities.[3] In practice, it appears to represent about what is observed for a line of moderate intensity. For strong lines, the effective mean position may be expected, for

---

[1] *Publications of the Carnegie Institution of Washington*, No. 153, 36–43, 1912.

[2] *Zeitschrift für Physik*, **15**, 189, 1923.

[3] H. Hönl, *Zeitschrift für Physik*, **31**, 340, 1925.

TABLE III

ZEEMAN PATTERNS FOR *Ti* II

TERMS	λ	OBSERVED		THEORY*		BLEND	
		p	n	p	n	p	n
$^2S_1-{}^2P_1$	4780	0.699	1.353	0.67	1.33		
$^2S_1-{}^2P_2$	4805	.347	0.993	.33	1.00		
			1.70		1.67		
$^2P_1-{}^2P'_1$	4316	0	0.671	.00	0.67		
$^2P_1-{}^2P'_2$	4330	.271	1.479	.33	1.00		
					1.67		
$^2P_2-{}^2P'_2$	4350	0	1.26	.00	1.33		
		0.185					
$^2P_1-{}^2D_2$	4873	?	0.87	.07	0.73	0	0.84
	4563	0	.81		.87		
$^2P_2-{}^2D_2$	4590	0.84	0.48	.27	0.53	0.66w	1.03w
			1.05	.80	1.07		
			1.60		1.60		
	4421	.33	1.12w				
	3706	0.62	0.90w_1				
$^2P_2-{}^2D_3$	4911	w_1	1.10	.07	1.00	0	1.10
	4533	w_1	1.011w_1	.20	1.13		
	4374	0	1.022		1.26		
					1.40		
$^2D_2-{}^2D'_2$	5226	0	0.804	.00	0.80		
	5010	0	.86				
	4337	0	.810				
	3757	0	0.86				
$^2D_2-{}^2D'_3$	4344	0.182	1.443	.20	0.60	w	1.50w
		0.597	1.875	.60	1.00		
	4287	w_3	1.72w_2		1.40		
	3776	w_1	1.45		1.80		
$^2D_3-{}^2D'_3$	5188	0	1.202	.00	1.20		
	5072	0	1.20				
	4294	0	1.220				
	3741	0	1.15				
$^2D_2-{}^2F_3$	5381	0	0.936	.03	0.77	0	0.90
	4443	0	.923	0.09	.83		
	4411	0	.887		.89		
	4171	0	0.89		0.94		

* The theoretical patterns given in the fifth and sixth columns and the computed blends in the last two columns apply equally to all of the lines having the same multiplet designation as indicated in the first column. Leaders in the fifth and sixth columns indicate the omission of one or more components from the theoretical pattern.

TABLE III—*Continued*

Terms	λ	Observed		Theory*		Blend	
		p	*n*	*p*	*n*	*p*	*n*
${}^2D_3-{}^2F_3$......	4450	0.82	1.20	0.17	0.34	0.69	1.03
				.51	0.69		
				.86	**1.03**		
					1.37		
					1.71		
${}^2D_3-{}^2F_4$......	5336	0	1.086	**.03**	**1.00**	0	1.07
	4488	0	1.072	.09	1.06		
	4395	0	1.079	.14	....		
	4163	0	1.04		1.29		
${}^2D_3-{}^2F_4$ ${}^2D_2-{}^2F_3$....	3685	0	1.05			0	1.00
${}^2F_3-{}^2F'_3$.......	3761.3	0	0.90	.00	0.86		
	3748	0	0.83				
${}^2F_3-{}^2F'_4$.......	3721	w_2	1.53	**.14**	0.43	w	1.50 w
				.43	....		
				.71	1.57		
					1.86		
${}^2F_4-{}^2F'_4$.......	3759	0	1.25	0.00	1.14		
	3761.8	0	1.10				
${}^2F_3-{}^2G_4$......	4501	0	0.910	**.02**	0.80	0	0.93
	4386	0	.934	.05	.84		
	4053	0	0.87	.08	....		
					.97		
${}^2F_4-{}^2G_4$.......	4444	0.76	$0.98w_2$	.13	0.25	0.70w	1.02w
				.38	....		
				.63	**1.02**		
				.89	....		
					1.78		
${}^2F_4-{}^2G_5$......	4468	0	1.050	**.02**	**1.00**	0	1.05
	4367	0	1.047	.05	1.03		
	4028	0	1.02	.08	....		
				.11	1.22		
${}^2G_4-{}^2G'_4$......	5185	0	0.886	0	0.89		
${}^2G_5-{}^2G'_5$......	5129	0	1.145	0	1.11		
${}^2G_4-{}^2H_5$......	4572	0	0.94	**0.01**	0.84	0	0.95
				.03	.86		
				....	....		
				0.07	**0.98**		

TABLE III—*Continued*

TERMS	λ	OBSERVED		THEORY*		BLEND	
		p	n	p	n	p	n
$^2G_5-{}^2H_5$……	4529	$0.83w_1$	$1.07w_2$	0.10 .30 .50 .71 **.91**	0.20 …… **1.01** …… 1.82	0.71w	1.01w
$^2G_5-{}^2H_6$……	4549	0	1.051	**.01** .03 …… 0.09	**1.00** 1.02 …… 1.18	0	1.04
$^4P_1-{}^4D_1$……	4314	1.308	1.304	1.33	1.33		
$^4P_1-{}^4D_2$……	4398 4301	0.71 .717	0.46 .500	0.73	**0.47** 1.93		
$^4P_2-{}^4D_1$……	4320	.845	0.861 2.586	.87	0.87 **2.60**		
$^4P_2-{}^4D_2$……	4409 4307	.78 0.773	? 0.942 1.478 1.976	.27 **.80**	0.93 **1.47** 2.00		
$^4P_2-{}^4D_3$……	4290	w_3	$0.95w_2$	**.18** .54	**0.83** 1.19 1.55 1.91	w	1.10w
$^4P_3-{}^4D_2$……	4330	w_3	$2.14w_2$	**.20** .60	1.00 1.40 1.80 2.20	w	1.90w
$^4P_3-{}^4D_3$……	4409 4312	0.54 0.52	1.65 1.48	.11 .34 **.57**	1.03 1.26 **1.48** 1.71 1.94	0.46w	1.48w
$^4P_3-{}^4D_4$……	4395 4300	w_1 $0w_2$	1.18 $1.157w_2$	**.09** .26 .43	**1.00** 1.17 …… 1.86	w	1.21w
$^4P_1-{}^2D_2$……	4568 4464	0.86 0.88	? 0.00 1.68	.93	0.13 **1.73**		
$^4P_2-{}^2D_2$……	4470	1.40	0.39 1.18 2.22	0.47 **1.40**	0.33 **1.27** 2.20		

TABLE III—*Continued*

Terms	λ	Observed		Theory*		Blend	
		p	*n*	*p*	*n*	*p*	*n*
$^4P_2-{}^2D_3$......	4417	0.263 .797	0.356 .731 0.923 1.464	0.27 .80	0.40 0.93 1.47 2.00		
$^2P_1-{}^4D_2$......	4394	.225	1.451	.27	0.93 1.47		
$^2P_2-{}^4D_2$......	4418	0.253	1.275	.07 .20	1.13 1.27 1.40	0.17	1.27
$^2P_2-{}^4D_3$......	4399	0	1.383	.02 .06	1.32 1.35 1.39 1.43	0	1.40
$^2D_3-{}^4D'_3$......	4173	0.34	1.27	.09 .26 .43	0.94 1.11 1.29 1.46 1.63	0.35	1.29
$^2D_3-{}^4D'_4$......	4161	w_2	$1.75w_2$	.11 .34 .57	0.86 .... 1.77 2.00	0w	1.72w
$^2F_3-{}^4F'_2$.......	3814	w_2	1.34	.23 .69	0.63 1.08 1.54	0w	1.31w
$^2F_4-{}^4F'_3$.......	3836	w_1	1.42	.06 .17 .28	0.86 0.97 .... 1.43	0w	1.29w
$^2F_4-{}^4F'_4$.......	3813	w_1	1.22	.05 .14 .24 .33	0.90 .... 1.19 .... 1.48	0w	1.19w
$^2F_3-{}^4G_3$......	4012	0.64	$0.75w_2$	.14 .43 .71	0.14 .43 0.71 1.00 1.29	0.64w	0.71w
$^2F_4-{}^4G_4$......	4025	0.49	1.00	.08 .24 .40 0.56	0.59 .... 1.06 .... 1.54	0.48w	1.06w

obvious reasons, to be nearer the weakest component, and for weak lines, nearer the strongest.

The agreement between the observed and computed separations is, in almost all cases, within the error of observation. It affords what is probably the most comprehensive test of Landé's formulae for the case of a doublet system that can at present be made. The agreement is also excellent for the two quartet multiplets, and for the intercombinations, many of which show unusual and interesting Zeeman patterns. Further observations, especially in the ultraviolet, would be of value. The unresolved pair at λ 3685 would be especially interesting; but very high resolving power would be required to separate the components. The observed resolution agrees tolerably with the anticipated blend. The line λ 4417 shows an *n* component at 0.731, which is not accounted for, and probably belongs to some neighboring line.

The only real discordances are for λλ 4330 ($b^2P'_1-a^2P_2$), 4350 ($b^2P'_2-a^2P_2$), and 4421 ($b^2P'_2-b^2D'_2$). The observations of the first and third are complicated by adjacent lines; but it appears probable that the g values for a^2P_2 and $b^2D'_2$ are abnormal. These two terms have the same inner-quantum number and closely adjacent energy-levels, and may perturb one another, as in the case studied by Back[1] in calcium. The intensities of some of the combinations involving these terms are abnormal; for example, $b^2D_2-a^2P_2$ and $a^2D_3-b^2D'_2$ are the strongest lines in the corresponding multiplets, though they should be weak. The assumption that $g=1.21$ for a^2P_2 (instead of 1.33) gives the patterns (0.27), 0.93, **1.48** for λ 4330, and (0.07, **0.19**), 1.14, **1.27**, 1.40 for λ 4350.

The unresolved pattern for λ 4421 suggests that $b^2D'_2$ has a g value about 1.0 instead of 0.80; but the data are insufficient for a determination.

7. THEORETICAL INTERPRETATION OF THE OBSERVED TERMS

Hund's theory[2] of the relation of spectral lines to electronic configurations in the atom finds an admirable confirmation in this spectrum. In the first long period, the orbits[1] of lowest total quantum number which the valency electron can occupy are 4s, 4p, 3d, and 4f. From general considerations based on our knowledge of other spectra it appears that the 3d and 4s electrons will be bound most closely, and almost equally so, and next the 4p's, while the 4f's will be much more loosely held. The atomic configurations of lowest energy will therefore involve only 3d and 4s electrons, and will give rise to terms of the "even" set—S, P′, D, F′, etc. These terms will not combine with one another, but will combine freely with higher-lying "odd" terms S′, P, D′, F, etc., arising from configurations containing one 4p electron. These again will combine with still higher even terms, corresponding to configurations in which one of the electrons is raised to a 5s or 4d orbit. Configurations containing more highly excited electrons, or two 4p orbits, or a 4f orbit, are likely to have such high energy as to give rise either to faint lines or to lines in the Schumann region.

---

[1] *Zeitschrift für Physik*, **33**, 579, 1925.

[2] *Ibid.*, p. 345; **34**, 296, 1925.

The lines which are to be expected from the various electronic configurations are given in Table IV. The groups of terms which should arise from the addition of a third electron to each of the spectroscopic terms of *Ti* III[2] corresponding to a given arrangement of the first two electrons are listed separately; thus the addition of a 4p electron to the configuration which gives the $^3F'$ term of *Ti* III (the normal state of the corresponding ion) gives triads of D′, F, G′ terms in the quartet and doublet systems. The electron which is supposed then to be added is the last in order in the configuration given in the first column. For the configurations $(3d)^3$, where Pauli's restriction is operative, such an assignment of the terms to particular terms in *Ti* III is impracticable.

The observed terms which are believed to correspond to the various predictions of theory are given in the last column of Table IV. In some instances the identifications are immediate; thus the term a^2H' belongs to the same set as the lowest terms in the atom and is evidently even; and it can be assigned only to the configuration $(3d)^3$. Similarly, a^2S, which is also low and even, must belong to $(3d)^2 4s$, and the odd terms a^4S', a^4G', a^2H to $(3d)^2 4p$, in the positions in which they are placed.

---

[1] The use of this convenient term indicates no dissent from the later "wave" theory.

[2] *Mt. Wilson Contr.*, No. 337; *Astrophysical Journal*, 66, 25, 1927.

TABLE IV

PREDICTED AND OBSERVED TERMS IN *Ti* II

Configuration	Limit in *Ti* III	Predicted Terms	Observed Terms
$(3d)^3$.......	....	$^4P'$, $^4F'$,	a^4P', b^4F'
		$^2P'$, ^2D, $^2F'$; ^2G, $^2H'$, ^2D	a^2P', b^2D, b^2F'; a^2G, a^2H', —
$(3d)^2 4s$.....	a^3P'	$^4P'$	b^4P'
		$^2P'$	b^2P'
	a^3F'	$^4F'$	a^4F'
		$^2F'$	a^2F'
	a^1S	^2S	a^2S
	a^1D	^2D	a^2D
	a^1G	^2G	b^2G
$3d(4s)^2$......	a^3D b^1D	^2D	c^2D
$(3d)^2 4p$.....	a^3P'	$^4S'$, ^4P, $^4D'$	a^4S', a^4P, b^4D'
		$^2S'$, ^2P, $^2D'$	a^2S', b^2P, c^2D'
	a^3F'	$^4D'$, ^4F, $^4G'$	a^4D', a^4F, a^4G'
		$^2D'$, ^2F, $^2G'$	a^2D', a^2F, a^2G'
	a^1S	^2P	....
	a^1D	^2P, $^2D'$, ^2F	a^2P, b^2D', b^2F
	a^1G	^2F, $^2G'$, ^2H	c^2F, b^2G', a^2H
$3d \cdot 4s \cdot 4p$....	a^3D	^4P, $^4D'$, ^4F	b^4P, c^4D', —
		^2P, $^2D'$, ^2F	c^2P, d^2D', d^2F
	b^1D	^2P, $^2D'$, ^2F	—, e^2D', e^2F
$(3d)^2 5s$......	a^3P'	$^4P'$	....
		$^2P'$	....
	a^3F'	$^4F'$	c^4F'
		$^2F'$	c^2F'
	a^1S	^2S	....
	a^1D	^2D	....
	a^1G	^2G	....
$(3d)^2 4d$......	a^3P'	$^4P'$, ^4D, $^4F'$	—, —, —
		$^2P'$, ^2D, $^2F'$	—, —, —
	a^3F'	$^4P'$, ^4D, $^4F'$, ^4G, $^4H'$	—, a^4D, d^4F', a^4G, a^4H'
		$^2P'$, ^2D, $^2F'$, ^2G, $^2H'$	—, —, d^2F', c^2G, b^2H'
	a^1S	^2D	....
	a^1D	^2S, $^2P'$, ^2D, $^2F'$, ^2G	—, —, —, —, —
	a^1G	^2D, $^2F'$, ^2G, $^2H'$, ^2I	—, —, —, —, —

In most cases, however, alternative possibilities are open, and further evidence is needed for the assignment. This can be obtained in several ways: (*a*) The terms formed by the addition of a p electron to a given term of the "parent spectrum" of the next highest degree of ionization form triads (except when the parent term is an S term). The terms of a given triad usually, though not always, lie at about the same level. (*b*) The terms which are produced by adding another electron to the arrangement corresponding to a given parent term combine with one another to give strong multiplets, while combinations with terms of different parentage usually give much weaker lines. The reason for this is evident; in the first case a single electron "jumps" without any rearrangement in the rest of the atom; in the second, more or less rearrangement takes place, which is statistically much less probable. (*c*) If the electron jump increases the azimuthal quantum number l (e.g., from an s to a p orbit), the multiplet in which the azimuthal quantum number L increases will be the strongest (e.g., the transition from F to G) and that in which it decreases, the weakest (F to D). But if the electron decreases its l, the opposite is the case. This rule was communicated to the writer by Dr. Otto Laporte. Like the preceding one, it is an obvious consequence of the correspondence principle. (*d*) Terms produced by adding an electron of a given kind (e.g., 4p) to various parent terms are usually, though not always, situated at about the same relative levels as the parent terms.

The parent terms in *Ti* III, with their relative levels (measuring upward from the lowest level, and taking the component of highest inner-quantum number), are:

$(3d)^2$		$3d \cdot 4s$	
$a^3F'_4$	422	a^3D_3	38,425
a^1D_2	8473	b^1D_2	41,704
$a^3P'_2$	10,721		
a^1S_0	14,053?		
a^1G_4	14,398		

As for the strength of the combinations, Table V gives the estimated intensity of the strongest line in each of the multiplets resulting from the combination of the terms which head the corresponding row and column, and provides the necessary data.

Beginning with the quartet terms of *Ti* II, we find obvious triads of odd terms, a^4D', a^4F, a^4G' and a^4S', a^4P, b^4D', which evidently belong to $(3d)^2 4p$ and are produced by the addition of a 4p electron to a^3F' and a^3P', respectively. The average term values for the two

TABLE V

LINE INTENSITIES *Ti* II

d^2p	ds^2	d^2s							d^3							$d^2\cdot d$							$d^2\cdot s$	
	c^2D	b^4P'	a^4F'	a^2S	b^2P'	a^2D	a^2F'	b^2G	a^4P'	b^4F'	a^2P'	b^2D	b^2F'	a^2G	a^2H'	a^4D	d^4F'	a^4G	a^4H'	d^2F'	c^2G	b^2H'	c^4F'	c^2F'
a^4S'	.....	30r				3			5															
a^4P	.....	35r		(1)		1			50ru		2													
b^4D'	.....	50r	(4)			2	5n		tr	30	(1)	3					(0)							
a^4D'	.....	2	75r			1	60		60	40ru	35	tr					4n			.....	.....	.....	1n	
a^4F	.....		75r			tr	4		(1)	75ru				tr		30	50n	50	2n	10			8n?	
a^4G'	.....		125r			(2)	4			30ru				tr			1	25	60	.....	.....	.....	8	
a^2S'	.....	(1)		(1)	2	0			6		100													
b^2P	0	.....	.....		20	4			0		5	6	(1)											
c^2D'	2	.....	.....		40	10	(2)		2		30	8	40											
a^2P	*i*	2		(1)	1	30r	8		tr		8	20												
b^2D'	*i*	(1)	tr		1	35r	15		1	(2)	8	50ru		4										
b^2F	(1)		2			40r	30r	7		tr*	2	60	1	35ru	(0)									
a^2D'	*i*	tr	12		(2)	50	250r		40	4	30	6	*i*	1		.....	.....	.....	.....	10			.....	8n
a^2F	*i*	tr	4			60	200r		(1)	0	tr	4	*i*	50		.....	.....	.....	.....	40	50n		.....	10n
a^2G'	.....		7				75r	2	.....	.....			*i*	70	60n	.....	.....	.....	.....		15	60	.....	4n
c^2F	15	.....	.....			1		50r	.....	.....	tr*	3	15											
b^2G'	.....	.....	.....				20	80r	.....	.....			15	70	35ru									
a^2H	.....	.....	.....					40r	.....	.....				3	50ru									
dsp																								
b^4P	.....	(5)				(1)			(1)															
c^4D'	(ou)	(3)	(3)			(1)	(0)																	
c^2P	(0)	.....	.....	1	3n																			
d^2D'	tr	.....	.....		0	(2)	(3)		.....	.....		(6)												
d^2F	1	.....	.....					(3)																
e^2D'	(2)																							
e^2F	(1)																							

* = Blend   *i* = Too far to red.

triads are (roughly) 31,400 and 41,000; their difference is 9600, while $a^3P'-a^3F'$ is 10,300. The two remaining odd quartet terms, b^4P and c^4D', may be assigned with confidence to the triad of origin 3d·4s·4p. Their mean level, 54,400, is 23,000 higher than that of the lowest triad, while a^3D is 38,000 higher than a^3F', but this difference is not beyond the limits of probability. The multiplet $a^4F'-c^4D'$ was found near λ 1900 in a list of lines measured by Professor Lang. The ^4F term, which should give another but fainter multiplet near by, could not be identified.

Of the pair of low $^4F'$ terms, one must arise from $(3d)^3$ and the other from $(3d)^2 4s$; and the same is true of the $^4P'$ terms. It appears from Table V that a^4F' gives a stronger combination with a^4G' than with a^4D', and b^4F' the contrary; hence the former must be assigned to $(3d)^2 4s$ and the latter to $(3d)^3$. In the case of the $^4P'$ terms, the situation is reversed; the higher one, b^4P', combines strongly with b^4D', while the combination from the lower one gives very faint lines. The resulting assignment is confirmed by the fact that b^4P' gives a strong multiplet with b^4P, and a^4P' a weak one. In the former case the transition is from the configuration $(3d)^2 4s$ to 3d·4s·4p, and involves only the jump of a single electron; in the latter the transition is from $(3d)^3$, involving a double electron jump.

Of the high even quartet terms, a^4H' and a^4G can arise only from $(3d)^2 4d$. These terms combine strongly with the triad a^4D', a^4F, a^4G', and so must belong to the parent term a^3F. There can be no doubt that a^4D and the two high $^4F'$ terms also belong to this sub-group, the former and one of the latter arising from $(3d)^2 4d$, and the other $^4F'$ term from $(3d)^2 5s$. Since an electron jump from p to d usually gives stronger lines than one from p to s, the term d^4F', which gives the stronger multiplets, may be assigned to the first configuration, and c^4F' to the second. This is confirmed by the fact that c^4F' combines most strongly with the G' term of the triad, and d^4F' with the F term. The latter is what might be expected in combinations between a triad and a pentad of terms of common origin, as has recently been shown in *Sc* II.[1]

All the known quartet terms have now been accounted for. The low even terms are theoretically complete, and all but one of the intermediate odd terms have been found. Of the high even terms, only those derived from the lowest parent terms in *Ti* III have been detected, and, of these, one member of the pentad is missing—it should give the faintest combinations of the five. The terms derived from the other terms of *Ti* III might be expected to give fainter combinations, and it is not surprising that they have not been detected.

---

[1] Russell and Meggers, *Scientific Papers of the Bureau of Standards*, 22, 329 (No. 558), 1927.

The numerous doublet terms present a more complicated problem. Among the odd terms, however, three conspicuous triads are present, each of which combines with one of the low even terms to give strong reversed lines, thus: a^2D', a^2F, a^2G' combine with a^2F'; a^2P, b^2D', b^2F with a^2D; and c^2F, b^2G', a^2H with b^2G. This makes it evident that each of these groups arises from a common parent term in *Ti* III; and these must evidently be a^3F', a^1D, and a^1G, the low terms being of origin $(3d)^2 4s$ and the others coming from $(3d)^2 4p$. Only three more levels remain below 50,000; these are a^2S', b^2P, and c^2D', which fit the requirements of the fourth triad, of origin $(3d)^2 4p$ and parent term a^3P'. The mean levels of the leading components of these four triads are 32,755, 39,718, 45,719, and 42,627. Subtracting the levels of the parent terms in *Ti* III, we find 32,333, 31,246, 31,321, and 31,906—a striking confirmation of rule (*d*).

The remaining odd terms, c^2P, d^2D', d^2F; e^2D', e^2F, fall naturally into place as a complete and incomplete triad arising from $3d \cdot 4s \cdot 4p$, though the assignment—and even the reality—of c^2P is somewhat doubtful. The rest of the low even terms are now easy to place. The term a^2S must be assigned to $(3d)^2 4s$. Of the terms a^2P', b^2P', the former combines most strongly with the first member of the triad a^2S', b^2P, c^2D', and the latter with the last. This assigns b^2P' to $(3d)^2 4s$ and a^2P' to $(3d)^3$. The remaining low even terms must arise from $(3d)^3$ or $3d(4s)^2$. Of these c^2D, which lies at the highest level and combines strongly with e^2D', e^2F, may be assigned with confidence to the latter configuration. It is noteworthy that this term combines more strongly with the higher triad of origin $3d \cdot 4s \cdot 4p$, than with the lower one, and that this is also the case in *Sc* I. The remaining doublet terms go by default to $(3d)^3$. As may be seen from Table V, the intensities of their combinations with the odd terms are in general less than for the terms of origin $(3d)^2 4s$ and are more irregular.

The few even high doublet terms which are known combine with the triad of parentage a^3F' and obviously arise from the configurations $(3d)^2 5s$ and $(3d)^2 4d$. As in the case of the quartets, there are two F' terms, of which the lower one, giving the weaker combinations, may be assigned to $(3d)^2 5s$.

All the known terms of *Ti* II are now accounted for theoretically. Conversely, all the low (even) terms which theory predicts have been found with the exception of one ^2D term of origin $(3d)^3$. Among the middle (odd) terms of origin $(3d)^2 4p$ only one ^2P term is lacking. The parent ^1S term in *Ti* III has been identified very doubtfully, if at all. The missing ^2P and ^4F terms arising from $3d \cdot 4s \cdot 4p$ should give faint multiplets. Of the high even terms, only those arising from the lowest parent term in *Ti* III have been observed, and some of these which should give the weaker combinations are missing.

In all points, therefore, the character of the spectrum is in exact accordance with the predictions of Hund's theory, including the fact that the $^4F'$ terms are lower than the $^4P'$ terms of the same origin, and that the quartet F' and P' terms are lower than the doublets which have the same parent term in *Ti* III.

8. SERIES AND IONIZATION POTENTIAL

According to the interpretation just given, the terms a^4F', c^4F' are successive members of a series, as are also a^2F', c^2F'. The limit of the series should be the lowest term a^3F' of *Ti* III, the components $^4F'_5$, $^2F'_4$ going to $a^3F'_4$ as limit; $^4F'_4$, $^2F'_3$ to $a^3F'_3$; and $^4F'_3$, $^4F'_2$ to $a^3F'_2$. Applying a Rydberg formula in the usual manner, determining the height of the limit above the lowest level in *Ti* II, and subtracting the quantities required to reduce all the results to determinations of the difference in level between the normal state of *Ti* II, $a^4F'_2$, and that of *Ti* III, $a^3F'_2$, we find:

Term	$^4F'_5$	$^4F'_4$	$^4F'_3$	$^4F'_2$	$^2F'_4$	$^2F'_3$
Limit..............	111,874	111,677	111,542	111,448	111,174	110,894
Correction.........	422	183	0	0	422	183
$a^3F'_2$–$a^4F'_2$..........	111,452	111,494	111,542	111,448	110,752	110,711

The results from the quartet and doublet terms agree quite as well as could be expected. The general mean is 111,233, corresponding to a value of 13.73 volts for the principal ionization potential of *Ti* II—that is, the energy required to pass from the normal state of *Ti* II to that of *Ti* III.

This value is, however, probably slightly too high, for in other cases when a Rydberg formula is applied to the first two terms in a series involving the removal of an s electron, the computed limit is usually higher than that given by a Ritz formula for the whole series.

For a number of spectra in which the ^1S term is the lowest, the percentage excess of the ionization potential calculated from the first two terms of the S series above that derived from the full series is as given below. The ionization potentials for the ionized atoms have been divided by 4 to make them comparable with the others.

Element	Ba^+	Sr^+	Ca^+	Mg^+	*Cs*	*Rb*	*K*
I/Z^2	2.49	2.74	2.96	3.74	3.88	4.16	4.32
Percentage error	+2.8	+1.4	+1.6	+0.7	+2.0	+1.6	+1.2

Element	*Na*	*Ag*	*Cu*	*Mg*	*Cd*	*Au*	*Zn*	*Hg*
I/Z^2	5.12	7.59	7.69	7.61	8.95	9.20	9.35	10.39
Percentage error	+0.6	+3.0	+2.2	+3.9	+4.7	+3.3	+4.1	+ 5.1

The percentage of error evidently increases with the ionization potential and with the atomic number. From a plot of the data it appears probable that the correction for *Ti* II lies between 1.0 and 1.5 per cent. The round number 110,000 for $a^3F'_2-a^4F'_2$, corresponding to a principal ionization potential of 13.58 volts, is probably as good a value as can at present be adopted.

No previous determination of the quantity has been made by physical methods. By the astrophysical method, based on the behavior of the lines of *Ti* II in stars of different spectral types, Menzel[1] derived the value 12.5 volts—a good approximation, but, like the astrophysical determinations for other elements, a little too low.

The only other series which might be represented among the observed terms in this spectrum involve the configurations $(3d)^3$ and $(3d)^2 4d$ with parent term a^3F' in *Ti* III; but any discussion of these is greatly complicated by the fact that Pauli's restriction operates upon the lower configuration—abolishing a large number of the terms which would otherwise appear and perhaps changing the energy-levels of the others. Of the four known members of the pentad, a^4D, d^4F', a^4G, a^4H', only the second can have a corresponding lower term, which must be b^4F'. Taking the leading components of these terms and referring them to the appropriate limit, $a^3F'_4$, which, with the adopted ionization potential, lies at the height 110,422 above the origin of measurement for *Ti* II, we find the term values for $b^4F'_5$, $d^4F'_5$ to be 109,207 and 41,341, giving the Rydberg denominators 2.004 and 3.257. These values indicate that the two terms are really in series—the lower one being bound with abnormal strength, presumably because it forms part of a "structural" group. This is the case in other spectra; for example, the analogous terms a^3F', b^3F' in *Sc* II give denominators 2.103, 3.284; and an instructive case in *Ti* I will be discussed later.

---

[1] *Harvard Circular*, No. 258, 1924.

Among the doublet terms of origin $(3d)^3$ the lowest is a^2G. If this is assumed to belong to the lowest limit, a^3F', it gives a denominator 2.081, while c^2G, which certainly belongs to this limit, gives the denominator 3.209; but whether the two terms are really in series cannot be definitely settled. Higher members of these series may well exist, but they would give lines in the Schumann region.

9. CAUSE OF THE COMPLEXITY OF THE SPECTRUM

In comparing a given spectrum with the spectra of neighboring elements, these may be taken either in the same state of ionization or in the states in which they have the same number of active electrons. In the latter case, the structure of the various spectra is very similar; in the former, the complexity increases rapidly as the incomplete shell of electrons begins to be filled.

The writer and Dr. Meggers[1] have called attention to the great increase in spectral complexity which attends the transition from the one-electron system of *Ca* II to the two-electron system of *Sc* II. In comparing such apparently dissimilar spectra, attention should be fixed, not upon spectroscopic terms, but upon electron jumps. For example, the H and K lines of *Ca* II correspond (in emission) to the falling back of a 4p electron into a 4s orbit. The corresponding orbital transition in *Sc* II may be associated with many different arrangements or rearrangements of the other electron orbit, and may give rise, not to 2 lines, but to 36, while the transition from a 4p to a 3d orbit gives 3 lines of *Ca* II and 50 of *Sc* II.

---

[1] *Loc. cit.*

In *Ti* II the complexity is much greater. The electron jump from 4p to 4s, which in *Ca* II gives only two lines—H and K—produces in *Ti* II all the combinations between terms of origin $(3d)^2 4p$ and $(3d)^2 4s$, and also those between groups of origin $3d \cdot 4s \cdot 4p$ and $3d\,(4s)^2$. From the list of terms in Table IV it may be shown without difficulty that the permissible transitions between the terms of the first two groups should give rise, theoretically, to 63 lines belonging to the quartet system, 107 doublet lines, and 150 intercombination lines—a total of 320. The other groups of terms give 20 doublets and 16 intercombinations, so that the whole number of possible lines corresponding to this single electron jump is no less than 356.

The jump from 4p to 3d gives 3 lines in *Ca* II (the infra-red group). In *Ti* II the transition between $(3d)^2 4p$ and $(3d)^3$ should give 73 lines belonging to the quartets, 140 doublets, and 173 intercombinations, while $3d \cdot 4s \cdot 4p$ to $(3d)^2 4s$ accounts for 34 quartets, 56 doublets, and 86 intercombinations—a total of 562 lines.

This computation takes no account of lines corresponding to changes in the "azimuthal" quantum number *L* by more than a unit (such as $^2G - {}^2D$) or of transitions involving a double electron jump, as from $3d \cdot 4s \cdot 4p$ to $(3d)^3$.

When these possibilities—many of which are actually realized—are taken into account, it appears that the possible changes from configurations containing one electron in a 4p orbit to those in which all the valency electrons are in 4s or 3d orbits are capable of producing more than 1000 lines in *Ti* II, as against 5 in *Ca* II. Not all these lines, of course, have actually been observed; most of the intersystem combinations, and many of those between terms of the same system which have different parent terms in *Ti* III, are too faint. It is none the less evident why the observed spectrum is so rich; the electron jump, in this more complex atom, may be accompanied by a great number of different arrangements or rearrangements of the orbits of the other valency electrons, each giving a different line. It is clear also that, if an atom can do but one thing at a time, the energy which in *Ca* II is concentrated into a few lines must in *Ti* II be distributed over a great many; which explains why there are no enhanced lines of titanium which have the enormous strength of H and K. The strongest lines should be, and are, those in which no rearrangement of the rest of the atom takes place when the electron jumps. The magnitude of the energy change, and hence the wavelength of the line, depends mainly on the nature of the electron jump, so that all these strong lines are crowded together in one part of the spectrum, the near ultra-violet. The leading lines of the multiplets corresponding to the transitions from each of the low terms of origin $(3d)^2 4s$ to the related triad are as follows:

a^4F'....	λλ 3349, 3234, 3088	a^2D.....	λλ 3190, 3278, 3239
b^4P'....	3248, 3106, 3332	a^2F'.....	3349, 3759, 3685
a^2S.....	3144	b^2G.....	3261, 3505, 3103
b^2P'....	3535, 3456, 4805		

The lines corresponding to an increase in the quantum number (which are the strongest of all) are given first in each row; thus λ 3349 is $a^4F'-a^4G'$, λ 3234 is $a^4F'-a^4F$, and λ 3088 is $a^4F'-a^4D'$.

With the exception of $b^2P'-a^2S'$, all these multiplets lie within a range of 700 A in the near ultra-violet. The principal lines (in the first column) range over less than 400 A.

The jump from 4p to 3d happens, in *Ti* II, to involve the liberation of nearly the same amount of energy as that from 4p to 4s. In *Ca* II and *Sc* II it liberates less; in *V* II and *Cr* II, more. Many of the strong lines arising from such transitions in *Ti* II therefore lie in the near ultra-violet and add to the concentration of strong lines in this region; a minority of these straggle into the violet and blue and account for the lines which are at present of most importance in stellar spectroscopy.

10. COMPARISON OF *Ti* II AND *Sc* I

The arc spectrum of scandium should be similar in general structure to the spark spectrum of titanium, and, since the former has recently been analyzed, it is of interest to compare the two. Quartet and doublet terms arising from similar electronic configurations have been identified in both, but the relative levels in the two are very different; thus the ^2D term of origin $3d(4s)^2$ is the lowest of all in *Sc* I, and the highest of the basal group in *Ti* II. This, and many differences of like nature, make the detailed structure of the two spectra appear very dissimilar; but the closeness of their actual relationship may be established by means of Moseley's law.

As applied to the optical spectra of elements of different atomic numbers, but with the same number of valency electrons remaining, this law states that the differences of $\sqrt{\nu/R}$ for corresponding spectroscopic terms of successive elements are substantially constant—where R is the Rydberg constant and ν the term value (measured from its own proper limit). This difference, $\Delta\sqrt{\nu/R}$, is almost exactly the same for all the various terms which can be produced by adding an electron of the same sort (e.g., 4p) to different limiting states of the atoms of the next degree of ionization; it is approximately the same for terms involving the addition of electrons of the same total quantum number (4s, 4p, 4d), but it decreases as the total quantum number increases.

Only two of the "three-electron" spectra, *Sc* I, *Ti* II, *V* III, ... , have been analyzed; but the test given in the last sentence is applicable. In applying it, it must be realized that a given term in *Ti* II may be derived in different ways from different terms in *Ti* III. For example, the term b^4P, arising from the configuration $3d\cdot4s\cdot4p$, may be produced by the addition of a 3d electron to the configuration $4s\cdot4p$ of *Ti* III—and, in particular, to the ^3P term arising from this configuration. It may also be produced by the addition of a 4s electron to the ^3P term arising from $3d\cdot4p$, and of a 4p electron to the ^3D term of origin $3d\cdot4s$. All three of these terms are known in *Ti* III,[1] and also the corresponding ones in *Sc* II,[2] so that three different values of ν are available for a test.

The identification of the parent terms is unambiguous in this case; but when Pauli's restriction operates, as in the passage from $(3d)^3$ to $(3d)^2$, it is harder to make. Here the terms $^4F'$, $^4P'$, $^2P'$, ^2D,

---

[1] Russell and Lang, *Mt. Wilson Contr.*, No. 337; *Astrophysical Journal*, **66**, 13, 1927.

[2] Russell and Meggers, *Scientific Papers of the Bureau of Standards*, **22**, 329 (No. 558), 1927.

$^2F'$, ^2G, $^2H'$, ^2D come from $^3F'$, $^3P'$, ^1S, ^1D, ^1G. The quartet terms can arise only from the triplets. It is natural, though not inevitable, to associate $^4F'$ with $^3F'$, and $^4P'$ with $^3P'$, and this is justified in the former case by the series relation discussed in section 8. The associations given below for the doublet terms are uncertain. Similarly, in the transition from $(3d)^2 4s$ ($^4F'$, $^4P'$, ^2S, $^2P'$, ^2D, $^2F'$, ^2G) to $3d \cdot 4s$ (^3D, ^1D), the quartets must go to the triplet terms, and the doublets may go to either. Fortunately, as is shown below by writing out one or two cases, this uncertainty makes very little difference in the value of $\Delta\sqrt{\nu/R}$.

The actual comparison is given in Table VI. The various values of ν are grouped according to the type of electron which is supposed to be removed, and again with respect to the electronic configurations involved.

To save printing, the letters which identify the specific terms and limits of scandium and those for titanium are placed together, separated by a comma; thus in the fourth line the terms a^2F' in *Sc* I and a^2F' in *Ti* II are referred, respectively, to the limits a^1D in *Sc* II and b^1D in *Ti* III.

The components of greatest inner-quantum number have been used in the calculations. In certain cases of ambiguity, when a doublet term has been referred to alternatively possible singlet and triplet limits, the two lines are connected by a bracket. Cases in which the term has not been identified in one of the two spectra, or when the term value cannot be assigned (as is the case for a^4P', a^4P, and a^4S' in *Sc* I, which could not be connected with any other terms), are represented by dashes. Many such terms which have been identified in one spectrum only are omitted to save space. The separations between the extreme components of the terms are given in the last three columns of the table.

It is evident that Moseley's law is very closely satisfied, the only serious discordances being for the two terms marked with colons, for both of which the assignment to the given electronic configuration is doubtful.

Taking means of these differences for the various groups (omitting the doubtful cases), we have the summary in Table VII. The

TABLE VI

COMPARISON OF *Sc* I AND *Ti* II

ELECTRON REMOVED	TERMS	LIMITS	$\sqrt{\nu/R}$			SEPARATIONS		
			Sc I	*Ti* II	DIFF.	*Sc* I	*Ti* II	RATIO
3d.....	$(3d)^2 4s$	$3d \cdot 4s$						
	a, a^4F'	a, a^3D	0.622	1.158	0.536	157	393	0.40
	a, b^4P'	a, a^3D	....	1.123	....	81	152	.53
	a, a^2F'	a, a^3D	.597	1.144	.547	115	269	.43
	a, a^2F'	a, b^1D	.615	1.157	.542			
	b, a^2D	a, b^1D	.600	1.142	.542	− 12	33	− .36
	a, b^2G	a, b^1D	.581	1.114	.533	− 3	− 8	.37
3d.....	$(3d)^3$	$(3d)^2$						
	b, b^4F'	a, a^3F'	.478	0.998	.520	143	308	.46
	b, a^4P'	a, a^3P'	.519	1.007	.488	80	155	.52
	d, b^2D	b, a^1D	.508:	0.982	.474:	54:	129	.42:
3d.....	$3d \cdot 4s \cdot 4p$	$4s \cdot 4p$						
	a, b^4P	b, b^3P	.826	1.322	.496	67	103	0.65
	a, c^4D'	b, b^3P	.838	1.335	.497	201	161	1.25
	a, c^2P	b, b^3P	.824	1.333:	.509:	145	7:	
	a, d^2D'	b, b^3P	.839	1.332	.493	− 74	− 43	1.72
	a, d^2F	b, b^3P	.812	1.310	.498	53	146	0.36
	b, e^2D'	b, b^3P	.789	1.275	.486	148	295	.50
	b, e^2F	b, b^3P	.785	1.270	.485	140	287	.49
4s.....	$3d(4s)^2$	$3d \cdot 4s$						
	a, c^2D	a, a^3D	.702	1.056	.354	168	232	0.73
	a, c^2D	a, b^1D	.717	1.074	.357			
4s.....	$(3d)^2 4s$	$(3d)^2$						
	a, a^4F'	a, a^3F'	.657	1.003	.346			
	b, a^2D	b, a^1D	.661	1.000	.339			
	a, a^2F'	a, a^3F'	.633	0.981	.348			
	a, b^2G	a, a^1G	.662	0.997	.335			
4s.....	$3d \cdot 4s \cdot 4p$	$3d \cdot 4p$						
	a, b^4P	a, b^3P	.772	1.109	.337			
	a, c^4D'	a, a^3D'	.775	1.110	.335			
	a, c^2P	a, a^1P	.774	1.130:	.356:			
	a, d^2D'	a, a^1D'	.762	1.094	.332			
	a, d^2F	a, a^1F	.770	1.104	.334			
	b, e^2D'	a, a^3D'	.721	1.036	.315			
	b, e^2F	a, a^3F	0.715	1.034	0.319			

TABLE VI—*Continued*

ELECTRON REMOVED	TERMS	LIMITS	$\sqrt{\nu/R}$			SEPARATIONS		
			Sc I	*Ti* II	DIFF.	*Sc* I	*Ti* II	RATIO
4p.....	3d·4s·4p	3d·4s						
	a, b^{4}P	a, a^{3}D	0.569	0.917	0.348			
	a, c^{4}D′	a, a^{3}D	.588	.935	.347			
	a, c^{2}P	a, a^{1}D	.586	.948:	.362:			
	a, d^{2}D′	a, a^{1}D	.608	.946	.338			
	a, d^{2}F	a, a^{1}D	.568	.917	.349			
	b, e^{2}D′	a, a^{3}D	.516	.848	.332			
	b, e^{2}F	a, a^{3}D	.509	.840	.331			
4p.....	(3d)^{2}4p	(3d)^2						
	b, a^{4}D′	a, a^{3}F′	.489	.841	.352	104	235	0.44
	b, a^{4}F	a, a^{3}F′	.502	.849	.347	176	464	.38
	a, a^{4}G′	a, a^{3}F′	.520	.855	.335	281	696	.40
	c, a^{2}D′	a, a^{3}F′	.480	.846	.366	92	269	.34
	c, a^{2}F	a, a^{3}F′	.484	.848	.364	125	283	.44
	a, a^{2}G′	a, a^{3}F′	.486	.831	.345	95	205	.46
	a, a^{4}S′	a, a^{3}P′	....	.858				
	c, a^{4}P	a, a^{3}P′	....	.846	....	87	212	.41
	—, b^{4}D′	a, a^{3}P′	....	.854	....	....	235	
	d, a^{2}P	b, a^{1}D	.504	.848	.344	− 39	− 71	.55
	d, b^{2}D′	b, a^{1}D	.505	.848	.343	105	243	.43
	—, b^{2}F	b, a^{1}D	....	.845	....	....	148	
	d, c^{2}F	a, a^{1}G	.509	.838	.329	8	−158	− .05
	b, b^{2}G′	a, a^{1}G	.513	.858	.345	31	40	.78
	a, a^{2}H	a, a^{1}G	.514	.846	.332	96	235	.41
5s.....	(3d)^{2}5s	(3d)^2						
	d, c^{4}F′	a, a^{3}F′	0.393	0.660	0.267	163	414	0.39

corresponding mean differences for two-electron and one-electron systems are added for comparison.[1]

It is evident that the relations are very regular. The configuration 3d·4s·4p gives somewhat smaller differences than the others. If the results obtained from this configuration, which cannot occur in the two- and one-electron systems, are omitted from the means, the differences become almost identical with those for the simpler atomic systems.

---

[1] Russell and Lang, *loc. cit.*, supplemented by unpublished studies on *Ca* I.

The separations of the terms in *Sc* I and *Ti* II also show a fairly close parallelism. Out of 27 cases (excluding the two doubtful ones) the ratio of the separations lies between 0.34 and 0.55 in no less than 20. The mean for these is 0.44. The mean ratio of the separations for 13 corresponding triplet terms in *Sc* II and *Ti* III is 0.49 (omitting one discordant case); for three corresponding terms in *Sc* III and *Ti* IV, it is 0.54—a remarkably regular progression.

TABLE VII

MOSELEY'S LAW

Added Electron	3d	4s	4p	5s
Configuration $(3d)^2$	0.504	0.342	0.346	0.267
Configuration 3d·4s	.539	.355	.331	....
Configuration 3d·4p	....	.328	....	....
Configuration 4s·4p	.493	....	....	....
Mean *Ti* II–*Sc* I	.512	.342	.338	.267
Mean *Sc* II–*Ca* I	.551	.351	.351	.265:
Mean *Ca* II–*K* I	0.535	0.369	0.353	0.263

It is worthy of special notice that the inverted terms in *Sc* I and *Ti* II, which are rather numerous, correspond either to inverted terms in the other spectra or to terms of very small separation. Whatever influence is at work to produce the inversion evidently acts in almost the same way in the two cases. All these inverted terms appear to be derived from limits belonging to the singlet systems of *Sc* II or *Ti* III.

There is, however, enough difference between the two spectra to show that the laws which govern the magnitude of the term separations must be rather complicated.

CARNEGIE INSTITUTION OF WASHINGTON
MOUNT WILSON OBSERVATORY
May 1927

Contributions from the Mount Wilson Observatory, No. 345
Reprinted from the *Astrophysical Journal*, Vol. LXVI, pp. 347–438, 1927
Printed in the U.S.A.

THE ARC AND SPARK SPECTRA OF TITANIUM

PART II. THE ARC SPECTRUM, *Ti* I

By HENRY NORRIS RUSSELL[1]

ABSTRACT

The *arc spectrum of titanium* is complicated. The identified terms include 43 singlets, 65 triplets, and 34 quintets. Combinations between these give 422 multiplets and account for 1394 lines. There are many intercombinations between singlets and triplets, and between triplets and quintets, but none between singlets and quintets.

The *lowest term* is a $^3F'$; next come a $^5F'$ and a ^1D.

Tables of these terms and of the classified lines similar to those in Part I are given, and the *methods* employed in the analysis are illustrated.

The *temperature classification* of the lines is again in agreement with their levels of origin, and the *Zeeman effect* accords with Landé's theory, except for a few terms with abnormal g values. *Tables* are given for more than 300 lines.

Hund's theory accounts for the observed terms in a completely satisfactory manner. The *electron configurations* corresponding to most of them can be assigned with certainty, and for the rest, with little ambiguity.

Seventeen *series* have been identified which converge to seven different limits, all terms of *Ti* II.

The *ionization potential* is 6.81 *volts.*

Comparison of the spectra of *Ti* I and *V* II shows the similarity of their structure, and indicates that the ionization potential of *V* II is approximately 14.1 volts.

I. INTRODUCTION

The present paper completes the investigation of the spectrum of titanium and deals with its most complicated portion—the spectrum of the neutral atom. A considerable part of this has been analyzed by Dr. and Mrs. Kiess,[2] who classified more than 350 lines, including most of the strongest. They proved the existence of triplet and quintet systems, and suspected that of singlets as well. The lowest term is a $^3F'$, the next $^5F'$, followed by a ^1D, a $^3P'$, and a second $^3F'$. About fifty multiplets were identified, resulting from combinations of the low triplet terms with higher ones of types S', P, D', F, and G'; quintet D', F, and G' terms combining with the low $^5F'$ term were found, and intercombinations between the triplets and quintets. A $^5P'$ term, combining with $^5S'$, ^5P, and $^5D'$ terms, was also found, but was not connected with the rest of the scheme.

---

[1] Research associate of the Mount Wilson Observatory, Carnegie Institution of Washington.

[2] *Journal of the Optical Society of America*, 8, 607, 1924.

The present investigation (which, as has previously been stated, was begun without the knowledge that Dr. and Mrs. Kiess were working on the spectrum) has confirmed their results in almost every detail. The low terms which they found are the most important in the spectrum, and almost all their higher terms have been verified. Both the triplet and quintet systems have, however, been much extended in the course of the present work, and the system of singlets has been worked out in detail. The terms now identified number 43 singlets, 65 triplets, and 34 quintets, or 142 in all, while the number of component levels, or separate energy states in which the neutral titanium atom can exist, which have actually been detected is 364. The combinations between these terms give rise to 422 multiplets and account in all for 1394 lines. Numerous intercombinations occur between the singlets and triplets and between the triplets and quintets, but none have been found between the singlets and quintets.

2. METHODS OF ANALYSIS

The analysis of so complicated a spectrum is not always easy, and some account of the methods employed may be of interest. A complete list of lines attributed to *Ti* I was prepared, and the wave numbers plotted on strips of co-ordinate paper, by means of lines drawn both above and below a longitudinal axis to a distance indicating the strength of the spectral line. The strips were then cut apart along their axes. By shifting one part past the other, after the fashion of a vernier, the search for pairs of lines with identical frequency differences was greatly facilitated. Strips 50 cm long on a scale of two frequency units per millimeter were found convenient. With their aid it is just as easy to "comb" the spectrum for a large known difference of several thousand units as for a small one, the lower half of one strip being set against the upper half of another at the appropriate shift. The temperature classes of the lines were indicated on the strips and all identifications were marked on them as fast as they were made. This method is particularly well adapted to the discovery of skew-symmetrical multiplets, and most of the important terms were found in this way. The isolated group of lines of class I near λ 5200, for example, led to the recognition of the lowest term (later known as a^3F'). Upon combing the spectrum with its frequency differences, 216 and 170, more than a dozen multiplets were found, each fixing a higher term, and, searching next with the characteristic interval separations of the strongest of these higher terms, the low terms b^3F' and a^3P' were found. Up to this point the *L* values for the various terms were unknown, but new combinations of the last-mentioned term were clearly PP' and PS groups, and the nature of the other terms followed.

The $^5F'$ and $^5P'$ terms were found in a similar fashion, aided in the second case by the Zeeman patterns, which are widely resolved. These two terms afford an excellent illustration of the separation of a given system into subsystems, each composed of terms having the same limit in the spark. The higher terms which combine strongly with the $^5P'$ terms combine very weakly with the $^5F'$, and vice versa. In such a case the multiplets resulting from combinations between the two subsystems may be so faint that only the strong "diagonal" lines are observable, and no satellites are available to exhibit the characteristic separations. The diagonal lines themselves, however, may be identified by their own separations, which are the differences of the separations of the components of the terms involved. For example, the low $^5F'$ term and the $^5D'$ term, which combines most strongly with the $^5P'$, have the separations

$^5F'$.............	100.21	81.79	62.17	41.97
$^5D'$............	104.56	75.81	49.38	24.36
Diff...........	−4.35	+ 5.98	+12.79	+17.61

Since the terms are "regular," i.e., the component of greatest inner-quantum number is at the highest level, the differences in wave number of the diagonal lines in the resulting multiplet will have the signs and values given above. By plotting five lines with these relative separations on a bit of paper and running this along one of the sets of strips mentioned above, it was very easy to find the following group of lines:

Intensity..	4 III	3 III A	2 III A	1 III A	tr III A
ν.........	28914.47	910.12	916.14	928.94	946.53
$\Delta\nu$........		−4.35	+6.02	+12.80	+17.59

which must evidently be the desired combination. In this particular case, some of the satellites have been observed, and the group could have been found by their aid; but in many other cases the method here suggested is the only available one.

This method is useful only for finding the connections between groups of terms which are already known. For the detection of new terms a similar method, which has proved very useful, may be illustrated by the search for a high $^3F'$ term. If such a term exists, it may be expected to combine with the lowest of the "middle terms" which themselves combine with the low $^3F'$ term. The term values for these terms, as already found from their combinations, are:

		Difference			Difference		
$a^3D'_3$ . . .	20126.13	552.17	a^3F_4	19573.96	2165.73	$a^3G'_5$ . . .	21739.69
$a^3D'_2$ . . .	20006.08	584.48	a^3F_3	19421.60	2166.86	$a^3G'_4$	21588.46
$a^3D'_1$ . . .	19937.88	614.90	a^3F_2	19322.98	2146.55	$a^3G'_3$ . . .	21469.53

The leading component $^3F'_4$ of the suspected term should combine with the leading components of these three terms, giving lines which should be the strongest in their different multiplets and should have the frequency differences indicated above. The other components, $^3F'_3$ and $^3F'_2$, should each give three lines near the first three and related by the corresponding frequency differences. A search for these differences reveals the lines

	Difference		Difference	
17698.51 (5 IV)	552.28	18250.79 (8 III)	2165.75	16085.04 (20 III)
17653.88 (4 III)	584.42	18238.30 (6 III)	2166.73	16071.57 (12 III)
17600.92 (2 III)	614.81	18215.73 (5 III)	2146.67	16069.06 (8 III)

A single coincidence of a frequency difference with a predicted value may well be a matter of chance—and a number of remarkable instances of this sort have appeared in the present work, sometimes leading it astray; but such coincidences as these, confirmed by the relative intensities and temperature classes of the lines, are all conclusive evidence of the new term (which is called c^3F' in Table I). By the application of these methods many additional terms of the triplet and quintet systems were found. Many faint lines, especially intercombinations, were found in the predicted places upon photographs of the spectrum prepared by Mr. King and Mr. Ellerman, and some, as faint solar lines greatly intensified, in the sun-spot spectrum, which were confirmed later on the laboratory plates.

Measures of these have added about 165 lines to the list of those known to belong to *Ti* I.

When all this had been done, a great many strong lines, some of them of classes I and II, remained outside the scheme, and both the isolation and the Zeeman effect of these lines confirmed Dr. and Mrs. Kiess's suspicion of the existence of a system of singlets, and showed that it must be extensive. The analysis of a singlet system is much more difficult than any other, for neither satellite separations nor Zeeman effects are available. Realizing this, the consideration of the subject was deferred until near the end of the work. By this time a considerable number of pairs of lines had been identified, which by their separations and temperature classes indicated that they were probably due to transitions from known terms of the triplet system to unclassified levels, which might well belong to the singlet system.

The outstanding lines were then examined for constant frequency differences, and two pairs of strong lines were found almost at once, with frequency differences of 1299.93 and 1299.92, which were separated by 6169.16 units. Many other pairs with separation 6169 were then found, showing that this must be the separation of two important low terms, while that of 1299 belongs to higher terms. Moreover, a separation of 1299.93 was found between two other lines, one of which belonged to a pair already identified as a combination with a low $^3H'$ term. The energy level for this term, and later for all the new singlet terms, could then be computed, and many other intercombinations with the triplets were found. Search among the remaining single lines, with the aid of the frequency differences of the higher singlet terms, resulted in the discovery of the lowest level in the singlet system and the classification of a number of conspicuous low-temperature lines arising from this level. More than twenty intercombinations with the triplet system were found, which definitely fixed the inner-quantum number j of this lowest level as 2. It is therefore recorded as a^1D.

The two low terms first mentioned combine with substantially the same higher terms, so that they must be of the same type. Their intercombinations with the triplets show that their j is either 4 or 5, and the fact that they combine with a number of terms which also combine with a^1D settles that $j=4$, and that the terms are G, a^1G, and b^1G. The higher terms just mentioned must be ^1F terms; the others which combine with the G's must be G' or H terms. Another low term, which combines with these and not with the ^1F terms, is clearly of type $^1H'$. A number of high terms combining with a^1D but not with the G terms were identified by means of their intercombinations with the low triplet terms, those which combined with a^3F' being evidently $^1D'$ terms, and the rest, which combined with a^3P' only, being recorded as ^1P. This assignment was later confirmed by the discovery of low $^1P'$ and ^1S terms. A number of still higher terms were also identified by combinations with those of the middle levels. The only strong outstanding line, λ 5120, was finally identified as $a^1H'-a^1I'$ by means of a very faint intercombination $a^3H'_5-a^1I'$, which was found in just the predicted place on King's photographs. The discrimination between the ^1H and $^1G'$ terms which combine with the low ^1G and $^1H'$ terms was difficult. The terms a^1G', d^1G' were identified by combinations with a^3F'; and b^1G', c^1G', a^1H, b^1H by the Zeeman patterns of their combinations with $a^3H'_4$, which showed that, for the first two, j was 4, while for the others it was not. Of the remaining terms e^1G', f^1G' combine with a^1F'. The identification of a^1F' itself is not free from ambiguity; so far as the observed combinations go, it might be a G term; and the fact that an F' term fits much better into Hund's theoretical scheme has largely influenced this assignment.

All told, even terms of types S, P', D, F', G, and H' and odd terms S', P, D', F, G', H, and I' have been found in the singlet system. A few outstanding, rather weak, isolated lines may be singlets, belonging here or in other places where they could be identified only by intercombinations much fainter than themselves.

3. TABLES OF TERMS AND LINES

A complete list of the terms which have been identified and those with which each term combines is given in Table I. The energy levels are counted upward from the normal state $a^3F'_2$. The largest number of them of any sort is 13 for $^3D'$; half of the alphabet is used up merely in labeling these terms for identification. The lowest term, a^3F', gives observable combinations with no less than 52 others; a^3P' combines with 41, and a^1D with 38.

Almost all the terms are regular, only three being wholly or partially inverted. Landé's interval rules are roughly obeyed, but there are noteworthy exceptions, such as c^3P', a^3H', c^3P, e^5D, and c^5D'.

It may be remarked that c^3S_1' and i^3D_3' have the same value. The combinations, especially with a^3P' and b^3P', show that there are really two different lines here, which are accidentally coincident. As in Part I, the numbers assigned to the multiplets in Table II are given below the combinations in Table I.

TABLE I

Ti I Terms and Combinations

Type	Term	Combinations				
aS_0....	15166.59	bP	cP	dP	eP	
		127	222	228	295	
aP'_1...	20062.98	aS′	aP	bP	cP	dP
		89	24	44	111	115
		eP	cD′	dD′	eD′	
		197	45	217	219	
bP'_1...	53663.32	aS′	bP	cP		
		49	101	41		
aD_2...	7255.29	aP	bP	cP	dP	eP
		269	291	361	365	395
		aD′	bD′	cD′	dD′	eD′
		43	143	296	398	401
		aF	bF	cF	dF	eF
		46	255	336	373	387
		fF	a^3S'	c^3P	d^3P	e^3P
		414	83	256	327	374
		f^3P	g^3P	b^3D'	c^3D'	d^3D'
		388	406	95	134	193
		e^3D'	f^3D'	g^3D'	h^3D'	i^3D'
		225	340	351	370	378
		j^3D'	k^3D'	e^3F	f^3F	h^3F
		389	390	275	338	385
		d^3G'	e^3G'	f^3G'		
		220	334	383		
bD_2...	20209.64	cP	dP	eP	eD′	bF
		104	114	195	216	18
		cF	dF	eF		
		79	133	161		
cD_2...	44581.16	aD′	bD′	aF		
		186	71	179		
dD_2...	50128.08	aP	aD′	aF		
		64	299	293		
aF'_3...	29818.31	eF	fF	eG′	fG′	
		8	99	31	63	
bF'_3...	41087.31	aD′	aF	aG′	a^3F	
		110	100	61	165	
cF'_3....	46650.26	aD′	aF	aG′		
		235	230	173		
aG_4...	12118.46	bF	cF	dF	eF	fF
		146	252	300	317	396
		aG′	bG′	cG′	eG′	fG′
		17	221	277	354	384
		aH	bH	cH	e^3F	d^3G'
		189	308	366	177	121
		c^3H				
		282				
bG_4...	18287.62	bF	cF	dF	fF	bG′
		40	118	174	332	84
		cG′	dG′	eG′	fG′	aH
		144	191	248	298	62
		bH	f^3G'	b^3H	c^3H	
		196	199	76	151	
cG_4...	46068.04	aF	aG′			
		218	160			
dG_4...	52125.98	aF	aG′	bG′		
		325	286	57		
aH'_5...	20795.65	bG′	cG′	dG′	eG′	fG′
		47	90	132	198	251
		aH	bH	cH	aI′	
		32	137	215	122	
bH'_5...	45485.35	aG′				
		150				
aS'_0....	38200.94	aP′	bP′			
		89	49			
aP_1...	33660.73	aP′	aD	dD	a^3P'	
		24	269	64	245	
bP_1...	34947.02	aS	aP′	bP′	aD	a^3P'
		127	44	101	291	266
cP_1...	39078.00	aS	aP′	bP′	aD	bD
		222	111	41	361	104
		a^3P'				
		337				
dP_1...	39265.80	aS	aP′	aD	bD	a^3P'
		228	115	365	114	342
eP_1...	42927.55	aS	aP′	aD	bD	a^3P'
		295	197	395	195	386
aD'_2...	22081.15	aD	cD	dD	bF′	cF′
		43	186	299	110	235
		a^3F'				
		169				
bD'_2...	27906.91	aD	cD	a^3P'	a^3F'	
		143	71	117	294	

TABLE I—*Continued*

Type	Term	Combinations
cD'_2...	35035.11	aP′ aD a^3P' a^3F' 45 296 270 391
dD'_2...	43710.28	aP′ aD 217 398
eD'_2...	43799.57	aP′ aD bD 219 401 216
aF_3...	22404.69	aD cD dD bF′ cF′ 46 179 293 100 230 cG dG a^3F' 218 325 175
bF_3...	32857.76	aD bD aG bG a^3F' 255 18 146 40 372
cF_3...	37622.63	aD bD aG bG a^3P' 336 79 252 118 311 a^3F' a^3G 404 184
dF_3...	40303.04	aD bD aG bG 373 133 300 174
eF_3...	41585.24	aD bD aF′ aG 387 161 8 317
fF_3....	48365.09	aD aF′ aG bG 414 99 396 332
aG'_4...	24694.81	bF′ cF′ aG cG dG 61 173 17 160 286 bH′ a^3F' 150 231
bG'_4...	36000.25	aG bG dG aH′ a^3G 221 84 57 47 149 a^3H' 86
cG'_4...	38959.53	aG bG aH′ b^3F' a^3H' 277 144 90 285 152
dG'_4...	40883.30	bG aH′ a^3F' 191 132 411
eG'_4...	43674.31	aF′ aG bG aH′ 31 354 248 198
fG'_4....	46257.67	aF′ aG bG aH′ a^3H' 63 384 298 251 301

Type	Term	Combinations
aH_5...	34700.31	aG bG aH′ b^3F' a^3H' 189 62 32 200 69
bH_5...	41039.93	aG bG aH′ a^3H' 308 196 137 203
cH_5...	44163.24	aG aH′ b^3F' 366 215 369
aI'_5....	40319.80	aH′ a^3H' 122 180
$a^3P'_2$... $a^3P'_1$... $a^3P'_0$...	8602.42 *109.94* 8492.48 *55.79* 8436.69	a^3S' b^3S' c^3S' d^3S' a^3P 60 276 367 397 73 b^3P c^3P d^3P e^3P f^3P 206 233 304 358 377 g^3P a^3D' b^3D' c^3D' d^3D' 400 5 72 103 155 e^3D' f^3D' g^3D' h^3D' i^3D' 190 315 331 349 363 j^3D' k^3D' l^3D' m^3D' f^3F 380 381 394 399 313 g^3F c^3G' aP bP cP 326 158 245 266 337 dP eP bD′ cD′ cF 342 386 117 270 311 a^5S' b^5S' a^5P b^5P b^5D' 66 306 116 292 77 c^5D' 162
$b^3P'_2$... $b^3P'_1$... $b^3P'_0$...	18145.40 *83.86* 18061.54 *65.79* 17995.75	b^3S' c^3S' b^3P f^3P g^3P 78 194 27 220 279 d^3D' e^3D' f^3D' g^3D' i^3D' 7 19 131 142 185
$c^3P'_2$... $c^3P'_1$... $c^3P'_0$...	18911.55 *85.66* 18825.89 *7.66* 18818.23	c^3S' c^3P d^3P e^3P g^3P 170 34 93 164 264 e^3D' h^3D' i^3D' b^5S' 14 148 166 96
$d^3P'_2$...	46244.60	a^3S' a^3D' 159 260
a^3D_3... a^3D_2... a^3D_1...	17540.33 *116.22* 17424.11 *54.52* 17369.59	b^3P c^3P d^3P e^3P f^3P 35 51 124 201 232 g^3P e^3D' f^3D' g^3D' h^3D' 290 26 140 156 178 i^3D' j^3D' d^3F e^3F f^3F 208 236 58 68 135 g^3F h^3F b^5S' 154 223 129

TABLE I—*Continued*

Type	Term	Combinations				
b^3D_3...	48839.74	a^3D'	d^3D'	a^3F	a^5D'	a^5F
	115.40	305	107	314	333	356
b^3D_2...	48724.34					
	−0.49					
b^3D_1...	48724.83					
c^3D_3...	49619.72	a^3D'	a^3F			
	48.03	318	330			
c^3D_2...	49571.69					
$a^3F'_4$...	386.88	a^3S'	a^3P	b^3P	a^3D'	b^3D'
	216.74	242	247	355	126	246
$a^3F'_3$...	170.14	c^3D'	d^3D'	e^3D'	f^3D'	g^3D'
	170.14	283	319	343	405	408
$a^3F'_2$...	0.00	h^3D'	i^3D'	j^3D'	k^3D'	l^3D'
		409	410	415	416	418
		m^3D'	a^3F	b^3F	c^3F	d^3F
		421	112	239	271	376
		e^3F	f^3F	g^3F	h^3F	i^3F
		382	403	407	413	417
		j^3F	a^3G'	b^3G'	c^3G'	d^3G'
		420	157	284	320	347
		e^3G'	f^3G'	g^3G'	a^3H	aD'
		402	412	419	353	169
		bD'	cD'	aF	bF	cF
		294	391	175	372	404
		aG'	dG'	a^5S'	a^5P	a^5D'
		231	411	243	288	91
		b^5D'	c^5D'	d^5D'	a^5F	b^5F
		249	323	393	65	302
		a^5G'	b^5G'			
		53	267			
$b^3F'_4$...	11776.89	a^3P	b^3D'	c^3D'	d^3D'	e^3D'
	137.04	30	28	52	88	119
$b^3F'_3$...	11639.85	f^3D'	g^3D'	h^3D'	i^3D'	j^3D'
	108.03	265	281	297	312	339
$b^3F'_2$...	11531.82	k^3D'	l^3D'	m^3D'	b^3F	c^3F
		341	371	379	22	48
		d^3F	e^3F	f^3F	g^3F	i^3F
		168	182	259	274	362
		j^3F	b^3G'	c^3G'	d^3G'	e^3G'
		375	54	94	123	257
		f^3G'	cG'	aH	cH	a^5S'
		321	285	200	369	23
		c^5D'	b^5G'			
		92	45a			
$c^3F'_4$...	37824.69	a^3D'	b^3D'	a^3F	c^3F	a^3G'
	164.72	82	13	87	2	56
$c^3F'_3$...	37650.97					
	121.26					
$c^3F'_2$...	37538.71					

Type	Term	Combinations				
$d^3F'_4$...	39785.94	b^3D'	b^3F	b^3G'		
	144.96	33	38	12		
$d^3F'_3$...	39640.98					
	114.09					
$d^3F'_2$...	39526.89					
$e^3F'_4$...	42107.06	a^3D'	a^3F	a^3G'	a^5D'	a^5F
	118.67	171	187	139	212	240
$e^3F'_3$...	41988.39					
	116.52					
$e^3F'_2$...	41871.87					
$f^3F'_4$...	46530.45	a^3D'	a^3F	a^3G'		
		268	280	238		
$g^3F'_4$...	47194.68	a^3F	a^3G'			
	156.52	289	250			
$g^3F'_3$...	47038.16					
a^3G_5...	15220.47	c^3F	d^3F	e^3F	f^3F	g^3F
	63.64	6	97	105	188	213
a^3G_4...	15156.83	h^3F	i^3F	b^3G'	c^3G'	d^3G'
	48.71	262	303	15	42	59
a^3G_3...	15108.12	e^3G'	g^3G'	a^3H	b^3H	c^3H
		183	310	70	138	224
		d^3H	cF	bG'		
		272	184	149		
b^3G_5...	36200.94	a^3F	b^3F	a^3G'		
	68.73	67	3	37		
b^3G_4...	36132.21					
	66.46					
b^3G_3...	36065.75					
c^3G_5...	41481.13	a^3F	a^3G'			
	112.27	167	125			
c^3G_4...	41368.86					
	174.44					
c^3G_3...	41194.42					
$a^3H'_6$...	18192.66	c^3G'	d^3G'	e^3G'	f^3G'	g^3G'
	51.29	10	20	120	205	261
$a^3H'_5$...	18141.37	a^3H	b^3H	c^3H	a^3I'	bG'
	104.09	29	80	153	141	86
$a^3H'_4$...	18037.28	cG'	fG'	aH	bH	aI'
		152	301	69	203	180
$b^3H'_6$...	45960.39	a^3G'				
	127.89	227				
$b^3H'_5$...	45832.50					
	110.61					
$b^3H'_4$...	45721.89					

TABLE I—*Continued*

Type	Term	Combinations				
a^3S_1'	24921.19	a^3P'	d^3P'	a^3F'	aD	
		60	159	242	83	
b^3S_1'	35439.43	a^3P'	b^3P'			
		276	78			
c^3S_1'	40844.19	a^3P'	b^3P'	c^3P'		
		367	194	170		
d^3S_1'	44857.89	a^3P'				
		397				
a^3P_2	25493.78	a^3P'	a^3F'	b^3F'		
	−43.61	73	247	30		
a^3P_1	25537.39					
b^3P_2	31805.94	a^3P'	b^3P'	a^3D	a^3F'	
	80.19	206	27	35	355	
b^3P_1	31725.75					
	39.85					
b^3P_0	31685.90					
c^3P_2	33114.49	a^3P'	c^3P'	a^3D	aD	
	23.94	233	34	51	256	
c^3P_1	33090.55					
	5.41					
c^3P_0	33085.14					
d^3P_2	37325.47	a^3P'	c^3P'	a^3D	aD	a^5P'
	152.44	304	93	124	327	210
d^3P_1	37173.03					
	82.38					
d^3P_0	37090.65					
e^3P_2	40467.04	a^3P'	c^3P'	a^3D	aD	
	82.46	358	164	201	374	
e^3P_1	40384.58					
	14.82					
e^3P_0	40369.76					
f^3P_2	41928.59	a^3P'	b^3P'	a^3D	aD	
	−15.36	377	220	232	388	
f^3P_1	41943.95					
	−15.51					
f^3P_0	41959.46					
g^3P_2	45178.06	a^3P'	b^3P'	c^3P'	a^3D	aD
	87.33	400	279	264	290	406
g^3P_1	45090.73					
	50.03					
g^3P_0	45040.70					

Type	Term	Combinations				
a^3D_3'	20126.13	a^3P'	d^3P'	b^3D	c^3D	a^3F'
	120.05	5	260	305	318	126
a^3D_2'	20006.08	c^3F'	e^3F'	f^3F'		
	68.20	82	171	268		
a^3D_1'	19937.88					
b^3D_3'	25643.76	a^3P'	a^3F'	b^3F'	c^3F'	d^3F'
	204.72	72	246	28	13	33
b^3D_2'	25439.04	aD	a^5F'			
	121.16	95	102			
b^3D_1'	25317.88					
c^3D_3'	27480.14	a^3P'	a^3F'	b^3F'	aD	a^5P'
	62.04	103	283	52	134	21
c^3D_2'	27418.10					
	62.94					
c^3D_1'	27355.16					
d^3D_3'	29912.33	a^3P'	b^3P'	b^3D	a^3F'	b^3F'
	143.63	155	7	107	319	88
d^3D_2'	29768.70	aD	a^5F'			
	107.44	193	204			
d^3D_1'	29661.26					
e^3D_3'	31206.08	a^3P'	b^3P'	c^3P'	a^3D	a^3F'
	15.36	190	19	14	26	343
e^3D_2'	31190.72	b^3F'	aD			
	6.71	119	225			
e^3D_1'	31184.01					
f^3D_3'	38159.71	a^3P'	b^3P'	a^3D	a^3F'	b^3F'
	182.93	315	131	140	405	265
f^3D_2'	37976.78	aD				
	124.87	340				
f^3D_1'	37851.91					
g^3D_3'	38764.96	a^3P'	b^3P'	a^3D	a^3F'	b^3F'
	65.01	331	142	156	408	281
g^3D_2'	38699.95	aD				
	45.72	351				
g^3D_1'	38654.23					
h^3D_3'	39715.51	a^3P'	c^3P'	a^3D	a^3F'	b^3F'
	29.41	349	148	178	409	297
h^3D_2'	39686.10	aD				
	23.95	370				
h^3D_1'	39662.15					
i^3D_3'	40844.19	a^3P'	b^3P'	c^3P'	a^3D	a^3F'
	173.59	363	185	166	208	410
i^3D_2'	40670.60	b^3F'	aD			
	114.53	312	378			
i^3D_1'	40556.07					

TABLE I—*Continued*

Type	Term	Combinations				
$j^3D'_3$...	42311.31	a^3P'	a^3D	a^3F'	b^3F'	aD
	104.43	380	236	415	339	389
$j^3D'_2$...	42206.88					
	60.49					
$j^3D'_1$...	42146.39					
$k^3D'_3$...	42376.71	a^3P'	a^3F'	b^3F'	aD	
	106.98	381	416	341	390	
$k^3D'_2$...	42269.73					
	75.79					
$k^3D'_1$...	42193.94					
$l^3D'_3$...	44233.15	a^3P'	a^3F'	b^3F'		
	153.76	394	418	371		
$l^3D'_2$...	44079.39					
	103.77					
$l^3D'_1$...	43975.62					
$m^3D'_3$..	45206.34	a^3P'	a^3F'	b^3F'		
	142.40	399	421	379		
$m^3D'_2$..	45063.94					
	97.58					
$m^3D'_1$..	44966.36					
a^3F_4...	19573.96	b^3D	c^3D	a^3F'	c^3F'	e^3F'
	152.36	314	330	112	87	187
a^3F_3...	19421.60	f^3F'	g^3F'	b^3G	c^3G	bF'
	98.62	280	289	67	167	165
a^3F_2...	19322.98	b^5D				
		192				
b^3F_4...	25388.39	a^3F'	b^3F'	d^3F'	b^3G	a^5F'
	161.13	239	22	38	3	98
b^3F_3...	25227.26					
	119.82					
b^3F_2...	25107.44					
c^3F_4...	27025.66	a^3F'	b^3F'	c^3F'	a^3G	a^5F'
	132.66	271	48	2	6	136
c^3F_3...	26893.00					
	89.52					
c^3F_2...	26803.48					
d^3F_4...	33700.87	a^3D	a^3F'	b^3F'	a^3G	
	20.55	58	376	168	97	
d^3F_3...	33680.32					
	24.35					
d^3F_2...	33655.97					
e^3F_4...	34205.06	a^3D	a^3F'	b^3F'	a^3G	aD
	126.41	68	382	182	105	275
e^3F_3...	34078.65	aG				
	98.02	177				
e^3F_2...	33980.63					

Type	Term	Combinations				
f^3F_4...	37852.47	a^3P'	a^3D	a^3F'	b^3F'	a^3G
	108.51	313	135	403	259	188
f^3F_3...	37743.96	aD				
	89.19	338				
f^3F_2...	37654.77					
g^3F_4...	38670.73	a^3P'	a^3D	a^3F'	b^3F'	a^3G
	126.35	326	154	407	274	213
g^3F_3...	38544.38					
	93.09					
g^3F_2...	38451.29					
h^3F_4...	41624.13	a^3D	a^3F'	a^3G	aD	
	166.51	223	413	262	385	
h^3F_3...	41457.62					
	120.19					
h^3F_2...	41337.43					
i^3F_4...	43744.55	a^3F'	b^3F'	a^3G		
	161.41	417	362	303		
i^3F_3...	43583.14					
	115.59					
i^3F_2...	43467.55					
j^3F_4...	45041.02	a^3F'	b^3F'			
	118.02	420	375			
j^3F_3...	44923.00					
	97.74					
j^3F_2...	44825.26					
$a^3G'_5$...	21739.69	a^3F'	c^3F'	e^3F'	f^3F'	g^3F'
	151.23	157	56	139	238	250
$a^3G'_4$...	21588.46	b^3G	c^3G	b^3H'	g^5F'	c^5H'
	118.93	37	125	227	273	263
$a^3G'_3$...	21469.53					
$b^3G'_5$...	27750.16	a^3F'	b^3F'	d^3F'	a^3G	a^5F'
	135.45	284	54	12	15	147
$b^3G'_4$...	27614.71					
	115.80					
$b^3G'_3$...	27498.91					
$c^3G'_5$...	30039.35	a^3P'	a^3F'	b^3F'	a^3G	a^3H'
	68.22	158	320	94	42	10
$c^3G'_4$...	29971.13	a^5F'				
	56.34	207				
$c^3G'_3$...	29914.79					
$d^3G'_5$...	31628.76	a^3F'	b^3F'	a^3G	a^3H'	aD
	139.27	347	123	59	20	229
$d^3G'_4$...	31489.49	aG				
	115.64	121				
$d^3G'_3$...	31373.85					

TABLE I—*Continued*

Type	Term	Combinations				
$e^3G'_5$	37690.37	a^3F'	b^3F'	a^3G	a^3H'	aD
	72.44	402	257	183	120	334
$e^3G'_4$	37617.93					
	62.94					
$e^3G'_3$	37554.99					
$f^3G'_5$	41341.62	a^3F'	b^3F'	a^3H'	aD	bG
	86.18	412	321	205	383	199
$f^3G'_4$	41255.44					
	85.62					
$f^3G'_3$	41169.82					
$g^3G'_5$	44375.57	a^3F'	a^3G	a^3H'		
	213.13	419	310	261		
$g^3G'_4$	44162.44					
a^3H_6	32013.61	a^3F'	a^3G	a^3H'		
	99.30	353	70	29		
a^3H_5	31914.31					
	84.33					
a^3H_4	31829.98					
b^3H_6	35685.23	a^3G	a^3H'	bG		
	125.57	138	80	76		
b^3H_5	35559.66					
	105.67					
b^3H_4	35453.99					
c^3H_6	39198.39	a^3G	a^3H'	aG	bG	
	46.25	224	153	282	151	
c^3H_5	39152.14					
	36.15					
c^3H_4	39115.99					
d^3H_6	41995.39	a^3G				
	100.24	272				
d^3H_5	41895.15					
	114.20					
d^3H_4	41780.95					
$a^3I'_7$	38779.97	a^3H'				
	110.94	141				
$a^3I'_6$	38669.03					
	96.28					
$a^3I'_5$	38572.75					
$a^5P'_3$	14105.68	a^5S'	b^5S'	a^5P	b^5P	b^5D'
	77.21	4	211	25	181	9
$a^5P'_2$	14028.47	c^5D'	d^5D'	d^3P	c^3D'	
	46.72	55	163	210	21	
$a^5P'_1$	13981.75					
$b^5P'_3$	42858.90	a^5D'				
	134.79	226				
$b^5P'_2$	42724.11					
	112.53					
$b^5P'_1$	42611.58					

Type	Term	Combinations				
b^5D_4	42184.66	a^5D'	a^5F	a^3F		
	131.94	214	244	192		
b^5D_3	42052.72					
	94.21					
b^5D_2	41958.51					
	57.15					
b^5D_1	41901.36					
	29.80					
b^5D_0	41871.56					
c^5D_4	44381.17	c^5D'	b^5F			
	126.78	36	50			
c^5D_3	44254.39					
d^5D_4	48186.11	a^5D'	a^5F			
	126.29	316	346			
d^5D_3	48059.82					
e^5D_4	49036.46	a^5D'	a^5F			
	12.03	335	360			
e^5D_3	49024.43					
	109.36					
e^5D_2	48915.07					
	55.56					
e^5D_1	48859.51					
	57.19					
e^5D_0	48802.32					
$a^5F'_5$	6843.00	a^5D'	b^5D'	c^5D'	d^5D'	e^5D'
	100.21	11	113	209	307	392
$a^5F'_4$	6742.79	a^5F	b^5F	b^5G'	b^3D'	d^3D'
	81.79	1	172	128	102	204
$a^5F'_3$	6661.00	b^3F	c^3F	b^3G'	c^3G'	
	62.17	98	136	147	207	
$a^5F'_2$	6598.83					
	41.97					
$a^5F'_1$	6556.86					
$b^5F'_5$	36351.43	a^5D'	a^5F	a^5G'		
	142.51	81	109	130		
$b^5F'_4$	36208.92					
	112.45					
$b^5F'_3$	36096.47					
	82.90					
$b^5F'_2$	36013.57					
	54.50					
$b^5F'_1$	35959.07					
$c^5F'_5$	39412.78	a^5D'	a^5F	a^5G'	b^5G'	
	110.42	145	176	202	16	
$c^5F'_4$	39302.36					
	87.98					
$c^5F'_3$	39214.38					
	65.12					
$c^5F'_2$	39149.26					
	42.01					
$c^5F'_1$	39107.25					

TABLE I—*Continued*

Type	Term	Combinations			
$d^5F'_5$...	43330.07	a^5D'	a^5F	b^5F	a^5G'
	98.08	234	258	39	278
$d^5F'_4$...	43231.99				
	83.84				
$d^5F'_3$...	43148.15				
	67.23				
$d^5F'_2$...	43080.92				
	46.84				
$d^5F'_1$...	43034.08				
$e^5F'_5$...	46157.76	a^5D'	a^5F	a^5G'	
	150.14	287	309	324	
$e^5F'_4$...	46007.62				
	114.36				
$e^5F'_3$...	45893.26				
	80.25				
$e^5F'_2$...	45813.01				
	48.30				
$e^5F'_1$...	45764.71				
$f^5F'_5$...	47777.32	c^5D'	b^5F		
		85	106		
$g^5F'_5$...	48462.11	a^5D'	a^5F	a^5G'	a^3G'
	133.30	322	350	364	273
$g^5F'_4$...	48328.81				
	119.94				
$g^5F'_3$...	48208.87				
	101.45				
$g^5F'_2$...	48107.42				
	48.57				
$g^5F'_1$...	48058.85				
$h^5F'_5$...	48771.73	a^5D'	a^5F	a^5G'	
	99.07	329	352	368	
$h^5F'_4$...	48672.66				
	84.38				
$h^5F'_3$...	48588.28				
	69.07				
$h^5F'_2$...	48519.21				
a^5G_6...	42019.22	a^5F	a^5G'		
	115.74	237	253		
a^5G_5...	41903.48				
	84.78				
a^5G_4...	41818.70				
	61.23				
a^5G_3...	41757.47				
	43.12				
a^5G_2...	41714.35				
b^5G_6...	45904.73	b^5F	b^5G'		
	148.28	74	108		
b^5G_5...	45756.45?				
	45.17				
b^5G_4...	45711.28				
	21.39				
b^5G_3...	45689.89				
c^5G_6...	47446.84	a^5F	a^5G'		
	166.15	328	344		
c^5G_5...	47280.69				
	140.83				
c^5G_4...	47139.86				
	109.58				
c^5G_3...	47030.28				
	86.37				
c^5G_2...	46943.91				
d^5G_6...	48233.47	a^5F	a^5G'		
	114.00	348	357		
d^5G_5...	48119.47				
	101.39				
d^5G_4...	48018.08				
	81.29				
d^5G_3...	47936.79				
	66.18				
d^5G_2...	47870.61				
$a^5H'_7$...	42205.59	a^5F	a^5G'		
	81.82	241	254		
$a^5H'_6$...	42123.77				
	105.76				
$a^5H'_5$...	42018.01				
	100.96				
$a^5H'_4$...	41917.05				
	93.86				
$a^5H'_3$...	41823.19				
$b^5H'_7$..	44134.65	b^5G'			
	83.28	75			
$b^5H'_6$...	44051.37				
	79.82				
$b^5H'_5$..	43971.55				
	69.81				
$b^5H'_4$...	43901.74				
	57.92				
$b^5H'_3$...	43843.82				
$c^5H'_7$...	48262.83	a^5F	a^5G'	a^3G'	
	156.00	345	359	263	
$c^5H'_6$...	48106.83				
	112.51				
$c^5H'_5$...	47994.32				
	80.71				
$c^5H'_4$...	47913.61				
	72.99				
$c^5H'_3$...	47840.62				
$a^5S'_2$...	25102.88	a^5P'	a^3P'	a^3F'	b^3F'
		4	66	243	23
$b^5S'_2$...	37359.13	a^5P'	a^3P'	c^3P'	a^3D
		211	306	96	129

TABLE I—*Continued*

Type	Term	Combinations				
a^5P_3...	27887.74	a^5P'	a^3P'	a^3F'		
	147.55	25	116	288		
a^5P_2...	27740.19					
	74.62					
a^5P_1...	27665.57					
b^5P_3...	36414.58	a^5P'	a^3P'			
	73.91	181	292			
b^5P_2...	36340.67					
	42.24					
b^5P_1...	36298.43					
$a^5D'_4$...	18695.23	b^5P'	b^5D	d^5D	e^5D	a^5F'
	101.24	226	214	316	335	11
$a^5D'_3$...	18593.99	b^5F'	c^5F'	d^5F'	e^5F'	g^5F'
	68.92	81	145	234	287	322
$a^5D'_2$...	18525.07	h^5F'	b^3D	a^3F'	e^3F'	
	42.21	329	333	91	212	
$a^5D'_1$...	18482.86					
	20.03					
$a^5D'_0$...	18462.83					
$b^5D'_4$...	25926.82	a^5P'	a^5F'	a^3P'	a^3F'	
	129.22	9	113	77	249	
$b^5D'_3$...	25797.60					
	97.65					
$b^5D'_2$...	25699.95					
	64.21					
$b^5D'_1$...	25635.74					
	30.71					
$b^5D'_0$...	25605.03					
$c^5D'_4$...	30060.34	a^5P'	c^5D	a^5F'	f^5F'	a^3P'
	74.10	55	36	209	85	162
$c^5D'_3$...	29986.24	a^3F'	b^3F'			
	78.95	323	92			
$c^5D'_2$...	29907.29					
	52.03					
$c^5D'_1$...	29855.26					
	26.10					
$c^5D'_0$...	29829.16					
$d^5D'_4$...	35757.51	a^5P'	a^5F'	a^3F'		
	104.56	163	307	393		
$d^5D'_3$...	35652.95					
	75.81					
$d^5D'_2$...	35577.14					
	49.38					
$d^5D'_1$...	35527.76					
	24.36					
$d^5D'_0$...	35503.40					

Type	Term	Combinations				
$e^5D'_4$...	42092.52	a^5F'				
	106.59	392				
$e^5D'_3$...	41985.93					
	79.32					
$e^5D'_2$...	41906.61					
	52.60					
$e^5D'_1$...	41854.01					
	31.02					
$e^5D'_0$...	41822.99					
a^5F_5...	17215.44	b^5D	d^5D	e^5D	a^5F'	b^5F'
	140.13	244	346	360	1	109
a^5F_4...	17075.31	c^5F'	d^5F'	e^5F'	g^5F'	h^5F'
	113.89	176	258	309	350	352
a^5F_3...	16961.42	a^5G	c^5G	d^5G	a^5H'	c^5H'
	86.23	237	328	348	241	345
a^5F_2...	16875.19	b^3D	a^3F'	e^3F'		
	58.00	356	65	240		
a^5F_1...	16817.19					
b^5F_5...	28896.08	c^5D	a^5F'	d^5F'	f^5F'	b^5G
	107.69	50	172	39	106	74
b^5F_4...	28788.39	a^3F'				
	85.69	302				
b^5F_3...	28702.70					
	63.88					
b^5F_2...	28638.82					
	42.37					
b^5F_1...	28596.45					
$a^5G'_6$...	16458.71	b^5F'	c^5F'	d^5F'	e^5F'	g^5F'
	191.20	130	202	278	324	364
$a^5G'_5$...	16267.51	h^5F'	a^5G	c^5G	d^5G	a^5H'
	161.43	368	253	344	357	254
$a^5G'_4$...	16106.08	c^5H'	a^3F'			
	130.49	359	53			
$a^5G'_3$...	15975.59					
	98.41					
$a^5G'_2$...	15877.18					
$b^5G'_6$...	26910.69	a^5F'	c^5F'	b^5G	b^5H'	a^3F'
	137.71	128	16	108	75	267
$b^5G'_5$...	26772.98	b^3F'				
	115.57	45a				
$b^5G'_4$...	26657.41					
	92.98					
$b^5G'_3$...	26564.43					
	70.06					
$b^5G'_2$...	26494.37					

Table II contains all the lines of Ti I which have been classified, and all the unclassified lines of intensity 3 or more on King's scale, or 2 or more on that of Meggers. The first column gives a reference to the source of the measures (see notes at end of the table); the second, the observed wave-length; the third, the excess in units of 0.01 A of this above the value computed from the term values of Table I. The fourth column gives the intensity, and the fifth the temperature class. When the latter is given, both data are taken from King's paper (or in a few instances from estimates made by the writer on the photographs, in which case the intensity in the furnace and the temperature class are given in brackets). Otherwise the intensity is that given by the observer mentioned in the first column. These latter intensities are far from homogeneous, but, as most of the lines are faint anyhow, it is not worth while to attempt to correct them. They are given in parentheses in the table. The sixth column gives the vacuum frequency, ν; and the seventh, the terms whose combination accounts for the line—two entries, in the cases where there is good reason to believe that the line is an unresolved blend. In the last column is an index number to facilitate the identification of the multiplets. The first line in the table and all lines in the same multiplet are numbered "1"; the next unappropriated line and all in the multiplet to which it belongs, "2"; and so on.

TABLE II

Ti I—IDENTIFIED ARC LINES

Source	Obs. λ (I.A.)	Δλ O−C	Int.	Temp. Class	ν	Designation	Multi-plet
6	9787.60	−3	(0)	....	10214.22	$a^5F'_3-a^5F_2$	1
6	9770.20	−8	(1)	....	10232.40	$a^5F'_5-a^5F_4$	1
1	9743.58	−3	(1h)	....	10260.36	$a^5F'_1-a^5F_1$	1
1	9728.33	−8	(1)	....	10276.44	$a^5F'_2-a^5F_2$	1
1	9705.63	−6	(1)	....	10300.48	$a^5F'_3-a^5F_3$	1
1	9675.57	+4	(1)	....	10332.48	$a^5F'_4-a^5F_4$	1
1	9647.55	+10	(1h)	....	10362.48	$a^5F'_2-a^5F_3$	1
1	9638.26	−3	(2h)	....	10372.47	$a^5F'_5-a^5F_5$	1
1	9599.44	−10	(1)	....	10414.42	$a^5F'_3-a^5F_4$	1
1	9546.06	0	(1)	....	10472.65	$a^5F'_4-a^5F_5$	1
1	9285.02	−9	(1)	....	10767.08	$c^3F_3-c^3F'_3$	2
1	9257.62	+7	(1)	....	10798.95	$c^3F_4-c^3F'_4$	2
1	9246.18	+21	(1)	....	10812.31	$b^3F_4-b^3G_5$	3
1	9167.55	−8	(1)	....	10905.05	$b^3F_3-b^3G_4$	3
1	9123.09	+10	(1)	....	10958.19	$b^3F_2-b^3G_3$	3
1	9090.68	−5	(1)	....	10997.26	$a^5P'_3-a^5S'_2$	4
1	9027.28	−7	(1)	....	11074.50	$a^5P'_2-a^5S'_2$	4
1	8989.40	−2	(2)	....	11121.16	$a^5P'_1-a^5S'_2$	4
6	8766.59	−12	(3−)	....	11403.82	$a^3P'_2-a^3D'_2$	5
1	8734.69	−5	(1h)	....	11445.47	$a^3P'_1-a^3D'_1$	5
1	8692.29	−7	(1)	....	11501.28	$a^3P'_0-a^3D'_1$	5
1	8682.93	−7	(2)	....	11513.69	$a^3P'_1-a^3D'_2$	5
1	8675.33	−5	(2)	....	11523.78	$a^3P'_2-a^3D'_3$	5
1	8548.06	+1	(2)	....	11695.35	$a^3G_3-c^3F_2$	6
1	8539.30	−14	(1)	....	11707.35	$b^3P'_1-d^3D'_2$	7
1	8518.20	−13	(4)	....	11736.35	$a^3G_4-c^3F_3$	6
1*	8495.94	−8 −12	(1)	....	11767.09	$b^3P'_2-d^3D'_3$ $aF'-eF$	7 8
1	8468.45	−8	(3)	....	11805.30	$a^3G_5-c^3F_4$	6
1	8467.13	......	(2)	....	11807.14	....	......
1	8457.03	−7	(2h)	....	11821.24	$a^5P'_3-b^5D'_4$	9
1	8450.89	−4	(3)	....	11829.82	$a^3H'_5-c^3G'_4$	10
1	8438.90	+4	(3)	....	11846.64	$a^3H'_6-c^3G'_5$	10
1	8435.64	−1	(5)	....	11851.21	$a^5F'_4-a^5D'_3$	11
1	8434.89	−2	(4)	....	11852.26	$a^5F'_5-a^5D'_4$	11
1	8426.46	−4	(4)	....	11864.13	$a^5F'_3-a^5D'_2$	11
1	8412.34	−1	(3)	....	11884.04	$a^5F'_2-a^5D'_1$	11
10	8402.47	−1	(0)	....	11898.00	$a^3H'_5-c^3G'_5$	10
1	8396.85	+1	(2)	....	11905.96	$a^5F'_1-a^5D'_0$	11
12*	8382.72	−2	(2)	....	11926.03	$a^5F'_1-a^5D'_1$	11
12*	8382.45	−13	(2)	....	11926.42	$a^5F'_2-a^5D'_2$	11
1	8377.83	0	(2)	....	11932.99	$a^5F'_3-a^5D'_3$	11
1	8364.18	−1	(2)	....	11952.46	$a^5F'_4-a^5D'_4$	11
1	8353.12	−6	(2)	....	11968.30	$a^5F'_1-a^5D'_2$	11
1	8334.42	+1	(2)	....	11995.15	$a^5F'_2-a^5D'_3$	11
1	8312.89	+4	(2)	....	12026.21	$b^3G'_4-d^3F'_3$	12
1	8311.71	+4	(2)	....	12027.92	$b^3G'_3-d^3F'_2$	12
1	8307.41	+6	(1)	....	12034.15	$a^5F'_3-a^5D'_4$	11
1	8306.27	−1	(2h)	....	12035.80	$b^3G'_5-d^3F'_4$	12
1	8207.32	+1	(1n?)	....	12180.91	$b^3D'_3-c^3F'_4$	13
1*	8180.45	+1 −6	(1n?)	....	12220.92	$b^3D'_2-c^3F'_3$ $b^3D'_1-c^3F'_2$	13 13

TABLE II—*Continued*

Source	Obs. λ (I.A.)	Δλ O−C	Int.	Temp. Class	ν	Designation	Multiplet
1........	8131.40	− 7	(1)	....	12294.64	$c^3P'_2-e^3D'_3$	14
12........	8089.71	+ 8	(0)	....	12358.00	$c^3P'_1-e^3D'_1$	14
12........	8084.96	−28	(1)	....	12365.25	$c^3P'_1-e^3D'_2$	14
12........	8084.42	−20	(0)	....	12366.09	$c^3P'_0-e^3D'_1$	14
1........	8068.21	− 9	(2)	....	12390.93	$a^3G_3-b^3G'_3$	15
1........	8064.09	......	(2)	....	12397.25	....	.....
1........	8024.83	− 1	(2)	....	12457.90	$a^3G_4-b^3G'_4$	15
1........	7996.49	+ 2	(3)	....	12502.06	$b^5G'_6-c^5F'_5$	16
1*.......	7978.87	+ 2 −19	(4)	....	12529.66	$a^3G_5-b^3G'_5$ $b^5G'_5-c^5F'_4$	15 16
1........	7961.59	+ 7	(2)	....	12556.86	$b^5G'_4-c^5F'_3$	16
1........	7949.11	−15	(3)	....	12576.58	$aG-aG'$	17
1........	7943.91	+ 1	(1h)	....	12584.81	$b^5G'_3-c^5F'_2$	16
1........	7926.34	+11	(1)	....	12612.70	$b^5G'_2-c^5F'_1$	16
12........	7903.98	−12	(0)	....	12648.31	$bD-bF$	18
12........	7663.38	+ 4	(0)	....	13045.26	$b^3P'_2-e^3D'_2$	19
1........	7654.46	− 1	(2)	....	13060.69	$b^3P'_2-e^3D'_3$	19
12........	7618.33	−10	(0)	....	13122.65	$b^3P'_1-e^3D'_1$	19
1........	7614.49	− 4	(1p?)	....	13129.25	$b^3P'_1-e^3D'_2$	19
12........	7580.55	+15	(1)	....	13188.01	$b^3P'_0-e^3D'_1$	19
1........	7496.12	0	(2)	....	13336.57	$a^3H'_4-d^3G'_3$	20
1........	7489.61	− 2	(2)	....	13348.16	$a^3H'_5-d^3G'_4$	20
1........	7474.93	+ 5	(1)	....	13374.37	$a^5P'_3-c^3D'_3$	21
1........	7440.58	− 1	(3)	....	13436.12	$a^3H'_6-d^3G'_5$	20
6........	7423.12	− 7	(2−)	....	13467.72	$b^3F'_3-b^3F_2$	22
1........	7366.58	− 2	(1)	....	13571.09	$b^3F'_2-a^5S'_2$	23
1........	7364.11	− 1	2	IV	13575.65	$b^3F'_2-b^3F_2$	22
1........	7357.73	0	3	IV	13587.41	$b^3F'_3-b^3F_3$	22
1........	7352.14	+ 1	(1)	....	13597.74	$aP'-aP$	24
1........	7344.69	− 2	4	IV	13611.54	$b^3F'_4-b^3F_4$	22
1........	7332.26	− 5	(1)	....	13634.61	$a^5P'_3-a^5P_2$	25
1........	7330.97	+ 5	(1)	....	13637.01	$a^5P'_2-a^5P_1$	25
12........	7323.71	− 8	(0)	....	13650.54	$a^3D_3-e^3D'_2$	26
1........	7318.43	+ 9	(2)	....	13660.38	$b^3P'_2-b^3P_2$	27
12........	7315.52	− 3	(1)	....	13665.81	$a^3D_3-e^3D'_3$	26
12........	7305.87	− 4	(1)	....	13683.90	$a^5P'_1-a^5P_1$	25
1........	7299.67	− 2	(2)	....	13695.48	$b^3F'_2-b^3F_3$	22
12........	7281.74	......	(3h)	....	13729.20	....	.....
3........	7273.76?	+ 8	(0)	....	13744.26	$b^3P'_1-b^3P_2$	27
3........	7271.47?	− 3	(0)	....	13748.60	$b^3F'_3-b^3F_4$	22
3........	7266.24?	− 3	(0)	....	13758.50	$a^5P'_1-a^5P_2$	25
12........	7265.32	−19	(0)	....	13760.25	$a^3D_2-e^3D'_1$	26
12........	7261.86	− 9	(1)	....	13766.78	$a^3D_2-e^3D'_2$	26
1*.......	7253.76	− 6 −10	(1)	....	13782.17	$a^5P'_3-a^5P_3$ $a^3D_2-e^3D'_3$	25 26
1........	7251.74	+ 3	8	III	13786.00	$b^3F'_2-b^3D'_1$	28
1........	7244.82	+ 1	10	III	13799.17	$b^3F'_3-b^3D'_2$	28
12........	7236.94	+12	(1)	....	13814.19	$a^3D_1-e^3D'_1$	26
12........	7233.44	+ 2	(1)	....	13820.91	$a^3H'_6-a^3H_6$	29
12........	7233.31	− 1	(1)	....	13821.14	$a^3D_1-e^3D'_2$	26
1........	7216.19	+ 1	5	III	13853.92	$b^3F'_3-a^3P_2$	30
12........	7214.97	−13	(0)	....	13856.25	$aF'-eG'$	31
12........	7213.3	−20	(1)	....	13859.66	$a^5P'_2-a^5P_3$	25

TABLE II—*Continued*

Source	Obs. λ (I.A.)	Δλ O−C	Int.	Temp. Class	ν	Designation	Multiplet
1	7209.44	− 2	20	III	13866.90	$b^3F'_4-b^3D'_3$	28
1	7189.92	+ 6	2	IV?	13904.54	$aH'-aH$	32
3	7188.59	+ 5	(0)	....	13907.12	$b^3F'_2-b^3D'_2$	28
6	7160.33	− 2	(2)	....	13962.00	$b^3F'_2-a^3P_2$	30
1	7138.92	+ 2	(1, Ti?)	....	14003.87	$b^3F'_3-b^3D'_3$	28
1	7069.11	+ 1	2	IV	14142.16	$b^3D'_3-d^3F'_4$	33
1	7050.68	− 6	(1)	....	14179.13	$c^3P'_2-c^3P_1$	34
3	7039.36?	0	(1)	....	14201.93	$b^3D'_2-d^3F'_3$	33
1	7038.83	− 2	6	IV	14202.99	$c^3P'_2-c^3P_2$	34
1	7035.85	0	(2)	....	14209.02	$b^3D'_1-d^3F'_2$	33
1	7010.94	−12	(1)	....	14259.50	$c^3P'_1-c^3P_0$	34
1	7008.32	− 8	(1)	....	14264.83	$c^3P'_1-c^3P_1$	34
12	7007.81	−14	(1)	....	14265.90	$a^3D_3-b^3P_2$	35
3	7006.68	0	(0)	....	14268.16	$c^5D'_3-c^5D_3$	36
3	7004.60	− 4	(1)	....	14272.41	$c^3P'_0-c^3P_1$	34
1	6996.69	+ 3	(1)	....	14288.54	$c^3P'_1-c^3P_2$	34
12	6990.31	0	(1)	....	14301.63	$a^3D_2-b^3P_1$	35
12	6983.23	+12	(1)	....	14316.07	$a^3D_1-b^3P_0$	35
12	6980.39	− 1	(1)	....	14320.85	$c^5D'_4-c^5D_4$	36
12	6963.93	+17	(0)	....	14355.80	$a^3D_1-b^3P_1$	35
12	6946.10	− 4	(0)	....	14392.61	$a^3G'_5-b^3G_4$	37
3	6943.71	0	(2)	....	14397.56	$b^3F_4-d^3F'_4$	38
3	6938.88?	......	(3)	....	14407.58	....	......
12	6935.88	− 3	(1)	....	14413.79	$b^3F_3-d^3F'_3$	38
12	6933.14	− 3	(1)	....	14419.51	$b^3F_2-d^3F'_2$	38
3	6926.16	− 3	(2)	....	14434.05	$b^5F_5-d^5F'_5$	39
11	6913.03	−10	(2)	....	14461.46	$a^3G'_5-b^3G_5$	37
3	6911.18	......	(2)	....	14465.33	....	......
3	6873.99	+ 8	(2)	....	14543.59	$a^3G'_4-b^3G_4$	37
1	6861.47	+ 1	6	III	14570.13	$bG-bF$	40
3	6854.30	− 2	(1)	....	14585.36	$cP-bP'$	41
12	6849.15	− 5	(2)	....	14596.33	$a^3G'_3-b^3G_3$	37
12	6841.65	+ 4	(0)	....	14612.40	$a^3G'_4-b^3G_5$	37
12	6818.12	− 4	(0)	....	14662.77	$a^3G'_3-b^3G_4$	37
12	6751.94	+ 7	(0)	....	14806.52	$a^3G_3-c^3G'_3$	42
12	6748.43	+ 5	(1)	....	14814.18	$a^3G_4-c^3G'_4$	42
12	6746.42	+13	(1)	....	14818.60	$a^3G_5-c^3G'_5$	42
1	6743.14	+ 3	10	III A	14825.80	$aD-aD'$	43
4	6716.68	− 8	(1)	....	14884.21	$aP'-bP$	44
3	6677.25	+ 1	(0)	....	14972.11	$aP'-cD'$	45
1	6666.57	0	(2n)	....	14996.09	$b^3F'_4-b^5G'_5$	45a
1	6599.12	+ 2	12	III A	15149.36	$aD-aF$	46
1	6575.19	+ 4	3	V	15204.50	$aH'-bG'$	47
3	6565.62	......	4	V	15226.65	....	......
1	6556.08	− 2	25	III	15248.81	$b^3F'_4-c^3F_4$	48
1	6554.23	+ 1	20	III	15253.13	$b^3F'_3-c^3F_3$	48
1	6546.26	− 1	20	III	15271.68	$b^3F'_2-c^3F_2$	48
1	6508.15	+ 3	3	III A	15361.11	$b^3F'_2-c^3F_3$	48
1	6497.71	0	3	III A	15385.80	$b^3F'_3-c^3F_4$	48
1	6465.56	+ 4	(2)	....	15462.29	$aS'-bP'$	49
1	6464.02	+ 1	(1)	....	15465.98	$b^5F_4-c^5D_3$	50
1	6456.06	+ 1	(2d?)	....	15485.06	$b^5F_5-c^5D_4$	50
1	6454.22	......	(2)	....	15489.47	....	......

TABLE II—*Continued*

Source	Obs. λ (I.A.)	Δλ O−C	Int.	Temp. Class	ν	Designation	Multiplet
1	6446.27	......	(2)	....	15508.57	....	......
12	6419.15	− 8	(2)	....	15574.35	$a^3D_3-c^3P_2$	51
12	6381.39	+ 5	(1)	....	15666.31	$a^3D_2-c^3P_1$	51
12	6371.75	+15	(1)	....	15690.02	$a^3D_2-c^3P_2$	51
1	6366.38	+ 3	8	III	15703.18	$b^3F'_4-c^3D'_3$	52
12†	6364.92	+13	[2]	[III A]	15706.73	$a^3F'_3-a^5G'_2$	53
12	6361.41	0	(1)	....	15715.55	$a^3D_1-c^3P_0$	51
12†	6359.88	+ 3	[8]	[II A]	15719.12	$a^3F'_4-a^5G'_4$	53
12	6359.20	− 1	(0)	....	15720.99	$a^3D_1-c^3P_1$	51
1	6336.10	+ 1	8	III	15778.22	$b^3F'_3-c^3D'_2$	52
12†	6325.22	+ 2	[10]	[II A]	15805.40	$a^3F'_3-a^5G'_3$	53
4	6318.00	− 3	5	III A	15823.42	$b^3F'_2-c^3D'_1$	52
1	6312.23	− 3	10	III	15837.89	$b^3F'_4-b^3G'_4$	54
12	6311.25	− 2	(1)	(III A)	15840.34	$b^3F'_3-c^3D'_3$	52
1	6303.76	− 4	10	III	15859.16	$b^3F'_3-b^3G'_3$	54
12	6298.07	0	(00)	....	15873.52	$a^5P'_1-c^5D'_1$	55
12†	6296.66	+ 6	[12]	[II A]	15877.04	$a^3F'_2-a^5G'_2$	53
12	6295.93	+ 9	(0)	....	15878.60	$a^5P'_2-c^5D'_2$	55
1*†‡	6295.30	+ 5 + 2	[2]	[III A]	15880.50	$a^3F'_4-a^5G'_5$ $a^5P'_3-c^5D'_3$	53 55
12	6277.51	+ 2	(00)	....	15925.49	$a^5P'_1-c^5D'_2$	55
12†	6273.39	0	[6]	[II A]	15935.94	$a^3F'_3-a^5G'_4$	53
12	6266.02	− 1	(1)	(III)	15954.69	$a^5P'_3-c^5D'_4$	55
12	6264.80	− 1	(0)	....	15957.80	$a^5P'_2-c^5D'_3$	55
1	6261.10	− 5	35	II	15967.22	$b^3F'_2-b^3G'_3$	54
1	6258.70	− 3	50	II	15973.35	$b^3F'_4-b^3G'_5$	54
1	6258.10	− 1	40	II	15974.88	$b^3F'_3-b^3G'_4$	54
12†	6257.72	+ 5	[2]	[III A]	15975.46	$a^3F'_2-a^5G'_3$	53
1	6222.56	......	(2)	....	16066.12	....	......
1	6221.42	+ 5	8	III	16069.06	$a^3G'_3-c^3F'_2$	56
1	6220.45	− 2	12	III	16071.57	$a^3G'_4-c^3F'_3$	56
1	6215.24	− 2	20	III	16085.04	$a^3G'_5-c^3F'_4$	56
2	6199.64	+ 8	(0)	....	16125.53	$bG'-dG$	57
1	6186.15	− 5	3	III	16160.68	$a^3D_3-d^3F_4$	58
1	6174.47	−31	(2n)	....	16191.25	$a^3G'_3-c^3F'_3$?	56
1	6159.02	0	(2n)	....	16231.86	$a^3D_2-d^3F_2$	58
1	6149.81	+ 2	2	III	16256.17	$a^3D_2-d^3F_3$	58
1	6146.22	+ 3	3	III	16265.66	$a^3G_3-d^3G'_3$	59
1	6138.38	− 2	1	IV	16286.44	$a^3D_1-d^3F_2$	58
1	6126.21	− 1	20	II	16318.80	$a^3P'_2-a^3S'_1$	60
1	6121.03	+ 2	3	III	16332.61	$a^3G_4-d^3G'_4$	59
1	6098.70	+ 3	7	III	16392.41	$aG'-bF'$	61
1	6092.79	− 1	4	III	16408.31	$a^3G_5-d^3G'_5$	59
1	6091.17	+ 1	20	III	16412.67	$bG-aH$	62
1	6085.22	0	20	II	16428.71	$a^3P'_1-a^3S'_1$	60
1	6081.31	+ 3	(1)	....	16439.28	$aF'-fG'$	63
1	6070.98	+ 4	(1)	....	16467.25	$aP-dD$	64
1	6064.64	− 1	9	II A	16484.47	$a^3P'_0-a^3S'_1$	60
12	6059.27	......	[2]	[III A]	16499.06	....	......
11†	6031.71	+ 3	(0)	....	16574.47	$a^3F'_4-a^5F_3$	65
3	6018.56?	−11	(0)	....	16610.69	$a^3P'_1-a^5S'_2$	66
12	6012.53	− 5	(1)	....	16627.11	$a^3F_4-b^3G_5$	67
3	6002.70?	− 1	(0)	....	16654.57	$a^3D_2-e^3F_3$	68

TABLE II—*Continued*

Source	Obs. λ (I.A.)	Δλ O−C	Int.	Temp. Class	ν	Designation	Multiplet
1........	5999.66	+ 1	8	III	16663.00	$a^3H_4'-aH$	69
7........	5999.00	− 4	4n	IV	16664.83	$a^3D_3-e^3F_4$	68
4........	5996.01	0	2	III	16673.15	$a^3G_4-a^3H_4$	70
4........	5995.68	+ 6	2	V	16674.07	$bD'-cD$	71
4........	5988.58	0	2	III	16693.83	$a^3G_5-a^3H_5$	70
11†.......	5984.59	+ 3	(1)	(III A)	16704.96	$a^3F_3'-a^5F_2$	65
12........	5982.52	− 2	(0)	(III A)	16710.66	$a^3F_3-b^3G_4$	67
12........	5980.89	+ 5	(1)	(III A)	16715.31	$a^3P_2'-b^3D_1'$	72
1........	5978.54	0	25	II	16721.87	$a^3G_3-a^3H_4$	70
12........	5971.07	− 1	(0)	....	16742.80	$a^3F_2-b^3G_3$	67
1........	5965.83	− 1	30	II	16757.50	$a^3G_4-a^3H_5$	70
1........	5953.16	− 1	30	II	16793.16	$a^3G_5-a^3H_6$	70
12†.......	5944.65	0	(0)	....	16817.20	$a^3F_2'-a^5F_1$	65
1........	5941.73	− 3	12	II A	16825.47	$a^3P_1'-b^3D_1'$	72
11†.......	5940.66	+ 2	(0)	....	16828.49	$a^3F_4'-a^5F_5$	65
1........	5937.79	0	6	III A	16836.62	$a^3P_2'-b^3D_2'$	72
1........	5922.11	− 1	18	II	16881.21	$a^3P_0'-b^3D_1'$	72
1........	5918.56	+ 1	10	II	16891.33	$a^3P_2'-a^3P_2$	73
11†.......	5913.71	0	(1)	....	16905.18	$a^3F_3'-a^5F_4$	65
1........	5903.33	+ 1	5	III A	16934.90	$a^3P_2'-a^3P_1$	73
1........	5899.29	+ 2	25	II	16946.50	$a^3P_1'-b^3D_2'$	72
1........	5880.30	+ 2	5	III A	17001.23	$a^3P_1'-a^3P_2$	73
3*.......	5877.77	+ 3 + 1	(1)	....	17008.55	$b^5F_5-b^5G_6$ $b^5F_3-b^5G_4$	74 74
1........	5866.45	− 1	35	II	17041.38	$a^3P_2'-b^3D_3'$	72
1........	5863.10	− 1	(1n)	....	17051.10	$b^5F_2-b^5G_3$	74
11........	5832.47	+ 1	(1)	(IV)	17140.66	$b^5G_6'-b^5H_6'$	75
1........	5823.76	+ 3	3	III	17166.29	$bG-b^3H_4$	76
12........	5814.00	0	(1)	(III A)	17195.13	$a^3P_2'-b^5D_3'$	77
2........	5812.83	0	(1)	(IV)	17198.58	$b^5G_5'-b^5H_5'$	75
12........	5809.75	− 6	(0)	(IV A)	17207.65	$a^3P_1'-b^5D_2'$	77
11........	5804.26	0	5n	IV	17223.96	$b^5G_6'-b^5H_7'$	75
2........	5797.45	+ 1	(1)	(IV)	17244.31	$b^5G_4'-b^5H_4'$	75
11........	5785.97	− 1	5n	IV	17278.41	$b^5G_5'-b^5H_6'$	75
12........	5785.66	+ 1	(1)	(IV)	17279.36	$b^5G_3'-b^5H_3'$	75
7........	5780.81	+ 6	2	III	17293.84	$b^3P_2'-b^3S_1'$	78
1........	5774.02	− 1	5n	IV	17314.17	$b^5G_4'-b^5H_5'$	75
1........	5766.33	+ 2	4n	IV	17337.26	$b^5G_3'-b^5H_4'$	75
1........	5762.25	− 3	4n	IV	17349.53	$b^5G_2'-b^5H_3'$	75
1........	5752.89	+ 5	1	IV	17377.75	$b^3P_1'-b^3S_1'$	78
1........	5741.28	+ 3	1	IV	17412.90	$bD-cF$	79
1........	5740.04	+ 1	4	IV	17416.67	$a^3H_4'-b^3H_4$	80
1........	5739.50	0	9	III	17418.30	$a^3H_5'-b^3H_5$	80
1........	5720.49	+ 1	3	III	17476.19	$a^5D_1'-b^5F_1'$	81
1........	5716.48	+ 2	4	III	17488.44	$a^5D_2'-b^5F_2'$	81
7........	5715.13	0	9	III	17492.57	$a^3H_6'-b^3H_6$	80
1........	5713.93	0	3	IV	17496.25	$a^5D_0'-b^5F_1'$	81
7........	5711.94	+ 5	4	IV	17502.34	$a^5D_3'-b^5F_3'$	81
1........	5708.27	+ 3	3	IV	17513.59	$a^5D_4'-b^5F_4'$	81
1........	5702.69	− 1	6	III	17530.73	$a^5D_1'-b^5F_2'$	81
1........	5689.47	− 2	10	III	17571.47	$a^5D_2'-b^5F_3'$	81
1........	5679.95	− 3	2	III	17600.92	$a^3D_1'-c^3F_2'$	82
1........	5675.41	− 3	9	III A	17615.01	$a^5D_3'-b^5F_4'$	81

TABLE II—*Continued*

Source	Obs. λ (I.A.)	Δλ O−C	Int.	Temp. Class	ν	Designation	Multiplet
4	5662.91	0	4	III	17653.88	$a^3D'_2-c^3F'_3$	82
1	5662.16	0	12	III	17656.21	$a^5D'_4-b^5F'_5$	81
12	5659.11	+5	(3)	(III A)	17665.74	$aD-a^3S'_1$	83
1	5648.63	+2	5	IV	17698.51	$a^3D'_3-c^3F'_4$	82
1	5644.14	+1	18	III	17712.59	$bG-bG'$	84
2	5642.79	+5	(1)	....	17716.83	$c^5D'_4-f^5F'_5$	85
1	5629.39	......	(2n?)	....	17759.00	....	.....
2	5600.80	......	(2)	....	17849.66	....	.....
1	5597.92	+1	(2n)	....	17858.84	$a^3H'_5-bG'$	86
2	5597.69	......	(3)	....	17859.57	....	.....
1	5565.48	+1	9	III	17962.93	$a^3H'_4-bG'$	86
2	5527.61	0	(1)	....	18086.00	$a^3F_4-c^3F'_3$	87
1	5514.54	0	25	II	18128.86	$b^3F'_3-d^3D'_2$	88
7	5514.36	0	20	II	18129.45	$b^3F'_2-d^3D'_1$	88
1	5512.54	0	25	II	18135.44	$b^3F'_4-d^3D'_3$	88
7	5511.80	+3	2	III A	18137.87	$aP'-aS'$	89
1	5503.89	−2	8	III	18163.93	$aH'-cG'$	90
11†	5490.82	−2	(1)	(I A)	18207.17	$a^3F'_4-a^5D'_3$	91
7	5490.16	−1	12	II	18209.37	$b^3F'_4-c^5D'_3$	92
7	5488.24	0	5	III	18215.73	$a^3F_2-c^3F'_2$	87
7	5481.90	+2	5	I A	18236.80	$b^3F'_2-d^3D'_2$	88
7	5481.45	+2	6	III	18238.30	$a^3F_3-c^3F'_3$	87
2	5477.70	−2	8	III	18250.79	$a^3F_4-c^3F'_4$	87
12	5474.52	+6	(1)	(IV)	18261.27	$c^3P'_2-d^3P_1$	93
7	5474.28	+8	6	II	18262.18	$b^3F'_4-c^3G'_5$	94
12	5473.56	+5	(1)	(IV)	18264.58	$c^3P'_1-d^3P_0$	93
4	5472.73	+3	2	III A	18267.35	$b^3F'_3-c^5D'_2$	92
7	5471.19	−1	5	III	18272.50	$b^3F'_3-d^3D'_3$	88
7‡	5460.51	+3	4	I A	18308.24	$a^3F'_4-a^5D'_4$	91
7	5453.67	+2	3	III A	18331.20	$b^3F'_3-c^3G'_4$	94
2	5451.97	+2	(1)	....	18336.93	$a^3F_2-c^3F'_3$	87
7	5449.19	+4	1	III A	18346.27	$b^3F'_3-c^5D'_3$	92
12	5448.85	0	(1)	(IV)	18347.13	$c^3P'_1-d^3P_1$	93
7*	5446.67	+1 +5	2	II A	18354.76	$c^3P'_0-d^3P_1$ $a^3F'_3-a^5D'_2$	93 91
7	5438.33	+2	1	III A	18382.90	$b^3F'_2-c^3G'_3$	94
7	5436.65	−4	1	III A	18388.60	$aD-b^3D'_3$	95
2	5432.32	−5	(0)	....	18403.25	$a^3F_3-c^3F'_4$	87
7	5429.15	−2	6	III	18413.99	$c^3P'_2-d^3P_2$	93
7	5426.27	+2	3	I A	18423.77	$a^3F'_3-a^5D'_3$	91
4	5419.22	−4	1	III A	18447.71	$c^3P'_2-b^5S'_2$	96
7	5409.62	−2	6	II	18480.47	$a^3G_5-d^3F_4$	97
11†	5408.93	+1	(1)	(I A)	18482.83	$a^3F'_2-a^5D'_1$	91
4	5404.03	0	2	IV	18499.58	$c^3P'_1-d^3P_2$	93
12	5401.32	−3	(1)	(III A)	18508.72	$a^5F'_2-b^3F_2$	98
4	5397.08	−2	4	III	18523.41	$a^3G_4-d^3F_3$	97
4*	5396.57	−3 −2	1	I A	18525.16	$a^3F'_2-a^5D'_2$ $a^3F'_3-a^5D'_4$	91 91
7	5390.26	−2	(2)	....	18546.84	$aF'-fF$	99
7	5390.00	+3	3	III	18547.74	$a^3G_3-d^3F_2$	97
4	5389.15	−2	2	III A	18550.66	$a^5F'_1-b^3F_2$	98
12	5384.63	+1	(1)	(III A)	18566.23	$a^5F'_3-b^3F_3$	98
12†	5376.58	−1	(0)	....	18594.04	$a^3F'_2-a^5D'_3$	91

TABLE II—*Continued*

Source	Obs. λ (I.A.)	Δλ O−C	Int.	Temp. Class	ν	Designation	Multi-plet
7	5369.65	......	4	III	18618.02	....	......
4	5366.63	− 2	2	III A	18628.51	$a^5F'_2-b^3F_3$	98
12†	5361.67	− 4	(1)	(III A)	18645.75	$a^5F'_4-b^3F_4$	98
7	5351.09	+ 1	4	III	18682.60	$aF-bF'$	100
4	5341.48	+ 2	1	IV?	18716.22	$bP-bP'$	101
12	5340.68	+ 1	(1)	(III A)	18719.02	$a^5F'_2-b^3D'_1$	102
4	5338.28	− 1	1	III A	18727.44	$a^5F'_3-b^3F_4$	98
12	5323.93	+ 4	(1)	(III A)	18777.91	$a^5F'_3-b^3D'_2$	102
12	5313.24	0	(2)	(III A)	18815.69	$a^3P'_2-c^3D'_2$	103
7‡	5299.98	− 2	1	III A	18862.76	$a^3P'_1-c^3D'_1$	103
7	5298.42	+ 1	4	III	18868.32	$bD-cP$	104
7	5297.29	+ 4	6	III	18872.35	$a^3G_3-e^3F_2$	105
7	5295.78	0	4	III	18877.72	$a^3P'_2-c^3D'_3$	103
7	5294.75	− 4	(2)	....	18881.39	$b^5F_5-f^5F'_5$	106
7	5289.28	+ 1	(1)	(III A)	18900.93	$a^5F'_4-b^3D'_3$	102
7	5284.39	+ 2	2	III A	18918.41	$a^3P'_0-c^3D'_1$	103
7	5283.45	+ 1	8	III	18921.78	$a^3G_4-e^3F_3$	105
7	5282.38	0	3	III A	18925.61	$a^3P'_1-c^3D'_2$	103
7	5281.93	+ 7	(2)	....	18927.22	$d^3D'_3-b^3D_3$	107
12	5269.93	+ 6	(1)	(III A)	18970.32	$a^3G_3-e^3F_3$	105
7	5266.28	0	(2)	....	18983.47	$b^5G'_5-b^5G_5$?	108
7	5265.97	0	10	III	18984.59	$a^3G_5-e^3F_4$	105
7	5263.50	− 1	3	III	18993.50	$a^5F_5-b^5F'_4$	109
7	5263.32	− 3	(2)	....	18994.14	$b^5G'_6-b^5G_6$	108
7	5259.97	− 2	3	IV	19006.25	$aD'-bF'$	110
4	5257.58	+ 4	(1)	....	19014.88	$aP'-cP$	111
7	5255.82	− 2	5	III	19021.25	$a^5F_4-b^5F'_3$	109
7	5252.11	+ 1	8	I A	19034.69	$a^3F'_4-a^3F_3$	112
12	5251.50	+ 1	(0)	(III A)	19036.89	$a^5F'_2-b^5D'_1$	113
4	5250.94	+ 1	2	III A	19038.93	$a^5F'_3-b^5D'_2$	113
11*†	5248.39	0 + 2	(1)	(III A)	19048.17	$a^5F'_1-b^5D'_0$ $a^3G_4-e^3F_4$	113 105
4	5247.30	+ 1	5	III	19052.13	$a^5F_3-b^5F'_2$	109
7	5246.81	− 1	(2)	....	19053.91	$b^5G'_4-b^5G_4$	108
4	5246.56	0	3	III A	19054.82	$a^5F'_4-b^5D'_3$	113
4	5246.14	− 5	2	V	19056.34	$bD-dP$	114
12	5239.94	− 1	(0)	....	19078.90	$a^5F'_1-b^5D'_1$	113
7*	5238.58	− 1 + 1	6	III A	19083.84	$a^5F'_5-b^5D'_4$ $a^5F_2-b^5F'_1$	113 109
12†	5233.81	− 4	(1)	(III A)	19101.25	$a^5F'_2-b^5D'_2$	113
7	5227.19	+ 1	(2)	....	19125.43	$b^5G'_3-b^5G_3$	108
7	5224.96	0	8	III	19133.60	$a^5F_4-b^5F'_4$	109
4	5224.57	+ 1	6	III	19135.03	$a^5F_3-b^5F'_3$	109
7	5224.32	+ 1	15	III	19135.94	$a^5F_5-b^5F'_5$	109
12†	5224.13	− 1	(0)	(IV A)	19136.63	$a^5F'_3-b^5D'_3$	113
7	5223.64	− 1	6	III	19138.43	$a^5F_2-b^5F'_2$	109
7	5222.68	− 2	6	III	19141.95	$a^5F_1-b^5F'_1$	109
7	5219.72	+ 1	8	I A	19152.80	$a^3F'_3-a^3F_2$	112
2	5212.27	......	3	III	19180.06	....	......
11†	5211.20	− 2	(1)	(III A)	19184.10	$a^5F'_4-b^5D'_4$	113
7	5210.39	0	40	I	19187.09	$a^3F'_4-a^3F_4$	112
4	5207.87	0	3	III	19196.38	$a^5F_1-b^5F'_2$	109
7	5206.09	− 4	5	III?	19202.95	$aP'-dP$	115

TABLE II—*Continued*

Source	Obs. λ (I.A.)	Δλ O−C	Int.	Temp. Class	ν	Designation	Multiplet
4	5201.12	0	4	III	19221.29	$a^{5}F_{2}-b^{5}F'_{3}$	109
4	5194.04	0	4	IV A	19247.49	$a^{5}F_{3}-b^{5}F'_{4}$	109
7	5192.98	+1	35	I	19251.42	$a^{3}F'_{3}-a^{3}F_{3}$	112
4	5186.32	−1	3	III	19276.15	$a^{5}F_{4}-b^{5}F'_{5}$	109
12	5183.79	−6	(1)	(III A)	19285.55	$a^{3}P'_{2}-a^{5}P_{3}$	116
12	5178.62	−9	[0]	[III A]	19304.81	$a^{3}P'_{2}-bD'$	117
7	5173.74	−1	30	I	19323.01	$a^{3}F'_{2}-a^{3}F_{2}$	112
12	5170.50	−5	(0)	....	19335.11	$bG-cF$	118
7	5152.18	−1	10	I A	19403.87	$a^{3}F'_{3}-a^{3}F_{4}$	112
7	5147.48	0	10	I A	19421.59	$a^{3}F'_{2}-a^{3}F_{3}$	112
7	5145.47	+1	12	II	19429.17	$b^{3}F'_{4}-e^{3}D'_{3}$	119
4	5132.96	+1	(1)	....	19476.52	$a^{3}H'_{5}-e^{3}G'_{4}$	120
11	5127.36	−2	(1)	....	19497.79	$a^{3}H'_{6}-e^{3}G'_{5}$	120
4	5124.08	+1	(1)	....	19510.28	$aG-d^{3}G'_{5}$	121
4	5122.09	−4	(1)	....	19517.86	$a^{3}H'_{4}-e^{3}G'_{3}$	120
7	5120.43	−1	12	III	19524.19	$aH'-aI'$	122
7	5113.45	+1	10	III	19550.84	$b^{3}F'_{3}-e^{3}D'_{2}$	119
4	5109.43	+1	4	III?	19566.21	$b^{3}F'_{3}-e^{3}D'_{3}$	119
7	5087.07	−1	8	III	19652.22	$b^{3}F'_{2}-e^{3}D'_{1}$	119
4	5085.35	+1	4	III	19658.87	$b^{3}F'_{2}-e^{3}D'_{2}$	119
7	5071.49	0	7	III	19712.59	$b^{3}F'_{4}-d^{3}G'_{4}$	123
11	5069.41	+10	5	IV	19720.68	$a^{3}D_{1}-d^{3}P_{0}$	124
2	5068.33	+1	3	IV	19724.87	$a^{3}G'_{3}-c^{3}G_{3}$	125
7	5066.01	+2	7	III	19733.92	$b^{3}F'_{3}-d^{3}G'_{3}$	123
7	5064.66	+2	25	I	19739.18	$a^{3}F'_{4}-a^{3}D'_{3}$	126
11	5064.07	−1	4	IV	19741.49	$a^{3}G'_{5}-c^{3}G_{5}$	125
7	5062.11	−5	7	III	19749.12	$a^{3}D_{2}-d^{3}P_{1}$	124
4*	5054.11	+1 +1	3	IV?	19780.38	$a^{3}G'_{4}-c^{3}G_{4}$ $aS-bP$	125 127
7	5052.88	−1	8	IV?	19785.19	$a^{3}D_{3}-d^{3}P_{2}$	124
4	5048.21	−2	(1)	....	19803.50	$a^{3}D_{1}-d^{3}P_{1}$	124
7	5045.43	0	5	III A	19814.41	$a^{5}F'_{5}-b^{5}G'_{4}$	128
4	5044.25	−6	2	IV	19819.05	$a^{3}D_{3}-b^{5}S'_{2}$	129
7	5043.59	0	7	III A	19821.64	$a^{5}F'_{4}-b^{5}G'_{3}$	128
7	5040.63	+2	6	III A	19833.28	$a^{5}F'_{3}-b^{5}G'_{2}$	128
7	5039.96	+1	22	I	19835.92	$a^{3}F'_{3}-a^{3}D'_{2}$	126
7	5038.41	+1	25	II	19842.01	$b^{3}F'_{2}-d^{3}G'_{3}$	123
7	5036.47	0	25	II	19849.65	$b^{3}F'_{3}-d^{3}G'_{4}$	123
7	5035.92	+1	25	II	19851.83	$b^{3}F'_{4}-d^{3}G'_{5}$	123
7	5025.58	+1	18	III	19892.67	$a^{5}G'_{6}-b^{5}F'_{5}$	130
7	5024.85	−1	20	II	19895.56	$a^{5}F'_{2}-b^{5}G'_{2}$	128
12	5023.39	0	(2)	....	19901.35	$a^{3}D_{2}-d^{3}P_{2}$	124
7	5022.87	+1	25	II	19903.41	$a^{5}F'_{3}-b^{5}G'_{3}$	128
7	5020.04	0	25	II	19914.62	$a^{5}F'_{4}-b^{5}G'_{4}$	128
7	5016.17	0	20	II	19929.99	$a^{5}F'_{5}-b^{5}G'_{5}$	128
11*†	5014.28	+1	(25)	(I)	19937.49	$a^{5}F'_{1}-b^{5}G'_{2}$	128
11*†	5014.19	+1	(25)	(I)	19937.83	$a^{3}F'_{2}-a^{3}D'_{1}$	126
7	5013.30	0	18	III	19941.40	$a^{5}G'_{5}-b^{5}F'_{4}$	130
7	5009.65	+2	7	I A	19955.92	$a^{3}F'_{3}-a^{3}D'_{3}$	126
2	5007.87	......	(2)	....	19963.01	....	......
7	5007.22	0	40	II	19965.61	$a^{5}F'_{2}-b^{5}G'_{3}$	128
7	5001.01	0	10	III A	19990.40	$a^{5}G'_{4}-b^{5}F'_{3}$	130
7	4999.51	0	45	II	19996.40	$a^{5}F'_{3}-b^{5}G'_{4}$	128

TABLE II—*Continued*

Source	Obs. λ (I.A.)	Δλ O−C	Int.	Temp. Class	ν	Designation	Multi-plet
7	4997.10	+1	8	I A	20006.05	$a^3F'_2-a^3D'_2$	126
12†	4995.08	+4	(1)	(III)	20014.15	$b^3P'_2-f^3D'_3$	131
7	4991.08	+1	50	II	20030.17	$a^5F'_4-b^5G'_5$	128
7	4989.16	+2	10	III	20037.89	$a^5G'_3-b^5F'_2$	130
7	4981.75	0	60	II	20067.69	$a^5F'_5-b^5G'_6$	128
7	4978.21	−1	10	III	20081.95	$a^5G'_2-b^5F'_1$	130
7	4977.75	+3	5	IV	20083.81	$a^5G'_5-b^5F'_5$	130
4	4976.82	+2	1	IV	20087.57	$aH'-dG'$	132
7	4975.36	−1	10	III	20093.45	$bD-dF$	133
7	4973.06	+2	6	III	20102.76	$a^5G'_4-b^5F'_4$	130
2	4968.57	−1	6	III	20120.92	$a^5G'_3-b^5F'_3$	130
12	4967.30	+2	(1)	(III A)	20126.04	$a^3F'_2-a^3D'_3$	126
7	4964.75	0	5	III	20136.40	$a^5G'_2-b^5F'_2$	130
4‡	4958.25	+1	2	III A	20162.79	$aD-c^3D'_2$	134
7	4948.21	−2	3	IV	20203.71	$a^3D_3-f^3F_3$	135
4	4948.01	+3	1	III A	20204.53	$a^5F'_2-c^3F_2$	136
12	4944.40	+1	(0)	....	20219.23	$a^5G'_2-b^5F'_3$	130
12†	4943.06	+2	(0)	(III A)	20224.75	$aD-c^3D'_3$	134
7	4941.58	−4	3	IV	20230.81	$a^3D_2-f^3F_2$	135
12	4941.32	+3	(1)	(III A)	20231.87	$a^5F'_3-c^3F_3$	136
12	4941.01	+4	(1)	....	20233.15	$a^5G'_3-b^5F'_4$	130
7	4938.31	+2	8	IV	20244.21	$aH'-bH$	137
12	4938.04	+1	(0n)	....	20245.31	$a^5G'_4-b^5F'_5$	130
7	4937.75	+3	4	III A	20246.50	$a^5F'_1-c^3F_2$	136
12	4928.89	+1	(0)	....	20282.82	$a^5F'_4-c^3F_4$	136
7	4928.36	+2	12	III	20285.09	$a^3D_1-f^3F_2$	135
7	4926.17	+2	4	III A	20294.10	$a^5F'_2-c^3F_3$	136
7	4925.42	−1	5	IV	20297.19	$a^3G_4-b^3H_4$	138
7	4921.79	−1	12	III	20312.16	$a^3D_3-f^3F_4$	135
7	4919.88	−5	10	III	20320.05	$a^3D_2-f^3F_3$	135
7	4915.24	−1	5	III	20339.23	$a^3G_5-b^3H_5$	138
7	4913.63	0	20	III	20345.89	$a^3G_3-b^3H_4$	138
4	4909.11	+1	2	III A	20364.62	$a^5F'_3-c^3F_4$	136
11†	4908.49	+4	(0)	....	20367.20	$a^3G'_5-e^3F'_4$	139
11†	4900.63	+2	(0)	....	20399.85	$a^3G'_4-e^3F'_3$	139
7	4899.93	0	20	III	20402.77	$a^3G_4-b^3H_5$	138
12	4893.90	−2	(1)	....	20427.89	$a^3D_2-f^3D'_1$	140
7	4893.06	−1	2	IV	20431.42	$a^3H'_5-a^3I'_5$	141
4	4891.85	−1	1	IV	20436.48	$a^3D_3-f^3D'_2$	140
7	4885.09	0	20	II	20464.75	$a^3G_5-b^3H_6$	138
7	4882.34	+2	2	IV	20476.28	$a^3H'_6-a^3I'_6$	141
7	4880.92	+2	3	IV	20482.25	$a^3D_1-f^3D'_1$	140
7	4870.14	+2	20	III	20527.58	$a^3H'_5-a^3I'_6$	141
7	4868.28	−1	18	III	20535.42	$a^3H'_4-a^3I'_5$	141
4	4864.22	+3	4	III	20552.56	$a^3D_2-f^3D'_2$	140
7	4856.01	0	20	III	20587.31	$a^3H'_6-a^3I'_7$	141
7	4848.46	0	8	IV	20619.36	$a^3D_3-f^3D'_3$	140
7	4843.99	0	2	IV	20638.39	$b^3P'_1-g^3D'_2$	142
7	4840.88	−1	25	I	20651.65	$aD-bD'$	143
12	4839.23	−6	(1)	....	20658.74	$b^3P'_0-g^3D'_1$	142
7	4836.13	0	6	III	20671.93	$bG-cG'$	144
4	4832.09	+2	(1)	....	20689.21	$a^5D'_2-c^5F'_3$	145
7	4827.60	−2	2	IV?	20708.46	$a^5D'_3-c^5F'_4$	145

TABLE II—*Continued*

Source	Obs. λ (I.A.)	Δλ O−C	Int.	Temp. Class	ν	Designation	Multiplet
11	4825.49	+ 1	3	IV	20717.51	$a^5D'_4-c^5F'_5$	145
12	4821.29	− 3	(1bd?)	....	20735.46	$a^3D_2-f^3D'_3$	140
7	4820.42	0	20	II	20739.30	aG−bF	146
11†	4812.89	0	(0)	(III A)	20771.71	$a^5F'_5-b^3G'_4$	147
7	4812.25	+ 1	5	III	20774.51	$c^3P'_2-h^3D'_2$	148
7	4811.09	+ 6	4	IV	20779.52	a^3G_5-bG'	149
7	4808.54	0	5	IV	20790.54	aG′−bH′	150
7	4805.43	− 1	12	III	20804.00	$c^3P'_2-h^3D'_3$	148
7	4799.81	0	12	III	20828.35	$bG-c^3H_4$	151
7	4797.99	0	5	III	20836.26	$c^3P'_1-h^3D'_1$	148
7	4796.22	− 1	6	III	20843.94	$c^3P'_0-h^3D'_1$	148
7	4792.50	+ 2	10	III	20860.13	$c^3P'_1-h^3D'_2$	148
6	4789.79	+ 1	(1−)	....	20871.90	$a^5F'_4-b^3G'_4$	147
12	4783.31	0	[2]	[III A]	20900.09	$a^5F'_2-b^3G'_3$	147
7	4781.73	+ 1	6	III A	20907.11	$a^5F'_5-b^3G'_5$	147
7	4778.27	0	10	III	20922.25	$a^3H'_4-cG'$	152
4	4771.13	+ 3	3	III A	20953.56	$a^5F'_3-b^3G'_4$	147
7	4769.78	0	4	III	20959.49	$a^3H'_6-c^3H_5$	153
7	4766.33	− 1	4	III	20974.65	$a^3H'_5-c^3H_4$	153
12	4759.74	+ 8	(1bd?)	....	21003.71	$a^3D_3-g^3F_3$	154
7	4759.28	0	25	III	21005.73	$a^3H'_6-c^3H_6$	153
7	4758.92	+ 1	4	III A	21007.32	$a^5F'_4-b^3G'_5$	147
7	4758.13	− 1	25	III	21010.81	$a^3H'_5-c^3H_5$	153
12	4754.38	− 3	(1bd?)	....	21027.32	$a^3D_2-g^3F_2$	154
7	4747.69	0	3	III	21057.01	$a^3H'_5-c^3H_6$	153
4	4747.29	+ 1	1	III A	21058.78	$a^3P'_2-d^3D'_1$	155
7	4742.80	0	20	III	21078.72	$a^3H'_4-c^3H_4$	153
7	4742.13	0	3	IV	21081.69	$a^3D_1-g^3F_2$	154
7	4734.68	0	3	IV?	21114.87	$a^3H'_4-c^3H_5$	153
7	4733.43	− 4	6	III?	21120.44	$a^3D_2-g^3F_3$	154
7	4731.18	− 2	9	III	21130.48	$a^3D_3-g^3F_4$	154
12	4724.68	+ 2	(2)	....	21159.53	$a^3D_3-g^3D'_2$	156
7	4723.18	0	10	III	21166.27	$a^3P'_2-d^3D'_2$	155
7	4722.63	+ 1	10	III	21168.74	$a^3P'_1-d^3D'_1$	155
7	4715.31	− 1	4	II A	21201.61	$a^3F'_4-a^3G'_4$	157
7*	4710.19	− 2 0	18	III	21224.64	$a^3P'_0-d^3D'_1$ $a^3D_3-g^3D'_3$	155 156
11	4708.97	− 1	1	IV?	21230.15	$a^3D_2-g^3D'_1$	156
12*†	4698.82	− 4	(6?)	....	21276.00	$a^3D_2-g^3D'_2$	156
7*	4698.79	+ 2	20	II	21276.14	$a^3P'_1-d^3D'_2$	155
7	4696.92	0	4	IV?	21284.62	$a^3D_1-g^3D'_1$	156
7	4693.68	+ 2	5	II A	21299.30	$a^3F'_3-a^3G'_3$	157
7	4691.34	0	20	II	21309.93	$a^3P'_2-d^3D'_3$	155
7	4690.81	+ 1	3	IV?	21312.34	$a^3P'_2-c^3G'_3$	158
4	4688.38	+ 1	3	IV?	21323.38	$a^3S'_1-d^3P'_2$	159
4	4686.92	0	4	IV?	21330.02	$a^3D_1-g^3D'_2$	156
4	4684.53	− 1	2	IV?	21340.90	$a^3D_2-g^3D'_3$	156
7	4681.91	− 1	30	I	21352.85	$a^3F'_4-a^3G'_5$	157
11	4677.42	− 3	2	IV?	21373.35	aG′−cG	160
11	4676.92	− 1	1	IV?	21375.64	bD−eF	161
7	4675.13	0	10	III	21383.82	$a^3P'_2-c^5D'_3$	162
4	4668.38	+ 2	2	IV?	21414.74	$a^3P'_1-c^5D'_2$	162
7	4667.59	− 1	25	I	21418.36	$a^3F'_3-a^3G'_4$	157

TABLE II—*Continued*

Source	Obs. λ (I.A.)	Δλ O−C	Int.	Temp. Class	ν	Designation	Multiplet
7	4656.47	+1	25	I	21469.50	$a^3F'_2-a^3G'_3$	157
7	4656.06	+2	6	III	21471.39	$a^5P'_3-d^5D'_2$	163
7	4655.70	−1	3	IV?	21473.06	$c^3P'_2-e^3P_1$	164
7	4650.02	0	10	III	21499.29	$a^5P'_2-d^5D'_1$	163
7	4645.19	0	12	III	21521.65	$a^5P'_1-d^5D'_0$	163
4	4640.37	−3	2	IV?	21543.99	$c^3P'_1-e^3P_0$	164
7	4639.94	0	15	III	21545.99	$a^5P'_1-d^5D'_1$	163
7	4639.66	0	15	III	21547.29	$a^5P'_3-d^5D'_3$	163
7	4639.36	0	18	III	21548.68	$a^5P'_2-d^5D'_2$	163
7	4637.88	−2	8	IV?	21555.57	$c^3P'_2-e^3P_2$	164
8	4637.24	+3	2	IV?	21558.57	$c^3P'_1-e^3P_1$	164
7	4635.55	−1	3	IV?	21566.39	$c^3P'_0-e^3P_1$	164
7	4629.34	+1	15	III	21595.33	$a^5P'_1-d^5D'_2$	163
7	4623.10	0	25	III	21624.48	$a^5P'_2-d^5D'_3$	163
4	4619.53	−1	3	IV?	21641.19	$c^3P'_1-e^3P_2$	164
7	4617.27	+1	30	II	21651.78	$a^5P'_3-d^5D'_4$	163
7	4614.29	−1	1	V	21665.77	a^3F_3-bF'	165
7	4599.23	......	5	IV	21736.71	....	......
11†	4576.52	+3	(0)	....	21844.57	$c^3P'_1-i^3D'_2$	166
7	4570.91	+1	3n	III	21871.38	$a^3F_2-c^3G_3$	167
7	4564.23	+1	1	III A	21903.39	$b^3F'_4-d^3F_3$	168
7	4563.44	0	5	III	21907.18	$a^3F_4-c^3G_5$	167
7	4562.63	−1	6	II A	21911.07	$a^3F'_3-aD'$	169
7	4559.94	0	6	III	21923.99	$b^3F'_4-d^3F_4$	168
7*	4558.12	−2 −2	2	IV	21932.75	$c^3P'_2-i^3D'_3$ $c^3P'_2-c^3S'_1$	166 170
4	4557.85	−1	2	IV	21934.05	$a^3D'_1-e^3F'_2$	171
7	4555.50	+1	30	II	21945.36	$a^5F'_5-b^5F_4$	172
7	4555.10	−1	3	III	21947.29	$a^3F_3-c^3G_4$	167
4	4553.41	0	(1)	....	21955.43	$aG'-cF'$	173
2	4552.45	−3	35	II	21960.07	$a^5F'_4-b^5F_3$	172
7	4548.77	0	35	II	21977.83	$a^5F'_3-b^5F_2$	172
4	4548.12	−1	2	III	21980.97	$a^3D'_3-e^3F'_4$	171
4	4547.86	+2	2	III	21982.23	$a^3D'_2-e^3F'_3$	171
7	4544.70	+2	30	II	21997.51	$a^5F'_2-b^5F_1$	172
4	4541.00	0	(1)	....	22015.43	$bG-dF$	174
7	4540.87	+1	1	III A	22016.06	$b^3F'_3-d^3F_2$	168
4	4540.48	−3	1	III A	22017.95	$a^3F'_4-aF$	175
2	4539.10	......	3	IV	22024.66	....	......
7	4536.00	−2	40	II	22039.71	$a^5F'_1-b^5F_1$	172
7	4535.92	−2	40	II	22040.10	$a^5F'_2-b^5F_2$	172
7	4535.58	−1	50	II	22041.75	$a^5F'_3-b^5F_3$	172
7	4534.78	−1	60	II	22045.63	$a^5F'_4-b^5F_4$	172
7	4533.25	0	80	II	22053.07	$a^5F'_5-b^5F_5$	172
11	4527.46	0	(4)	(III A?)	22081.17	$a^3F'_2-aD'$	169
7	4527.32	0	35	II	22081.95	$a^5F'_1-b^5F_2$	172
4*	4526.36	0 −1	1	III A	22086.63	$a^5F_5-c^5F'_4$ $aG-e^3F_4$	176 177
7‡	4522.80	−4	40	II	22104.07	$a^5F'_2-b^5F_3$	172
7	4518.69	0	8	III	22124.13	$b^3F'_2-d^3F_2$	168
7	4518.03	+1	50	II	22127.36	$a^5F'_3-b^5F_4$	172
2	4515.61	−3	1	IV A	22139.22	$a^5F_4-c^5F'_3$	176
4	4513.71	−1	1	IV A	22148.53	$b^3F'_2-d^3F_3$	168

TABLE II—*Continued*

Source	Obs. λ (I.A.)	Δλ O−C	Int.	Temp. Class	ν	Designation	Multiplet
7	4512.74	0	40	II	22153.30	$a^5F'_4-b^5F_5$	172
7	4511.18	......	3	IV	22160.96	....	.....
7	4508.28	−1	1	IV	22175.22	$a^3D_3-h^3D'_3$	178
7	4508.04	+1	2	IV	22176.40	$aF-cD$	179
12	4507.64	+1	[00]	....	22178.38	$a^3H'_5-aI'$	180
4	4505.71	0	1	IV	22187.86	$a^5F_3-c^5F'_2$	176
7	4503.78	−1	4n	IV	22197.37	$a^5F_5-c^5F'_5$	176
7	4497.75	−2	3	III	22227.13	$a^5F_4-c^5F'_4$	176
8	4496.24	−1	2	III A	22234.59	$a^3F'_3-aF$	175
7	4496.15	−1	20	III	22235.04	$a^5P'_3-b^5P_2$	181
7	4495.02	......	4	III	22240.63	....	.....
7	4492.56	+3	3	III	22252.80	$a^5F_3-c^5F'_3$	176
12	4490.69	0	(2)	....	22261.98	$a^3D_2-h^3D'_2$	178
7	4489.10	0	20	III	22269.96	$a^5P'_2-b^5P_1$	181
2	4485.01	−4	1	IV A	22290.24	$a^5F_1-c^5F'_1$	176
12	4484.53	−2	(2)	....	22292.66	$a^3D_1-h^3D'_1$	178
7	4482.69	−1	10	III	22301.80	$b^3F'_4-e^3F_3$	182
7	4481.27	+1	30	III	22308.87	$a^5P'_3-b^5P_3$	181
7	4480.61	+1	5	III A	22312.15	$a^5P'_2-b^5P_2$	181
7	4479.70	0	9	III	22316.68	$a^5P'_1-b^5P_1$	181
4	4475.51	−2	1	IV	22337.58	$a^5F_4-c^5F'_5$	176
7*	4474.86	−1 +2	8	III	22340.83	$b^3F'_3-e^3F_2$ $a^5F_3-c^5F'_4$	182 176
7	4471.24	0	20	III	22358.91	$a^5P'_1-b^5P_2$	181
7	4465.80	−1	20	III	22386.15	$a^5P'_2-b^5P_3$	181
7	4463.55	+1	8	III	22397.43	$a^3G_5-e^3G'_4$	183
7	4463.39	−1	8	III	22398.23	$a^3G_4-e^3G'_3$	183
7	4462.08	−2	(3)	(III A)	22404.81	$a^3F'_2-aF$	175
7	4457.42	−1	40	II	22428.23	$b^3F'_4-e^3F_4$	182
7	4455.32	0	30	II	22438.80	$b^3F'_3-e^3F_3$	182
7	4453.70	−2	20	III	22446.97	$a^3G_3-e^3G'_3$	183
7	4453.32	−1	30	II	22448.87	$b^3F'_2-e^3F_2$	182
7	4450.90	0	25	III	22461.09	$a^3G_4-e^3G'_4$	183
7	4449.99	+2	1	IV	22465.68	a^3G_4-cF	184
7	4449.13	−2	30	III	22470.02	$a^3G_5-e^3G'_5$	183
2	4444.27	−2	(1)	....	22494.61	$b^3P'_1-i^3D'_1$	185
7	4443.20	0	(3)	....	22500.01	$aD'-cD$	186
7	4441.26	−1	4	IV	22509.84	$a^3G_3-e^3G'_4$	183
7	4440.34	0	10	III	22514.50	a^3G_3-cF	184
7	4438.23	0	2	IV	22525.21	$b^3P'_2-i^3D'_2$	185
12	4436.64	−3	(1)	(III?)	22533.23	$a^3F_4-e^3F'_4$	187
7	4436.59	0	4	III	22533.53	$a^3G_4-e^3G'_5$	183
7*	4433.99	+2 −2	15	III A	22546.74	$b^3F'_2-e^3F_3$ $a^3G_3-f^3F_2$	182 188
7	4433.58	+1	3	III	22548.83	$a^3F_2-e^3F'_2$	187
7	4431.28	−4	4	III	22560.53	$b^3P'_0-i^3D'_1$	185
7	4430.37	+1	7	III A	22565.17	$b^3F'_3-e^3F_4$	182
7	4430.03	−2	3	III	22566.90	$a^3F_3-e^3F'_3$	187
7	4427.10	0	40	III	22581.83	$aG-aH$	189
7	4426.05	−1	10	II?	22587.18	$a^3G_4-f^3F_3$	188
7	4425.83	0	3	III A	22588.31	$a^3P'_2-e^3D'_2$	190
7	4424.40	+1	2	III	22595.62	$bG-dG'$	191
7	4422.82	−1	10	II	22603.69	$a^3P'_2-e^3D'_3$	190

TABLE II—*Continued*

Source	Obs. λ (I.A.)	Δλ O−C	Int.	Temp. Class	ν	Designation	Multiplet
7........	4421.75	− 2	6	III	22609.16	$b^3P'_1-i^3D'_2$	185
7........	4421.47	+ 2	1	IV	22610.60	$a^3F_4-b^5D_4$	192
12........	4417.43	− 3	(1n)	....	22631.27	$a^3F_3-b^5D_3$	192
7........	4417.28	− 1	15	III	22632.04	$a^3G_5-f^3F_4$	188
7........	4416.54	0	4	III?	22635.83	$a^3G_3-f^3F_3$	188
7........	4412.43	+ 3	1	III A	22656.90	$aD-d^3D'_3$	193
7........	4405.70	0	2	III A	22691.52	$a^3P'_1-e^3D'_1$	190
4‡........	4404.91	+ 1	5	III	22695.59	$a^3G_4-f^3F_4$	188
4........	4404.40	+ 1	5	III A	22698.21	$a^3P'_1-e^3D'_2$	190
7*........	4404.27	− 2	10	III	22698.89	$b^3P'_2-c^3S'_1$ $b^3P'_2-i^3D'_3$	194 185
7........	4400.60	+ 2	(2)	....	22717.82	$bD-eP$	195
12........	4394.85	− 4	(2)	(III A)	22747.54	$a^3P'_0-e^3D'_1$	190
7........	4393.93	0	8	III	22752.30	$bG-bH$	196
7........	4388.09	+ 1	3	III	22782.58	$b^3P'_1-c^3S'_1$	194
7........	4375.44	+ 2	1	IV	22848.44	$b^3P'_0-c^3S'_1$	194
7........	4372.40	+ 4	3	IV	22864.34	$aP'-eP$	197
7........	4369.70	+ 4	5n	IV	22878.46	$aH'-eG'$	198
7........	4368.97	− 2	2	IV	22882.28	$bG-f^3G'_3$	199
7........	4361.15	+ 2	1	IV	22923.31	$b^3F'_4-aH$	200
7........	4360.51	+ 1	4	III?	22926.68	$a^3D_3-e^3P_2$	201
7........	4355.32	+ 1	1	IV A	22954.00	$a^5G'_6-c^5F'_5$	202
7........	4354.08	− 1	3	III	22960.54	$a^3D_2-e^3P_1$	201
7........	4346.60	+ 2	1	IV	23000.05	$a^3D_1-e^3P_0$	201
7........	4346.13	+ 2	5	IV	23002.53	$a^3H'_4-bH$	203
4........	4343.80	+ 2	1	IV	23014.87	$a^3D_1-e^3P_1$	201
7........	4340.06	+ 3	1	IV?	23034.71	$a^5G'_5-c^5F'_4$	202
7........	4338.50	− 1	1	IV?	23042.99	$a^3D_2-e^3P_2$	201
7........	4334.86	+ 2	2	III A	23062.33	$a^5F'_2-d^3D'_1$	204
7........	4326.98	+ 1	2	III A	23104.34	$a^5F'_1-d^3D'_1$	204
7........	4326.35	0	9	II	23107.70	$a^5F'_3-d^3D'_2$	204
7........	4325.13	− 3	9n	III	23114.21	$a^3H'_5-f^3G'_4$	205
7........	4323.44	+ 1	1	III A	23123.25	$a^3P'_2-b^3P_1$	206
7........	4321.70	− 1	8n	III	23132.58	$a^3H'_4-f^3G'_3$	205
7........	4318.64	0	10n	III	23148.95	$a^3H'_6-f^3G'_5$	205
7*........	4314.80	0 + 6	25	II	23169.55	$a^5F'_4-d^3D'_3$ $a^5F'_2-d^3D'_2$	204 204
7........	4314.34	− 1	5	III A	23172.03	$a^5F'_4-c^3G'_3$	207
7........	4311.65	0	2	IV	23186.47	$a^3D_1-i^3D'_1$	208
7........	4310.36	0	1	III A	23193.42	$a^3P'_1-b^3P_0$	206
7........	4309.09	0	1	IV	23200.25	$a^3H'_5-f^3G'_5$	205
4........	4308.47	− 1	2	III A	23203.60	$a^3P'_2-b^3P_2$	206
4........	4306.92	− 2	1	III A	23211.94	$a^5F'_1-d^3D'_2$	204
7........	4305.91	− 1	60	II	23217.39	$a^5F'_5-c^5D'_4$	209
4........	4305.43	− 3	2	III A	23219.97	$a^5P'_3-d^3P_2$	210
4........	4302.97	0	1n	III A	23233.25	$a^3P'_1-b^3P_1$	206
7........	4301.08	0	50	II	23243.46	$a^5F'_4-c^5D'_3$	209
7........	4300.55	− 1	50	II	23246.32	$a^5F'_3-c^5D'_2$	209
7........	4299.64	+ 2	15	III	23251.24	$a^5F'_3-d^3D'_3$	204
7‡........	4299.24	+ 1	15	III	23253.39	$a^5P'_3-b^5S'_2$	211
7........	4298.67	− 1	40	II	23256.49	$a^5F'_2-c^5D'_1$	209
7........	4295.75	0	22	II	23272.30	$a^5F'_1-c^5D'_0$	209
4........	4292.64	− 2	1	III A	23289.16	$a^3P'_0-b^3P_1$	206

TABLE II—*Continued*

Source	Obs. λ (I.A.)	Δλ O−C	Int.	Temp. Class	ν	Designation	Multiplet
4........	4291.88	− 2	(1)	....	23293.28	$a^5D'_4-e^3F'_3$	212
2*.......	4291.21	+ 1 − 7	5n	IV	23296.92	$a^5P'_2-d^3P_2$ $a^5F'_4-c^3G'_5$	210 207
7........	4290.93	− 1	22	II	23298.44	$a^5F'_1-c^5D'_1$	209
7........	4289.92	− 1	3	III	23303.92	$a^3D_3-i^3D'_3$	208
7........	4289.08	− 1	25	II	23308.50	$a^5F'_2-c^5D'_2$	209
7*.......	4288.18	+ 1 + 2	3	III A	23313.38	$a^3P'_1-b^3P_2$ $a^5F'_2-d^3D'_3$	206 204
7........	4287.41	0	22	II	23317.57	$a^5F'_4-c^5D'_4$	209
7........	4286.01	+ 1	25	II	23325.19	$a^5F'_3-c^5D'_3$	209
7........	4284.99	− 1	8	III	23330.73	$a^5P'_2-b^5S'_2$	211
7........	4282.72	+ 1	12	III	23343.10	$a^3G_3-g^3F_2$	213
7‡.......	4281.40	+ 2	10	III	23350.30	$a^5F'_1-c^5D'_2$	209
7........	4280.08	0	2n	III	23357.50	$a^5D'_4-b^5D_3$	214
7........	4278.81	+ 1	3n	III	23364.44	$a^5D'_3-b^5D_2$	214
7‡.......	4278.23	0	7	IV	23367.60	$aH'-cH$	215
7........	4276.66	0	2	III	23376.18	$a^5D'_2-b^5D_1$	214
7........	4276.44	0	8	III	23377.38	$a^5P'_1-b^5S'_2$	211
7*.......	4274.60	+ 2 − 1	15	III	23387.44	$a^3G_4-g^3F_3$ $a^5F'_2-c^5D'_3$	213 209
2........	4274.41	+ 4	(1n)	(III)	23388.50	$a^5D'_1-b^5D_0$	214
7........	4273.31	− 2	2	IV	23394.50	$a^5D'_3-e^3F'_3$	212
7........	4272.44	+ 1	8	III A	23399.27	$a^5F'_3-c^5D'_4$	209
7........	4270.14	− 1	7n	IV	23411.86	$a^5D'_4-e^3F'_4$	212
12........	4268.92	− 1	(1n)	(III)	23418.55	$a^5D'_1-b^5D_1$	214
7........	4266.21	0	3n	IV	23433.44	$a^5D'_2-b^5D_2$	214
7........	4265.71	+ 1	4	IV	23436.19	$a^3G_3-g^3F_3$	213
4........	4265.28	0	3n	III	23438.55	$a^5D'_0-b^5D_1$	214
7........	4263.14	− 1	15	III	23450.31	$a^3G_5-g^3F_4$	213
7........	4261.61	0	5n	III	23458.73	$a^5D'_3-b^5D_3$	214
2........	4260.74	− 4	2	IV	23463.52	$a^5D'_2-e^3F'_3$	212
7........	4258.53	− 1	4n	IV	23475.70	$a^5D'_1-b^5D_2$	214
7........	4256.04	+ 1	8n	III	23489.43	$a^5D'_4-b^5D_4$	214
7........	4251.76	0	2n	III	23513.07	$a^5D'_3-e^3F'_4$	212
7........	4251.60	− 1	3	III	23513.96	$a^3G_4-g^3F_4$	213
7........	4249.13	0	5n	III	23527.63	$a^5D'_2-b^5D_3$	214
7........	4237.88	− 3	7	III	23590.09	$bD-eD'$	216
2........	4237.79	+ 1	(2)	(III)	23590.62	$a^5D'_3-b^5D_4$	214
7........	4227.64	+ 1	5	III	23647.22	$aP'-dD'$	217
7........	4224.78	+ 2	5	IV	23663.23	$aF-cG$	218
7........	4211.72	0	4	III	23736.61	$aP'-eD'$	219
11........	4203.46	− 1	8	IV	23783.25	$b^3P'_2-f^3P_2$	220
7........	4200.79	+ 3	6	III	23798.37	$b^3P'_2-f^3P_1$	220
7........	4188.69	− 1	5	III	23867.12	$b^3P'_1-f^3P_2$	220
7‡.......	4186.12	+ 1	25	III	23881.76	$aG-bG'$	221
7........	4183.29	0	4	III	23897.92	$b^3P'_1-f^3P_0$	220
7........	4180.86	− 7	(3)	....	23911.80	$aS-cP$	222
4........	4180.52	− 7	(1)	....	23913.74	$a^3D_2-h^3F_2$	223
4........	4179.91	+ 1	(1)	....	23917.24	$a^3D_3-h^3F_3$	223
12........	4177.36	− 4	(2)	....	23931.88	$a^3G_5-c^3H_5$	224
7........	4174.47	− 4	3	III	23948.40	$b^3P'_0-f^3P_1$	220
2§.......	4174.09	− 2	(1)	(III A)	23950.93	$aD-e^3D'_3$	225
12........	4172.54	+ 4	(2)	....	23958.94	$a^3G_4-c^3H_4$	224

TABLE II—*Continued*

Source	Obs. λ (I.A.)	Δλ O−C	Int.	Temp. Class	ν	Designation	Multiplet
7	4171.02	−7	8	III	23968.26	$a^3D_1-h^3F_2$	223
7	4169.33	0	7	III	23977.93	$a^3G_5-c^3H_6$	224
4	4166.32	+1	6	III	23995.26	$a^3G_4-c^3H_5$	224
4	4164.14	+1	4	III	24007.82	$a^3G_3-c^3H_4$	224
4	4159.64	−5	9	III?	24033.79	$a^3D_2-h^3F_3$	223
7	4150.97	−3	10	III	24083.98	$a^3D_3-h^3F_4$	223
7	4150.54	0	3	III	24086.49	$a^5D'_2-b^5P'_1$	226
2	4149.45	−1	(1)	....	24092.84	$a^3G'_5-b^3H'_5$	227
2	4148.39	+4	(1)	....	24098.97	$aS-dP$	228
4	4145.03	+1	(1)	....	24118.50	$aD-d^3G'_3$	229
7	4143.28	+1	3	III	24128.68	$a^5D'_1-b^5P'_1$	226
7	4143.04	+1	7n	III	24130.09	$a^5D'_3-b^5P'_2$	226
2	4142.48	+2	2	IV	24133.34	$a^3G'_4-b^3H'_4$	227
4‡	4139.83	−1	2	IV	24148.80	$a^5D'_0-b^5P'_1$	226
7	4137.29	+1	10n	III	24163.62	$a^5D'_4-b^5P'_3$	226
7	4131.26	+2	4	III	24198.90	$a^5D'_2-b^5P'_2$	226
2	4129.17	......	4	III	24211.15	....	.....
7	4127.54	0	15	III	24220.70	$a^3G'_5-b^3H'_6$	227
12	4124.00	−3	(1n)	(V)	24241.42	$a^5D'_1-b^5P'_2$	226
7‡	4123.57	+1	10	III?	24244.05	$a^3G'_4-b^3H'_5$	227
7	4123.31	+1	5n	IV	24245.54	$aF-cF'$	230
2	4122.14	−1	10	III	24252.40	$a^3G'_3-b^3H'_4$	227
7	4121.64	......	4	III	24255.37	....	.....
4	4120.01	−1	2	III	24264.96	$a^5D'_3-b^5P'_3$	226
7	4112.73	0	20	II	24307.92	$a^3F'_4-aG'$	231
7	4099.17	−1	8	III	24388.32	$a^3D_3-f^3P_2$	232
7	4082.46	0	20	III	24488.15	$a^3P'_2-c^3P_1$	233
7	4079.73	−1	6	III	24504.53	$a^3D_2-f^3P_2$	232
7	4078.47	−1	30	III	24512.10	$a^3P'_2-c^3P_2$	233
7	4077.15	−3	4	IV	24520.04	$a^3D_2-f^3P_1$	232
4	4076.38	0	4	III A	24524.67	$a^3F'_3-aG'$	231
5	4074.36	−1	3	IV	24536.84	$a^5D'_4-d^5F'_4$	234
7	4071.48	−1	2	IV	24554.19	$a^5D'_3-d^5F'_3$	234
4	4071.26	−1	2	IV	24555.51	$a^5D'_2-d^5F'_2$	234
7	4069.00	−1	4n	IV	24569.15	$aD'-cF'$	235
4	4068.65	0	(1)	....	24571.27	$a^5D'_0-d^5F'_1$	234
7	4068.14	0	3	IV	24574.34	$a^3D_1-f^3P_1$	232
12	4065.57	0	(0)	....	24589.88	$a^3D_1-f^3P_0$	232
7	4065.11	0	15	III	24592.66	$a^3P'_1-c^3P_0$	233
7	4064.22	0	15	III	24598.05	$a^3P'_1-c^3P_1$	233
7	4060.27	+1	20	III	24621.97	$a^3P'_1-c^3P_2$	233
7	4058.15	0	7	IV	24634.84	$a^5D'_4-d^5F'_5$	234
7	4057.64	+1	5	III	24637.93	$a^5D'_3-d^5F'_4$	234
7	4055.02	0	20	III	24653.86	$a^3P'_0-c^3P_1$	233
7	4052.95	+2	2	III	24666.44	$a^3D_3-j^3D'_2$	236
7	4049.39	−1	2n	III	24688.13	$a^5F_5-a^5G_5$	237
7	4043.77	−2	2	IV	24722.43	$a^3D_2-j^3D'_1$	236
7	4040.33	−2	4n	III	24743.50	$a^5F_4-a^5G_4$	237
7	4035.84	−1	10	III	24771.02	$a^3D_3-j^3D'_3$	236
7	4034.92	+2	5	III	24776.66	$a^3D_1-j^3D'_1$	236
7	4033.92	0	6	III	24782.80	$a^3D_2-j^3D'_2$	236
2	4032.63	0	3n	V	24790.75	$a^3G'_5-f^3F'_4$	238
7	4031.77	0	3n	III	24796.03	$a^5F_3-a^5G_3$	237

TABLE II—*Continued*

Source	Obs. λ (I.A.)	Δλ O−C	Int.	Temp. Class	ν	Designation	Multiplet
7	4030.53	+2	25n	III	24803.65	$a^5F_5-a^5G_6$	237
2	4027.43	......	4	IV	24822.77	....	......
7	4026.54	−1	25n	III	24828.22	$a^5F_4-a^5G_5$	237
7	4024.57	0	35	II	24840.37	$a^3F'_4-b^3F_3$	239
4	4021.87	+4	25n	III	24857.06	$a^5F_3-a^5G_4$	237
7	4017.78	−1	15n	III	24882.35	$a^5F_2-a^5G_3$	237
7	4016.99	−1	3	III	24887.25	$a^3D_2-j^3D'_3$	236
7	4016.30	+1	6	III	24891.53	$a^5F_5-e^3F'_4$	240
7	4015.40	+1	12n	III	24897.11	$a^5F_1-a^5G_2$	237
7	4013.60	+1	12n	III	24908.27	$a^5F_5-a^5H'_6$	241
7	4012.81	−1	3	III	24913.17	$a^5F_4-e^3F'_3$	240
12	4011.55	+3	[3]	[III A]	24921.01	$a^3F'_2-a^3S'_1$	242
7	4009.68	+2	15	II	24932.63	$a^3F'_3-a^5S'_2$	243
7‡	4008.94	+1	35	II	24937.23	$a^3F'_3-b^3F_2$	239
7	4008.07	+1	9n	III	24942.63	$a^5F_4-a^5H'_5$	241
7	4007.21	0	3n	IV	24947.99	$a^5F_2-a^5H'_3$	241
7	4005.98	0	6n	III	24955.65	$a^5F_3-a^5H'_4$	241
4	4003.80	0	10n	III	24969.24	$a^5F_5-b^5D_4$	244
7	4002.50	+1	9n	III	24977.34	$a^5F_4-b^5D_3$	244
7‡	3999.34	0	7n	III	24997.11	$a^5F_3-b^5D_2$	244
7	3998.65	+2	100R	II	25001.40	$a^3F'_4-b^3F_4$	239
7*	3994.70	+14 +1	4n	III	25026.12	$a^5F_3-e^3F'_3$ $a^5F_2-b^5D_1$	240 244
4	3993.79	−1	1	IV	25031.83	$a^5F_4-e^3F'_4$	240
12	3990.18	−2	(1n)	(III)	25054.47	$a^5F_1-b^5D_0$	244
7	3989.77	+1	80r	II	25057.04	$a^3F'_3-b^3F_3$	239
2	3989.58	0	(1)	(III A)	25058.28	$a^3P'_2-aP$	245
2	3985.43	......	3	III	25084.25	....	......
2	3985.25	......	3	III	25085.49	....	......
7	3984.33	+1	3	III	25091.25	$a^5F_3-b^5D_3$	244
7	3982.54	+6	30	II	25102.53	$a^3F'_2-a^5S'_2$	243
7	3981.77	+1	70r	II	25107.38	$a^3F'_2-b^3F_2$	239
2	3981.47	+1	(1)	(III)	25109.27	$a^5F_4-b^5D_4$	244
12	3972.10	−4	(0)	(III A)	25168.52	$a^3P'_1-aP$	245
7	3964.27	+1	35	II	25218.21	$a^3F'_3-b^3F_4$	239
12	3963.33	+3	(0)	(III A)	25223.87	$a^3P'_0-aP$	245
7	3962.85	0	35	II	25227.26	$a^3F'_2-b^3F_3$	239
7	3958.21	+1	80	II	25256.83	$a^3F'_4-b^3D'_3$	246
7	3956.28	−4	60	II	25269.14	$a^3F'_3-b^3D'_2$	246
7	3948.66	0	60	II	25317.91	$a^3F'_2-b^3D'_1$	246
7	3947.75	−2	40	II	25323.75	$a^3F'_3-a^3P_2$	247
4	3937.97	+1	2n	IV	25386.63	$bG-eG'$	248
7	3934.23	−1	9	III	25410.76	$a^3F'_4-b^5D'_3$	249
7	3929.87	+1	40	II	25438.95	$a^3F'_2-b^3D'_2$	246
9	3928.18	−3	(0)	....	25449.90	$a^3G'_4-g^3F'_3$?	250
12	3927.40	−1	(2)	....	25455.07	$a^3G'_5-g^3F'_4$	250
7	3926.32	+1	10	IV	25461.95	$aH'-fG'$	251
7	3924.51	−1	50	II	25473.69	$a^3F'_3-b^3D'_3$	246
7	3921.42	0	30	II	25493.77	$a^3F'_2-a^3P_2$	247
7	3919.82	0	5	III	25504.17	$aG-cF$	252
2	3916.11	......	3	IV	25528.37	....	......
7	3915.88	0	3	III A	25529.83	$a^3F'_3-b^5D'_2$	249
7	3914.72	0	5	III	25537.40	$a^3F'_2-a^3P_1$	247

TABLE II—*Continued*

Source	Obs. λ (I.A.)	Δλ O−C	Int.	Temp. Class	ν	Designation	Multiplet
7	3914.33	0	35	II	25539.94	$a^3F'_4-b^5D'_4$	249
7	3912.58	−3	2	IV	25551.38	$a^5G'_5-a^5G_4$	253
12	3911.37	0	(2)	(IV)	25559.27	$a^5G'_6-a^5H'_5$	254
7	3911.18	0	8n	III	25560.51	$a^5G'_6-a^5G_6$	253
7	3904.77	0	40n	II	25602.47	$aD-bF$	255
7	3900.96	0	12	II	25627.47	$a^3F'_3-b^5D'_3$	249
2*	3899.67	−3 0	(2)	......	25635.97	$a^3F'_2-b^5D'_1$ $a^5G'_5-a^5G_5$	249 253
7	3898.49	+1	8	III	25643.72	$a^3F'_2-b^3D'_3$	246
7	3897.58	−2	1	IV	25649.70	$a^5G'_5-a^5H'_4$	254
7	3897.32	0	1	IV	25651.40	$a^5G'_4-a^5G_3$	253
7	3895.24	−1	30n	III	25665.11	$a^5G'_6-a^5H'_6$	254
7	3889.96	0	6	III (A)	25699.94	$a^3F'_2-b^5D'_2$	249
7	3888.04	0	4n	IV	25712.64	$a^5G'_4-a^5G_4$	253
12	3887.33	−3	(1n)	....	25717.34	$a^5G'_4-a^5H'_3$	254
7	3884.04	−5	(2)	....	25739.12	$a^5G'_3-a^5G_2$	253
5	3882.87	0	20n	III?	25746.87	$a^5G'_6-a^5H'_7$	254
5	3882.34	+2	10n	III?	25750.39	$a^5G'_5-a^5H'_5$	254
5	3882.13	−1	15n	III?	25751.78	$a^5G'_5-a^5G_6$	253
4	3881.41	+2	4	IV?	25756.56	$a^3F'_3-b^5D'_4$	249
5	3877.60	0	2n	IV	25781.87	$a^5G'_3-a^5G_3$	253
7*	3875.29	+6 +3	20n	III	25797.23	$a^3F'_2-b^5D'_3$ $a^5G'_4-a^5G_5$	249 253
4	3873.25	+2	10n	III	25810.82	$a^5G'_4-a^5H'_4$	254
4	3869.60	+2	2n	IV?	25835.16	$aD-c^3P_1$	256
5	3869.32	+2	5n	IV?	25837.03	$a^5G'_2-a^5G_2$	253
4	3868.42	+1	10n	IV?	25843.04	$a^5G'_3-a^5G_4$	253
4	3867.77	+3	3	IV?	25847.39	$a^5G'_3-a^5H'_3$	254
4	3866.45	+1	15n	IV?	25856.20	$a^5G'_5-a^5H'_6$	254
4	3866.00	0	1	IV?	25859.22	$aD-c^3P_2$	256
4	3862.84	−1	10n	III	25880.38	$a^5G'_2-a^5G_3$	253
2	3861.08	......	3n	IV?	25892.18	....	......
4	3858.12	−1	15n	III	25912.03	$a^5G'_4-a^5H'_5$	254
5	3857.89	−1	2	III A?	25913.58	$b^3F'_4-e^3G'_5$	257
4	3853.74	0	10n	III	25941.49	$a^5G'_3-a^5H'_4$	254
4	3853.05	−2	10n	IV	25946.12	$a^5G'_2-a^5H'_3$	254
4	3848.29	−2	2	IV	25978.22	$b^3F'_3-e^3G'_4$	257
2	3846.44	......	6n	IV	25990.73	....	......
2	3842.61	−1	(3)	....	26016.61	$a^5F_5-d^5F'_4$	258
4	3841.67	+3	(1)	....	26022.99	$b^3F'_2-e^3G'_3$	257
2	3836.76	......	5	IV	26056.27	....	......
5	3833.91	−1	3	IV?	26075.65	$b^3F'_4-f^3F_4$	259
2	3833.67	......	4	III	26077.26	....	......
2	3833.19	......	4	IV	26080.59	....	......
4	3829.70	−3	2	IV?	26104.33	$b^3F'_3-f^3F_3$	259
7	3828.17	−2	3	III?	26114.75	$a^5F_5-d^5F'_5$	258
4	3827.62	0	1	IV?	26118.50	$a^3D'_3-d^3P'_2$	260
2	3827.48	+1	1	IV?	26119.45	$a^5F_3-d^5F'_2$	258
4	3826.95	−2	1	IV?	26123.08	$b^3F'_2-f^3F_2$	259
2	3822.03	−1	(2)	....	26156.73	$a^5F_4-d^5F'_4$	258
7	3821.74	+3	2	IV?	26158.69	$a^5F_2-d^5F'_1$	258
2	3818.20	0	(1)	....	26182.89	$a^3H'_6-g^3G'_5$	261
4	3817.65	0	5	IV?	26186.71	$a^5F_3-d^5F'_3$	258

TABLE II—*Continued*

Source	Obs. λ (I.A.)	Δλ O−C	Int.	Temp. Class	ν	Designation	Multiplet
7	3814.86	−2	4	IV?	26205.86	$a^5F_2-d^5F_2'$	258
2	3813.26	+1	(0)	....	26216.85	$a^5F_1-d^5F_1'$	258
2	3811.39	−7	4	IV?	26229.76	$a^3G_3-h^3F_2$	262
5*	3807.78	+2 +1	1	IV?	26254.59	$a^5F_4-d^5F_5'$ $a^3G_5'-c^5H_5'$	258 263
5	3806.45	−1	1	IV?	26263.77	$a^5F_1-d^5F_2'$	258
5	3806.04	−1	1	IV?	26266.59	$c^3P_2'-g^3P_2$	264
7	3805.48	+2	1	IV?	26270.45	$a^5F_3-d^5F_4'$	258
7	3805.13	+1	1	IV?	26272.87	$a^5F_2-d^5F_3'$	258
7	3801.07	−2	3	IV	26300.93	$a^3G_4-h^3F_3$	262
4	3798.29	−1	6	IV	26320.18	$b^3F_2'-f^3D_1'$	265
4	3795.87	−1	7	IV	26336.97	$b^3F_3'-f^3D_2'$	265
4‡	3794.74	−3	(1)	(IV)	26344.80	$a^3P_2'-bP$	266
4	3793.67	−1	(1)	....	26352.24	$c^3P_1'-g^3P_2$	264
4	3789.28	+1	8	IV	26382.77	$b^3F_4'-f^3D_3'$	265
8	3788.80	0	2	III A	26386.11	$a^3F_4'-b^5G_5'$	267
7	3786.27	−1	3	IV	26403.74	$a^3G_5-h^3F_4$	262
12	3786.16	−2	(1)	(V)	26404.49	$a^3D_3'-f^3F_4'$	268
7	3786.03	0	20	II	26405.41	$aD-aP$	269
7	3782.14	+2	2	III A	26432.57	$a^3P_2'-cD'$	270
4	3779.03	+3	(1)	(V)	26454.33	$a^3P_1'-bP$	266
4	3774.32	−1	1n	IV	26487.35	$a^3F_3'-b^5G_4'$	267
7	3771.64	0	25	I	26506.15	$a^3F_4'-c^3F_3$	271
7	3766.46	0	3	IV A	26542.61	$a^3P_1'-cD'$	270
4	3754.93	0	1	IV	26624.11	$a^3G_4-d^3H_4$	272
7	3753.63	0	25	I	26633.33	$a^3F_3'-c^3F_2$	271
7	3752.87	+1	8or	I	26638.72	$a^3F_4'-c^3F_4$	271
4	3748.07	0	6n	IV	26672.84	$a^3G_3-d^3H_4$	272
4	3747.80	−1	1	IV	26674.76	$a^3G_5-d^3H_5$	272
7	3741.14	+3	1	IV	26722.24	$a^3G_5'-g^5F_5'$	273
7	3741.06	+1	6or	I	26722.81	$a^3F_3'-c^3F_3$	271
7	3738.90	+1	5n	IV	26738.25	$a^3G_4-d^3H_5$	272
2	3735.66	......	4n	IV	26761.45	....	......
7	3733.78	0	4n	IV	26774.92	$a^3G_5-d^3H_6$	272
7	3729.77	−3	5or	I	26803.71	$a^3F_2'-c^3F_2$	271
11	3728.66	−3	1	IV	26811.68	$b^3F_3'-g^3F_2$	274
12	3727.05	+1	(1)	(III A)	26823.30	$aD-e^3F_3$	275
7	3725.12	−2	20	III	26837.17	$a^3P_2'-b^3S_1'$	276
4	3724.59	+1	20	III	26840.99	$aG-cG'$	277
4	3722.58	+1	15?	II?	26855.47	$a^3F_3'-c^3F_4$	271
8	3720.38	0	2	IV	26871.36	$a^5G_6'-d^5F_5'$	278
7	3717.39	0	20	I	26892.97	$a^3F_2'-c^3F_3$	271
8	3717.26	−1	1	IV A	26893.91	$b^3F_4'-g^3F_4$	274
8	3715.79	0	1	IV A	26904.55	$b^3F_3'-g^3F_3$	274
7	3715.33	......	3n	IV	26907.88	....	......
4	3713.70	−3	1	IV A	26919.68	$b^3F_2'-g^3F_2$	274
12	3710.17	−1	(0)	....	26945.39	$b^3P_2'-g^3P_1$	279
7	3709.95	+1	20	III	26946.89	$a^3P_1'-b^3S_1'$	276
2	3708.63	0	4n	IV	26956.52	$a^3F_4-f^3F_4'$	280
7*	3707.53	0	10n	IV	26964.49	$a^5G_5'-d^5F_4'$	278
4‖	3705.53	+2	(1)	....	26979.03	$b^3P_1'-g^3P_0$	279
7	3704.29	0	15	III	26988.06	$b^3F_4'-g^3D_3'$	281
7	3702.98	−1	2	IV	26997.62	$aG-c^3H_4$	282

TABLE II—*Continued*

Source	Obs. λ (I.A.)	Δλ O−C	Int.	Temp. Class	ν	Designation	Multi-plet
7	3702.29	+1	10	III	27002.65	$a^3P'_0-b^3S'_1$	276
7	3700.05	......	4n	IV	27018.99	....	......
6	3698.41	−1	(1−)	....	27030.97	$b^3F'_3-g^3F_4$	274
7	3698.17	−1	3	IV	27032.73	$b^3P'_2-g^3P_2$	279
7	3696.88	−1	2	IV	27042.16	$a^5G'_4-d^5F'_3$	278
7	3694.43	0	10	III	27060.10	$b^3F'_3-g^3D'_2$	281
7	3689.89	−2	15	I	27093.39	$a^3F'_4-c^3D'_3$	283
12	3689.67	0	(0)	....	27095.00	$b^3P'_0-g^3P_1$	279
4	3687.38	+3	5	III A	27111.83	$a^3F'_4-b^3G'_3$	284
12	3686.71	−3	(0)	....	27116.75	$b^3P'_1-g^3P_2$	279
7	3685.95	+1	2	IV A	27122.35	$b^3F'_2-g^3D'_1$	281
5	3681.23	−3	1	IV	27157.12	$a^5G'_2-d^5F'_1$	278
7	3679.68	......	3	IV	27168.57	....	......
5	3677.75	−2	tr	IV A	27182.82	$b^3F'_4-cG'$	285
7	3671.66	−1	20	I	27227.91	$a^3F'_4-b^3G'_4$	284
7	3668.95	−1	15	I	27248.01	$a^3F'_3-c^3D'_2$	283
7	3660.62	0	12	I	27310.02	$a^3F'_3-c^3D'_3$	283
7	3658.14	+3	20	I	27328.54	$a^3F'_3-b^3G'_3$	284
7	3654.58	0	15	I	27355.15	$a^3F'_2-c^3D'_1$	283
7	3653.49	−1	100r	I	27363.32	$a^3F'_4-b^3G'_5$	284
7	3646.19	0	12	I	27418.10	$a^3F'_2-c^3D'_2$	283
7	3644.69	......	4	IV	27429.37	....	......
7	3644.46	+1	1	IV	27431.10	$aG'-dG$	286
7	3642.68	+1	80r	I	27444.52	$a^3F'_3-b^3G'_4$	284
4	3640.33	+4	1	IV	27462.24	$a^5D'_4-e^5F'_5$	287
7	3637.97	+1	10	II	27480.05	$a^3F'_2-c^3D'_3$	283
7	3635.47	−1	80r	I	27498.95	$a^3F'_2-b^3G'_3$	284
7	3635.20	−2	8	II	27500.98	$a^3F'_4-a^5P_3$	288
4	3633.45	......	5	IV	27514.24	....	......
4	3632.00	......	3	IV	27525.22	....	......
7	3626.09	0	4	III A	27570.08	$a^3F'_3-a^5P_2$	288
4	3623.10	......	3	IV	27592.83	....	......
5	3620.00	+1	1	IV	27616.46	$a^3F_3-g^3F'_3$	289
7	3619.45	+1	1	IV	27620.65	$a^3F_4-g^3F'_4$	289
4	3617.21	0	1	IV	27637.76	$a^3D_3-g^3P_2$	290
7	3614.20	......	3	IV	27660.77	....	......
11	3613.44	0	(1u)	....	27666.59	$a^3D_2-g^3P_1$	290
9	3612.84	−1	(0u)	....	27671.19	$a^3D_1-g^3P_0$	290
4‡	3610.16	0	12	III	27691.73	$aD-bP$	291
4	3609.61	+1	1	IV A	27695.95	$a^3P'_2-b^5P_1$	292
7	3607.12	+1	2	IV	27715.07	$a^3F_2-g^3F'_3$	289
4	3606.81	+2	4	III A	27717.45	$a^3F'_3-a^5P_3$	288
7	3606.06	+2	1	IV	27723.21	$aF-dD$	293
7	3604.30	0	8	III	27736.75	$a^3F'_3-bD'$	294
4	3603.86	+1	2	III A	27740.14	$a^3F'_2-a^5P_2$	288
9	3602.02	−5	(0u)	....	27754.30	$a^3D_2-g^3P_2$	290
5	3601.16	+1	1	IV	27760.92	$aS-eP$	295
7	3598.71	0	15	III	27779.84	$aD-cD'$	296
7	3585.86	......	4	III?	27879.38	....	......
4	3578.25	−1	3	IV?	27938.67	$b^3F'_4-h^3D'_3$	297
8	3574.24	+1	8	III	27970.01	$bG-fG'$	298
6‡	3564.51	−3	(1−)	....	28046.46	$b^3F'_3-h^3D'_2$	297
4	3564.4	−4	1	IV?	28047.23	$aD'-dD$	299

TABLE II—*Continued*

Source	Obs. λ (I.A.)	Δλ O−C	Int.	Temp. Class	ν	Designation	Multiplet
5........	3558.51	......	6?	IV	28093.65	....	......
4........	3556.17	......	3	IV	28112.13	....	......
6........	3553.82	− 5	(1)	....	28130.74	$b^3F'_2-h^3D'_1$	297
7........	3547.01	− 2	15	IV	28184.73	$aG-dF$	300
4........	3542.51	− 2	3	IV?	28220.53	$a^3H'_4-fG'$	301
7........	3530.58	− 1	1	III A	28315.89	$a^3F'_4-b^5F_3$	302
8........	3525.16	0	3	III	28359.42	$a^3G_3-i^3F_2$	303
8........	3519.94	0	1	III A	28401.47	$a^3F'_4-b^5F_4$	302
7........	3516.84	− 3	3	IV	28426.52	$a^3G_4-i^3F_3$	303
8........	3511.64	+ 1	3	III A	28468.60	$a^3F'_3-b^5F_2$	302
7........	3507.43	......	3	IV	28502.77	....	......
7........	3506.64	0	8	I	28509.20	$a^3F'_4-b^5F_5$	302
8........	3504.78	− 3	2	III A	28524.33	$a^3G_5-i^3F_4$	303
4........	3503.76	− 1	1	III A	28532.62	$a^3F'_3-b^5F_3$	302
7........	3499.10	0	8	III	28570.62	$a^3P'_2-d^3P_1$	304
8........	3495.94	0	2	III A	28596.45	$a^3F'_2-b^5F_1$	302
7........	3495.73	0	6	III A	28598.17	$a^3P'_1-d^3P_0$	304
7........	3493.27	− 1	4	II A	28618.31	$a^3F'_3-b^5F_4$	302
8........	3490.77	0	1	III A	28638.81	$a^3F'_2-b^5F_2$	302
7........	3485.69	0	6	III	28680.54	$a^3P'_1-d^3P_1$	304
4........	3483.00	0	(1)	....	28702.69	$a^3F'_2-b^5F_3$	302
7........	3481.68	0	3	IV	28713.58	$a^3D'_3-b^3D_3$	305
8........	3481.11	0	3	IV	28718.27	$a^3D'_2-b^3D_2$	305
7........	3480.53	0	12	III	28723.06	$a^3P'_2-d^3P_2$	304
7........	3478.92	0	6	III A	28736.35	$a^3P'_0-d^3P_1$	304
7........	3476.45	− 1	3	III A	28756.77	$a^3P'_2-b^5S'_2$	306
4........	3472.81	0	2	IV	28786.91	$a^3D'_1-b^3D_1$	305
8........	3467.26	0	6	III A	28832.98	$a^3P'_1-d^3P_2$	304
8........	3463.20	− 2	1	III A	28866.79	$a^3P'_1-b^5S'_2$	306
8........	3459.41	......	3	III	28898.42	....	......
8........	3458.01	0	3	III A	28910.12	$a^5F'_4-d^5D'_3$	307
7........	3457.49	0	4	III	28914.47	$a^5F'_5-d^5D'_4$	307
8........	3457.29	0	2	III A	28916.14	$a^5F'_3-d^5D'_2$	307
8........	3456.65	0	6	III	28921.49	$aG-bH$	308
8........	3455.76	0	1	III A	28928.94	$a^5F'_2-d^5D'_1$	307
8........	3455.43	+ 2	1	IV	28931.70	$a^5F_3-e^5F'_3$	309
8........	3455.37	+ 1	2	IV	28932.21	$a^5F_4-e^5F'_4$	309
8........	3454.73	+ 3	tr	IV	28937.56	$a^5F_2-e^5F'_2$	309
8*.......	3454.17	+ 1 − 3	1	III A	28942.25	$a^5F_5-e^5F'_5$ $a^3G_5-g^3G'_4$	309 310
8........	3453.66	0	tr	III A	28946.53	$a^5F'_1-d^5D'_0$	307
4........	3453.55	+ 1	(1)	....	28947.44	$a^5F_1-e^5F'_1$	309
8........	3450.75	0	1	III A	28970.93	$a^5F'_1-d^5D'_1$	307
8........	3449.87	0	2	III A	28978.32	$a^5F'_2-d^5D'_2$	307
8........	3448.25	0	1	III A	28991.93	$a^5F'_3-d^5D'_3$	307
8........	3446.6	− 2	2	IV	29005.81	$a^3G_4-g^3G'_4$	310
8........	3445.55	+ 1	1	III A	29014.65	$a^5F'_4-d^5D'_4$	307
8........	3444.89	0	tr	IV A	29020.22	$a^3P'_2-cF$	311
8........	3444.41	0	3	III A	29024.26	$b^3F'_2-i^3D'_1$	312
7........	3443.64	0	5	III	29030.74	$b^3F'_3-i^3D'_2$	312
7........	3439.30	− 1	8	III	29067.39	$b^3F'_4-i^3D'_3$	312
4........	3435.40	......	3	III	29100.38	....	......
12........	3431.86	− 3	(1)	....	29130.40	$a^3P'_1-cF$	311

TABLE II—*Continued*

Source	Obs. λ (I.A.)	$\Delta\lambda$ O−C	Int.	Temp. Class	ν	Designation	Multiplet
8	3430.88	+1	2	III	29138.71	$b^3F'_2-i^3D'_2$	312
8	3430.54	−1	1	III A	29141.60	$a^3P'_2-f^3F_3$	313
7	3428.95	0	4	III	29155.12	$a^3G_5-g^3G'_5$	310
8	3428.12	+1	1	IV A	29162.18	$a^3P'_1-f^3F_2$	313
8	3423.18	+1	2	IV A	29204.25	$b^3F'_3-i^3D'_3$	312
7	3415.99	+1	5	IV	29265.72	$a^3F_4-b^3D_3$	314
7	3411.67	0	5	IV	29302.77	$a^3F_3-b^3D_2$	314
7	3405.09	0	5	III A	29359.40	$a^3P'_1-f^3D'_1$	315
7	3403.36	0	4	III A	29374.33	$a^3P'_2-f^3D'_2$	315
4	3400.14	−3	3	IV	29402.14	$a^3F_2-b^3D_1$	314
7	3398.62	−1	8	III	29415.28	$a^3P'_0-f^3D'_1$	315
8	3392.79	0	1	IV	29465.83	$a^5D'_3-d^5D_3$	316
8	3392.71	+3	10	III	29466.53	$aG-eF$	317
7	3390.67	0	10	III	29484.27	$a^3P'_1-f^3D'_2$	315
8	3389.90	−1	1n	IV	29490.96	$a^5D'_4-d^5D_4$	316
8	3389.60	0	1	IV	29493.57	$a^3D'_3-c^3D_3$	318
7	3385.93	−1	40r	II	29525.53	$a^3F'_4-d^3D'_3$	319
8	3385.66	0	12	I	29527.89	$a^3F'_4-c^3G'_3$	320
7	3382.30	+1	15	II	29557.22	$a^3P'_2-f^3D'_3$	315
8	3381.44	0	2	IV	29564.74	$b^3F'_4-f^3G'_5$	321
8	3381.35	+1	1	IV	29565.52	$a^3D'_2-c^3D_2$	318
8	3380.12	−3	1	IV	29576.28	$a^5D'_1-g^5F'_1$	322
8	3379.43	0	1	IV	29582.32	$a^5D'_2-g^5F'_2$	322
7	3379.20	−1	15	I	29584.33	$a^3F'_4-c^3G'_4$	320
8	3377.57	−1	30r	I	29598.62	$a^3F'_3-d^3D'_2$	319
8	3377.48	−1	20	I	29599.41	$a^3F'_4-c^5D'_3$	323
8	3375.69	−2	3n	III	29615.09	$a^5D'_3-g^5F'_3$	322
8	3374.60	−1	1	IV	29624.66	$a^5D'_1-g^5F'_2$	322
8*	3373.58	0 +2	1	IV	29633.61	$a^5D'_4-g^5F'_4$ $a^3D'_1-c^3D_2$	322 318
7	3371.44	+1	80R	II	29652.43	$a^3F'_4-c^3G'_5$	320
7	3370.42	−2	40r	II	29661.41	$a^3F'_2-d^3D'_1$	319
8	3369.05	0	1	III A	29673.46	$a^3F'_4-c^5D'_4$	323
7	3367.87	−1	3n	III	29683.86	$a^5D'_2-g^5F'_3$	322
7§	3366.17	+2	5	III E	29698.84	$a^5G'_6-e^5F'_5$	324
8	3363.60	−3	2n	IV	29721.54	$aF-dG$	325
7	3362.10	0	3	III	29734.80	$a^5D'_3-g^5F'_4$	322
7	3361.82	−1	10	I	29737.27	$a^3F'_3-c^5D'_2$	323
8	3361.50	0	1	III A	29740.11	$a^5G'_5-e^5F'_4$	324
12¶	3361.27	+1	40r	I	29742.14	$a^3F'_3-d^3D'_3$	319
4	3361.00	+1	10	I	29744.53	$a^3F'_3-c^3G'_3$	320
7	3358.47	−1	8n	IV	29766.94	$a^5D'_4-g^5F'_5$	322
7	3358.26	−1	10	I	29768.79	$a^3F'_2-d^3D'_2$	319
8	3356.18	−1	2	III	29787.25	$a^5G'_4-e^5F'_3$	324
7	3354.64	+1	60r	II	29800.92	$a^3F'_3-c^3G'_4$	320
7	3352.92	+1	6	I A	29816.21	$a^3F'_3-c^5D'_3$	323
8	3350.53	−1	2	IV	29837.47	$a^5G'_3-e^5F'_2$	324
12	3349.24	0	(?)	(III A)	29848.88	$a^3P'_2-g^3F_2$	326
8	3348.52	−1	5	II A	29855.38	$a^3F'_2-c^5D'_1$	323
8	3344.91	−1	1	III A	29887.60	$a^5G'_2-e^5F'_1$	324
8	3344.7	+8	tr	IV A	29889.49	$a^5G'_5-e^5F'_5$	324
8	3343.34	−1	tr	IV A	29901.64	$a^5G'_4-e^5F'_4$	324
7	3342.70	−1	2	II A	29907.36	$a^3F'_2-c^5D'_2$	323

TABLE II—*Continued*

Source	Obs. λ (I.A.)	Δλ O−C	Int.	Temp. Class	ν	Designation	Multiplet
7	3342.14	0	6	I A	29912.37	$a^3F'_2-d^3D'_3$	319
7**	3341.87	0	50r	II	29914.79	$a^3F'_2-c^3G'_3$	320
8*	3341.54	0 −1	1	III A	29917.74	$aD-d^3P_1$ $a^5G'_3-e^5F'_3$	327 324
12	3340.77	−2	(1)	(V)	29924.58	$a^5F_5-c^5G_4$	328
8	3339.5	−2	1n	IV	29936.03	$a^5G'_2-e^5F'_2$	324
8	3338.82	−2	2	III A	29942.13	$a^3P'_2-g^3F_3$	326
8	3337.40	+1	1n	IV	29954.86	$a^5F_4-c^5G_3$	328
8	3336.94	−2	1	IV A	29958.99	$a^3P'_1-g^3F_2$	326
8	3334.88	−1	1	IV	29977.49	$a^5D'_4-h^5F'_4$	329
12	3334.35	+3	(1n)	(IV)	29982.25	$a^5F_3-c^5G_2$	328
8	3333.91	0	2	III A	29986.21	$a^3F'_2-c^5D'_3$	323
8*	3333.02	+1 −1	2n	IV	29994.22	$a^5D'_3-h^5F'_3$ $a^5D'_2-h^5F'_2$	329 329
8	3328.34	−1	1	IV	30036.40	$a^5D'_1-h^5F'_2$	329
8	3327.3	0	1n	IV	30045.77	$a^3F_4-c^3D_3$	330
8	3326.64	+1	2	III A	30051.74	$a^3P'_2-g^3D'_1$	331
8	3325.37	0	1n	IV	30063.23	$a^5D'_2-h^5F'_3$	329
8	3325.22	0	3	IV	30064.58	$a^5F_4-c^5G_4$	328
8	3325.15	0	3	IV	30065.21	$a^5F_5-c^5G_5$	328
8*	3324.74	−2 −1	4	III	30068.93	$a^5F_2-c^5G_2$ $a^5F_3-c^5G_3$	328 328
8	3324.61	+1	1	III A	30070.09	$aD-d^3P_2$	327
8	3323.89	−1	2	IV A	30076.61	$a^5D'_4-h^5F'_5$	329
8	3323.80	+1	4	III	30077.42	$bG-fF$	332
8	3323.66	0	2n	IV	30078.68	$a^5D'_3-h^5F'_4$	329
7	3321.58	0	8	III	30097.53	$a^3P'_2-g^3D'_2$	331
7	3318.35	−1	4	IV	30126.82	$a^5F_1-c^5G_2$	328
8	3316.38	−2	1	IV	30144.71	$a^5D'_4-b^3D_3$	333
8	3315.78	−1	2n	IV	30150.17	$a^3F_3-c^3D_2$	330
8	3315.22	−2	2	IV	30155.26	$a^5F_2-c^5G_3$	328
8	3314.50	−1	8	III	30161.82	$a^3P'_1-g^3D'_1$	331
8	3314.42	0	10	I	30162.55	$a^3P'_2-g^3D'_3$	331
7	3312.68	+1	5	III	30178.37	$a^5F_3-c^5G_4$	328
7	3309.71	−1	6	III	30205.46	$a^5F_4-c^5G_5$	328
4	3309.49	0	15	I	30207.46	$a^3P'_1-g^3D'_2$	331
7	3308.38	−1	10	III	30217.61	$a^3P'_0-g^3D'_1$	331
7	3306.87	0	10	III	30231.40	$a^5F_5-c^5G_6$	328
8	3305.75	−2	2	IV	30241.63	$a^5D'_1-b^3D_2$	333
8	3305.29	−1	2	IV	30245.86	$a^5D'_3-b^3D_3$	333
8	3299.41	−1	10	III	30299.75	$aD-e^3G'_3$	334
8	3297.78	−1	1	IV	30314.72	$a^5D'_2-b^3D_3$	333
8	3297.24	−1	1	IV	30319.69	$a^5D'_1-e^5D_0$	335
8	3297.08	−1	1	IV	30321.16	$a^5D'_3-e^5D_2$	335
12	3296.21	0	(1)	....	30329.18	$a^5D'_4-e^5D_3$	335
8	3295.64	0	1	IV A	30334.42	$a^5D'_2-e^5D_1$	335
7	3294.89	−1	6	IV	30341.32	$a^5D'_4-e^5D_4$	335
7	3292.06	−1	20	I	30367.40	$aD-cF$	336
12	3291.07	+1	(0)	....	30376.52	$a^5D'_1-e^5D_1$	335
12	3289.58	−3	(0)	....	30390.26	$a^5D'_2-e^5D_2$	335
12	3288.89	0	(1)	....	30396.67	$a^5D'_0-e^5D_1$	335
7	3288.13	......	3	IV	30403.69	....	......

TABLE II—*Continued*

Source	Obs. λ (I.A.)	Δλ O−C	Int.	Temp. Class	ν	Designation	Multiplet
8	3285.24	0	2	IV	30430.44	$a^5D_3'-e^5D_3$	335
8	3285.04	−1	1	IV	30432.29	$a^5D_1'-e^5D_2$	335
8	3283.94	0	2	IV	30442.49	$a^5D_3'-e^5D_4$	335
8	3280.38	+1	2	III A	30475.52	$a^3P_2'-cP$	337
8	3278.96	0	[12]	III A	30488.71	$aD-f^3F_3$	338
12	3277.82	0	(1)	(IV)	30499.40	$a^5D_2'-e^5D_3$	335
4	3274.05	0	(5)	(III A)	30534.44	$b^3F_4'-j^3D_3'$	339
7	3270.56	0	3	III A	30567.03	$b^3F_3'-j^3D_2'$	339
8	3268.60	+2	1	III A	30585.35	$a^3P_1'-cP$	337
8	3267.41	+1	tr	IV A	30596.50	$aD-f^3D_1'$	340
8	3267.06	+1	2n	III	30599.77	$b^3F_4'-k^3D_3'$	341
8	3265.46	−2	2	III A	30614.75	$b^3F_2'-j^3D_1'$	339
8	3263.83	−2	2n	III	30630.05	$b^3F_3'-k^3D_2'$	341
8	3262.63	0	1	IV A	30641.31	$a^3P_0'-cP$	337
8	3260.39	−3	1	IV	30662.37	$b^3F_2'-k^3D_1'$	341
8§	3260.26	−2	3	III E	30663.59	$a^3P_2'-dP$	342
8	3259.41	−1	2	IV	30671.58	$b^3F_3'-j^3D_3'$	339
8	3259.04	0	1	IV A	30675.06	$b^3F_2'-j^3D_2'$	339
7§	3248.60	−3	15	III Er	30773.63	$a^3P_1'-dP$	342
8	3243.80	0	4	III A	30819.18	$a^3F_4'-e^3D_3'$	343
8	3243.51	+1	3	III	30821.93	$a^5G_6'-c^5G_5$	344
7	3238.20	−1	4	IV	30872.47	$a^5G_5'-c^5G_4$	344
8	3236.21	−1	tr	III A	30891.45	$a^5F_5-c^5H_6'$	345
12	3233.62	−1	(1)	....	30919.08	$a^5F_4-c^5H_5'$	345
8	3232.78	0	3	IV	30924.23	$a^5G_4'-c^5G_3$	344
8	3229.86	0	tr	IV A	30952.18	$a^5F_3-c^5H_4'$	345
8	3228.17	−1	2	III	30968.39	$a^5G_3'-c^5G_2$	344
8	3227.94	+1	2N	III	30970.60	$a^5F_5-d^5D_4$	346
8	3226.49	0	1N	IV	30984.52	$a^5F_4-d^5D_3$	346
8	3226.22	−1	1	III A	30987.11	$a^3F_4'-d^3G_3'$	347
7	3226.11	0	12	III	30988.16	$a^5G_6'-c^5G_6$	344
8	3223.51	0	10	III	31013.16	$a^5G_5'-c^5G_5$	344
8	3223.00	0	2N	III	31018.06	$a^5F_5-d^5G_6$	348
8	3222.74	0	3	II A	31020.57	$a^3F_3'-e^3D_2'$	343
7	3221.37	0	10	III	31033.77	$a^5G_4'-c^5G_4$	344
8	3221.14	0	2	III A	31035.98	$a^3F_3'-e^3D_3'$	343
8	3220.28	−1	1	III A	31044.26	$a^5F_4-d^5G_5$	348
8	3219.33	0	1n?	III	31053.43	$a^5F_1-d^5G_2$	348
7	3219.21	+1	8	III	31054.58	$a^5G_3'-c^5G_3$	344
8	3218.98	−1	2N	III	31056.80	$a^5F_3-d^5G_4$	348
8	3218.67	−1	tr	IV A	31059.79	$a^3P_2'-h^3D_1'$	349
12	3218.47	−1	(0N)	(IV)	31061.70	$a^5F_2-d^5G_3$	348
7	3217.95	0	8	III	31066.74	$a^5G_2'-c^5G_2$	344
8	3216.19	−1	3	III A	31083.74	$a^3P_2'-h^3D_2'$	349
7	3214.23	−1	12	I	31102.70	$a^3F_4'-d^3G_4'$	347
7*	3213.14	−2 +1	8	III	31113.25	$a^3P_2'-h^3D_3'$ $a^5F_5-g^5F_4'$	349 350
8	3211.07	+3	1n	IV	31133.30	$a^5F_4-g^5F_3'$	350
7	3209.02	−1	4	IV	31153.20	$a^5G_2'-c^5G_3$	344
7	3207.90	+2	5	IV	31164.06	$a^5G_3'-c^5G_4$	344
7	3207.33	+1	5	III	31169.60	$a^3P_1'-h^3D_1'$	349
7	3206.82	+1	5	IV	31174.56	$a^5G_4'-c^5G_5$	344
7	3206.34	+1	5	IV	31179.23	$a^5G_5'-c^5G_6$	344

TABLE II—*Continued*

Source	Obs. λ (I.A.)	$\Delta\lambda$ O−C	Int.	Temp. Class	ν	Designation	Multiplet
7........	3205.85	0	5	II	31184.00	$a^3F'_2-e^3D'_1$	343
8........	3205.15	−1	2	III A	31190.80	$a^3F'_2-e^3D'_2$	343
7........	3204.87	+1	6	III	31193.52	$a^3P'_1-h^3D'_2$	349
7........	3203.82	0	15	I	31203.75	$a^3F'_3-d^3G'_3$	347
7........	3201.59	0	5	III	31225.49	$a^3P'_0-h^3D'_1$	349
7........	3199.91	0	100R	II	31241.88	$a^3F'_4-d^3G'_5$	347
8........	3199.43	+1	1n	IV A	31246.58	$a^5F_5-g^5F'_5$	350
12........	3199.34	0	(1n)	(IV A)	31247.45	$a^5F_3-g^5F'_3$	350
8........	3198.71	−1	1n	IV A	31253.61	$a^5F_4-g^5F'_4$	350
7........	3192.00	+1	80R	II	31319.29	$a^3F'_3-d^3G'_4$	347
7........	3186.45	0	60r	II	31373.83	$a^3F'_2-d^3G'_3$	347
7........	3179.28	+1	3	III A	31444.59	$aD-g^3D'_2$	351
7........	3172.72	+1	4	III A	31509.61	$aD-g^3D'_3$	351
8........	3172.38	0	1n	IV	31512.99	$a^5F_4-h^5F'_3$	352
7........	3170.92	−1	3	III A	31527.49	$a^3F'_4-a^3H_5$	353
8*.......	3168.04	+1 −3	2n	IV	31556.15	$a^5F_5-h^5F'_5$ $aG-eG'$	352 354
8........	3163.92	+1	1	IV	31597.24	$a^5F_4-h^5F'_4$	352
12........	3160.95	−1	(0)	(IV)	31626.93	$a^5F_3-h^5F'_3$	352
8........	3160.09	+3	tr	III A	31635.54	$a^3F'_3-b^3P_2$	355
8........	3157.66	0	1	III A	31659.88	$a^3F'_3-a^3H_4$	353
7........	3153.59	......	3	III A	31700.75	....	......
8........	3151.11	+1	tr	IV A	31725.69	$a^3F'_2-b^3P_1$	355
8........	3147.42	+1	1	IV A	31762.87	$a^5F_3-b^3D_2$	356
7........	3147.26	−1	3	IV A	31764.49	$a^5F_4-b^3D_3$	356
8........	3146.24	0	3N	IV	31774.80	$a^5G'_6-d^5G_6$	357
8........	3145.51	0	1	IV A	31782.18	$a^3P'_2-e^3P_1$	358
8........	3143.34	0	12N	IV	31804.12	$a^5G'_6-c^5H'_7$	359
7........	3141.67	0	10	IV	31821.01	$a^5F_5-e^5D_4$	360
7........	3141.51	+1	15	II	31822.63	$aD-cP$	361
8........	3139.87	+1	10N	IV	31839.25	$a^5G'_5-c^5H'_6$	359
4........	3138.87	+2	(1)	....	31849.40	$a^5F_2-b^3D_1$	356
8........	3138.62	0	1n	IV A	31851.94	$a^5G'_5-d^5G_5$	357
12........	3137.36	−1	(1)	....	31864.72	$a^3P'_2-e^3P_2$	358
4*.......	3136.03	0 +1	2	IV	31878.25	$a^3P'_1-e^3P_0$ $a^5F_3-b^3D_3$	358 356
8........	3135.05	0	8N	IV	31888.20	$a^5G'_4-c^5H'_5$	359
8........	3134.66	−1	1	IV A	31892.17	$a^3P'_1-e^3P_1$	358
8........	3133.13	−1	1	IV A	31907.74	$a^5F_1-b^3D_1$	356
8........	3132.71	0	6N	IV	31912.03	$a^5G'_4-d^5G_4$	357
8........	3132.1	......	3N	IV	31918.23	....	......
8††......	3130.81	......	15?	IV	31931.39	....	......
8........	3130.38	0	1	IV A	31935.78	$b^3F'_2-i^3F_2$	362
8........	3130.16	0	8N	IV	31938.02	$a^5G'_3-c^5H'_4$	359
8........	3129.62	−2	1	IV A	31943.53	$b^3F'_3-i^3F_3$	362
7........	3129.07	0	7	IV	31949.14	$a^5F_4-e^5D_3$	360
7*.......	3128.64	+1 +1	8	IV	31953.53	$a^3P'_2-i^3D'_1$ $a^5F_3-e^5D_2$	363 360
8*.......	3127.90	+1 +1	5	IV	31961.09	$a^5F_4-e^5D_4$ $a^5G'_3-d^5G_3$	360 357
8........	3127.67	0	8N	IV	31963.44	$a^5G'_2-c^5H'_3$	359
8........	3127.43	+1	?	IV A	31965.90	$a^5G'_5-d^5G_6$	357
8........	3127.23	−3	2	IV	31967.94	$b^3F'_4-i^3F_4$	362

TABLE II—*Continued*

Source	Obs. λ (I.A.)	Δλ O−C	Int.	Temp. Class	ν	Designation	Multiplet
12‡‡	3125.64	+1	(2)	(IV)	31984.23	$a^5F_2-e^5D_1$	360
8	3125.55	0	2	IV	31985.13	$a^5F_1-e^5D_0$	360
8	3124.74	0	1	IV A	31993.41	$a^5G'_2-d^5G_2$	357
7	3123.76	−1	20n	IV	32003.45	$a^5G'_6-g^5F'_5$	364
7	3123.07	0	15	II	32010.51	aD−dP	365
8	3122.80	+1	tr	IV A	32013.29	$a^5G'_4-d^5G_5$	357
8	3120.21	0	3	IV	32039.85	$a^5F_2-e^5D_2$	360
8*	3119.97	0 +2	2	IV	32042.32	$a^5F_1-e^5D_1$ $a^5G'_3-d^5G_4$	360 357
8	3119.73	0	15	III	32044.78	aG−cH	366
7	3118.13	+1	15	IV	32061.23	$a^5G'_5-g^5F'_4$	364
8	3117.89	−1	5	III A	32063.70	$a^3P'_1-i^3D'_1$	363
7	3117.45	0	6	III	32068.22	$a^3P'_2-i^3D'_2$	363
7	3114.09	0	20n	IV	32102.82	$a^5G'_4-g^5F'_3$	364
7	3112.48	−1	8	III	32119.44	$a^3P'_0-i^3D'_1$	363
7	3111.28	0	10n	IV	32131.83	$a^5G'_3-g^5F'_2$	364
8§	3110.61	......	4	IV	32138.74	....	......
7	3109.58	......	8n	IV	32149.39	....	......
7	3107.45	+2	12n	IV	32171.42	$a^5G'_2-g^5F'_1$	364
7	3106.80	0	8	III A	32178.15	$a^3P'_1-i^3D'_2$	363
8	3105.22	+1	2n	IV	32194.52	$a^5G'_5-g^5F'_5$	364
8	3102.50	0	3n	III	32222.74	$a^5G'_4-g^5F'_4$	364
8	3101.77	−1	1n	IV A	32230.33	$a^5G'_2-g^5F'_2$	364
8	3101.48	−1	4n	III	32233.35	$a^5G'_3-g^5F'_3$	364
8*	3100.67	0 0	12	III A	32241.76	$a^3P'_2-c^3S'_1$ $a^3P'_2-i^3D'_3$	367 363
8	3093.83	0	3n	IV	32313.04	$a^5G'_6-h^5F'_5$	368
7	3090.13	0	8	III	32351.73	$a^3P'_1-c^3S'_1$	367
8	3086.82	−1	1	IV A	32386.42	$b^3F'_4$−cH	369
8	3085.03	0	2n	IV	32405.20	$a^5G'_5-h^5F'_4$	368
7	3084.81	0	4	III A	32407.52	$a^3P'_0-c^3S'_1$	367
8	3082.62	+2	2	III A	32430.55	aD−$h^3D'_2$	370
7	3080.17	−1	1	III	32456.34	$b^3F'_4-l^3D'_3$	371
8	3079.82	+2	1	III A	32460.03	aD−$h^3D'_3$	370
12	3077.72	0	(1)	(IV)	32482.17	$a^5G'_4-h^5F'_3$	368
12	3071.92	+1	(0)	(IV)	32543.50	$a^5G'_3-h^5F'_2$	368
7	3042.54	0	3	III A	32857.73	$a^3F'_2$−bF	372
8	3025.06	+1	2	III	33047.59	aD−dF	373
8	3021.56	......	3	IV	33085.89	....	......
8	3015.55	......	4n	IV	33151.81	....	......
8	3010.12	+1	tr	IV A	33211.61	aD−e^3P_2	374
8	3007.48	......	4N	IV	33240.78	....	......
8	3005.37	0	2n	IV A	33264.10	$b^3F'_4-j^3F_4$	375
8	3003.65	0	2n	IV A	33283.15	$b^3F'_3-j^3F_3$	375
7*	3002.73	+1 +1	3	III A	33293.36	$a^3F'_4-d^3F_3$ $b^3F'_2-j^3F_2$	376 375
7	3000.87	0	20	II	33313.98	$a^3F'_4-d^3F_4$	376
8	2999.78	+1	tr	IV A	33326.08	$a^3P'_2-f^3P_2$	377
8	2998.41	+2	tr	IV A	33341.31	$a^3P'_2-f^3P_1$	377
8	2995.75	......	4	IV	33370.95	....	......
8	2993.94	+1	tr	IV A	33391.09	$b^3F'_2-j^3F_3$	375
8	2993.05	+1	tr	IV A	33401.01	$b^3F'_3-j^3F_4$	375
8	2991.79	+2	1	IV A	33415.08	aD−$i^3D'_2$	378

TABLE II—*Continued*

Source	Obs. λ (I.A.)	Δλ O−C	Int.	Temp. Class	ν	Designation	Multiplet
8........	2990.98	0	3	IV A	33424.13	$b^3F'_3-m^3D'_2$	379
8........	2990.48	−3	3	IV A	33429.73	$b^3F'_4-m^3D'_3$	379
8........	2990.03	−2	3	IV A	33434.75	$b^3F'_2-m^3D'_1$	379
8........	2989.91	0	tr	IV A	33436.10	$a^3P'_1-f^3P_2$	377
8........	2985.46	−1	3	III A	33485.94	$a^3F'_3-d^3F_2$	376
7........	2983.29	−1	20	II	33510.29	$a^3F'_3-d^3F_3$	376
12§§......	2981.45	−2	(2)	(III A)	33530.98	$a^3F'_3-d^3F_4$	376
8........	2980.28	−2	tr	IV A	33544.14	$a^3P'_2-j^3D'_1$	380
8........	2976.32	+1	2	III A	33588.75	$aD-i^3D'_3$	378
7........	2974.93	0	4	III A	33604.46	$a^3P'_2-j^3D'_2$	380
7........	2970.55	−1	4	III A	33654.00	$a^3P'_1-j^3D'_1$	380
7........	2970.38	0	10	II A	33655.93	$a^3F'_2-d^3F_2$	376
8........	2969.37	−1	1	IV A	33667.37	$a^3P'_2-k^3D'_2$	381
7........	2968.23	0	4	III A	33680.30	$a^3F'_2-d^3F_3$	376
7........	2967.22	0	25	II	33691.77	$a^3F'_4-e^3F_3$	382
8........	2966.38	+1	1	IV	33701.31	$a^3P'_1-k^3D'_1$	381
8........	2965.72	+1	15	III	33708.80	$a^3P'_2-j^3D'_3$	380
7........	2965.68	+5	8	III	33709.26	$a^3P'_0-j^3D'_1$	380
4........	2965.24	+1	(6)?	....	33714.27	$a^3P'_1-j^3D'_2$	380
8........	2961.48	+2	2	III A	33757.06	$a^3P'_0-k^3D'_1$	381
8........	2959.98	+1	5	III A	33774.17	$a^3P'_2-k^3D'_3$	381
8........	2959.71	0	3	III A	33777.25	$a^3P'_1-k^3D'_2$	381
7........	2956.80	0	25	II	33810.50	$a^3F'_3-e^3F_2$	382
7........	2956.13	0	70R	II	33818.16	$a^3F'_4-e^3F_4$	382
7........	2948.25	0	60r	II	33908.55	$a^3F'_3-e^3F_3$	382
8........	2947.72	−1	3	III A	33914.63	$aD-f^3G'_3$	383
7........	2941.99	−1	60r	II	33980.69	$a^3F'_2-e^3F_2$	382
7........	2937.30	0	25	II	34034.96	$a^3F'_3-e^3F_4$	382
7........	2933.53	0	25	II	34078.68	$a^3F'_2-e^3F_3$	382
7........	2928.32	−1	30	III	34139.31	$aG-fG'$	384
8........	2922.92	−1	2	IV A	34202.39	$aD-h^3F_3$	385
8........	2912.47	0	2	IV A	34325.12	$a^3P'_2-eP$	386
7........	2912.07	+1	40	III	34329.80	$aD-eF$	387
7........	2905.65	......	5	IV A	34405.66	....	.....
8........	2903.17	0	2	IV	34435.04	$a^3P'_1-eP$	386
12........	2892.77	......	[3]	[IV A]	34558.84	....	.....
8........	2883.23	+1	1	IV A	34673.18	$aD-f^3P_2$	388
8........	2881.94	0	1	IV A	34688.70	$aD-f^3P_1$	388
8........	2860.27	+1	2	IV A	34951.49	$aD-j^3D'_2$	389
8........	2855.13	0	1	IV	35014.42	$aD-k^3D'_2$	390
8........	2853.43	−1	1	IV A	35035.27	$a^3F'_2-cD'$	391
8........	2836.60	0	1	IV A	35243.14	$a^5F'_4-e^5D'_3$	392
8........	2836.40	0	1n	IV A	35245.61	$a^5F'_3-e^5D'_2$	392
8........	2836.09	0	1	IV A	35249.47	$a^5F'_5-e^5D'_4$	392
8........	2835.63	0	2	IV	35255.19	$a^5F'_2-e^5D'_1$	392
8........	2834.75	0	2	IV A	35266.13	$a^5F'_1-e^5D'_0$	392
8........	2832.26	0	1n	IV A	35297.13	$a^5F'_1-e^5D'_1$	392
8........	2831.40	−1	1n	IV A	35307.85	$a^5F'_2-e^5D'_2$	392
8........	2830.03	0	2n	IV A	35324.95	$a^5F'_3-e^5D'_3$	392
8*.......	2828.05	+1 0	2	IV A	35349.68	$a^5F'_1-e^5D'_2$ $a^5F'_4-e^5D'_4$	392 392
8........	2826.37	0	tr	IV A	35370.69	$a^3F'_4-d^5D'_4$	393
8........	2825.06	0	1	IV A	35387.09	$a^5F'_2-e^5D'_3$	392

TABLE II—*Continued*

Source	Obs. λ (I.A.)	Δλ O−C	Int.	Temp. Class	ν	Designation	Multiplet
8	2823.46	− 1	1	IV A	35407.13	$a^3F'_3-d^5D'_2$	393
8	2821.51	− 1	1	IV A	35431.61	$a^5F'_3-e^5D'_4$	392
6	2817.83	− 7	(1)	....	35477.85	$a^3P'_2-l^3D'_2$	394
6	2817.37	− 4	(1)	....	35483.64	$a^3P'_1-l^3D'_1$	394
7	2812.96	− 3	2	IV A	35539.31	$a^3P'_0-l^3D'_1$	394
7	2809.15	− 5	5	III	35587.50	$a^3P'_1-l^3D'_2$	394
7	2805.68	− 6	6	III	35631.51	$a^3P'_2-l^3D'_3$	394
7	2802.47	0	15	III	35672.31	$aD-eP$	395
4	2758.06	0	20	III	36246.68	$aG-fF$	396
4	2757.40	+ 1	6	III	36255.37	$a^3P'_2-d^3S'_1$	397
4	2749.04	− 1	5	III	36365.60	$a^3P'_1-d^3S'_1$	397
8	2744.85	+ 1	5	....	36421.11	$a^3P'_0-d^3S'_1$	397
4	2742.30	0	15	III	36454.99	$aD-dD'$	398
12	2741.82	+ 1	(1)	....	36461.35	$a^3P'_2-m^3D'_2$	399
12	2740.88	0	(2)	....	36473.86	$a^3P'_1-m^3D'_1$	399
8	2739.80	+ 1	15	III	36488.24	$a^3P'_2-g^3P_1$	400
12	2736.71	+ 2	(2)	....	36529.40	$a^3P'_0-m^3D'_1$	399
7	2735.61	+ 1	6	III	36544.12	$aD-eD'$	401
7	2735.29	0	10	III	36548.27	$a^3P'_1-g^3P_0$	400
8	2733.27	+ 1	30	III	36575.48	$a^3P'_2-g^3P_2$	400
8	2731.59	+ 3	7	III	36597.91	$a^3P'_1-g^3P_1$	400
8	2731.14	0	4	....	36603.86	$a^3P'_2-m^3D'_3$	399
7	2727.38	− 3	8	III	36654.40	$a^3P'_0-g^3P_1$	400
8	2725.08	+ 2	10	III	36685.33	$a^3P'_1-g^3P_2$	400
4	2688.83	......	10	....	37179.88	....	......
12	2685.14	+ 1	(3)	....	37230.97	$a^3F'_4-e^3G'_4$	402
4	2684.85	......	5	....	37234.99	....	......
8	2679.95	+ 3	20	IV	37303.07	$a^3F'_4-e^3G'_5$	402
12	2676.09	+ 1	(1)	....	37356.89	$a^3F'_4-f^3F_3$	403
8	2669.61	+ 2	15	IV	37447.55	$a^3F'_3-e^3G'_4$	402
8	2669.27	+ 1	2	....	37452.32	$a^3F'_3-cF$	404
12	2668.36	+ 3	(1)	....	37465.11	$a^3F'_4-f^3F_4$	403
4	2661.98	+ 1	10	IV	37554.87	$a^3F'_2-e^3G'_3$	402
12	2660.66	+ 2	(1)	....	37573.51	$a^3F'_3-f^3F_3$	403
8	2657.19	0	10	IV	37622.58	$a^3F'_2-cF$	404
8	2656.92	......	4	....	37626.39	....	......
8	2656.38	......	4	....	37634.04	....	......
8	2654.93	+ 1	5	....	37654.59	$a^3F'_2-f^3F_2$	403
12	2653.02	+ 4	(2)	....	37681.71	$a^3F'_3-f^3F_4$	403
8	2649.60	......	3	....	37730.33	....	......
4	2649.31	......	4	....	37734.47	....	......
12	2648.65	+ 1	(1)	....	37743.82	$a^3F'_2-f^3F_3$	403
8	2646.65	+ 3	40	II	37772.39	$a^3F'_4-f^3D'_3$	405
8	2644.28	+ 2	40	II	37806.31	$a^3F'_3-f^3D'_2$	405
8	2641.12	+ 3	40	II	37851.48	$a^3F'_2-f^3D'_1$	405
12	2636.16	+ 1	(1)	....	37922.69	$aD-g^3P_2$	406
8	2632.42	+ 2	15	....	37976.55	$a^3F'_2-f^3D'_2$	405
4	2631.55	+ 3	(1)	....	37989.12	$a^3F'_3-f^3D'_3$	405
8	2619.94	0	10	IV	38157.45	$a^3F'_4-g^3F_3$	407
4	2611.47	0	8	....	38281.20	$a^3F'_3-g^3F_2$	407
8	2611.29	0	25	IV	38283.84	$a^3F'_4-g^3F_4$	407
4	2605.16	+ 2	25	IV	38373.92	$a^3F'_3-g^3F_3$	407
12	2604.88	0	(3)	....	38378.07	$a^3F'_4-g^3D'_3$	408

TABLE II—*Continued*

Source	Obs. λ (I.A.)	Δλ O−C	Int.	Temp. Class	ν	Designation	Multiplet
8	2599.91	−1	25	IV	38451.40	$a^3F'_2-g^3F_2$	407
8	2596.60	+1	10	....	38500.40	$a^3F'_3-g^3F_4$	407
12	2594.63	+1	(2)	....	38529.65	$a^3F'_3-g^3D'_2$	408
4	2593.66	+2	(1)	....	38544.04	$a^3F'_2-g^3F_3$	407
8	2590.27	+2	5	....	38594.57	$a^3F'_3-g^3D'_3$	408
12	2586.26	−1	(3)	....	38654.35	$a^3F'_2-g^3D'_1$	408
8	2583.22	+1	2	....	38699.82	$a^3F'_2-g^3D'_2$	408
8	2580.81	......	5	....	38735.95	....	......
12	2578.91	+3	(2)	....	38764.48	$a^3F'_2-g^3D'_3$	408
8	2541.92	+1	20	....	39328.54	$a^3F'_4-h^3D'_3$	409
4	2529.86	0	(1)	....	39516.00	$a^3F'_3-h^3D'_2$	409
8	2527.99	+1	5	....	39545.24	$a^3F'_3-h^3D'_3$	409
8	2520.54	0	10	....	39662.11	$a^3F'_2-h^3D'_1$	409
12¶¶	2519.07	+6	(8)	....	39685.24	$a^3F'_2-h^3D'_2$	409
12	2517.14	−1	(1)	....	39715.70	$a^3F'_2-h^3D'_3$	409
8	2504.52	......	3	....	39915.78	....	......
12	2470.98	−1	(3)	....	40457.53	$a^3F'_4-i^3D'_3$	410
10	2468.60	−1	(1)	....	40496.57	$a^3F'_4-dG'$	411
8	2468.36	0	2	....	40500.50	$a^3F'_3-i^3D'_2$	410
8	2464.98	0	2	....	40556.03	$a^3F'_2-i^3D'_1$	410
12	2458.00	−3	(2)	....	40671.14	$a^3F'_2-i^3D'_2$	410
12	2457.80	−2	(2)	....	40674.44	$a^3F'_3-i^3D'_3$	410
12	2446.12	−1	(2)	....	40868.67	$a^3F'_4-f^3G'_4$	412
8	2440.98	0	10	....	40954.74	$a^3F'_4-f^3G'_5$	412
12	2438.28	−2	(2)	....	41000.10	$a^3F'_3-f^3G'_3$	412
8	2434.09	+1	3	....	41070.65	$a^3F'_4-h^3F_3$	413
8	2433.23	+1	6	....	41085.16	$a^3F'_3-f^3G'_4$	412
12	2431.78	+1	(1)	....	41109.64	$aD-fF$	414
6	2428.36	−1	(1)	....	41167.51	$a^3F'_3-h^3F_2$	413
8	2428.24	+1	2	....	41169.59	$a^3F'_2-f^3G'_3$	412
8	2424.26	0	10	....	41237.17	$a^3F'_4-h^3F_4$	413
8	2421.31	0	10	....	41287.44	$a^3F'_3-h^3F_3$	413
8	2418.37	−1	10	....	41337.60	$a^3F'_2-h^3F_2$	413
6	2411.58	0	(1)	....	41454.04	$a^3F'_3-h^3F_4$	413
8	2411.37	0	2	....	41457.61	$a^3F'_2-h^3F_3$	413
8	2384.52	0	4	....	41924.36	$a^3F'_4-j^3D'_3$	415
6	2380.80	0	(2)	....	41989.81	$a^3F'_4-k^3D'_3$	416
8	2378.15	+1	3	....	42036.65	$a^3F'_3-j^3D'_2$	415
6	2374.59	0	(1)	....	42099.59	$a^3F'_3-k^3D'_2$	416
6	2372.23	−2	(1)	....	42141.47	$a^3F'_3-j^3D'_3$	415
6	2371.95	0	(2)	....	42146.43	$a^3F'_2-j^3D'_1$	415
6	2369.29	0	(1)	....	42193.92	$a^3F'_2-k^3D'_1$	416
6*	2368.57	$\left\{\begin{matrix}+1\\-1\end{matrix}\right\}$	(1)	....	42206.74	$\left\{\begin{matrix}a^3F'_2-j^3D'_2\\a^3F'_3-k^3D'_3\end{matrix}\right.$	415 416
12	2365.04	0	(1)	....	42269.73	$a^3F'_2-k^3D'_2$	416
6	2314.27	−4	(2)	....	43196.92	$a^3F'_4-i^3F_3$	417
6	2308.88	−2	(2)	....	43297.73	$a^3F'_3-i^3F_2$	417
8	2305.69	0	12	....	43357.59	$a^3F'_4-i^3F_4$	417
8	2302.75	0	10	....	43412.96	$a^3F'_3-i^3F_3$	417
8	2299.86	0	10	....	43467.49	$a^3F'_2-i^3F_2$	417
8	2294.24	+2	3	....	43573.97	$a^3F'_3-i^3F_4$	417
8	2293.78	+2	3	....	43582.71	$a^3F'_2-i^3F_3$	417
8	2280.00	+1	12	....	43846.09	$a^3F'_4-l^3D'_3$	418

TABLE II—*Continued*

Source	Obs. λ (I.A.)	Δλ O−C	Int.	Temp. Class	ν	Designation	Multiplet
8	2276.75	+ 3	10	....	43908.67	$a^3F'_3-l^3D'_2$	418
8	2273.33	+ 5	8	....	43974.73	$a^3F'_2-l^3D'_1$	418
6	2272.63	+ 2	(4)	....	43988.33	$a^3F'_4-g^3G'_5$	419
6	2272.45	+ 2	(1)	....	43991.82	$a^3F'_3-g^3G'_4$	419
6	2268.78	0	(2)	....	44062.96	$a^3F'_3-l^3D'_3$	418
6	2267.98	+ 5	(2)	....	44078.50	$a^3F'_2-l^3D'_2$	418
8	2264.07	......	5	....	44154.56	....	......
6	2260.08	+ 3	(1−)	....	44232.52	$a^3F'_2-l^3D'_3$	418
8	2246.14	......	4	....	44506.98	....	......
6	2244.69	+ 2	(4)	....	44535.69	$a^3F'_4-j^3F_3$?	420
6*	2238.73	0 + 5	(4)	....	44654.22	$a^3F'_4-j^3F_4$ $a^3F'_3-j^3F_2$	420 420
6	2238.20	......	(3)	....	44664.79	....	......
6	2233.79	0	(4)	....	44752.94	$a^3F'_3-j^3F_3$	420
6	2230.48	+ 1	(4)	....	44819.33	$a^3F'_4-m^3D'_3$	421
6	2230.18	− 1	(4)	....	44825.36	$a^3F'_2-j^3F_2$	420
6	2229.67	......	(4)	....	44835.61	....	......
6	2227.91	− 2	(1+)	....	44871.22	$a^3F'_3-j^3F_4$	420
6	2226.77	− 2	(3)	....	44894.18	$a^3F'_3-m^3D'_2$	421
6	2225.11	......	(4)	....	44927.67	....	......
6	2223.19	0	(4)	....	44966.45	$a^3F'_2-m^3D'_1$	421
6	2221.48	......	(4)	....	45001.07	....	......
6	2219.75	0	(3)	....	45036.12	$a^3F'_3-m^3D'_3$	421
6	2218.38	0	(3)	....	45063.92	$a^3F'_2-m^3D'_2$	421
6	2211.36	− 3	(1−)	....	45206.94	$a^3F'_2-m^3D'_3$	421
6	2143.52	......	(3)	....	46637.44	....	......
6	2126.05	......	(3)	....	47020.76	....	......
6	2123.50	......	(4)	....	47077.21	....	......
6	2121.90	......	(3)	....	47112.70	....	......
6	2117.01	......	(3)	....	47221.49	....	......

* Blend.

† Lines from sun-spot spectrum.

‡ Error in λ corrected.

§ Blend with enhanced line.

|| May be *Fe* 3705.57.

¶ Measured in low-temperature furnace. "λ 3361.30 measured in high-temperature furnace, a difficult blend" (King).

** Apparently coincides exactly with *Ti*+line.

†† Blend with enhanced line. Enhanced line to violet.

‡‡ Not *Fe* 3125.66; unresolved, but double.

§§ Blend with *Fe* 2981.45 but too strong in furnace for the latter.

¶¶ Too strong; may be a blend.

TABLE II*a*

LINES MASKING *Ti* I LINES

Obs. λ (I.A.)	Element	ν	Designation	Multiplet
6905.94	*Cu*	14476.23	$a^3G'_4-b^3G_3$	37
6743.14	*Ti*	14825.80	$bD-cD'$	....
6292.82	*V*	15886.78	$b^3F'_2-c^3D'_2$	52
5194.04	*Ti*	19247.49	$a^3P'_1-a^5P_2$	116
4848.46	*Ti*	20619.36	$b^3P'_2-g^3D'_3$	142
4667.59	*Ti*	21418.36	$a^3P'_0-c^5D'_1$	162
4535.92	*Ti*	22040.10	$b^3F'_3-d^3F_3$	168
4518.03	*Ti*	22127.36	$a^3H'_6-aI'$	180
4488.32	*Ti*+	22273.84	$a^5F_2-c^5F'_2$	176
4427.10	*Ti*	22581.83	$a^3P'_2-e^3D'_1$	190
4300.55	*Ti*	23246.32	$a^3D_2-i^3D'_2$	208
4290.93	*Ti*	23298.44	$bG-eF$	....
4186.12	*Ti*	23881.76	$b^3P'_1-f^3P_1$	220
4064.22	*Ti*	24598.05	$a^5D'_1-d^5F'_2$	234
4060.27	*Ti*	24621.97	$a^5D'_2-d^5F'_3$	234
4025.13	*Ti*+	24836.93	$a^3D_1-j^3D'_2$	236
3475.45	*Fe*	28765.00	$aG-dG'$	....
3375.69	*Ti*	29615.09	$b^3F'_3-f^3G'_4$	321
3117.89	*Ti*	32063.70	$a^5F_3-e^5D_3$	360
3017.63	*Fe*	33128.96	$aD-e^3P_1$	374
2983.57	*Fe*	33507.15	$a^3P'_0-f^3P_1$	377
2834.75	*Ti*	35266.13	$a^3F'_4-d^5D'_3$	393
2809.15	*Ti*	35587.50	$a^3F'_3-d^5D'_4$	393
2733.58	*Fe*	36571.26	$a^3P'_1-m^3D'_2$	399

NOTES ON TABLE II

1. Bureau of Standards, *Scientific Papers of the Bureau of Standards*, **16**, 54 (No. 372), 1920.
2. Crew, *Astrophysical Journal*, **60**, 108, 1924.
3. Evans, in Kayser, *Handbuch der Spectroscopie*, **6**, 655, 1912.
4. Exner and Haschek, *ibid.*
5. Hasselberg, *ibid.*
6. Kiess, unpublished material.
7. Kilby, *Astrophysical Journal*, **30**, 243, 1909.
8. King, *Mt. Wilson Contr.*, No. 76; *Astrophysical Journal*, **39**, 139, 1914. Also *Mt. Wilson Contr.*, No. 274; *Astrophysical Journal*, **59**, 155, 1924, and unpublished material.
9. Lohse, in Kayser, *Handbuch der Spectroscopie*, **6**, 655, 1912.
10. Miss Moore, unpublished material.
11. Rowland, in Kayser, *Handbuch der Spectroscopie*, **6**, 655, 1912.
12. Russell, unpublished material.

The energy levels and relations of the various terms are shown graphically in Figures 1–3. There are far too many terms to show on a single Bohr-Grotrian diagram, and so the singlet, triplet, and quintet terms are plotted separately. Terms of the same sort, e.g., ^3F or $^3F'$, are plotted on the same vertical line and distinguished by the letters used to designate them in the tables. Those triplet terms which combine with higher singlet terms are, however, plotted on the singlet diagram (Fig. 1), the intercombinations being indicated by dotted lines; and similarly in the other cases. In a few cases, where terms lie close together, the plotted points have been slightly shifted to avoid confusion. These diagrams illustrate in an expressive fashion the great complexity of the spectrum.

4. TEMPERATURE CLASSIFICATION AND ZEEMAN EFFECT

The relation between the temperature classification of the lines and their level of origin is, as usual, very close. It is well known[1] that the appearance of emission lines in the furnace is limited by its temperature—the limit extending steadily toward the ultra-violet as this is increased—while absorption lines may be found, even at low temperatures, as far as the observations can be made.

King's data reproduced in Table II were derived from emission spectra. It is therefore immediately comprehensible why the lines originating (in absorption) in the lowest level a^3F', which are of class I or I A in the visible region, gradually become of class II in the ultra-violet, while the the fainter lines there are of class III, or beyond λ 2200 even of class IV. The lines originating in a^5F', which lies higher by 0.82 volts, are of class II in the visible and class III or IV A in the ultra-violet, and, as Grotrian[2] has found, are much more feebly absorbed by the vapor of the metal at 2000°C.

For the next levels, a^1D (0.90 volts) and a^3P' (1.05), much the same is the case, while the lines coming from b^3F' (1.44 volts) and a^1G (1.50) are divided between classes II and III, even in the visible. There are very few lines of class II belonging to a^5P' (1.73) or a^3G (1.87); the higher levels give, at best, lines of class III; and the highest

---

[1] King, *Mt. Wilson Contr.*, Nos. 150 and 247; *Astrophysical Journal*, **48**, 13, 1918; **56**, 320, 1922.

[2] *Zeitschrift für Physik*, **25**, 342, 1924.

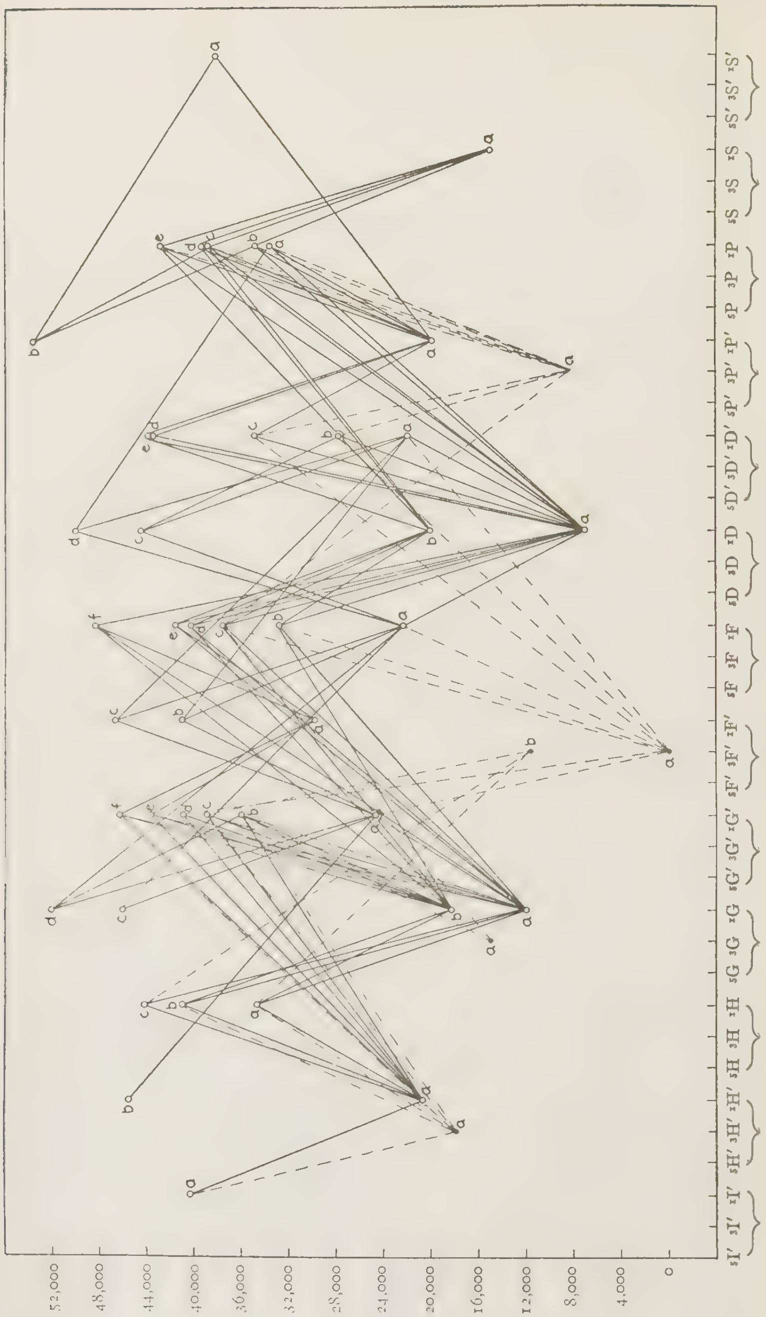

FIG. 1.—*Ti* Singlet combinations

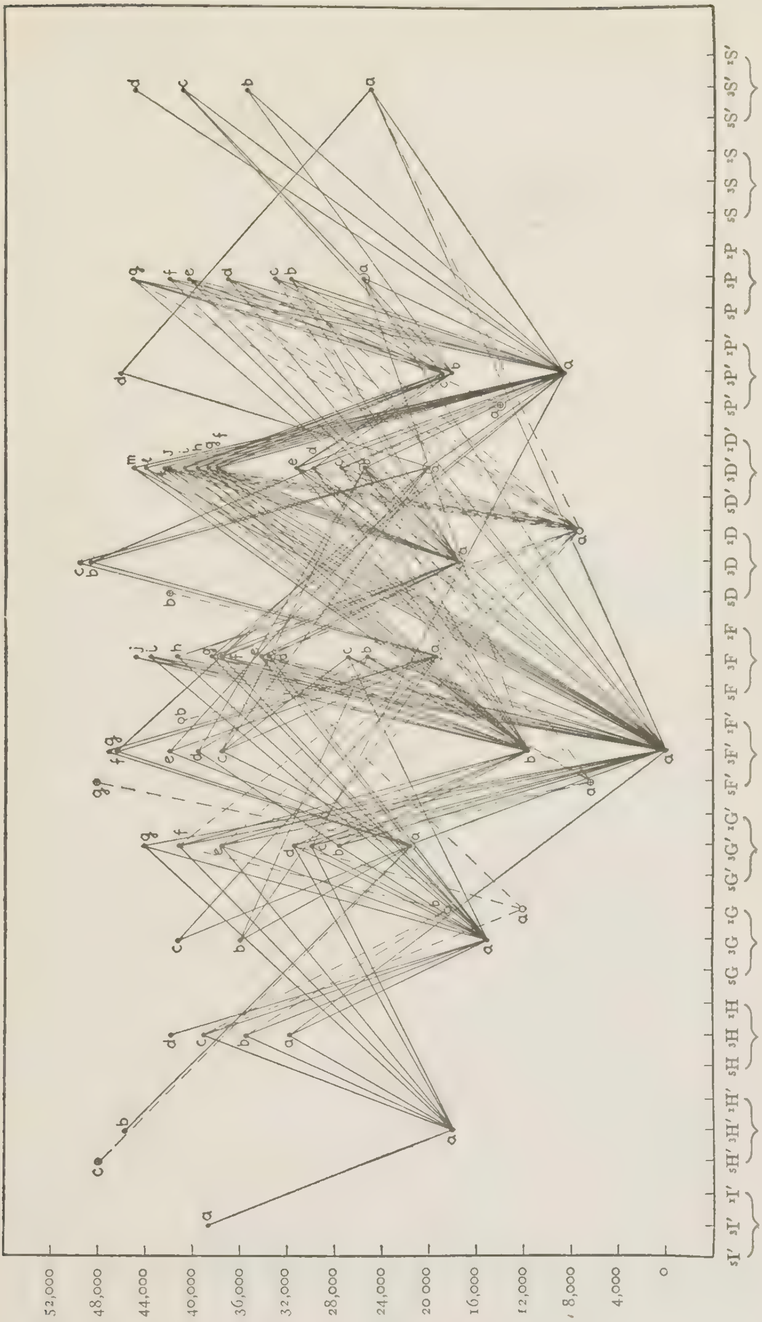

FIG. 2.—*Ti* Triplet combinations

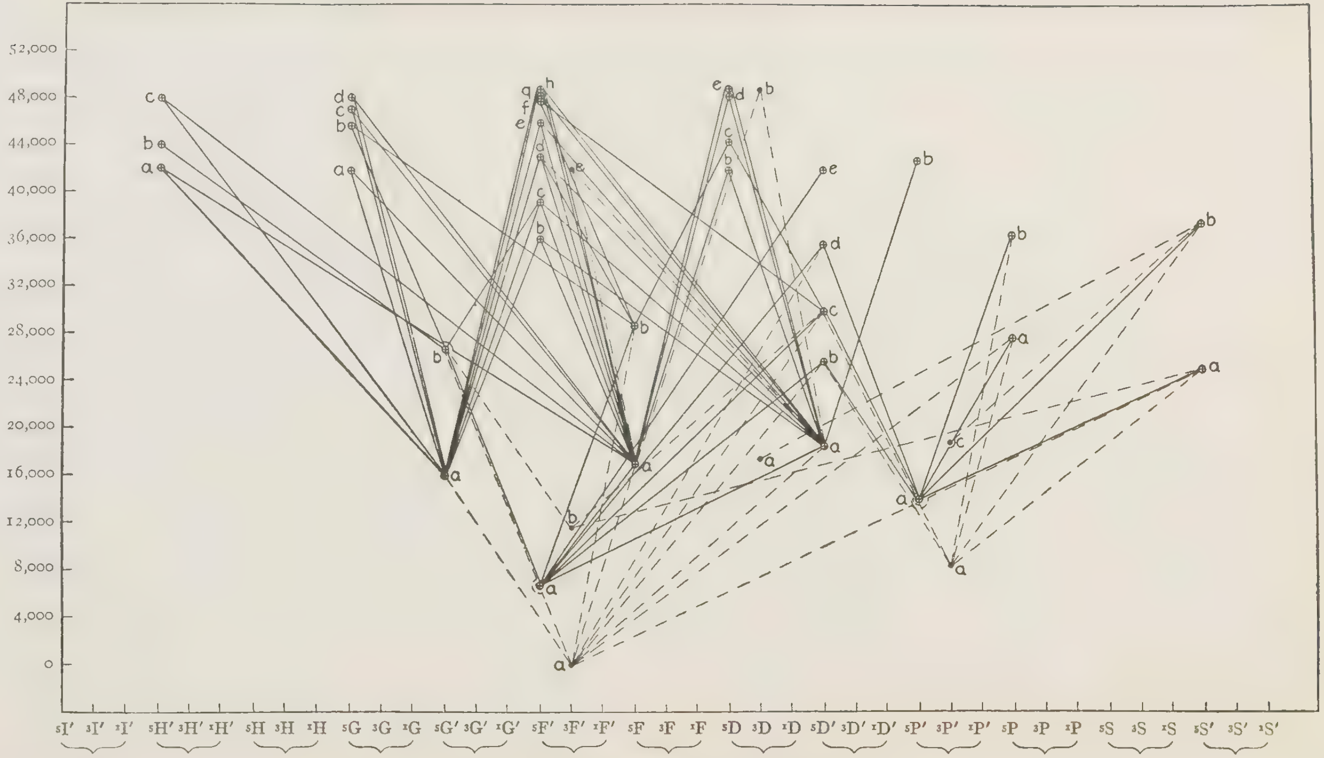

FIG. 3.—*Ti* Quintet combinations

from which transitions upward have been detected, such as b^3D' (3.16) and b^5G' (3.29), give lines of class IV exclusively. The behavior of the titanium lines in sun-spots closely parallels the temperature classification. Those frequenting low atomic levels are greatly strengthened in the spots (especially the weaker lines). This effect diminishes for the lines arising from higher terms, but even those from the highest levels are decidedly intensified.

Extensive measures of the Zeeman effect have been made by King[1] and by Babcock.[2] A comparison of the observed patterns with those calculated by Landé's theory is given in Table III, which is arranged like the similar table for *Ti* II. All combinations between levels of any given sorts, e.g., $^3P_2$ and $^3D_3$, are listed together, no matter which term happens to be the lower, or whether they are primed or unprimed, since in any of these cases they should show the same Zeeman pattern. Babcock's observed data are given to three decimal places; King's, to two. The "blends," given in the last two columns to represent the complex patterns, are derived on the assumption that the center of gravity of the unresolved mass is one-quarter of the way from the strongest component toward the weakest. This rule accords well with the theoretical intensities and with the observations for the majority of the lines. For faint lines, however, or for those in which the pattern is near the limit of resolution, the observed blend is likely to be nearer to the stronger component than the rule would indicate. Such cases are often observed.

---

[1] *Carnegie Institution of Washington Publications*, No. 153, 1912.

[2] Unpublished material.

TABLE III

OBSERVED AND COMPUTED ZEEMAN EFFECTS IN *Ti* I

TERMS	λ	OBSERVED		THEORY*		BLEND	
		p	*n*	*p*	*n*	*p*	*n*
$^1P-^1P'$	5206	0	1.06	0	1.00		
	4372	0	1.00				
$^1P-^1D$	3786	0	0.98	0	1.00		
$^1D-^1D'$	6743	0	1.02	0	1.00		
	4840	0	1.004				
	4237	0	0.98				
$^1D-^1F$	6599	0	1.00	0	1.00		
	5259	0	0.95				
	4975	0	1.054				
	3904	0	0.97				
$^1F-^1F'$	5351	0	1.026	0	1.00		
$^1F-^1G$	6098	0	0.991	0	1.00		
	4820	0	1.016				
$^1G-^1G'$	5644	0	1.021	0	1.00		
	4836	0	0.96				
	4424	0	.95				
	4186	0	0.99				
	3724	0	1.07				
$^1G-^1H$	6091	0	1.067	0	1.00		
	5503	0	1.031				
	4427	0	1.000				
	4393	0	1.03				
	4369	0	0.98				
	3926	0	0.98				
$^1H-^1H'$	4938	0	1.061	0	1.00		
	4278	0	1.02				
$^1H-^1I$	5120	0	1.024	0	1.00		
$^3F_3-^1D_2$	4562	0	1.25	**0.00** .08 .17	0.92 .... 1.17 **1.25**	0	1.17
$^3F_4-^1G_4$	4112	0.86	$1.09W_2$	.25 .50 0.75 **1.00**	0.25 .... **1.00** **1.25** 2.00	0.81	1.12W

PLATE V

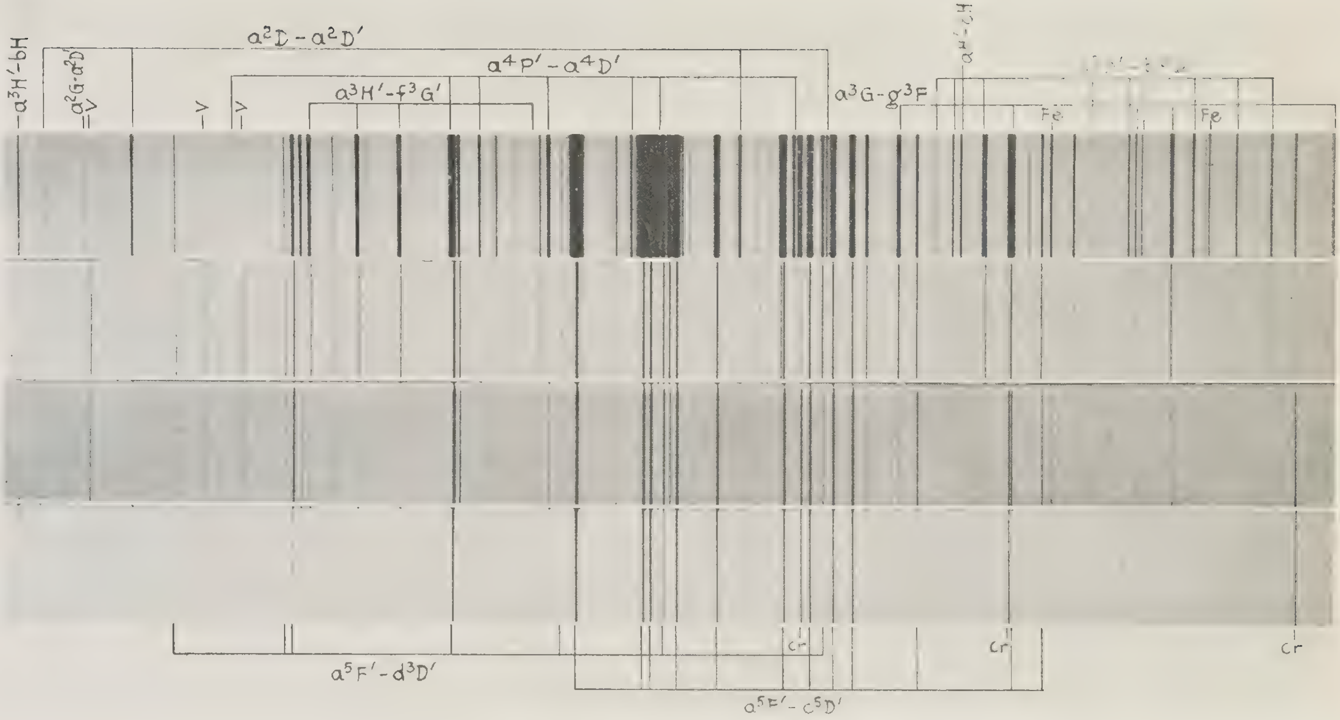

Arc and Furnace Spectrum of Ti λ 4347 to λ 4251

Multiplets of the arc and spark spectra are indicated, including singlets, doublets, triplets, quartets, quintets, and various inter-system combinations.

TABLE III—*Continued*

TERMS	λ	OBSERVED		THEORY*		BLEND	
		p	*n*	*p*	*n*	*p*	*n*
$^3G_3-{}^1F_3$.......	4440	0.52	0.84w_1	0.25	0.25	0.62	0.87w
				.50	.50		
				.75	0.75		
					1.00		
					1.25		
					1.50		
$^3H_4-{}^1G_4$......	5565	.561	.920	.20	0.20	0.65	0.90
	4778	0.491	0.943	.40	....		
				.60	0.80		
				.80	1.00		
					....		
					1.60		
$^3H_4-{}^1H'_5$......	5999	w_2	1.467w_1	.00	0.20	0w	1.40w
	4346	w_2	1.47w_1	.20	....		
				....	1.60		
				.80	1.80		
$^3S_1-{}^3P_0$.......	6064	0	1.954	.00	2.00		
$^3S_1-{}^3P_1$.......	6085	0.501	1.496	.50	1.50		
			1.985		2.00		
$^3S_1-{}^3P_2$.......	6126	0	0.998	.00	1.00	0w	1.25w
		0.497	1.490	0.50	1.50		
	3725	w_1	1.15		2.00		
$^3P_0-{}^3P'_1$.......	4065	0	1.47	0	1.50		
	4055	0	1.47				
$^3P_1-{}^3P'_1$.......	4064	0	1.47	0	1.50		
$^3P_1-{}^3P'_2$.......	5903†	0	1.491	0	1.50		
	5880†	0	1.425				
	4323	0	1.52				
	4082	0	1.47				
	4060	0	1.47				
$^3P_2-{}^3P'_2$.......	5918	0	1.489	0	1.50		
	5429	0	1.542				
	4078	0	1.46				
$^3P_0-{}^3D_1$......	5922	0	0.492	0.00	0.50		
	5069	0	.56				
	4796	0	.52w_1				
	4710	0	0.506				
$^3P_1-{}^3D_1$.......	5941	0.990	0.489	1.00	0.50		
			1.527		1.50		
	4797	1.03	0.58				
			1.58				
	4722	1.07	0.62				
			1.53				
	4405	0.99	w_2				

TABLE III—*Continued*

TERMS	λ	OBSERVED		THEORY*		BLEND	
		p	n	p	n	p	n
$^3P_1-{}^3D_2$	5899	0	1.127	0.00	0.83	0w	1.00w
	5062	w_1	0.99	.33	1.17		
	4792	w_3	0.918w_2		1.50		
	4698	w_2	1.02w_2				
$^3P_2-{}^3D_2$	5937	0.39	1.46w_2	.33	0.83	0.59w	1.33w
	4723	0.62	1.24w_2	.67	**1.17**		
					1.50		
					1.83		
$^3P_2-{}^3D_3$	5866	0	1.169w_2	.00	**1.00**	0w	1.17w
	5295	w_1	1.23w_1	.17	1.17		
	5052	w_1	1.08	.33	1.34		
	4805	w_1	1.08		1.50		
	4691	w_1	1.23		1.67		
	4422		1.18				
$^3P_2-{}^3F_2$	3921†	–?	0.00	0.83	−0.17	0.93‡	−0.27
			0.78	**1.67**	**0.67**	**1.87**	**0.67**
			1.68		**1.50**		**1.60**
			2.64		2.33		2.53
$^3P_2-{}^3F_3$	3947†	w_2	0.39w_2	**0.00**	**0.25**	**0.00‡**	**0.05**
				.42	0.67	0.52	0.56
				.83	1.08	1.04	1.08
					1.50		1.60
					1.92		2.12
$^3D_1-{}^3D_1'$	4880	0	.51	.00	0.50		
	4696	0	.54				
	4311	w_1	0.49				
$^3D_2-{}^3D_2'$	4864	0	1.14	.00	1.17		
$^3D_3-{}^3D_3'$	4848	0	1.35	.00	1.33		
	4710	0	1.333				
	4035	0	1.33				
$^3D_1-{}^3F_2$	6318	0	0.734	**.00**	0.50	0	0.75
	5514	0	.73	.17	.67		
	5087	0	.78		**.83**		
	4928	0	.732				
	4171	0	.74				
	3948	0	.73				
$^3D_2-{}^3F_2$	4997	1.02	?	0.50	.17	0.87w	.92w
	3929†	1.16	.00	1.00	**0.67**	0.68§	−0.02
			0.75		**1.17**	**1.37**	**0.67**
			1.46		1.67		**1.35**
			2.10				2.03

TABLE III—*Continued*

TERMS	λ	OBSERVED		THEORY*		BLEND	
		p	*n*	*p*	*n*	*p*	*n*
$^3D_2-{}^3F_3$.......	6336	0	0.936	**0.00**	**0.92**	0	1.00w
	5514	0	0.94	.08	1.00		
	5113	0	1.01	.17	....		
	5039	0	0.993		1.25		
	4919	0	.988			**0.00§**	**0.55**
	4733	0	.975			.27	0.81
	4159	0	.93			.54	....
	3956†	0	0.90				1.62
$^3D_3-{}^3F_3$.......	5009	0.68	?	.25	0.58	0.62w	1.21w
	3924	0.65	$1.16w_2$	.50	....		
				.75	**1.08**		
					1.33		
					....		
					1.83		
$^3D_3-{}^3F_4$.......	6366	0	1.016	**.00**	**1.00**	0	1.12w
	5648	0	1.160	.08	1.08		
	5512	0	1.15	.17	....		
	5145	0	1.14	.25	1.50		
	5064	0	1.119				
	4921	0	1.088				
	4731	0	1.094				
	4150	0	1.09				
	3958	0	1.12				
$^3F_2-{}^3F'_2$.......	6546	0	0.673	.00	0.67		
	5488	0	.676				
	5173	0	.667				
	4518	0	.66				
	4453	0	.649				
	3981†	0	.73				
	3729	0	0.63				
$^3F_2-{}^3F'_3$.......	6508	w_3	$1.91w_3$	**.00**	.25	0w	1.50 w
	5219	w_2	1.20	.42	0.67		
			1.48	.83	1.08		
			1.83		1.50		
	5147	w_3	$1.86w_2$		**1.92**		
	4474	w_3	$1.56w_1$				
	4008	w_2	$1.32w_2$				
	3962†	w_2	$1.80w_2$				
	3753	w_2	1.63				
$^3F_3-{}^3F'_3$.......	6554	0	1.046	0.00	1.08		
	5481	0	1.121				
	5192	0	1.080				
	4455	0	1.106				
	3989	0	1.06				
	3741	0	1.09				

TABLE III—*Continued*

Terms	λ	Observed		Theory*		Blend	
		p	*n*	*p*	*n*	*p*	*n*
$^3F_3-^3F'_4$.......	6497	0	1.76	0.00	0.75	0w	1.50w
	5252	w_2	1.52w_2	.17	0.92		
	5152	w_1	1.55w_1	.33	....		
	4482	w_2	1.52w_1	.50	1.58		
	4430	w_2	1.46w_1		1.75		
	4024	w_1	1.49w_1				
	3964	w_1	1.40w_1				
	3771	w_1	1.54				
	3722†	w_1	0.64				
$^3F_4-^3F'_4$.......	6556	0	1.232	.00	1.25		
	5477	0	1.270				
	5210	0	1.250				
	4559	0	1.32				
	4457	0	1.242				
	3998†	0	1.06				
	3752	0	1.21				
$^3F_2-^3G_3$.......	6261	0	0.833	.00	0.58	0	0.83
	6221	0	.801	.08	.67		
	5390	0	.794	.17	.75		
	5297	0	.843		.83		
	5038	0	.833		.92		
	4656	0	.83				
	4433	0	.830				
	4282	0	.82				
$^3F_3-^3G_3$.......	6303	0.86	.87w_3	.33	.08	0.83w	0.91w
	5066	?	.97	0.67	.42		
				1.00	0.75		
					1.08		
					1.42		
					1.75		
$^3F_3-^3G_4$.......	6258	0	.987	0.00	0.95	0	1.00
	6220	0	0.987	.03	0.98		
	5397	0	1.010	.07	....		
	5283	0	1.000	.10	1.12		
	5036	0	1.004		1.15		
	4667	0	0.98				
	4426	0	1.004				
	4274	0	0.97				
$^3F_4-^3G_4$.......	6312	0.658	1.272	.20	0.45	0.65w	1.15w
	5071	0.66	1.12w_2	.40	....		
	4404‖	0	1.00	.60	1.05		
				0.80	1.25		
					....		
					1.85		

TABLE III—*Continued*

Terms	λ	Observed		Theory*		Blend	
		p	*n*	*p*	*n*	*p*	*n*
$^3F_4-{}^3G_5$......	6258	0	1.098	0.00	1.00	0	1.10
	6215	0	1.057	.05	1.05		
	5474	0	1.061	.10	....		
	5409	0	1.107	.15	1.35		
	5265	0	1.067	.20	1.40		
	5035	0	1.101				
	4681	0	1.12				
	4417	0	1.087				
	4263	0	1.12				
$^3G_3-{}^3G'_3$......	6146	0	0.750	.00	0.75		
	4453¶	0.175	0.760				
$^3G_3-{}^3G'_4$......	4463¶	W_2	$1.57W_1$	.00	0.15	0W	1.50W
	4441	W_2	$1.28W_1$	.30	....		
				.60	1.65		
				.90	1.95		
					....		
$^3G_4-{}^3G'_4$......	6121	0	1.02	.00	1.05		
	4450	0	1.057				
$^3G_4-{}^3G'_5$......	4463¶	W_1	1.57	.00	0.60	0W	1.50W
	4436	W_2	$1.45W_1$	.15	....		
				....	1.65		
				.60	1.80		
					....		
$^3G_5-{}^3G'_5$......	6092	0	1.185	.00	1.20		
	4449	0	1.212				
$^3G_3-{}^3H_4$......	5978	0	0.874	.00	0.65	0	0.87
	4913	0	0.879	.05	....		
	4321	0	1.02	....	.90		
	4122	0	0.94	.15	.95		
$^3G_4-{}^3H_4$......	4925	0.92	?	.25	....	0.75W	0.92W
				.50	0.80		
				0.75	1.05		
				1.00	....		
$^3G_4-{}^3H_5$......	5965	0	1.000	0.00	0.97	0	1.00
	4899	0	1.007	.02	0.98		
	4325	0	1.002	....	1.00		
	4123	0	0.95	.07	....		
					1.10		
$^3G_5-{}^3H_5$......	4915	0.59	$1.05W_2$	.17	....	0.67W	1.12W
				....	1.03		
				.67	1.20		
				0.83	....		

TABLE III—*Continued*

TERMS	λ	OBSERVED		THEORY*		BLEND	
		p	n	p	n	p	n
$^3G_5-{}^3H_6$......	5953	0	1.088	**0.00**	**1.00**	0.00	1.08
	4885	0	1.098	.03	1.03		
	4318	0	1.054	....	....		
	4127	0	1.05	.17	1.33		
$^3H_4-{}^3H'_4$......	5740	0	0.805	.00	0.80		
	4742	0	0.840				
$^3H_5-{}^3H'_5$......	5739	0	1.034	.00	1.03		
	4758	0	1.023				
$^3H_5-{}^3H'_6$......	4769	w_2	1.57w_2	**.00**	0.50	0w	1.50w
				.13	....		
				....	1.70		
				.67	**1.83**		
$^3H_6-{}^3H'_6$......	5715	0	1.17	.00	1.17		
	4759	0	1.181				
$^3H_4-{}^3I_5$.......	4868	0	0.821	**.00**	0.70	0	0.90
				.03	.73		
				....	....		
				.10	.93		
				.13	**.97**		
$^3H_5-{}^3I_6$.......	4870	0	1.010	**.00**	**.976**	0	1.00
				.010	0.986		
				....	....		
				.038	1.062		
				.048	1.072		
$^3H_6-{}^3I_7$.......	4856	0	1.078	**.00**	**1.00**	0	1.07
				.02	1.02		
				....	....		
				.12	1.26		
				.14	1.29		
$^3P_2-{}^5D_3$.......	4675	0	1.42	0.00	1.50		
$^3F_2-{}^5S_2$.......	3982†	2.19	**0.57**	1.33	−0.67	0.17**	−0.50
			1.83	**2.66**	**0.67**	2.33	**0.67**
			3.03		**2.00**		**1.83**
					3.33		3.00
$^3F_3-{}^5S_2$.......	4009†	?	0.33	**0.00**	**−0.75**	0.00**	**−0.42**
				0.92	0.17	0.75	0.33
				1.83	1.08	1.50	1.08
					2.00		1.83
					2.92		2.58

** $g=1.83$

TABLE III—*Continued*

TERMS	λ	OBSERVED		THEORY*		BLEND	
		p	*n*	*p*	*n*	*p*	*n*
$^3F_4-^5D_4$	3914	0.83	1.41w$_2$	0.25 .50 0.75 **1.00**	0.50 .... **1.25** **1.50** 2.25	0.81w	1.38w
$^3F_4-^5D_3$	5490	w$_3$	0.80w$_2$	**0.00** .25 .50 .75	**0.50** 0.75 .... 2.00	w	0.87w
$^5F_3-^3D_2$	4326	0	1.314	**.00** .08 .17	1.08 .... 1.33 **1.42**	0	1.33
$^5F_3-^3D_3$	4299¶	w$_1$	1.18	.08 .17 **.25**	1.08 .... **1.25** **1.33** 1.50	w	1.29w
$^5F_4-^3D_3$	4314	0	1.372	**.00** .02 .... .05	1.30 .... 1.38 **1.40**	0	1.37
$^5F_2-^3F'_3$	4926	0	1.27	**.00** .08 .17	0.92 .... 1.17 **1.25**	0	1.17
$^5F_4-^3G_5$	4291¶	0	0.77	**.00** .15 .60	**0.60** 0.75 1.80	0w	0.90w
$^5F_5-^3G_5$	4781	0.84w$_2$	w$_3$	.20 .40 .60 0.80 **1.00**	0.40 .... **1.20** **1.40** 2.20	0.80w	1.30w
$^5S_2-^5P_1$	4276	w$_2$	1.49w$_1$	**0.00** .50	**1.50** 2.00 2.50	w	1.75w
$^5S_2-^5P_2$	4284	w$_1$	1.89	.16 **0.33**	1.67 **1.83** **2.00** 2.17	w	1.91w

TABLE III—*Continued*

Terms	λ	Observed		Theory*		Blend	
		p	*n*	*p*	*n*	*p*	*n*
$^5S_2-{}^5P_3$	4299¶	W_2	1.43	**0.00** .33 .67	**1.00** 1.33 1.67 2.00 2.33		
$^5P_1-{}^5P'_1$	4479	o	2.53	.00	2.50		
$^5P_1-{}^5P'_2$	4489	**0.00** .653	**1.150** 1.82 2.61	**.00** .67	**1.17** 1.83 2.50		
	4471	**.00** 0.654	**1.151** 1.825 2.54				
$^5P_2-{}^5P'_2$	4480	o	1.87	.00	1.83		
$^5P_2-{}^5P'_3$	4496	o	1.50	**.00** .17 0.33	**1.33** 1.50 .... 2.00	ow	1.50w
	4465	W_1	$1.48W_1$				
$^5P_3-{}^5P'_3$	4481	o	1.665	o	1.67		
$^5P_1-{}^5D_0$	4645	o	2.50	o	2.50		
$^5P_1-{}^5D_1$	4639¶	1.01	1.52 2.46	1.00	1.50 2.50		
$^5P_1-{}^5D_2$	4629	**0.00** 1.03	**0.50** 1.53 2.50	**0.00** 1.00	**0.50** 1.50 2.50		
$^5P_2-{}^5D_1$	4650	W_2	$2.08W_1$	**0.00** .33	1.50 1.83 **2.16**	w	2.00w
$^5P_2-{}^5D_2$	4639¶	0.64	$1.69W_3$	.33 .67	1.17 **1.50** **1.83** 2.16	0.59w	1.67w
$^5P_2-{}^5D_3$	4623	W_3	$1.09W_2$	**.00** .33 .67	**0.83** 1.17 .... 2.16	w	1.17w
$^5P_3-{}^5D_3$	4639¶	?	1.56	.17 .33 **0.50**	1.17 .... **1.50** **1.67** 2.00	0.42w	1.58w

TABLE III—*Continued*

TERMS	λ	OBSERVED		THEORY*		BLEND	
		p	*n*	*p*	*n*	*p*	*n*
$^5P_3-{}^5D_4$	4617	w_2	1.16w_1	0.00	1.00	w	1.25 w
	4137	0	1.31	.17	1.17		
				.33	....		
				0.50	2.00		
$^5D_3-{}^5D'_3$	4261†	w_1	1.09w_1	0	1.50		
$^5D_4-{}^5D'_4$	4256†	0	1.34w_1	0	1.50		
$^5D_0-{}^5F_1$	5713	0	0	0.00	0.00		
	4295	0	0				
$^5D_1-{}^5F_1$	5720	1.65	0.00	1.50	0.00		
			1.77		1.50		
	4290	1.48	0.00				
			1.47				
$^5D_1-{}^5F_2$	5702	w_2	0.68w_3	0.00	0.50	w	0.75w
	4298	0.00	.48	.50	1.00		
		.48	.97		1.50		
$^5D_2-{}^5F_1$	4281	0.00	0.00	0.00	0.00		
		1.50	1.48	1.50	1.50		
			3.00		3.00		
$^5D_2-{}^5F_2$	5716	0.94	1.26w_3	0.50	0.50	0.87w	1.25w
	4289	.47	0.48	1.00	1.00		
		0.96	1.02		1.50		
			1.48		2.00		
			1.96				
$^5D_2-{}^5F_3$	5689	w_2	0.98w_2	0.00	0.75	0.0w	1.00w
	4300	w_2	0.88w_1	.25	1.00		
				.50	....		
					1.75		
$^5D_3-{}^5F_3$	5711	0.68	1.49	.25	0.75	0.62w	1.37w
	4286	0.55	1.34w_2	.50	....		
				.75	1.25		
					1.50		
					....		
					2.00		
$^5D_3-{}^5F_4$	5675	w_1	1.08w_1	.00	0.90	0w	1.12w
	4301	w_1	1.182w_1	.15	1.05		
				....	....		
				.45	1.80		
$^5D_4-{}^5F_3$	4272	w_3	1.22w_2	.00	0.75	0w	1.88?
				.25	....		
				....	2.00		
				0.75	2.25		

TABLE III—*Continued*

Terms	λ	Observed		Theory*		Blend	
		p	*n*	*p*	*n*	*p*	*n*
$^5D_4-^5F_4$	5708	0.70	1.59w_2	0.15	0.90	0.49w	1.42w
	4287	0.49	1.40w_2	....	....		
				.45	**1.35**		
				.60	**1.50**		
					....		
					1.95		
$^5D_4-^5F_5$	5662	w_1	1.30w_1	**.00**	**1.00**	0w	1.20w
	4305	w_2	1.21w_1	.10	1.10		
				....	....		
				.40	1.80		
$^5F_1-^5F'_1$	5222	0	0.00	.00	0.00		
	4536	0	.00				
$^5F_1-^5F'_2$	5238†	w_1	.85w_1	**0.00**	0.00		
	4544	**0.00**	0.00	1.00	1.00		
		1.00	1.00		**2.00**		
			1.98				
	4527	**0.00**	0.00				
		1.002	0.992				
			2.000				
$^5F_2-^5F'_2$	5223†	0	1.097	0.00	1.00		
	4535	0	0.982				
$^5F_2-^5F'_3$	5247†	w_2	1.72w_2	**.00**	0.75	0w	1.50w
	5201†	w_1	0.86w_1	.25	....		
	4548	w_2	1.66w_1	.50	1.50		
	4522	w_2	1.51w_1		**1.75**		
$^5F_3-^5F'_3$	5224¶	0	1.265	.00	1.25		
	4535	0	1.241				
$^5F_3-^5F'_4$	5255	w_1	1.44w_1	**.00**	1.05	0w	1.50w
	4552	w_1	1.51	.10	....		
	4518	w_1	1.50	....	1.55		
				.30	**1.65**		
$^5F_4-^5F'_4$	5224¶	0	1.375	.00	1.35		
	4534	0	1.326				
$^5F_4-^5F'_5$	5263	0	1.55w_1	**.00**	1.20	0	1.50
	4555	0	1.50	.05	....		
	4512	0	1.501	....	1.55		
				.20	**1.60**		
$^5F_5-^5F'_5$	5224¶	0	1.425	.00	1.40		
	4533	0	1.376				
$^5F_1-^5G_2$	5014¶	0.00	.53	**.00**	0.00	0w	0.50w
	4978	w_1	0.59w_1	0.33	.33		
					0.67		

TABLE III—*Continued*

TERMS	λ	OBSERVED		THEORY*		BLEND	
		p	*n*	*p*	*n*	*p*	*n*
$^5F_2-{}^5G_2$.......	5024	0.65	**0.341**	0.67	−0.33		
		1.348	1.050	**1.33**	**0.33**		
			1.741		**1.00**		
					1.67		
$^5F_2-{}^5G_3$.......	5007	0.00	0.838	**0.00**	**0.75**	0	0.83
	4989	.00	0.836	.08	0.83		
				.17	....		
					1.08		
$^5F_3-{}^5G_3$.......	5022	$0.90w_1$	$1.13w_3$	.33	0.25	0.83w	1.08w
				0.67	....		
				1.00	**0.92**		
					1.25		
					....		
					1.92		
$^5F_3-{}^5G_4$.......	5001	w_1	0.99	**0.00**	**0.85**	0	1.01w
	4999	0	1.01	.10	0.95		
				....	....		
				.30	1.45		
$^5F_4-{}^5G_4$.......	5020	0.711	$1.202w_3$	.20	0.55	0.65w	1.25w
				....	....		
				.60	**1.15**		
				.80	**1.35**		
					....		
					1.95		
$^5F_4-{}^5G_5$.......	5013	0	1.072	**.00**	**0.93**	0	1.10w
	4991	0	1.151	.08	1.02		
	4026†	0	0.83	....	....		
				.33	1.60		
$^5F_5-{}^5G_5$.......	5016	0.559	1.308	.13	0.73	0.53	1.33
				....	....		
				.53	**1.27**		
				.67	**1.40**		
					....		
					1.93		
$^5F_5-{}^5G_6$......	5025	0	1.115	**.00**	**1.00**	0	1.17
	4981	0	1.196	.07	1.07		
	4030†	w_1	$0.92w_1$	....	....		
				.33	1.67		
$^5G_3-{}^5G'_4$......	3868	w_1	1.40	**.00**	0.45	0w	1.50w
				.23	....		
				....	1.62		
				0.70	1.85		

TABLE III—*Continued*

Terms	λ	Observed		Theory*		Blend	
		p	*n*	*p*	*n*	*p*	*n*
$^5G_4-{}^5G'_5$......	3875	0	1.32	**0.00**	0.80	0w	1.50w
				.12	....		
				....	1.62		
				.47	**1.73**		
$^5G_5-{}^5G'_6$......	3882¶	0	1.32	**.00**	1.00	0	1.50w
				.07	....		
				....	1.60		
				.33	**1.67**		
$^5G_3-{}^5H_4$......	5766	0	0.917	**.00**	**0.85**	0	0.87
	3853	w1	1.10	.02	.87		
				....	....		
				.05	.95		
$^5G_4-{}^5H_5$......	5774	0	1.028	**.00**	**.90**	0	1.00
	3858	w1	1.14	.05	0.95		
				....	....		
				.20	1.30		
$^5G_5-{}^5H_5$......	3882¶	w2	1.62w1	.17	0.43	0.67w	1.19w
				....	....		
				.67	**1.10**		
				.83	**1.27**		
					....		
					1.93		
$^5G_5-{}^5H_6$......	5785	0	1.097	**.00**	**0.95**	0	1.08
	3866	0	1.16	.05	1.01		
				....	....		
				.26	1.48		
$^5G_6-{}^5H_6$......	3895	w1	1.25	.12	0.62	0.56w	1.28w
				....	....		
				.60	**1.22**		
				.71	**1.33**		
					....		
					1.93		
$^5G_6-{}^5H_7$......	5804	0	1.157	**.00**	**1.00**	0	1.14
	3882¶	0	1.13	.05	1.05		
				....	....		
				0.29	1.57		

---

* The theoretical patterns given in the fifth and sixth columns and the computed blends in the last two columns apply equally to all of the lines having the same multiplet designation as indicated in the first column.

† g value abnormal.

‡ $g=1.60$.

§ $g=1.35$.

‖ Blend.

¶ Measures disturbed by components of neighboring line.

** $g=1.83$.

A similar comparison has been made by Dr. and Mrs. Kiess for many of the lines identified by them.

For the great majority of the more than 300 lines included in Table III, the Zeeman effect appears to be in full agreement with Landé's theory. For a few lines marked with a dagger (†) in the table the patterns appear to be abnormal. If these are set aside for the moment and means are taken for the separations of the stronger lines, the 28 singlet lines give a mean separation of 1.007 and an average deviation, without regard to sign, of ± 0.029 from the theoretical value 1.00; further, 9 lines belonging to $^3P^3P'$ groups give a mean separation of 1.485 instead of 1.500. For the leading components of the principal multiplets of the triplet system, observation and theory compare as indicated in Table IV. The components are arranged in order of decreasing inner-quantum number in each multiplet. For the skew-symmetrical groups the separations should be equal to Landé's g's, and they are so with remarkable accuracy. For the other multiplets the agreement with the values calculated from the table for blending, given above, suffices to show that, on the average, this rule gives a very good approximation to the facts. All the g's for the triplet system as far as the H terms, and many of those for the quintets, could be determined from these data alone.

TABLE IV

Mean Zeeman Separations—Triplet System

Type	PD			DD′			DF		
No.	(6)	(4)	(4)	(3)	(1)	(3)	(9)	(7)	(6)
Obs.	1.16	1.01	0.52	1.34	1.14	0.51	1.11	0.96	0.74
Comp.	1.17	1.00	0.50	1.33	1.17	0.50	1.12	1.00	0.75
Type	FF′			FG			GG′		
No.	(6)	(4)	(4)	(9)	(8)	(8)	(2)	(2)	(2)
Obs.	1.25	1.08	0.66	1.09	0.99	0.82	1.20	1.04	0.75
Comp.	1.25	1.08	0.67	1.10	1.00	0.83	1.20	1.05	0.75
Type	GH			HH′			HI		
No.	(4)	(4)	(4)	(2)	(2)	(2)	(1)	(1)	(1)
Obs.	1.08	0.99	0.93	1.18	1.03	0.82	1.08	1.01	0.82
Comp.	1.08	1.00	0.87	1.17	1.03	0.80	1.07	1.00	0.90

A few terms exhibit abnormal g values. The most notable are

a^3P_2, for which g appears to be about 1.60 instead of 1.50; b^3D_2, 1.35 instead of 1.17; and a^5S_2, 1.89 instead of 2.00. These terms have the same inner-quantum number and very nearly the same energy level, and it appears probable that they perturb one another in some way, as in the case studied in calcium by Back.[1] The first and last of these terms give abnormally strong combinations with a^3F. There is some evidence that some of the components of b^3F, which also lies at very nearly the same level, are also affected. A detailed study of these peculiarities would not be difficult, as the Zeeman patterns are very open, and might be of considerable theoretical interest.

Some of the high-lying quintet lines, such as b^5D and a^5G, appear also to have abnormal g's, and for these, too, the intensities in the multiplets are abnormal.

5. THEORETICAL INTERPRETATION OF THE OBSERVED TERMS: THE QUINTET SYSTEM

The terms which are to be expected in the spectrum of *Ti* I, according to Hund's theory,[2] are listed in Table V, together with the observed terms which are believed to represent them. They are grouped in accordance with the electronic configurations which produce them and the terms in *Ti* II to which they go as limits. These all belong to the low even set, and their assignment to the various configurations appears to be free from uncertainty. The first column gives the configuration; the second, the limit when the last-mentioned electron is removed; the third, the terms which are theoretically to be expected, and the fourth, those observed terms which have been identified with them. One term, which is predicted but not observed in *Ti* II, is put in brackets.

For a number of the higher configurations, only the terms which arise from the lowest terms of *Ti* II are listed, since none of the numerous terms corresponding to other limits have been identified. For the last entry the limit is taken to be the term in *Ti* III obtained by removing the two 4p electrons.

The reasons for assigning the various observed terms to the given configurations may now be given.

---

[1] *Zeitschrift für Physik*, **33**, 579, 1925.

[2] *Linienspektren*, pp. 184 ff.

TABLE V

Predicted and Observed Terms in *Ti* I

Configuration	Limit *Ti* II	Predicted Terms	Observed Terms
$(3d)^2\ (4s)^2$...	a^4F' a^2F'	$^3F'$	a^3F'
	b^4P' b^2P'	$^3P'$	a^3P'
	a^2S	^1S	a^1S
	a^2D	^1D	a^1D
	b^2G	^1G	a^1G
$(3d)^3\ 4s$.....	b^4F'	$^5F'$; $^3F'$	a^5F'; b^3F'
	a^4P'	$^5P'$; $^3P'$	a^5P'; c^3P'
	a^2P'	$^3P'$; $^1P'$	b^3P'; a^1P'
	b^2D	^3D; ^1D	a^3D; b^1D
	b^2F'	$^3F'$; $^1F'$	—; a^1F'
	a^2G	^3G; ^1G	a^3G; b^1G
	a^2H'	$^3H'$; $^1H'$	a^3H'; a^1H'
	(^2D)	^3D; ^1D	—; —
$(3d)^4$........	....	^5D; $^3P'$ $^3F'$	—; — —
		$^3P'$ ^3D $^3F'$ ^3G $^3H'$	— b^3D? — b^3G —
		^1S ^1D ^1G	— — —
		^1S ^1D $^1F'$ ^1G ^1I	— — — — —
$(3d)\ (4s)^2\ 4p$.	c^2D	^3P, $^3D'$ ^3F; ^1P, $^1D'$, ^1F	g^3P e^3D i^3F; — — —
$(3d)^2\ 4s\ 4p$...	a^4F'	$^5D'$ ^5F $^5G'$; $^3D'$ ^3F $^3G'$	a^5D' a^5F, a^5G'; b^3D' b^3F c^3G'
	b^4P'	$^5S'$ ^5P $^5D'$; $^3S'$ ^3P $^3D'$	a^5S' a^5P b^5D'; b^3S' c^3P f^3D'
	a^2S	^3P ^1P	—; e^1P?
	b^2P'	$^3S'$ ^3P $^3D'$; $^1S'$ ^1P $^1D'$	a^3S' a^3P c^3D'; — b^1P c^1D'
	a^2D	^3P $^3D'$ ^3F; ^1P $^1D'$ ^1F	b^3P e^3D' d^3F; a^1P, b^1D' c^1F
	a^2F'	$^3D'$ ^3F $^3G'$; $^1D'$ ^1F $^1G'$	a^3D' a^3F a^3G'; a^1D' a^1F a^1G'
	a^2G	^3F $^3G'$ ^3H; ^1F $^1G'$ ^1H	e^3F d^3G' a^3H; e^1F c^1G' c^1H
$(3d)^2\ 4s\ 5p$...	a^4F'	$^5D'$ ^5F $^5G'$; etc.	e^5D' — —;
$(3d)^3\ 4p$.....	b^4F'	$^5D'$ ^5F $^5G'$; $^3D'$ ^3F $^3G'$	c^5D' b^5F b^5G'; d^3D' c^3F b^3G'
	a^4P'	$^5S'$ ^5P $^5D'$; $^3S'$ ^3P $^3D'$	b^5S' b^5P d^5D'; c^3S' d^3P h^3D'
	a^2P'	$^3S'$ ^3P $^3D'$; $^1S'$ ^1P $^1D'$	d^3S' f^3P i^3D'; a^1S' d^1P d^1D'
	b^2D'	^3P $^3D'$ ^3F; ^1P $^1D'$ ^1F	e^3P j^3D' f^3F; c^1P e^1D' $d\,^1F$
	b^2F'	$^3D'$ ^3F $^3G'$; $^1D'$ ^1F $^1G'$	g^3D' h^3F, —; — f^1F? f^1G'?
	a^2G	^3F $^3G'$ ^3H; ^1F $^1G'$ ^1H	g^3F e^3G' b^3H; b^1F b^1G' a^1H
	a^2H'	$^3G'$ ^3H $^3I'$; $^1G'$ ^1H $^1I'$	f^3G c^3H a^3I'; e^1G' b^1H a^1I'
	(^2D)	^3P $^3D'$ ^3F; ^1P $^1D'$ ^1F	— — — ; — — —
$(3d)^2\ 4s\cdot 5s$...	a^4F'	$^5F'$; $^3F'$	b^5F'; c^3F'
	b^4P'	$^5P'$; $^3P'$	—; d^3P'
	a^2S	^3S; ^1S	—; —
	b^2P'	$^3P'$; $^1P'$	—; —
	a^2D	^3D; ^1D	—; c^1D
	a^2F'	$^3F'$; $^1F'$	d^3F'; b^1F'
	b^2G	^3G; ^1G	—; d^1G
$(3d)^2\ 4s\cdot 6s$ ..	a^4F'	$^5F'$; $^3F'$	e^5F'; f^3F'

TABLE V—*Continued*

Configuration	Limit *Ti* II	Predicted Terms	Observed Terms
$(3d)^2\,4s\cdot 4d$..	a^4F'	$^5P'\ ^5D\ ^5F'\ ^5G\ ^5H'$ $^3P'\ ^3D\ ^3F'\ ^3G\ ^3H'$	$b^5P'\ b^5D\ d^5F'\ a^5G\ a^5H'$ — — $e^3F'\ c^3G$ —
	a^2F'	$^3P'\ ^3D\ ^3F'\ ^3G\ ^3H'$ $^1P'\ ^1D\ ^1F'\ ^1G\ ^1H'$	— — g^3F' — b^3H' — — $c^1F'\ c^1G\ b^1H'$
$(3d)^2\,4s\cdot 5d$..	a^4F'	$^5P'\ ^5D\ ^5F'\ ^5G\ ^5H'$	— $e^5D\ h^5F'\ d^5G\ c^5H'$
$(3d)^3\,5s$.....	b^4F' b^2D a^2P'	$^5F'$; $^3F'$ ^3D; ^1D $^3P'$; $^1P'$	c^5F'; d^3F' c^3D; — —; b^1P'
$(3d)^3\,6s$.....	b^4F'	$^5F'$; $^3F'$	f^5F'; —
$(3d)^3\,4d$.....	b^4F'	$^5P'\ ^5D\ ^5F'\ ^5G\ ^5H'$	— c^5D — $b^5G\ b^5H'$
$(3d)^2\,(4p)^2$...	a^3F' (*Ti* III)	$^5D\ ^5F'\ ^5G$; $^3D\ ^3F'\ ^3G$; $^1D\ ^1F'\ ^1G$	$d^5D\ g^5F'\ c^5G$; — — — — — —

The quintet system.—As is usual in complex spectra, the system of highest multiplicity has the simplest structure. Only two low even terms are to be anticipated (arising from $(3d)^3 4s$), and these must evidently be a^5F' and a^5P'. Among the odd terms, at a middle level, four triads are to be anticipated, two of D′FG′ terms, combining strongly with a^5F', and the other two, of S′PD′ terms, combining strongly with a^5P', and exactly these terms are observed. For the triads of origin $(3d)^3 4p$ the electron jump for the low term is from s to p, and the multiplets of highest L value should be the strongest. This is the case for the higher of each pair of triads, as is illustrated in Table VI and also by the fact that the multiplet $a^5F'-b^5G'$ includes the *raies ultimes* of *Ti* I in the visible region. The other two triads must then arise from $(3d)^2 4s\cdot 4p$, and for these the multiplets of lowest L value should be the strongest. This is clearly so for $a^5P'-a^5S'$, which is recorded as equally strong photographically with $a^5P'-b^5D'$, though the former lies far in the infra-red. For the other triad, $a^5F'-a^5D'$ is very strong; the combination with a^5F is at the limit of observation and with a^5G' beyond it. This disposes of all the even terms except e^5D', which may be attributed to $(3d)^2 4s\cdot 5p$, with limit a^4F'. This conclusion is confirmed by series relations (sec. 8). The other terms of the triad, which should give weaker multiplets, have not been found.

The high even terms fall into two sharply separated groups, the larger composed of terms which combine with the lowest odd triad a^5D', a^5F, a^5G' and but weakly with anything else; the smaller, of terms which combine most strongly with the triad c^5D', b^5F, b^5G' and weakly with the lower triad. It is evident that these groups of terms must be derived from the same limits as these triads, namely, a^4F' and b^4F'. From the first limit we have the configurations $(3d)^2 4s \cdot ms$, giving an isolated $^5F'$ term, and $(3d)^2 4s \cdot md$, giving a pentad, $^5P'$, ^5D, $^5F'$, ^5G, $^5H'$. The term b^5F' meets the condition for the first, giving the strongest combination with a^5G', as it should.

The first pentad, of terms lying almost at the same level, is also immediately recognizable. The terms belonging to it alternate in level in the characteristic manner observed in other spectra. Four of the five terms belonging to it give multiplets consisting of decidedly fuzzy lines, denoted by "n" in Table VI.

The higher isolated term e^5F', which behaves like b^5F' but gives much fainter combinations, is apparently in series with it, and four out of the five members of the pentad, which is in series with the one already found, can easily be identified, giving, as they do, the most diffuse lines in the whole spectrum. In this pentad also the energy levels alternate, and the differences in level are about half those in the lower one.

Among the terms of the second group, which evidently arise from the configurations $(3d)^3 ms$ and $(3d)^3 md$, the term c^5F', although originally identified by means of its combinations with the lower triad, is shown to belong here by the strength of its combination with b^5G' in the deep red.

For the term next in series with it, f^5F', only the leading component has been identified, but the agreement with a series formula (sec. 8) makes its reality probable. Three of the five members of the pentad of origin $(3d)^3 4d$ have also been recognized.

This leaves three high even terms unclassified, e^5D, g^5F', c^5G. They lie nearly at the same level, give strong multiplets, and are evidently related to one another. All the configurations containing an excited s or d electron which are at all likely to give strong lines have already been accounted for, but the configuration $(3d)^2(4p)^2$ should produce terms of exactly the observed types. Similar terms arising from the configurations involving two p electrons have been identified in *Ca* I[1] and *Sc* I.[2] It is of much interest to note that the relative intensities of the different multiplets resulting from the

TABLE VI

Ti I, Intensities of Strongest Lines, Quintet System*

		$(3d)^2 4s\cdot 4p$						$(3d)^3 4p$						$(3d)^2 4s\cdot 5p$
		a^5S'	a^5P	b^5D'	a^5D'	a^5F	a^5G'	b^5S'	b^5P	d^5D'	c^5D'	b^5F	b^5G'	e^5D'
$(3d)^3 4s$	a^5P'	(2)	(1)	(2)	*i*			15	30	30	(1)			
	a^5F'			3	(5)	(2h)	*i*			4	60	80	60	2
$(3d)^3 5s$	c^5F'	....	....	....	3	4n	1	....	....	....	*i*	*i*	(3)	
$(3d)^3 6s$	f^5F'	....	....	....	....	....	....	....	....	....	(1)	(2)		
$(3d)^3 4d$	c^5D	....	....	....	....	....	....	....	....	....	(1)	(2)		
	b^5G	....	....	....	....	....	....	....	....	....		(1)	(2)	
	b^5H'	....	....	....	....	....	....	....	....	....			5n	
$(3d)^2 4s\cdot 5s$.	b^5F'	....	....	....	12	15	18	....	....	....	*i*	*i*	*i*	
$(3d)^2 4s\cdot 6s$.	e^5F'	....	....	....	1	2	2							
$(3d)^2 4s\cdot 4d$.	b^5P'	....	....	....	10n									
	b^5D	....	....	....	8n	10n								
	d^5F'	....	....	....	7	5	2							
	a^5G	....	....	....		25n	15n							
	a^5H'	....	....	....		12n	30n							
$(3d)^2 4s\cdot 5d$.	d^5D	....	....	....	1n	2N								
	h^5F'	....	....	....	2n	1n	3n							
	d^5G	....	....	....		2N	6N							
	c^5H'	....	....	....		(1)	12N							
$(3d)^2(4p)^2$ ..	e^5D	....	....	....	6	10								
	g^5F'	....	....	....	8n	1n	20n							
	c^5G	....	....	....		10	12							

* The table gives the intensity of the strongest unblended line in each multiplet; *i* denotes that the corresponding multiplet is in the infra red.

combinations of the terms arising from configurations such as $(3d)^2 4s\cdot 4p$ and $(3d)^2 4s\cdot ms$, $(3d)^2\cdot 4s\cdot mp$ and $(3d)^2\cdot 4p\cdot md$, are remarkably similar to those of the individual lines resulting from the combination of a P term with S, P′, or D terms in a system of high multiplicity—the *L* values for the various terms of the triads or pentads taking the place of the *j* value for the components of the individual terms. The multiplet involving the greatest values of *L* is always the strongest, and even the finer details, such as the weakness of the middle line in a PP′ multiplet, and of the outer members of the middle set of three in a PD group, are faithfully reproduced. This relation, it is believed, was first noticed by the writer in *Sc* II. It is probably of general validity.

---

[1] Russell and Lang, *Mt. Wilson Contr.*, No. 337; *Astrophysical Journal*, **66**, 13, 1927.

[2] Russell and Meggers, *Scientific Papers of the Bureau of Standards*, **22**, 329 (No. 558), 1927.

The quintet system is now satisfactorily interpreted. All the observed terms have been accounted for, and all the electronic configurations that might be expected to give lines of any strength have been identified, e.g., those terms, at least, which should theoretically be most prominent, except for $(3d)^4$. The reason why this has not been found will be discussed in section 9.

6. THEORETICAL INTERPRETATION OF THE OBSERVED TERMS: THE SINGLET SYSTEM

The singlet system is next in order of complexity. The low terms to be expected are S, D, G from the configuration $(3d)^2(4s)^2$, and P′, D, F′, G, H′, D from $(3d)^3 4s$. The terms of the former group may be expected to be the lower, since the second of a pair of equivalent s electrons is usually more tightly bound than the first. The first group may therefore be assigned as a^1S, a^1D, a^1G, leaving a^1P', b^1D, a^1F', b^1G, a^1H' for the other, and accounting for all the theoretical even terms except one ^1D term. This corresponds to a limiting term in *Ti* II which has not been observed, and which must give faint lines and be statistically improbable, so that the absence of the related term in *Ti* I is not surprising.

Confirming evidence in favor of this assignment is found in the relative levels of these terms and of the limits in *Ti* II. Subtracting the term values in *Ti* I from those in *Ti* II, we obtain a set of numbers which (since both sets of term values are measured upward from the lowest level) show how much greater or less is the energy involved in passing from a given term to its limit than from the lowest level in *Ti* I to that in *Ti* II. The resulting values for the first group are $a^1S+6172$, $a^1D+1489$, $a^1G+3139$, and for the second, $a^1P'-$

10087, $b^1D - 7451$, $a^1F' - 8927$, $b^1G - 9169$, $a^1H' - 8021$. The binding of the second 4s electron therefore involves more energy than that of the first by about 11,000 frequency units, or 1.35 volts.

Passing to the odd terms at middle levels, we must seek for triads related to the various limiting terms of *Ti* III. Some are easy to identify; for example, the three lowest odd terms, a^1D', a^1F, a^1G', which combine with a number of high even terms, clearly come from the lowest limit in *Ti* II, a^2F'.

The next lowest limit, a^2D, should give a triad combining with a^1D, to produce some of the strongest lines in the spectrum; a^1P, b^1D', b^1F (or perhaps c^1F) satisfy this condition. The middle term of the triad is more than 5000 frequency units below the other two, but similar differences are known in other spectra. From the limit b^2D should come a triad combining strongly with b^1D. The terms d^1F and e^1D' must belong to this (as the intensities given in Table VII show), and the most probable third member is c^1P (although d^1P might pass). To the limit a^2P' corresponds a triad combining with a^1P'. The unappropriated terms a^1S', d^1P, and d^1D' give the strongest combinations with this low term and may be placed here.

There should be a second S′PD′ triad, with limit b^2P', which, coming from $(3d)^2 4s \cdot 4p$, should combine more strongly with a^1S and a^1D than with a^1P'. The terms b^1P, c^1D' satisfy this test and may be placed here provisionally. The ${}^1S'$ term of this triad would be hard to identify and has not been found.

We may next seek the triads having the limits a^2H', a^2G, and b^2G. The first should be composed of G′, H, and I′ terms, combining strongly with a^1H'; a^1I' must certainly be assigned here, and b^1H very probably.

The terms derived from a^2G should combine strongly with b^1G, which has the same limit; and the intensities of the lines place a^1H and b^1G' unquestionably here. The last term to fill out the triad is b^1F, leaving c^1F for the triad with limit a^2D. The other FG′H triad should combine strongly with a^1G, and, when permissible, with a^1D. Here we must now place c^1H; and c^1G' and e^1F appear to complete the group satisfactorily, leaving e^1G', which combines more strongly with a^1H' than with anything else, for the corresponding triad. For the remaining terms we might expect theoretically an isolated P term with limit a^2S, and triads $D'FG'$ with limit b^2F', and $PD'F$ from c^2D. These limiting terms lie high, especially the last. The observed terms which are still unassigned are e^1P, f^1F, d^1G', and f^1G'. It is not practicable to allocate these with any confidence; f^1G' may belong to b^2F', and so may f^1F, although the combinations of both with a^1G are stronger than might be expected; e^1P may be associated with either a^1S' or c^1D'. The remaining term d^1G' depends only on three faint lines and may not even be real.

The high even terms remain to be discussed. Evidence will be given in section 8 that c^1D is in series with a^1D, and d^1G with a^1G. Most of the other terms combine with the lowest odd triad, and must, like this, have the limit a^2F'. The addition of a 4d electron to this should give a pentad, to which c^1F', c^1G, and b^1H' belong, as is indicated by their levels, the intensity of their combinations, and the term values given in section 8. The term b^1H' depends on a single observed line, $a^1G'-b^1H'$; but this should be the strongest combination between the triad and the pentad, and no other available line is in the proper region with the right intensity and Zeeman pattern.

Adding a 5s electron to a^2F' gives an isolated $^1F'$ term, which should be some 6000 units below the pentad; b^1F' is in just the right place for this. Finally, d^1D is at about the right level for a 4d derivative of a^2D, but its combinations do not fit this identification. It may arise from $(3d)^4$. The term b^1P' may arise from the addition of a 3d electron to a^2P. It combines most strongly with a^1S', as it should on this hypothesis, and is at the right level (sec. 6).

The arrangement of the terms which has finally been adopted is given in Table VII. It should be borne in mind that in some cases, especially in those marked with colons, the assignment of the terms to a given limit is less certain than in the case of the quintets; but the energy levels of the terms assigned to the same triad are usually near together, and the intensities appear to run satisfactorily, increasing, in general, with the L values in each principal triad of combinations, as they ought to do, since all the electron jumps are from s to p.

Some of the lines corresponding to double electron jumps are strong, but this is also the case in other spectra; for example, for the PP' group near λ 3000 in *Ca* I.

TABLE VII

Ti I, INTENSITIES OF SINGLET LINES

CONFIGURATION		$(3d)^2(4s)^2$			$(3d)^3 4s$					$(3d)^2 4s\cdot 5s$			$(3d)^2 4s\cdot 4d$			$(3d)^2 4d$	?
Limit	Term	a^{1}S	a^{1}D	a^{1}G	a^{1}P′	b^{1}D	a^{1}F′	b^{1}G	a^{1}H′	c^{1}D	b^{1}F′	d^{1}G	c^{1}F′	c^{1}G	b^{1}H′	b^{1}P′	d^{1}D
	$(3d)^2 4s\cdot 4p$																
a^{2}S..........	e^{1}P:	1	15		3	(2)											
b^{2}P′.........	—																
	b^{1}P	3	12		(1)					……	……	……	……	……	……	1	
	c^{1}D′		15		(0)					……	……	……	……	……	……	*m*	
a^{2}D..........	a^{1}P		20		(1)					……	……	……	……	……	……	……	(1)
	b^{1}D′		25		*i*					2			……	……	……	m	
	c^{1}F		20	5		1	*i*	(0)									
a^{2}F′.........	a^{1}D′		10		*i*					(3)	3		4n			……	1
	a^{1}F		12	*i*			*i*	*i*		2	4	2n	5n	5		……	1
	a^{1}G′			(3)			*i*	*i*	*i*		7	1	(1)	2	5		
b^{2}G..........	e^{1}F		40	10		1	(1)	*m*									
	c^{1}G′			20			*i*	6	8								
	c^{1}H			15					7								
	$(3d)^3 4p$																
a^{2}P′.........	a^{1}S′	……	……	……	2					……	……	……	……	……	……	(2)	
	d^{1}P	(1)	15		5	2				……	……	……	……	……	……	*m*	
	d^{1}D′		15		5					……	……	……	……	……	……	*i*	
b^{2}D.........	c^{1}P	(3)	15		(1)	4				……	……	……	……	……	……	(1)	
	e^{1}D′		6		4	7											
	d^{1}F		2	15		10	*i*	(1)									

b^2F'	—										
	f^1F:	(1)	20		(2)	4					
	f^1G':		30		(1)	8	10				
a^2G..........	b^1F	40n	20	(2)	*i*	6					
	b^1G'		25		*i*	18	3	(0)			
	a^1H		40			20	2				
a^2H'.........	e^1G'		2n		(0)	2n	5n				
	b^1H		6			8	8				
	a^1I'	....					12				
?............	d^1G'		*m*			2	1				

i, in infra-red; *m*, masked by stronger line.

7. THEORETICAL INTERPRETATION OF THE OBSERVED TERMS: THE TRIPLET SYSTEM

The triplet system is much the most intricate, since triplet terms may arise from both doublet and quartet limits in *Ti* II. The lowest terms may be expected to come from the configuration $(3d)^2(4s)^2$, and to be of types $^3P'$, $^3F'$, the latter being the lower. These must obviously be the terms a^3P', a^3F'. From $(3d)^3 4s$ we should have, from the quartet terms in *Ti* II, $^3P'$ and $^3F'$, and, from the doublet terms, $^3P'$, ^3D, $^3F'$, ^3G, $^3H'$. All these are observed, except one $^3F'$ term. The terms a^3D, a^3G, and a^3H' fall naturally into the second group, while b^3F', which is at a lower level, evidently comes from the low limit, b^4F'. The limits a^2P' and a^4P' are very close together, and so are the terms b^3P' and c^3P', which are doubtless derived from them. Which belongs to which limit is hard to tell. As good a guide as any may be found in the differences of the energy levels in *Ti* I and the limits in *Ti* II. Taking differences of term values, as before, we find, for the transitions involving the completion of a pair of 4s electrons,

$$b^4P' - a^3P' = +1422; \qquad a^4F' - a^3F' = +7.$$

For those where a single s electron is added and the multiplicity of the term increases, we have

$$b^2D - a^3D = -4782, \quad a^2G - a^3G = -6102, \quad a^2H' - a^3H' = -5418\,.$$

For comparison we have

$$a^4P' - a^5P' = -4587\,, \quad b^4F' - a^5F' = -5628\,.$$

For the transitions in which one s electron is added but the multiplicity decreases, the difference is considerably greater (meaning that the energy of binding of the electron is less than when the multiplicity increases). We have $b^4F' - b^3F' = -10{,}561$, while the mean for five transitions from doublets to singlets (sec. 6) is -8919.

We should therefore expect differences of about -9200 for the term derived from a^4P' and -5300 for that coming from a^2P', putting them at levels near 18,700 and 15,300, respectively. The actual difference in level is much less, but it seems best to assign b^3P' to a^2P', giving a difference of -8170, and c^3P' to a^4P', with a difference of −9393. On the same basis the level of the ${}^3F'$ term derived from b^2F' should be about 26,000—which means that all its stronger combinations with the known odd terms should be in the infra-red, so that it is not surprising that it has not been detected.

The odd triplet terms should contain a great number of triads. Those which combine with the low F' terms should be especially conspicuous. We may expect to find two of origin $(3d)^2 4s \cdot 4p$ and limits a^4F' and a^2F', and two of origin $(3d)^3 4p$ and limits b^4F' and b^2F', the last high-lying and perhaps inconspicuous. The first pair of triads should combine very strongly with a^3F', and the second strongly with b^3F'. The strongest combinations of this term are with d^3D', c^3F, b^3G', and e^3F. The first three of these lie at nearly the same level, and evidently form the triad with limit b^4F'. They combine very strongly with a^3F' also. Another obvious triad is a^3D', a^3F, a^3G', which, like similar triads in the singlet and quintet systems, contains the lowest odd terms.

Another triad, which gives extremely strong combinations with a^3F' and relatively weak ones with b^3F', is formed by b^3D', b^3F, and c^3G'. This may be accepted as the second triad of origin $(d)^2 s \cdot p$. Which of these triads belongs to the limit a^4F', and which to a^2F', can hardly be determined from the data on the spectrum of *Ti* alone, extensive as they are; but a comparison of all the spectra from *Ca* to *Cu* shows conclusively[1] that the higher-lying triad, which gives the stronger combinations, belongs to the limit of higher multiplicity.

The limit a^2H' should give a $G'HI'$ triad, combining strongly with a^3H'. Much the strongest combinations from this level are with f^3G', c^3H, and a^3I', which are thus identified. There should be two $FG'H$ triads with limits a^2G and b^2G. Both should combine strongly with a^3G (the electron jumping from 4s to 4p in the first case, and 3d to 4p in the second); but the second should combine more strongly with a^3F' than the first. There is only one strong GG' multiplet involving e^3G', which evidently belongs in the first triad, and leaves available for the second only d^3G', which combines very strongly with a^3F', but much more weakly with a^3G than might be expected.

The strong GH multiplets involve a^3H and b^3H. The former term combines with a^3F', in spite of the unusual transition, and must be assigned to the second triad and b^3H to the first. The second triad is naturally completed by e^3F, which combines very strongly with a^3F'. For the other, f^3F or g^3F are at the right level; the latter has been adopted, and, like e^3G', it gives a much stronger combination with a^3F' than with b^3F'. The triads with large values of L are thus satisfactorily identified; those with small L's are harder to pick out.

---

[1] *Mt. Wilson Contr.*, No. 341; *Astrophysical Journal*, **66**, 184, 1927.

There should be four $S'PD'$ triads, of origin $(3d)^2 4s \cdot 4p$ and limits b^4P', b^2P', and of origin $(3d)^3 4p$ with limits a^4P', a^2P'. The four known $^3S'$ terms show that all four triads exist, but to identify them completely is difficult. By analogy with the $D'FG'$ triads we might expect the one with limit b^2P' to be the lowest, and to give combinations of only moderate strength. The terms a^3S', a^3P, c^3D' fit these conditions. Except for the first, their combinations with a^3P' are faint; all three of them also combine with a^3F' and give groups with abnormal intensities.

The triad with limit b^4P' should give the strongest combinations with a^3P'. It seems clear that c^3P must belong to this triad. Unless the levels are very irregular, b^3S' must do so too. For the third term, f^3D', which combines strongly with both a^3P' and a^3F', appears to be the best choice.

The other two triads, with limits a^2P' and a^4P', should give distinctive combinations with b^3P' and c^3P', respectively. It is probable that f^3P and i^3D' belong to the first of these. The second should include h^3D' and either d^3P or e^3P. As the former gives a strong combination with a^3P', it is chosen in preference to the latter. It then appears reasonable, from consideration of energy levels, to put c^3S' in the latter triad and d^3S' in the former. It should be freely admitted, however, that the arrangement of these upper $S'PD'$ triads is subject to considerable uncertainty.

There should be two $PD'F$ triads, with limits a^2D and b^2D, the latter giving strong combinations with a^3D. The unassigned terms e^3P and j^3D' fit in well here, as would either f^3F or h^3F. The former has been adopted because, like i^3D', it combines weakly with a^3F'. The other triad might be expected to be lower, and there are three unclassified terms, b^3P, e^3D', d^3F, which look well enough as regards energy level. Their combinations, however, are weaker than might be expected, and not very satisfactory in intensity, so that this triad must remain doubtful.

Three more triads involving a 4p electron are to be anticipated, with limits c^2D, b^2F', and an unobserved ^2D term. The last is not likely to give identifiable terms; the second probably gives inconspicuous ones, but the first, coming from the configuration $3d(4s)^24p$, may combine with the low term of origin $(3d)^2(4s)^2$ and give strong multiplets. There are three terms at a very high level which give such strong combinations—g^3P, l^3D', and i^3F, and these have been grouped together. Among the remaining terms, those which give the strongest combinations are g^3D' and h^3F. These may be placed tentatively in the triad with limit b^2F'.

There remain the odd terms k^3D', m^3D', j^3F, g^3G', and d^3H, all of which give faint combinations. These probably arise from configurations containing a 5p electron, and it will be seen in section 8 that m^3D', j^3F, g^3G' are probably in series with the triad d^3D', c^3F, b^3G', and have the limit b^4F'. The other two terms have not been placed.

Fewer high even triplet terms have been found than might have been expected. There are several groups of three neighboring unclassified faint lines in the arc spectrum which point to the existence of other triplet terms, probably belonging to this group, but they cannot be definitely located. Of the known terms, c^3F' and f^3F' are in series with a^3F with limit a^4F', and a^3F' and d^3F' with limit a^2F' (sec. 8). The fragmentary terms c^3D and d^3P' appear to be the series members following a^3D and a^3P' (sec. 8). All the rest combine mainly, if not exclusively, with the low odd triad, a^3D', a^3F, a^3G'. This suggests that they belong to the pentads formed by adding a d electron to a^4F' or a^2F', and the term values indicate that e^3F' and c^3G probably belong to the first, and g^3F' and b^3H' to the second.

This leaves outstanding b^3G and b^3D. The former lies much too low to be derived from any of the terms of *Ti* II by adding either a 5s or a 4d electron, and can arise only from the configuration $(3d)^4$. This is confirmed by the comparison with *V* II given in section 9. It is highly probable that b^3D, which does not fit in well otherwise, comes from the same configuration.

The arrangement which has finally been adopted for the triplet terms is given in Table VIII, which is arranged like Tables VI and VII.

Practically all the observed terms of *Ti* I have now found their place in the scheme provided by Hund's theory. For a large majority of the terms the identification of the electronic configuration corresponding to each term is definite; for the remainder, although some ambiguity exists, it involves only the choice between interpretations, both of which are consistent with theory. The representation of the structure of this complex spectrum by Hund's theory leaves therefore nothing to be desired.

8. SERIES AND IONIZATION POTENTIAL

The foregoing analysis indicates that a considerable number of series can be identified in this spectrum. Only two of these, however, can be followed beyond the second member. These begin, as might have been anticipated, with the terms which give the strongest lines in the spectrum (a^3F' and a^5F') and, even so, the third members give such faint lines that only the leading component of the multiple terms could be found (by searching in the region predicted by a Rydberg formula). In both cases, however, the reality of these terms appears to be confirmed by the combinations in which they appear.

The term values of the leading components of a^3F', c^3F', f^3F' are exactly represented by the Ritz formula

$$x=A-\frac{R}{\{m+q+K(A-x)\}^2}\,,$$

if $A=55{,}384$, $q=0.5403$, $K=-2.36\times10^{-6}$; while for a^5F', c^5F', f^5F' the constants are

$$A=56{,}500\,,\quad q=0.5586\,,\quad K=-1.46\times10^{-6}\,.$$

The values of A give the heights of the limits of the two series above the lowest level, $a^3F'_2$ in *Ti* I. These limits are the terms $a^4F'_4$ and $b^4F'_5$ of *Ti* II which lie at heights 393 and 1216 above the lowest level $a^4F'_2$ of *Ti* II. The difference of the lowest levels in *Ti* I and *Ti* II is therefore 54,991 from the triplet, and 55,284 from the quintet series, corresponding to ionization potentials of 6.79 and 6.83 volts,

TABLE VIII

Ti I, INTENSITIES OF STRONGEST LINES, TRIPLET SYSTEM

CONFIGURATION		$(3d)^2(4s)^2$		$(3d)^3 4s$						$(3d)^4$	
Limit		b^4P'	a^4F'	a^4P'	b^4F'	a^2P'	b^2D	a^2G	a^2H'		
		a^3P'	a^3F'	c^3P'	b^3F'	b^3P'	a^3D	a^3G	a^3H'	b^3D	b^3G
$(3d)^2 4s \cdot 4p$											
b^4P'.......	b^3S'	20				2					
	c^3P	30		(1)			(2)				
	f^3D'	15	40		8	1	8				
a^4F'.......	b^3D'	35	80	*i*	20	*i*	*i*				
	b^3F		100R		4		*i*	*i*			(1)
	c^3G'		80R		6			(1)	(3)		
b^2P'.......	a^3S'	20	(3)	*i*		*i*					
	a^3P	10	40	*i*	5	*i*	*i*				
	c^3D'	4	15	*i*	8	*i*	*i*				
a^2D.......	b^3P	2	tr			(2)	(1)				
	e^3D'	10	5	(1)	12	(2)	(1)				
	d^3F		20		8		3	6			
a^2F'.......	a^3D'	(3)	25	*i*	*i*	*i*	*i*			3	
	a^3F		40		*i*		*i*	*i*		5	(1)
	a^3G'		30		*i*			*i*	*i*		(2)
b^2G.......	e^3F		70R		40		4n	10			
	d^3G'		100R		25			4	(3)		
	a^3H		3					30	(1)		
$(3d)^3 4p$											
a^4P'.......	c^3S'	8				3					
	d^3P	12		6			8				
	h^3D'	6	20	12	3		(2)				
b^4F'.......	d^3D'	20	40r		25	(1)				(2)	
	c^3F		80r		25		*i*	(4)			
	b^3G'		100r		50			(4)	*i*		
a^2P'.......	d^3S'	6									
	f^3P	tr				8	8				
	i^3D'	12	(3)	2	8	6	3				
b^2D.......	e^3P	1		8			4				
	j^3D'	15	4		(5)		10				
	f^3F	1	5		3		12	15			
b^2F'.......	g^3D'	15	5		15	2	4				
	h^3F		10				10	4			
a^2G.......	g^3F	2	25		1		9	15			
	e^3G'		20		2			30	(1)		
	b^3H							20	9		

TABLE VIII—*Continued*

Configuration		$(3d)^2(4s)^2$		$(3d)^3 4s$						$(3d)^4$	
Limit		b^4P'	a^4F'	a^4P'	b^4F'	a^2P'	b^2D	a^2G	a^2H'		
		a^3P'	a^3F'	c^3P'	b^3F'	b^3P'	a^3D	a^3G	a^3H'	b^3D	b^3G
a^2H'	f^3G'		10		2				10n		
	c^3H							7	25		
	a^3I'								20		
$3d\,(4s)^2\,4p$											
c^2D	g^3P	30		1		3	1				
	l^3D'	6	12		1						
	i^3F		12		2			3			
$(3d)^3 \cdot 5p$											
b^4F'	m^3D'	(4)	(7)		3						
	j^3F		(8)		2n						
	g^3G'		(3)					4			
?	k^3D'	5	(4)		2n						
	d^3H							6n			

		$(3d)^2 4s \cdot 5s$			$(3d)^2 4s \cdot 6s$	$(3d)^2 4s \cdot 4d$				$(3d)^3 5s$
		a^4F'	a^2F'	b^4P'	a^4F'	a^4F'		a^2F'		a^2D
		c^3F'	d^3F'	d^3P'	f^3F'	e^3F'	c^3G	g^3F'	b^3H'	c^3D
$3d \cdot 4s \cdot 4p$										
a^4F'	a^3D'	5		1	(1)	2				1
	a^3F	8			4n	3	5	2		2n
	a^3G'	20			3n	(0)	4	(2)	15	
a^2F'	b^3D'	(1n)	2							
	b^3F		(2)							
	c^3G'	*i*	*i*							
b^4P'	a^3S'			3						
$(3d)^3 4p$										
b^4F'	c^3F	(1)								
	b^3G'	*i*	(2h)							

respectively. The agreement is satisfactory, and we may adopt the mean, 6.81 volts, as the principal ionization potential of the neutral atom of titanium, or, which comes to the same thing, adopt $a^4F'_2 - a^3F'_2 = 55{,}138$.

It is now possible to locate accurately all the terms in *Ti* II with respect to the scale of levels employed for *Ti* I. For those terms which have appeared above as limits of possible series in *Ti* I, we find by adding 55,138 to the levels referred to $a^4F'_2$ and taking always the component of greater inner-quantum number,

$a^4F'_5$	55,531	a^2S	76,476	b^2D_3	67,896	a^2G_5	64,256
$b^4F'_5$	56,354	$a^2P'_2$	65,114	c^2D_3	80,331	b^2G_5	70,396
$a^4P'_3$	64,656	$b^2P'_2$	71,763	$a^2F'_4$	60,036	$a^2H'_6$	67,913
$b^4P'_3$	65,163	a^2D_3	63,882	$b^2F'_4$	76,030		

We may now compute the true term values and the Rydberg denominators for all the terms which have been classified in section 7. The results for those terms which form series are given in Table IX. The various series are arranged according to the types of electrons which shift, and, to save printing, only the Rydberg denominators are given. The term values can be found by subtracting the values given in Table I, taking always the component of highest inner-quantum number, from the appropriate limit, as listed above.

Seventeen series have been identified. The successive terms of each lie in the same horizontal row. When an s electron is involved the fractional part of the denominator is nearly the same for the terms of a given series. For a 5p electron it is greater by about 0.12 than for a 4p. For 4d and 5d it is nearly the same, but for 3d it is much less, showing that, as usual, the electron is much more firmly bound when it goes into a group of similar electrons than when it stands alone.

It should be noted that a^3F' is the leading term of two different series, one converging to a^4F' and the other to a^2F'. This arises from the fact that, by Pauli's restriction, the addition of a 4s electron to either of these terms of *Ti* II can give only this term in *Ti* I, while the addition of a 5s electron to the two gives four different terms, all of which have been identified.

The quantum defects are nearly the same for all the terms involving s electrons, considerably smaller for the p's, and smaller yet for the d's (excepting 3d). To complete the data regarding them, the denominators for the remaining terms are given in Table X, which is arranged in fashion very similar to Table IX. All the terms arising from the addition of 4s and 4p electrons are given; those from 3d electrons are given only when they do not appear in

Table IX. Certain cases, in which it is doubtful whether the term belongs in the assigned place, are marked with a question mark (?).

It appears from this table that the denominators are smaller and the quantum defects greater for those terms which originate from the configuration $(3d)^2 4s$ than for those which come from $(3d)^3$; i.e., an additional electron is more firmly bound to the first configuration than the second. The binding is also closer when the multiplicity increases on adding the new electron than when it decreases. The mean values of the quantum defect, omitting the doubtful cases, are as shown in Table XI, the number of cases being indicated by figures in parentheses. These values may be taken as a measure of the failure of complete screening of the attraction of the nucleus by the outer electrons. The screening is of course greatest for the d, and least for the s orbits; conversely, an electron already in the

TABLE IX

RYDBERG DENOMINATORS FOR SERIES TERMS

SERIES LIMIT	ELECTRON					
	4s		5s		6s	
a^4F'	a^3F'	1.410	c^3F'	2.489	f^3F'	3.490
			b^5F'	2.456	e^5F'	3.420
b^4F'	a^5F'	1.489	c^5F'	2.544	f^5F'	3.576
b^4P'	a^3P'	1.392	d^3P'	2.408		
a^2D	a^1D	1.392	c^1D	2.384		
b^2D	a^3D	1.476	c^3D	2.450		
a^2F'	a^3F'	1.356	d^3F'	2.327		
			b^1F'	2.406		
b^2G	a^1G	1.372	d^1G	2.450		
	4p		5p			
a^4F'	a^5D'	1.726	e^5D'	2.856		
b^4F'	d^3D'	2.040	m^3D'	3.136		
	c^3F	1.934	j^3F	3.114		
	b^3G'	1.958	g^3G'	3.026		
	3d		4d		5d	
a^4F'	....		b^5D	2.866	d^5D	3.860
	a^5F'	1.516	d^5F'	2.998	h^5F'	4.027
			a^5G	2.849	d^5G	3.875
			a^5H'	2.869	c^5H'	3.883
	b^3F'	1.583	e^3F'	2.858		

TABLE X

Rydberg Denominators for Other Terms

Series Limit	Electron							
	4s		4p		4p		4d	
a^4F'	a^3F'	1.410	a^5D'	1.726	b^3D'	1.916	b^5P'	2.941
			a^5F	1.692	b^3F	1.908	c^3G	2.794
			a^5G'	1.675	c^3G'	2.074		
b^4F'	a^5F'	1.489	c^5D'	2.042	d^3D'	2.040	c^5D	3.027
	b^3F'	1.568	b^5F	1.989	c^3F	1.934	b^5G	3.240
			b^5G'	1.930	b^3G'	1.958	b^5H'	2.996
a^4P'	a^5P'	1.474	b^5S'	2.006	c^3S'	2.146		
	c^3P'	1.548	b^5P	1.971	d^3P	2.003		
			d^5D'	1.948	h^3D'	2.097		
b^4P'	a^3P'	1.392	a^5S'	1.655	b^3S'	1.921		
			a^5P	1.716	c^3P	1.850		
			b^5D'	1.672	f^3D'	2.015		
a^2S	a^1S	1.337	....		e^1P	1.808?		
a^2P'	b^3P'	1.528	d^3S'	2.327	a^1S'	2.018	b^1P'	3.095
	a^1P'	1.560	f^3P	2.175	d^1P	2.060		
			i^3D'	2.124	d^1D'	2.264		
b^2P'	a^3P'	1.318	a^3S'	1.530				
			a^3P	1.540	b^1P	1.726		
			c^3D'	1.574	c^1D'	1.728		
a^2D	a^1D	1.392	b^3P	1.849	a^1P	1.905	d^1D	2.824?
			e^3D'	1.832	b^1D'	1.746		
			d^3F	1.906	c^1F	2.043		
b^2D	a^3D	1.476	e^3P	2.000	c^1P	1.951		
	b^1D	1.517	j^3D'	2.070	e^1D'	2.134		
			f^3F	1.911	d^1F	1.994		
c^2D	....		g^3P	1.766				
			l^3D'	1.743				
			i^3F	1.731				
a^2F'	a^3F'	1.356	a^3D'	1.658	a^1D'	1.700	g^3F'	2.923
			a^3F	1.646	a^1F	1.707	b^3H'	2.791
			a^3G'	1.692	a^1G'	1.772	c^1F'	2.862
							c^1G	2.802
							b^1H'	2.745
b^2F'	b^1F'	1.541	g^3D'	1.716?	f^1F	1.991?		
			h^3F	1.785?	f^1G'	1.921?		
a^2G	a^3G	1.496	g^3F	2.070	b^1F	1.861		
	b^1G	1.545	e^3G'	2.032	b^1G'	1.970		
			b^3H	1.959	a^1H	1.927		
b^2G	a^1G	1.372	e^3F	1.741	e^1F	1.951		
			d^3G'	1.661	c^1G'	1.868		
			a^3H	1.690	c^1H	2.045		
a^2H'	a^3H'	1.485	f^3G'	2.032	e^1G'	2.127		
	a^1H'	1.526	c^3H	1.954	b^1H	2.020		
			a^3I'	1.940	a^1I'	1.994		

atom in a 3d orbit produces more screening upon an added electron of whatever sort than does one in a 4s orbit. For the terms which have been tentatively assigned to the addition of a 4p electron to the term c^2D (arising from $3d(4s)^2$), the mean quantum defect is 2.255, indicating a still smaller screening and confirming this interpretation. Since the assignment of the various terms to their limits was made primarily on the basis of the intensities of their combinations, the systematic character of the results just obtained may be taken as further and convincing evidence of the general correctness of the interpretation.

TABLE XI

Quantum Defects

Electron Added	Configuration (*Ti* II)			
	$(3d)^2 4s$		$(3d)^3$	
4s	2.632	(7)	2.481	(13)
5s	2.583	(7)	2.503	(2)
6s	2.545	(2)	2.424	(1)
4p	2.219	(35)	1.975	(36)
5p	2.144	(1)	1.908	(3)
3d	1.450	(2)	....	....
4d	1.145	(13)	0.910	(4)
5d	1.089	(4)	....	....

Odd terms, arising from configurations involving a 4f electron, might theoretically be expected; but for such terms the quantum defect should be small. The term values should therefore be of the order of 7000, referred to their own limits, and the lowest of them should be at least 48,000 above the base-level used in Table I. None of the odd terms which have been observed lie so high. The terms with limit a^4F' should give combinations with a^3P, lying near λ 2050, where the arc spectrum is unknown; those with limit b^4F' should give combinations with a^5F' lying near λ 2350 and with d^3F' near λ 2650, but nothing of the sort can be recognized there.

9. COMPARISON OF *Ti* I AND *V* II

The analysis of the principal terms of the spark spectrum of vanadium by Meggers[1] invites comparison with the titanium arc.

---

[1] *Zeitschrift für Physik*, **33**, 509, 1925; **39**, 114, 1926.

The most satisfactory method is the application of Moseley's law, as discussed in Part I of this paper.[1] From the run of the values for spectra of elements earlier in the first long period there given it appears that in this case the differences $\Delta\sqrt{\nu/R}$, for terms derived from their limits by the addition of a 3d, 4s or 4p electron, should be very close to 0.51, 0.34, and 0.33, respectively.

TABLE XII

TERMS OF *V* II

Term	Level	Term	Level	Term	Level
a^5D_4	339	$a^3F'_4$	9097	a^3G_5	14,655
$a^5F'_5$	3163	$a^3P'_2$	11,908	b^3G_5	16,532
$a^5P'_3$	13,741	$b^3F'_4$	13,608	$a^3H'_6$	20,363
$a^5G'_6$	35,483	$a^3D'_3$	36,919	a^3P_2	46,123
a^5F_5	37,352	$b^3D'_3$	37,205	a^3H_6	47,607
$a^5D'_4$	37,531	$a^3G'_5$	39,612	$a^3I'_7$	52,252
$b^5D'_4$	47,420	a^3F_4	40,430	$b^3I'_7$	53,319
a^5P_3	47,051			$a^3S'_1$	58,461
$a^5S'_2$	49,731				

No series are known in *V* II, and it is necessary, in order to apply Moseley's law, to identify the electronic configurations corresponding to some at least of the terms, assume that the law holds for these, derive the corresponding ionization potential, and then test our assumptions by the values of $\Delta\sqrt{\nu/R}$ for other terms.

The known terms of *V* II, with their levels referred to the lowest term $^5D_0$, are listed in Table XII. Only the leading components are given, and Meggers' notation of primed and unprimed terms is reversed to correspond with Heisenberg's general rule. Designating letters—always an "a"—have been added in some cases when Meggers has not used them.

From analogy with other spectra it is practically certain that the lowest terms of *V* III will be a $^4F'$ and $^4P'$ derived from the configuration $(3d)^3$, the former being the lower. The $^4F'$ term identified by Gibbs and White[2] arises from $(3d)^2 4s$ and probably lies much higher.

---

[1] *Mt. Wilson Contr.*, No. 344; *Astrophysical Journal*, **66**, 283, 1927.

[2] *Physical Review*, Ser. 2, **29**, 658, 1927.

In *V* II the low terms should come from $(3d)^4$ and $(3d)^3 4s$, the former giving ^5D, $^3F'$, $^3P'$, $^3P'$, ^3D, $^3F'$, ^3G, $^3H'$, and the latter $^5F'$, $^5P'$, $^3P'$, ^3D, $^3F'$, ^3G, $^3H'$, ^3D, neglecting singlet terms.

The three low quintet terms are exactly what is to be expected,[1] and the higher odd quintet terms evidently form the two triads of origin $(3d)^3 4p$ and limits $^4F'$ and $^4P'$. Among the low triplet terms all that can be said with certainty is that one ^3G term must come from $(3d)^4$ and the other from $(3d)^3 4s$. The intensities of the combinations, as Meggers points out, show that a^3F' and a^3G are related, and also b^3F' and b^3G, the former combining strongly with a^3D', b^3D', a^3F, and a^3G', as far as the ordinary rules permit, and the latter only with a^3F. It may be noted in passing that there is place for only one odd $^3I'$ term in Hund's scheme, namely, that derived from $(3d)^3 4p$. The term called by Meggers a^3I' appears actually to combine with b^3G', giving lines observed in the spark by Exner and Haschek; so it is probably a ^3H term, which removes the discrepancy.

The terms a^5F' in *Ti* I and a^5F' in *V* II are evidently homologous, and b^3F' and a^3F' look promising. For the first the value of $\sqrt{\nu/R}$ is 0.671 in *Ti* I. Adding 0.34, we have 1.01 for the second, indicating that the limit $^4F'_5$ is higher than the term $^5F'_5$ in *V* II by 111,800 units, or above the low level of *V* II by 115,000 (to the nearest hundred). From a consideration of certain similar cases, the value 114,600 was adopted for this quantity, corresponding to an ionization potential of 14.1 volts. The values of $\sqrt{\nu/R}$ can then be computed for all the terms of *V* II which may be legitimately associated with the lowest limit a^4F' in *V* III. Strictly speaking, these are rather few, but such terms as $^5P'$ and the low $^3D'FG'$ triad, which arise from the same electronic configuration, are likely to give nearly the same $\Delta\sqrt{\nu/R}$ when referred to a^4F' as when referred to their proper limits (a^4P' or a^2F'), since the differences in level of the limits in *Ti* II and *V* III increase almost *pari passu* with the term values.

We thus obtain the comparison given in Table XIII, which is arranged similarly to Table VI in Part I of this paper. The designations in the second column give first the term in *Ti* I, then the corresponding one in *V* II. The differences in $\sqrt{\nu/R}$ run with remarkable smoothness, averaging 0.341 for the 4s electron and 0.339 for 4p. For the first two entries in the table the agreement with the expected values is forced, but free for all the others. A change of the assumed ionization potential by ±0.5 volts would alter the mean values by approximately ±0.019 for 4s and ±0.022 for 4p. They accord so well with the values to be expected from comparison with other spectra as to indicate that the assumed value is probably correct within ±0.5 volts.

---

[1] Hund, *op. cit.*, p. 159.

TABLE XIII

COMPARISON OF *Ti* I AND *V* II

ELECTRON REMOVED	TERMS	LIMIT	$\sqrt{\nu/R}$			SEPARATIONS		
			Ti I	*V* II	DIFF.	*Ti* I	*V* II	Ratio
4s....	$(3d)^3\ 4s$							
	a, a^5F'	$^4F'$	0.671	1.008	0.337	286	558	0.51
	a, a^5P'	$^4F'$	.620	0.959	.339	124	230	.54
	b, a^3F'	$^4F'$	.638	.980	.342	245	458	.54
	a, a^3G	$^4F'$	.612	.954	.342	112	194	0.58
	a, a^3H'	$^4F'$	.590	.933	.343	155	121	(1.28)
4p....	$(3d)^3\ 4p$							
	c, a^5D'	$^4F'$	.489	.839	.350	231	429	0.54
	b, a^5F	$^4F'$	.501	.840	.339	108	(202)	.53*
	b, a^5G'	$^4F'$	.518	.850	.332	426	891	.48
	b, a^5S'	$^4F'$	.417	.769	.352			
	b, a^5P	$^4F'$	.426	.785	.359	116	298	.39
	d, b^5D'	$^4F'$	.434	.784	.350	254	834	.30
	d $\{$ a^3D'	$^4F'$	.522	.841	.319	251	430	0.58
	b	$^4F'$	.522	.840	.318	251	247	(1.02)
	c, a^3F	$^4F'$	.496	.823	.327	222	428	0.52
	b, a^3G'	$^4F'$	.503	0.827	.324	251	379	.66
3d....	$(3d)^4$							
	—, a^5D	$^4F'$	....	1.021	....	....	339	
	—, b^3F'	$^4F'$	....	0.960	....	....	118	
	b, b^3G	$^4F'$	0.429	.946	0.517	135	191	0.71
	—, a^3P'	$^4F'$	....	0.968	....	....	613	

* Separation of the first two components; the rest have not been identified in *V* II.

The ratios of the extreme separations of the multiple terms are given in the last column. Most of these are near to the value 0.5, which might have been anticipated (cf. Part I, sec. 10). The principal exceptions involve the terms a^3H' in *Ti* I and b^5D' in *V* II, both of which have very abnormal intervals.

There appear, therefore, to be strong reasons for assigning the designated terms in *V* II to the configurations $(3d)^3 4s$ and $(3d)^3 4p$. An exception should be noted in the case of a^3F, for which the intensities of the combinations indicate a different origin, which must be $(3d)^2 4s \cdot 4p$. It looks also as if b^3D' might belong to this configuration, while a^3D' fits in well with the other. As for the configuration $(3d)^4$, there can be no hesitation in assigning to it the terms here listed for *V* II. (The ^3P term is much too low to be the one homologous with b^3P' in *Ti* I, for which $\sqrt{\nu/R}$ is 0.590). The only term identified during the analysis of *Ti* I as certainly due to this configuration is b^3G, which gives the expected value of $\Delta\sqrt{\nu/R}$. If this difference is the same for the terms in *Ti* I homologous with the other known terms of *V* II, the ^5D term (referred to the lowest level in *Ti* I) should lie at the level 28,500, and all its combinations of any strength must be in the infra-red, which explains why it has not been detected. The $^3P'$ and $^3F'$ terms should lie at about 34,100 and 34,800. They would combine strongly only with terms of origin $(3d)^3 4p$, and these again give infra-red lines. It is not surprising that their faint combinations with the low odd terms of origin $(3d)^2 4s \cdot 4p$ have been missed.

10. SUMMARY

It may be appropriate in conclusion to summarize the results obtained in the discussion of the spectra of titanium in the various degrees of ionization, as is done in Table XIV. The number of energy levels, or separate components of the terms, represents the number of distinct states in which the atom in this degree of ionization is known to exist. The whole number of such states, for all four degrees of ionization together, is 545; of multiplets which have been identified, 629; and of lines classified, 2044.

As the number of valency electrons increases, the complexity of the spectrum becomes great. The number of terms and multiplets is very large, and that of the various identifiable electron configurations in the atom increases. It is worthy of remark, however, that a greater variety of electron orbits has been identified in the simple "stripped" atom *Ti* IV than in any other state.

The final outcome of this long investigation may be summarized in a sentence. The present theories of atomic and spectral structure suffice to give a most satisfactory account, in full and complete detail, of all the features of the very complex spectrum of titanium.

TABLE XIV

SUMMARY

Systems Present	*Ti* I; Quintets Triplets, Singlets	*Ti* II; Quartets Doublets	*Ti* III; Triplets Singlets	*Ti* IV; Doublets
Types of terms	S to H S′ to I′	S to H S′ to H′	S to G P′ to D′	S to H
Number of terms	142	49	19	12
Number of energy levels	364	123	40	18
Number of multiplets	422	164	28	15
Number of lines classified	1394	529	90	31
Number of series found	17	4	2	4
Ionization potential, volts	6.81	13.58	27.6	43.08
Electron configurations:				
Low even	$(3d)^2 4s^{2*}$	$(3d)\,(4s)^2$		
	$(3d)^3 4s$	$(3d)^2\, 4s^*$	$3d\, 4s$	$4s$
	$(3d)^4$	$(3d)^3$	$(3d)^{2*}$	$3d^*$
Odd	$(3d)^2 4s \cdot 4p^*$	$3d \cdot 4s \cdot 4p$	$4s \cdot 4p$	$4p$
	$(3d)^3 4s \cdot 5p$	$(3d)^2 \cdot 4p^*$	$3d \cdot 4p^*$	$5p$
	$(3d)^3 4p$	....	....	$4f$
	$(3d) \cdot {}^3 5p$			
High even	$(3d)^2 4s \cdot 5s^*$	$(3d)^2 \cdot 5s^*$	$3d \cdot 4d$	$5s$:
	$(3d)^2 4s \cdot 6s$	$(3d)^2 \cdot 4d$	....	$6s$:
	$(3d)^2 4s \cdot 4d$	....	....	$4d$
	$(3d)^2 4s \cdot 5d$	....	....	$5d$
	$(3d)^2 (4p)^2$	....	....	$5g$
	$(3d)^3 5s$	....	....	$6h$
	$(3d)^3 6s$	....	....	....
	$(3d)^3 4d$	....	....	$7h$

* This configuration gives the lowest energy level among the group in which it falls.

All the lines of any prominence have been classified, and it is reasonably certain that no important low terms have escaped notice. There are many faint unidentified lines, however, and a few stronger ones in the arc spectrum in the far ultra-violet, which show that there is still more work to be done, presumably in the study of the higher energy levels. The data already obtained, however, should suffice for astrophysical investigation, and they afford extensive material for both observational and theoretical studies of line intensities, term separations, and relative levels of terms arising from the same configuration.

To the writer's many colleagues, who have generously supplied him with material and aided in many other ways, he desires to record once more his gratitude; for himself the interest of the work itself has been an abundant reward.

Carnegie Institution of Washington
Mount Wilson Observatory
May 23, 1927

INDEX TO VOLUME XV

Nos. 327 to 345

AUTHORS

PAGE

Babcock, Harold D.—
  Secondary Standards of Wave-Length; Interferometer Measurements of Iron and Neon Lines 307
  A Study of the Infra-Red Solar Spectrum with the Interferometer . 11

Bowie, William—Measurements of Length of Line Used in Determination of Velocity of Light 48

Duncan, John Charles. *See* Hubble, Edwin

Hubble, Edwin, and John Charles Duncan—The Nebulous Envelope around Nova Aquilae No. 3 145

Lang, R. J. *See* Russell, Henry Norris

Merrill, Paul W.—Stars Whose Spectra Have Bright Iron Lines . 135

Michelson, A. A., Assisted by F. Pearson—Measurement of the Velocity of Light between Mount Wilson and Mount San Antonio 35

Pearson, F. *See* Michelson, A. A.

Pettit, Edison—Transmission Properties of Some Filters . . 151

Russell, Henry Norris—
  The Arc and Spark Spectra of Titanium
    Part I: The Spark Spectrum, *Ti* II 335
    Part II: The Arc Spectrum, *Ti* I 381
  On the Relations between Period, Luminosity, and Spectrum among Cepheids 221
  Related Lines in the Spectra of the Elements of the Iron Group . 249
  Series and Ionization Potentials of the Elements of the Iron Group . 283

Russell, Henry Norris, and R. J. Lang—On the Spectra of Doubly and Trebly Ionized Titanium (*Ti* III and *Ti* IV) 167

Sanford, Roscoe F.—
  On the Radial Velocity and Spectrum of the Cepheid Variable T Monocerotis 235
  Spectrographic Orbits of the Two Components of Boss 5683 . . 129

Schilt, J.—The Short-Period Variable Star RV Canum Venaticorum . 57

PAGE

Strömberg, Gustaf—
  The Absolute Magnitudes of Giant M Stars 1
  The Motions of Giant M Stars 101

Struve, Otto—Interstellar Calcium 63

Van Maanen, Adriaan—Investigations on Proper Motion. Twelfth Paper: The Proper Motions and Internal Motions of Messier 2, 13, and 56 197

SUBJECTS

Absolute magnitudes, of giant M stars, 1
Arc spectrum, of titanium, 381
Binaries, spectroscopic, orbits of two components of Boss 5683; 129
Calcium, interstellar, 63
RV Canum Venaticorum, 57
Cepheids, radial velocity and spectrum of T Monocerotis, 235
———, relations between period, luminosity, and spectrum, 221
Filters, transmission properties, 151
Giant M stars, absolute magnitudes, 1
———, motions, 101
Infra-red solar spectrum, studied with interferometer, 11
Interferometer, used to study infra-red solar spectrum, 11
Interferometer measurements, of iron and neon lines, 307
Ionization potentials of elements of iron group, 283
Iron group, elements, related lines in spectra, 249
———, ———, series and ionization potentials, 283
Iron lines, interferometer measurements, 307
Light, velocity, measured between Mount Wilson and Mount San Antonio, 35
Lines, bright iron, in stellar spectra, 135
———, iron and neon, interferometer measurements, 307
———, related, in spectra of elements of iron group, 249
Magnitudes, absolute, of giant M stars, 1
Messier 2, 13, 56, internal and proper motions, 197
T Monocerotis, radial velocity and spectrum, 235
Motions, internal, of Messier 2, 13, 56; 197
———, of giant M stars, 101
———, proper, of Messier 2, 13, and 56; 197
Nebulous envelope, around Nova Aquilae No. 3; 145
Neon lines, interferometer measurements, 307
Nova Aquilae No. 3, surrounding nebulous envelope, 145
Radial velocity, of T Monocerotis, 235
Series and ionization potentials of elements of iron group, 283
Spark spectrum, of titanium, 335
Spectra, of doubly and trebly ionized titanium, 167
———, of elements of iron group, related lines, 249
———, stellar, having bright iron lines, 135
Spectroscopic binaries, orbits of two components of Boss 5683; 129
Spectrum, arc, of titanium, 381

Spectrum, of T Monocerotis, 235
———, solar, studied in infra-red with interferometer, 11
———, spark, of titanium, 335
Standards of wave-length, secondary, 307
Stars, giant M, absolute magnitudes, 1
———, ———, motions, 101
———, short-period variable, RV Canum Venaticorum, 57
———, variable, radial velocity and spectrum of T Monocerotis, 235
———, ———, relations between period, luminosity, and spectrum among Cepheids, 221
———, with spectra having bright iron lines, 135
Sun, infra-red spectrum, studied with interferometer, 11
Titanium, arc spectrum, 381
———, doubly and trebly ionized, spectra, 167
———, spark spectrum, 335
Transmission properties of filters, 151
Variable stars, Cepheid, radial velocity and spectrum of T Monocerotis, 235
———, ———, relations between period, luminosity, and spectrum, 221
———, short-period, RV Canum Venaticorum, 57
Velocity of light, measured between Mount Wilson and Mount San Antonio, 35
Wave-length, secondary standards, 307

a39001 006937273b

522 19 C28 V15
MOUNT WILSON OBSERVATORY CONTRIBUTION

INSERT BOOK
MASTER CARD
FACE UP IN
FRONT SLOT
OF S.R. PUNCH

MASTER CARD

GLOBE 901144-0

ESTABLISHED 1885

UNIVERSITY OF ARIZ
LIBRARY